AFFDL-TR-79-3045
Volume II

ANGULAR VIBRATION OF AIRCRAFT
Volume II — Prediction Methods for Angular Vibration

ANAMET LABORATORIES, INC.
APPLIED MECHANICS DIVISION
SAN CARLOS, CALIFORNIA 94070

April 1979

TECHNICAL REPORT AFFDL-TR-79-3045, Volume II
Final Report for Period August 1977 to April 1979

Approved for public release; distribution unlimited.

AIR FORCE FLIGHT DYNAMICS LABORATORY
AIR FORCE WRIGHT AERONAUTUICAL LABORATORIES
AIR FORCE SYSTEMS COMMAND
WRIGHT-PATTERSON AIR FORCE BASE, OHIO 45433

NOTICE

When Government drawings, specifications, or other data are used for any purpose other than in connection with a definitely related Government procurement operation, the United States Government thereby incurs no responsibility nor any obligation whatsoever; and the fact that the government may have formulated, furnished, or in any way supplied the said drawings, specifications, or other data, is not to be regarded by implication or otherwise as in any manner licensing the holder or any other person or corporation, or conveying any rights or permission to manufacture, use, or sell any patented invention that may in any way be related thereto.

This report has been reviewed by the Information Office (OI) and is releasable to the National Technical Information Service (NTIS). At NTIS, it will be available to the general public, including foreign nations.

This technical report has been reviewed and is approved for publication.

Lt. Michael W. Obal

LT MICHAEL W. OBAL
Project Engineer

Ralph N. Bingman

RALPH N. BINGMAN
Technical Manager

Ralph L. Kuster Jr.

RALPH L. KUSTER, JR., Colonel, USAF
Chief, Structures and Dynamics Division

Copies of this report should not be returned unless return is required by security considerations, contractual obligations, or notice on a specific document.

AIR FORCE/56780/5 July 1979 — 150

UNCLASSIFIED

SECURITY CLASSIFICATION OF THIS PAGE (When Data Entered)

REPORT DOCUMENTATION PAGE

READ INSTRUCTIONS BEFORE COMPLETING FORM

1. REPORT NUMBER AFFDL-TR-3045, Volume II	2. GOVT ACCESSION NO.	3. RECIPIENT'S CATALOG NUMBER
4. TITLE (and Subtitle) ANGULAR VIBRATION OF AIRCRAFT Volume II - Prediction Methods for Angular Vibration		5. TYPE OF REPORT & PERIOD COVERED Final Report 8/77 to 4/79 6. PERFORMING ORG. REPORT NUMBER
7. AUTHOR(s) Conor D. Johnson, Ernest B. Paxson, Warren C. Gibson, David Kienholz		8. CONTRACT OR GRANT NUMBER(s) F33615-77-C-3050
9. PERFORMING ORGANIZATION NAME AND ADDRESS Anamet Laboratories, Inc. 100 Industrial Way San Carlos, California 94070		10. PROGRAM ELEMENT, PROJECT, TASK AREA & WORK UNIT NUMBERS Project 2401 Task 240104 W.U. 24010408
11. CONTROLLING OFFICE NAME AND ADDRESS Air Force Flight Dynamics Laboratory AFSC/AFWAL, United States Air Force Wright-Patterson AFB, Ohio 45433		12. REPORT DATE April 1979 13. NUMBER OF PAGES 433
14. MONITORING AGENCY NAME & ADDRESS(if different from Controlling Office)		15. SECURITY CLASS. (of this report) UNCLASSIFIED 15a. DECLASSIFICATION/DOWNGRADING SCHEDULE

16. DISTRIBUTION STATEMENT (of this Report)

Approved for public release; distribution unlimited.

17. DISTRIBUTION STATEMENT (of the abstract entered in Block 20, if different from Report)

18. SUPPLEMENTARY NOTES

19. KEY WORDS (Continue on reverse side if necessary and identify by block number)

Angular Vibration
Finite Element
Statistical Energy Analysis
Structural Analysis
Structural Dynamics
Angular Measurement
NASTRAN
Structural Test
Semi-Loof

20. ABSTRACT (Continue on reverse side if necessary and identify by block number)

This report describes development work in several distinct areas, all related to prediction of angular vibration of aircraft structures. Angular vibration in this context refers to dynamic rotations or changes in slope at specific points on a vibrating structure. It is of interest primarily in connection with high resolution optical and electro-optical systems. Efforts were directed at both low frequency vibration, where individual normal modes are known, as well as high frequency vibration where they are not. For low frequency predictions, improved accuracy per unit cost was sought by an evolutionary improvement to an

DD FORM 1473, 1 JAN 73 — EDITION OF 1 NOV 65 IS OBSOLETE

UNCLASSIFIED

SECURITY CLASSIFICATION OF THIS PAGE (When Data Entered)

existing finite element code. A state-of-the-art shell element, the Semi-Loof, was incorporated into NASTRAN by means of pre- and post-processors and DMAP instructions. Its accuracy is tested against both closed form solutions for simple cases and experiment for an actual fuselage. For high frequency predictions the method of Statistical Energy Analysis was pursued. A demonstration case involving two coupled plates is presented to show how SEA may be used to predict angular vibration in a situation where normal modes are too numerous to be predicted individually. Relationships between linear and angular vibration were developed for various structural forms. Theoretical error bounds are also derived for spectral measurements of angular vibration which are obtained by differencing of signals from translational sensors.

AD071749

FOREWORD

This report describes an investigation into the prediction methods of angular vibration of aircraft, performed by Anamet Laboratories, Inc., San Carlos, California, for the Air Force Flight Dynamics Laboratory, Air Force Systems Command, Wright-Patterson Air Force Base, Ohio, under Contract F33615-77-C-3050. This research was conducted under Project 2401, "Structural Mechanics," Task 240104, "Vibration Prediction and Control, Measurement and Analysis," Work Unit 24010408, "Angular Vibration of Aircraft." Lt. Michael W. Obal, (AFFDL/FBG) was the project engineer. This report is in two volumes: Volume I - Executive Summary; Volume II - Prediction Methods for Angular Vibration.

This program was conducted by the Applied Mechanics Division of Anamet Laboratories. Program Manager was Dr. Conor Johnson and Principal Investigators were Dr. Warren Gibson, Dr. David Kienholz, and Dr. Ernest Paxson. This research was performed between August 1977 and April 1979.

This report was submitted by the authors on 2 April 1979 for publication as an AFFDL Technical Report.

TABLE OF CONTENTS

TABLE OF CONTENTS (Continued)

TABLE OF CONTENTS (Continued)

TABLE OF CONTENTS (Concluded)

LIST OF ILLUSTRATIONS

LIST OF ILLUSTRATIONS (Continued)

LIST OF ILLUSTRATIONS (Continued)

LIST OF ILLUSTRATIONS (Continued)

LIST OF ILLUSTRATIONS (Concluded)

LIST OF TABLES

LIST OF SYMBOLS

a	Coordinate location (x=a) of concentrated random load
A	Cross-section area of beam (Section V)
A	Amplitude coefficient on the noise power spectrum (Section VI)
A_i	Stiffener area
A_{ij}, B_{ij}, D_{ij}	Force-strain parameters for stiffened shells
$A_{ijk\ell}$	Finite element master matrix
A_p	Plate area
b_i	Stiffener spacing
B	Amplitude coefficient on the signal power spectrum
B_{ij}	Finite element master vector
c	Transducing scale factor, engineering units/volt (Section VI)
c, c_1, c_2	Spring damping constants (Section V)
$c(f)$	Nominal frequency response of transducing channel
c_b	Phase velocity of flexural wave
c_ℓ	Extentional wave speed for a material, $\sqrt{E/\rho}$
C_i	Stiffener eccentricity
$C_i(f)$	Complex functions of frequency defined by Eq. (6.17)
$C_1 = \frac{\Lambda}{k} K_1$, $C_2 = \frac{\Lambda}{k} K_2$	Modal damping factors
D	Amplitude of flexural wave
$e_i(t)$	Voltage produced by transducer channel i
e_o	Difference signal

LIST OF SYMBOLS (continued)

$\vec{e}_x, \vec{e}_y$	Unit vectors in x and y directions
E	Modulus of elasticity
$E_i(f)$	Fourier transform of $e_i(t)$
$E_i(t)$	Energy of i^{th} mode (in Section 4.4.1)
$E^{(i)}(t)$	Energy of i^{th} mode (in Section 4.5.1)
$E_A(f)$	Spectral density of total energy of body A
$E_A(t)$	Total energy (kinetic plus potential) of body A
f	Frequency in cycles/unit time
f_b	Center frequency of band b
f_c	Center frequency of a specified band
$f_i, f^{(i)}$	i^{th} natural frequency
$f_{\ell.m.}$	Log mean frequency of a band
f_r	r^{th} resonant frequency
F	Energy density interior to a structure
F_1, F_2	Forces at ends of rigid bar
g	Gravitational constant (396.04 lb_m-in/lbf-sec^2)
G	Energy density on the boundary of a structure (Section III)
G	Shear modulus (Appendix A)
h	Plate thickness
$h_i(\tau)$	Impulse response to transducer channel i
h_1, h_2	Response single degree-of-freedom system to unit impulse
$H(f)$	Fourier transform of $h(\tau)$
H_i	Weighting factors for Gaussian integration
$H_i(f), c_i(f)$	Frequency response of transducer channel i

LIST OF SYMBOLS (continued)

$H_{oi}(f)$	Displacement/force frequency response between points o and i
H_A	Mechanical admittance of body A at a coupling degree of freedom ($=Z_A^{-1}$)
$H_1(\omega),H_2(\omega)$	Complex frequency responses
$H_1^*(\omega),H_2^*(\omega)$	Complex conjugates of H_1 and H_2, respectively
i	$\sqrt{-1}$, also used as the mode index
I	Area moment of inertia of cross-section of beam about neutral axis
I_c	Mass moment of inertia for rigid bar about CG
I_i	Stiffener moment of inertia
J_i	Stiffener torsion constant
k	Exponent of envelope of signal power spectrum (Section VI)
k,k_1,k_2	Spring stiffness constants (Section V)
k_c	Stiffness of coupling spring
k_{xi},k_{yi}	Wavenumbers in the x and y direction corresponding to the i^{th} mode
K_1,K_2	Modal stiffness constants
$\ell(t)$	Force input
$\ell_a(t),\ell_b(t)$	Coupling forces acting at points a and b of bodies A and B
$\ell_c(t)$	Force in a massless coupling element
$\ell_o(t)$	Prescribed input force
L	Length of rigid bar, length of finite beam
L(f)	Fourier transform of $\ell(t)$
$L_a(f),L_b(f)$	Fourier transforms of loads $\ell_a(t)$ and $\ell_b(t)$

LIST OF SYMBOLS (continued)

L_1, L_2	Distances from opposite ends to CG of rigid bar
m	Mass per unit length of beam (Section V)
m	Exponent of envelope of noise power spectrum (Section VI)
m_i	i^{th} diagonal entry of mass matrix $\underset{\sim}{M}$ (Section 4.2) or i^{th} modal mass (Section 4.4.1)
m_A	Total mass of body A
M	Mass of rigid bar
$\underset{\sim}{M}$	Mass matrix
M_o	Minimum allowable value of flexural modulation function
M_1, M_2	Elements of mass matrix for spring-supported rigid bar system (Section V)
M_1, M_2, M_{12}	Shell moment resultants (Appendix A)
$n_i(t)$	Noise in channel i
$N_i(f)$	Fourier transform of $n_i(t)$
$N_{ij}(\xi,\eta)$	Finite element shape functions
N_A	Number of normal modes of body A within a specified frequency band
N_1, N_2, N_{12}	In-plane shell force resultants
$P(t)$	Temporally random concentrated load
$q(x)$	Spatial distribution of load on beam
q_n, q_k	Fourier coefficients for load function on beam
q_o	Constant representing load intensity on beam
q_1, q_2	Normal coordinates for spring supported rigid bar system
$R_{v\ell}(t)$	Cross correlation between $v(t)$ and $\ell(t)$

LIST OF SYMBOLS (continued)

$R_x(\tau)$	Auto correlation of x(t)
$S_{\bar{e}}(f)$	Average of $S_{e_1}(f)$ and $S_{e_2}(f)$
$S_p(\omega)$	Spectral density of random concentrated force
S_{po}	Constant value of spectral density for White Noise
$S_u(f)$	Autopower spectral density of u(t)
$S_{uv}(f)$	Cross power spectral density of u(t) and v(t)
$S_x(\omega), S_y(\omega)$	Spectral densities of x(t) and y(t), respectively
$S_{w_r}, S_{\theta_\theta}, S_{\theta_z}$	Spectral density of w_r, θ_θ, θ_z, respectively
$S_{NR}(f)$	Narrow-band signal-to-noise ratio for a quantity obtained by differencing
t	Time (Section IV)
t	Shell thickness (Appendix A)
T	Averaging time (Section 4.3.2) or sampling interval (Section 4.6.2)
$T_A(t)$	Kinetic energy of structure A
$u_i(\xi,\eta)$	Displacements
$\hat{u}_{k\ell}$	Finite element degrees of freedom
$U_A(f)$	Spectral density of $U_A(t)$
$U_A(t)$	Potential energy of body A
$v_a(t), v_b(t)$	Velocities at coupling points a and b of bodies A and B
$v_b^{(\ell_c)}(t)$	Velocity of coupling point b of body B when B is acted on only by the coupling force ℓ_c
$V_a(f), V_b(f)$	Fourier transforms of $v_a(t)$ and $v_b(t)$
w	Transverse shell displacement
w(x,y)	Out-of-plane displacement of a plate

LIST OF SYMBOLS (continued)

w_r	Displacement of panel normal to surface
x	Independent coordinate along undeformed beam neutral axis
$\underset{\sim}{x}$	Vector of displacements
x,y	Rectangular coordinates (in Section 4.4.1)
$x(t)$	Vertical displacement of CG of rigid bar
$x_a(t),x_b(t)$	Displacements at coupling points a and b of bodies A and B
x_1,x_2	Vertical displacement of ends of rigid bar
$\overline{x^2}$	Temporal mean of $[x(t)]^2$
$X_a(f),X_b(f)$	Fourier transform of $x_a(t)$ and $x_b(t)$
$\underset{\sim}{X}_9,\underset{\sim}{Y}_9$	Unit vectors at the center point of a Semi-Loof shell element
$y(t)=L\theta(t)$	Relative displacement of one end of rigid bar with respect to opposite end
$y(x,t)$	Lateral displacement of beam longitudinal axis
$y_i(t)$	Displacement of channel i transducer
$\overline{y^2}$	Temporal mean of $[y(t)]^2$
$Y_i(f)$	Fourier transform of $y_i(t)$
Z_a	Mechanical impedance of body A at a coupling degree of freedom a
$\alpha(f)$	Spectral discrete difference function defined by Eq. (6.26)
α_i	Gauss points
α_1,α_2	Ratios L_1/L and L_2/L such that $\alpha_1+\alpha_2=1$
β	Ratio of c_2/c_1 for rigid bar system, damping factor for beam material

LIST OF SYMBOLS (continued)

$\tilde{\beta}_1, \tilde{\beta}_2$	Modal damping factors
γ	Ratio of k_2/k_1
$\underset{\sim}{\gamma}$	Transverse shear strain vector resultant
$\gamma^2_{uv}(f)$	Coherence between u(t) and v(t)
$\underset{\sim}{\gamma}_{XZ}$	Transverse shear strain on the boundary of an element
$\Gamma^2(f)$	Real function of frequency defined by Eq. (6.49)
$\delta(f)$	Complex channel mismatch function defined by Eq. (6.23)
$\delta(\xi)$	Discontinuity along an element edge $-1 \leq \xi \leq 1$
Δf	Width of a frequency band used to define the $< >_t$ operator
Δx	Separation distance for transducers
$\varepsilon_1, \varepsilon_2, \varepsilon_{12}$	In-plane shell strains
ζ_r	Viscous damping ratio of r^{th} mode
η	Ratio of distance to P(t) from CG of rigid bar/ length L
$\eta_i^{(t)}, \eta^{(i)}(t)$	i^{th} generalized coordinate
η_A	Internal loss factor for body A
η_{AB}	Coupling loss factor for power transmission from body A to body B
$\theta(t)$	Angular displacement of rigid bar (Section V)
$\theta(t)$	Rotation angle to be measured (Section VI)
$\theta(x,t)$	Angular displacement of beam longitudinal axis (Section V)
$\theta(x,y,t)$	∇w, gradient of w(x,y,t) (Section IV)
θ_z	Angular displacement of panel about z-axis

LIST OF SYMBOLS (continued)

$\hat{\theta}_A$	Estimate of $\ddot{\theta}$ obtained with an actual transducing system
$\hat{\theta}$	Estimate of $\ddot{\theta}$ obtained with an ideal transducing system
θ_θ	Angular displacement of panel about θ-axis
κ	Radius of gyration for the cross-section of a beam or plate
λ	Wavelength of flexural wave
λ_n	Roots of characteristic frequency equation for FREE-FREE beam
Λ	Proportionality constant between spring damping and spring stiffnesses
ν	Poisson's ratio
ξ,η	Curvilinear shell coordinates
$\xi^{(i)}$	Viscous damping ratio of the i^{th} mode
π	Energy functional (Section III)
π	3.1416 (Sections IV and VI)
$\pi^{(i)}(t)$	Power input to the i^{th} mode
$\pi_{A,DIS}$	Power dissipated internally by body A
$\pi_{A,IN}$	Power input to body A from prescribed sources
$\pi_{AB,TRAN}$	Power transmitted from body A to body B
$\Pi_{AB}(f)$	Spectral density of power transmitted from A to B
ρ	Density of beam material
$\sigma^2_{e_i}$	Mean square signal in channel i
σ^2_n	Mean square noise
σ^2_u	Mean square value of the zero-mean variable u(t)
τ	Lag time in the correlation function

LIST OF SYMBOLS (continued)

$\phi(\xi,\eta)$	Any function to be integrated over an element domain
Φ_n, Φ_k	Eigenfunctions for FREE-FREE beam
$\chi_1, \chi_2, \chi_{12}$	Shell curvatures
$\psi_i(x,y)$	i^{th} normal mode shape
$\psi_o^{(r)}, \psi_i^{(r)}$	Amplitude of r^{th} normal mode shape at points o and i
ω	Frequency in radians/unit time
$\omega_i, \omega^{(i)}$	i^{th} natural frequency (Section IV)
ω_n, ω_k	Natural frequencies of n and k mode shapes for beam (Section V)
ω_r	$2\pi f_r$
Ω	Weighting factor for the centerpoint of Gaussian integration
$\mathcal{L}(u_i)$	Differential operator governing the interior of a structure
$\mathcal{B}(u_i)$	Differential operator governing the boundary of a structure
$\langle\ \rangle_t$	Expectation with respect to time, usually of the portion of a positive definite quantity within a specified frequency band
$\mathcal{F}(\ )$	Fourier transform
$\mathcal{F}^{-1}(\ )$	Inverse Fourier transform
Re( )	Real part of
Im( )	Imaginary part of
$\lvert\ \rvert$	Modulus of
$\bar{\ }$ (overbar)	Smoothing with respect to frequency

LIST OF SYMBOLS (Concluded)

< >	Ensemble averaging (when applied to products of Fourier transforms)
∇	Gradient operator in two dimensions
E[ ]	Expectation
$(\ )_{rms}$	Square root of the temporal mean of $(\ )^2$
$(\dot{\ })$	Time derivative of ( )
( )'	Spatial derivative
^	Denotes estimate
*	Convolution operator
*	Complex conjugate (used as superscript)
$M(\cdot)$	Modulation function $\sin(\cdot)/(\cdot)$

SECTION I
INTRODUCTION

With the design and development of inertial sensing systems and laser beam control systems, angular vibration measurements and predictions have become as important, and in some cases more important, than translational vibration measurements and predictions. Also, very small amplitudes of angular vibration, on the order of a few microradians, have become important, especially in the design of airborne laser beam control systems. Angular vibration is the major factor in beam jitter of laser systems. Beam jitter is dynamic misalignment of a laser beam due to dynamic motion of the components of the optical train through which it passes. Beam jitter is normally random in time and is specified by the root mean square value. The optical train consists of both stationary and servo-controlled mirrors and sensors from beam initiation in the laser device through the pointing and tracking system.

Beam jitter is dependent on a number of factors. Among these are mechanical resonances of individual optical components and their supporting structures, dynamic behavior of the entire structure system, spacing of the optical components, mounting system characteristics, dynamic characteristics of the aircraft, and frequency content of loads. Since the laser or electro-optical system is mounted to the aircraft, and the aircraft is subjected to many loads, such as gusts, turbulence, etc., the dynamics of the aircraft must be predicted accurately. The dynamic characteristics of the aircraft that are used for design and analysis consist of both translational and angular vibrations. The elastic modes of an aircraft may be as low as 1 or 2 Hz. The lowest elastic modes of individual components of a laser system may be in the 150 to 300 Hz range. Therefore,

to perform complete frequency response analysis may require modal information from 1 Hz to 1000 to 2000 Hz.

The objectives of this contract were (1) to develop techniques for predicting the low and high frequency angular environment of aircraft; (2) to develop accurate angular vibration measurement techniques; (3) to develop techniques for predicting the low and high frequency angular vibration of combined airframe and electro-optical systems; and (4) to demonstrate these techniques by applying them to an aircraft-like structure and comparing the results with measured data. For this report, low frequencies are defined as those frequencies for which individual normal mode shapes can be predicted accurately or determined by tests.

The work on this contract was subdivided into three phases. The objective and accomplishment of Phase I was to identify methods which could be used to predict angular vibration for both low and high frequencies. Literature searches were performed to obtain information on past experience in the area of angular vibration. Also searched were methods and improvements to methods which may be useful in the prediction of angular vibration at low and high frequencies. For low frequencies, it was decided the main thrust should be directed towards obtaining more accuracy per degree of freedom in finite element analysis. This approach satisfies all of the objectives for the low frequency method and also gives a method which is flexible and adaptable for application to complex structures. The Semi-Loof shell element and its companion beam element were selected as the most promising candidates to meet this objective. The technique selected for combining components or structures, such as an aircraft and an electro-optical system, into a system analysis for low frequencies was component mode synthesis. The component mode synthesis technique treats each component or structure in terms of its modal description (obtained either from tests or

analysis). For high frequency analysis, statistical energy analysis (SEA) was selected. SEA treats the structure in terms of some averaged, or statistical, description. One of the most important features of the SEA method is its ability for making use of whatever level of detail is available in the description of a structure.

The major emphasis of Phase II was the detailed development of the methods chosen during Phase I. For the low frequency method, the approach taken was to implement Semi-Loof into the finite element code, NASTRAN. As originally derived, the Semi-Loof element was for use on static problems only. Therefore, the mass matrices for the elements had to be incorporated. To be able to model complex structures such as airframes, other enhancements to the element had to be made. Among these were orthotropic material properties, offset beams, smeared stiffeners, variable thicknesses for the shell elements, non-prismatic beam geometry, and distributed loads. The input was developed using NASTRAN bulk data card formats. A stress recovery and a rotational recovery capability were added. The element is incorporated into NASTRAN by means of pre- and post-processors and NASTRAN DMAP instructions. The processors incorporate a matrix assembly routine, and an extensive error checking capability. A User's Manual for Semi-Loof was written and is included in this report as Appendix A. During Phase II a number of sample problems were executed and the results were compared to NASTRAN solutions and tests. The results showed good improvement in accuracy per degree of freedom.

As stated earlier, statistical energy analysis (SEA) had been chosen as the best approach to predict the angular vibration environment of aircraft when only an averaged or statistical description of the structures is known. SEA has been used as a tool for acoustical analysis in the past but no work had been done toward employing this method to predict angular vibration environments. The theory of SEA was studied and the essential features of SEA which make it attractive for the

present purpose were identified. A formula for estimating coupling loss factor by the wave transmission method was rederived without assuming response to be in the form of traveling waves. An experiment was conducted where the wave transmission method was used to predict transmitted power and the equilibrium energy ratio between two coupled plates. This experiment demonstrated that SEA could be used to predict the energy ratio and power transfer coefficient between coupled plates in a high frequency region where finite element modeling was impractical. A relation was derived between the r.m.s. angle and the vibrational energy in frequency bands. An experiment was conducted to test this relation and show how r.m.s. angular displacement can be obtained from SEA results without detailed knowledge of individual mode shapes or natural frequencies. Software was developed for the minicomputer-based equipment used to perform these experiments.

A study was also conducted on relationships between linear and angular vibration for various structural components. A detailed study of the simplest structural system possessing both linear and angular degrees of freedom was conducted. The ratio of the mean square angular to mean square linear displacement was investigated for simply-supported beams, a simply-supported flat plate, a free-free beam, and a curved stiffened panel. A simple relation between mean square angular to mean square linear displacement was derived using wave theory.

In order to verify the prediction methods developed, reliable experimental data had to be obtained, especially dynamic rotations at specific points. The measurement method used to obtain these rotations was differencing of translational acceleration signals. A better quantitative understanding of limitations and error sources was desirable. Therefore, theoretical derivations were developed for estimating errors introduced by noise in individual channels, frequency-dependent gain and phase mismatching between channels, and flexure of the mounting surface. Effects of the first two error sources were

demonstrated by experiment and it was demonstrated that mismatch error can be reduced by appropriate data processing. Also, an expression was derived for coherence of a measured angular frequency response when angular response was obtained by differencing.

The major objective of Phase III was to apply the methods developed to a complex structure. A fuselage section of a fighter aircraft was chosen as the test structure. This structure was chosen because it was a fairly complex structure to analyze. A finite element model of the fuselage was developed using the Semi-Loof elements. All of the features that were developed for this element were employed in the modeling. An eigenvalue analysis of the structure was performed to determine the normal modes. A frequency response analysis was performed with random noise input at three different points. The responses at a number of translational and rotational degrees of freedom were output. A test of the fuselage was also performed. The fuselage was supported on a low stiffness mounting system and driven by a small shaker system at three different locations. Both force to linear acceleration and force to angular acceleration transfer functions were measured for drive and response points corresponding to points in the Semi-Loof model. After processing the data on the minicomputer-based modal analysis equipment, the experimental data was compared to the results predicted by Semi-Loof.

Section II of this report described the literature searches performed to obtain information on past experience in the area of angular vibration. Also searched were methods and improvements to methods which might have been useful in the prediction of angular vibration at low and high frequencies. This section also discusses some of the methods looked at and discarded, and the reasons behind the selection of the methods chosen for further study.

Section III describes the work performed on the Semi-Loof elements, which was the main low frequency method. This section gives a review of the theory of finite elements in general and the Semi-Loof element in particular. The implementation of Semi-Loof into NASTRAN is described in detail. Comparisons and evaluations are made using small simple problems, results of analysis using other elements, and test results.

Section IV describes the high frequency method, which is statistical energy analysis (SEA). A brief summary of the theory of SEA is presented. Derivations of relations and experiments are described which predict transmitted power, the equilibrium energy ratio, and angular response between two coupled plates.

Section V is a study of the relationship between linear and angular vibration for various structural components.

Section VI describes the work performed on some quantitative methods of estimating the reliability of measured power spectral density functions or frequency response functions for the case where the response quantity is an angular motion obtained by differencing of signals from linear transducers.

Section VII describes the fuselage finite element model and the dynamic test performed on this fuselage. A comparison of the results of the test and analysis is given.

Section VIII gives a summary of the work, draws conclusions from the progress made, and briefly describes additional work which should be done in the future.

SECTION II
BACKGROUND

2.1 LITERATURE SEARCH

The first task started in Phase I was a literature search to determine what had been done in the past for predicting angular vibration as well as high frequency translational vibration. As usual in an extensive literature search, one source led to another, often via topics which were not directly related to the immediate problem. Some of the most useful information and sources were obtained through personal communication.

Initial searching revealed little on angular vibration as such which was not previously known. However, numerous possibilities were identified within the overall field of vibration analysis which might lead to improved methods for prediction of angular vibration.

The data bases searched included DDC Technical Reports, NTIS, NASA, and COMPENDEX. The DDC (Defense Documentation Center) Technical Reports data bank contains more than 1,200,000 records dating back to March, 1953. DDC receives these reports from defense facilities and their contractors who are required to submit to DDC copies of each report that records scientific and technical data from defense sponsored research, development test, and evaluation. NTIS (National Technical Information Service) contains the complete Government Reports Announcements (GRA) file from the National Technical Information Service. It contains 641,000 citations of government research from over 240 agencies. The file, which dates back to 1964, is updated every two weeks, and is growing at the rate of 78,000 abstracts per year. The NASA data base contains the results of worldwide research and development activities in aeronautics, space, and supporting disciplines. It now contains nearly a million

documents which are abstracted and indexed. COMPENDEX is a machine readable version of the Engineering Index data base which provides abstracts and an index to the world's significant engineering literature and conference proceedings covering the time span of 1970 to the present. This data base covers 3,500 journals, publications, and papers from the proceedings of conferences as well as selected government reports and books. It contains over 90,000 abstracts and 655,000 citations.

The major topics that were searched included (1) linear vibration of aircraft, (2) angular vibrations, (3) finite elements or finite differences in combination with angular vibration, high frequencies, and statistics, (4) high frequency methods, (5) acoustical methods, and (6) statistical energy methods. These major topics led to many minor topics which were investigated to the extent of determining the usefulness in predicting angular vibration.

Automated searching on the key phrases "finite element" and "angular vibration" was unproductive. "Angular vibration" often turns out to mean torsional vibration of shafts. There simply does not seem to have been any finite element or other numerical work that focused specifically on angular vibrations as that term is understood in the current effort. Consequently, the searching strategy for the analytical portion of this effort was shifted rather early toward developments that might contribute indirectly to angular vibration predictions. This broadened the possibilities immensely (for example, a DDC search listed some 1300 references under "finite element"). Narrowing the search to shell elements, searching continued mostly in a manual mode, with many papers leading to others through references. Most of these were concerned with isoparametric elements which have received the most attention from researchers. A number of papers in this vein were reviewed. However, the Semi-Loof element, which was adopted for study and implementa-

tion, was obtained through a personal communication. Subsequently, other papers on Semi-Loof were discovered in the literature.

As noted previously in this section, literature searching under key words such as "angular vibration" yielded almost no research or development work not previously known. The few references uncovered on angular vibration of any kind were concerned with specific pieces of hardware rather than prediction methods. For high frequency angular vibration, the search strategy was to investigate high frequency and statistical methods in general without reference to any particular type of response variable. A list of key words and phrases used in the computer-aided searches is given in Table 1.

TABLE 1

KEY WORDS USED FOR HIGH-FREQUENCY VIBRATION LITERATURE SEARCH

angular vibration
high frequency vibration
high frequency response
blast response
(statistical) and (vibrations)
statistical energy methods
high frequency approximations
mode slopes
mode rotations
(regression analysis) and (vibrations)
spatial averaging
spatial covariance
mode [modal] averaging
mode [modal] covariance
(statistical) and (structures)

spatial [spatially] random processes
(covariance) and (vibration[s])
(autocovariance) and (vibration[s])
Sommerfeld-Watson transformation
Poisson summation

It quickly became apparent during the literature search that a well developed body of theory called Statistical Energy Analysis (SEA) already existed and was at least partially applicable to the current problem. It also became clear that a survey of this field was not necessary because an excellent survey and tutorial report had been prepared for AFFDL in 1974 by R. H. Lyon of M.I.T. [1]*. This report was extremely valuable in acquiring a basic understanding of the underlying theory. An extensive bibliography organized by subject within SEA is contained in Reference [1].

2.2 SELECTION OF LOW FREQUENCY METHODS

The finite element method has risen to prominence in aircraft structural analysis in parallel with advancing computer capabilities. Its primary appeal lies in its generality and relative ease of use. Literature searching revealed thousands of titles containing the term "finite element" of which a large fraction would no doubt have some bearing on the problems at hand. Thus, there was never any question that this method would be the analysis tool used in the low frequency end of the angular vibration spectrum, with perhaps some exceptions for special cases or crude approximations.

With finite elements so widespread, there has been a gradual shift of emphasis away from purely theoretical developments toward questions like cost effectiveness and adaptability to well-established codes. In the present work, the goal was

---

* Numbers in brackets designate References at end of report.

to bring some advanced finite element technology from a "laboratory" status to a production environment. In practice, this means testing, evaluating, and "idiot-proofing" an element, and above all, tying it to an existing software system so as to take advantage of the large investment in auxiliary functions that such systems have.

While a number of theoretically appealing elements were reviewed, many of them were rejected mainly because they could not be used with NASTRAN. The goal of NASTRAN compatibility was adopted as it became clear that any other approach to assembling finite element software would be prohibitive in terms of the effort required in coding, checking, training users, and gaining their acceptance.

Implicit in this approach is the proposition that angular problems are not fundamentally distinguished from those of translational vibrations. There is no way to divorce an angular deformation from the associated translational deformation. Mathematically, one is the derivative of the other. Hence, the pursuit of better angular vibration was embodied in a search for better finite element methods in general. In other words, an evolutionary approach was taken rather than revolutionary.

The authors began this work with considerable experience in application of finite element techniques to aircraft structural analysis, much of it using NASTRAN. Following is a summary of the procedures and rules of thumb evolved by the authors in the course of this work.

First, the choice of mesh depends on a number of factors. The areas where response is more of interest need a finer mesh. Also, angular vibrations generally require a finer mesh than translational vibrations, and if the anticipated rotation is primarily about one axis, refinement perpendicular to that axis may be in order.

Boundary conditions must be handled carefully, often using auxiliary coordinate systems, in order that the allowable

motions in the model reflect the actual situation as nearly as possible.

Eigensolution strategies must be chosen carefully. When relatively high frequencies are desired, a sweeping procedure such as the Givens method is in order. In this case, a condensation step is usually called for. This may take the form of Guyan reduction, or generalized "dynamic reduction," both available in NASTRAN.

The debugging stage is just as important as the modeling stage. Following are some of the checks that Anamet personnel routinely use in verifying a finite element model:

(1) Apsect ratios and degrees of skew are checked for plane and solid elements using a preprocessor developed by Anamet.

(2) Plots of the undeformed structure are generated. Anamet's preprocessors NASSET and SAPLOT are sometimes used to generate partial views.

(3) The weight calculated from the finite element model is compared with the actual weight of the structure.

(4) Diagonals of the master stiffness and mass matrix are checked if a singularity or near-singularity is suspected.

(5) Simple static cases are run, usually with dead weight acting, before dynamics is attempted.

(6) For every NASTRAN matrix decomposition, the maximum ratio of matrix diagonal to factor diagonal is noted, as a check on the conditioning of the matrix.

(7) The quantity ε_o is noted. For static runs where an equation of the form $K\tilde{u} = \tilde{\rho}$ is solved, a residual vector $\delta P = \rho - K^{-1}\tilde{u}$ is calculated. This vector, which would be zero if no arithmetic round-off were present, has the form of a load vector. Its magnitude is assessed by comparing the work done by δP to that done by the actual load $\tilde{\rho}$, i.e. $\varepsilon_o = \delta P^T\tilde{u}/\rho\tilde{u}$. For dynamic runs the rigid body matrix X should be singular. Its norm is calculated and compared to the stiffness matrix for the rigid-body coordinates, i.e. $\varepsilon_o = ||X||/||K_{rr}||$. In both cases, for a successful

solution, ε_o should be near the order of computer precision, i.e. 10^{-10} to 10^{-14}.

(8) When eigenvalues are extracted, the off-diagonal modal mass term is noted. This quantity indicates how nearly orthogonal the eigenvectors are.

(9) When rigid-body modes are anticipated, the corresponding eigenvectors are checked to be sure that they are actually pure translations and/or rotations.

(10) The first few elastic modes are checked for reasonableness. Frequencies can often be checked against estimates made by hand. Mode shapes are checked with plots.

(11) Reaction forces are printed to insure that a constraint introduced for the purpose of eliminating a singularity has not inadvertently caused a spurious reaction force.

(12) Strain energies are sometimes checked. A high concentration of strain energy in one or a few elements sometimes indicates a modeling error.

In angular vibration applications of finite elements it is important to assess the quality of the mode shapes that have been computed. Ideally one would like to be able to divide mode shapes into three groups. First, "good" modes; second, modes that individually are questionable, but as an aggregate possess reliable statistical characteristics; and third, unreliable modes. One rough rule that can be applied is to assume that only a certain percentage of the analysis set represents good modes. A clue to the unreliable modes (at high frequency) is a sudden fall off in modal density. Also, one should bear in mind the importance of mode shapes with respect to the response of interest. This may be assessed by requesting mode normalization such that each mode has a value of one at a specified degree of freedom. The modal mass would then be an indication of the importance a particular mode plays with respect to a particular degree of freedom. This assessment could be made for a number of degrees of freedom, including loaded d.o.f. as well as response d.o.f.

Very large finite element models, or models which combine finite element models with test data, may be executed with the technique of component modal synthesis. In component modal synthesis, each component is characterized in terms of a number of natural frequencies and associated mode shapes, modal masses, modal stiffnesses, and modal damping. This can be done in three different ways:

(1) Perform a test using either a shaker or impulse loading. Record the modal information listed above.

(2) Perform a computer analysis using a finite element or other appropriate program.

(3) Analyze the component by hand.

There are two major advantages to describing a component in modal formulation. First, the equations governing the dynamic behavior of the component become uncoupled. Second, in the modal formulation it is possible to obtain adequate accuracy by using only a subset of the total modes of the component.

The components are then combined into a system analysis by writing equations of constraint between the interconnecting degrees of freedom of each component. These equations of constraint are the equations transforming the physical degrees of freedom to modal degrees of freedom. For each equation for the physical degree of freedom, the coefficients of the modal degrees of freedom are the components of the eigenvectors associated with that physical degree of freedom.

The accuracy of the component modal synthesis technique is dependent on several factors. First, the individual eigenvectors of the components must be accurately calculated, especially at the connection degrees of freedom (both translational and rotational). To model a system up to a given frequency, (i.e., N Hz.) each component's modal description must contain information greater than this frequency. A good rule of thumb is to pass to the system analysis modes for each

component up to one and a half times the highest frequency of interest. However, this is very dependent on the problem and the number of connection degrees of freedom. The greater the number of connection points, the greater the number of modes that must be passed. Not including the higher modes in the system analysis leads to a formulation which is too stiff (i.e., the predicted frequencies will be higher than the actual).

Using the procedures and techniques described, it is seen that large models may be solved, and the accuracy of the solution is realistic when compared with the elements used. Therefore, the kinds of advances that may bear on angular vibration problems include more accuracy per degree of freedom, judicious approximations that improve cost effectiveness, better numerical solution methods, and better ways of recovering dependent response quantities (in this case, angular deformations). It was decided that more accuracy per degree of freedom would be the most promising area, and that led to a selection of a new element described in Section III.

2.3 SELECTION OF APPROACH FOR HIGH FREQUENCY PREDICTION

The selection of an approach for prediction of so-called high frequency angular vibration was conditioned by the definition of low vs. high frequency as stated in the previous section. Modeling of a small stiff structure with a fundamental mode at 500 Hz. is not necessarily more difficult than modeling a larger structure with its first resonance at 5 Hz. The difficulty occurs when a model must be capable of predicting response to inputs over a frequency range which contains a very large number of modes. Angular responses are particularly difficult to predict because their modal series representations tend to converge more slowly than do those for translational responses and thus more modes must be known. Higher order modes will be sensitive to structural details which are too small to model economically and may not even be identical for structures built

from the same design. In effect, for high frequencies, one does not have a fixed description of the structure even in physical coordinates. The distinction between low and high frequencies for the purposes of this work is thus a functional one. Low frequency analysis implies that properties of individual vibration modes can be obtained, either by analysis or test. High frequency analysis presupposes that this level of detailed knowledge is unavailable.

This definition does not rule out the possibility of a purely empirical approach to high frequency prediction. In fact, this has been the basis for much high frequency translational vibration work in the past. One could collect the available data and attempt to correlate vibration levels with flight conditions, aircraft type, and some general structural description. It was decided in Phase I that this approach was not appropriate for the current contract. It would duplicate work being done already at AFFDL.

Based on the above considerations, it was decided during Phase I that the method of Statistical Energy Analysis (SEA) was the most promising candidate. While much of the specific SEA theory was unfamiliar to the investigators at this point, a number of attractive features were clear:

(1) The method does not necessarily require information about individual normal modes of a structure in order to make response predictions. The lack of such information inevitably introduces some uncertainty into the predictions but this may be acceptable for many cases. The point is that averaged descriptor quantities such as approximate model density and total mass may be sufficient to make useful first estimates of response.

(2) High model densities may actually be an advantage. Each mode contributing to response acts something like a statistical degree of freedom. As more modes contribute, their variability (i.e. the uncertainty as to the properties of any single mode) tends to become less important. For example, early SEA work was often associated with room acoustics where mode counts in the audio band may be in the hundreds of thousands.

(3) It appeared that deterministic methods of analysis with which the investigators were intimately familiar could be used to good effect in SEA modeling. In particular, certain aspects of large scale finite element analysis and minicomputer-based experimental modal analysis appeared promising. It was suspected that a higher level of structural detail could be incorporated into an SEA model by utilizing these technologies which were not available when most of the basic SEA theory was worked out.

(4) SEA modeling can be attempted using structural descriptions of varying detail. This was considered essential if a method were to be usable during both preliminary and prototype stages of design.

In hindsight, the investigators are convinced that the decision to focus on SEA for high frequency predictions was correct.

SECTION III
LOW FREQUENCY METHODS

Dynamic problems in general, and angular vibration in particular, require different approaches for different frequency ranges. We may classify these two approaches as deterministic and statistical. In a deterministic approach, the analyst models the entire structure mathematically in a way that strives to represent the behavior of any part of it under the most general loading. There are, of course, limits on the capability of any mathematical model in terms of the amount of detail that can be achieved in the predicted response. Ideally, the analyst knows that he can achieve greater accuracy as the mesh is refined, and can determine some error bounds for his model. In the frequency domain, these limitations can be expressed in terms of upper bounds on frequency. The lowest vibration modes almost always involve gross motions of the entire structure, and these modes are easy to predict analytically (for example, a simple beam model may be adequate to pick up a few modes of a complicated fuselage). With increasing frequency, mode shapes begin to have wavelengths at or below the mesh spacing, so that the model necessarily begins to break down. Aside from modeling errors, eigenvalue subroutines often have numerical trouble with the higher modes. Beyond the range where individual modes can be calculated accurately it may be possible to extract further information using aggregates of mode shapes.

However, the point is that a deterministic model must break down, and it is at this point (or hopefully before) that statistical approaches begin to make sense. The situation is analogous to the transition from microscopic to macroscopic thermodynamics where at some scale one must abandon any attempt to look at individual particles and start to look at averaged quantities.

Statistical methods will be taken up in Section IV. The rest of this section is devoted to a discussion of the finite element method in vibration problems, and to a new finite element that has been applied to angular vibration problems.

3.1 FINITE ELEMENT REVIEW

The finite element method is the dominant but not exclusive method in use today for numerical solutions to boundary value problems. Its popularity stems from its extreme flexibility with regard to the range of shapes and boundary conditions that may be handled. Before proceeding to a discussion of the Semi-Loof shell and beam elements, we review very briefly the mathematical foundations of the finite element method. Some understanding of these foundations is necessary in order to appreciate the development of the Semi-Loof elements. It may be fair to say that some users of finite elements need a better mathematical understanding of the method. Without this knowledge, users with a superficial view of finite elements as "building blocks" may misapply the method.

A finite element formulation may be derived beginning with an energy functional. For a two dimensional (ξ,η) problem, for example, one would have

$$\pi(u_i) = \iint F\,[u_i(\xi,\eta)]\,d\xi d\eta + \int G\,[u_i(\xi,\eta)]dS \qquad (3.1)$$

where the u_i are independent variables (functions of ξ,η), F represents energy in the interior, and G the boundary of the region. At this point the problem could be one of thermodynamics, electrostatics, elasticity, or any other field where an energy principle governs. For structures problems, Eq. (3.1) most commonly is the potential energy, and the u_i are displacements.

In the traditional calculus of variations approach, a formal variation is carried out in terms of the variations of each independent function u_i. Setting the coefficients of

each δu_i to zero then yields the Euler equations, which are the differential equations and boundary conditions governing the problem.

$$\delta\pi = 0 = \sum_i \frac{\partial\pi}{\partial u_i} \delta u_i \tag{3.2}$$

$$\begin{aligned} \mathcal{L}_i(u_j) &= 0 \\ \mathcal{B}_i(u_j) &= 0 \end{aligned} \tag{3.3}$$

At this point the finite element approximation functions are introduced

$$u_i(\xi,\eta) \simeq \sum_j N_{ij}(\xi,\eta)\, \hat{u}_{ij}, \qquad i = 1,2,\ldots \tag{3.4}$$

wherein $\hat{u}_{ij}$ are undetermined coefficients, or independent variables, and the N_{ij} are shape functions, usually polynomials in ξ and η. For a linear displacement formulation of a structures problem it is necessary that these functions satisfy displacement boundary conditions (prescribed boundary conditions) exactly while force (or "natural") boundary conditions are usually only approximated. We also note that the use of double subscripts is entirely arbitrary at this point.

Substitution of Eq. (3.4) into Eq. (3.3) then yields algebraic equations which may be written

$$\sum_{k,\ell} A_{ijk\ell}\, \hat{u}_{k\ell} + B_{ij} = 0, \qquad i,j = 1,2,\ldots \tag{3.5}$$

which may then be solved numerically. Equation (3.5) is meant to represent a static, free vibration, transient dynamic, or frequency response problem, with time variation implicit in the $A_{ijk\ell}$ and B_{ij}.

An alternative approach is possible. Instead of taking the variation first and then introducing approximation functions, one can reverse these steps. That is, introducing Eq. (3.4) into Eq. (3.1) renders it a function of the $\hat{u}_{ij}$,

after the integration has been carried out. One may then set the partial derivatives of it with respect to each u_{ij} to zero to obtain the same algebraic Eq. (3.5). This alternative is attractive particularly when nonlinear terms are present, making it possible to apply minimization techniques directly to the potential energy. The two approaches are summarized in Figure 1.

The foregoing development is a description of the more general Rayleigh-Ritz method, and as yet nothing has been said about the essential feature of the finite element method. We now examine the nature of the approximation functions $N_i(\xi,\eta)$ and the independent variables (undetermined coefficients) that multiply them. Consider for illustration a plate bending problem. The plate is divided into finite elements by mesh lines. The shape functions are such that each function has a value only at one of the node points of the mesh, and in the interior of elements surrounding that node point (see Figure 2). The node point value is the independent variable $\hat{u}_{ij}$ associated with that shape function. It is possible to consider the shape functions within only a single element, provided continuity requirements have been met. That is, two elements with a common edge must both predict the same displacement values at any point along that edge, given values for the corner-point degrees of freedom at either end of that edge. This being the case, it is possible to make models with elements of any size and shape, and to form matrices for the entire system by accumulating matrices generated for individual elements.

In recent years the "patch test" has come into favor as a means of evaluating a proposed finite element. It is based on the stipulation that any element must represent both rigid-body motion and constant-strain deformation in order to assure that a finer mesh yields a better solution. This is like saying that a series approximation needs to have at least the constant and first-order terms correct. In the patch test,

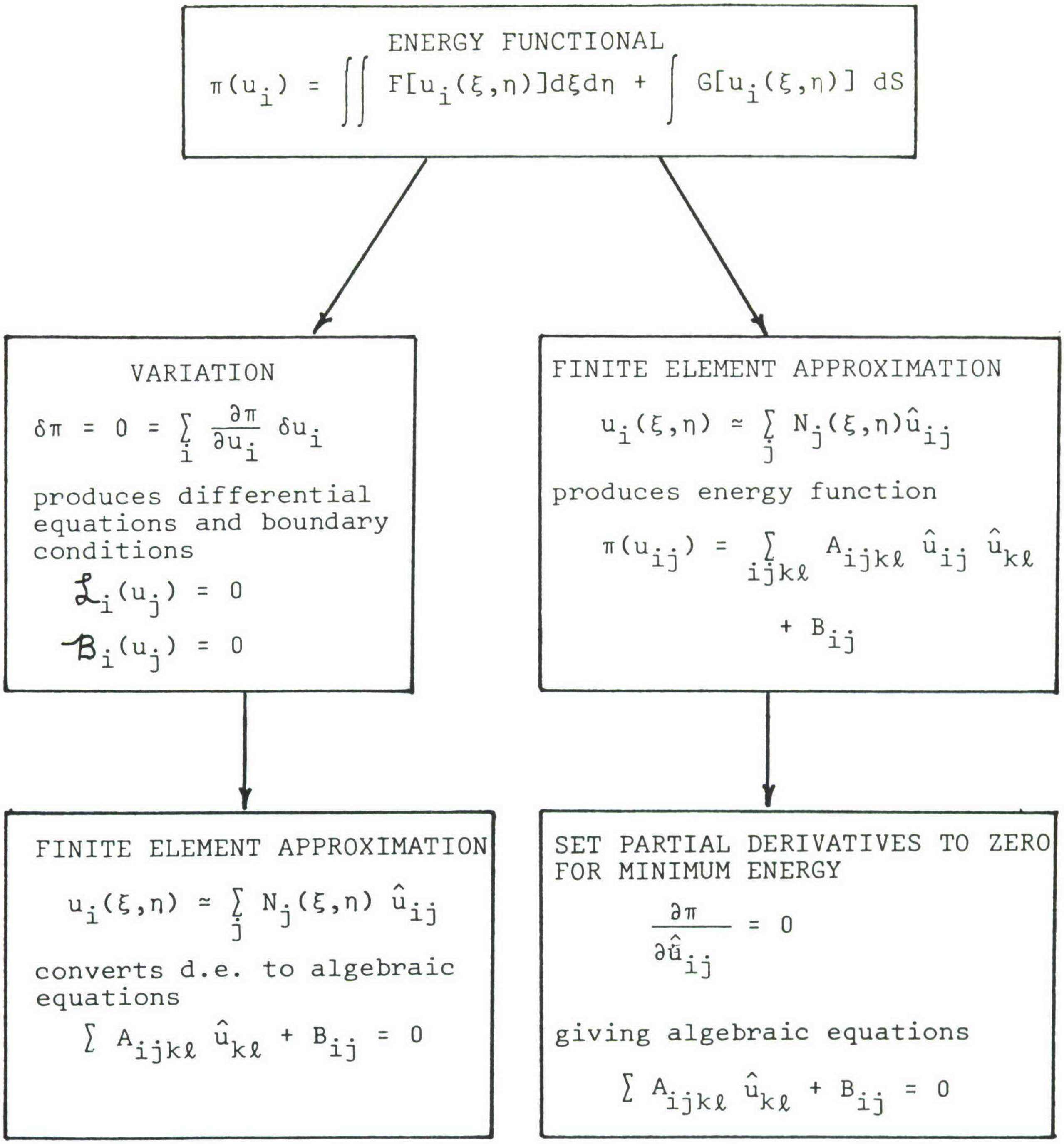

Figure 1 Finite Element Mathematical Derivation

these conditions are tested by taking a "patch" of elements and imposing rigid body or constant strain motions on the points on the boundary of the patch. The elements in the interior should then reproduce that state exactly.

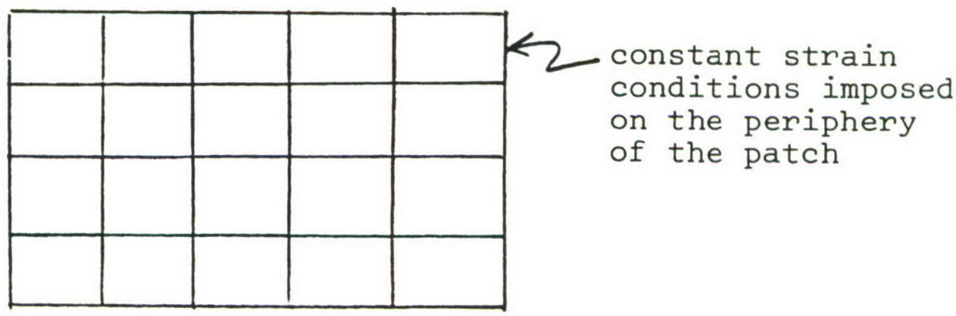

Figure 2 The Patch Test

3.2 THE SEMI-LOOF ELEMENTS

This section presents some of the background of the Semi-Loof elements that have been utilized in the present work. These elements were developed by Prof. Bruce Irons and his co-workers, and are best documented in Reference [2]. The developers are engineers and they are willing to venture into realms of approximations and adaptations where mathematicians might fear to tread, given the less than rigorous theoretical justifications. If past history is repeated, mathematicians will develop the missing theoretical basis for these and other advanced elements after engineers have been applying them successfully for some time.

First, the Semi-Loof shell elements are isoparametric elements, meaning that the functions used to describe the undeformed shape are the same as those used to describe displacements (i.e., the shape functions). This is a well known approach to shell elements, explained in texts such as Chapter 8 of Reference [3]. Also commonplace is the use of Gaussian quadrature for integration of element stiffness and mass. This is a form of numerical integration where the locations and weighting factors for sampling functions are chosen such as to minimize truncation errors when the integrands are polynomials. The locations are known as Gauss points. For two-point integration of a function on a normalized interval (-1,1), for example, the Gauss points are located at $\pm 1/\sqrt{3}$ and the weighting factors are both unity.

The Semi-Loof elements begin to deviate from orthodox elements with the question of inter-element compatibility, or conformity as it is sometimes called. This concept was introduced in Section 3.1 and it asserts that displacements (and slopes, for bending elements) must be continuous across element boundaries as a condition of admissibility of the shape functions. The Semi-Loof elements are basically non-conforming

elements, but the non-conformity is of a special kind: such that any discontinuity and its first moment integrate to zero between elements. That is, if ξ is the normalized arc length along an element interface ($-1 \leq \xi \leq 1$), and $\delta(\xi)$ is a discontinuity, then

$$\int_{-1}^{1} \delta(\xi)\, d\xi = 0$$

and (3.6)

$$\int_{-1}^{1} \xi\delta(\xi)\, d\xi = 0$$

so that the elements can pass the patch test. This property is made possible by the use of Loof nodes which are located at the Gauss points along each element edge (i.e., $\xi = \pm 1/\sqrt{3}$). This idea stems from an early development by H. W. Loof [4] who proposed very high order elements providing exact solutions in element interiors, with shape functions collocated at a number of points along element interfaces.

A Semi-Loof isoparametric quadrilateral begins with 17 nodes and 43 degrees of freedom. The node points include four corner nodes, four midside nodes, and a center node (see Figure 3). The degrees of freedom are:

3 translations at each midside and corner mode	3x8 = 24
Rotations about two axes at each Loof node and the corner node	2x(8+1) = 18
The "bubble function" $w = (1-\xi^2)(1-\eta^2)$ required by the patch test	= 1
TOTAL	= 43

The 43 degrees are then reduced to 32 by imposition of the following constraints:

First, rotations about the normals at all eight Loof nodes are set to zero. These rotations introduce transverse shear strains, which are small for thin shell theory (8 constraints).

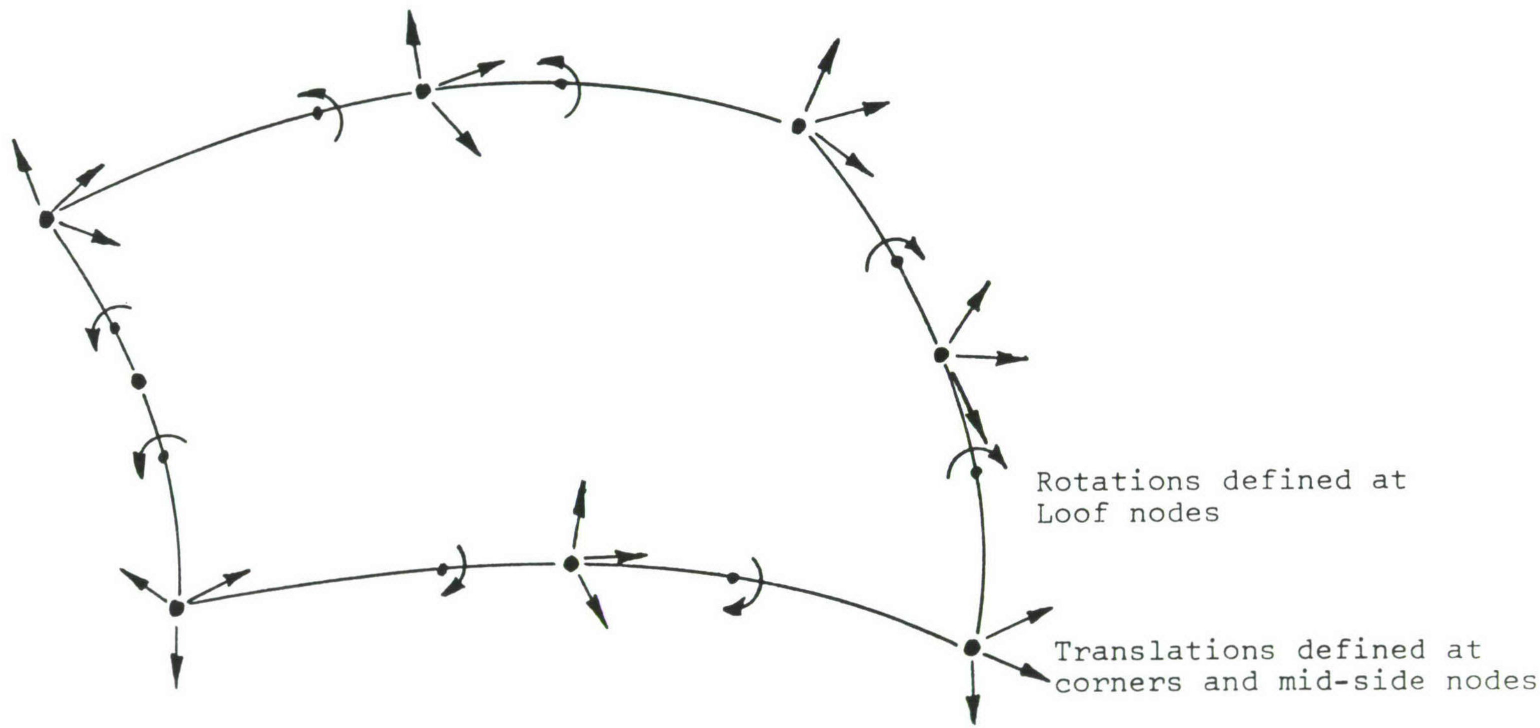

Figure 3 Semi-Loof Quadrilateral Element Degrees of Freedom

Second, two constraints are used to reduce out the center point rotations. These are:

$$\int \underset{\sim}{X}_9 \cdot \underset{\sim}{\gamma} \, d(\text{area}) = \int \underset{\sim}{Y}_9 \cdot \underset{\sim}{\gamma} \, d(\text{area}) = 0 \tag{3.7}$$

where $\underset{\sim}{X}_9$ and $\underset{\sim}{Y}_9$ are unit vectors at the center point in the ξ = constant and η = constant directions, and $\underset{\sim}{\gamma}$ is the vector resultant of the two transverse shear strains. Irons found through experience that constraining this average shear strain produced better results than simply eliminating the two center point shear strains.

Finally, the constraint

$$\int \nabla \cdot \underset{\sim}{\gamma} \, d(\text{area}) = 0 \tag{3.8}$$

is transformed into a boundary integral by Green's theorem

$$\int (\text{thickness}) \, \gamma_{XZ} \, d(\text{boundary}) = 0 \tag{3.9}$$

and used to reduce out the bubble function leaving 43-8-2-1=32 degrees of freedom. These are shown in Figure 3.

Ideally, the stiffness matrix for the quadrilateral would have a rank of 26 (32 nodal variables minus 6 rigid body motions). But each integrating point can contribute, at most, six (the rank of the modulus matrix) for a total of 24 with 2x2 Gaussian quadrature. Thus, under these circumstances, the element contains two spurious mechanisms; that is, deformation states for which the predicted strain energy is zero. Experience has shown that for many cases this is not a problem, particularly when stresses are of primary interest. Nevertheless, this situation is unacceptable in a production environment. Two remedies are presently available, neither of which is ideal. The first is to introduce, somewhat arbitrarily, a fifth integration point at the center, with a small weighting factor, Ω,

by

$$\int_{-1}^{1}\int_{-1}^{1} \phi(\xi,\eta)d\xi d\eta = \Omega\phi(0,0) + (1-\Omega/4)\sum_{1}^{4} \phi(\pm\frac{1}{\sqrt{3}}\ \pm\frac{1}{\sqrt{3}}) \qquad (3.10)$$

The second alternative is to resort to 3 x 3 integration, for which the integration formula (taken from Table 8.1, Reference [3]) is

$$\int_{-1}^{1}\int_{-1}^{1} \phi(\xi,\eta)\, d\xi d\eta \simeq \sum_{i,j=1}^{3} H_i H_j \phi(\alpha_i)\phi(\alpha_j) \qquad (3.11)$$

where the Gauss points are

$$\begin{aligned} \alpha_1 &= .7745966692 \\ \alpha_2 &= 0.0 \\ \alpha_3 &= -\alpha_1 \end{aligned} \qquad (3.12)$$

and the weighting factors are

$$\begin{aligned} H_1 &= 5/9 \\ H_2 &= 8/9 \\ H_3 &= 5/9 \end{aligned} \qquad (3.13)$$

In the NASTRAN implementation of Semi-Loof to be discussed subsequently, the choice of integration rules has been left to the user (2x2, 2x2+1, or 3x3).

Triangular elements have not yet been introduced yet. These elements are a fairly straightforward extension of the quadrilateral element. There are 24 degrees of freedom, including three displacements at each of three corner nodes and each of three midside nodes, plus six Loof rotations (Figure 4). There is no problem with spurious mechanisms, since three integration points provide a matrix rank of 3 x 6 = 18, plus six rigid body modes = 24, the size of the matrix.

The third Semi-Loof element is the curved beam, which is meant to join with the shell elements along their edges. This

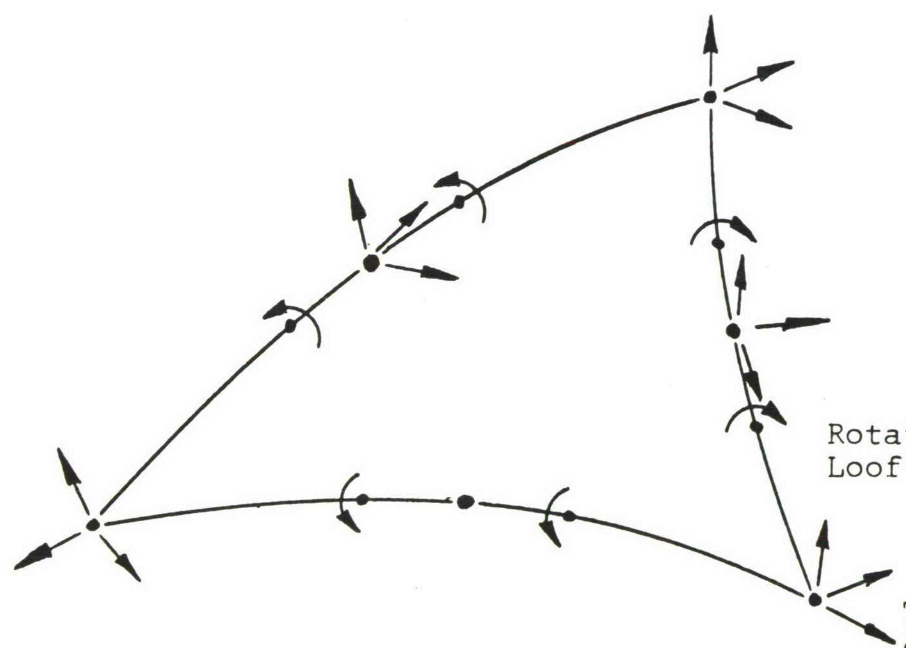

Figure 4 Semi-Loof Triangular Element Degrees of Freedom

element is documented in Reference [5]. Like the shell element, constraints are used to reduce out unwanted degrees of freedom. The element has two end nodes, a center node, and two Loof nodes, like the edge of a shell element. This is shown in Figure 5.

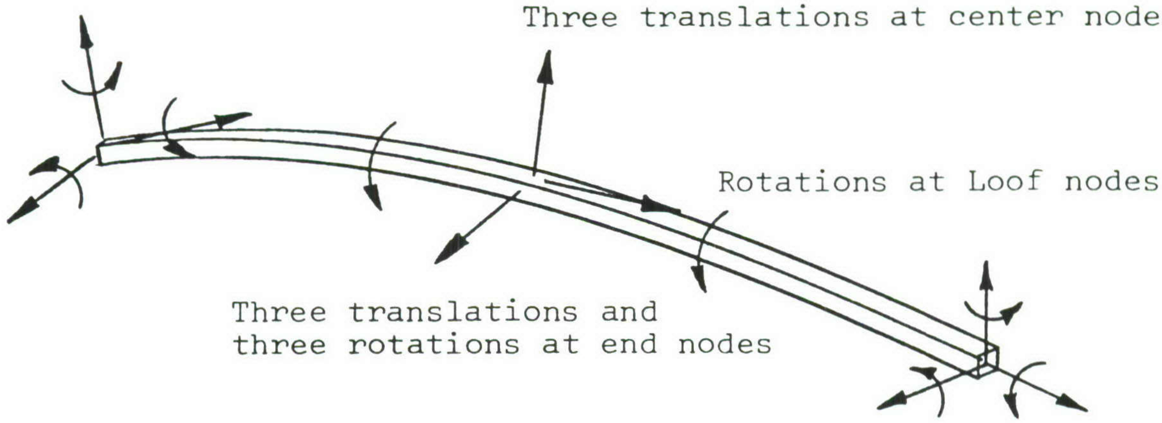

Figure 5   Semi-Loof Beam Element Degrees of Freedom

There are initially three displacements and three rotations at each end point, three displacements at the center point, and three rotations at each Loof node. Gauss point transverse shear strains are zeroed out, eliminating two unwanted rotation degrees of freedom at each Loof node. The final element has quadratic variation of both bending and torsion strains.

Prof. Irons has made available his shape function subroutines. When supplied with element geometry and isoparametric coordinates ξ,η, they return values of all the shape functions and their derivatives so that an engineer/programmer may change the integration method, or form different integrals without disturbing the basic shape function computations. These subroutines are the heart of the PRELOOF code, developed as part of this effort and described in Appendix A of this report.

3.3 COMPARISON AND EVALUATION OF SEMI-LOOF ELEMENTS

A number of evaluations and comparisons of Semi-Loof elements have been published in the literature. At the time, Semi-Loof was in a "laboratory development" stage, and had not been applied much in production situations. Many of the elements that were compared to it were not in production status either. Additional evaluations were carried out as part of this effort with the specific aim of comparing Semi-Loof with the widely used plate elements in NASTRAN, since the final goal was to make Semi-Loof available to NASTRAN users.

We summarize very briefly some of the results reported in the literature. Irons [2] reports on a cantilever cylinder (Figure 6) with end moments. A very coarse mesh (60° elements) gave stresses accurate to within 1%. This is a rather spectacular result. Uniformly loaded square and circular plates also give excellent results. On the other hand, a point-loaded square plate is much less satisfying, though still acceptable (Figure 7). This may be a consequence of the fact that Semi-Loof corners can hinge. In practical situations, point loads are usually carried by beams, however.

Martins and Owen [6] compare Semi-Loof's performance with several other elements with respect to vibration of a square plate and of a cantilever cylindrical panel. Comparisons were presented as plots of relative error versus number of degrees of freedom employed, and each problem showed a substantial improvement for Semi-Loof over most other elements. The same authors [7] report favorable results for both elasto-plastic and geometrically nonlinear problems. In this case, comparison with other elements is more difficult.

As an initial comparison of Semi-Loof with the standard QUAD2 (COSMIC NASTRAN) and QUAD4 (MSC/NASTRAN) plate elements, a simple plate bending problem was run. The results (Figure 8) were encouraging in that Semi-Loof outperformed both NASTRAN elements. A surprising result was that the QUAD4 did not converge any faster than QUAD2, although it did better for the

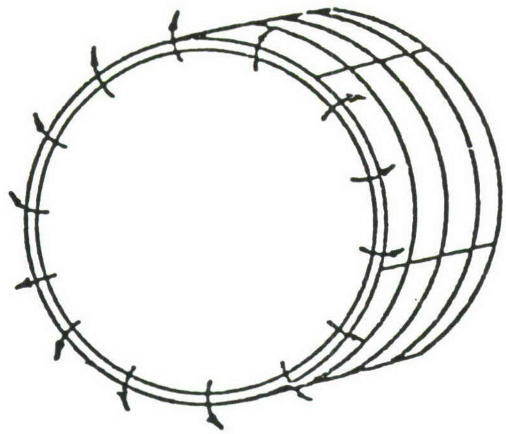

Radius = 10"
Length from fixed end = 8"
Thickness = 0.8"
Poisson's Ratio = 0.3

Figure 6 Cantilever Cylinder

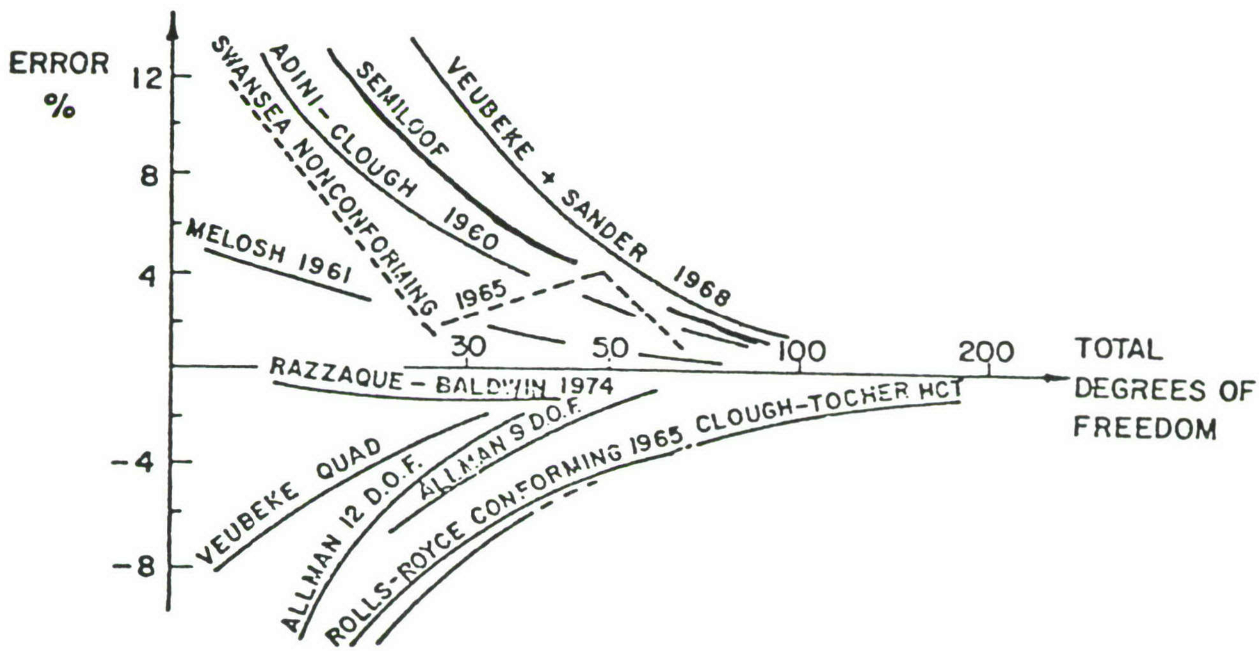

Figure 7 Point-loaded Plate Evaluation

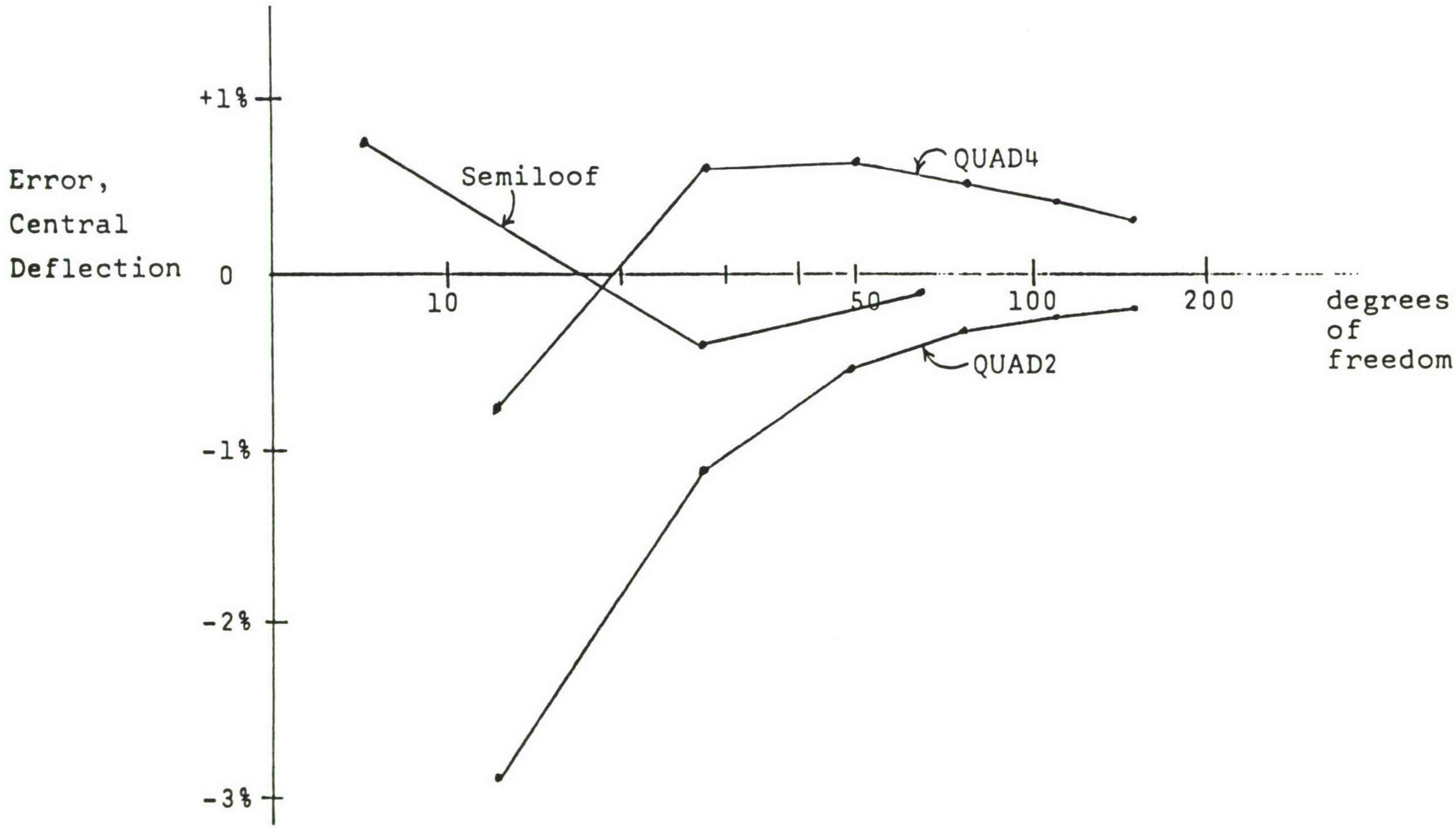

Figure 8 Plate Element Convergence Study

coarse mesh. Incidentally, the degree-of-freedom counts for these runs excluded in-plane displacements.

Next, Problem 3-1-1 of the NASTRAN Demonstration Problem Manual [8] was run. This is a vibration problem for a flat plate. The following frequencies were obtained:

Mode	Theoretical	QUAD1 10x20 Mesh 590 DOF	QUAD1 20x40 Mesh ~1200 DOF	Semi-Loof 4x7 Mesh 196 DOF
1	0.9069	0.9056	0.9066	0.9069
2	2.2672	2.2634		2.2632
3	4.5345	4.5329		4.5302

Although this exercise was mainly intended to check out the mass matrix coding and not necessarily to compare the two elements, there is some evidence of increased efficiency for Semi-Loof.

The third academic test problem that was selected was a cantilever cylinder with varying thickness. Although no analytical solution is known, it was possible to observe the rate of convergence (of the first fundamental frequency) as the models were refined (Semi-Loof versus QUAD4). The following table summarizes these runs:

	Semi-Loof	QUAD4
First Frequency	770.6	767.8
Degrees of Freedom (before omit)	504	900
Degrees of Freedom (after omit)	504	457
Number of Modes Computed	2	1
Total Run "Cost" Including Matrix Generation	$8.70	$21.30

As a final test problem, a curved, stiffened aluminum panel was fabricated (see Figure 9). The panel was tested in the laboratory and was analyzed with both QUAD4 and Semi-Loof elements. The first few frequencies were:

Mode	Description	Experimental	QUAD4 710 DOF	Semi-Loof 500 DOF
1	First twisting	66.2	68.1	67.1
2	First bending	194.4	194.7	186.9
3	Second bending	228.1	239.0	232.5
4	Second twisting	241.9	247.3	241.8
5	Third bending	275.0	284.9	281.3

Note that the Semi-Loof model reproduces the twisting modes somewhat better than the bending modes. This is thought to be a reflection of an early deficiency in the Semi-Loof beam element: the lack of an offset specification to represent eccentric stiffeners. There was some difficulty in choosing accurate equivalent non-eccentric beam properties to model the stiffener. This deficiency was remedied later in the program and the appropriate code was added to PRELOOF.

During Phase I it was thought that rotary inertia, which is usually neglected in finite element mass matrices, might have more importance in angular vibration problems than is generally the case. Rotary inertia is the moment induced in a shell due to a unit angular acceleration about a line tangent to the shell's middle surface. If the two orthogonal rotations for a shell are $\partial w/\partial x$ and $\partial w/\partial y$, then, integrating over the shell surface, we would add the term

$$\iint [(\frac{\partial w}{\partial x})^2 + (\frac{\partial w}{\partial y})^2] \frac{\rho t^3}{12} \, d\xi d\eta$$

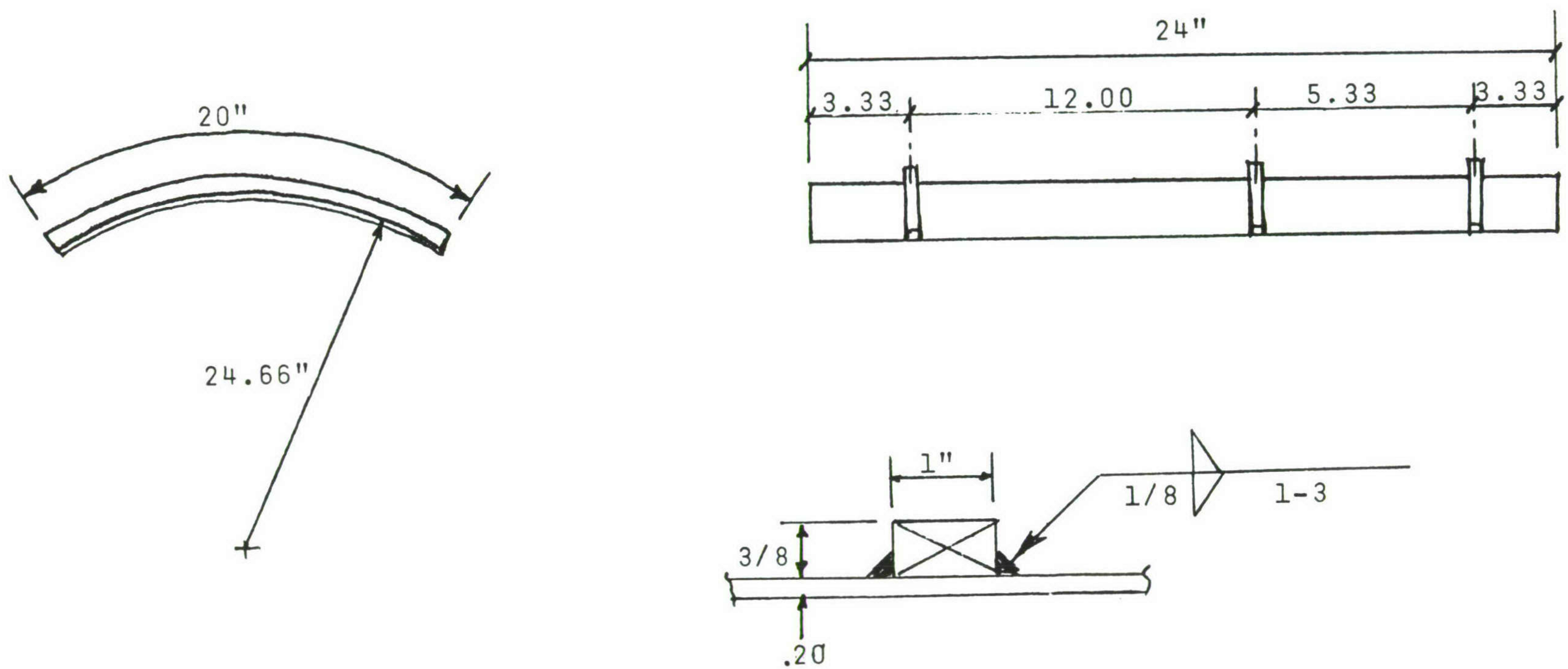

Stiffener Section (Typical)

Material - Aluminum

Figure 9 Curved Panel Configuration

to the mass matrix, where the thickness, t , may vary with ξ and η. In a test case where rotary inertia was added, the natural frequencies changed in only the fourth decimal place. Rotation degrees-of-freedom typically changed in the sixth or seventh decimal place. For a thin shell it is clear that rotary inertia is entirely insignificant. For rotary inertia to be significant, either thicknesses or rotations would have to be large. If thicknesses were large, then the assumptions about zero transverse shear strain would be wrong. If rotations were large, then the linear strain-displacement relations would no longer hold. Although it costs virtually nothing to add rotary inertia to Semi-Loof, it would provide no real payoff and would be inconsistent with the assumptions underlying the stiffness formulation.

3.4 IMPLEMENTATION INTO NASTRAN

The subroutines supplied by Irons do the basic work of defining shape functions for Semi-Loof elements and applying constraints to reduce out unwanted degrees of freedom. A primary goal of this effort was to make Semi-Loof elements available to NASTRAN users. Considerable effort was involved in writing code around the shape function routines to make this possible.

One of the first decisions faced was whether to modify NASTRAN at the source code level. This would have produced the "cleanest" result in that no interfacing would have been necessary. The alternative was to generate matrices in a pre-processing program and read them into NASTRAN. The former alternative was rejected for the following reasons:

(1) There are two major versions of NASTRAN, MSC/NASTRAN and COSMIC NASTRAN. MSC/NASTRAN, used by most industrial and some government users, is not available at the source code level, and these users would presumably be shut out by a development limited to COSMIC NASTRAN, for which source code is available.

(2) There would be no guarantee that future modifications to NASTRAN would be compatible with modifications made for Semi-Loof.

(3) Link-editing NASTRAN is a time-consuming process, most likely an overnight computer run. This would hamper debugging and checkout considerably.

The NASTRAN DMAP language allows the user access to any matrix or table at any stage of execution. However, it is difficult to access element matrices and assembly tables. Consequently, it was decided that not only would element matrices be generated by PRELOOF, the preprocessing routine, but would be assembled into master matrices as well. This still allows for connection of Semi-Loof elements to other NASTRAN elements since the matrices read from PRELOOF are added to the matrices generated by NASTRAN for any additional elements that may be present. In addition to PRELOOF, a post-processing routine, POSTLOOF, was written for the purposes of recovering stresses and/or angular deformations. The latter are not independent variables at node points; hence, the option to recover them as secondary variables.

The file handling required to transfer information from PRELOOF to NASTRAN and from NASTRAN to POSTLOOF has been made painless by means of packaged control card procedures and DMAP Alters. Experience has shown that there is practically no penalty for doing preprocessing and post-processing outside of NASTRAN as a result.

PRELOOF and POSTLOOF input are described in Appendix A. Some programming notes for PRELOOF are given there, also. Briefly, PRELOOF does the following:

(1) Reads and checks input data in NASTRAN Bulk Data format.

(2) Sorts grid point numbers and establishes a sequencing table for degrees of freedom.

(3) Generates PLOTEL cards to enable plotting of shell elements, if desired.

(4) Generates element stiffness matrices and, if requested, element mass matrices and/or load vectors. This involves formation of modulus matrices, generation of shape functions at integration points, and accumulation of stiffness terms.

(5) Assembles element matrices into global matrices, which are written out to a file six columns at a time, in a form acceptable to NASTRAN.

3.5 SUMMARY

There has been considerable research activity in finite element analysis, but the results of these efforts have been disappointingly slow in reaching the production user. The demands made upon analysts by angular vibration problems in aircraft require that the best tools be available. Millions of dollars have been invested in finite element software, and the vast majority of these funds have been devoted to matters other than the mathematical formulation of elements; that is, such things as input checking, sorting, sequencing, matrix decomposition techniques, spill logic, internal file handling, and output formatting. It would be foolish to attempt to duplicate this massive investment just for the sake of introducing a new element; hence, the motivation for using NASTRAN with its full complement of solution strategies, output options, etc. It is believed that real progress has been made in delivering a new tool to the analyst for angular vibration and other structural problems. However, this new tool, in turn, intensifies the requirement that the analyst "know his elements." Semi-Loof by nature is more sophisticated than simple plate elements, especially with regard to integration procedures.

Part of a fighter fuselage was obtained and tested in the laboratory. The fuselage was modeled and analyzed with Semi-Loof elements, and tested in the laboratory. Section VII is a discussion and comparison of these results.

SECTION IV
HIGH FREQUENCY METHODS

4.1 INTRODUCTION

A basic assumption from the beginning of Anamet's work on angular vibration has been that deterministic methods of structural modeling would not, by themselves, be sufficient. Experience with airborne optical systems has shown that high frequency, low amplitude motion of optical components can seriously degrade system performance. This high frequency motion represents the aggregate contribution of numerous high order modes of vibration which are too sensitive to small details of construction to be reliably modeled by deterministic methods. While motions induced by high frequency disturbances may be small compared to low frequency contributions, the active servomechanisms used to control the optical beam have their own frequency limitations. They cannot effectively suppress and may actually amplify the effect of disturbances at frequencies beyond a few hundred Hz.

Typical cumulative power data for in-flight vibration at a particular fuselage station is shown in Figures 10 and 11 for a translational and rotational displacement, respectively. (Data courtesy of AFFDL.) It may be observed that the normalized cumulative power ($\int_0^f S(f)df/\sigma^2$) of the rotation converges to unity somewhat more slowly than does the corresponding function of the translation. In both cases only a few percent of total signal power is beyond 50 Hz. Nevertheless, the ability to accurately predict this portion of a response PSD is quite important.

Historically, prediction methods for high frequency vibration environments of airborne equipment have been based on empirical correlations of actual flight test data. While this approach has proven to be useful in many cases, it was considered outside the scope of the current contract. Efforts at

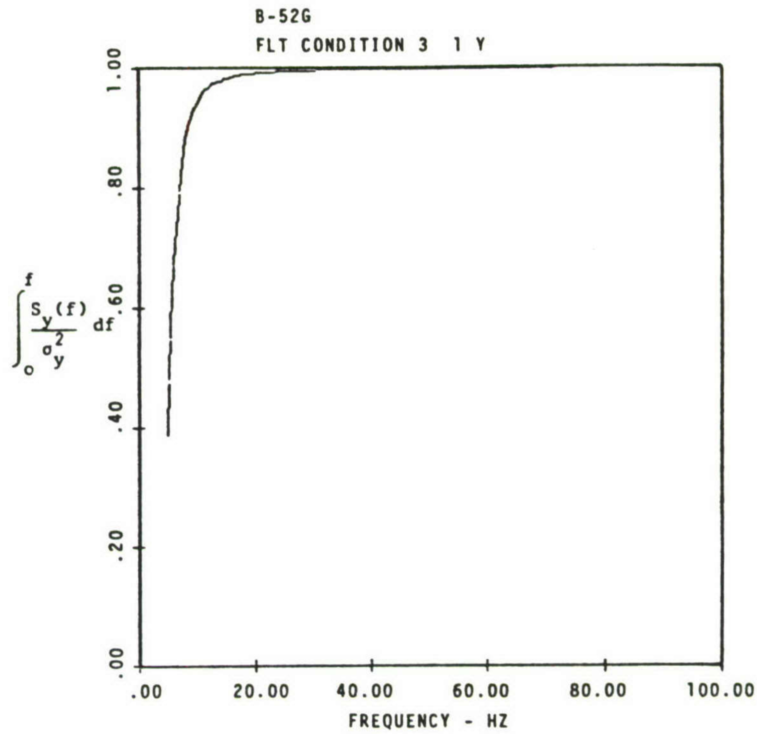

Figure 10 Cumulative Power of Typical Translational Variable for In-flight Vibration.

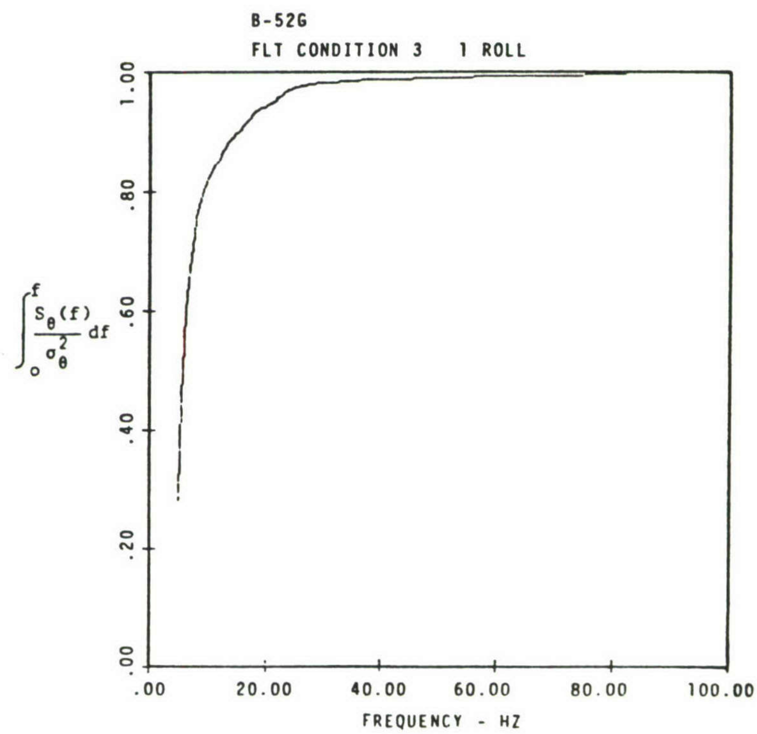

Figure 11 Cumulative Power of Typical Rotational Variable for In-flight Vibration.

Anamet have, therefore, concentrated on more general analytical methods derivable from first principles. The use of experimental data and, in particular, structural models assembled from test data, has by no means been ruled out, however.

The distinction between so-called high frequency and low frequency prediction methods which has been adopted in the current studies is a functional one and does not necessarily involve specific frequency ranges. High frequency prediction methods are defined simply as those which do not necessarily involve knowledge of individual normal modes of a structure. Low frequency methods are those which are based upon such knowledge whether it be obtained through analysis or test.

4.1.1 Statistical Energy Analysis

The definition of high frequency methods stated above leads inevitably to approaches which treat a structure in terms of some averaged, or statistical, description. In Phase I it was decided that the method of Statistical Energy Analysis offered the most promise for predicting high frequency angular vibration. A significant portion of the total effort in Phase II, as well as Phase I, was expended in gaining an understanding of the theoretical and practical basis of the method. This in itself has proven to be a formidable task, mainly because the theory is made up of contributions from several related but diverse fields: classical vibrations, random processes, wave mechanics, mechanical impedance methods, and acoustics. Reference [1] was found to be a most useful document in this regard due to its thoroughness and extensive bibliography.

The single most appealing feature of the SEA approach is its apparent facility for making use of whatever level of detail is available in the description of a structure. This was considered essential since a mode-by-mode description will, by assumption, not be known. The method also appears well suited to situations where a small, indirectly excited structure, such

as an optical element, is attached to a much larger structure, such as an airframe, by a small number of common degrees of freedom.

Section 4.2 of this chapter is devoted to a brief summary of the fundamentals of SEA. It is not intended to describe the entire basis of the method, but rather to point out the essential features which make it attractive for the present purpose. Attention will be focused on a case similar to that described in the preceding paragraph. A wave transmission method for obtaining coupling loss factors is reviewed in Section 4.3.1 and an alternate set of assumptions is presented in Section 4.3.2 which allows a similar formula for coupling loss factor to be obtained by considering a modal coordinate description. It is demonstrated how a convenient measurement procedure can be used to obtain the internal loss factor for a component. In Section 4.6 an experiment is described where the wave transmission method is used to predict transmitted power and equilibrium energy ratio between two coupled plates. Finally, an expression is derived and tested experimentally for predicting the r.m.s. angular displacement in frequency bands at an interior point of a uniform plate under broadband random excitation, given the total vibrational energy.

The purpose of the experiment was to gain some first-hand experience with SEA and to estimate its potential usefulness as a day-to-day engineering tool. In this regard, the use of minicomputer-based FFT methods is described as they pertain to the experiment.

4.2 FUNDAMENTALS OF SEA

Statistical Energy Analysis of vibration is set apart from classical deterministic methods by its use of time-averaged component energies and power flows between components as primary variables. If a component is a distinct mechanical substructure, its energy under stationary random vibration is always expressible as some form of inner product. For example, if component

A is a substructure described by an Nx1 vector $\underset{\sim}{x}$ of displacements and a lumped mass matrix $\underset{\sim}{M}$, the time averaged kinetic energy of A is

$$T_A = \frac{1}{2} \langle \dot{\underset{\sim}{x}}^T \underset{\sim}{M} \dot{\underset{\sim}{x}} \rangle_t = \frac{1}{2} \sum_{i=1}^{N} m_i \langle \dot{x}_i^2 \rangle_t \tag{4.1}$$

where m_i = i'th diagonal entry of $\underset{\sim}{M}$

$$\dot{x}_i = \frac{dx_i}{dt}$$

$\langle \; \rangle_t$ = expectation with respect to time

The time-averaging and summing operations (4.1) represent the transformation between the individual $\dot{x}_i$ or $\langle \dot{x}_i^2 \rangle_t$ variables of classical deterministic analysis and the energy variables T_A of an SEA model. In general the sum as determined from an SEA model cannot be separated into its individual terms and hence, the identity of individual spatial points is lost. For situations where individual modes are unavailable, this mixing or averaging process is basic to the method in that it allows equilibrium equations for component energies to be obtained under varying levels of assumptions regarding the nature of the substructure. The wave transmission method, for example, makes rather gross simplifying assumptions by assuming two uniform structures of infinite size. This is appropriate for very high frequency analysis since complications, such as shell curvature or lumped mass concentrations, tend to either have less effect than at low frequencies, or to affect response in only a local area with little change in total energy.

A second inherent characteristic of an SEA model is the decomposition of energy and power flow quantities by frequency. This is analogous to the decomposition of the mean square value

of a zero-mean stationary random quantity into its power spectral density.

$$\sigma_x^2 = \int_o^\infty S_x(f)\, df = \int_o^{f_1} S_x(f)\, df + \int_{f_1}^{f_2} S_x(f)\, df + \ldots \quad (4.2)$$

It is possible to write equilibrium equations for component energies and inter-component power flow for linear structures under stationary excitation, in terms of frequency bands. The variables are energy or power between specified frequency limits. It should be noted that the terms power spectral density and energy spectral density now mean exactly what they say. This is in contrast to the more common usage of stochastic processes where $S_x(f)$ is called the PSD of x even though x^2 does not have the dimensions of power.

Equilibrium equations are written in terms of simple power balance relations for each component. Suppose two components A and B are connected by a light spring and component A is directly excited (Figure 12).

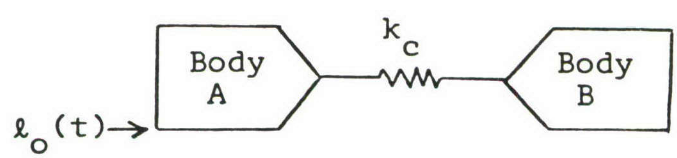

Figure 12 Two Bodies with Stiffness Coupling and Direct Excitation of One Body

$$\langle \pi_{A,IN} \rangle_t = \langle \pi_{A,DIS} \rangle_t + \langle \pi_{AB,TRAN} \rangle_t \quad (4.3)$$

$$\langle \pi_{B,IN} \rangle_t = \langle \pi_{B,DIS} \rangle_t + \langle \pi_{BA,TRAN} \rangle_t \quad (4.4)$$

where

$<\pi_{A,IN}>_t$ = input power to body A from all ideal sources (in this case $\ell_o(t)$)

$<\pi_{A,DIS}>_t$ = power dissipated internally by body A

$<\pi_{AB,TRAN}>_t$ = power transmitted from body A to body B

with similar definitions for $<\pi_{B,IN}>_t$, $<\pi_{B,DIS}>_t$, and $<\pi_{BA,TRAN}>_t$.

In equations (4.3) and (4.4) the $< >_t$ operator implies time-averaged power in some frequency band . A separate set of equations may be written for each band of interest.

The power quantities on the right hand side of (4.3) and (4.4) are next expressed in terms of component energies by making use of two other basic SEA principles.

As usual in linear vibrations, the energy dissipated per cycle at a given frequency is assumed to be proportional to the amount present at that frequency. The proportionality constant for body A is called $\eta_A(f)$, the internal loss factor at frequency f. As usual, the equation is written in terms of energy and power within specific frequency bands.

$$<\pi_{A,DIS}>_t = 2\,\pi f_c \eta_A(f_c) <E_A>_t$$
$$<\pi_{B,DIS}>_t = 2\,\pi f_c \eta_A(f_c) <E_A>_t \qquad (4.5)$$

where

$<E_A>_t$, $<E_B>_t$ = time-averaged total energies of A and B (kinetic + potential) within a frequency band

f_c = center frequency of band

The relation between transmitted power and component energies represents the unique element of SEA analysis. It may be thought of as defining the so-called coupling loss factors $\eta_{AB}(f_c)$ and $\eta_{BA}(f_c)$

$$\langle \pi_{AB,TRANS} \rangle_t = 2\pi f_c [\eta_{AB} \langle E_A \rangle_t - \eta_{BA} \langle E_B \rangle_t] \tag{4.6}$$

For multi-mode structures η_{AB} represents the coupling of each mode of A to all modes of B and thus is a function of $N_B(f_c)$, the number of modes of B occurring within the band about f_c which was used to define the $\langle\ \rangle_t$ operator. All modes of a component have also been assumed to have equal energies which implies η_{AB} is directly proportional to N_B. Many methods have been used to estimate coupling loss factors. One of the simplest methods (which therefore makes relatively gross assumptions about the structure and excitations) is explained in Section 4.3.

4.2.1 SEA Parameters

For the simplest case where body B is driven only by its connection to body A, it is often assumed that $<E_B>_t$ is small compared to $<E_A>_t$ and that η_{BA}/η_{AB} is not large compared to unity. In this case (4.6) can be simplified to yield

$$<\pi_{AB,TRANS}>_t = 2\ \pi f_c \eta_{AB} <E_A>_t \qquad (4.7)$$

If B is not directly excited $<\pi_{B,IN}>_t = 0$ and (4.4) becomes, after combining with (4.5) and rearranging

$$<E_B>_t = <E_A>_t \left[\frac{\eta_{AB}}{\eta_B + \eta_{BA}}\right] \qquad (4.8)$$

It can be shown [9] that equipartition of energy between modes leads to a reciprocity relation between coupling loss factors

$$N_A\ \eta_{AB} = N_B\ \eta_{BA} \qquad (4.9)$$

Combining (4.8) and (4.9)

$$<E_B>_t = <E_A>_t \left[\frac{\eta_{AB}}{\eta_B + (N_A/N_B)\ \eta_{AB}}\right] \qquad (4.10)$$

Finally, if the previous assumption of $\eta_{BA} <E_B>_t << \eta_{AB} <E_A>_t$ is applied to (4.6) and the result combined with (4.4) and (4.5)

$$<E_A>_t = \frac{<\pi_{A,IN}>_t}{\omega(\eta_A + \eta_{AB})} \qquad (4.11)$$

Equations (4.7), (4.10) and (4.11) can give some physical insight into the SEA parameters. For a given level of power input to A from the external source, the equilibrium energy level of A is set by the sum of η_A and η_{AB} (4.11). With $<E_A>_t$ set, the power transmitted to B is proportional to η_{AB} (4.7). Also for a given level $<E_A>_t$, the equilibrium energy level of the indirectly excited body $<E_B>_t$ is set by a combination of

η_B, η_{AB}, and the mode counts (4.10). In the limit as the internal damping of B goes to zero, its energy level does not go to infinity as it would for a single body driven by an ideal source. Rather, the energy per mode $\langle E_B \rangle_t / N_B$ of the receptor body B becomes equal to $\langle E_A \rangle_t / N_A$, the energy per mode of the transmitter body. This last conclusion is a fundamental SEA result and is particularly significant in view of the difficulty of predicting internal loss factors in lightly damped structures. It implies that an error in η_B will produce a smaller percentage error in $\langle E_B \rangle_t$ (which is usually the quantity of most interest) and even an assumed value of zero internal loss in B will still produce an answer.

4.3 ESTIMATION OF COUPLING LOSS FACTOR BY THE WAVE TRANSMISSION METHOD

4.3.1 Derivation in Terms of Waves

One of the simplest methods for estimating the coupling loss factors for point-connected structures is the so-called wave transmission approach. It treats the motion of the coupled bodies in terms of traveling waves and represents the coupling loss factor in terms of mechanical impedance or admittance functions at the coupling points. It implies rather extreme simplifying assumptions when applied to real structures since simple traveling wave solutions exist only for structures with a high degree of uniformity. Examples would be infinite plates and beams of uniform section. Nevertheless, the method was pursued for several reasons:

a. The simplicity of the model made the method a good first step in gaining familiarity with SEA.

b. It appeared to be adaptable to one of the objectives of the SEA work; investigating the use of interactive minicomputer processing of test data to predict coupling loss factors.

c. For sufficiently high frequency, the simplifying assumption of uniform structure may be quite reasonable for structures such as curved stiffened shells which are distinctly non-uniform at lower frequency.

The derivation of coupling loss factor in terms of coupling impedance using a wave model is given in Reference [10] and will not be repeated here except to slightly rearrange the final result. Equation 11 of Reference [10] is (refer to Figure 12):

$$2\pi f_c \eta_{AB} = \frac{1}{m_A} \left| \frac{Z_A Z_B'}{Z_A + Z_B'} \right|^2 \mathrm{Re}\left(\frac{1}{Z_B}\right) \qquad (4.12)$$

where

m_A = mass of body A

Z_A = impedance of body A at the degree of freedom to which one end of the coupling spring in attached

Z_B' = impedance looking into the series combination of body B and the coupling spring

We note that a typographical error occurred in Eq. 11 of Reference [10] and so it differs slightly from (4.12) [11]. If Z_B is the impedance of body B at the point where it attaches to the light spring, then

$$\frac{1}{Z_{B^T}} = \frac{1}{Z_B} + \frac{1}{Z_c} \tag{4.13}$$

where

$$Z_c = Z_c(f) \doteq \frac{k_c}{i2\pi f}$$

k_c = stiffness of coupling spring

Combining (4.12) with (4.13) and using the definition of mobility H(f) as the reciprocal of impedance Z(f):

$$2\pi f_c \eta_{AB} = \frac{1}{m_A} \frac{Re(H_B)}{\left|H_A+H_B+H_C\right|^2} \tag{4.14}$$

Equation 4.14 is nearly the formula for coupling loss factor upon which the experiment described in section 4.4 is based. However for application to real (i.e. finite) structures, an important modification is necessary. The explanation of this will follow more naturally after an alternate derivation has been given.

4.3.2 Derivation in Terms of Normal Modes

The formula for coupling loss factor, Eq. (4.14), may be derived without explicit reference to traveling waves. The procedure is similar in principal to Reference [10] except that the notions of normal modes and power spectral density functions are used rather than waves of complex exponential amplitude. It is felt that the former terminology would allow a clearer explanation of the experiment which follows.

Consider two structures A and B of Figure 12 connected by a light spring of stiffness k_c. Body A only is directly excited by load $\ell_o(t)$.

Replacing the coupling spring by its force $\ell_c(t)$

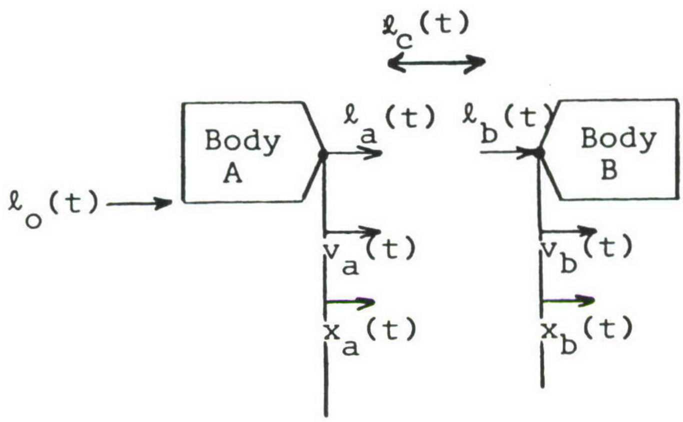

where

$\ell_a(t)$, $\ell_b(t)$ = forces on bodies A and B at the connect points

$v_a(t)$, $v_b(t)$ = velocities of the connect points

$x_a(t)$, $x_b(t)$ = displacements at the connect points

$\ell_o(t)$ = external force on body A

$\ell_c(t)$ = coupling force in spring

Then if $\ell_c > 0$ implies tension in the spring

$$\ell_a = \ell_c \tag{4.15}$$

$$\ell_b = -\ell_c \tag{4.16}$$

The mechanical impedance of body B at the attachment point b is defined as

$$Z_b(f) \triangleq \frac{L_b(f)}{V_b(f)} \tag{4.17}$$

where

f = frequency

$L_b(f)$ = Fourier transform of $\ell_b(t)$

$= \mathcal{F}[\ell_b(t)]$

$V_b(f)$ = Fourier transform of $v_b(t)$

$= \mathcal{F}[v_b(t)]$

It should be noted that the definition of $Z_b(\omega)$ implies that $v_b(t)$ is the velocity of B at b when $\ell_b(t)$ is the <u>only</u> force acting on B. To emphasize this fact, we will write $v_b^{(\ell_b)}(t)$ to denote the velocity of b under this condition. The superscript in parenthesis will also carry over to Fourier transforms.

Transforming (4.16) and combining with (4.17)

$$Z_b(f) = \frac{-L_c(f)}{V_b^{(\ell_c)}(f)} \tag{4.18}$$

Similarly

$$Z_a(f) = \frac{L_c(f)}{V_a^{(\ell_c)}(f)} \tag{4.19}$$

The coupling force is

$$\ell_c(t) = k_c[x_b(t) - x_a(t)] \tag{4.20}$$

Transforming (4.20)

$$L_c(f) = k_c[X_b(f) - X_a(f)] \tag{4.21}$$

Using the derivative relation for Fourier transforms

$$V(f) = i2\pi f X(f) \tag{4.22}$$

gives

$$L_c = \frac{k_c}{i2\pi f} (V_b - V_a) \tag{4.23}$$

If both structures are assumed to behave linearly we may use superposition

$$\begin{aligned} v_a &= [v_a \text{ due to } \ell_o \text{ with } \ell_c = 0] \\ &\quad + [v_a \text{ due to } \ell_c \text{ with } \ell_o = 0] \end{aligned} \tag{4.24}$$

Putting (4.24) in terms of the notation previously defined

$$v_a = v_a^{(\ell_o)} + v_a^{(\ell_c)} \tag{4.25}$$

Transforming (4.25)

$$V_a(f) = V_a^{(\ell_o)}(f) + V_a^{(\ell_c)}(f) \tag{4.26}$$

From (4.26) and (4.19), dropping the argument

$$V_a = V_a^{(\ell_o)} + \frac{L_c}{Z_a} \tag{4.27}$$

Similarly

$$V_b = V_b^{(\ell_o)} - \frac{L_c}{Z_b} \tag{4.28}$$

But $V_b^{(\ell_o)} = 0$ since body B won't move if ℓ_c is removed. Then

$$V_b = -\frac{L_c}{Z_b} \tag{4.29}$$

Combining (4.23), (4.27) and (4.29)

$$L_c = \frac{-V_a^{(\ell_o)}}{\frac{1}{Z_a} + \frac{1}{Z_b} + \frac{1}{Z_c}} \tag{4.30}$$

where

$Z_c(f) \triangleq$ impedance of spring element with one end fixed

$$= \frac{k_c}{i2\pi f}$$

Next, we find an expression for $<\pi_{AB}>_t$ in terms of $V_a^{(\ell_o)}$. $<\pi_{AB}>_t$ is the time averaged power being transmitted from body A to body B through the coupling spring. If $\pi_{AB}(t)$ is the instantaneous power being received at b then

$$\pi_{AB}(t) = v_b(t)\ \ell_b(t) \tag{4.31}$$

$$= -v_b(t)\ \ell_c(t) \tag{4.32}$$

If the vibration is assumed to be stationary random and ergodic, we can time average (4.32) to get

$$<\pi_{AB}>_t = \lim_{T\to\infty} \frac{-1}{T} \int_o^\infty v_b \ell_c dt = - <v_b \ell_c>_t \tag{4.33}$$

Introducing the definition of cross correlation

$$R_{v_b \ell_c}(\tau) \triangleq <v_b(t)\ \ell_c(t+\tau)>_t \tag{4.34}$$

From (4.33) and (4.34)

$$<\pi_{AB}>_t = - R_{v_b \ell_c}(0) \tag{4.35}$$

The correlation $R(\tau)$ is related to power spectral density $S(f)$ by Wiener's theorem

$$R_{xy}(\tau) = \mathcal{F}^{-1}[S_{xy}(f)] \tag{4.36}$$

$$= \int_{-\infty}^{\infty} S_{xy}(f)e^{i2\pi f\tau}df \tag{4.37}$$

$$= \int_{-\infty}^{\infty} \langle X^*(f)Y(f)\rangle e^{i2\pi f\tau}df \tag{4.38}$$

where the last equation makes use of the stationarity assumption Then letting $\tau = 0$ in (4.34) and (4.38) and combining with (4.33) gives

$$\langle\pi_{AB}\rangle_t = - \int_{-\infty}^{\infty} \langle L_c^* V_b\rangle \, df \tag{4.39}$$

where * denotes complex conjugate and < > applied to products of Fourier transforms denotes ensemble averaging.

Now $v_b(t)$ and $\ell_c(t)$ are both real so $V_b(f)$ and $L_c(f)$ both have Hermetian symmetry; that is, $V_b(-f) = V_b^*(f)$ and $L_c(-f) = L_c^*(f)$. The integral in (4.39) is then

$$\int_{-\infty}^{\infty} \langle L_c^* V_b\rangle \, df = 2\mathrm{Re}\left[\int_{0}^{\infty} \langle L^* V_b\rangle df\right] \tag{4.40}$$

Then

$$\langle\pi_{AB}\rangle_t = - 2\mathrm{Re}\int_{0}^{\infty} \langle L_c^* V_b\rangle df \tag{4.41}$$

(4.41)suggests that we define $\Pi_{AB}(f)$, the spectral density of transmitted power, as

$$\Pi_{AB}(f) \overset{\Delta}{=} -2\mathrm{Re}\,\langle L_c^* V_b\rangle \tag{4.42}$$

The convention implied in (4.42), namely that Fourier transforms are double-sided and spectral density functions are single-sided, will be followed throughout this chapter.

From (4.41) and (4.42)

$$\langle\pi_{AB}\rangle_t = \int_0^\infty \Pi_{AB}(f)df \tag{4.43}$$

Since $\ell_c(t)$ is the only force acting on body B we can write, from (4.42)

$$\Pi_{AB} = -2\text{Re}\ \langle L_c^* V_b^{(\ell_c)}\rangle \tag{4.44}$$

Combining (4.18) and (4.44)

$$\Pi_{AB}(f) = 2\langle|L_c(f)|^2\rangle\ \text{Re}(\frac{1}{Z_b(f)}) \tag{4.45}$$

Next define $E_A^{(\ell_o)}(f)$ as the spectral density of the time-averaged total energy (kinetic and potential) of body A with the coupling removed. That is, if $T_A^{(\ell_o)}(f)$ and $U_A^{(\ell_o)}(f)$are respectively the spectral densities of kinetic and potential energies of the uncoupled body A

$$T_A^{(\ell_o)}(f) + U_A^{(\ell_o)}(f) = E_A^{(\ell_o)}(f) \tag{4.46}$$

It may be shown [12] that for the uncoupled body A driven only by $\ell_o(t)$ the time averaged kinetic and potential energies in any frequency band are equal.

$$T_A^{(\ell_o)} = U_A^{(\ell_o)} \tag{4.47}$$

Then from (4.46) and (4.47

$$2T_A^{(\ell_o)}(f) = E_A^{(\ell_o)}(f) \tag{4.48}$$

Next, consider the quantity $<|V_a^{(\ell_o)}|^2>$. If the modal density of body A is very high in the frequency band of interest, and the mass distribution is fairly uniform, then the vibration field will be homogeneous. That is, the temporal mean square velocity in a frequency band will not vary much over the structure. Then, with the coupling spring detached, point a on body A is just a typical point whose velocity spectrum is a good estimate of the mass-averaged velocity spectrum of the whole structure. Thus, if m_A is the mass of body A

$$T_A^{(\ell_o)}(f) = m_A <|V_A^{(\ell_o)}(f)|^2> \tag{4.49}$$

It should be noted that the above assumptions are just those which are needed to admit a simple traveling wave description of the motion of body A. Thus, it is not surprising that the end result is similar to equation 11 of Reference [10], which was obtained using a wave approach.

From Eqs. (4.48) and (4.49)

$$E_A^{(\ell_o)}(f) = 2m_A <|V_A^{(\ell_o)}(f)|^2> \tag{4.50}$$

The fundamental theorem of SEA is

$$\int_{\Delta f} \Pi_{AB}(f)df = 2\pi f_c[\eta_{AB}(f_c)\int_{\Delta f} E_A(f)df - \eta_{BA}(f_c)\int_{\Delta f} E_B(f)df] \tag{4.51}$$

where $\eta_{AB}(f_c)$ and $\eta_{BA}(f_c)$ are the coupling loss factors evaluated for the frequency band Δf centered at f_c. It must be noted that equation (4.51) holds only in the mean. Each of the three terms represents an estimate of the mean value of a random variable and thus the terms are themselves random variables. In practical terms this implies that the product of modal density and Δf must be large enough to allow many modes to contribute if (4.51) is to hold for a particular trial [13].

When the coupling is light and only one body is directly excited, it is commonly assumed that the coupled and uncoupled energies of the directly excited body (body A) are essentially equal. Also, the energy of the indirectly excited body is assumed to be small compared to that of the directly excited. Under these assumptions (4.51) becomes

$$\int_{\Delta f} \Pi_{AB}(f)df = 2\pi f_c \; \eta_{AB} \int_{\Delta f} E_A^{(\ell_o)}(f)df \tag{4.52}$$

Combining (4.45) and (4.30)

$$\Pi_{AB}(f) = \frac{2<|V_a^{(\ell_o)}|^2>}{\frac{1}{Z_a} + \frac{1}{Z_b} + \frac{1}{Z_c}} \quad Re(\frac{1}{Z_b}) \tag{4.53}$$

Substituting (4.53) and (4.50) into (4.52) and introducing the velocity admittance $H = Z^{-1}$ (also called the mobility) in place of impedance gives

$$\int_{\Delta f} \frac{2<|V_A^{(\ell_o)}|^2 \quad Re(H_b)df}{|H_a + H_b + H_c|^2}$$

$$= \quad 4\pi f_c \; m_A \; \eta_{AB} \int_{\Delta f} <|V_a^{(\ell_o)}|^2>df \tag{4.54}$$

The mobility functions are defined at every frequency f both inside and outside the integration band Δf. For structures with the assumed high modal density, $H_A(f)$ and $H_B(f)$ can be expected to vary rapidly within the band and thus the factor $Re(H_B)/|H_A+H_B+H_C|^2$ cannot be taken outside the integral on the left side of (4.54). However, if one returns to the basic assumptions of SEA the next step is clear. The energy equilibrium equations of the form (4.3)-(4.4) are written for frequency bands of finite width on the assumption that internal and

coupling loss coefficients can be treated as constant over each of these frequency bands. Thus, consistency requires that the quantity $\mathrm{Re}(H_B)/|H_A+H_B+H_C|^2$ be replaced by a constant value which is, in some sense, best over the frequency band Δf. Intuitively, one suspects that the frequency average over Δf of the whole quantity would be appropriate. However, a slightly different approach is suggested by Manning [11] and is the one actually taken. The individual frequency responses $H_A(f)$, $H_B(f)$, and $H_C(f)$ are replaced by their frequency averages over the band Δf and centered at f. It can be shown [14] that for many types of structures, the mobility function of a finite structure, when averaged over a band which contains many modes, will equal the mobility of an infinite extension of the structure. Thus, replacing $H(f)$ by $\overline{H}(f_c)$ where

$$\overline{H}(f_c) = \frac{1}{\Delta f} \int_{f_c - \frac{\Delta f}{2}}^{f_c + \frac{\Delta f}{2}} H(f)df \tag{4.55}$$

amounts to replacing the actual structure by an equivalent one which is a best uniform approximation in a particular frequency range. Making the above substitutions for $H_A(f)$, $H_B(f)$ and $H_C(f)$ allows the mobilities to be taken outside the integral on the left. The remaining integrals then cancel and the result is

$$2\pi f_c\ \eta_{AB} = \frac{1}{m_A} \frac{\mathrm{Re}[\overline{H}_B(f_c)]}{|\overline{H}_A(f_c)+\overline{H}_B(f_c)+\overline{H}_C(f_c)|^2} \tag{4.56}$$

Note that this result is identical to Eq. (4.14) except that the admittance functions H_A, H_B and H_C have been replaced by their smoothed (i.e., averaged with respect to frequency) counterparts. The final test of the approximations described above must, of course, be by experiment. One such experiment is described in Section 4.5.

4.4 ESTIMATION OF ANGULAR RESPONSE

In Section 4.3 of this report a method is described for calculating coupling loss factor in a particular situation. From the discussion of Section 4.2 it may be seen that this factor, along with internal (damping) loss factors, can be used to set up an SEA model for a simple two-component system coupled at a single degree of freedom. The solution of the SEA equilibrium equations will then be component energies and the inter-component power flow in frequency bands. However, these are not usually the quantities of direct interest. In the present case we would like to estimate mean square angular response and, if possible, its spectral distribution at specific points on a structure. In Section 4.5, the SEA modeling described in Sections 4.2 and 4.3 is carried out for a simple system consisting of two uniform plates coupled at one point. In this section we derive an expression for angular response in terms of component energy for this demonstration case. Its validity was tested by experiment and results are reported in Section 4.5.4.

4.4.1 Relation Between Angular Response and Total Energy For A Uniform Plate

Suppose a uniform rectangular plate is excited by broadband random forces. Assume that the smoothed spectral density of the total vibrational energy is fairly flat well into the frequency range where modal density (averaged over the smoothing bandwidth) is constant. Let the dynamic response of the plate be represented as

$$w(x,y,t) = \sum_{i} \eta_i(t)\ \psi_i(x,y) \tag{4.57}$$

where

x, y = coordinates parallel to plate edges

t = time

w = normal displacement of plate midplane

$\psi_i(x,y)$ = shape function of i^{th} normal mode of plate

$\eta_i(t)$ = amplitude of i^{th} normal mode.

It is assumed that if the support conditions allow rigid body modes, the forcing is such that their response is negligible compared to flexural modes in the high frequency range of interest. The desired response quantity is the amplitude of the total angle between the instantaneous normal to the plate at a point (x,y) and the normal to the undisturbed plate at that point.

$$|\theta(x,y,t)| = |\nabla w| \tag{4.58}$$

where

∇ = gradient operator

$$= \vec{e}_x \frac{\partial}{\partial x} + \vec{e}_y \frac{\partial}{\partial y}$$

$\vec{e}_x$, $\vec{e}_y$ = unit vectors in x and y directions

combining Eqs. (4.57) and (4.58), squaring, and taking the expectation with respect to time.

$$\langle\theta^2(x,y,t)\rangle_t = \sum_i \sum_j \langle\eta_i\eta_j\rangle_t \frac{\partial\psi_i}{\partial x}\frac{\partial\psi_j}{\partial x} + \sum_i \sum_j \langle\eta_i\eta_j\rangle_t \frac{\partial\psi_i}{\partial y}\frac{\partial\psi_j}{\partial y} \tag{4.59}$$

For light damping, each of the mean square modal responses will have spectral densities which have large values in the neighborhood of their respective natural frequencies but are much smaller elsewhere. This implies

$$\langle\dot{\eta}_i^2\rangle_t \simeq \omega_i^2 \langle\eta_i^2\rangle_t \tag{4.60}$$

and

$$\langle\eta_i\eta_j\rangle_t = 0 \text{ for } \omega_i \neq \omega_j \tag{4.61}$$

The time-averaged total energy of vibration in a lightly damped structure can be represented in modal coordinates as

$$\langle E\rangle_t = \sum_i \langle E_i\rangle_t = \sum_i m_i \langle \dot{\eta}_i^2\rangle_t \tag{4.62}$$

where

$\langle E\rangle_t$ = time-averaged total energy, kinetic plus potential, of the plate

$\langle E_i\rangle_t$ = time-averaged energy of i^{th} mode

$\dot{\eta}_i = \frac{d\eta_i}{dt}$

m_i = modal mass of i^{th} mode.

As usual in SEA work, the $\langle\ \rangle_t$ operator applied to a positive definite quantity implies the division of that quantity by frequency bands; that is, if $G_u(f)$ is a single-sided spectral density function, then

$$\langle u^2\rangle_t = \int_{f_c - \frac{\Delta f}{2}}^{f_c + \frac{\Delta f}{2}} G_u(f)\, df \tag{4.63}$$

Equation (4.63)defines the common SEA notation even though the center frequency f_c and bandwidth Δf are not expressly noted in the left-hand side. We assume that N modes are resonant within Δf and that only their responses need be considered in forming $\langle\theta^2\rangle_t$.

Combining Equations (4.59) and (4.61) and simplifying

$$\langle\theta^2(x,y,t)\rangle_t = \sum_{i=1}^{N} \langle\eta_i^2\rangle\ |\nabla\psi|^2 \tag{4.64}$$

Combining Equations (4.60), (4.62) and (4.64)

$$\langle\theta^2(x,y,t)\rangle_t = \sum_{i=1}^{N} \frac{\langle E_i\rangle_t}{m_i\omega_i^2}\ |\nabla\psi_i|^2 \tag{4.65}$$

Next we invoke the basic SEA assumption of equipartition of energy between the N modes of a single component in a band.

$$<E_i>_t = \frac{<E>_t}{N} \tag{4.66}$$

From Equations (4.65) and (4.66), writing out $|\nabla\psi|^2$

$$<\theta^2(x,y,t)>_t = \sum_{i=1}^{N} \frac{<E>_t}{m_i\omega_i^2 N} \left[\left(\frac{\partial\psi_i}{\partial x}\right)^2 + \left(\frac{\partial\psi_i}{\partial y}\right)^2\right] \tag{4.67}$$

The frequency range of interest is high compared to the fundamental mode of the plate. Therefore, away from the boundaries the mode shapes will be approximately sinusoidal regardless of boundary conditions.

$$\psi_i(x,y) = \sin(k_{xi}x)\sin(k_{yi}y) \tag{4.68}$$

where k_{xi} and k_{yi} are allowable wavenumbers in the x and y directions. Their exact values will depend on boundary conditions, but in the high frequency regime, only their average density in wavenumber space is important. This density is independent of boundary conditions. In addition, by assuming a traveling wave solution, we may write the dispersion relation for a plate independent of the type of supports.

$$\omega_i^2 = (k_{xi}^2 + k_{yi}^2)^2 \frac{\kappa^2 c_\ell}{(1-\nu^2)} \tag{4.69}$$

where

ω_i = natural radian frequency of i^{th} mode

κ = radius of gyration of plate cross section

= $h/2\sqrt{3}$

h = plate thickness

c_ℓ = extensional wave speed

E = plate elastic modulus

ρ = plate mass density

ν = Poisson's ratio

Combining Equations (4.67) and (4.68)

$$\langle\theta^2(x,y,t)\rangle_t = \sum_{i=1}^{N} \frac{\langle E\rangle_t}{m_i\omega_i^2 N} [k_{xi}^2 \cos^2(k_{xi}x)\sin^2(k_{yi}y) + k_{yi}^2 \sin^2(k_{xi}x)\cos^2(k_{yi}y)] \quad (4.70)$$

In the wave transmission method for finding power transfer coefficients, it is assumed that many modes fall within the frequency band Δf and thus N is large compared to 1. We, therefore, assume that the "typical" point (x'y') falls on the different mode shapes at points such that the quantities $k_{xi}x'$ and $k_{yi}y'$ are uniformly distributed over the range from 0 to 2π. Under this assumption we may replace the $|\nabla\psi_i|^2$ quantity on the right hand side of Equation (4.70) by its spatial average taken over many cycles in both x and y directions. We may also drop the x,y arguments on the left hand side, requiring only that x' y' be well away from the plate boundaries. In that case

$$\langle\theta^2\rangle_t = \sum_{i=1}^{N} \frac{\langle E\rangle_t}{m_i\omega_i^2 N} \frac{(k_{xi}^2 + k_{yi}^2)}{4} \quad (4.71)$$

For a uniform mass density, the modal mass corresponding to mode shapes given by Equation (4.68) is

$$m_i = \frac{M}{4} \quad (4.72)$$

where M is the plate physical mass. Combining Equations (4.69), (4.71) and (4.72)

$$\langle\theta\rangle_t = \frac{\langle E\rangle_t\sqrt{1-\nu^2}}{NM\kappa c_\ell} \sum_{i=1}^{N} \frac{1}{2\pi f_i} \quad (4.73)$$

Once again, the assumption of high modal density can be used to simplify the result. If the natural frequencies f_i are assumed to be uniformly distributed over the frequency band Δf we have

$$\sum_{i=1}^{N} \frac{1}{f_i} \simeq \frac{N}{\Delta f} \int_{f_c - \frac{\Delta f}{2}}^{f_c + \frac{f_c}{2}} \frac{df}{f} \tag{4.74}$$

Note that $N/\Delta f$ is the average modal density and $\Delta f/N$ is the average mode spacing. Combining Eqs. (4.73) and (4.74) and carrying out the integration.

$$\langle\theta^2\rangle_t = \frac{\langle E\rangle_t \sqrt{1-\nu^2}}{2\pi M\kappa c_\ell} \frac{\ln\left[\frac{f_c + \frac{\Delta f}{2}}{f_c - \frac{\Delta f}{2}}\right]}{\Delta f} \tag{4.75}$$

or

$$\langle\theta^2\rangle_t = \frac{\langle E\rangle_t \sqrt{1-\nu^2}}{2\pi M\kappa c_\ell f_{\ell.m.}} \tag{4.76}$$

where $f_{\ell.m.}$ is the log mean frequency of the band. For the bandwidths and center frequencies used in the coupled plate experiment, it is essentially equal to the arithmetic mean f_c. The final result is then

$$\langle\theta^2\rangle_t = \frac{\langle E\rangle_t \sqrt{1-\nu^2}}{2\pi M\kappa c_\ell f_c} \tag{4.77}$$

The r.m.s. value of θ is obtained by summing $\langle\theta^2\rangle$ over all bands and taking the square root.

$$\theta_{r.m.s.} = \frac{(1-\nu^2)^{1/4}}{(2\pi M\kappa c_\ell)^{1/2}} \left(\sum_b \frac{\langle E_b\rangle}{f_b}\right)^{1/2} \tag{4.78}$$

where

$\theta = |\nabla \omega|$, angle between the instantaneous normal to plate at a point x, y, and the normal to the undisturbed plate at that point

w = out-of-plane displacement

ν = Poisson's ratio

M = total plate mass

$\kappa = h/2\sqrt{3}$, radius of gyration of plate cross section

h = plate thickness

$c_\ell = \sqrt{E/\rho}$, extensional wave speed

E = elastic modulus

ρ = mass density

$\langle E_b \rangle$ = temporal mean energy in a frequency band b

f_b = center frequency of band b

In a sense, the derivation leading to Eq. (4.78) is similar to the method of Lee and Whaley [15] for estimating angular vibration from translational vibration. Like Lee and Whaley's method, it is based on a particular structural form (i.e., a beam or plate) and uses the idea of summing or averaging translational response over that form. However, it differs in that mass-weighted velocity PSD's are added to obtain the spectral density of the vibrational energy. Also, this method does not require knowledge of boundary conditions or individual normal modes. Rather, it is assumed that many modes contribute and that low order modes are not dominant.

4.5 ESTIMATION OF INTERNAL LOSS FACTOR

In assembling an SEA model of a real structure, the most formidable task is usually the calculation of the coupling loss factors. However, the accuracy of the model in predicting equilibrium component energies is also quite dependent on the accuracy of internal loss factors which are input to the model. The damping mechanisms in built up structures are usually complex. Estimates of internal loss factor are almost always

empirical in nature. Measurements must be made on the structure in question if it is available or inferred from previous measurements on similar structures. In either case, a convenient method of obtaining damping data suitable for SEA modeling is highly desirable. Recent developments in mini-computer-based dynamic testing have provided a method which seems promising. It is described in the next section.

4.5.1 Measurement and Use of Modal Damping Ratios

While it was assumed at the outset that complete descriptions of individual normal modes of interacting structures would not, in general, be known, it is also true that this is a practical rather than a theoretical restriction. Modal densities of airframe structures may be high, but they are finite. It is quite easy to see the contributions of individual modes in the mobility function measured at a coupling degree of freedom if the measured function is sufficiently well resolved in frequency. It is also possible to estimate the equivalent viscous modal damping ratios of individual modes by trial-and-error fitting of a curve of specific mathematical form to the measured function [16, 17]. Again, the measurement may require a high degree of frequency resolution but this can be accommodated by commercially available hardware/software packages which implement the so-called "zoom" discrete Fourier transform [18]. In theory, each modal damping ratio is characteristic of the entire structure and is independent of the excitation used to measure it. In practice, one will obtain reliable modal damping estimates only for modes with significant amplitude at the coupling point. However, these are exactly the modes which will determine the properties of the coupled system, so obtaining their damping ratios should be adequate.

For the two component system which was tested, the desired damping quantity is

$$\omega_c \eta_B = \frac{\langle \pi_{AB} \rangle_t}{\langle E_B \rangle_t} \tag{4.79}$$

At first glance it might appear that the internal loss factor η_B could be obtained from the modal damping ratios $\xi^{(i)}$ simply by averaging $2\xi^{(i)}$ over all modes resonant in the band of interest. However, this method yields poor agreement with direct experimental measurement of η_B via Eq. (4.79) [19]. A better method, suggested by Manning [11], has been found to give excellent agreement and is explained below.

Since essentially all the vibrational energy of a particular mode is in a narrow band about its natural frequency, we may write, for the frequency band which contains $\omega^{(i)}$

$$\langle E_B^{(i)} \rangle_t = \frac{\langle \pi_{AB}^{(i)} \rangle_t}{\omega^{(i)} \eta^{(i)}} \tag{4.80}$$

where

$\langle E_B^{(i)} \rangle_t$ = averaged energy in i^{th} mode of B

$\langle \pi_{AB}^{(i)} \rangle_t$ = averaged power input to i^{th} mode

$\omega^{(i)}$ = natural radian frequency of i^{th} mode

$\eta_B^{(i)}$ = loss factor for i^{th} mode of B

$= 2\xi_B^{(i)}$

$\xi_B^{(i)}$ = viscous damping ratio of i^{th} mode

If the total energy of the component is $\langle E_B \rangle_t$, then

$$\langle E_B \rangle_t = \sum_i^{N_B} \langle E_B^{(i)} \rangle_t \tag{4.81}$$

where the summation is over all N_B modes which are resonant within the band. From Eqs. (4.80) and (4.81)

$$\langle E_B \rangle_t = \sum_{i=1}^{N_B} \frac{\langle \pi_{AB}^{(i)} \rangle_t}{\omega^{(i)} \eta^{(i)}} \tag{4.82}$$

The input power to a specific mode will depend on its properties such as shape and modal mass, which are presumably not available. We, therefore, approximate $\langle \pi_{AB}^{(i)} \rangle_t$ for all i by an averaged value $\langle \pi_{AB} \rangle_t / N_B$ where $\langle \pi_{AB} \rangle_t$ is the total input power. Making this substitution in Eq. (4.82) as well as replacing $\eta^{(i)}$ by $2\xi^{(i)}$ and $\omega^{(i)}$ by $2\pi f^{(i)}$

$$\frac{\langle \pi_{AB} \rangle_t}{\langle E_B \rangle_t} = 4\pi \left[\frac{1}{N_B} \sum_{i=1}^{N_B} \frac{1}{f^{(i)} \xi^{(i)}} \right]^{-1} \tag{4.83}$$

Comparing Eqs. (4.79) and (4.83)

$$\omega_c \eta_B = 4\pi \left[\frac{1}{N_B} \sum_{i=1}^{N_B} \frac{1}{f^{(i)} \xi^{(i)}} \right]^{-1} \tag{4.84}$$

The left-hand side of Eq. (4.83) is the quantity desired for SEA modeling. The right-hand side is data available from the complex curve fitting routine.

It should be noted that a fitting algorithm of the type described in [16] will return more complex poles than the structure actually has modes. This is necessary in order to obtain a good fit in the presence of the inevitable noise contamination of the measurement. However, it is usually a simple matter to pick out the correct complex poles by examination of the peaks in the frequency response and the complex residues associated with each indicated pole. A test of Eq. (4.83) is described in a later section where $\langle \pi_{AB} \rangle_t / \langle E_B \rangle_t$ is measured directly and compared with an estimate made by curve fitting of a single admittance function.

4.6 SEA WAVE TRANSMISSION EXPERIMENT

4.6.1 Objective

During Phases II and III of this contract an experiment was carried out to test the theoretical developments (described in Sections 4.3 and 4.4). The specific objectives of the exercise were quite numerous. As a whole, it was intended to be a first step towards the development of SEA modeling techniques, based on a combination of theory and experiment, which could be used in the development of airborne optical systems. More specific objectives included:

(1) Compare SEA predictions with measurements for transmitted power and energy of an indirectly excited body over various frequency bands. It was later decided to make the comparisons on the basis of $\langle\pi_{AB}\rangle_t/\langle E_A\rangle_t$ and $\langle E_B\rangle_t/\langle E_A\rangle_t$ to reduce the time and cost of the experiment. In this latter format no prediction for $\langle E_A\rangle_t$ itself is needed and some ambiguity is removed from the results.

(2) Compare predictions of angular response made from Eq. (4.78) and measured energy with directly measured values.

(3) Acquire some hands-on experience with applying an SEA model to a real structure, albeit a very simple one.

(4) Test the limits of the assumptions built into the wave transmission formula Eq. (4.56). In particular, the test was run with rather heavy coupling (stiff coupling spring) so that $\langle E_B\rangle_t/\langle E_A\rangle_t$ was about 0.2 over most frequency bands. In developing the SEA model $\langle E_B\rangle_t \ll \langle E_A\rangle_t$ had been assumed.

(5) Investigate the usefulness of interactive minicomputer processing of test data for SEA modeling. Since SEA models are always constructed individually for different frequency bands, it was felt that FFT methods could be put to good use both in developing the model and in processing of test data for comparison with model predictions.

(6) Develop preliminary software. A number of subroutines were written for tasks which have a high

probability of occurring in any future investigation of more sophisticated SEA methods.

(7) Evaluate numerical procedures for damping measurement. The definition of internal loss factor η_B as utilized in the two-component SEA model of Figure 12 is

$$\eta_B(f_c) = \frac{<\pi_{AB}>_t}{2\pi f_c <E_B>_t} \qquad (4.79)$$

Measurement of η_B directly from this definition is time-consuming even for a simple structure. It may be impractical for anything resembling an airframe since $<E_B>_t$ must be assembled as a mass-weighted sum of smoothed velocity PSD's from many response points. A more practical method involving only measurement of coupling point mobilities was described in Section 4.5.

A word of caution is needed on two points regarding the experiment. While the software which was produced is supplied as an appendix to this report, it cannot be considered a finished product. Its purpose so far has been investigation of a method of analysis. A great deal more work can be anticipated prior to producing software suitable for SEA modeling of anything resembling an actual aircraft and optical system. The uniform plates chosen as test structures are not represented as being dynamically similar to the airframe-optical systems which motivate the overall effort. They are of interest simply because they are typical "high frequency" structures; that is, many modes contribute to response and properties of each individual mode are impractical to obtain, either by analysis or test.

Secondly, one should be aware of what constitutes a "correct" SEA prediction. For complex multi-modal structures, any SEA model is by necessity built up from a coarse and incomplete description of the actual. SEA theory is then used to estimate average or typical component energies and infer from them the mean square response (translation or rotation) at an

average or typical point. However, as Lyon [1] points out repeatedly, the analyst is not interested in averages. He desires to predict response for one specific realization; namely response at a transducer mount point on the prototype sitting in the lab. Thus, the variance of a particular trial about the mean must be considered. The derivation of confidence bands for estimates has not been made for the coupled-plate experiment. Rather, for this initial investigation, the test structure was simply chosen to have higher modal density and be much more uniform than a typical airframe. Both properties tend to reduce response variance. It was simply assumed that such variance as remained was held small enough to allow evaluation of the practical potential of SEA.

4.6.2 Experimental Hardware

The experimental set-up is shown in Figures 13 and 14. Two rectangular aluminum plates of slightly different sizes are suspended in parallel vertical planes by hanging them by long, compliant cords. Pendulum frequencies are low enough that in the frequency range of interest the plates behave as if they were in a free-free configuration. Plate dimensions are 65.12" x 48.12" x 0.090" and 79.12" x 48.12" x 0.090". The coupling link was constructed from 3/8" diameter aluminum rod, 5" in length, with a miniature preloaded universal joint at one end to reduce the moment transmitted into the indirectly excited plate (Figure 14). The connection to both plates is slightly off-center to avoid discriminating against either symmetric or antisymmetric bending modes. The connection to the indirectly excited plate is made by means of a short piece of 10-32 threaded rod which passes through a drilled hole in the plate and clamps it between an accelerometer on one side and a load cell on the other. The load cell then connects to one end of the universal joint. It was originally intended to use a light spring as the coupling element, but some difficulty was encountered in fabricating a spring which would behave as a pure

Figure 13 Couples Plates Used for SEA Wave Transmission Experiment

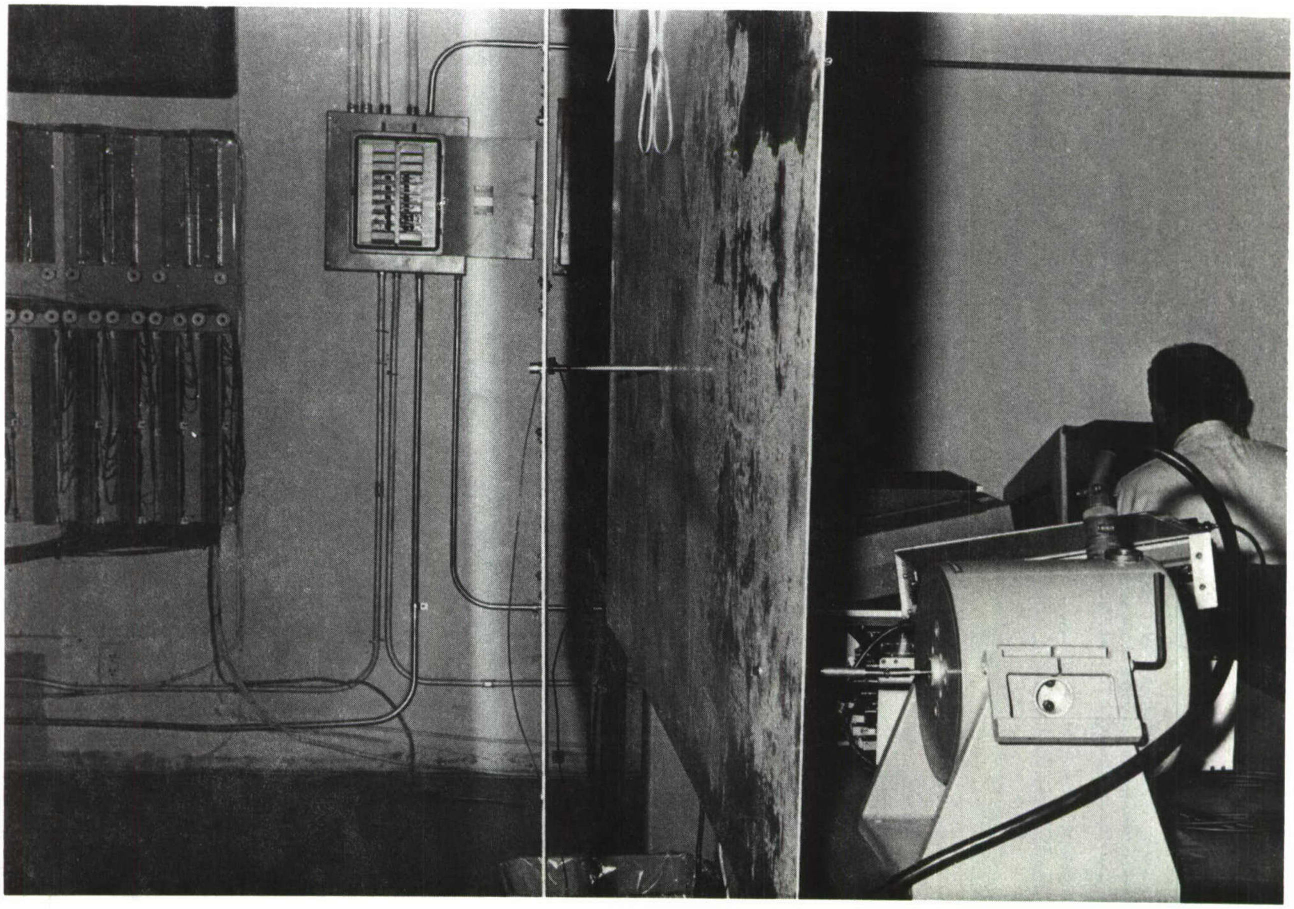

Figure 14 Close-Up of Connecting Link Instrumented to Measure Instantaneous Force and Acceleration

compliance over the desired 100-1000 Hz. band. An attempt was made to use a ring-shaped spring of 163 lbf/in. stiffness which would theoretically have given light coupling (i.e., $H_c >> H_B$) above 350 Hz. The attempt failed due to resonances of the spring itself well below 1000 Hz. The exercise was, nonetheless, instructive and is described in Section 4.6.4.4.

Body A (the larger plate) was directly excited by a small electrodynamic shaker coupled through a universal joint. The drive signal was white Gaussian noise with band-limiting to 150-1000 Hz. Total power input to plate A was about 1 milliwatt and force level was about 0.3 lbf (rms).

The stiffness of the solid link was measured dynamically as 6163 lbf/in. While this implies fairly heavy coupling throughout the band, it was decided that it should be used, nonetheless. Since real structures are likely to be coupled simply by rigid or near-rigid connection of one or more degrees-of-freedom, it was felt that a deliberate violation of the $H_c >> H_B$ assumption might be instructive. It may be noted from the derivation in Section 4.3.2 that $\langle E_B \rangle_t / \langle E_A \rangle_t << 1$ is the actual format of the light coupling assumption. Data presented later in this section show that this was not grossly violated.

The choice of structures for the wave transmission experiment was based on satisfying, as much as possible, the assumptions which are built into the derivation of Eq. 4.56. It was felt that this would allow attention to be focused on the more specialized question of assembling an SEA model from test data. A prerequisite for the test structures is that modal densities be high. For a uniform plate of finite size, the modal density n(f) in modes per Hz. is [20]:

$$n(f) = \frac{\sqrt{3}\, A_p}{h c_\ell} \qquad (4.85)$$

This implies modal densities of about 24 and 29 modes per 80 Hz. frequency band for the smaller (body B) and larger (body A) plates, respectively.

4.6.3 Experimental Procedure

The test procedure consisted basically of 12 steps.

(1) Set up plates in the coupled configuration and establish a suitable drive level and drive spectrum shape.

(2) Measure the smoothed spectral density of transmitted power from force and acceleration signals at the coupling point of plate B.

(3) Measure the smoothed spectral density of total vibrational energy of each plate from accelerometer signals. A uniform grid of 40 locations on plate A and 35 locations on plate B was used.

(4) Remove the coupling link and arrange the shaker, force cell, and accelerometer to measure the mobility function looking into the coupling point of plate B.

(5) Repeat step (4) on plate A.

(6) Compute frequency-averaged mobility functions for the desired frequency bands using the results of steps (4) and (5).

(7) Compute the predicted coupling loss factor weighted by $2\pi f_c$ from the results of step (6) and Eq. (4.56).

(8) Form the actual internal loss factor of plate B as $<\pi_{AB}>_t/<E_B>_t = 2\pi f_c \eta_B(f_c)$.

(9) Compute the predicted energy ratio $<E_B>_t/<E_A>_t$ using the results of steps (7) and (8) and Eq. (4.10).

(10) Use the results of steps (2) and (3) to compute actual transmitted power and component energy in frequency bands. Form the ratios $<\pi_{AB}>_t/<E_A>_t$ and $<E_B>_t/<E_A>_t$ for frequency bands.

(11) Make comparison plots of actual and predicted values of $<E_B>_t/<E_A>_t$ and $<\pi_{AB}>_t/<E_A>_t$.

(12) Rearrange the hardware to drive a single plate (the larger) and measure steady state energy and angular response at an interior point. Plot data as smoothed spectral densities to verify Eq. (4.78).

In principle, step (12) could have been carried out using an indirect drive to the plate to obtain a more nearly end-to-end comparison between theory and experiment. In fact, this step was carried out as something of an afterthought and the direct drive was used to reduce experimental time and cost. It was noted, however, that the smoothed PSD of force input to the plate was similar for either direct or indirect drive, so the comparison of predicted and measured $\langle\theta^2\rangle_t$ and θ r.m.s. should be representative.

An error analysis of the differential acceleration method used to measure the spectral density of angular response is given as an example in Section 6.2.1.

In reference to step (11), a second set of predicted values for $\langle E_B\rangle_t/\langle E_A\rangle_t$ and $\langle\pi_{AB}\rangle_t/\langle E_A\rangle_t$ was computed using the theoretical mobility functions for infinite plates of the same material and thickness as the actual plates [21]. Thus, three sets of data are available for the comparison quantities noted in step (11):

(a) Actual, as measured experimentally.

(b) Predicted, using a theoretical infinite uniform plate approximation.

(c) Predicted, using an infinite uniform structure approximation defined by frequency averaging of measured mobility functions.

Virtually all of the power and energy measurements were accomplished by first obtaining a discrete approximation to their spectral density functions by means of digital discrete Fourier transform (DFT) processing with ensemble averaging. This function could then be integrated over any desired frequency band to obtain the $\langle\ \rangle_t$ quantities of the SEA equilibrium equations. The only restrictions were that the desired frequency band must lie entirely below 1/2T and be an integer multiple of 1/NT where T is the sampling interval and N is the

time domain block size. Using digital methods, it was not necessary to specify either integration bandwidth or band center frequencies prior to data acquisition. In effect, many very narrow bands were defined and combined afterwards to obtain the desired bandwidth for the SEA model.

Source code listings and a description of a typical test run are provided in Appendix C. These are recommended as being the most detailed documentation of the procedure.

Spectral densities and mobility functions were measured with a 2.5 Hz. frequency resolution up to 1280 Hz. and then smoothed over 32 spectral lines (80 Hz.). A constant bandwidth was chosen in order to keep the number of interacting modes per band roughly constant. An interesting aspect of the digital procedure is that it is not necessary to restrict oneself to 1280/80 = 16 frequency bands. It is actually more convenient to consider an 80 Hz. averaging band centered over each spectral line at 2.5 Hz. intervals. Thus the results, both predicted and actual, have the appearance of continuous curves, but actually represent a series of heavily overlapped discrete bands. A 40 Hz. band at either end of the base 0-1280 Hz. analysis range must, of course, be excluded from the smoothed results, but this is of no consequence for the intended purpose.

The DFT resolution band of 2.5 Hz. was chosen for a specific reason. It was known that this would be small compared to the smoothing band but still inadequate to obtain a good representation of the rapidly fluctuating mobility function for the lightly damped plates. However, it was desired to measure the effect of this shortcoming on the smoothed version of the function from which the coupling loss factors are actually estimated. If this moderate level of resolution could yield reasonable results, it would have important practical implications for testing of real structures. It should be noted that the actual power and energy comparison quantities are essentially invariant

with respect to DFT resolution. This is so because the smoothing with respect to frequency can be shown to be equivalent to starting with the same time data but dividing it into a larger number of shorter records. The shorter records would produce a coarser frequency resolution but the statistical confidence of the estimate of power within a given frequency band would remain the same.

4.6.4 Experimental Results

4.6.4.1 Principal Results

Figures 15 and 16 present the main results of the wave transmission experiment. Figure 15 compares the actual ratio of transmitted power to transmitting body energy with predicted values obtained using two different representations for coupling point mobility. Figure 16 shows a similar comparison for normalized receptor body energy, and is based on actual measured damping in plate B, as calculated by Eq. (4.79). Disagreement between between measured mobility is about 1.5 to 6 dB (factor of 1.4 to 4) in the range beyond 300 Hz. The predicted value of $\langle\pi_{AB}\rangle_t/\langle E_A\rangle_t$ using an infinite plate approximation is somewhat better at 0 to 5 dB error (factor of 1 to 3.2). For $\langle E_B\hat{}_t/\langle E_A\rangle_t$ the corresponding agreement figures are 0 to 3 dB for both prediction methods. In general, it appears at this point that the infinite plate approximation is the better of the two. However, some further data presented in the next section suggests that better DFT frequency resolution in the measurement of H_A and H_B would improve the accuracy of the frequency-averaged measured mobility approach. It also appears that a wider smoothing bandwidth would be appropriate and would improve the accuracy of both methods. At any rate, the results are quite encouraging. The receptor body energy is within a factor of two of the measured value in all frequency bands, which implies that a

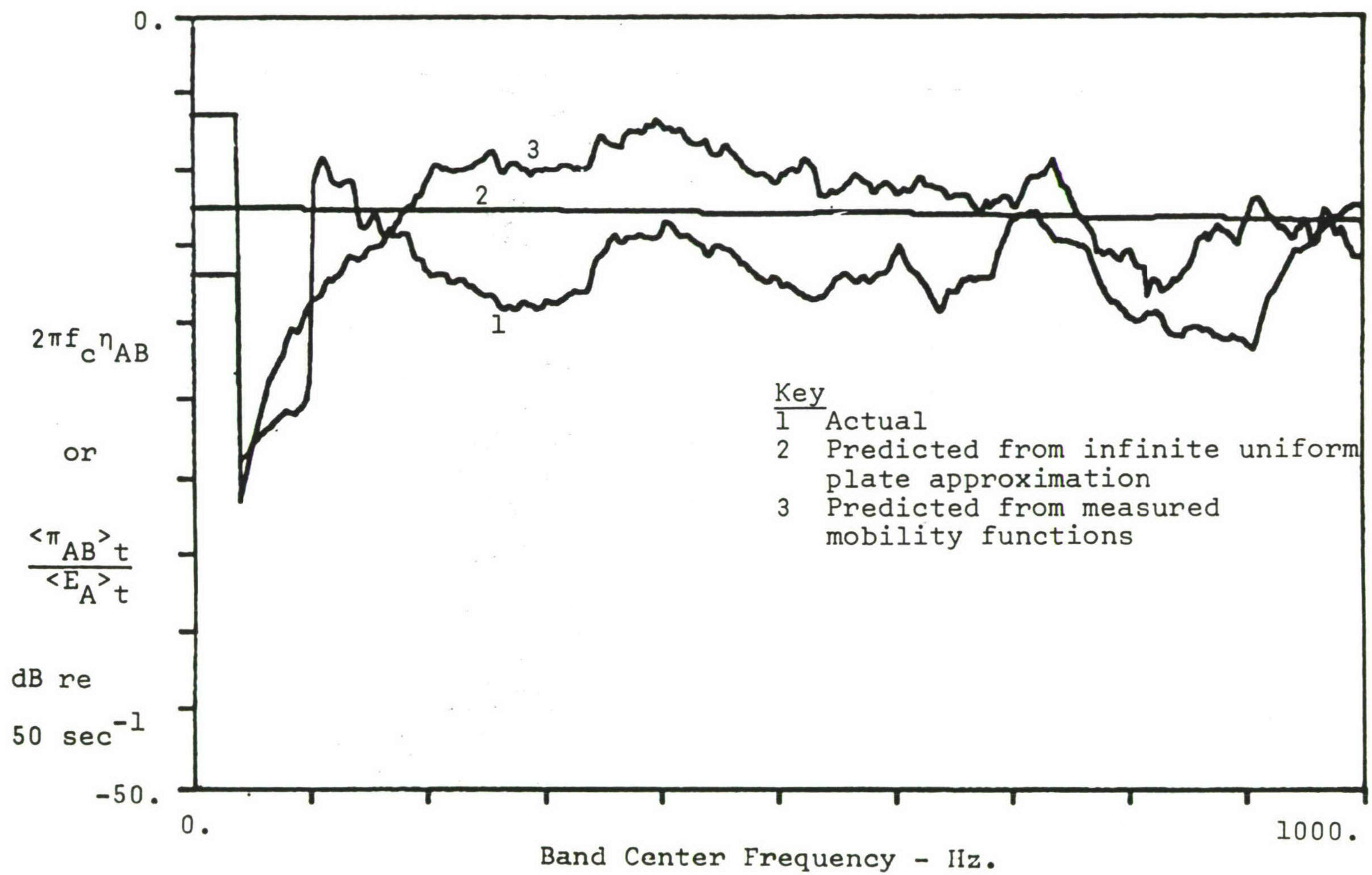

Figure 15 Normalized Transmitted Power $\langle \pi_{AB} \rangle_t / \langle E_A \rangle_t$

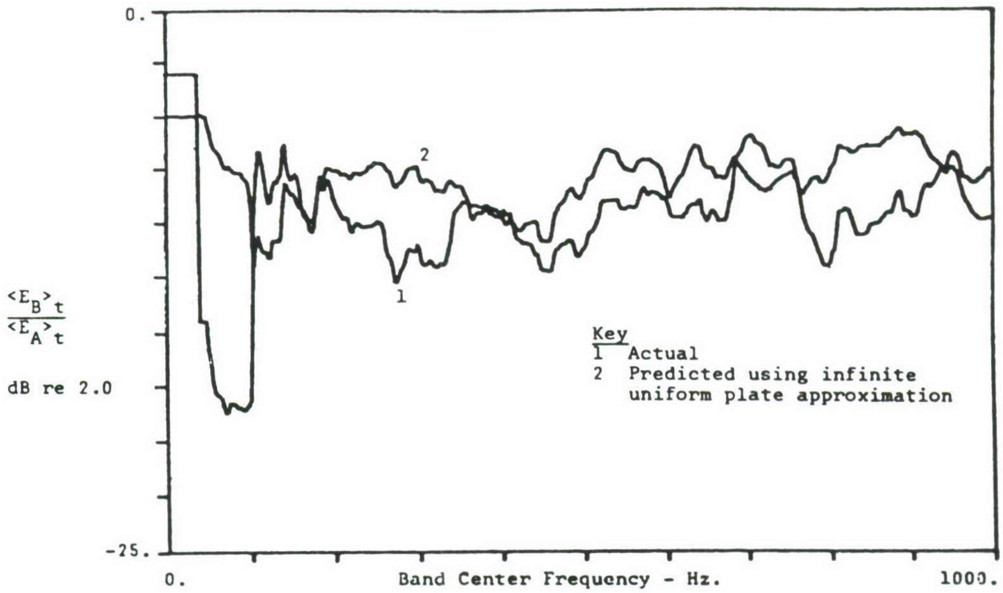

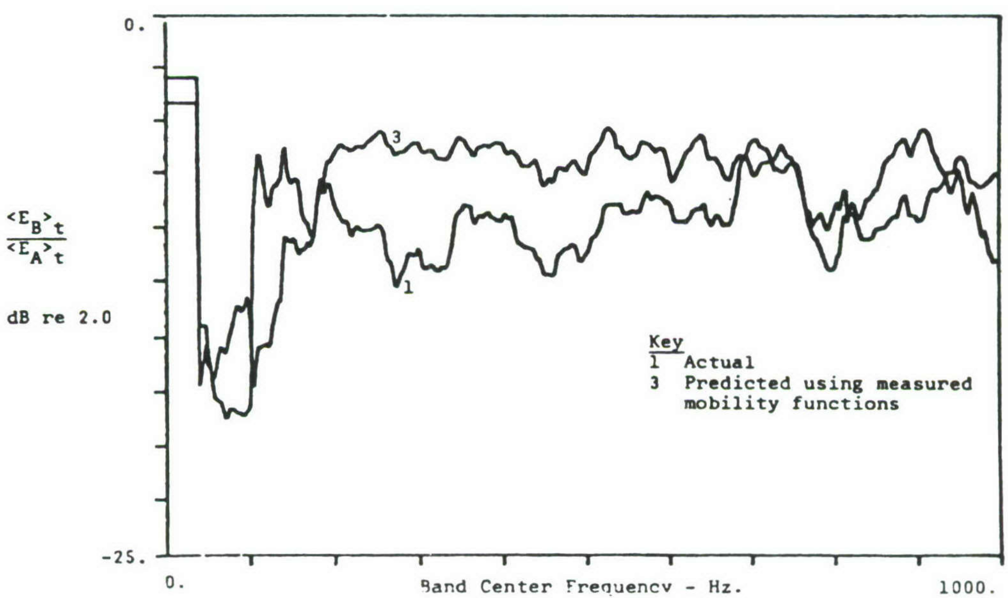

Figure 16 Normalized Energy of Indirectly Excited Body. Actual Damping Used.

spatially-averaged r.m.s. displacement or velocity would be within 41%.

The comparison of angular response, actual vs. estimated from measured energy, is given in terms of smoothed spectral density functions and r.m.s. values in Figure 17.

Predicted r.m.s. angular displacement is within 8% of actual. Most of the discrepancy appears to be due to a single mode around 250 Hz. which contributes disproportionately to mean square angle at the particular point chosen for comparison. Errors of this type are inherent in the SEA procedure if individual mode shapes are not known. This is discussed extensively in Chapter 4 of Lyon [13].

4.6.4.2 Measurement of Internal Loss Factor

Figure 18 shows a comparison of internal loss factor (weighted by band center frequency) as measured by two different methods. The continuous curve is $\langle \pi_{AB} \rangle_t / \langle E_B \rangle_t$ obtained by direct measurement of the numerator and denominator and is, by definition, the correct quantity for SEA modeling. $\langle E_B \rangle_t$ is obtained as a mass-weighted sum of velocity PSD's for forty points arranged over the plate. The symbol ⊢⊖⊣ indicates $\omega_c \eta_B$ estimated by curve-fitting to the measured coupling point mobility and using Eq. (4.83). The width of the symbol indicates the frequency range over which $H_B(f)$ was measured using a high-resolution DFT. Natural frequencies and modal damping ratios as estimated by curve fitting are tabulated in Table 2 for the four bands shown.

Agreement between the two measurement methods is excellent. The 0 to 1 dB difference is better than typical repeatability of damping measurements. This result is quite encouraging because measurement by curve fitting was about ten times faster for this simple case. For a more complex structure, the advantage would be even greater due to the effort of assembling a mass matrix which is circumvented in the curve fitting method.

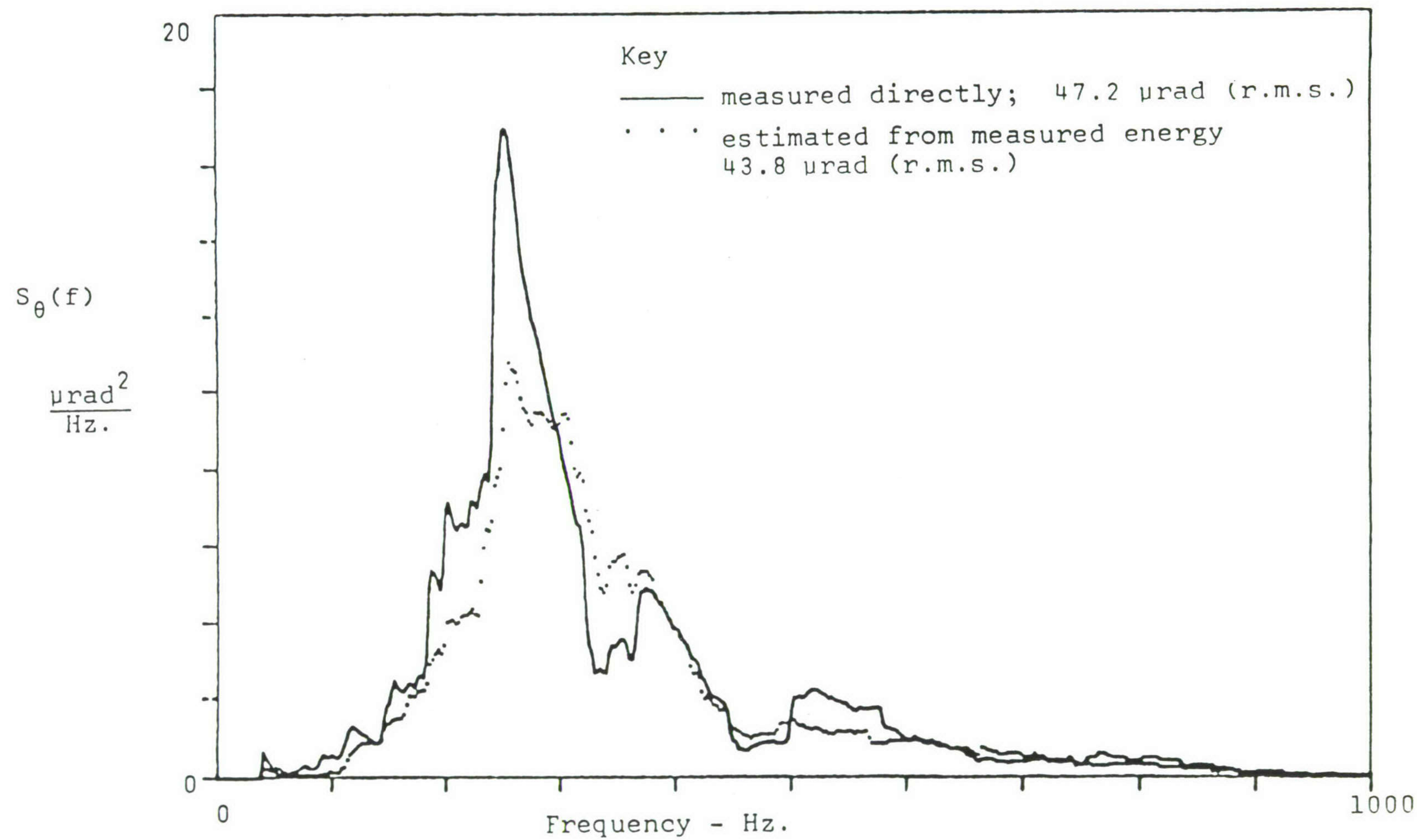

Figure 17 Smoothed Power Spectral Density and R.M.S. Value of High-Frequency Angular Vibration at a Typical Point of a Uniform Rectangular Plate

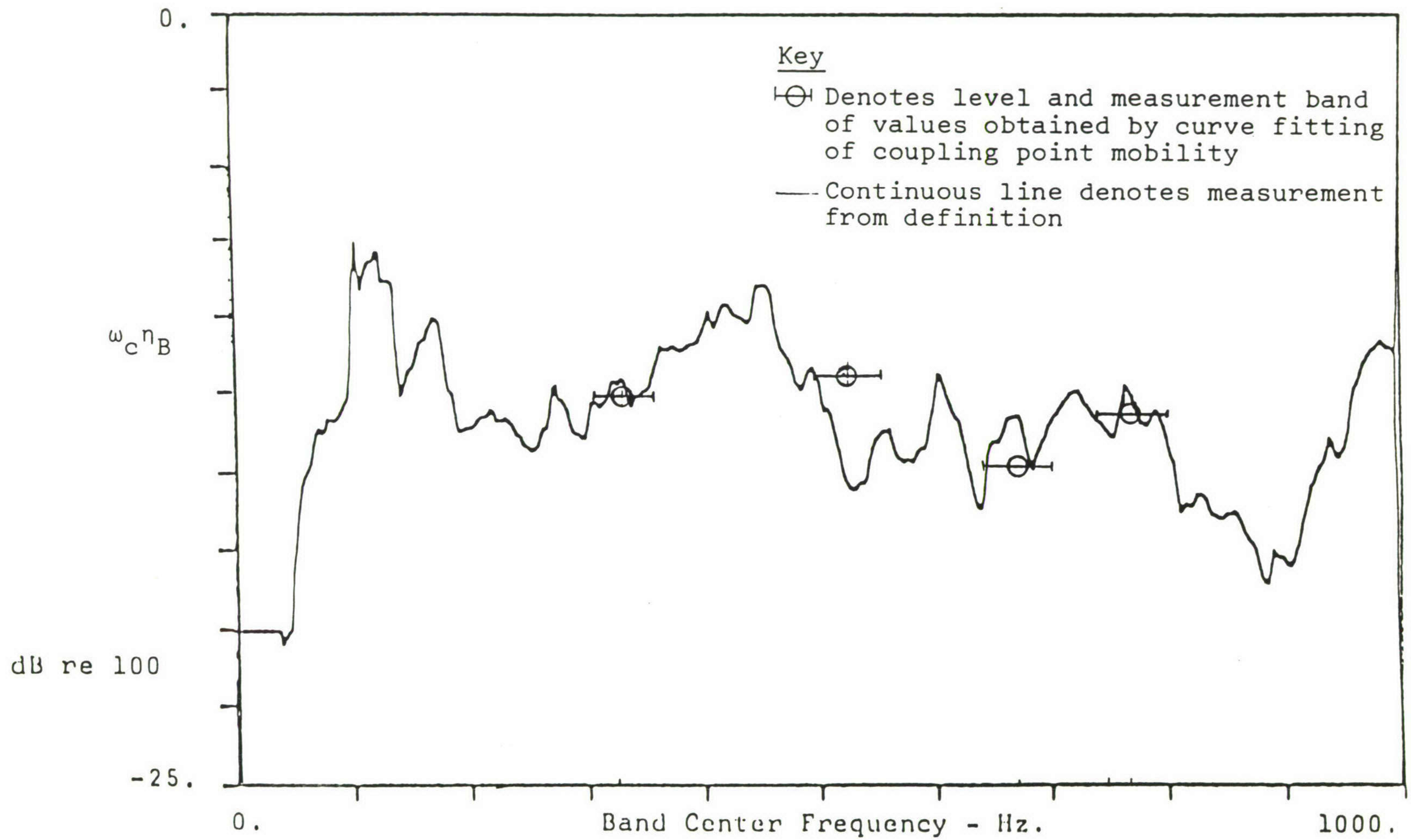

Figure 18 Internal Loss Factor vs. Frequency of Indirectly Excited Plate

TABLE 2

NATURAL FREQUENCIES
AND MODAL DAMPING RATIOS FOR PLATE B

Band 1	300-340 Hz
$f^{(i)}$, Hz	$\xi^{(i)}$
303.9	.00329
306.3	.00497
309.8	.00123
325.8	.00283
326.8	.00125
330.3	.00037
336.9	.00182

Band 2	505-540 Hz
$f^{(i)}$, Hz	$\xi^{(i)}$
509.0	.00380
511.7	.00059
521.3	.00059
522.9	.00173
531.3	.00086
533.6	.00134
542.4	.00098

Band 3	650-700 Hz
$f^{(i)}$, Hz	$\xi^{(i)}$
654.3	.00092
657.3	.00062
659.4	.00106
663.5	.00096
669.5	.00106
676.2	.00007
679.9	.00064
682.3	.00086
686.5	.00032
689.2	.00070

Band 4	750-800 Hz
$f^{(i)}$, Hz	$\xi^{(i)}$
756.5	.00035
758.6	.00095
760.1	.00040
766.4	.00035
770.6	.00031
772.0	.00061
775.9	.00043
784.3	.00046
789.8	.00099

4.6.4.3 Other Results

Figure 19 indicates the probable effect of inadequate DFT resolution in measuring mobilities $H_A(f)$ and $H_B(f)$. The data shown is modulus of the acceleration admittance rather than real part of velocity admittance (mobility) but the implication is still quite clear. Decreasing the frequency resolution will suppress the peaks in H(f) without filling in the valleys. The frequency averaged version of H(f) will thus be reduced and $\omega\eta_{AB}$ predicted from it by Eq. (4.56) will be increased. In Figure 15 the predicted value of $\omega_c\ \eta_{AB}$ follows the actual but is higher over a broad range of frequencies. It thus appears that a smaller DFT resolution element would result in improved accuracy.

A closer examination of the measured $\overline{H}_B(f_c)$ function shows another peculiarity. It is plotted in Figure 20 in both real-imaginary and modulus formats. In theory, from Reference [14], the real part of $\overline{H}_B(f_c)$, called the conductance, should approach a constant with increasing f_c while the imaginary part, or susceptance, goes to zero. From Figure 20, the modulus approaches a fairly constant value but neither $Re[\overline{H}_B(f_c)]$ nor $Im[\overline{H}_B(f_c)]$ behave as predicted. Identical behavior was observed with $\overline{H}_A(f_c)$. It appears that some further work on measurement of averaged mobility of high modal density structures will be in order if wave transmission methods are to be pursued further.

The spectral density of transmitted power and its smoothed version are shown in Figure 21. Spectral densities of total vibration energy for the A and B plates are shown in Figure 22. Two observations may be made:

(1) The distributions of energy and power with respect to frequency are reasonably even. In testing the SEA model with broadband excitation, one is essentially running several experiments simultaneously, one in each frequency band. Some care must be taken so that a large signal in one band does not cause error in another due to dynamic range limitations.

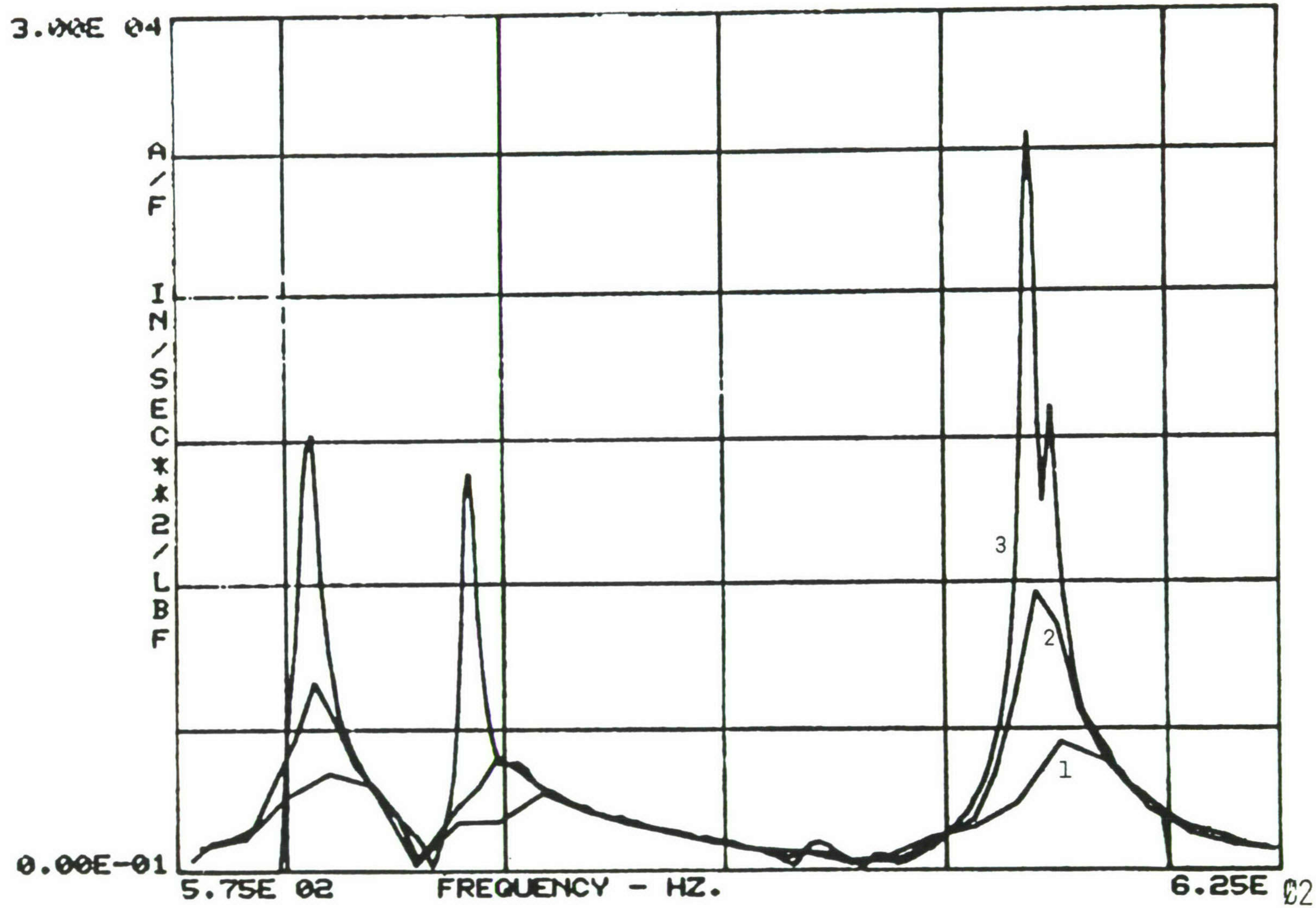

Figure 19 Modulus of Acceleration Admittance at Center Point of Large Plate.
Measured with Frequency Resolution of (1) 1.94 Hz.
(2) 0.94 Hz.
(3) 0.20 Hz.

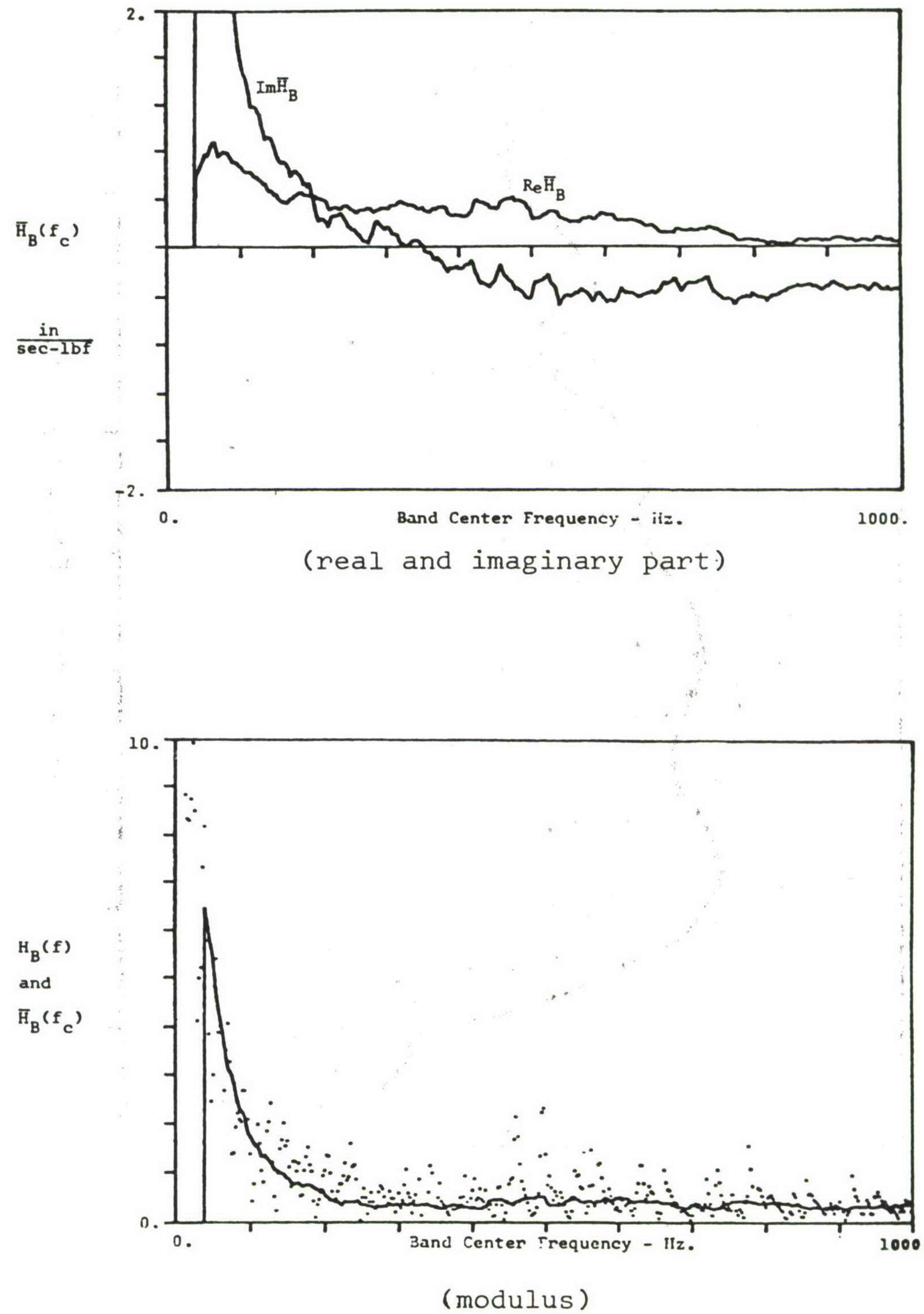

Figure 20 Measured Coupling Point Mobility of Small Plate After Smoothing

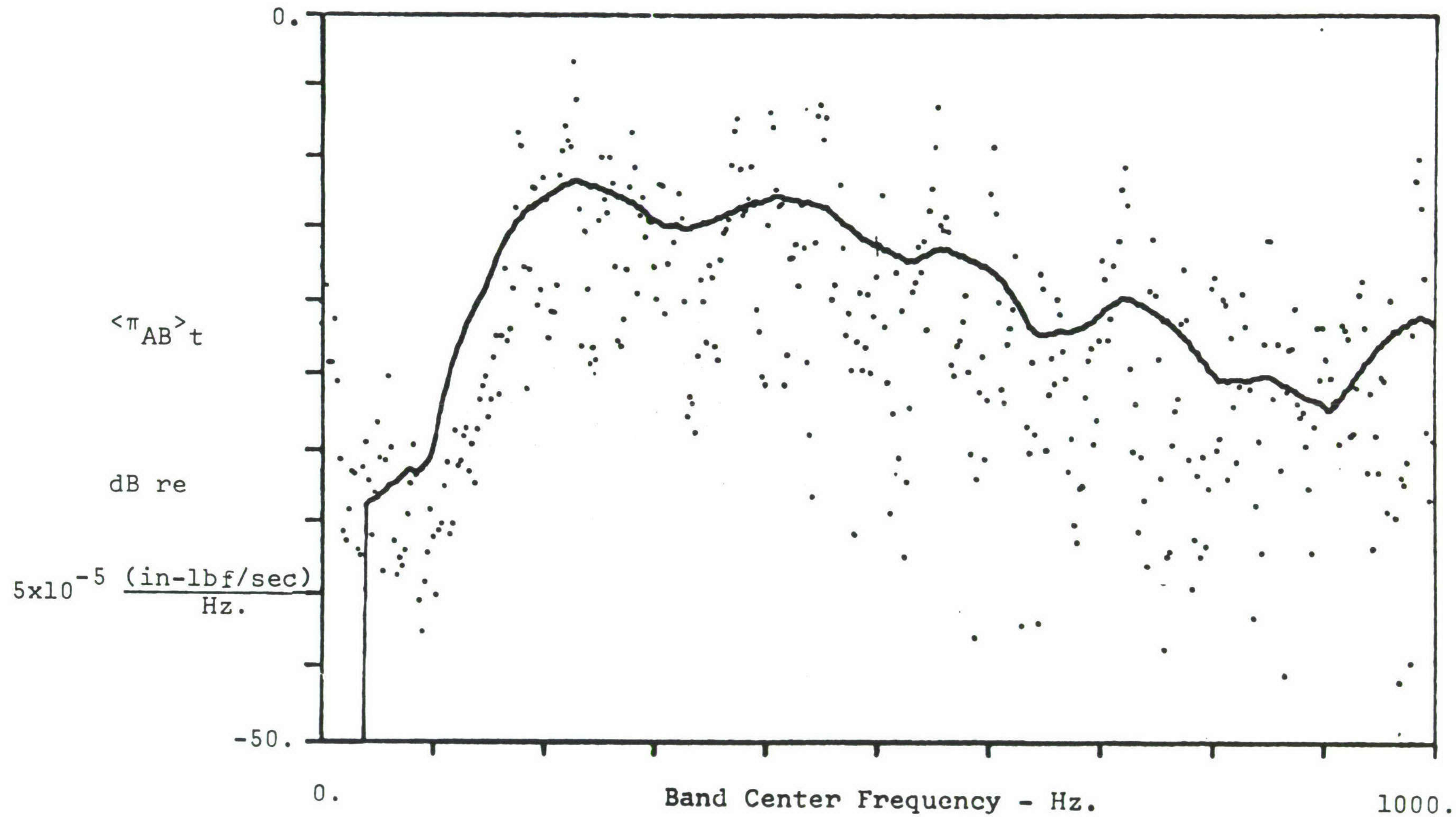

Figure 21 Spectral Density of Transmitted Power, Smoothed and Unsmoothed Versions

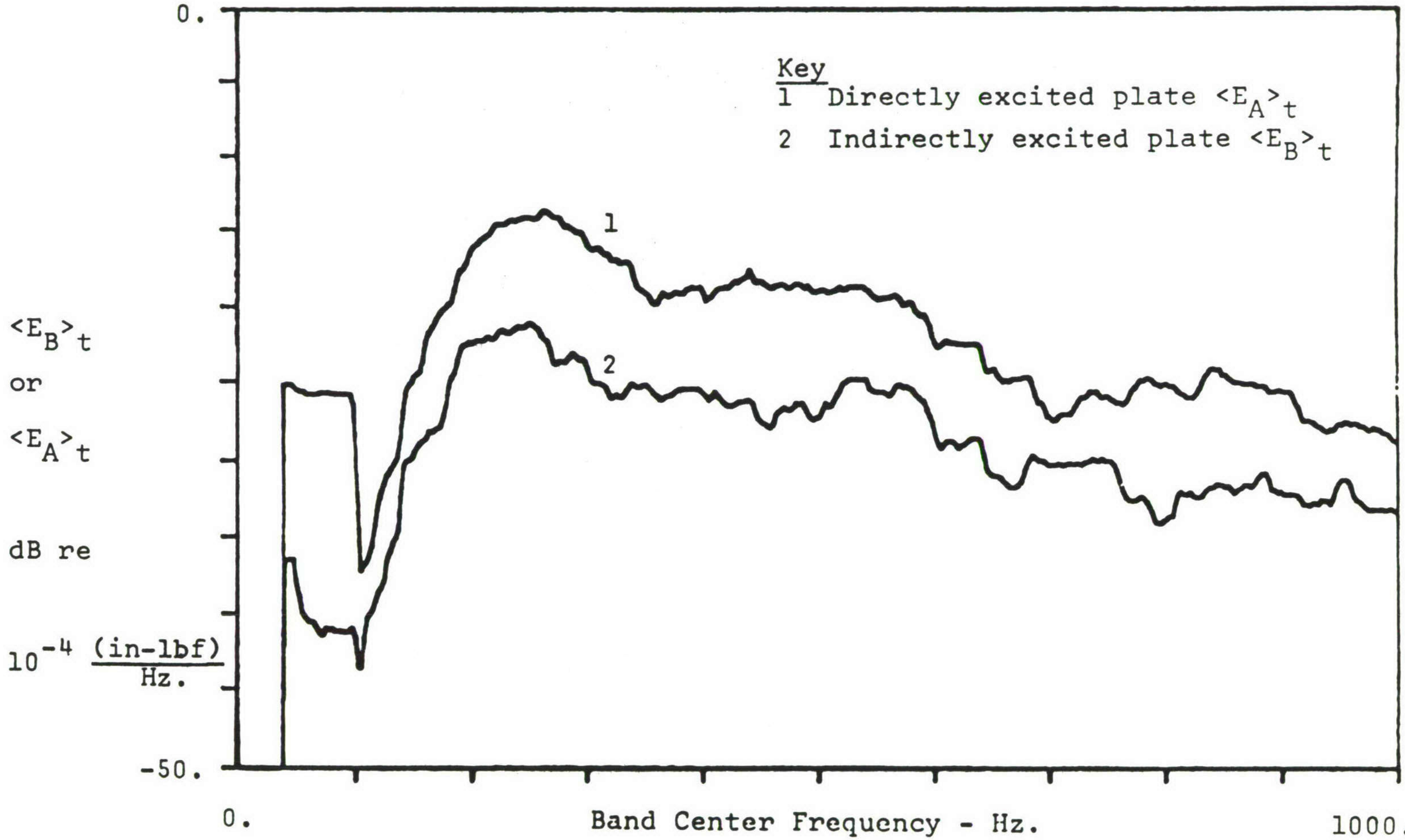

Figure 22 Smoothed Spectral Density of Total Vibration Energy.

This is particularly true with the fixed point arithmetic built into most minicomputer DFT software. Figures 21 and 22 show less than 40 dB of range, which should cause no problems.

(2) The validity of the assumption $\langle E_A \rangle_t \gg \langle E_B \rangle_t$ may be checked using Figure 22. Over most of the range above 200 Hz the ratio of $\langle E_A \rangle_t / \langle E_B \rangle_t$ is in the range of 4 to 6. Therefore, the assumption is being violated but not grossly.

4.6.4.4 Results for Lightly Coupled Case

An unsuccessful attempt was made to predict coupling loss factors for light coupling between the two plates. A light fiberglas spring of ring shape with k_c(static) = 163 lbf/in. was substituted for the aluminum coupling rod. Figure 23 shows the results. The disparity between curves 1 and 2 is caused by the fact that the actual $H_c(f)$ is much higher than $i2\pi f/k_c$ for frequencies over 200 Hz. In effect, the ring mass is not negligible and the dynamics of the coupling element are not of the simple form assumed in deriving Eq. (4.56).

Curve 3 of Figure 23 resulted from trying to remedy the above problem in a simple way. The B structure was redefined as the series combination of the spring and smaller plate. $H_B(f)$ for this combination was measured in the usual way. The combination was then considered to be attached to plate A by a spring of infinite stiffness and, thus, $H_c = 0$. The poor accuracy of $\omega_c \eta_{AB}$ computed under these assumptions is shown by curve 3. It is probably due to the fact that the coupling point to the new B structure is no longer a "typical" point and, thus, another assumption built into Eq. (4.56) is violated.

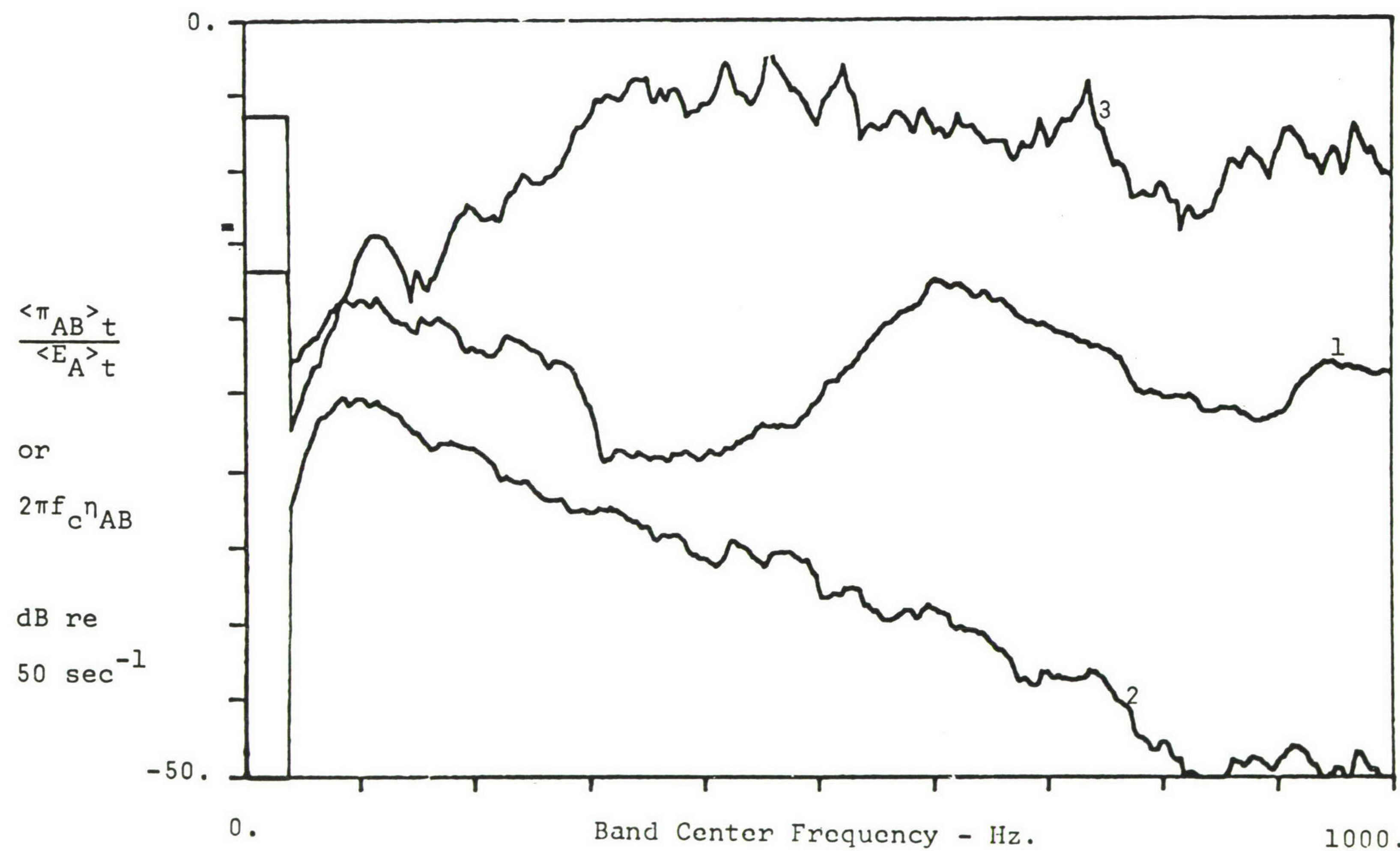

Figure 23 Normalized Transmitted Power With Light Coupling Spring

4.7 CONCLUSION

4.7.1 Summary

The motivation for study of high frequency methods in the current effort has been summarized and the method of Statistical Energy Analysis has been selected for further study. The basic principles of SEA have been reviewed within the context of analysis of airborne optical systems.

The wave transmission method for prediction of coupling loss factors has been reviewed and an alternate derivation of the principal result, without reference to waves, has been presented. It has been applied to a simple system involving two coupled plates of high modal density. Coupling loss factors have been predicted for the case of one plate only receiving direct excitation. Predictions have been made on the basis of modeling each plate either as an infinite uniform extension of the real plate or simply as an infinite uniform structure equivalent to the actual in the sense of having the same frequency-averaged mobility at the coupling point. The basic assumptions of SEA have been used to derive a simple formula for inferring r.m.s. angular response from component energy for the test case of a uniform plate. They have also been used to estimate a global internal loss factor from a single coupling point mobility measurement.

An experiment has been carried out to test various theoretical predictions described above for the case of two coupled uniform plates. Agreement with respect to component energy and transmitted power was generally encouraging, although it is suspected that some improvement in the test procedure itself may be possible. Prediction of angular response from the energy resultant was quite accurate, although it must be noted that this was essentially a demonstration case since the method used is restricted to uniform beams or plates. It was shown that excellent accuracy is possible in obtaining internal loss factor

via curve-fitting of the measured coupling-point mobility function.

At this point it is appropriate to review what has and has not been accomplished to date by the work on high frequency angular vibration. It would not be accurate to say that a first generation method has been developed for prediction of high frequency vibration, angular or otherwise. That goal, in retrospect, was simply unrealistic in view of the complexity and size of the problem relative to the resources allocated to it under this contract. What has been accomplished is, nevertheless, necessary and useful in the pursuit of that end. It has been demonstrated that angular vibration, in the form of a coarsely resolved power spectrum and associated r.m.s. value, can be predicted in a high frequency situation; i.e., one where deterministic modeling would be impractical. Wave transmission, one of the simplest methods for obtaining coupling loss factor for single point connections, has been recast in a format suitable for structures with large but finite modal densities. The new interpretation does not require modeling explicitly in terms of traveling waves and should be easier to relate to practical structures. Finally, data acquisition and processing software has been developed and used for tasks which have a high probability of occurring in the development of more general SEA methods. The usefulness of interactive digital signal processing technology for SEA modeling has thus been demonstrated. On the whole, it is the opinion of the investigators that the original decision to pursue SEA as the most promising method for high frequency prediction has been reinforced by this work.

4.7.2 Suggestions For Future Work

The work performed to date on high frequency methods has been quite useful in identifying specific areas where additional effort could be cost-effective. The ultimate goal is the

development of methods which are practical, though based on a solid theoretical foundation, for prediction of high frequency vibration of airborne optical systems. To this end, the following specific areas are suggested:

(1) It may be possible to model individual normal modes as SEA components. This seems natural when an optical system with known normal modes is connected to a complex airframe with modes which are numerous and not individually known.

(2) The basic idea of the wave transmission method might be extended to cover the case where components are connected at more than one degree of freedom. An admittance matrix formulation seems to be called for. It may be anticipated that this effort would be quite software-intensive.

(3) It might be possible to incorporate finite element results into an SEA model. An interface format suggested by work to date is the mechanical admittance function averaged with respect to frequency [22]. It is suspected on theoretical grounds that this quantity can be predicted by a finite element model which is too coarse to accurately predict individual normal modes.

(4) The coupled plate experiment suggested numerous improvements in the acquisition and processing of experimental data to obtain coupling loss factors. Several avenues were identified but not pursued due to time restrictions.

SECTION V

RELATIONSHIPS BETWEEN LINEAR AND ANGULAR VIBRATION IN AIRCRAFT STRUCTURAL COMPONENTS

Because of the predominant availability of linear vibration data as compared to that for angular vibration of structural components, the task of finding a usable and correct relationship between these two vibration quantities appears to be justifiable on the basis that we could use linear vibration data to determine angular vibrations for those portions of the aircraft structure which are of interest. It seemed like an appropriate way to attack the problem would be to investigate the behavior of the simplest two degree-of-freedom (DOF) model of a structural component, which would be a spring-supported rigid bar, subjected to a temporally random concentrated load. In this way one could begin to obtain a feel for how a linear-to-angular relationship would depend upon the load and structural parameters (i.e. mass, stiffness, geometry) for a simple system. The next step was to proceed to more complex structural components and to determine linear-to-angular relationships for them as a function of position on the structure. This was done for a beam with simple-support boundary conditions, a plate with simple-support boundaries, and a beam with free-free boundary conditions all subjected to temporally random, spatially deterministic loading conditions. Some of the results of this study are presented here. However, the reader is referred to Reference [19] for the detailed results. In order to examine a structural form somewhat more representative of an aircraft structural component, a NASTRAN analysis of a stiffened curved panel subjected to a concentrated temporally random load was completed to round out the effort.

5.1 LINEAR-TO-ANGULAR RELATIONSHIP OF SPRING-SUPPORTED RIGID BAR SUBJECTED TO TEMPORALLY RANDOM CONCENTRATED LOAD

The simplest structural system possessing both linear and angular degrees of freedom is a spring-supported rigid bar as pictured below in Figure 24.

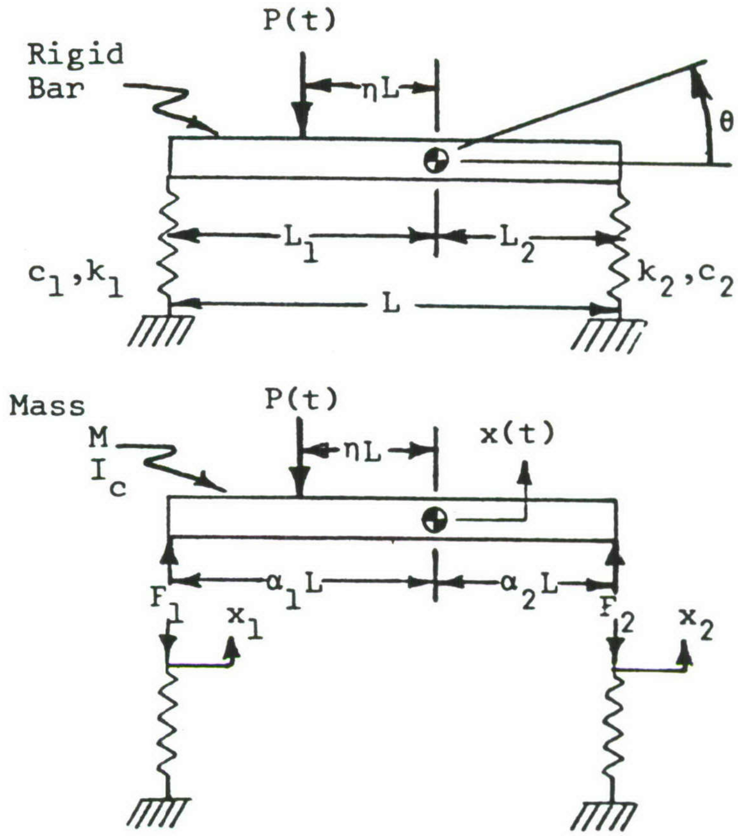

Figure 24 Spring Supported Rigid Bar

The spring and damping constants are defined as follows:

$$k_1 = k \quad ; \quad c_1 = c$$

$$k_2 = \gamma k \quad ; \quad c_2 = \beta c \tag{5.1}$$

where $0 < \beta$ and $0 < \gamma$. The assumptions made in the subsequent analysis of this structure are (1) no gravity forces are present, and (2) angular displacements are small such that $\sin\theta \simeq \theta$.

The differential equations of motion governing this system may be written in matrix form as

$$\begin{bmatrix} M & 0 \\ 0 & \frac{I_c}{L^2} \end{bmatrix} \begin{bmatrix} \ddot{x} \\ \ddot{y} \end{bmatrix} + c \begin{bmatrix} (1+\beta) & (\beta\alpha_2-\alpha_1) \\ (\beta\alpha_2-\alpha_1) & (\alpha_1{}^2+\beta\alpha_2{}^2) \end{bmatrix} \begin{bmatrix} \dot{x} \\ \dot{y} \end{bmatrix}$$

$$+ k \begin{bmatrix} (1+\gamma) & (\gamma\alpha_2-\alpha_1) \\ (\gamma\alpha_2-\alpha_1) & (\alpha_1{}^2+\gamma\alpha_2{}^2) \end{bmatrix} \begin{bmatrix} x \\ y \end{bmatrix} = \begin{bmatrix} -P \\ -P\eta \end{bmatrix} \tag{5.2}$$

where $y = L\theta$. In order to facilitate the solution of Eq. (5.2) one may employ the linear coordinate transformation from physical to normal coordinates

$$\begin{bmatrix} x \\ y \end{bmatrix} = \begin{bmatrix} u_{11} & u_{12} \\ u_{21} & u_{22} \end{bmatrix} \begin{bmatrix} q_1 \\ q_2 \end{bmatrix} \tag{5.3}$$

which will uncouple the system. In normal coordinates, the set of D.E.'s Eq. (5.2) will take on the form

$$\begin{bmatrix} 1 & 0 \\ 0 & 1 \end{bmatrix} \begin{bmatrix} \ddot{q}_1 \\ \ddot{q}_2 \end{bmatrix} + \begin{bmatrix} C_1 & 0 \\ 0 & C_2 \end{bmatrix} \begin{bmatrix} \dot{q}_1 \\ \dot{q}_2 \end{bmatrix} + \begin{bmatrix} K_1 & 0 \\ 0 & K_2 \end{bmatrix} \begin{bmatrix} q_1 \\ q_2 \end{bmatrix} = \begin{bmatrix} u_{11} & u_{21} \\ u_{12} & u_{22} \end{bmatrix} \begin{bmatrix} -P \\ -P\eta \end{bmatrix} \tag{5.4}$$

If the following substitutions are made

$$2\tilde{\beta}_1=C_1;\ 2\tilde{\beta}_2=C_2;\ \text{and}\ \tilde{\omega}_1{}^2=K_1;\ \tilde{\omega}_2{}^2=K_2 \tag{5.5a}$$

and

$$a_1= -(u_{11} + \eta u_{21});\quad a_2= -(u_{12} + \eta u_{22}) \tag{5.5b}$$

Equation (5.4) becomes

$$\ddot{q}_1 + 2\tilde{\beta}_1\dot{q}_1 + \tilde{\omega}_1{}^2 q_1 = a_1 P(t) \tag{5.6}$$

$$\ddot{q}_2 + 2\tilde{\beta}_2\dot{q}_2 + \tilde{\omega}_2{}^2 q_2 = a_2 P(t) \tag{5.7}$$

for which the solutions are

$$q_1(t) = a_1\int_0^{\infty} h_1(\phi)P(t-\phi)d\phi \tag{5.8}$$

$$q_2(t) = a_2\int_0^{\infty} h_2(\phi)P(t-\phi)d\phi \tag{5.9}$$

where

$$h_1(t) = \frac{e^{-\tilde{\beta}_1 t}}{\tilde{\omega}_1'} \sin \tilde{\omega}_1' t ; \quad h_2(t) = \frac{e^{-\tilde{\beta}_2 t}}{\tilde{\omega}_2'} \sin \tilde{\omega}_2' t$$

$$\text{and} \quad \tilde{\omega}_1' = \sqrt{\tilde{\omega}_1^{\,2} - \tilde{\beta}_1^{\,2}} \quad ; \quad \tilde{\omega}_2' = \sqrt{\tilde{\omega}_2^{\,2} - \tilde{\beta}_2^{\,2}} \tag{5.10}$$

The next question to answer is what form x and y will take if P(t) is a random function (stationary and ergodic). At this point one might ask about making $\eta = \eta(t)$ thereby allowing the load to be random as to its point of application as well as its magnitude; however, this will not be done here.

Working with x(t) first and substituting Eqs. (5.8) and (5.9) in Eq. (5.3) gives

$$x(t) = \int_0^{\infty} [u_{11}a_1h_1(\phi) + u_{12}a_2h_2(\phi)]P(t-\phi)d\phi \tag{5.11}$$

Since P(t) is random and is usually assumed to have a Gaussian distribution about its mean value, x(t) will also be Gaussian, if our structural system is linear. One can calculate the auto correlation of x(t) then to be

$$\begin{aligned} E[x(t)x(t+\tau)] = E\Big[\int_0^{\infty}\int_0^{\infty} &\{u_{11}a_1h_1(\phi_1) + u_{12}a_2h_2(\phi_1)\}\cdot \\ \cdot\{u_{11}a_1h_1(\phi_2) + u_{12}a_2h_2(\phi_2)\}&P(t-\phi_1)P(t+\tau-\phi_2)d\phi_1 d\phi_2\Big] \end{aligned} \tag{5.12}$$

which can be written

$$R_x(\tau) = \int_0^\infty\int_0^\infty R_p(\tau+\phi_1-\phi_2)\{u_{11}{}^2 a_1{}^2 h_1(\phi_1)h_1(\phi_2)$$

$$+ u_{11}a_1u_{12}a_2[h_1(\phi_1)h_2(\phi_2) + h_1(\phi_2)h_2(\phi_1)]$$

$$+ u_{12}{}^2 a_2{}^2 h_2(\phi_1)h_2(\phi_2)\}d\phi_1 d\phi_2 \tag{5.13}$$

In terms of spectral densities, the Wiener-Khintchine relation states that

$$S_x(\omega) = \frac{1}{2\pi}\int_{-\infty}^{\infty} R_x(\tau)e^{-i\omega\tau}d\tau \tag{5.14}$$

Substituting Eq. (5.13) for $R_x(\tau)$ into Eq. (5.14) and integrating yields

$$\begin{aligned} S_x(\omega) = {} & [u_{11}{}^2 a_1{}^2 |H_1(\omega)|^2 + u_{12}{}^2 a_2{}^2 |H_2(\omega)|^2]S_p(\omega) \\ & + u_{11}a_1u_{12}a_2[H_1(\omega)H_2{}^*(\omega) + H_2(\omega)H_1{}^*(\omega)]S_p(\omega) \end{aligned} \tag{5.15}$$

where

$$H_1(\omega) = \frac{1}{\tilde{\omega}_1{}^2-\omega^2+2i\tilde{\beta}_1\omega} \quad ; \quad H_2(\omega) = \frac{1}{\tilde{\omega}_2{}^2-\omega^2+2i\tilde{\beta}_2\omega} \tag{5.16}$$

and $H_1{}^*(\omega)$ and $H_2{}^*(\omega)$ are the complex conjugates of $H_1(\omega)$ and $H_2(\omega)$. Similarly, one would find

$$\begin{aligned} S_y(\omega) = {} & [u_{21}{}^2 a_1{}^2 |H_1(\omega)|^2 + u_{22}a_2{}^2 |H_2(\omega)|^2]S_p(\omega) \\ & + u_{21}a_1u_{22}a_2[H_1(\omega)H_2{}^*(\omega) + H_2(\omega)H_1{}^*(\omega)]S_p(\omega) \end{aligned} \tag{5.17}$$

For white noise forcing with constant spectral density, $S_p(\omega) = S_{po}$, the next step would be to determine the mean square responses

$$\overline{x^2} = \int_{-\infty}^{\infty} S_x(\omega)d\omega \tag{5.18}$$

$$\overline{y^2} = \int_{-\infty}^{\infty} S_y(\omega)d\omega \tag{5.19}$$

If one lets

$$\hat{H}_{11} = \int_{-\infty}^{\infty} |H_1(\omega)|^2 d\omega \quad ; \quad \hat{H}_{12} = \int_{-\infty}^{\infty} H_1(\omega)H_2^*(\omega)d\omega$$

$$\hat{H}_{21} = \int_{-\infty}^{\infty} H_2(\omega)H_1^*(\omega)d\omega; \quad \hat{H}_{22} = \int_{-\infty}^{\infty} |H_2(\omega)|^2 d\omega \tag{5.20}$$

Equations (5.18) and (5.19) become

$$\overline{x^2} = [u_{11}{}^2 a_1{}^2 \hat{H}_{11} + u_{11}a_1u_{12}a_2(\hat{H}_{12}+\hat{H}_{21}) + u_{12}{}^2 a_2{}^2 \hat{H}_{22}]S_{po} \tag{5.21}$$

$$\overline{y^2} = [u_{21}{}^2 a_1{}^2 \hat{H}_{11} + u_{21}a_1u_{22}a_2(\hat{H}_{12}+\hat{H}_{21}) + u_{22}{}^2 a_2{}^2 \hat{H}_{22}]S_{po} \tag{5.22}$$

Taking the ratio of mean square angular to mean square linear displacement, one obtains

$$\frac{y_{rms}}{x_{rms}} = \sqrt{\frac{u_{21}{}^2 a_1{}^2 \hat{H}_{11} + u_{21}u_{22}a_1a_2(\hat{H}_{12}+\hat{H}_{21}) + u_{22}{}^2 a_2{}^2 \hat{H}_{22}}{u_{11}{}^2 a_1{}^2 \hat{H}_{11} + u_{11}u_{12}a_1a_2(\hat{H}_{12}+\hat{H}_{21}) + u_{12}{}^2 a_2{}^2 \hat{H}_{22}}} \tag{5.23}$$

where

$$\hat{H}_{11} = \pi/C_1K_1 \quad ; \quad \hat{H}_{22} = \pi/C_2K_2 \tag{5.24}$$

$$\hat{H}_{12} = 2\pi(C_1+C_2)/\{[K_1-K_2-\tfrac{1}{2}C_1(C_1+C_2)]^2+(C_1+C_2)^2(K_1-\frac{C_1{}^2}{4})\} \tag{5.25}$$

$$\hat{H}_{21} = 2\pi(C_1+C_2)/\{[K_2-K_1-\tfrac{1}{2}C_2(C_1+C_2)]^2+(C_1+C_2)^2(K_2-\frac{C_2{}^2}{4})\} \tag{5.26}$$

Calculating the coefficients of $\hat{H}_{ij}$ in terms of M_1 and M_2, one arrives at

$$u_{21}{}^2 a_1{}^2 = \frac{1}{4M_2}\left[\left(\frac{1}{M_1} - \frac{1}{M_2}\right)\frac{1}{1+a^2} + 2\left(\frac{\eta}{\sqrt{M_1M_2}}\sqrt{\frac{1}{1+a^2}} + \frac{1}{M_2}\right)\left(1-\sqrt{1-\frac{1}{1+a^2}}\right)\right] \tag{5.27}$$

$$u_{21}u_{22}a_1a_2 = \frac{1}{4M_2}\left[\left(\frac{1}{M_1} + \frac{\eta^2}{M_2}\right)\frac{1}{1+a^2} + \frac{2\eta}{M_1M_2}\sqrt{\frac{1}{1+a^2}}\sqrt{1-\frac{1}{1+a^2}}\right] \tag{5.28}$$

$$u_{22}^2\, a_2{}^2 = \frac{1}{4M_2}\left[\left(\frac{1}{M_1} - \frac{1}{M_2}\right)\frac{1}{1+a^2} - 2\left(\frac{\eta}{\sqrt{M_1M_2}}\sqrt{\frac{1}{1+a^2}} - \frac{1}{M_2}\right)\left(1+\sqrt{1-\frac{1}{1+a^2}}\right)\right] \tag{5.29}$$

$$u_{11}^2 a_1^2 = \frac{1}{4M_1}\left[\left(\frac{1}{M_2} - \frac{1}{M_1}\right)\frac{1}{1+a^2} + 2\left(\frac{\eta}{\sqrt{M_1M_2}}\sqrt{\frac{1}{1+a^2}} + \frac{1}{M_1}\right)\left(1 + \sqrt{1-\frac{1}{1+a^2}}\right)\right] \tag{5.30}$$

$$u_{11}u_{12}a_1a_2 = -\frac{1}{4M_1}\left[\left(\frac{1}{M_1} + \frac{\eta^2}{M_2}\right)\frac{1}{1+a^2} + \frac{2\eta}{\sqrt{M_1M_2}}\sqrt{1-\frac{1}{1+a^2}}\right] \tag{5.31}$$

$$u_{12}{}^2 a_2{}^2 = \frac{1}{4M_1}\left[\left(\frac{1}{M_2}-\frac{1}{M_1}\right)\frac{1}{1+a^2} - 2\left(\frac{\eta}{\sqrt{M_1M_2}}\sqrt{\frac{1}{1+a^2}} - \frac{1}{M_1}\right)\left(1-\sqrt{1-\frac{1}{1+a^2}}\right)\right] \tag{5.32}$$

where

$$a = \frac{1}{2(\gamma\alpha_2 - \alpha_1)}\left(\alpha_1^2 + \gamma\alpha_2^2 - \frac{M_2}{M_1}(1+\gamma)\right) \tag{5.33}$$

and $M_1 = M$; $M_2 = I_c/L^2$.

If one assumes that the damping is proportional, then

$C_1 = \frac{\Lambda}{k} K_1$ and $C_2 = \frac{\Lambda}{k} K_2$ (Λ a constant)

where

$$K_1 = \frac{\tilde{k}_1}{2M_1}\left(1+\sqrt{1-\frac{1}{1+a^2}}\right) + \frac{\tilde{k}_2}{\sqrt{M_1M_2}}\sqrt{\frac{1}{1+a^2}} + \frac{\tilde{k}_3}{2M_2}\left(1-\sqrt{1-\frac{1}{1+a^2}}\right) \quad (5.34)$$

$$K_2 = \frac{\tilde{k}_1}{2M_1}\left(1-\sqrt{1-\frac{1}{1+a^2}}\right) - \frac{\tilde{k}_2}{\sqrt{M_1M_2}}\sqrt{\frac{1}{1+a^2}} + \frac{\tilde{k}_3}{2M_2}\left(1+\sqrt{1-\frac{1}{1+a^2}}\right) \quad (5.35)$$

and

$$\begin{aligned}\tilde{k}_1 &= (1+\gamma)k\\ \tilde{k}_2 &= (\gamma\alpha_2 - \alpha_1)k\\ \tilde{k}_3 &= (\alpha_1^2 + \gamma\alpha_2^2)k\end{aligned} \quad (5.36)$$

There is a special case which one might examine. When $\gamma = \frac{\alpha_1}{\alpha_2}$, which implies that $\beta = \frac{\alpha_1}{\alpha_2}$ for proportional damping, the DE Eq. (5.2) automatically uncouple; and the elements of the transformation matrix reduce to:

$$u_{11} = \sqrt{1/M_1} \quad ; \quad u_{22} = \sqrt{1/M_2} \quad ; \quad u_{12} = u_{21} = 0 \quad (5.37)$$

Also

$$a_1 = -u_{11} \quad ; \quad a_2 = -\eta u_{22} \quad (5.38)$$

$$\hat{H}_{11} = \pi/C_1K_1 = (\pi/\Lambda k)(1 + \alpha_1/\alpha_2)^2/M^2 \quad (5.39)$$

$$\hat{H}_{22} = \pi/C_2K_2 = (\pi/\Lambda k)(\alpha_1^2 + \alpha_1\alpha_2)^2\, L^4/I_c^2 \quad (5.40)$$

Equation (5.23) then reduces to

$$\frac{y_{rms}}{x_{rms}} = \frac{\eta ML^2}{I_c}\sqrt{\frac{I_c^2(1+\alpha_1/\alpha_2)^2}{(\alpha_1^2+\alpha_1\alpha_2)^2L^4M^2}} = \frac{\eta(1+\alpha_1/\alpha_2)}{\alpha_1\alpha_2(1+\alpha_1/\alpha_2)} \quad (5.41)$$

or

$$\frac{y_{rms}}{x_{rms}} = \frac{\eta}{\alpha_1\alpha_2} \quad ; \quad y_{rms} = L\theta_{rms} \quad (5.42)$$

for the condition $\gamma = \frac{\alpha_1}{\alpha_2}$, which physically represents that case where the spring and damping forces at each end of the bar exactly match the translational inertia reactions at those points.

One might observe that y_{rms}/x_{rms} may vary between zero and a finite number depending upon the location of P. Equation (5.42) also portends a rather significant variance depending upon the values for α_1 and α_2. The occurrence of such large variances would suggest that spatially averaged values for random locations of P(t) are subject to question.

5.2 BEHAVIOR OF BEAMS SUBJECTED TO TEMPORALLY RANDOM LOADING CONDITIONS

Lee and Whaley had already laid some of the ground work for beams in their paper [23]. One of the major analytical problems with more complex structures is that the loading conditions can be random in space as well as random in time. Lee and Whaley assumed that load q(x) on the beam was random in space such that the Fourier coefficient q_n was completely uncorrelated with q_k, i.e. $\langle q_n q_k \rangle = o$ for $n \neq k$, which reduced the double summations to single summations (and provided one way to circumvent spatial randomness). An equally realistic approach seemed to be that of assuming that the load would be deterministic in space but random in time, since most experimental investigations·of angular vibrations in structures would have to proceed on that path anyway.

In order to assess the effect of various generalized coordinate loading factors q_n, two spatially deterministic, temporally random loading conditions on a beam with simple support were considered and the spatial variation of the ratio of r.m.s. angular to r.m.s. linear displacement along the beam was examined. This spatial variation was compared with Lee and Whaley's "beam averaged r.m.s. amplitudes."

The derivation of the ratio of r.m.s. angular to r.m.s. linear displacement along the beam has been presented in detail in Reference [19], the Phase II Interim report on this contract. For white noise forcing with constant spectral density, this ratio was found to be

$$\frac{\theta_{rms}}{y_{rms}} = \frac{\pi}{L}\sqrt{\frac{\sum\limits_n \sum\limits_k q_n q_k I_{nk} nk \cos\frac{n\pi x}{L} \cos\frac{k\pi x}{L}}{\sum\limits_n \sum\limits_k q_n q_k I_{nk} \sin\frac{n\pi x}{L} \sin\frac{k\pi x}{L}}} \tag{5.43}$$

where

$$I_{nk} = 8\pi\beta/[(\omega_n^2-\omega_k^2-4\beta^2)^2 + (4\beta\omega_n')^2]$$

and $$\omega_n' = \sqrt{\omega_n^2 - \beta^2} \quad ; \quad \omega_n^2 = n^4 \frac{EI\pi^4}{mL^4} \tag{5.44}$$

In order to obtain the spatial variation in θ_{rms}/y_{rms}, the following parameters for the beam were used:

$L = 100$ in. $\rho = 0.10$ lbm/in.^{3}

$E = 10 \times 10^6$ psi. $g = 386.04$ lbm-in/lbf-sec.^{2}

$I = 5.00$ in.^{4} $A = 1.25$ in.^{2}

$\beta = 38.78$ sec.$^{-1}$

It was decided to subject the beam to two spatially determinant loading conditions: (a) The first was

$$q(x) = q_o \tag{5.45}$$

which when represented by Fourier sine series takes on the form

$$q(x) = \sum_{n=1}^{\infty} q_n \sin \frac{n\pi x}{L} \quad \text{where} \quad q_n = \frac{2q_o}{n\pi}(1-\cos n\pi) \tag{5.46}$$

(b) The second loading condition was given by

$$q(x) = q_o \sum_{n=1,3,5}^{\infty} \sin \frac{n\pi x}{L} \tag{5.47}$$

A plot of Eq. (5.43) under these two loading conditions is shown in Figure 25, where $k_{max} = n_{max} = 7$.

As a comparison, Lee and Whaley propose a spatially averaged value of

$\theta_{rms}/y_{rms} = 1.17\ \pi/L = 0.0367$ in.$^{-1}$ which is also shown on Figure 25.

Now consider the special case of a load condition which contains only a single harmonic

$$q(x) = q_{n_o} \sin \frac{n_o \pi x}{L} \tag{5.48}$$

Eq. (5.43) would then become

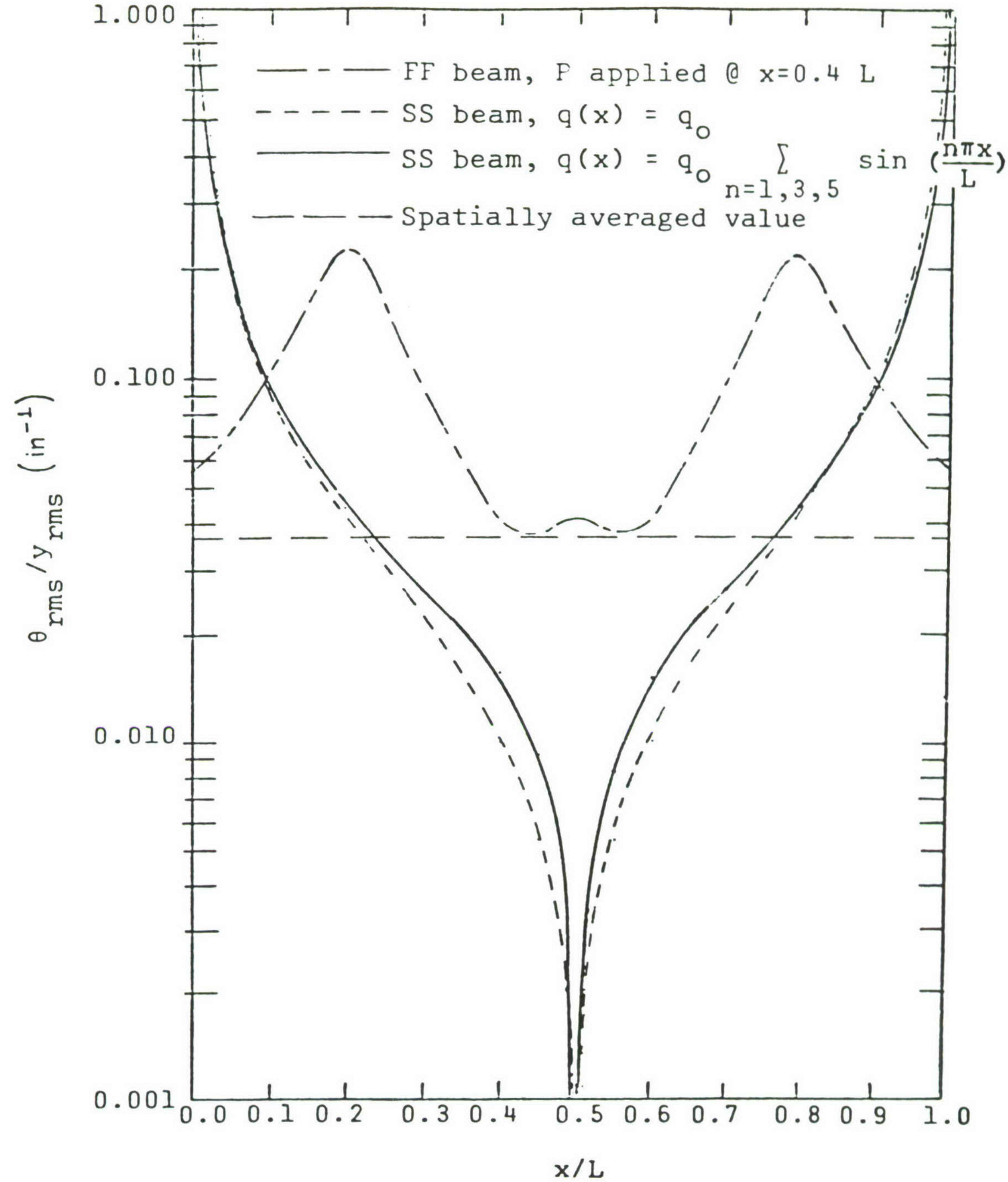

Figure 25 Plot of θ_{rms}/y_{rms} for Simply-Supported and Free-Free Beams Subjected to Temporally Random Loads

$$\frac{\theta_{rms}}{y_{rms}} = \frac{n_o \pi}{L} \cot \frac{n_o \pi x}{L} \tag{5.49}$$

For this loading condition, one sees that θ_{rms}/y_{rms} varies between $\pm\infty$.

As one studies the results of considering the previous loading conditions on a beam with simple support, one may conclude that any load which is symmetrically distributed with respect to the center of the beam will have a variation of θ_{rms}/y_{rms} between, at least, 0 and $+\infty$. Here again, the use of a spatially averaged θ_{rms}/y_{rms} value is subject to question; but, in this case the support condition of $y(o) = y(L) = o$ and the spatial symmetry of loading are the main source of the extreme variance. For this reason it was thought that a beam in the free-free vibration condition would furnish a more representative variation of θ_{rms}/y_{rms} relative to beam station in comparison to aircraft structural components, which do not normally have simple-support conditions.

One may assess the effects of support conditions by considering the beam in the free-free condition. However, since the panels or beams in an aircraft structure are elastically supported, a question may be raised as to how applicable such analytical results based on free-free conditions might be (notwithstanding the whole airplane which could be in the free-free condition). The justification for using free-free conditions is that the variation in the r.m.s. angular to r.m.s. linear displacement ratio along the beam or over the plate surface is more representative of actual aircraft structural components. Even though there will be discrepancies at the boundaries, they are far less for free-free solutions than they will be for solutions based on simple-support conditions.

For a free-free beam subjected to a concentrated load, P, at any point, x=a, the θ_{rms}/y_{rms} ratio is obtained in Reference [19] as

$$\frac{\theta_{rms}}{y_{rms}} = \sqrt{\frac{\sum\limits_{nk}\sum q_n q_k \Phi_n' \Phi_k' I_{nk}}{\sum\limits_{nk}\sum q_n q_k \Phi_n \Phi_k I_{nk}}} \tag{5.50}$$

where

$$q_n = \frac{P}{L}[\cos\frac{a\lambda_n}{L} + \text{Cosh}\frac{a\lambda_n}{L} + \alpha_n(\sin\frac{a\lambda_n}{L} + \text{Sinh}\frac{a\lambda_n}{L})] \tag{5.51}$$

$$\Phi_n(x) = \cos\frac{\lambda_n x}{L} + \text{Cosh}\frac{\lambda_n x}{L} + \alpha_n(\sin\frac{\lambda_n x}{L} + \text{Sinh}\frac{\lambda_n x}{L}) \tag{5.52}$$

$$\Phi_n'(x) = \frac{\lambda_n}{L}[-\sin\frac{\lambda_n x}{L} + \text{Sinh}\frac{\lambda_n x}{L} + \alpha_n(\cos\frac{\lambda_n x}{L} + \text{Cosh}\frac{\lambda_n x}{L})] \tag{5.53}$$

and

$$\alpha_n = \frac{\sin\lambda_n + \text{Sinh}\lambda_n}{\cos\lambda_n - \text{Cosh}\lambda_n} \tag{5.54}$$

I_{nk} may be expressed in the form

$$I_{nk} = 8\pi\beta/[\omega_n^{\,2}-\omega_k^{\,2})^2 + 8\beta^2(\omega_n^{\,2}+\omega_k^{\,2})] \tag{5.55}$$

where

$$\omega_n^{\,2} = \frac{\lambda_n^4}{L^4}\cdot\frac{EI}{m} \tag{5.56}$$

and λ_n represents the roots of the frequency equation

$$1 = \text{Cosh}\lambda_n \cos\lambda_n \tag{5.57}$$

The ratios of angular r.m.s. to linear r.m.s., Eq. (5.50) at different stations along the beam, have been calculated for the beam properties given previously and are presented in Table 3 is $k_{max} = n_{max} = 1,2,3,4$, and 6. This ratio is $k_{max} = n_{max}$ is also shown on Figure 25.

As one examines the θ_{rms}/y_{rms} ratios in Table 3 for the one-term approximation one sees that they get quite large as the node points for the first free-free mode shape are approached. With the additional higher frequency mode shapes

TABLE 3

θ_{rms}/y_{rms} FOR FREE-FREE BEAM SUBJECT TO CONCENTRATED LOAD

(a/L = 0.4)

x/L	θ_{rms}/y_{rms} $n_{max}=k_{max}=1$	θ_{rms}/y_{rms} $n_{max}=k_{max}=2$	θ_{rms}/y_{rms} $n_{max}=k_{max}=3$	θ_{rms}/y_{rms} $n_{max}=k_{max}=4$	θ_{rms}/y_{rms} $n_{max}=k_{max}=6$
0	0.0465	0.0507	0.0518	0.0550	0.0563
0.10	0.0851	0.0961	0.0981	0.1014	0.1014
0.15	0.1415	0.1568	0.1562	0.1504	0.1506
0.16	0.1630	0.1766	0.1741	0.1645	0.1655
0.17	0.1922	0.1999	0.1942	0.1799	0.1820
0.18	0.2345	0.2258	0.2152	0.1961	0.1993
0.19	0.3013	0.2514	0.2342	0.2111	0.2153
0.20	0.4230	0.2697	0.2461	0.2222	0.2267
0.21	0.7159	0.2725	0.2460	0.2262	0.2299
* 0.22	2.4141	0.2572	0.2332	0.2215	0.2235
0.23	1.7015	0.2304	0.2121	0.2090	0.2091
0.24	0.6199	0.2007	0.1833	0.1919	0.1906
0.25	0.3750	0.1733	0.1655	0.1732	0.1712
0.30	0.1166	0.0898	0.0913	0.0992	0.0998
0.35	0.0603	0.0551	0.0583	0.0595	0.0627
0.40	0.0332	0.0389	0.0414	0.0409	0.0416
0.45	0.0151	0.0317	0.0325	0.0374	0.0383
0.50	0.0000	0.0299	0.0296	0.0385	0.0414
0.55	0.0151	0.0321	0.0329	0.0379	0.0387
0.60	0.0332	0.0394	0.0421	0.0415	0.0423
0.65	0.0603	0.0558	0.0591	0.0602	0.0634
0.70	0.1166	0.0906	0.0921	0.0999	0.1005
0.75	0.3749	0.1739	0.1654	0.1734	0.1712
0.76	0.6197	0.2009	0.1876	0.1913	0.1901
0.77	1.6999	0.2297	0.2105	0.2077	0.2079
* 0.78	2.4173	0.2551	0.2305	0.2193	0.2213
0.79	0.7161	0.2689	0.2422	0.2234	0.2271
0.80	0.4231	0.2654	0.2418	0.2191	0.2235
0.81	0.3014	0.2472	0.2302	0.2081	0.2123
0.82	0.2346	0.2223	0.2418	0.1934	0.1967
0.83	0.1922	0.1971	0.1915	0.1778	0.1799
0.84	0.1630	0.1745	0.1721	0.1628	0.1638
0.85	0.1415	0.1552	0.1547	0.1491	0.1493
0.90	0.0851	0.0956	0.0976	0.1010	0.1010
1.00	0.0465	0.0506	0.0518	0.0550	0.0564

considered, the extreme variation in θ_{rms}/y_{rms} as a function of x/L is attenuated, but the fundamental mode shape still retains a significant influence on the shape of the curve. Nevertheless, the variation between the maximum and minimum values of θ_{rms}/y_{rms} along the beam length is finite but of sufficient magnitude to imply that a spatially averaged value could have significant error.

5.3 NASTRAN ANALYSIS OF STIFFENED CURVED PANEL SUBJECTED TO TEMPORALLY RANDOM CONCENTRATED LOAD

In order to assess the linear-to-angular relationship in a structural component of a somewhat more complex geometry, it was decided to analyze a stiffened curved panel. A NASTRAN finite element model of the curved panel was developed and is shown in Figure 26. The model consists of 726 degrees of freedom, 100 quadrilateral bending elements, and 30 beam elements. This panel was assumed to be in the free-free condition with the random concentrated load applied at grid point station 406. The response of the curved panel was evaluated for a 20-2560 Hz. band width and for the seven octaves in between as follows:

(a) 20 - 40 Hz
(b) 40 - 80 Hz
(c) 80 - 160 Hz
(d) 160 - 320 Hz
(e) 320 - 640 Hz
(f) 640 - 1280 Hz
(g) 1280 - 2560 Hz

The output of the NASTRAN analysis included the following quantities:

(a) w_{rrms} - temporal average of displacement normal to plate

(b) $\theta_{\theta rms}$ - temporal average of angular displacement about θ-axis

(c) θ_{zrms} - temporal average of angular displacement about z-axis

at each of the following sets of grid points:

(a) 106, 206, 306, ... 1106
(b) 401, 402, 403, ... 411
(c) 104, 204, 304, ... 1104

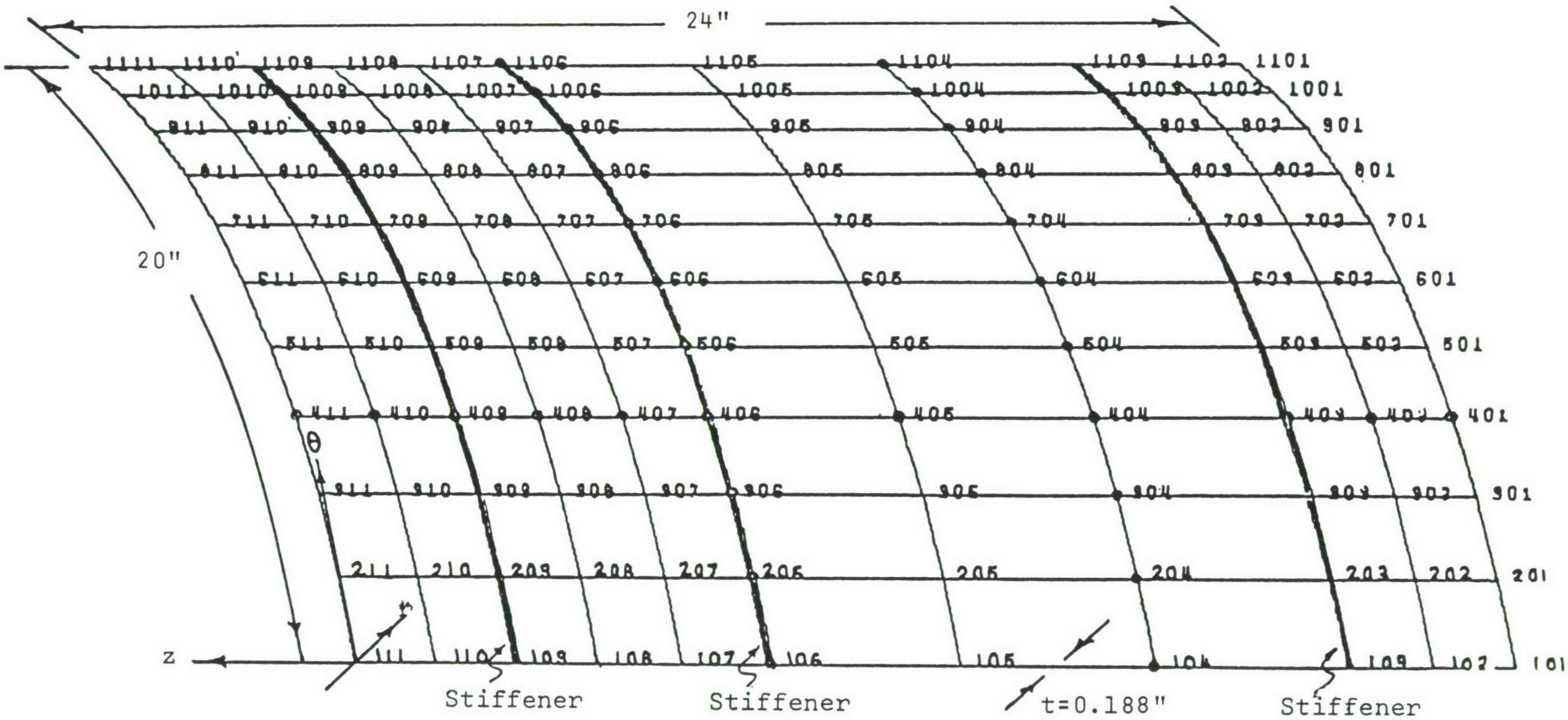

Figure 26 NASTRAN Model of Stiffened Curved Panel

Figure 27 shows the ratio of RMS total resultant angular displacement to RMS linear displacement vs. grid point station for 20-2560 Hz. frequency band for the bare curved panel. In this figure the straight lines plotted are the <u>spatial average</u> as represented by the quantity

$$\frac{\sum_{106}^{1106}\sqrt{\int_{\omega_1}^{\omega_2} S_{\theta_\theta}\, d\omega + \int_{\omega_1}^{\omega_2} S_{\theta_z}\, d\omega}}{\sum_{106}^{1106}\sqrt{\int_{\omega_1}^{\omega_2} S_{w_r}\, d\omega}} \quad \text{for Stations 106 to 1106} \tag{5.58}$$

where

$$\omega_1 = 20 \text{ Hz}$$
$$\omega_2 = 2560 \text{ Hz} \tag{5.59}$$

and

$$\overline{w_r^2} = \int_{\omega_1}^{\omega_2} S_{w_r}\, d\omega \quad ; \quad \overline{\theta_\theta^2} = \int_{\omega_1}^{\omega_2} S_{\theta_\theta}\, d\omega \quad ; \quad \overline{\theta_z^2} = \int_{\omega_1}^{\omega_2} S_{\theta_z}\, d\omega \tag{5.60}$$

This particular method of averaging corresponds to that of Lee and Whaley in their aforementioned report.

Figure 28 presents the ratio of RMS angular displacement component to spatially averaged RMS linear displacement vs. grid point station for 20-2560 Hz. for the curved panel. The straight lines plotted are the spatial averages as given by the expressions

$$\frac{\theta_{\theta rms_{avg}}}{w_{rrms_{avg}}} = \frac{\sum_{106}^{1106}\sqrt{\int_{\omega_1}^{\omega_2} S_{\theta_\theta}\, d\omega}}{\sum_{106}^{1106}\sqrt{\int_{\omega_1}^{\omega_2} S_{w_r}\, d\omega}} \tag{5.61}$$

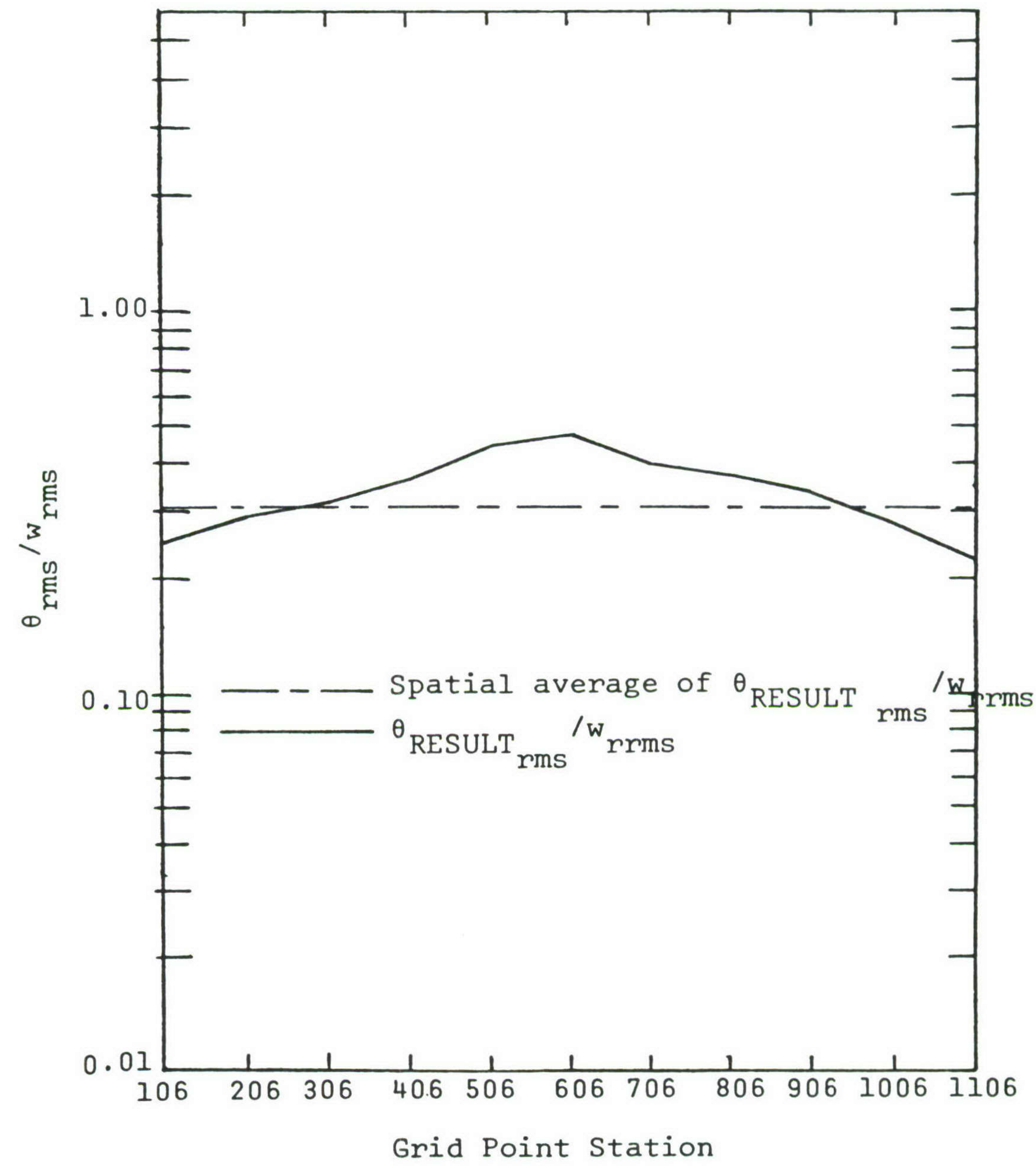

Figure 27 Ratio of RMS Resultant Angular Displacement to RMS Linear Displacement vs. Grid Point Station for Curved Plate with Stiffeners, 20-2560 Hz.

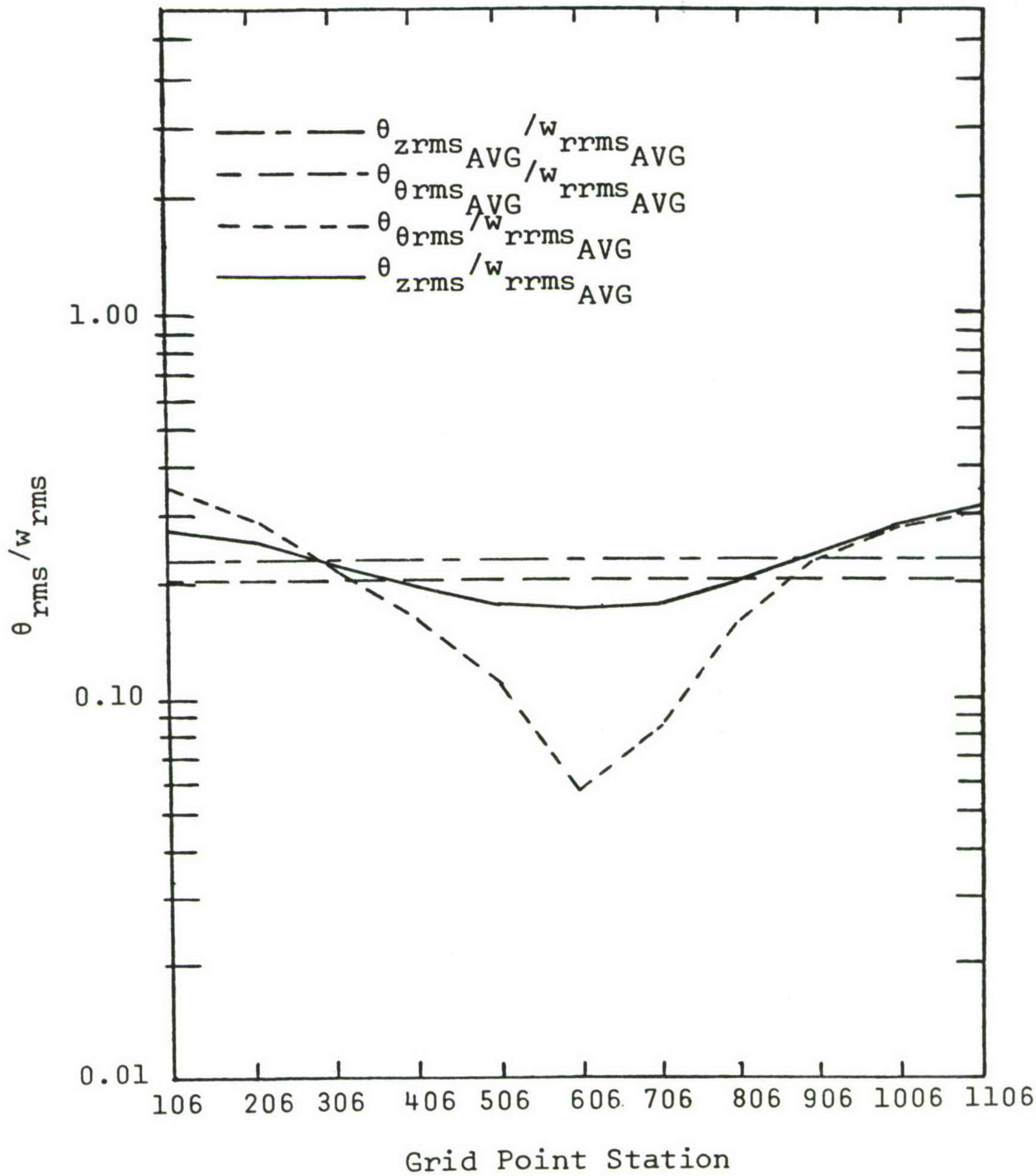

Figure 28 Ratio of RMS Angular Displacement to Spatially Average RMS Linear Displacement vs. Grid Point Station for Curved Plate with Stiffeners, 20-2560 Hz.

$$\frac{\theta_{zrms_{avg}}}{y_{rms_{avg}}} = \frac{\sum_{106}^{1106} \sqrt{\int_{\omega_1}^{\omega_2} S_{\theta_z} \, d\omega}}{\sum_{106}^{1106} \sqrt{\int_{\omega_1}^{\omega_2} S_{w_r} \, d\omega}} \tag{5.62}$$

for stations 106 to 1106. The variable quantity is actually the angular displacement component at each station except that it has been normalized by the spatial average of the linear displacement in accordance with the ratios

$$\frac{\theta_{\theta rms}}{\sum_{106}^{1106} \sqrt{\int_{\omega}^{\omega_2} S_{w_r} \, d\omega}} \quad \text{and} \quad \frac{\theta_{zrms}}{\sum_{106}^{1106} \sqrt{\int_{\omega_1}^{\omega_2} S_{w_r} \, d\omega}} \tag{5.63}$$

The subsequent plots, Figures 29 through 36, present the angular-displacement-component-to-linear-displacement ratios of $\theta_{\theta rms}/w_{rrms}$ and θ_{zrms}/w_{rrms} as a function of grid point stations 106 through 1106 for the frequency band width of 20-2560 Hz. and the seven octaves in between. In each of these plots, the straight lines represent the spatial average of the RMS angular component divided by the spatial average of the RMS linear displacement. For the 20-2560 Hz. case, there are two additional lines plotted which represent the spatial average of all grid points considered in this study on the curved panel.

An examination of the plots for the 20-2560 Hz. band widths (Figures 27 through 29) reveal a somewhat mild spatial variation in the linear-to-angular relationships for the stiffened curved panel subjected to the temporally random concentrated load. However, as one studies the response of the panel to the narrow band octaves, e.g. Figure 30, the maximum value for the r.m.s. angular-to-r.m.s. linear displacement ratio (θ_{zrms}/w_{rrms}) was almost 100 times greater than the minimum value. Thus, for narrow band random excitation, the results

definitely preclude the use of a spatial average as a representative value for the stiffened curved panel subjected to the aforementioned loading condition.

Additional plots for stations 401 through 411 and 104 through 1104 may be found in Reference [24]. Also, a study where mass was added to the panel was reported in this reference.

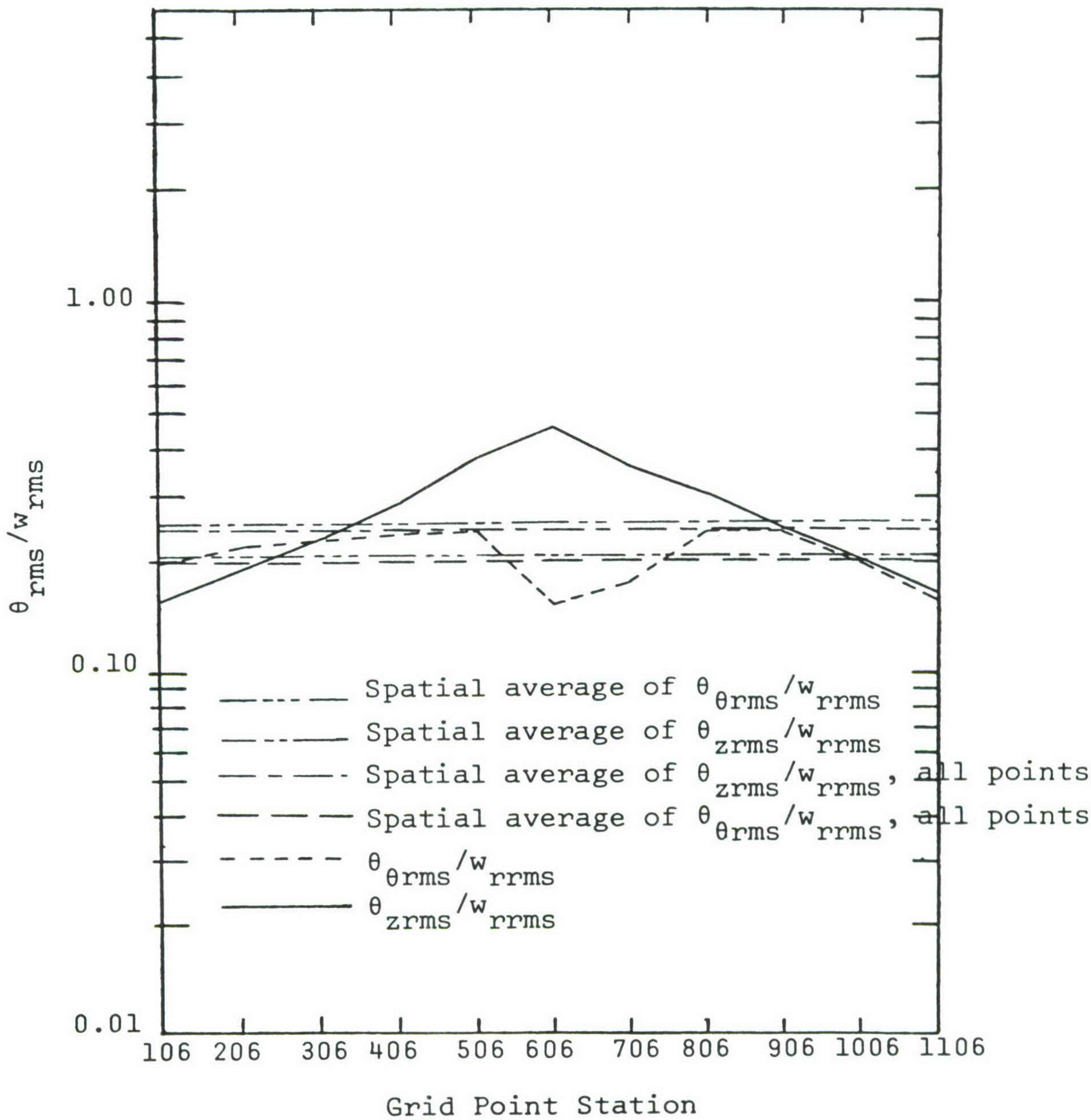

Figure 29 Ratio of RMS Angular Displacement to RMS Linear Displacement vs. Grid Point Station for Curved Plate with Stiffeners, 20-2560 Hz.

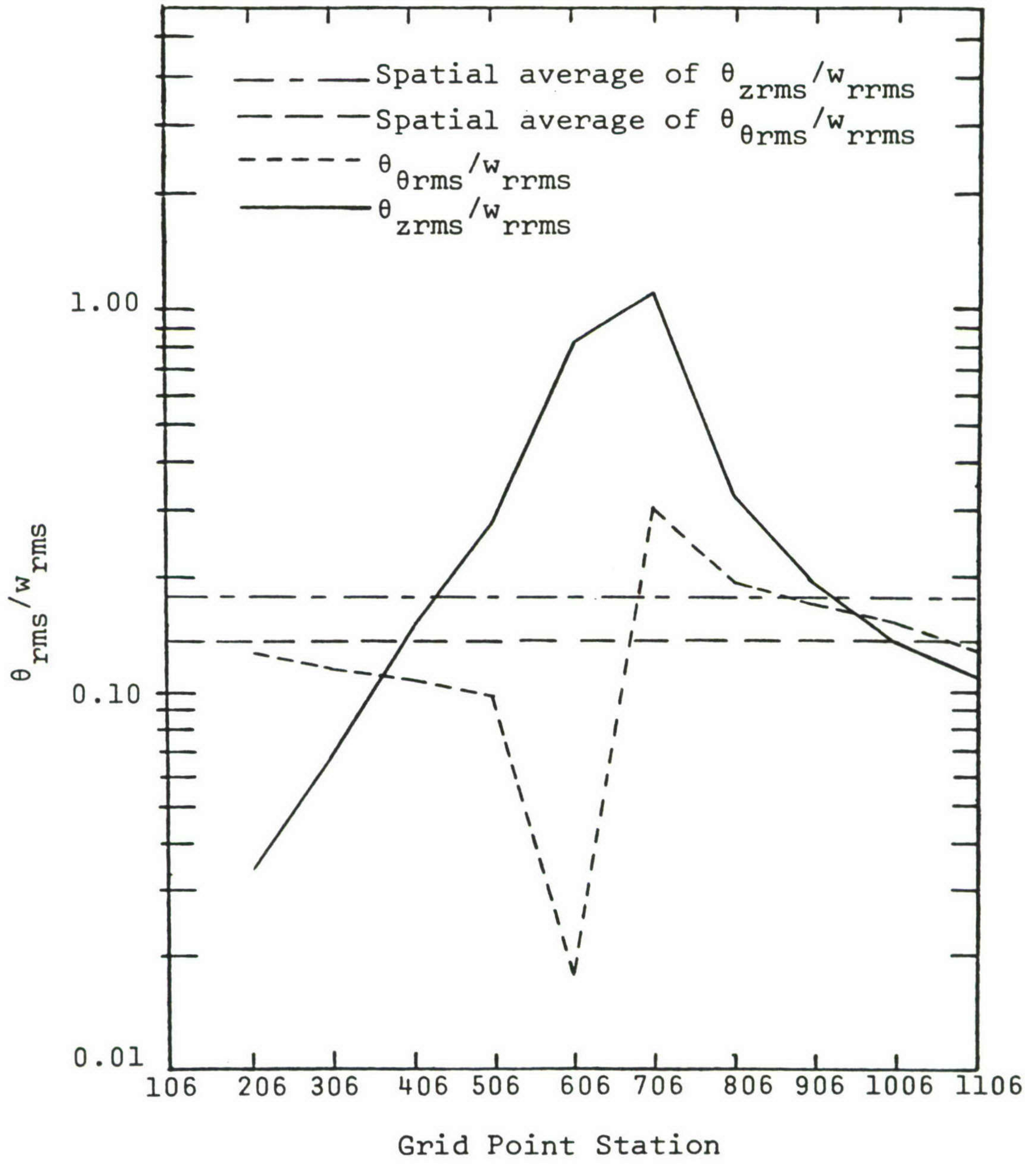

Figure 30 Ratio of RMS Angular Displacement to RMS Linear Displacement vs. Grid Point Station for Curved Plate with Stiffeners, 20-40 Hz.

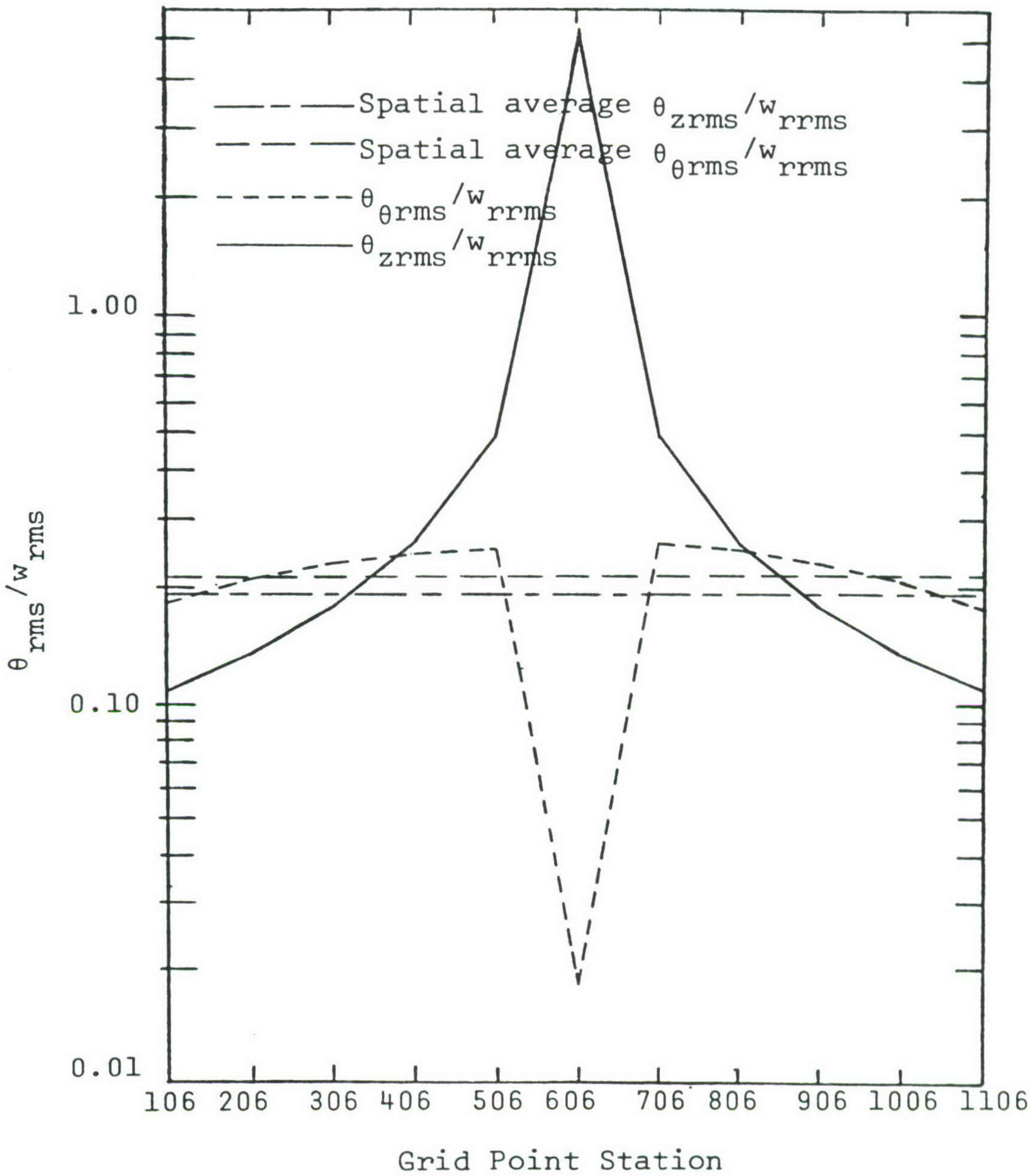

Figure 31 Ratio of RMS Angular Displacement to RMS Linear Displacement vs. Grid Point Station for Curved Plate with Stiffeners, 40-80 Hz.

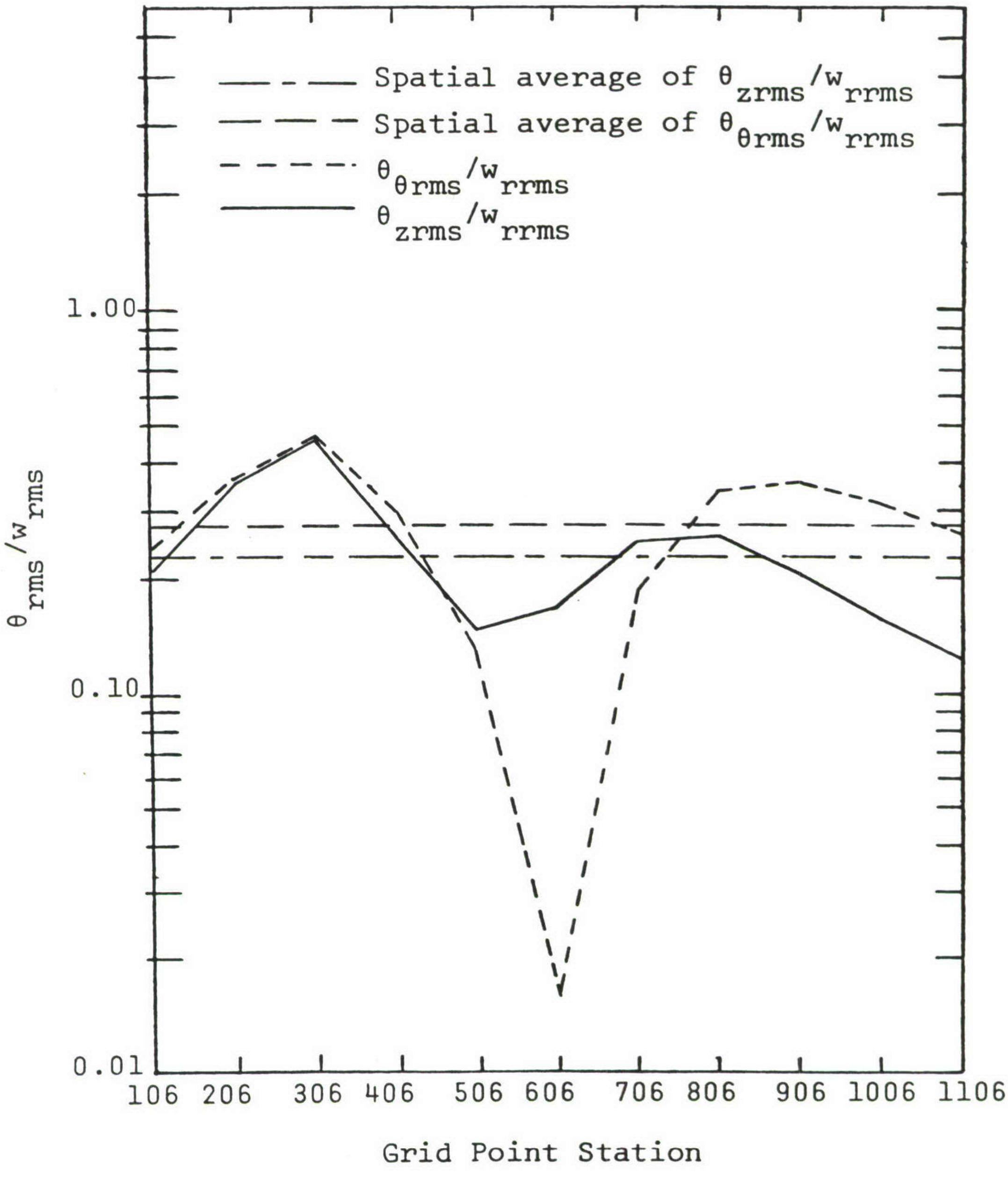

Figure 32 Ratio of RMS Angular Displacement to RMS Linear Displacement vs. Grid Point Station for Curved Plate with Stiffeners, 80-160 Hz.

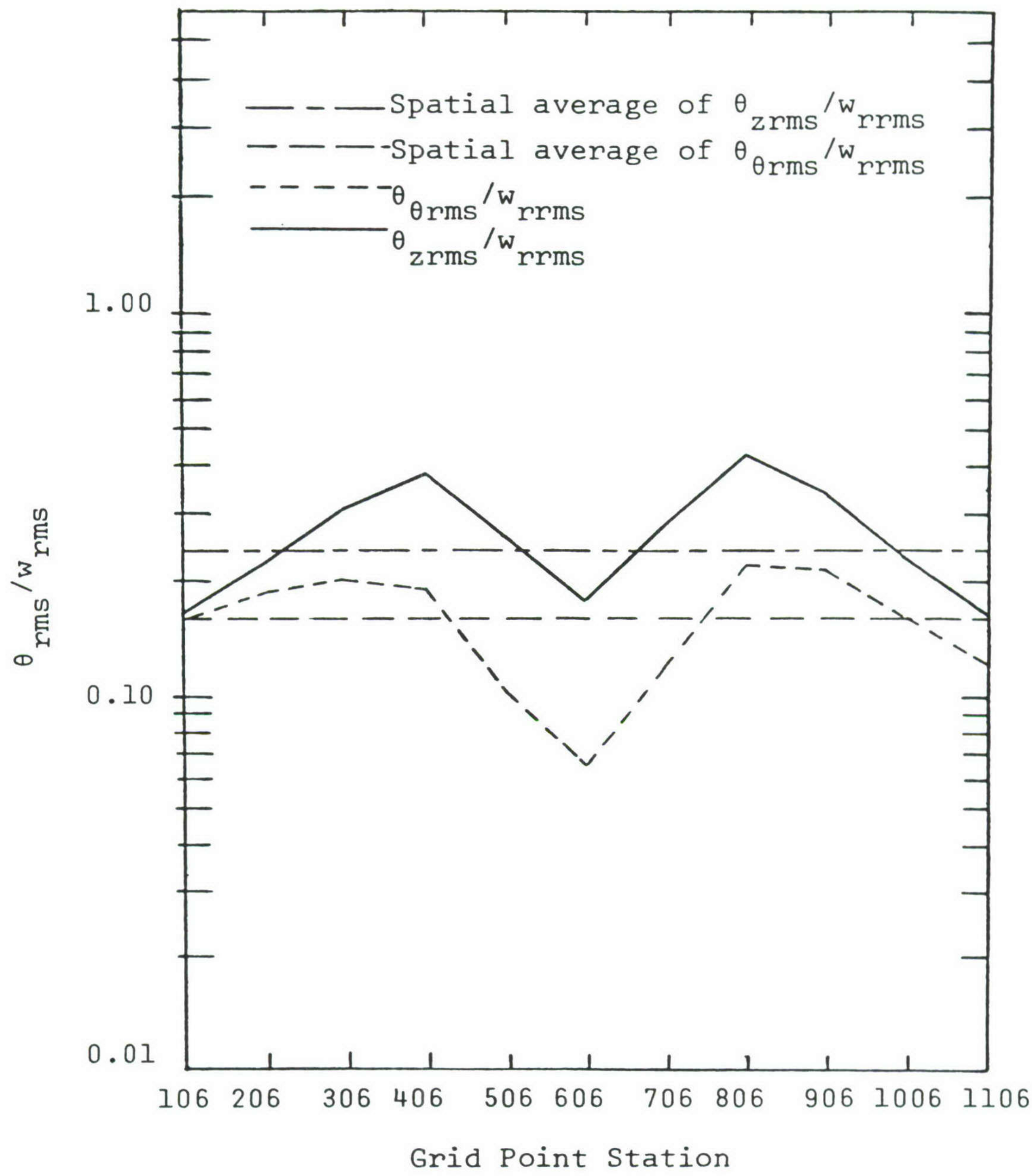

Figure 33 Ratio of RMS Angular Displacement to RMS Linear Displacement vs. Grid Point Station for Curved Plate with Stiffeners, 160-320 Hz.

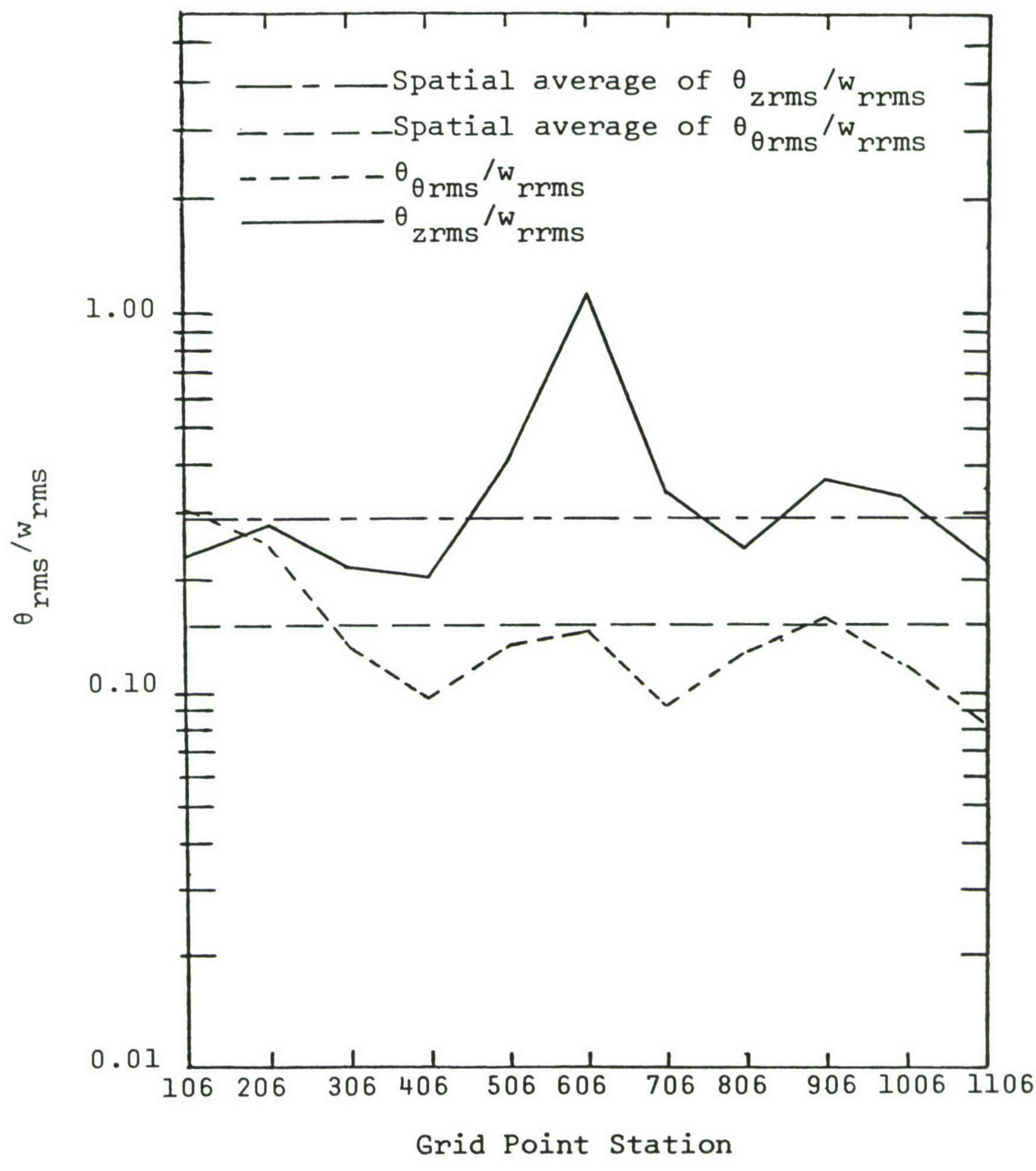

Figure 34 Ratio of RMS Angular Displacement to RMS Linear Displacement vs. Grid Point Station for Curved Plate with Stiffeners, 320-640 Hz.

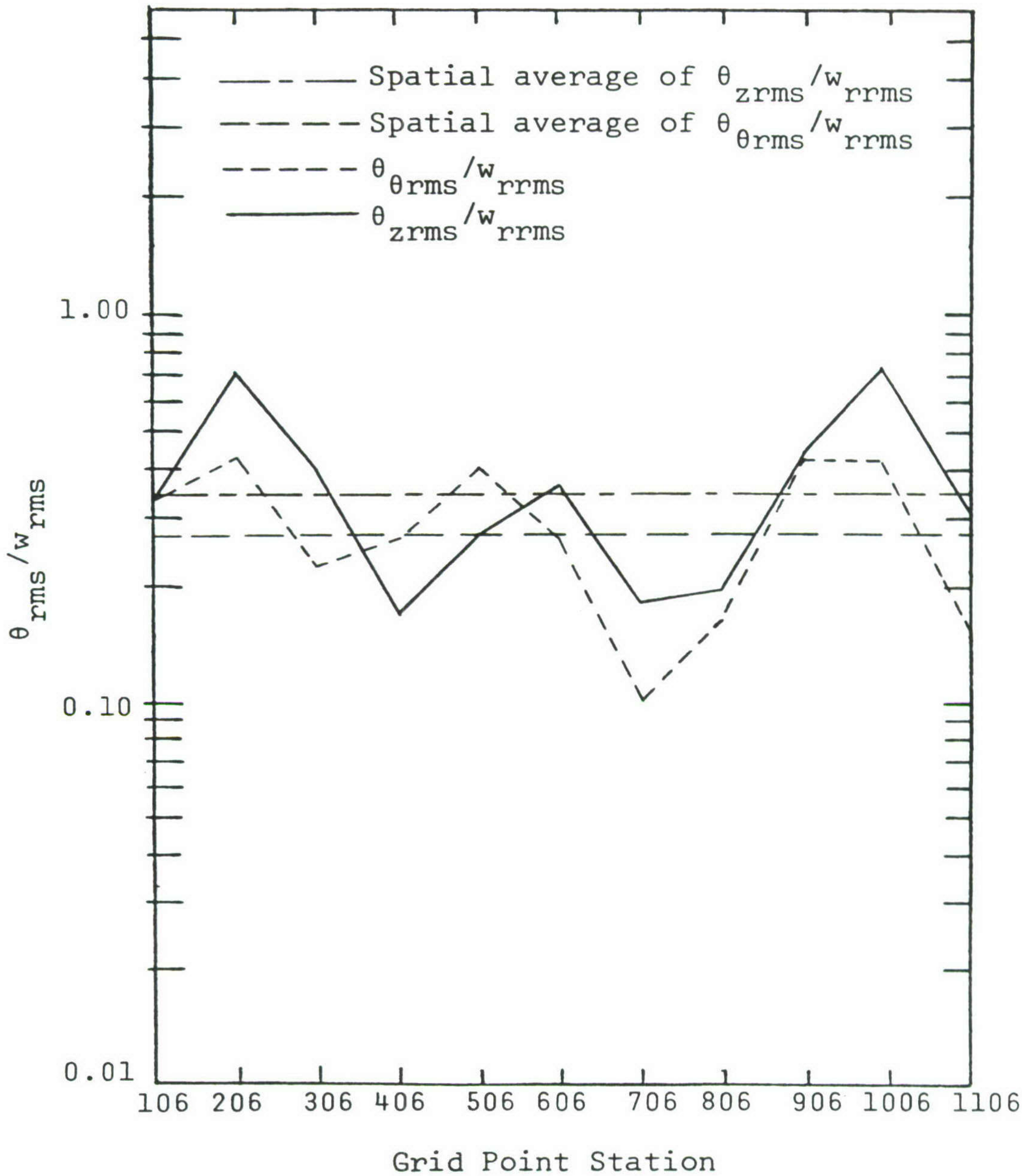

Figure 35 Ratio of RMS Angular Displacement to RMS Linear Displacement vs. Grid Point Station for Curved Plate with Stiffeners, 640-1280 Hz.

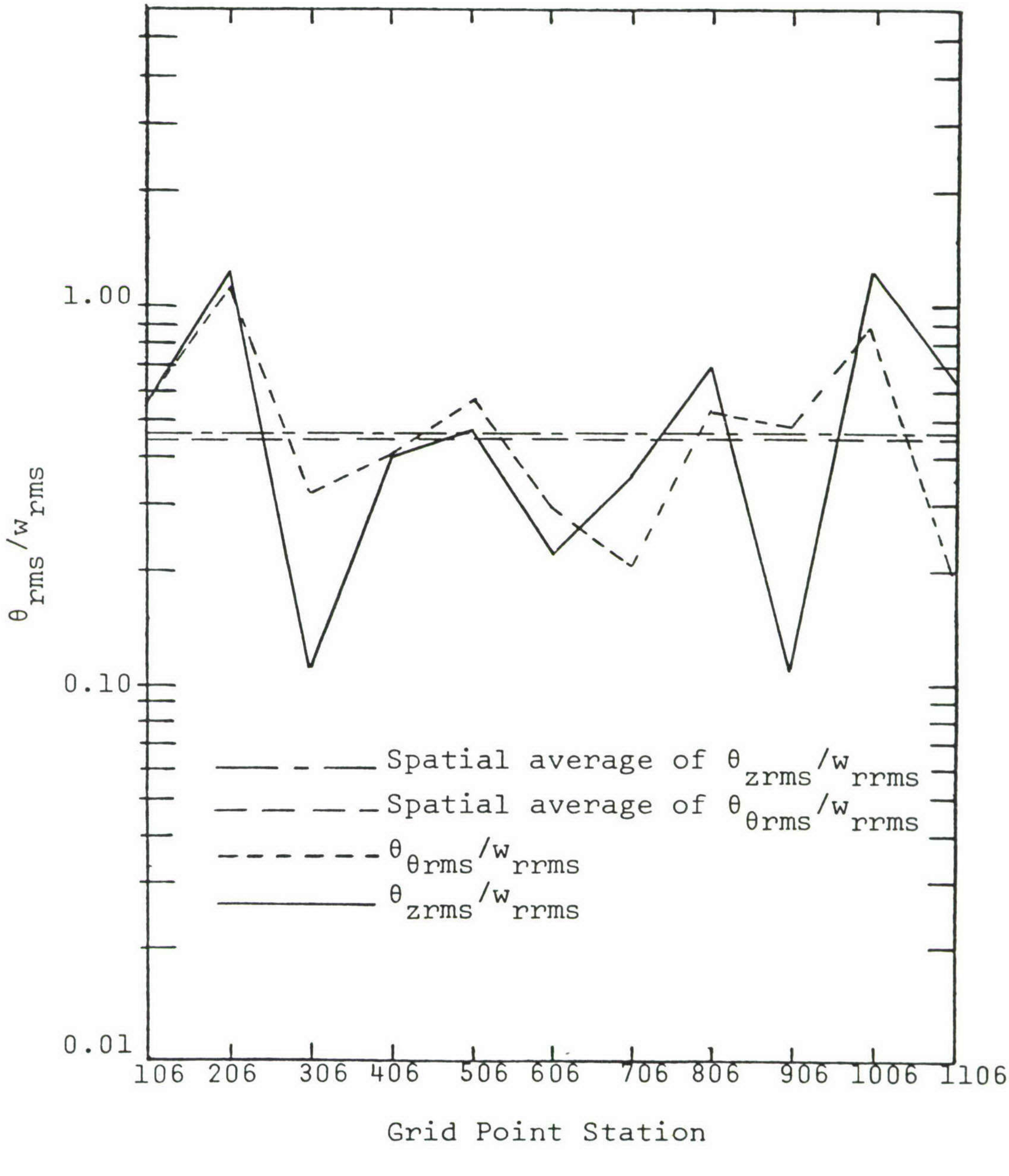

Figure 36 Ratio of RMS Angular Displacement to RMS Linear Displacement vs. Grid Point Station for Curved Plate with Stiffeners, 1280-2560 Hz.

5.4 VARIATION OF ANGULAR TO LINEAR DISPLACEMENT RATIOS IN STRUCTURAL COMPONENTS

As one studies the results of the analytical investigation for random vibrations of a rigid bar on springs, a simple-supported beam and a free-free beam, the conclusion would be made that the spatial variance of the r.m.s. angular-to-r.m.s. linear displacement ratio is significant enough to warrant not using a spatial average for these structures if great accuracy is desired. If large errors (for the free-free beam this would be a factor of 7 between the maximum r.m.s. amplitude occurring and Lee & Whaley's proposed spatial average) can be tolerated, then a single spatial average for the structure is convenient to use; but, it seems the behavior of the structure ought to be understood in some detail so that the applicability of the spatial average is assessed. In the panel example, the ratio was formed by actually computing (via a finite element model for a specific random load case) both r.m.s. angular and linear responses at many points. The conclusion which may be drawn from the example is that even if one has knowledge of the ratio of averages, that quantity is not a particularly good estimation of the ratio at a given point as indicated by those plots encompassing octave bands. The spatial average might be considered an acceptable quantity when considering the 20-2560 Hz. case, but it is felt that the response of different structures under random loading should be investigated before a definite conclusion is drawn. The examples investigated in the previous paragraphs also show cases when the ratio is quite sensitive to structural parameters, load distribution, and the frequency bands.

One means of eliminating the effects of end conditions is by simply considering an infinitely long beam. For this case a traveling wave solution may be written. For sinusoidal excitation at a single point

$$y = Ae^{i(kx-\omega t)} \tag{5.64}$$

where the wave number k is related to frequency by the usual dispersion relation for one-dimensional bending waves:

$$(2\pi f)^2 = k^4 \kappa^2 c_\ell^2 \tag{5.65}$$

In this expression, κ is the radius of gyration and c_ℓ is the extensional wave speed. From (5.64), one may compute $\theta = \frac{dy}{dx}$

$$\theta = ikAe^{i(kx-\omega t)} = iky \tag{5.66}$$

The factor i simply comes from using complex arithmetic to keep track of phase in time and space. It will drop out when temporal averaging is performed to obtain r.m.s. values.

$$\frac{\theta_{rms}}{y_{rms}} = \sqrt{\frac{2\pi f}{\kappa c_\ell}} \tag{5.67}$$

For random steady state excitation at a point we note that, by linearity, the portion of response in a frequency band Δf is due only to the excitation in that band so we may write

$$\frac{S_\theta(f)}{S_y(f)} = \frac{2\pi f}{\kappa c_\ell} \tag{5.68}$$

This ratio does not vary in space and requires only intensive beam parameters κ and c_ℓ rather than a global length L. It can be expected to hold for beams of finite length at frequencies sufficiently high that $L \gg \lambda$.

The infinite beam may be thought of as having an infinite number of natural frequencies which are spaced infinitesimally close together. Since for this case, an exact relation exists between $S_y(f)$ and $S_\theta(f)$, one might expect that a long beam with a large but finite modal density might show approximately this ratio. It is shown in Section IV that, for a plate with high modal density, one may indeed exploit this idea to estimate angular response from component energy expressed as a mass-weighted mean square translational velocity.

SECTION VI
ANGULAR VIBRATION MEASUREMENT

The major objective of the contract effort was the development of methods for prediction of angular vibration. However, it was known from the beginning that some attention would have to be given to purely measurement problems. This view was motivated by two factors:

(1) The scarcity of experimental data suitable for testing of analytical methods meant that Anamet had to be capable of performing its own verification tests. This capability had to be ready when analytical work reached the testing stage in order to produce a reliable and timely product.

(2) Modern methods of structural response prediction, angular or otherwise, often depend on models built entirely or in part from measured data. Two examples are experimental modal analysis and statistical energy analysis where component SEA parameters are obtained by measurement.

The measurement of dynamic rotations at specific points on an elastic structure is not new although concern about angular displacements at the microradian level seems to be confined to optical system applications. Historically, three basic methods of measurement have been used.

(1) Outputs of translational motion sensors mounted a known distance apart may be differenced.

(2) A light beam may be reflected off the point in question and its lateral displacement measured.

(3) Inertia torque on a suspended seismic mass may be sensed.

The most critical angular measurements on airborne optical or laser systems are generally those where motion of a reflecting surface is transduced. Typical requirements in this case may include:

(1) Bandwidth. As usual in structural dynamics, the frequency composition of unwanted motion often contains information which is highly useful to the designer attempting to reduce such motion. Frequency components in the 0.1 to 1.0 kHz range may be particularly important since, in general, they cannot be effectively removed by active servo systems.

(2) Size and Weight. Mirror assemblies as small as 0.1 m (4 in.) and weighing less than 1 kg (2.2 lb.) must be instrumented. Transducers must neither change the dynamic properties of the assembly nor interfere with the intended optical function.

(3) Flexibility of use. During development of component assemblies, sensors must be installed and removed quickly and easily without the requirement of elaborate fixturing. This tends to favor inertially-referenced methods over optical sensing. Furthermore, the sensing of displacement by optical systems rather than velocity or acceleration may make high frequency measurements difficult.

(4) Cost. As usual, the use of standard devices made in production quantities and usable for other purposes is desirable.

It quickly became clear that differencing of translational acceleration signals was the most appropriate method for the present effort. Other investigators [25, 26] have used the method and have concluded that it is quite practical. However, it appeared that a better quantitative understanding of limitations and error sources was desirable. The work described in this chapter was intended to develop that understanding.

Theoretical derivations are presented for estimating errors introduced by noise in individual channels, frequency dependent gain and phase mismatching between channels, and flexure of the mounting surface. Effects of the first two error sources are demonstrated by experiment and it is demonstrated that mismatch error can be reduced by appropriate data processing. Finally, an expression is derived for coherence of a measured angular frequency response when angular response is obtained by differencing.

6.1 THEORETICAL ERROR ANALYSIS

Figure 37 shows a typical arrangement for measuring dynamic rotation. The linear sensors must often be spaced quite closely, either to obtain a good discrete approximation to the angle of rotation at a point, or simply due to space constraints. The difference signal may be much smaller than either of the individual signals. The question then arises, "How 'good' must the individual linear sensing channels be in order that their difference can provide a meaningful estimate of angular motion?"

In attempting to understand the dynamic behavior of a structure, spectral measurements obtained through discrete Fourier transforms are often used. The two most common types of frequency domain data are the power spectral densities of response variables and complex frequency response functions measured for spatially fixed excitations. The intent of this section is to present some quantitative methods for estimating the reliability of these two data types for the case where the response quantity is an angular motion obtained by differencing of signals from translational motion sensors.

The figures of merit used are narrow band signal power/noise power for PSD estimates and the ordinary coherence function for frequency response estimates. Both are derived for the special case of differential sensing in terms of the corresponding quantities for the individual channels.

6.1.1 Narrow-Band Signal-to-Noise Ratio

In Figure 37 two single axis translation accelerometers are mounted a distance Δx apart and their output signals are conditioned and subtracted. The pair then form a differential acceleration sensing system. Each leg is assumed to be a linear, time-invariant system with impulse response $h_i(\tau)$ and frequency response $H_i(f)$. In general, $H_1(f)$ and $H_2(f)$ will be slightly different and will both show a weak dependence on frequency in the range of interest. Noise in each channel is simulated by $n_1(t)$ and $n_2(t)$ as shown. Noise sources are assumed to be

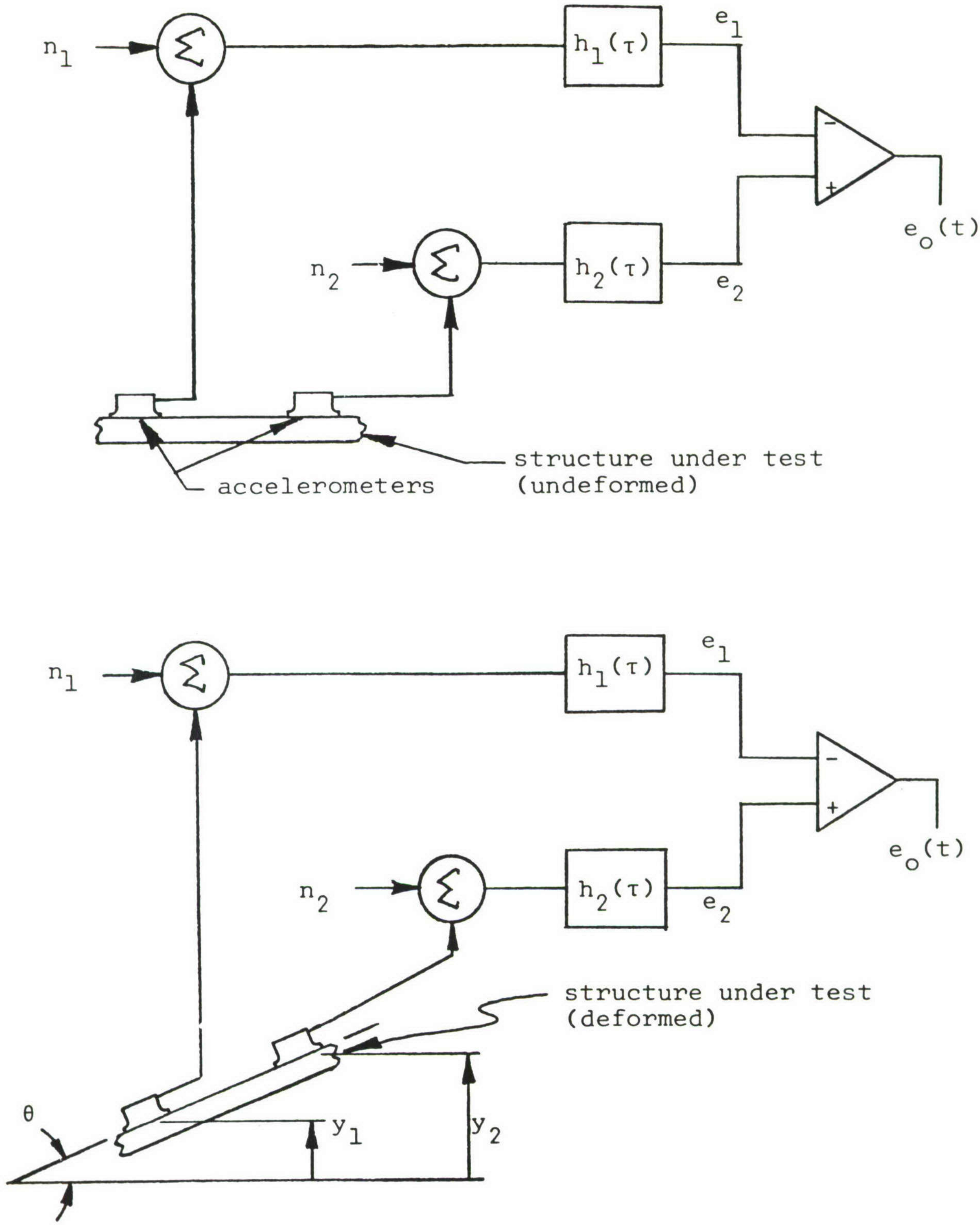

Figure 37 Measurement of Angular Acceleration by Differencing

correlated neither with the measurands $\ddot{y}_1$ and $\ddot{y}_2$ nor with each other.

One component of the angular acceleration at the point midway between the transducers can be estimated as

$$\hat{\ddot{\theta}}(t) = e_0/c\Delta x \tag{6.1}$$

where c is constant and equal to some nominal value of $|H_1|$ or $|H_2|$. If $\ddot{\theta}(t)$ is the true value of angular acceleration, the estimate $\hat{\ddot{\theta}}(t)$ which one obtains from $e_0(t)$ will deviate from $\ddot{\theta}(t)$ due to imperfections introduced by noise sources n_1 and n_2 as well as differences between c and $H_{1_{actual}}$ and $H_{2_{actual}}$. We therefore define an ideal transducing system which has $n_1 = n_2 = 0$ and $H_{1_{ideal}} = H_{2_{ideal}} = c$ where c is close to $H_{1_{actual}}$ and $H_{2_{actual}}$. This definition will allow calculation of a figure of merit for the actual system.

The figure of merit will be called narrow-band signal-to-noise ratio and is a function of frequency defined as

$$S_{NR}(f)_{dB} = 10 \log \left[\frac{S_{\hat{\theta}_I}(f)}{S_{(\hat{\ddot{\theta}}_A - \hat{\ddot{\theta}}_I)}(f)}\right] \tag{6.2}$$

where

$S_{NR}(f)$ = narrow-band signal-to-noise ratio

$\hat{\ddot{\theta}}_I(t)$ = estimate of $\ddot{\theta}(t)$ which would be obtained with an ideal system

$S_{\hat{\theta}_I}(f)$ = power spectral density of $\hat{\ddot{\theta}}_I$

$\hat{\ddot{\theta}}_A(t)$ = estimate of $\ddot{\theta}(t)$ obtained with the actual system

$S_{(\hat{\ddot{\theta}}_A - \hat{\ddot{\theta}}_I)}(f)$ = power spectral density of $\hat{\theta}_A - \hat{\theta}_I$

The quantity $\hat{\theta}_A - \hat{\ddot{\theta}}_I$ is a residual random variable similar to those used to define partial and multiple coherence functions (Reference [27]).

It should be clear that S_{NR} will be degraded only by mismatching between H_1 and H_2. If they are perfectly matched and both equal to c, a small shift in c will have no effect. Thus, there is no loss of generality in allowing c to be a complex function of frequency although Eq. (6.1) should properly be written in terms of Fourier transforms.

In all of the following, the power spectral density of a time history will be represented simply by the ensemble averaged value of the squared magnitude of its Fourier transform. This ignores a number of important mathematical details [28] but is appropriate since virtually all applied work will be carried out using digital FFT methods. The normalizing factor which is needed to compensate for finite record length when using a discrete Fourier transform is also omitted. This simplifies the algebra and is allowable since the final results are arranged in dimensionless form where this factor would cancel out.

If the impulse response of each leg of the ideal system is $h(\tau)$, then

$$h(\tau) = \mathcal{F}^{-1}(c(f)) \tag{6.3}$$

and

$$e_i(t) = h_i(t) * \ddot{y}_i(t) \quad , \quad i = 1,2 \tag{6.4}$$

where $*$ is the convolution operator and $\mathcal{F}^{-1}(\ )$ is the inverse Fourier transform operator. Taking the Fourier transform of Eq. (6.4)

$$E_i(f) = -(2\pi f)^2\ c(f)\ Y_i(f), \quad i = 1,2 \tag{6.5}$$

where

$$E_i(f) = \mathcal{F}[(e_i(t)]$$

$$Y_i(f) = \mathcal{F}[y_i(t)]$$

From Figure 37, for either the actual or ideal system

$$(\Delta x)\ \ddot{\theta}(t) = \ddot{y}_2 - \ddot{y}_1 \tag{6.6}$$

or

$$(\Delta x)\ \theta(f) = Y_2(f) - Y_1(f) \tag{6.7}$$

For the ideal system, Eqs. (6.5) and (6.7) may be combined

$$-(2\pi f)^2 \; \hat{\Theta}_I = \frac{E_2 - E_1}{c\Delta x} \tag{6.8}$$

where

$$\hat{\Theta}_I = \mathcal{F}[\hat{\theta}_I]$$

Forming the conjugate square of Eq. (6.8)

$$|-4\pi^2 f^2 \hat{\Theta}|^2 = \frac{|E_2|^2 + |E_1|^2 - 2\mathrm{Re}[E_1{*}E_2]}{|c|^2 (\Delta x)^2} \tag{6.9}$$

where

$*$ = complex conjugate

Ensemble averaging Eq. (6.8) and using the derivative relation for power spectral density

$$S_{\ddot{u}}(f) = (2\pi f)^4 \; S_u(f) \tag{6.10}$$

gives

$$S_{\hat{\theta}_I} = \frac{S_{e_2} + S_{e_1} - 2\mathrm{Re}[S_{e_1 e_2}]}{|c|^2 (\Delta x)^2} \tag{6.11}$$

An expression for $S_{(\hat{\hat{\theta}}_A - \hat{\hat{\theta}}_I)}$ is obtained in a similar way. For the actual system

$$e_i = h_i * (\ddot{y}_i + n_i) \quad , \quad i = 1,2 \tag{6.12}$$

Transforming Eq. (6.12)

$$E_i = H_i[-(2\pi f)^2 \; Y_i + N_i] \quad , \quad i = 1,2 \tag{6.13}$$

Combining Eqs. (6.7) and (6.13)

$$-(2\pi f)^2 \Delta x \; \hat{\Theta}_A = [\frac{E_2}{H_2} - N_2] - [\frac{E_1}{H_1} - N_1] \tag{6.14}$$

By linearity of the Fourier transform

$$\mathcal{F}(\hat{\theta}_A - \hat{\theta}_I) = \hat{\Theta}_A - \hat{\Theta}_I \quad (6.15)$$

From Eqs. (6.8) and (6.14)

$$-(2\pi f)^2 \; \Delta x(\hat{\Theta}_A - \hat{\Theta}_I) = E_2[\frac{1}{H_2} - \frac{1}{c}] - E_1[\frac{1}{H_1} - \frac{1}{c}] - N_2 + N_1 \quad (6.16)$$

Now define complex functions of frequency $C_1(f)$ and $C_2(f)$ where

$$C_i(f) \overset{\Delta}{=} (\frac{1}{H_i(f)} - \frac{1}{c(f)})^{-1}, \qquad i = 1,2 \quad (6.17)$$

Substituting Eq. (6.17) into (6.16) and taking the conjugate square of both sides

$$(2\pi f)^4 \; (\Delta x)^2 \; |\hat{\Theta}_A - \hat{\Theta}_I|^2 = \left|\frac{E_2}{C_2}\right|^2 + \left|\frac{E_1}{C_1}\right|^2 + |N_2|^2 + |N_1|^2$$

$$-[\frac{E_1}{C_1}]^* \frac{E_2}{C_2} - \frac{E_2 N_2^*}{C_2} + \frac{E_2 N_1^*}{C_2} - \frac{E_1 E_2^*}{C_1 \; C_2} + \frac{E_1 N_2^*}{C_1} - \frac{E_1 N_1^*}{C_1}$$

$$- \frac{N_2 E_2^*}{C_2} + \frac{N_2 E_1^*}{C_1} - N_1^* N_2 + \frac{N_1 E_2^*}{C_2} - \frac{N_1 E_1^*}{C_1} - N_1 N_2^* \quad (6.18)$$

After ensemble averaging, dropping uncorrelated products, and using the derivative relations for power spectra

$$(\Delta x)^2 S_{(\hat{\theta}_A - \hat{\theta}_I)} = \frac{S_{e_1}}{|C_1|^2} + \frac{S_{e_2}}{|C_2|^2} - 2\mathrm{Re}\;[\frac{S_{e_1 e_2}}{C_1 C_2}] + 2\; S_n \quad (6.19)$$

Combining Eqs. (6.2), (6.11), and (6.19)

$$S_{NR} = \frac{S_{e_1} + S_{e_2} - 2\mathrm{Re}[S_{e_1 e_2}]}{\frac{|c|^2}{|C_1|^2} S_{e_1} + \frac{|c|^2}{|C_2|^2} S_{e_2} - 2|c|^2 \mathrm{Re}[\frac{S_{e_1 e_2}}{C_1^* C_2}] + 2|c|^2 S_n} \quad (6.20)$$

Equation (6.20) is the desired quantity but it can be simplified considerably. Let the frequency response of each leg of the ideal system be chosen as the average of the two legs of the actual system.

$$c(f) = \frac{H_1(f) + H_2(f)}{2} \tag{6.21}$$

Also define the average of the single channel power spectra as $S_{\bar{e}}$ where

$$S_{\bar{e}} \triangleq \frac{S_{e_1} + S_{e_2}}{2} \tag{6.22}$$

Finally, let the channel mismatch be specified in terms of a single complex function of frequency $\delta(f)$ where

$$\delta(f) = \frac{H_2(f)}{H_1(f)} - 1 \tag{6.23}$$

From Eqs. (6.17), (6.21), and (6.23)

$$\frac{c}{C_1} = \frac{\delta}{2}$$

$$\frac{c}{C_2} = -\frac{\delta}{2}\,[1 - \delta + \delta^2 - \ldots] \tag{6.24}$$

where the expansion for c/C_2 can be shown to converge for δ anywhere inside the circle $|\delta| = 1$. Using Eq. (6.22) and Eq. (6.24) to simplify Eq. (6.20) gives, after dropping third and higher order terms in δ

$$S_{NR} = \frac{4\left[1 - \dfrac{R_e(S_{e_1 e_2})}{S_{\bar{e}}}\right]}{\left[|\delta|^2\left(1 + \dfrac{Re(S_{e_1 e_2})}{S_{\bar{e}}}\right) + 4\dfrac{|c|^2 S_n}{S_{\bar{e}}}\right]} \tag{6.25}$$

The quantity $\mathrm{Re}(S_{e_1 e_2})/S_{\bar{e}}$ is a dimensionless function which indicates the amount of angular acceleration which may be measured by finite spatial differencing at a given frequency. It occurs in other developments and will be called the spectral discrete difference and given the symbol α.

$$\alpha\,(f) \stackrel{\Delta}{=} \mathrm{Re}[S_{e_1 e_2}(f)]/S_{\bar{e}}\,(f) \tag{6.26}$$

Combining Eqs. (6.25) and (6.26)

$$S_{NR} = \frac{4\,(1 - \alpha)}{[|\delta|^2(1 + \alpha) + 4\,\dfrac{|c|^2 S_n}{S_{\bar{e}}}]} \tag{6.27}$$

This is then the final result. The narrow-band discrete angle signal-to-noise ratio is expressed in terms of a corresponding single channel quantity $S_{\bar{e}}/|c|^2 S_n$, the complex channel mismatch parameter δ, and a new quantity called the spectral discrete difference. All variables in Eq. (6.27) are functions of frequency.

A simple interpretation of the quantity $\alpha(f)$ may be obtained from the following identity. For any two stationary random signals e_1 and e_2

$$1 - \alpha(f) = \frac{S_{(e_1 - e_2)}}{S_{e_1} + S_{e_2}} \tag{6.28}$$

The quantity $1 - \alpha$ is thus simply the nondimensional size of the PSD of a difference. In the present case $1 - \alpha$ will tend to zero as either Δx or the true angle go to zero. As $1 - \alpha$ goes to zero we may expect poor accuracy in our estimate of $S_{(e_1 - e_2)}$.

If the numerator and denominator in Eq. (6.27) are thought of as dimensionless signal power and dimensionless noise power, then the noise power can be divided. It is composed of a signal-

correlated noise term $|\delta|^2 (1 + \alpha)$ induced by mismatching of channel gain and phase characteristics and an uncorrelated noise term $c^2 S_n / S_{\bar{e}}$ which depends only on single channel noise performance.

Some numerical examples are useful to compare the degradation caused by incoherent single channel noise, gain mismatching between channels, and phase mismatching. Suppose one is attempting to measure $S_{\ddot{\theta}}(f)$ at a frequency where single channel S/N is quite good, say 60 dB. Then

$$\frac{|c|^2 S_n}{S_{\bar{e}}} = 10^{-60/10} = 10^{-6}$$

Suppose further that $\alpha = 0.98$. It is shown later that values closer to unity (i.e. worse) than this can be expected to occur routinely in practice. Now consider four situations regarding channel mismatch.

1) Perfect matching. Differential narrow-band S/N is

$$S_{NR}\Big|_{dB} = 10 \log \left[\frac{4(1-.98)}{4 \times 10^{-6}}\right] = 43.0 \text{ dB}$$

(17.0 dB worse than single channel)

2) Perfect phase matching but 1.5% gain mismatch. In this case

$$\frac{H_2}{H_1} = 1.015 + i0, \quad \delta = \frac{H_2}{H_1} - 1 = 0.015 + i0$$

$$|\delta| = 0.015$$

$$S_{NR}\Big|_{dB} = 10 \log \left[\frac{4(1-.98)}{.015^2(1+.98) + 4 \times 10^{-6}}\right]$$

$= 22.5$ dB (37.5 dB worse than single channel)

3) Perfect gain matching but 2° of phase error.

$$\frac{H_2}{H_1} = 1 \angle 2° = .9994 + i\ .0349$$

$$\delta = -.0006 + i\ .0349 = .0349 \angle 91.0°$$

$$S_{NR}\big|_{dB} = 10 \log \left[\frac{4(1-.98)}{.0349^2(1+.98) + 4 \times 10^{-6}}\right]$$

$$= 15.2 \text{ dB } (44.8 \text{ dB worse than single channel})$$

4) Phase mismatch of 2° and gain mismatch of 1.5%.

$$\frac{H_2}{H_1} = 1.015 \angle 2° = 1.0144 + i\ .0354$$

$$\delta = .0144 + i\ .0354 = .0382 \angle 67°$$

$$S_{NR}\big|_{dB} = 10 \log \left[\frac{4(1-.98)}{.0382^2(1+.98) + 4 \times 10^{-6}}\right]$$

$$= 14.4 \text{ dB } (45.6 \text{ dB worse than single channel})$$

The latter values for noise and mismatch parameters are probably typical for a differential sensing system where each leg consists of a piezoelectric accelerometer, charge converter, voltage amplifier, anti-aliasing filter, and A/D converter. If, in addition, individual channels are passed through analog tape, the situation could be considerably worse.

Eq. (6.27) has been used to compute a set of plots which may be used for quick reference in setting up an experiment where the PSD of a difference quantity is to be measured. These are displayed as Figures 38 through 41.

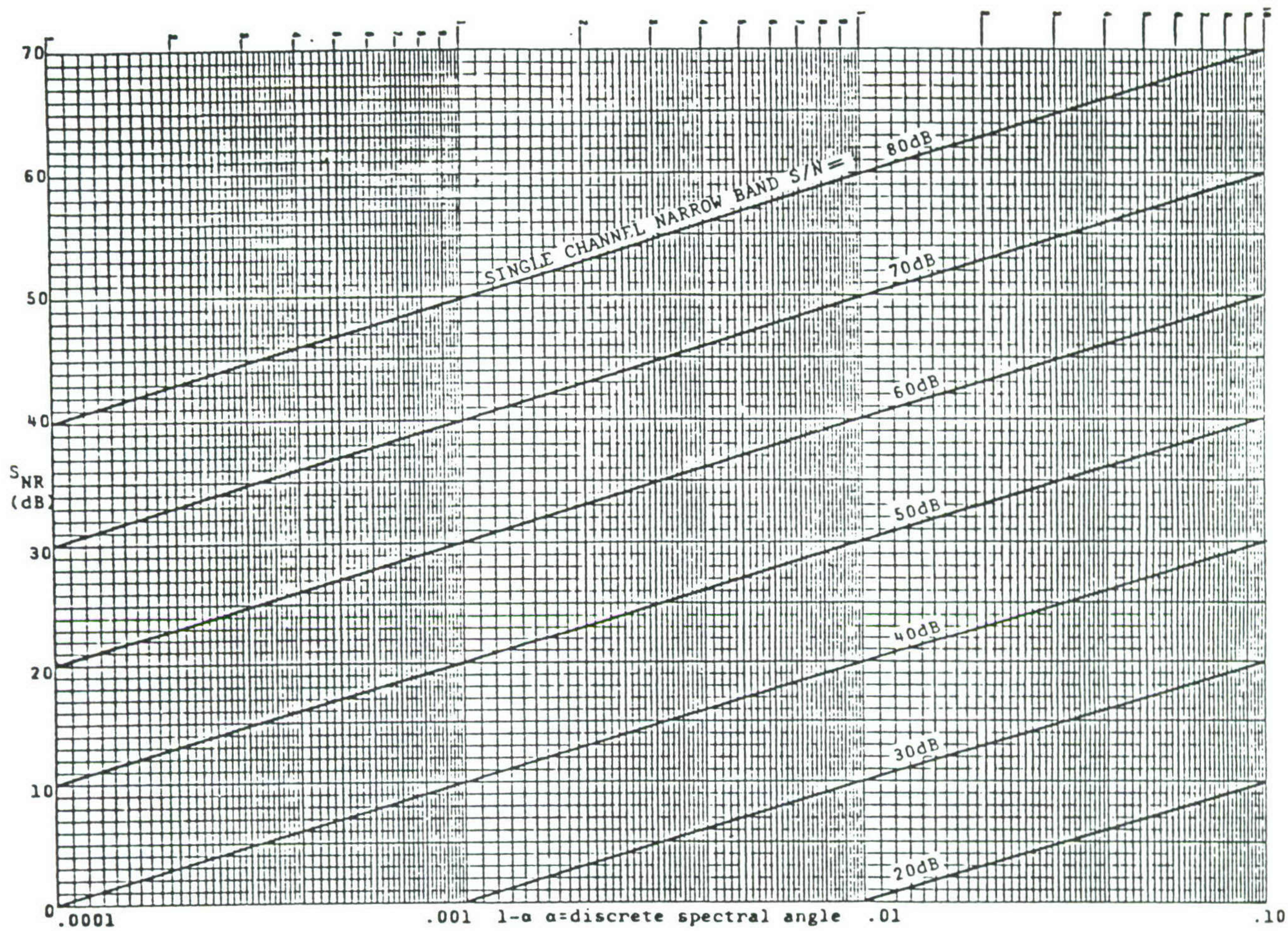

Figure 38 Narrow-Band Signal-to-Noise Ratio of Angular Acceleration Estimate Obtained by Differencing of Linear Accelerations

$|\delta| = 0.000$

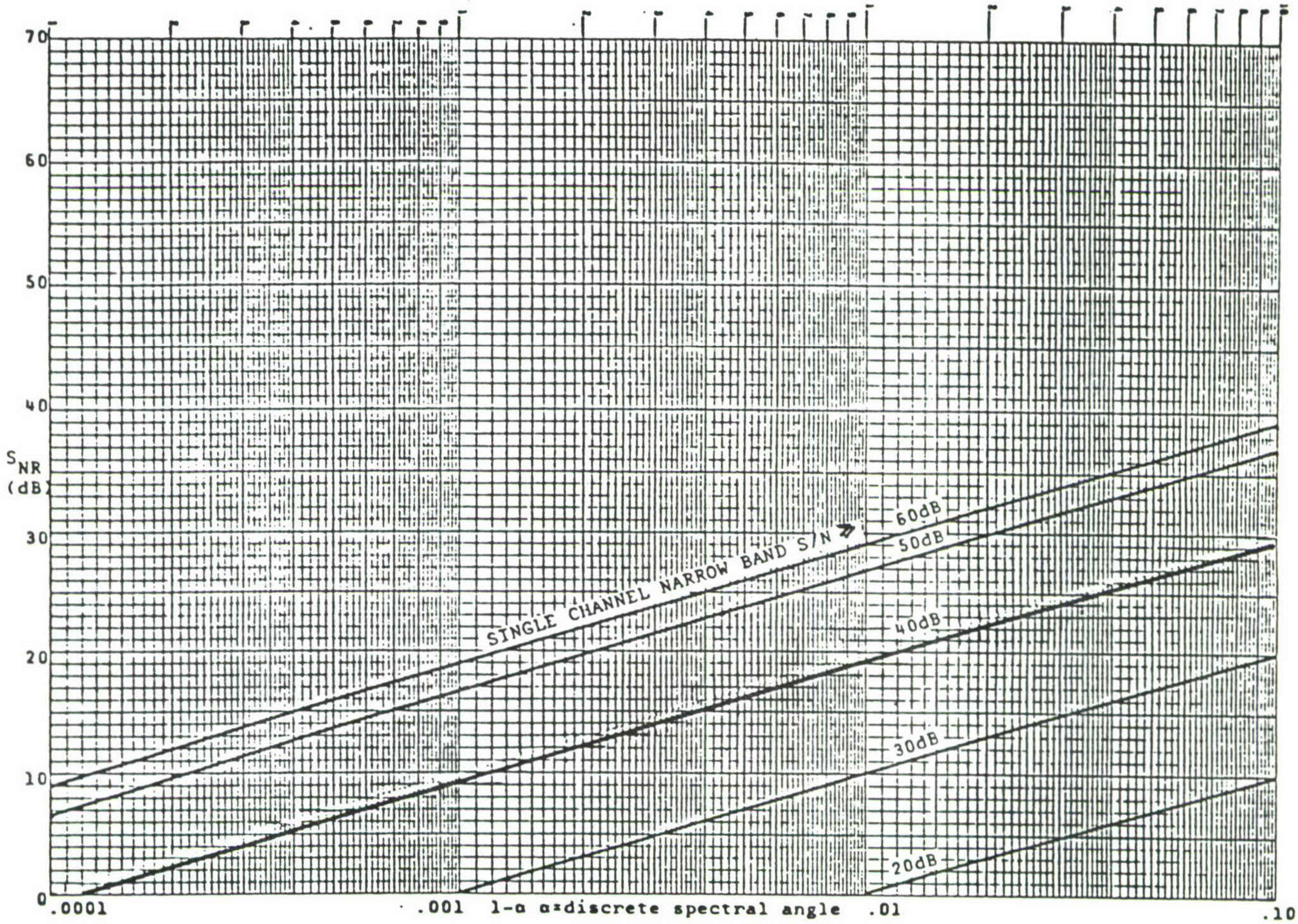

Figure 39 Narrow-Band Signal-to-Noise Ratio of Angular Acceleration Estimate Obtained by Differencing of Linear Accelerations
$|\delta| = 0.005$

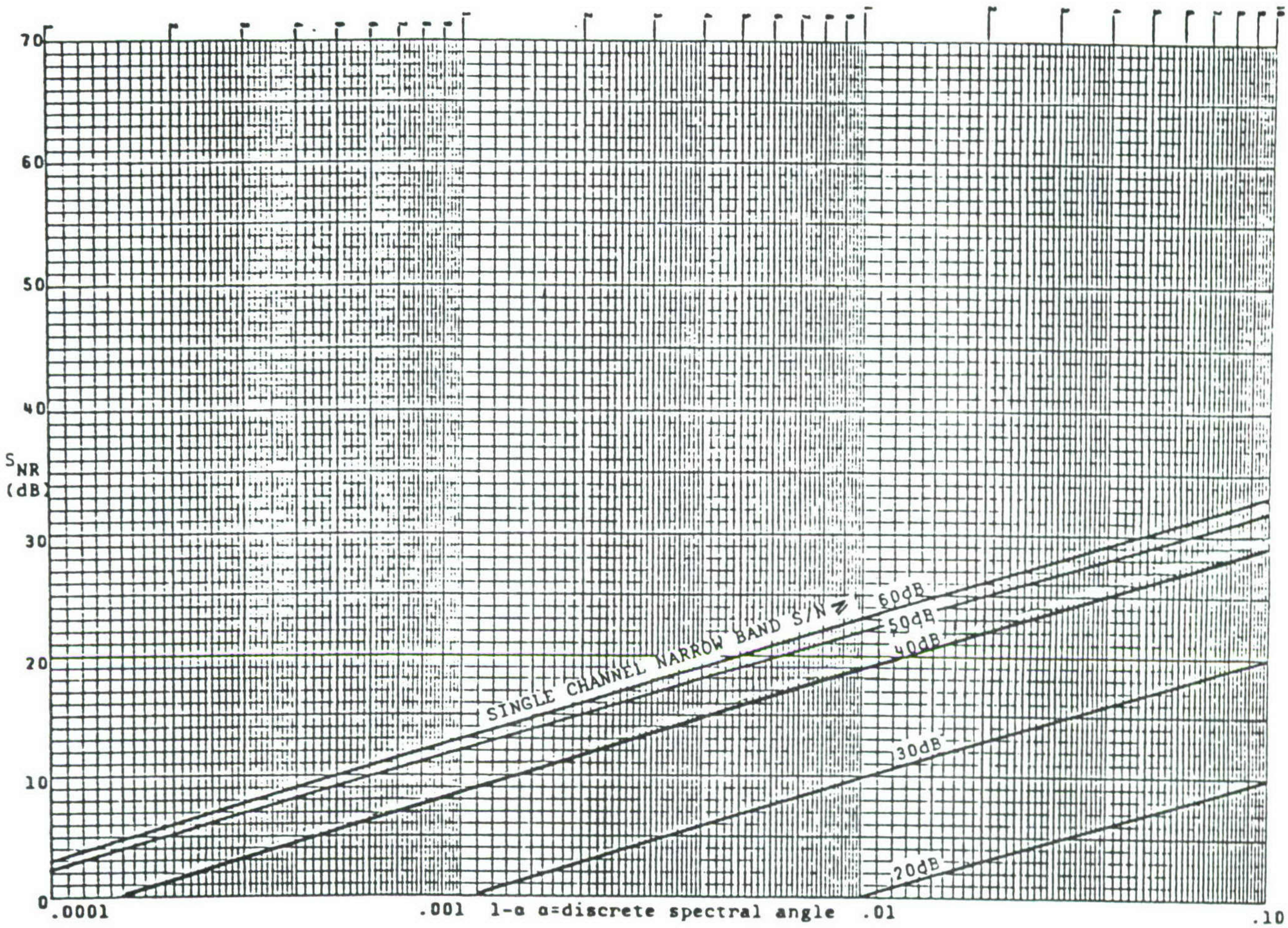

Figure 40 Narrow-Band Signal-to-Noise Ratio of Angular Acceleration Estimate Obtained by Differencing of Linear Accelerations
$|\delta| = 0.01$

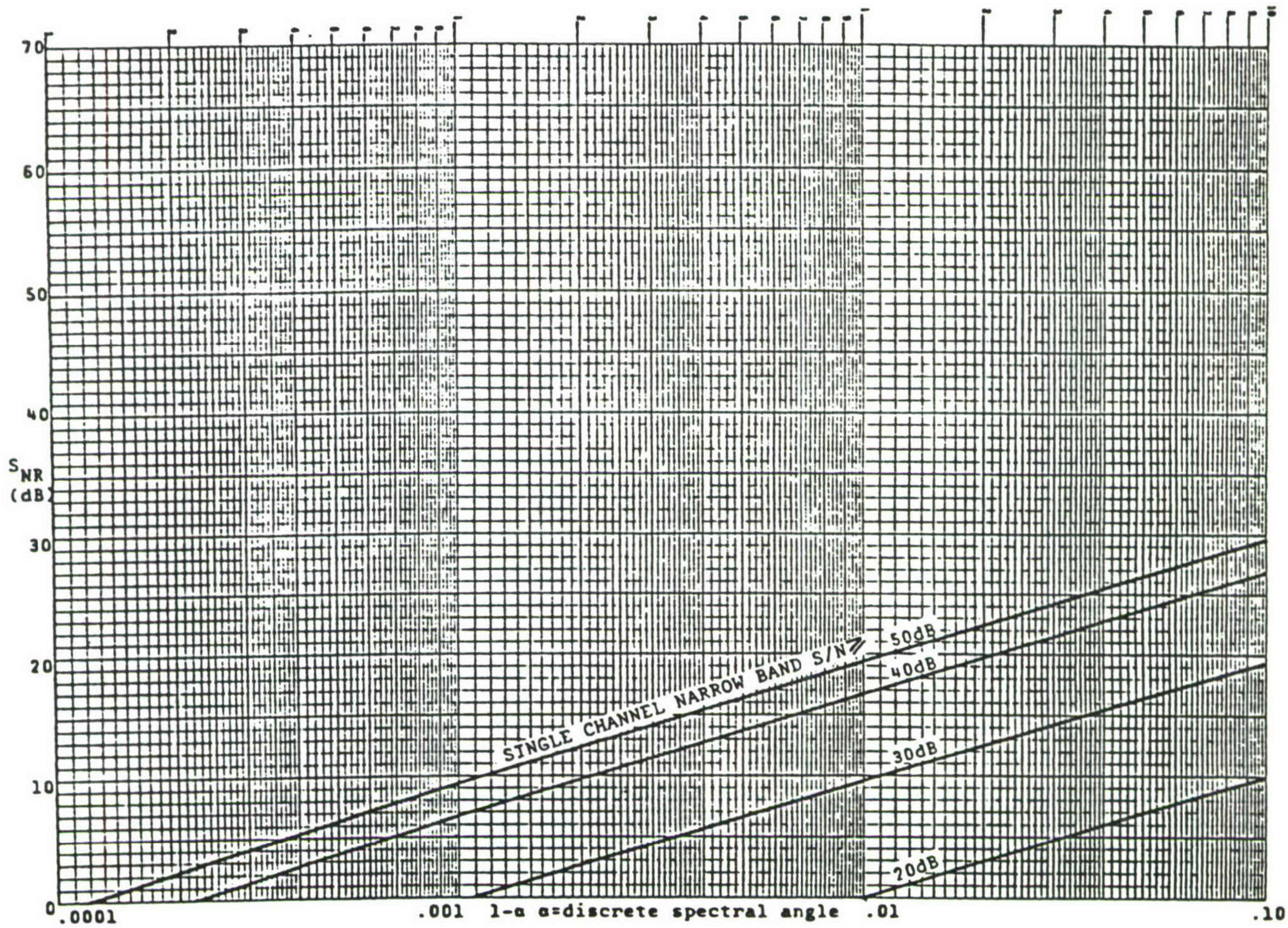

Figure 41 Narrow-Band Signal-to-Noise Ratio of Angular Acceleration Estimate Obtained by Differencing of Linear Accelerations
$|\delta| = 0.015$

The transducer separation distance Δx does not appear explicity in Eq. (6.27). Its effect is included in the spectral discrete difference α. As Δx is increased, a difference appears between e_1 and e_2 which causes α to drop below unity. It is shown in a later paragraph that α may be very close to unity for practical cases. It should be noted that while $\alpha(f)$ is a useful concept for quantifying errors, its measurements is not necessarily straightforward. Experiments have indicated that accurate determination of $\alpha(f)$ is at least as difficult as the measurement of $S_\theta(f)$ itself.

One additional plot is provided as Figure 42 to aid in estimating narrowband signal-to-noise ratio at a given frequency. It is intended for use with piezoelectric accelerometers where essentially all of the incoherent noise power is below 100 Hz and a high pass filter is incorporated to suppress very low frequency noise below about 1 Hz. A typical noise power spectrum for this type of instrument is of the form

$$S_n(f) = A\, f^{-m} \tag{6.29}$$

If the total noise power σ_n^2 between $f_{min} = 1$ Hz and $f_{max} = 100$ Hz is known, the quantity A in Eq. (6.29) can be obtained in terms of σ_n^2 and m from

$$\sigma_n^{\ 2} = \int_{f_{min}}^{f_{max}} S_n(f)\, df \tag{6.30}$$

From Eqs. (6.29) and (6.30)

$$A = \frac{(1 - m)\, \sigma_n^{\ 2}}{(f_{max}^{\ 1-m} - f_{min}^{\ 1-m})} \tag{6.31}$$

Measurements of noise spectra for a variety of piezoelectric transducers have indicated that m = 1.32 is a representative value. This was used in the calculation of Figure 42.

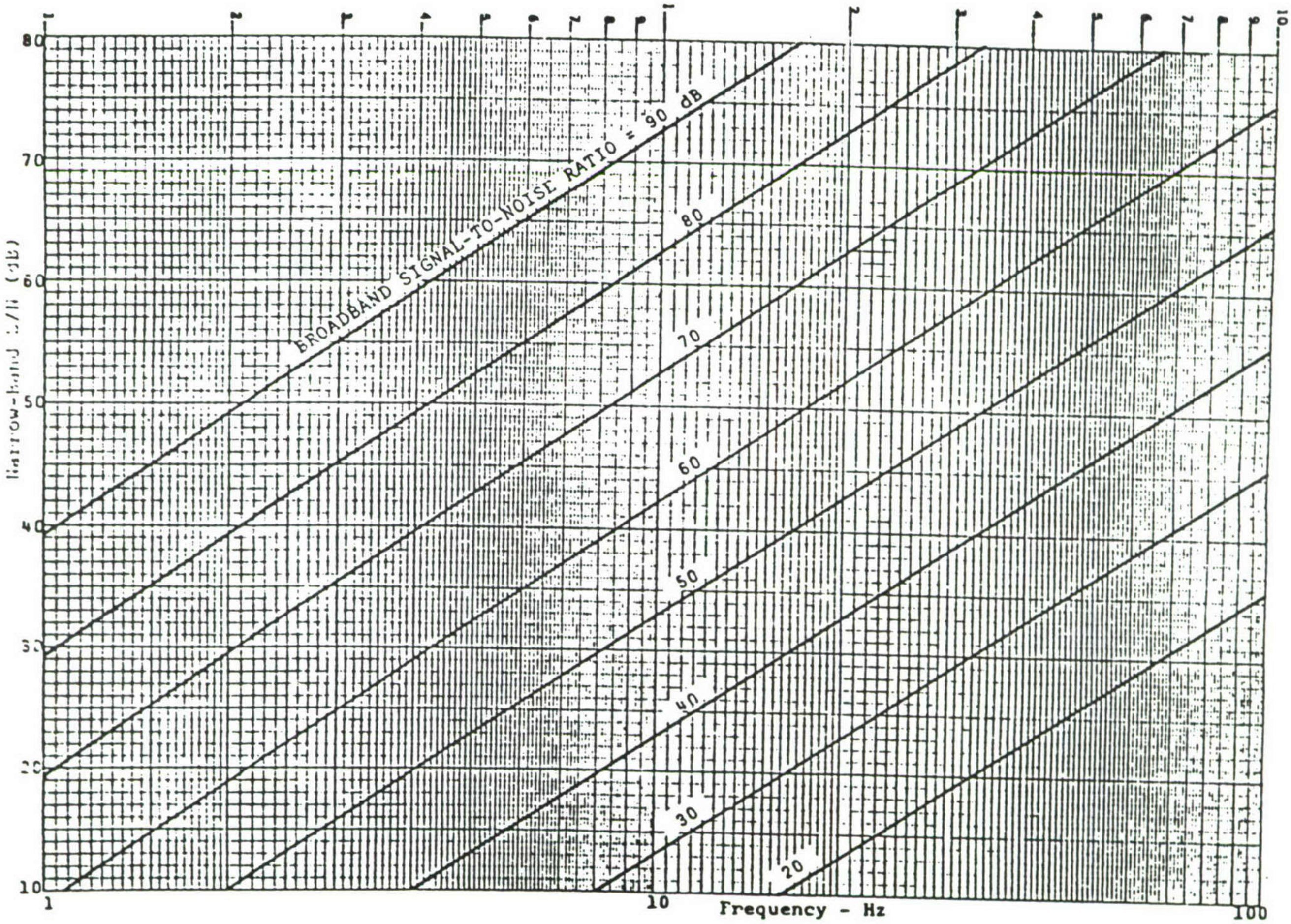

Figure 42 Typical Narrow-Band Signal-to-Noise for Piezoelectric Accelerometers

For an infinite plate, the mechanical impedance (ratio of input force to response velocity at a given frequency) can be shown to be independent of frequency [21]. Thus, for a structure built up of plate elements, it is reasonable to expect the envelope of the PSD acceleration response under random excitation to increase with frequency as ω^2 once the region of reasonably high modal density has been reached. The signal power spectrum will therefore be approximated as

$$S_{e_i} = Bf^k \qquad , \; i = 1,2 \tag{6.32}$$

with k = 2. Then if σ_e^2 is the total signal power in the band of interest, B can be found from

$$\sigma_{e_i}^2 = \int_{f_{min}}^{f_{max}} Bf^k \tag{6.33}$$

or

$$B = \frac{(k + 1)\,\sigma_{e_i}^2}{(f_{max}^{k+1} - f_{min}^{k+1})} \tag{6.34}$$

In the current case $f_{min} \approx 1$ Hz and $f_{max} = 100$ Hz, so with negligible error

$$B = \frac{(k + 1)\,\sigma_{e_i}^2}{f_{max}^{k+1}} \tag{6.35}$$

In addition, the use to which $c^2 S_n/S_{e_i}$ will be put does not require extreme accuracy so A will be approximated as

$$A \simeq \frac{(m - 1)\,\sigma_n^2}{f_{min}^{1-m}} \tag{6.36}$$

Combining Eqs. (6.29), (6.31), (6.32), and (6.34)

$$\frac{S_e}{c^2 S_n} = \left(\frac{k+1}{m-1}\right)\left(\frac{f_{min}}{f_{max}}\right)\left(\frac{f}{f_{min}}\right)^m \left(\frac{f}{f_{max}}\right)^k \left(\frac{\sigma_e^2}{c^2\sigma_n^2}\right) \tag{6.37}$$

The quantity $\sigma_e^2/c^2\sigma_n^2$ is the single channel broadband signal-to-noise ratio which may be quickly measured or estimated from experience in setting up an experiment. Eq. (6.37) simply quantifies the effect of the noise power spectrum being shaded towards low frequencies and the signal power spectrum towards high frequencies. From Figure 42 it may be observed that, for the values of m, k, f_{min}, and f_{max} used, the narrowband signal-to-noise ratio is worse than the broadband below about 34 Hz. At 5 Hz, which is still high enough to be important for airborne optical system applications, the narrowband S/N is approximately 27 dB worse.

6.1.2 Coherence Function for Angular Frequency Response

In establishing a mathematical model from test data or for verifying an analytical model, some form of standardized, measurable input-output relationship is needed. For linear structures this is usually taken as the frequency response. If angular response can be reliably measured by differencing of linear signals then one important use of these angular data would be to compute the frequency response of angular degrees of freedom to spatially fixed force inputs. The ordinary coherence function [29] is a standard method of checking the consistency of frequency responses measured by the DFT cross-spectral averaging method. In this section, an expression is obtained for the coherence function of a differentially measured angular frequency response in terms of the coherence functions associated with the individual channels.

Suppose $\ell(t)$ with Fourier transform L(f) is a force input producing two acceleration outputs $\ddot{y}_1(t)$ and $\ddot{y}_2(t)$ which are differenced to estimate $\ddot{\theta}(t)$ according to Eq. (6.6). The definition of coherence for this output quantity is

$$\gamma_{\ell\ddot{\theta}} = \frac{|S_{\ell\ddot{\theta}}|^2}{S_{\ddot{\theta}} S_{\ell}} \tag{6.38}$$

Relating this to single channel quantities

$$(\Delta x) S_{\ell\ddot{\theta}} = \overline{L^*(\ddot{Y}_z - \ddot{Y}_1)} = \overline{L^*\ddot{Y}_2} - \overline{L^*\ddot{Y}_1} = S_{\ell\ddot{y}_2} - S_{\ell\ddot{y}_1} \tag{6.39}$$

$$(\Delta x)^2 S_{\ddot{\theta}} = \overline{(\ddot{Y}_2 - \ddot{Y}_1)^* (\ddot{Y}_2 - \ddot{Y}_1)} = S_{\ddot{y}_1} + S_{\ddot{y}_2} - 2\mathrm{Re}(S_{\ddot{y}_1\ddot{y}_2}) \tag{6.40}$$

Combining Eqs. (6.38), (6.39), and (6.40)

$$\gamma_{\ell\ddot{\theta}} = \frac{|S_{\ell\ddot{y}_2}|^2 + |S_{\ell\ddot{y}_1}|^2 - 2\mathrm{Re}(S^*_{\ell\ddot{y}_2} S_{\ell\ddot{y}_1})}{S_{\ell}[S_{\ddot{y}_1} + S_{\ddot{y}_2} - 2\mathrm{Re}(S_{\ddot{y}_1\ddot{y}_2})]} \tag{6.41}$$

The effect of channel sensitivity mismatching is to introduce signal-correlated noise. Since this will not be detected by the coherence function there is nothing to be gained by considering $H_1 \neq H_2$ in simplifying Eq. (6.41). So let $H_1 = H_2 = c$. Then since

$$|S_{\ell y_i}|^2 = |c|^2 |S_{\ell e_i}|^2 \tag{6.42}$$

$$S_{\ell\ddot{y}_i} = c\, S_{\ell e_i}$$

etc.

we have from Eq. (6.41) after canceling $|c|^2/|c|^2$

$$\gamma^2_{\ell\ddot{\theta}} = \frac{|S_{\ell e_1}|^2 + |S_{\ell e_2}|^2 - 2\mathrm{Re}(S^*_{\ell e_2} S_{\ell e_1})}{S_{\ell}[S_{e_1} + S_{e_2} - 2\mathrm{Re}(S_{e_1 e_2})]} \tag{6.43}$$

Introducing the definitions of average signal power spectrum $S_{\bar{e}}$ from Eq. (6.22) and spectral discrete difference α from Eq. (6.26) into Eq. (6.43)

$$\gamma^2_{\ell\ddot{\theta}} = \frac{1}{2(1-\alpha)}\left[\frac{|S_{\ell e_1}|^2}{S_\ell S_{\bar{e}}} + \frac{|S_{\ell e_2}|^2}{S_\ell S_{\bar{e}}} - \frac{2Re(S^*_{\ell e_2}\ S_{\ell e_1})}{S_\ell S_{\bar{e}}}\right] \quad (6.44)$$

Combining this with the definition of the single channel coherence function

$$\gamma^2_{\ell e_i} = \frac{|S_{\ell e_i}|^2}{S_\ell S_{e_i}} \quad (6.45)$$

$$\gamma^2_{\ell\ddot{\theta}} = \frac{1}{2(1-\alpha)}\left[\frac{S_{e_2}}{S_{\bar{e}}}\gamma^2_{\ell e_2} + \frac{S_{e_1}}{S_{\bar{e}}}\gamma^2_{\ell e_1} - \frac{2Re(S^*_{\ell e_2}\ S_{\ell e_1})}{S_\ell S_{\bar{e}}}\right] \quad (6.46)$$

Since there is no reason to expect the individual channel coherences to be different any more than the individual channel noises, they will be assumed equal, that is

$$\gamma^2_{\ell e_1} = \gamma^2_{\ell e_2} = \gamma^2_{\ell e} \quad (6.47)$$

Then

$$\gamma_{\ell\ddot{\theta}} = \frac{1}{(1-\alpha)}\left[\gamma^2_{\ell e} - \frac{Re(S_{\ell e_1}\ S^*_{\ell e_2})}{S_\ell S_{\bar{e}}}\right] \quad (6.48)$$

The second term in the brackets is a real, dimensionless function of frequency with both numerator and denominator being products of two power spectra (except for the Re($\cdot$) operator). In these respects, it resembles an ordinary coherence function. It will therefore be given the symbol Γ

$$\Gamma^2 \triangleq \frac{Re(S_{\ell e_1}\ S^*_{\ell e_2})}{S_\ell S_{\bar{e}}} \quad (6.49)$$

With this notation

$$\gamma^2_{\ell\ddot{\theta}} = \frac{\gamma^2_{\ell e} - \Gamma^2}{1-\alpha} \tag{6.50}$$

This is the desired result although it will likely be a poorly conditioned calculation because $\gamma^2_{\ell e}$, Γ^2 and α will all be close to unity for small transducer separation.

6.1.3 Typical Value of Spectral Discrete Difference

The narrowband signal-to-noise ratio S_{NR} and input-output coherence function $\gamma_{\ell\ddot{\theta}}$ for angular responses obtained by differencing have been shown to depend on the spectral discrete difference α. Both of these quantities are of particular interest for the frequency range around a structural resonance. In this section a simple expression is obtained for α in terms of the mode shape associated with a particular resonant frequency. This is useful in order to gain some idea of the difficulty to be expected in measuring α, or more specifically $1-\alpha$.

Suppose a structure is excited at a single degree of freedom by a load $\ell(t)$ with a Fourier transform $L(f)$. Let L be broad band with unit amplitude in the frequency range around an isolated resonance at $f_r = \omega_r/2\pi$. Assume perfect coherence between ℓ and each of the responses $\ddot{y}_1$ and $\ddot{y}_2$. Then

$$\begin{aligned} Y_1 &= H_{01}\, L \\ Y_2 &= H_{02}\, L \end{aligned} \tag{6.51}$$

The subscript 0 in Eq. (6.51) refers to the driving point. Then

$$S_{y_1 y_2} = \overline{Y_1^{*} Y_2} = H_{01}^{*}\, H_{02}\, S_{\ell} \tag{6.52}$$

By the assumption of perfect coherence

$$S_{y_1} = |H_{01}|^2 \, S_\ell$$
$$S_{y_2} = |H_{02}|^2 \, S_\ell \qquad (6.53)$$

Then from Eqs. (6.26), (6.52), and (6.53)

$$\alpha = \frac{2\mathrm{Re}(H_{01}^{*} \, H_{02})}{|H_{01}|^2 + |H_{02}|^2} \qquad (6.54)$$

If f_r is the resonant frequency associated with a normal mode shape vector $\underset{\sim}{\psi}^{(r)}$, the frequency response has the form

$$H_{0i}\ (\omega) = \sum_{r=1}^{N} \frac{\psi_0^{(r)} \psi_i^{(r)}}{(\omega^2 - \omega_r^2) + j\ 2\zeta_r \omega\omega_r} \qquad (6.55)$$

where

$\psi_0^{(r)}$, $\psi_i^{(r)}$ = 0 and i'th entries in mode vector which is asssumed to be real and normalized to unit modal mass

ζ_r = modal damping ratio

For very light damping H_{0i} can be approximated by the rth term of its modal series for $\omega \approx \omega_r$. Using this approximation along with Eq. (6.54)

$$\alpha = \frac{2(\frac{\psi_2}{\psi_1})}{1 + (\frac{\psi_2}{\psi_1})^2} \qquad (6.56)$$

$$1 - \alpha = \frac{(1 - \frac{\psi_2}{\psi_1})^2}{1 + (\frac{\psi_2}{\psi_1})^2} \qquad (6.57)$$

Figure 43 shows a plot of dimensionless signal $1-\alpha$ versus $\frac{\psi_2}{\psi_1} - 1$. This result shows the problem inherent in angular measurement since α departs from unity much more slowly than does ψ_2/ψ_1. To obtain $1-\alpha$ of even .01 requires $\psi_2/\psi_1 = 1.153$. Unless points 1 and 2 on the mode shape ψ fall close to a node point, one can expect the differential signal-to-noise ratio to be markedly worse than that for individual channels.

6.1.4 Flexural Error

At higher frequencies, the magnitude of uncorrelated noise will diminish to insignificance. However, a new limitation will arise. An error limit will be established by the discrete angle approximation itself. In this section, a chart is presented for choosing a separation distance for a given error.

At high frequencies, the bending mode shapes of plates or beams are affected by boundary conditions only near the edges. For a time-random load applied well inside the boundary the high frequency behavior can be interpreted in terms of an infinite plate or beam. The power input at a frequency f will be propagated outward by waves of length λ where λ and f are related by the dispersion relation for bending of beams or plates. If the acceleration distribution is one dimensional (straight crested waves in a plate) with wavelength λ

$$\ddot{y}\,(x) = D \sin \frac{2\pi x}{\lambda} \qquad (6.58)$$

The finite difference approximation to angular acceleration is

$$\hat{\theta} = \frac{\ddot{y}(x_2) - \ddot{y}(x_1)}{\Delta x} = \frac{D}{\Delta x}\left[\sin\left(\frac{2\pi x_2}{\lambda}\right) - \sin\left(\frac{2\pi x_1}{\lambda}\right)\right] \qquad (6.59)$$

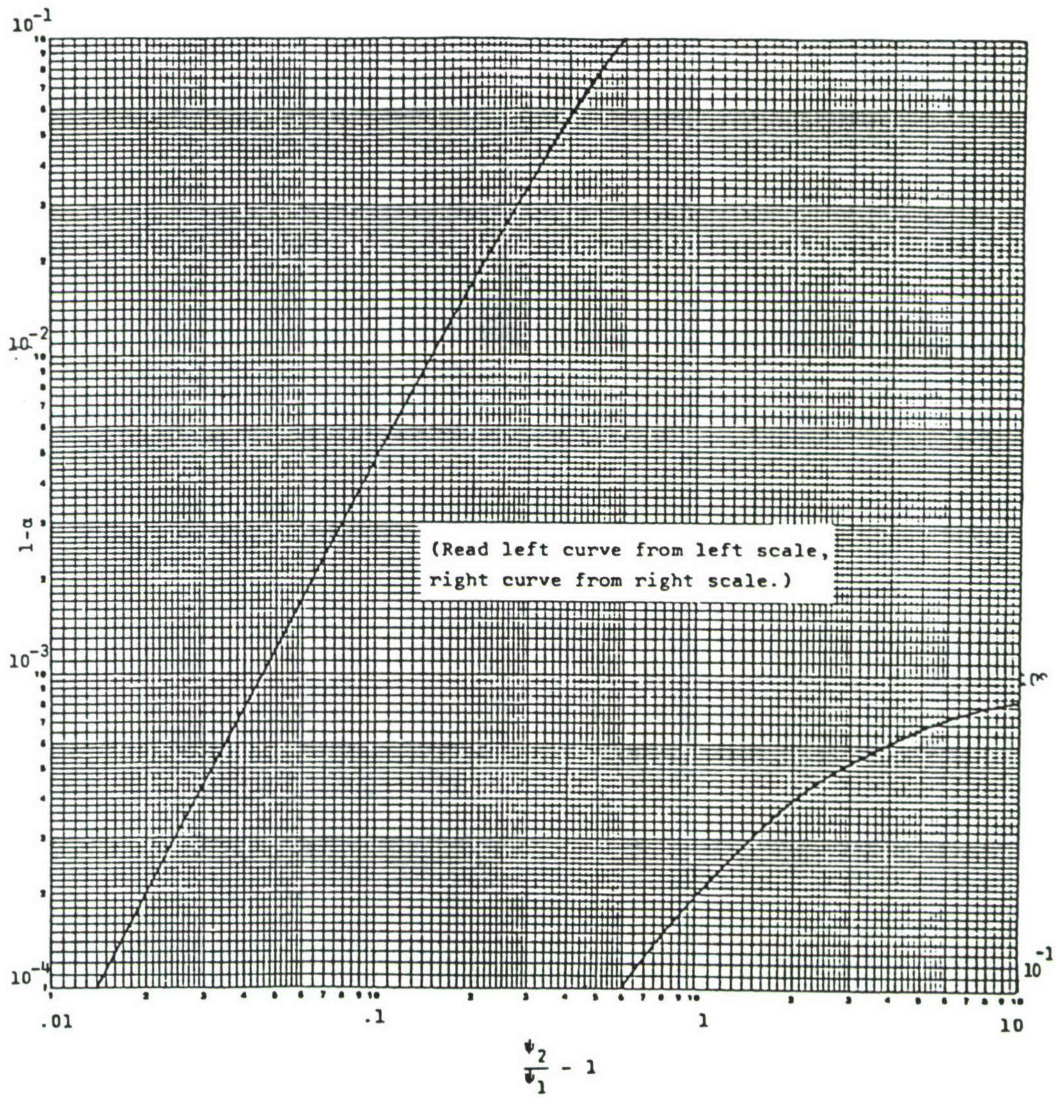

Figure 43 Dimensionless Difference Signal $1-\alpha$ vs. Mode Shape $\underset{\sim}{\psi}$

then if

$$x_2 = x_c + \frac{\Delta x}{2}$$
$$x_1 = x_c - \frac{\Delta x}{2} \qquad (6.60)$$

Equation (6.59) can be rearranged as

$$\hat{\theta} = \frac{2D}{\Delta x} \cos(\frac{2\pi x_c}{\lambda}) \sin(\frac{\pi \Delta x}{\lambda}) \qquad (6.61)$$

The true angular acceleration at $x = x_c$ is

$$\ddot{\theta}(x_c) = \frac{d\ddot{y}}{dx} = \frac{2\pi D}{\lambda} \cos\frac{2\pi x_c}{\lambda} \qquad (6.62)$$

From Eqs. (6.61) and (6.62)

$$\hat{\ddot{\theta}} = [\frac{\sin \frac{\pi \Delta x}{\lambda}}{(\frac{\pi \Delta x}{\lambda})}] \ddot{\theta} \qquad (6.63)$$

The quantity in brackets is the familiar modulation function which occurs when sampling is performed by averaging over a finite interval. Call it $M(\cdot)$.

$$M(\cdot) \stackrel{\Delta}{=} \frac{\sin(\cdot)}{(\cdot)} \qquad (6.64)$$

For straight crested waves in a plate, the dispersion relation is the same as for a simple beam if the Poisson effect is neglected [30].

$$c_b = \sqrt{2\pi f \kappa c_\ell} \qquad (6.65)$$

c_b = phase velocity of bending waves

f = frequency

κ = radius of gyration of section

c_ℓ = extensional wave speed $\sqrt{E/\rho}$

If M_0 is the minimum allowable value of the modulation function ($1 - M_0$ = fractional error), then Eqs. (6.63), (6.64), and (6.65) may be combined to find the frequency above which this error will be exceeded.

$$f = \frac{2}{\pi} c_{\ell} \kappa \left[\frac{M^{-1}(M_0)}{\Delta x}\right]^2 \tag{6.66}$$

Arranging in dimensionless form

$$\left(\frac{f\kappa}{c_{\ell}}\right) = \frac{2}{\pi}\left(\frac{\Delta x}{\kappa}\right)^{-2} [M^{-1}(M_0)]^2 \tag{6.67}$$

This relation is plotted in Figure 44 for various dimensionless separation distance ($\Delta x/\kappa$). For airborne optical system work the areas where one would be likely to place differential transducers are usually on fairly thick, stiff components. Thus, the upper half of Figure 44 is probably the most relevant.

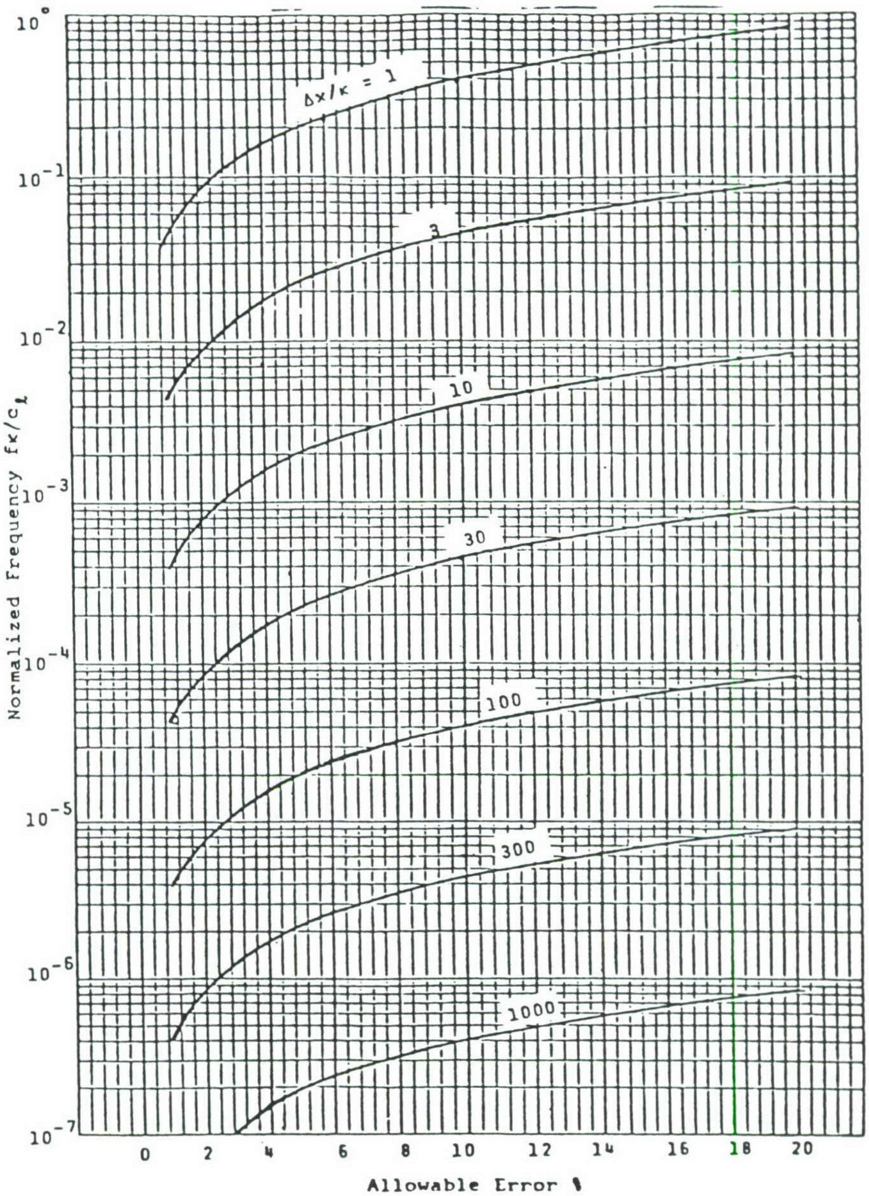

Figure 44 Upper Frequency Limit for Differential Sensing of Angular Vibration

6.2 EXAMPLES

In this section some examples are presented to illustrate the practical meaning of the error sources described in Section 6.1. In addition, a method is demonstrated for reducing the effect of one error source, the interchannel gain and phase mismatch.

6.2.1 Use of Error Formulas

In Section 4.6 of this report, an experiment is described which involves measurement of the PSD of angular acceleration at an interior point on a uniform plate. Error bands for this measurement situation are calculated here as an example. The following data are known:

Plate characteristics	
material	aluminum
thickness	0.090 in.
Young's modulus	10×10^6 lbf/in.^{2}
mass density	2.6×10^{-4} lbf-sec.^{2}/in.^{4}
Poisson's ratio	0.3
Measurement requirements	
minimum frequency	100 Hz.
maximum frequency	1000 Hz.
transducer separation	1.40 in.

It is desired to estimate the differential narrowband signal/noise ratio at the low end of the frequency band and the flexural error at the high end.

The noise spectrum of the accelerometer/signal conditioning system was not measured. However, the transducer sensitivity was less than that of transducer A (see Figure 45) by about a factor of 100. If the curve for transducer A is extrapolated to 100 Hz. and noise power/Hz. is assumed to be proportional to (sensitivity)$^{-2}$, then we may estimate the noise power spectrum at 100 Hz. to be about $2.0 \times 10^{-9} \frac{G^2}{Hz.}$ or 3.0×10^{-4} (in/sec.^{2})^2/Hz. The r.m.s. force input was about

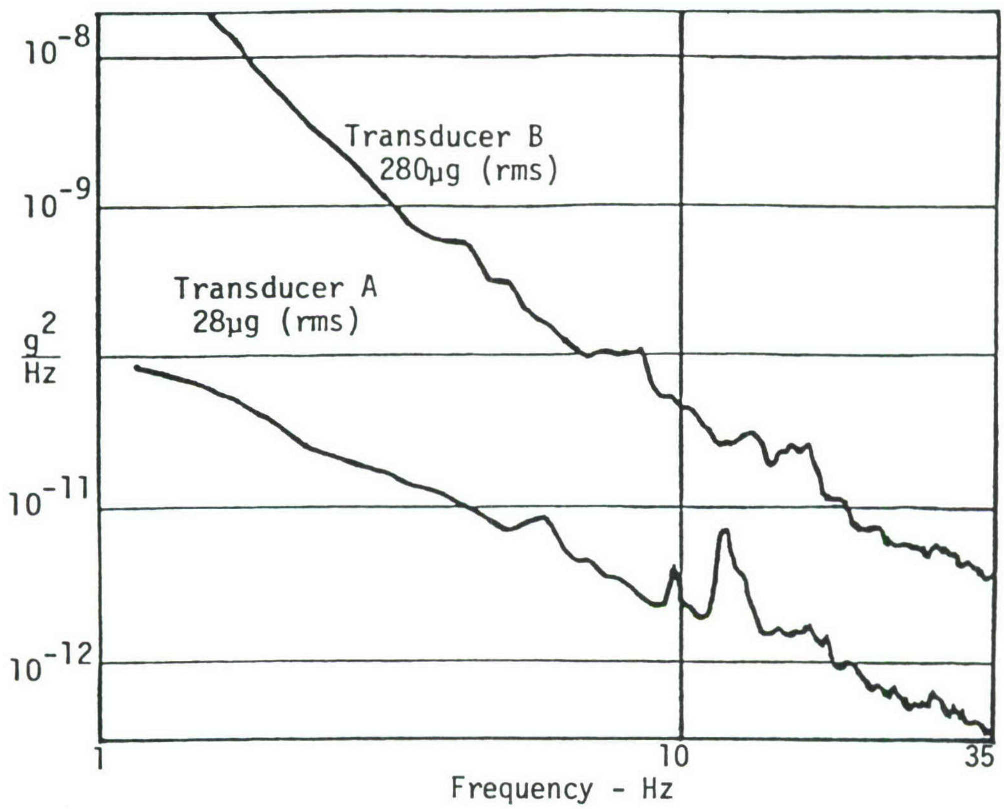

Figure 45 Noise PSD for Two Different Piezoelectric Accelerometers

0.3 lbf. If the force p.s.d. is taken to be constant over 0-1000 Hz. and the plate is approximated as infinite in extent with the thickness and material properties of the actual plate, then the velocity p.s.d. at the drive point is [21]

$$S_{\dot{y}} = \frac{S_f}{(8\rho h\kappa c_\ell)^2}$$

or

$$S_{\ddot{y}} = \frac{S_f\omega^2}{(8\rho h\kappa c_\ell)^2}$$

Computing the signal power/Hz. at 100 Hz.

$$\kappa = \frac{h}{2\sqrt{3}} = \frac{0.090}{2\sqrt{3}} = 0.0260 \text{ in.}$$

$$c_\ell = \sqrt{\frac{E}{\rho}} = \sqrt{\frac{10 \times 10^6}{2.6 \times 10^{-4}}} = 1.96 \times 10^5 \text{in/sec.}$$

$$S_f = \frac{(0.3)^2 \text{ lbf}^2}{1000 \text{ Hz.}} = 9.0 \times 10^{-5} \frac{\text{lbf}^2}{\text{Hz.}}$$

$$S_{\ddot{y}} = \frac{S_f\omega^2}{(8\rho h\kappa c_\ell)^2} = \frac{(9.0)(10^{-5})[(2\pi)(100)]^2}{[(8)(2.6)(10^{-4})(0.090)(0.026)(1.96)(10^{+5})]^2}$$

$$= 39.0 \frac{(\text{in/sec.}^2)^2}{\text{Hz.}}$$

The worst case single channel narrowband noise/signal ratio is thus estimated as

$$\frac{|c^2|S_n}{S_{\bar{e}}} = \frac{3.0 \times 10^{-4}}{39.0} = 7.69 \times 10^{-6} \text{ (-52 dB)}$$

The sensing channels were gain-matched at 300 Hz. prior to use. so residual mismatch will be taken as 0.5% gain and 1.5° phase. The mismatch parameter δ is then

$$\delta = 1.005 \angle 1.5° - 1.000$$

$$= 0.0267 \angle 80.0°$$

$$|\delta|^2 = 7.14 \times 10^{-4}$$

The spectral discrete difference α could be estimated as anything between -1 and +1 since there is no way of knowing where the accelerometers will be placed relative to the shapes of modes which are resonant around 100 Hz. In deriving Eq. (4.78) (which is the prediction this measurement was intended to verify) it was assumed that mode shapes would vary sinusoidally in space in directions parallel to the plate edges. We therefore assume that the mid-point between the accelerometers is halfway between the peak and zero of a sine wave. Some modes will be worse (closer to the peak) and some will be better. The most important modes, i.e. those contributing the most to $\langle\theta^2\rangle_t$, will be those where the transducers are closer to a node. The midway assumption should therefore be conservative. The appropriate wave-length λ can be found from the dispersion relation, Eq. (6.65), and the elementary relation $c_b = f\lambda$.

$$\lambda = \frac{2\pi\kappa c_\ell}{f}$$

$$\lambda = \frac{(2\pi)(0.026)(1.96)(10^5)}{100}$$

$$\lambda = 17.9 \text{ in.}$$

The values of $k_{xi}x$ (see Section 4.4) corresponding to the transducer locations are thus $\frac{\pi}{8} \pm \frac{2\pi\Delta x}{2\lambda}$ or

$$\frac{\pi}{8} \pm \frac{2\pi\Delta x}{2\lambda} = \frac{\pi}{8} \pm \frac{(2\pi)(1.40)}{(2)(17.9)} = 0.146,\ 0.638 \text{ radians}$$

The representative value of α is then, by Eq. (6.56)

$$\alpha = \frac{2[\frac{\sin(.638)}{\sin(.146)}]}{1 + [\frac{\sin(.638)}{\sin(.146)}]^2} = 0.461$$

The worst case differential narrowband signal/noise ratio is, by Eq. (6.27)

$$S_{NR} = \frac{4(1-\alpha)}{|\delta|^2 (1+\alpha) + 4(\frac{|c|^2 S_n}{S_{\bar{e}}})}$$

$$= \frac{4(1 - 0.461)}{[(7.14)(10^{-4})(1 + 0.461) + 4(7.69)(10^{-6})]}$$

$$= 2.01 \times 10^3 \text{ (33.0 dB)}$$

This level of signal fidelity should be quite adequate for the intended purpose.

To compute worst-case flexural error, we calculate the wavelength associated with the highest frequency of interest, 1000 Hz.

$$\lambda = \frac{2\pi\kappa c_\ell}{f} = \frac{(2\pi)(0.026)(1.96)(10^5)}{1000} = 5.66 \text{ in.}$$

Then, using Eq. (6.63)

$$\frac{\hat{\ddot{\theta}}}{\ddot{\theta}} = \frac{\sin(\frac{\pi\Delta x}{\lambda})}{\frac{\pi\Delta x}{\lambda}} = \frac{\sin[\frac{\pi(1.40)}{5.66}]}{[\frac{\pi(1.40)}{5.66}]} = 0.902$$

The effective reduction will actually be even less than 10% since the dominant contributions to $\theta_{r.m.s.}$ come from frequencies well below 1000 Hz. (see Figure 17).

6.2.2 Effect of Single Channel Noise

To illustrate the effect of uncorrelated noise in individual accelerometer channels, a simple experiment was performed.

A slender aluminum I-beam was suspended in a horizontal position by long cords to simulate a free-free condition. It was vibrated by a small shaker driving in the beam's weak direction at a point slightly off midspan. A time-random force

signal was input and rotations at various points along the beam's length were sensed by analog differencing of accelerometer outputs. Frequency responses between angular acceleration output and point force input were measured and curve-fitted to estimate the first few normal mode shapes in slope coordinates [16]. The experiment was repeated with two different accelerometer pairs of substantially different noise performance. Measured noise power spectra for both are shown in Figure 45. The force input was identical in both cases and was much smaller than one would normally use in modal survey work in order to emphasize the effect of random noise in the sensor channels. The shape of the second bending mode as measured by each transducer pair is shown in Figure 46. Since the beam was uniform, any deviation from a smooth curve indicates error in the measurement. The improvement with lower noise transducers is evident.

6.2.3 Effect of Interchannel Gain and Phase Mismatch

The derivation leading to Eq. (6.27) suggests a method for removing, or at least reducing, signal-correlated error due to mismatching. The method is basically to measure the complex (i.e., both gain and phase) mismatch between the two sensing channels as a function of frequency and use it to apply a small correction to the data coming from one channel prior to differencing. Mathematically, if we define a correction function H_c as $H_c(f) = H_2(f)/H_1(f)$, then the corrected PSD of $(e_2 - e_1)$ may be calculated either as

$$S_{(e_2-e_1)} = S_{e_2} + |H_c|^2 S_{e_1} - 2 \text{ Re}[H_c S_{e_2e_1}] \tag{6.68}$$

or as

$$S_{(e_2-e_1)} = \overline{|E_2 - H_cE_1|^2} \tag{6.69}$$

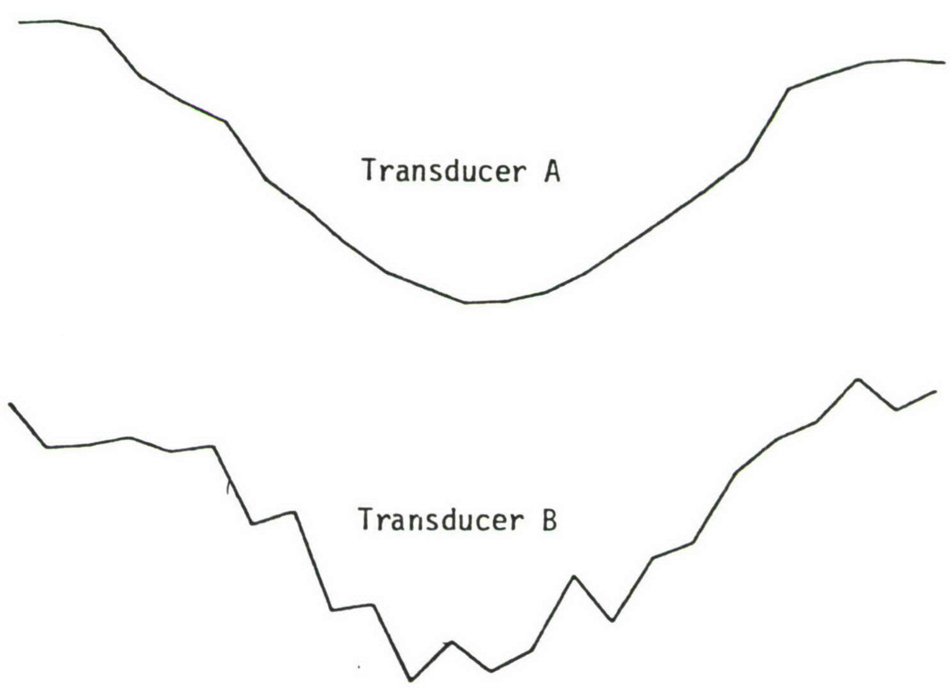

Figure 46 Second Bending Mode in Slope Coordinates of Free-Free Beam Measured with Accelerometers of Different Noise Performance
Beam Length = 610 cm.
Section Radius of Gyration = 1.47 cm.
Mode Frequency = 18.7 Hz.

The former implementation is computationally faster since only ensemble averages are corrected rather than the discrete Fourier transform of each frame of data. However, the latter is far less sensitive to digital round-off error. It has been found to be superior for use with the 10 or 12 bit A/D converters and 16 bit word length generally found in minicomputer-based laboratory data systems.

The measurement of H_c is of course quite critical in the method. It is accomplished by using a shaker to input exactly the same broadband random acceleration to both transducers. H_c is then computed simply as $S_{e_1 e_2}/S_{e_1}$ for this excitation. It should be noted that the correction function measured in this way will include mismatch between the low-pass anti-aliasing filters which must be inserted prior to digitizing. Their mismatch will generally be larger than the combined mismatch of all other elements in the channels. Thus, it is not correct to use H_c measured by this method to compute $\delta(f)$ in Eq. (6.27) if analog differencing prior to digitization is to be used. It is correct if differencing is to be done after digitization, although this would clearly be an inferior method.

A second experiment was performed to illustrate the effects of interchannel mismatch and to test the correction method described above.

A short section of aluminum I-beam was mounted as shown in Figure 47. Dimensions and mounting were chosen so as to approximate pinned-free end conditions. It was driven in the stiff direction by a shaker attached at the point calculated to be a node of the first flexural mode. Frequency responses between acceleration outputs at various points along the beam and force input were measured over 0 - 1.5k Hz. It was established that by careful adjustment of the mounting, it was possible to obtain a frequency response which was flat within a few percent up to 700 Hz. The amplitude of the function was also found to be directly proportional to the distance from the

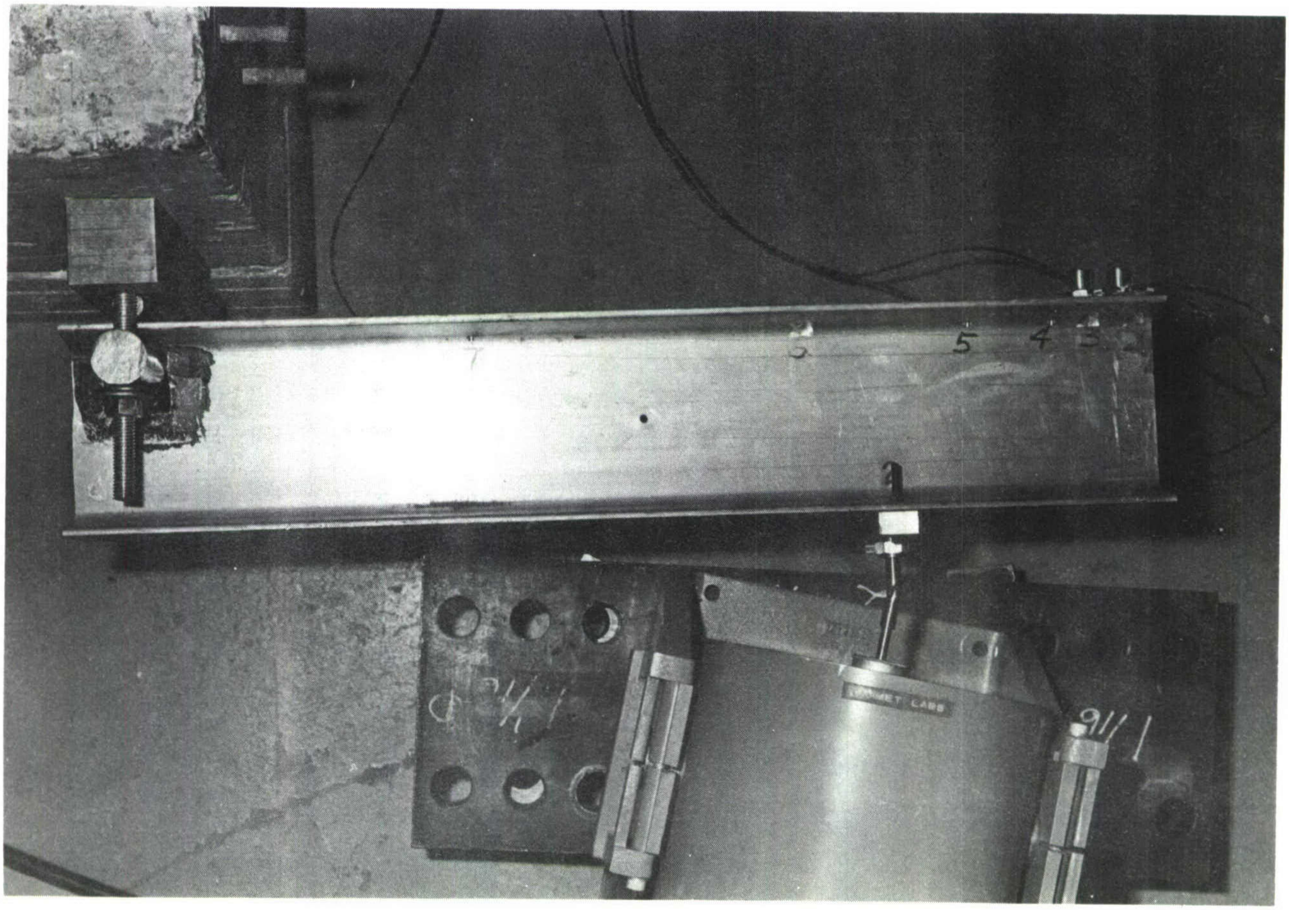

Figure 47 Test Structure for Evaluating Angular Acceleration Measurement Methods. Short I-Beam is Mounted in a Fixed-Free Condition and Driven by a Small Shaker.

pivot point to the acceleration sensor. Thus, it could be concluded that over this frequency range the beam behaves as a rigid body with a fixed axis of rotation. This implied that angular acceleration and its PSD could be accurately measured without differencing using only a single translational sensor. This measurement could then be used to check measurements made by differencing. In addition, dimensionless difference signal $1 - \alpha$ for any separation distance could be computed from Eq. (6.57) by taking ψ_2 and ψ_1 as the distances from the pivot point to the sensors. The experiment was set up and a time-random drive signal with a highly repeatable spectrum was established. Angular acceleration and its PSD were then measured by four methods.

1. Acceleration at a single point was measured and scaled by $1/x_p$ where x_p was the distance from pivot to sensor.

2. Accelerations at two points along the beam were transduced, analog differenced, and the result scaled by $1/\Delta x$ where Δx was the sensor separation distance. Channel gains upstream from the differencing amplifier were set according to the transducer manufacturers calibration data.

3. Procedure was identical to 2 except that the gain of one signal channel (transducer plus charge amplifier) was adjusted to exactly match the other at one frequency (300 Hz.). This required a gain adjustment of 0.4% relative to that used in 2.

4. A correction function H_c was measured for the two sensing channels at their nominal gains. Data from both channels were digitized and the PSD of their difference, corrected for mismatch error, was computed per Eq. (6.69). It was then scaled by $1/(\Delta x)^2$.

Two different separation distances were used for methods 2, 3, and 4. Data from method 1 is considered to be the most accurate and may be used to evaluate the other methods. Some details of the setup are given in Table 4.

TABLE 4

TEST CONDITIONS FOR SHORT BEAM EXPERIMENT USED TO INVESTIGATE MISMATCHING ERROR

Case	ψ_1 cm.(in.)	ψ_2 cm.(in.)	$1 - \alpha$
A	58.57(23.061)	60.96(24.000)	0.000796
B	50.55(19.900)	60.96(24.000)	0.0174

Case A is a fairly demanding measurement situation because of the combination of moderately high frequency and small dimensionless difference signal. Case B is probably more typical of day-to-day applications in optical systems. Results are shown in Figure 48 for Case A ($1-\alpha = 0.0008$) and Case B ($1-\alpha = 0.0174$). For Case B, analog differencing with no special attention to balancing is satisfactory. For Case A, a drastic improvement is realized by more careful analog balancing but some error is still evident. Digital frequency compensation shows the best performance in this difficult case. All PSD's were measured by ensemble averaging of 300 frames with 2.25 Hz. frequency resolution. These were then smoothed by averaging in frequency over 16 spectral lines. The resultant estimate is thus based on 9600 statistical degrees of freedom which provides the smooth curves desirable for comparison.

In summary, it appears that the extra setup effort and data processing required by the frequency compensation method are justified only in severe cases. Such cases may be identified as those involving small transducer separations (a few cm. or less), high frequencies (200 Hz. or more), or high common mode accelerations. It may also be worthwhile if sensors of different types or low resonant frequencies (less than ten times the desired data bandwidth) are to be paired. Attention to accurate gain matching, however, is always worthwhile if analog differencing is used.

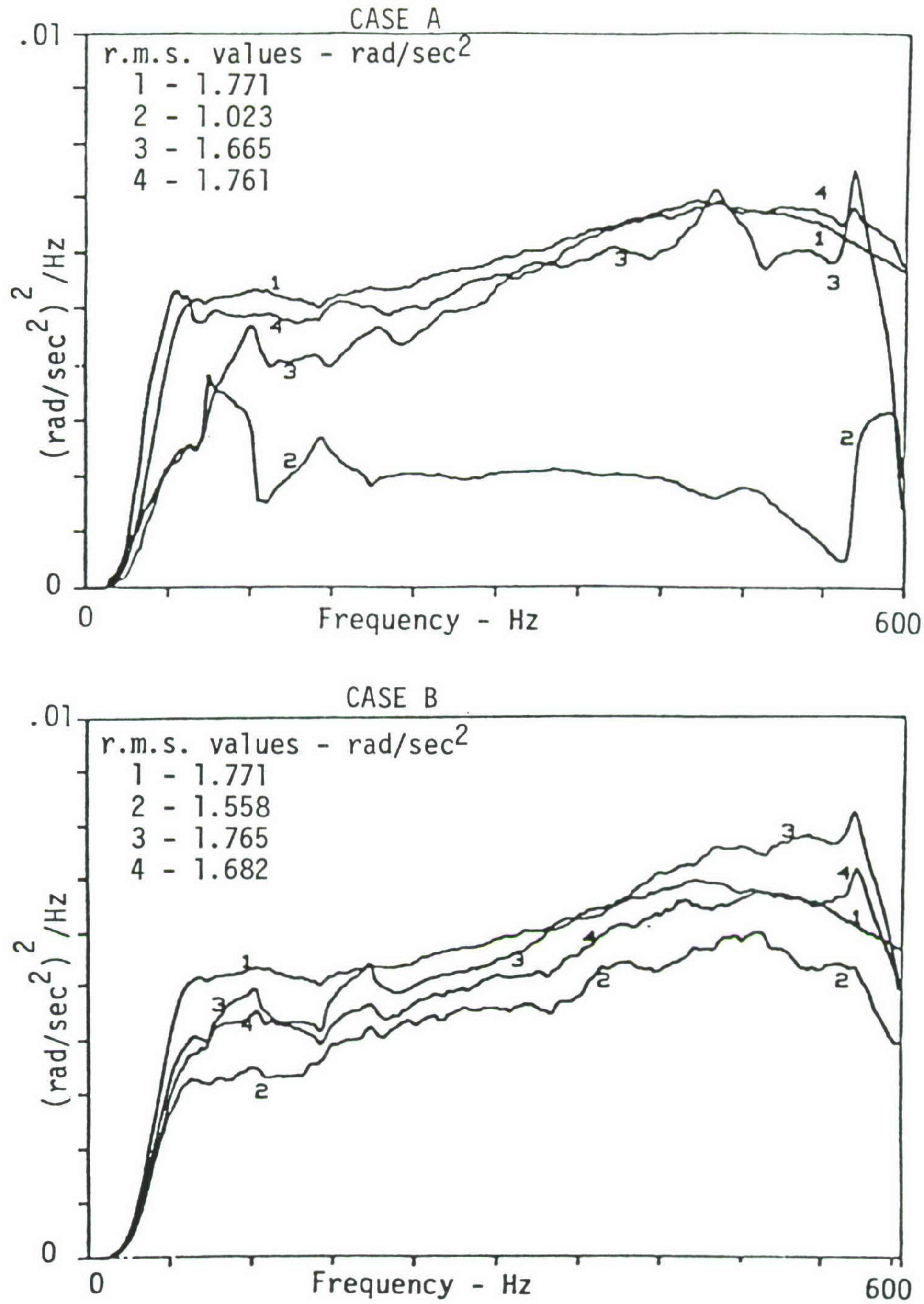

Key
1 = scaled from single point acceleration
2 = analog differenced with nominal channel gains
3 = analog differenced with gains matched at 300 Hz.
4 = digital differenced in frequency domain after correction

Figure 48 Measured PSD of Angular Acceleration of a Rigid Body with One Axis Fixed

6.3 CONCLUSION

Theoretical expressions have been developed for use in evaluating or predicting the validity of two types of angular acceleration spectral data obtained by differencing of linear transducer outputs. These are response power spectra and single input-single output frequency responses. A non-dimensional difference signal quantity α and a coherence-like quantity Γ have been defined. They are indices which may be used to compute figures of merit in the process of measuring power spectra and frequency responses of differential quantities by digital Fourier transform methods.

Experiments have been carried out to demonstrate the undesirable effects of single channel noise and interchannel mismatch as well as to test a method of reducing errors due to the latter.

The work described in this chapter has led to three principal conclusions regarding angular vibration measurement:

(1) Measurement by analog differencing of accelerometer signals is, in general, an excellent method for day-to-day development work provided frequencies are not below 30-50 Hz., transducers with good noise performance are used, and some attention is paid to analog gain matching.

(2) For certain critical measurements such as high-frequency angular vibration of mirror surfaces, differencing of acceleration signals may be the only practical method.

(3) Errors in differential measurement due to channel mismatching may be reduced by digital frequency domain processing although this is warranted only in difficult measurement situations.

SECTION VII

TEST AND EVALUATION OF PREDICTION METHOD

During Phase III of this contract, a test was performed to assess the accuracy and usability of prediction techniques for angular vibration which were developed during Phases I and II. Initially, it was expected that tests of both low and high frequency methods would be performed during Phase III, and that the procedure would involve forced vibration tests of a fairly complex airframe-like structure. The test plan was later reduced in scope to concentrate on evaluation of Semi-Loof/NASTRAN methods for low frequency prediction. This decision was made at the end of Phase II after consultation with AFFDL. It was motivated by several factors.

(1) Since the Semi-Loof implementation had nearly reached the status of a deliverable product, its testing and evaluation were given priority over that of high frequency methods where the work was still relatively basic and exploratory.

(2) The SEA work had not yet reached the stage where application to a realistic airframe structure would be meaningful. It was felt that, at a minimum, an SEA model should be able to account for connections between components at multiple degrees of freedom in order to be worth testing on a simulated airframe/optical system.

(3) The time and cost of completing the Semi-Loof development, modeling a reasonable airframe section, and testing to evaluate the model were thought to be fairly predictable. Together with reporting requirements, they accounted for about 85% of the available Phase III man-hours. Thus, there was no real possibility of significant further SEA development, let alone its testing, during Phase III.

For these reasons, the Phase III test was confined to measurement and prediction of low frequency response of a section of an aircraft fuselage under known excitation.

Section 7.1 describes the test object and its preparation. Section 7.2 describes the Semi-Loof finite element model and demonstrates the use of the pre- and post-processors with NASTRAN. In Section 7.3, the experimental procedure and equipment are described, and Section 7.4 presents the comparison of predicted and measured responses.

7.1 DESCRIPTION OF THE TEST OBJECT

The structure chosen as a test case for the Semi-Loof element was a rear fuselage section of a 1950 vintage Marine fighter aircraft. It was located at the Alameda Naval Property Disposal Yard. With the cooperation of AFFDL/FBG, it was acquired and transported to Anamet's laboratory in San Carlos, California. It is shown, as received, in Figures 49 and 50, and after preparation in Figures 51 - 53. The preparation consisted of removing all wiring and hydraulics, general cleaning, and removal of several feet from the front, as well as the vertical stabilizer, in order to reduce the specimen to manageable size. The prepared structure weighed 334 pounds.

The structure is made up primarily of flat and singly curved panels with extensive stiffeners. There are a number of major ring stiffeners which probably carried concentrated loads, as well as numerous short minor stiffeners attached to individual panels. A box section built into the floor appears to have been an electronics bay. The top of the box also served as the rear engine mount.

While the test structure is by definition aircraft-like in construction, it may not be entirely typical. The fuselage section contains heavy forgings which carried concentrated loads from the vertical stabilizer, the carrier arresting hook, and the jet engine. However, these forgings are tied together by shell structure, which should make the overall object a good test case for Semi-Loof modeling. In addition, the nearly-rigid forgings make excellent response points for measuring angular vibration.

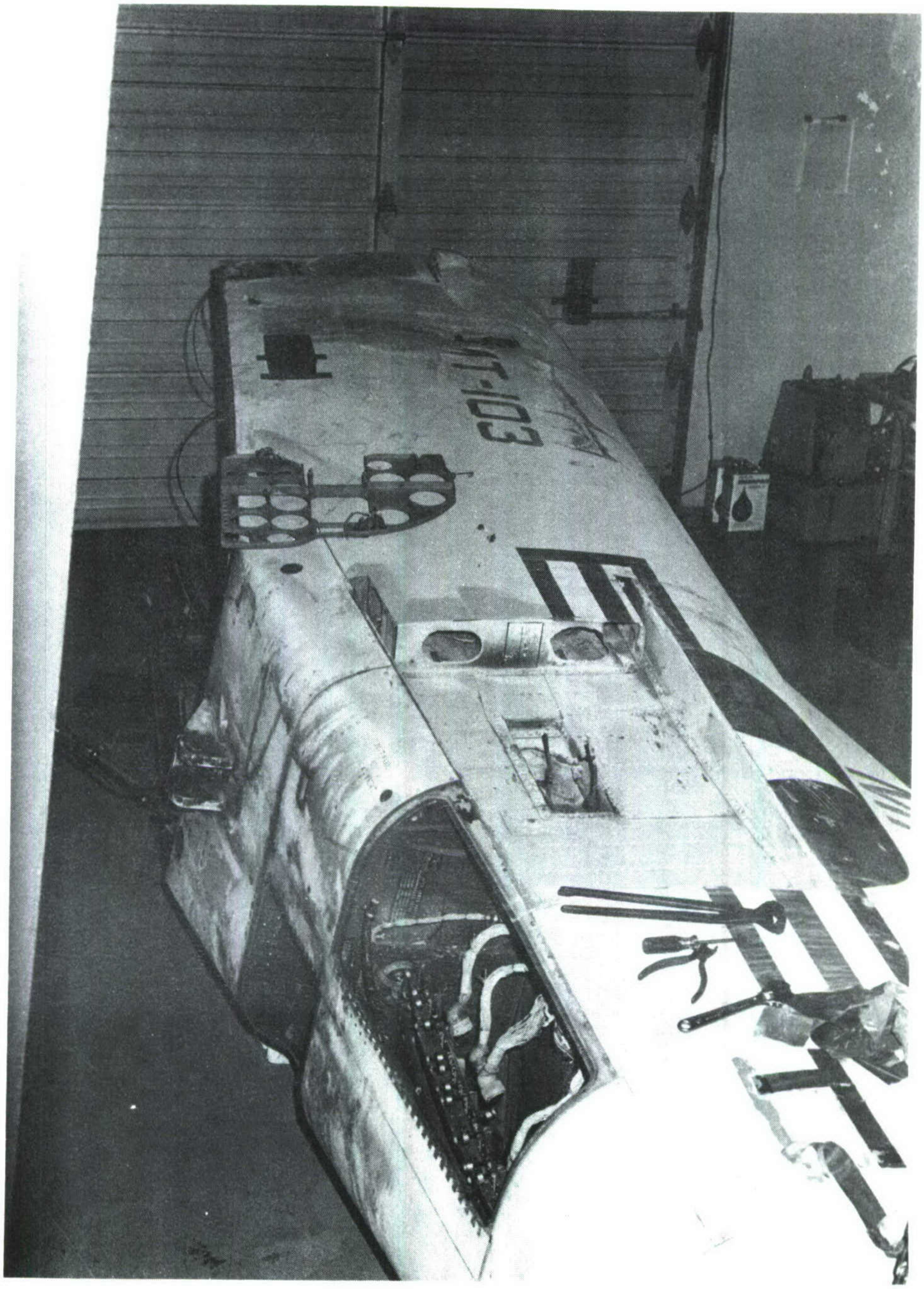

Figure 49 Exterior View of Test Fuselage in As-received Condition

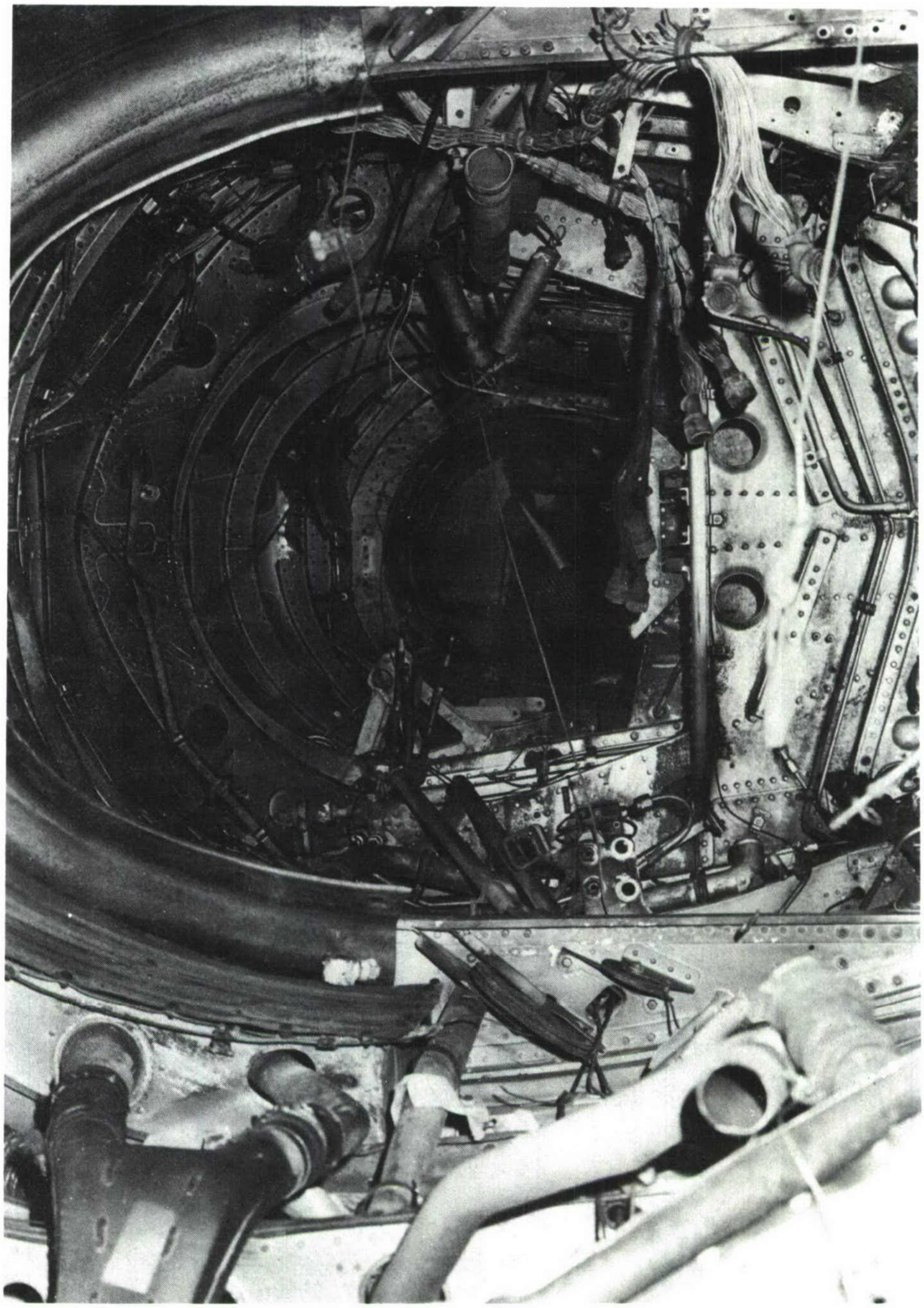

Figure 50 Interior View of Test Fuselage in As-received Condition

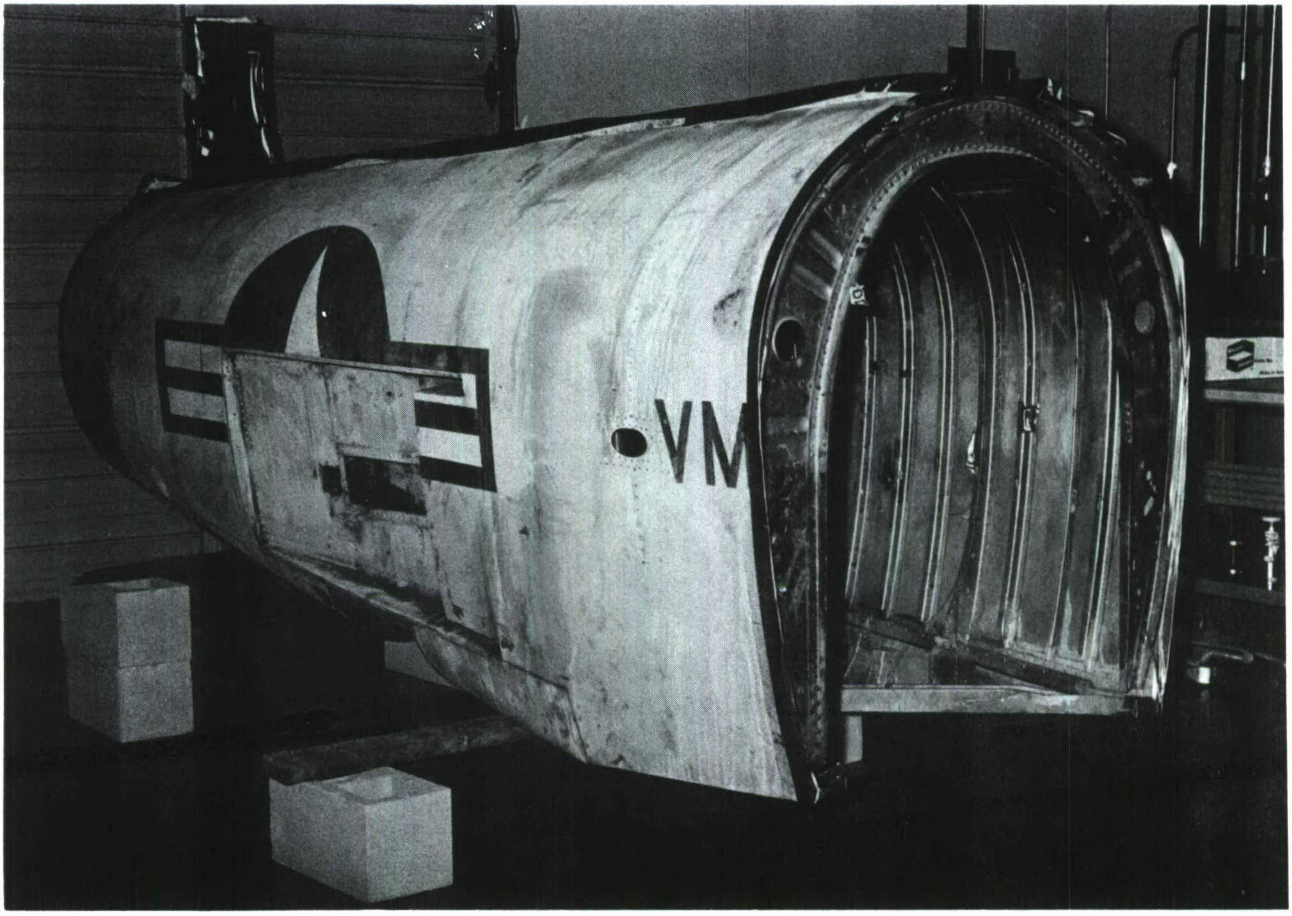

Figure 51 External View of Prepared Test Fuselage

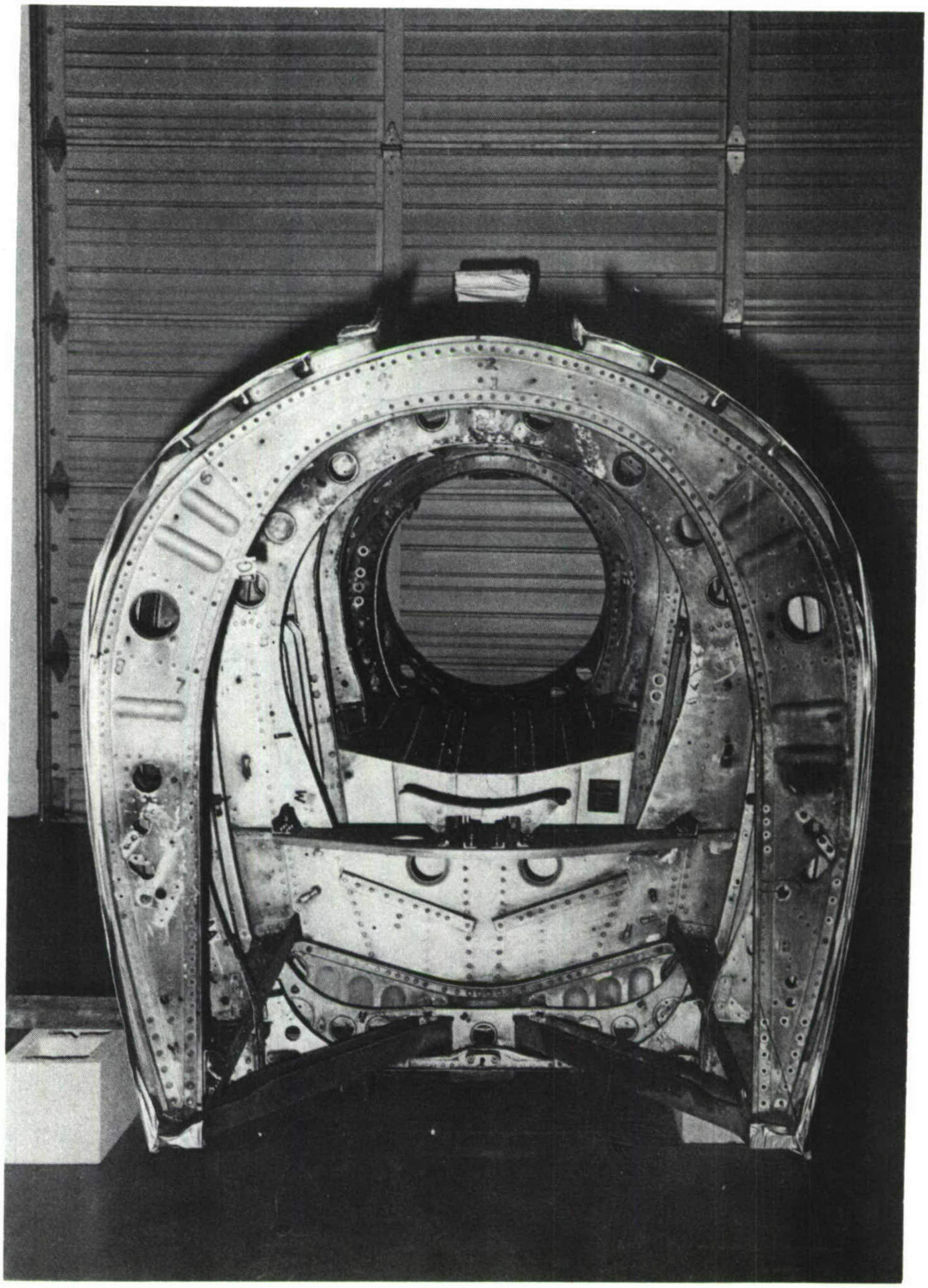

Figure 52 Internal View of Prepared Test Fuselage

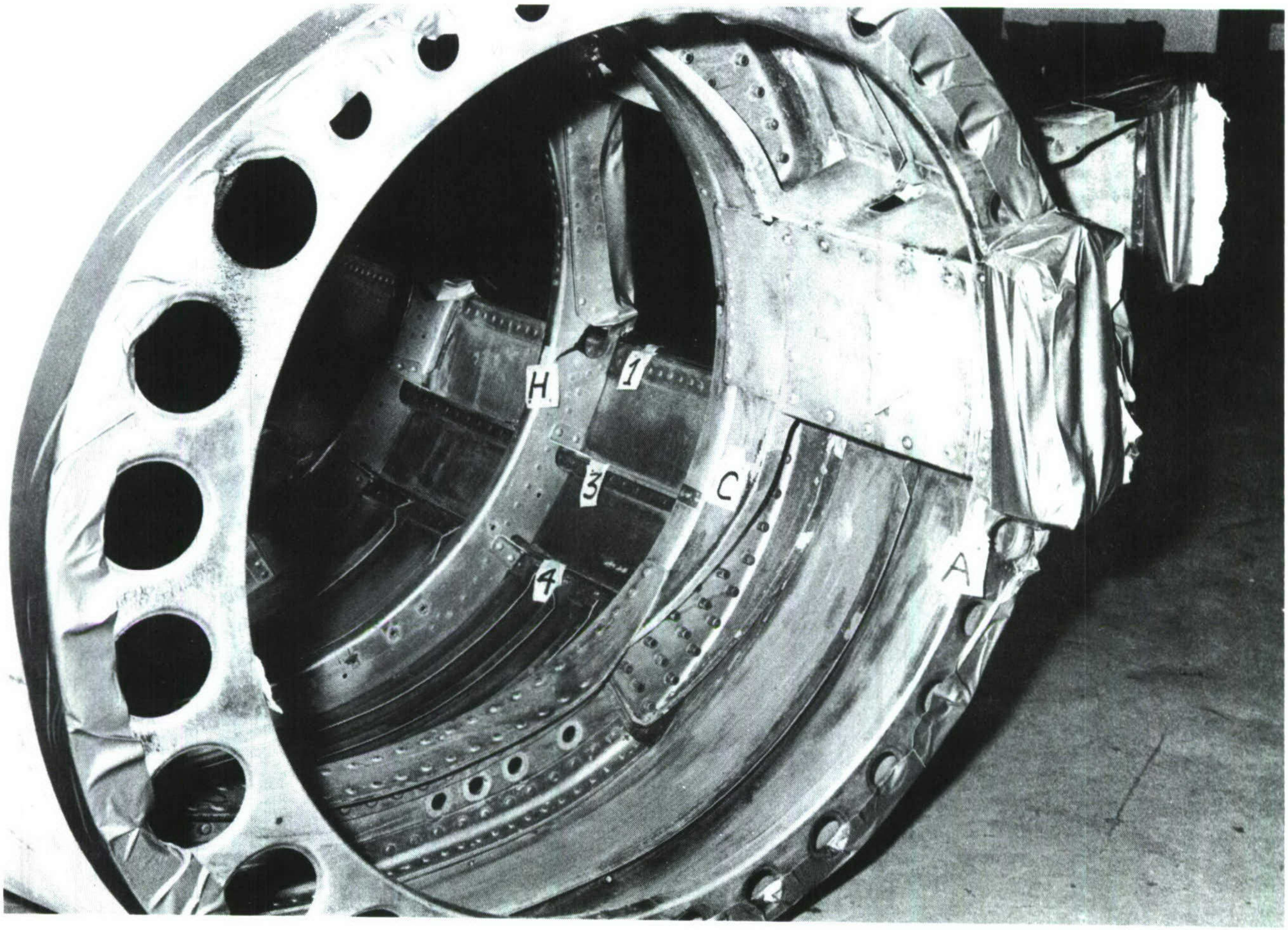

Figure 53 Rear View of Prepared Test Fuselage Showing Construction Details

7.2 FINITE ELEMENT MODEL

An outline of the Semi-Loof model of the fuselage is shown in Figure 54. The lines shown are the boundaries of the shell elements used. Beam elements are not shown. Symmetry was assumed about a vertical plane running along the axis of the fuselage, in spite of some minor differences between one side and the other. While the structure is geometrically symmetric, or nearly so, individual mode shapes are either symmetric or anti-symmetric. Two options were available for handling the symmetry plane. One was to compute two distinct sets of vibration nodes: one with symmetric boundary conditions [$f(y)=f(-y)$], and one with anti-symmetric boundary conditions [$f(y)=-f(-y)$]. These sets would then have to be merged prior to performing frequency response analysis. Although this approach was feasible, it was discarded because of the uncertain logistics involved in merging the two sets of nodes. Instead, the other side of the fuselage was generated by reflection about the symmetry plane, using a small Fortran program. A complete listing of the input data can be found in Appendix C.

Major rib stiffeners were modeled by offset curved LOOF3 beam elements. The skin was modeled by a single row of LOOF8 (and some LOOF6) curved shell elements between major ribs. Most of the skin was stiffened by minor ribs and/or stringers, mostly with a "Z" cross-section. These minor stiffeners were "smeared" into the shell structure using the procedure outlined in Appendix A for calculating equivalent homogeneous orthotropic shell properties based on stiffener section properties, stiffener spacing, and skin properties. In fact, the PLOOFX data card described in Appendix A was developed specifically for this application. In all, the model contains 585 grid points, 142 LOOF8 quadrilaterals, 57 LOOF6 triangles, and 194 LOOF3 beam elements.

Additional LOOF8 elements were used for the floor, mentioned previously, and miscellaneous beams and rigid masses were used as needed. Material density was increased 5% to

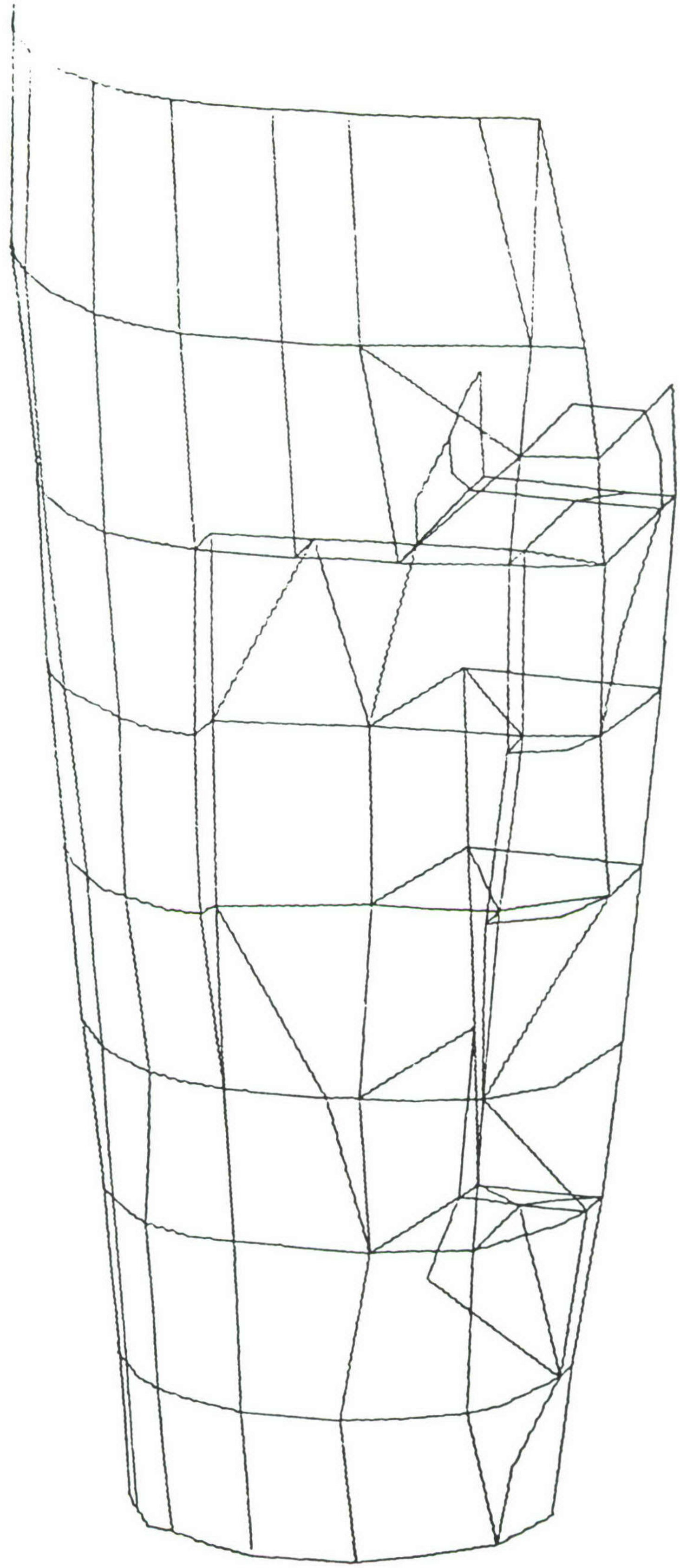

Figure 54   Semi-Loof Fuselage Model

account for rivets. With this adjustment, the total weight predicted by the model was 321 lbs. versus 334 lbs. measured.

The BANDIT node resequencing program was modified to recognize Semi-Loof elements and was used to generate SEQGP cards, which reorder the grid points for minimum bandwidth and thus reduced solution times.

Following usual analysis procedures, a static run with uniform external pressure was made to check out the connections and support conditions of the model. Following this a free vibration run was performed to extract natural frequencies and mode shapes. Finally, several short runs were made to produce frequency response and PSD curves. These latter runs used the NASTRAN Checkpoint/Restart feature to use information saved from the free vibration run. In each case, responses were computed over a range of 40 to 160 Hz. The 0-40 band was eliminated because the "free-free" modes actually had frequencies up to about 5 Hz. due to finite stiffness of the supports, and no attempt was made to model these supports with finite elements. Approximate modal damping values were used, based on experimental values. Damping was quite light and thus rather insignificant except perhaps for the heights of peak responses.

7.3 TEST DESCRIPTION

A series of forced vibration tests were carried out on the aircraft fuselage section described in Section 7.1. The tests were designed to furnish data for evaluating the Semi-Loof finite element model described in Section 7.2 and thereby, the Semi-Loof element itself. The experimental procedure and equipment are described in this section. Experimental results and comparisons with predictions are in Section 7.4.

7.3.1 Overview

Most linear dynamic response simulation under NASTRAN is done by normal mode methods. Thus, in developing a new element, one would like to make measured-vs.-predicted comparisons in terms of properties of individual modes. However, in the current case, this approach was not practical. In principle, it should be sufficient to compare predicted and measured values of natural frequencies and selected entries of the mode shape vectors (after normalizing to equal modal mass) which correspond to critical displacements and rotations. This implies that only a cursory modal survey covering the selected response points should be necessary. However, for a complex structure with numerous normal modes such as the fuselage, the task is not this easy. Unless natural frequency predictions are known in advance to be quite accurate, one is never sure which predicted normal mode should be compared with which measured mode. The usual solution is to measure mode vector entries for enough response locations to obtain a reliable physical picture of the overall mode shape. For example, one might identify a particular mode as the "first twisting" or "first bending" mode. Unfortunately, the time and cost allotted to testing of the fuselage under this contract were not adequate to allow a modal survey of this order, even with modern computer-based methods.

The approach actually taken was to perform a test which would measure the accuracy of the finite element model in an

end-to-end sense. What was given up in order to meet time and cost limits was detailed information about individual modes which one might use to improve the model.

The test consisted of mounting the fuselage on a soft suspension to simulate a free-free condition and measuring a number of acceleration/force frequency responses. Both linear and angular accelerations were taken as response variables. Input was a single point force in all cases. The frequency responses were measured in digital form and stored on disc for later processing and comparison with NASTRAN predictions. The functions were converted digitally to displacement/force frequency responses and these were used to predict displacement PSD's and r.m.s. values for a specified force input PSD. This computational procedure facilitated comparison with NASTRAN predictions in terms of output PSD and r.m.s. quantities. An important practical advantage is that NASTRAN and experimental output quantities could be compared on the basis of identical input force PSD without requiring precise closed loop control of the experimental input.

7.3.2 Test Procedure

Diagrams of the test object showing input and response point locations are presented as Figures 55 through 57. Table 5 gives the location, direction, and type (translation or rotation) of all degrees of freedom. Table 6 shows which of the possible entries of the frequency response matrix were actually measured. Each column represents a different input degree of freedom (shaker location) and each row represents a different response quantity. A total of 3 shaker locations were used in an attempt to acquire at least one frequency response function with a significant contribution from each mode in the 0-160 Hz measurement band. A total of 16 response degrees of freedom were used, of which 8 represented translations and 8 represented rotations. From Table 6 it may be observed that

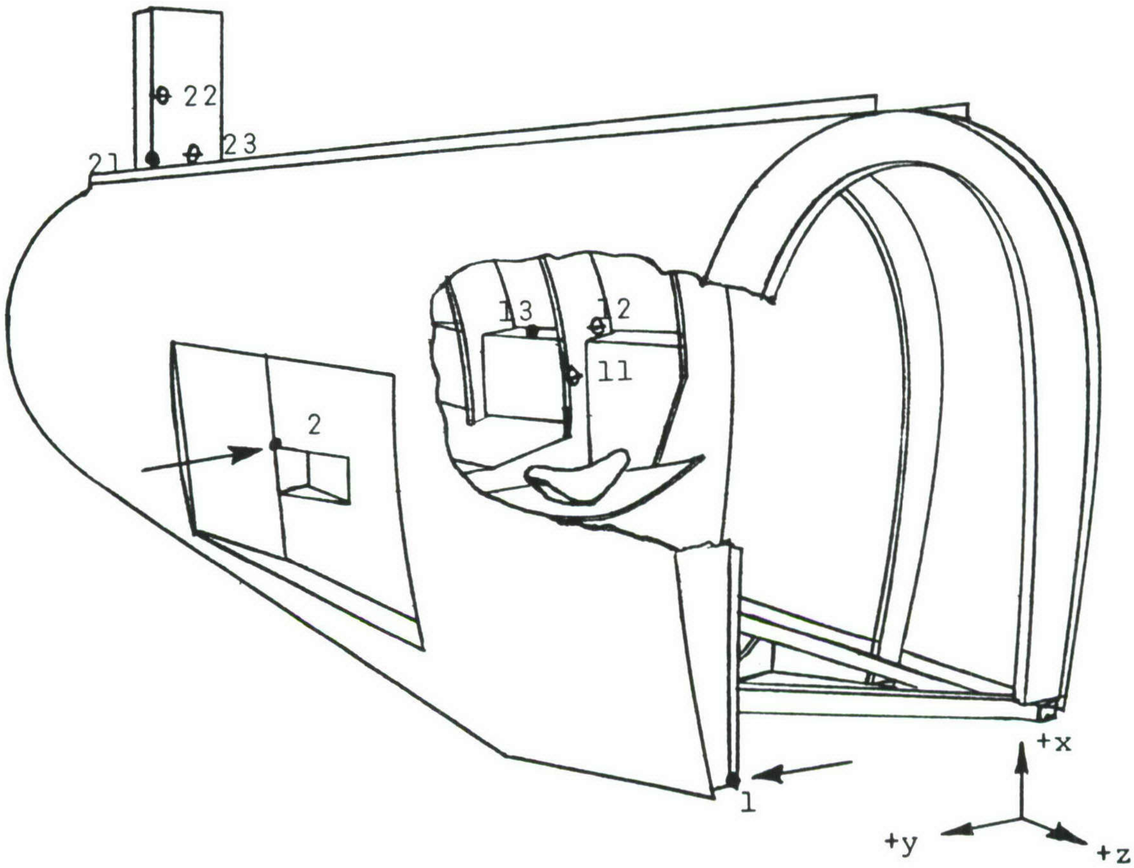

Figure 55 Sketch of Test Object Showing Input Force Location and Direction (Arrow), Translational Response Sensor •, and Rotational Response Sensor θ

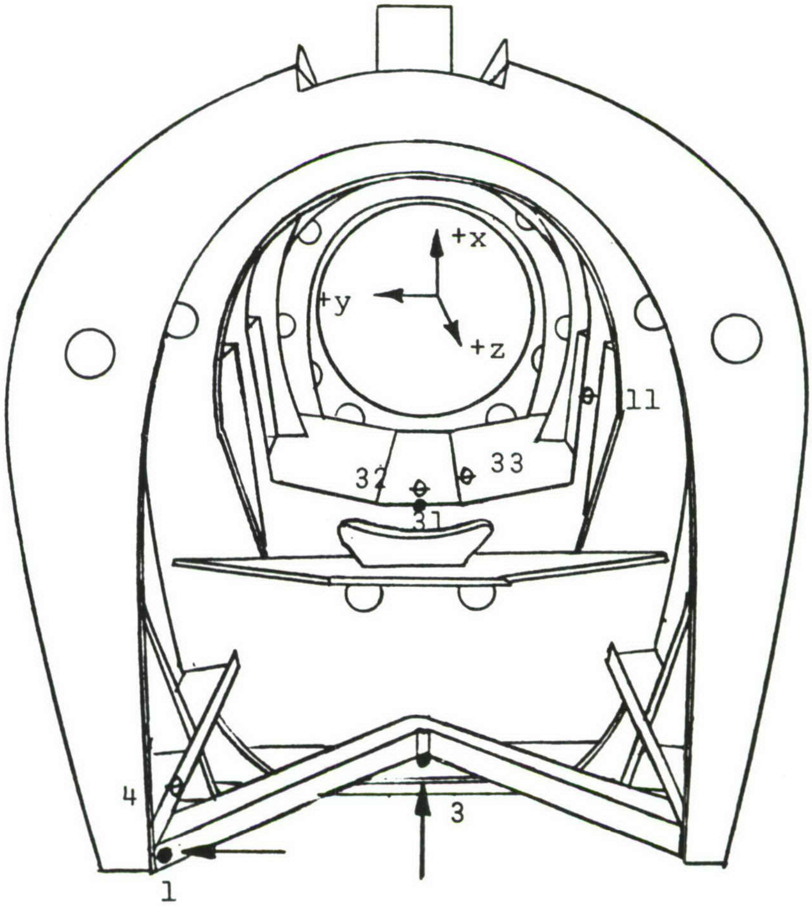

Figure 56 Front View Sketch of Test Object Showing Input Force Location and Direction (Arrow), Translational Response Sensor •, and Rotational Response Sensor θ

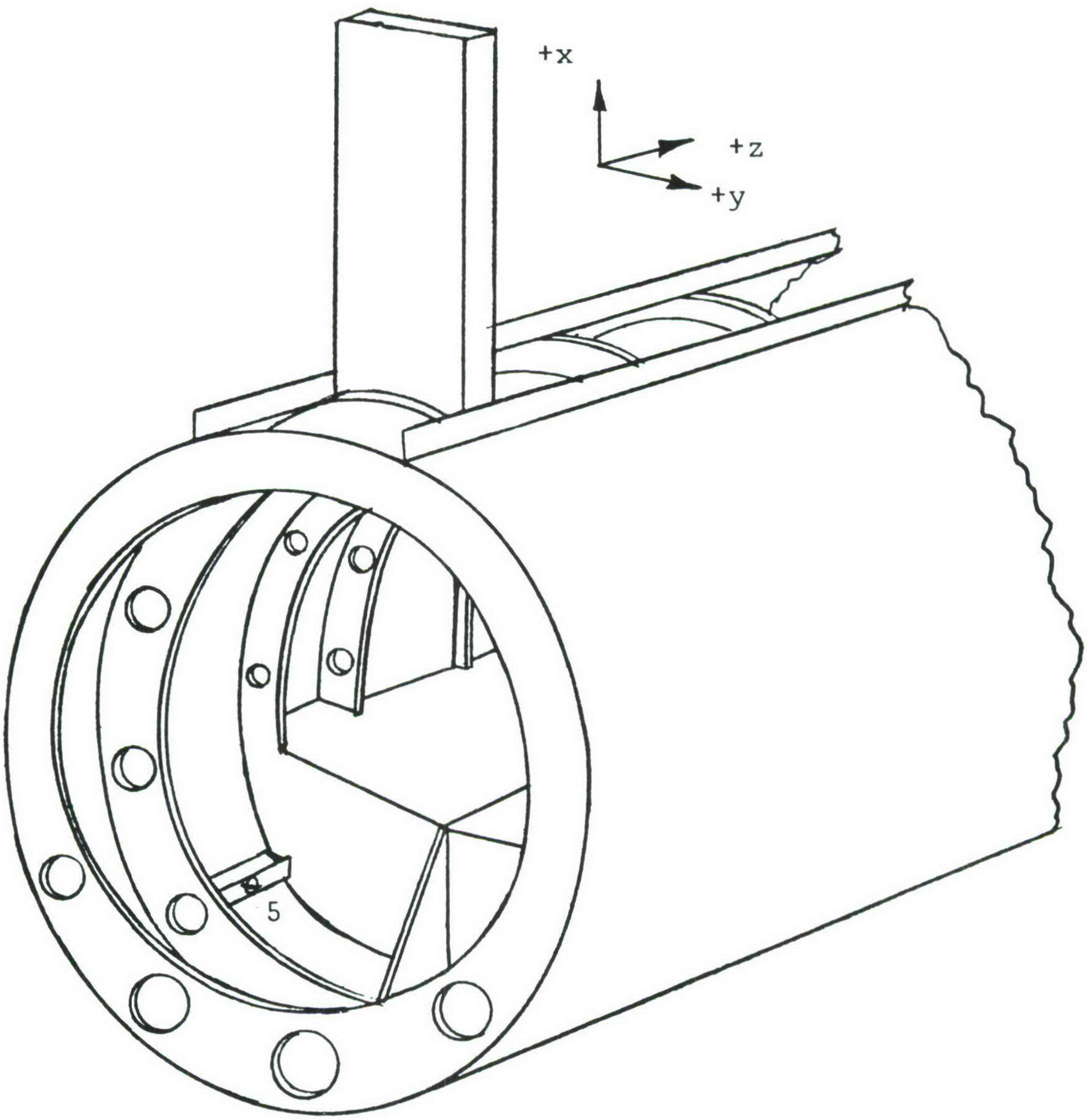

Figure 57   Partial Sketch of Test Object Showing Location of Rotational Sensor No. 5

TABLE 5

DESCRIPTION OF RESPONSE VARIABLES

Number & Direction	Type	Location
1y	trans.	Inside fuselage at extreme lower right front on end of heavy wishbone beam.
2y	trans.	Outside of fuselage, right side, near box section reinforcement for airbrake pivot bolt.
3x	trans.	Outside bottom of fuselage, near arresting hook bracket.
4x	rot.	Yaw at extreme lower right front on heavy beam outside wishbone.
5x	rot.	Yaw on major longitudinal stiffener at lower left, just behind electronics enclosure.
11z	rot.	Roll on major rib stiffener S, left inside of fuselage over electronics enclosure.
12y	rot.	Pitch at junction between major rib stiffener S and top of left airbrake box.
13x	trans.	Top of left airbrake box inside fuselage between ribs O and S.
21x	trans.	Outward normal direction (slightly to the right of vertical) on rib C near lower right corner of stabilizer stub.
21y	trans.	Lower right side of stabilizer stub.
21z	trans.	Lower right front of stabilizer stub.
22y	rot.	Pitch at base of stabilizer stub.
23x	rot.	Yaw at base of stabilizer stub.
31x	trans.	Top center front of electronics enclosure.
32z	rot.	Roll at top front center of electronics enclosure.
33y	rot.	Pitch at top front of electronics enclosure on stringer slightly left of center.

TABLE 6

MEASURED FREQUENCY RESPONSES

Response	Input 1y	Input 2y	Input 3x
1y	x		
2y		x	
3x			x
4x		x	
5x		x	
11z	x	x	x
12y	x	x	x
13x	x	x	x
21x	x	x	x
21y	x	x	x
21z	x	x	x
22y	x	x	x
23x	x	x	x
31x	x	x	x
32z	x	x	x
33y	x	x	x

a total of 38 different input/output pairs were used. Random excitation was provided by an electrodynamic shaker of 50 lbf (peak) capacity. Typical drive levels were 3-10 lbf (r.m.s.), depending on input and response locations. This drive level was found to give excellent coherence ($\gamma^2 > 0.97$) between force and acceleration over the frequency range of 50 to 160 Hz when the shaker drive signal was bandlimited to 5-180 Hz. However, a separate run with all drive power concentrated in the 5-60 Hz band was needed to get good coherence below 50 Hz.

Frequency responses for the 38 input/output pairs were measured over 0 to 160 Hz. The measurement was made using both a baseband FFT (Δf = 0.312 Hz) and a high resolution or zoom FFT (Δf = 0.1 Hz). The wideband measurements were intended as quick-look data, and the zoomed functions for estimation of modal parameters, such as damping. It was found that, in most cases, the wideband functions could be used to compute output PSD and r.m.s. quantities with negligible error.

A typical run was made by first setting the drive signal passband to 5-60 Hz and adjusting the force amplitude to about 10 lbf (r.m.s.). A baseband, 512 spectral line frequency response over 0-60 Hz was then measured and stored. The drive passband was next opened up to 5-180 Hz, and the amplitude adjusted as required. 400 seconds of the force and response signal, sampled at 640 Hz, were digitized and throughput to disc in real time. The shaker was then shut down and a stored program was run. It processed the stored data to obtain a 512 line baseband frequency response over 0-160 Hz, as well as five zoomed frequency responses of 200 spectral lines each, spaced over 60-80, 80-100, 100-120, 120-140, and 140-160 Hz. While this processing was taking place, the operator was free to move the sensors or shaker to the location desired for the next run.

A potential problem with the procedure as described above involves the rigid body modes of the test object. It is desirable that the actual test object and its NASTRAN idealization be identical with respect to support conditions. However, boundary conditions such as free or fixed which are easy to analyze may be quite difficult to implement. Likewise, a condition which is readily constructed may be impractical to model. The solution for this case was to use a soft, pneumatic suspension and model it as free-free. This implies that pure rigid body modes at zero frequency will be suppressed, but will reappear as nearly rigid modes at low frequency. Also, some slight modification of flexural modes will occur due to constraint forces. Some care is required if predicted-vs.-measured comparisons are made on the basis of displacement, which may be dominated by contributions from rigid body modes which were modeled only approximately. Two measures were taken to minimize this problem:

(1) The hypothetical input force PSD used for measured-vs.-predicted comparison was taken to be zero below 40 Hz. Since the highest rigid body mode was at about 5 Hz. and the lowest elastic mode was at 45 Hz, this reduced the effect of rigid body modes considerably.

(2) Frequency responses selected for comparison were those where, within the 40-160 Hz comparison band, contributions from elastic modes were large relative to those from rigid body modes.

It is possible to further reduce the effect of support conditions on the measured frequency response functions by careful data processing. A parametric representation of each function may be obtained by curve fitting a complex partial fraction expansion to the measured version. The analytic form represents the contribution of each mode, flexural or rigid, by a pair of terms. The function may then be resynthesized including only the terms corresponding to straining modes. While the data taken was sufficient to carry out this procedure, it was not done due to time and cost limitations.

7.3.3 Test Equipment

Figure 58 is a schematic of the test setup. A list of equipment used is supplied as Table 7.

Because of the low excitation force level available relative to the mass of the test object, it was found that very low-noise acceleration sensing was necessary. The combination of Endevco 2207-200 transducers and 2735 charge amplifiers was found to give an instrumentation noise level of about 28 μg (r.m.s.). High coherence measurements were possible for all input-output pairs as long as the available force was concentrated in the frequency band of interest and some effort was made to maintain a quiet test environment.

Angular acceleration was sensed by analog differencing of translational acceleration signals. Analog gain balancing was performed at 100 Hz prior to testing. Residual unbalance was estimated as less than 0.5% gain and 0.5° phase.

Typical r.m.s. response levels were on the order of 0.04 g. The lowest observed elastic mode of the fuselage was at 45 Hz. We may use Eqs. (6.27) and (6.37) of this report to estimate that at this frequency a differential narrowband signal/noise ratio of 30 dB could be maintained down to a dimensionless difference signal level of $1-\alpha = 0.05$ and 20 dB could be maintained down to $1-\alpha = 0.005$. This was considered adequate for the purpose at hand. Transducer separation varied for the different response locations, but was always in the 6.5 - 10.5 inch range. Flexural error was estimated using Figure 44 of this report and was found to be less than 10% for all cases. However, data from location 11z was eventually discarded because it was decided that the beam flange, on which the transducers were mounted, was too flexible to give a good approximation to a one-dimensional beam.

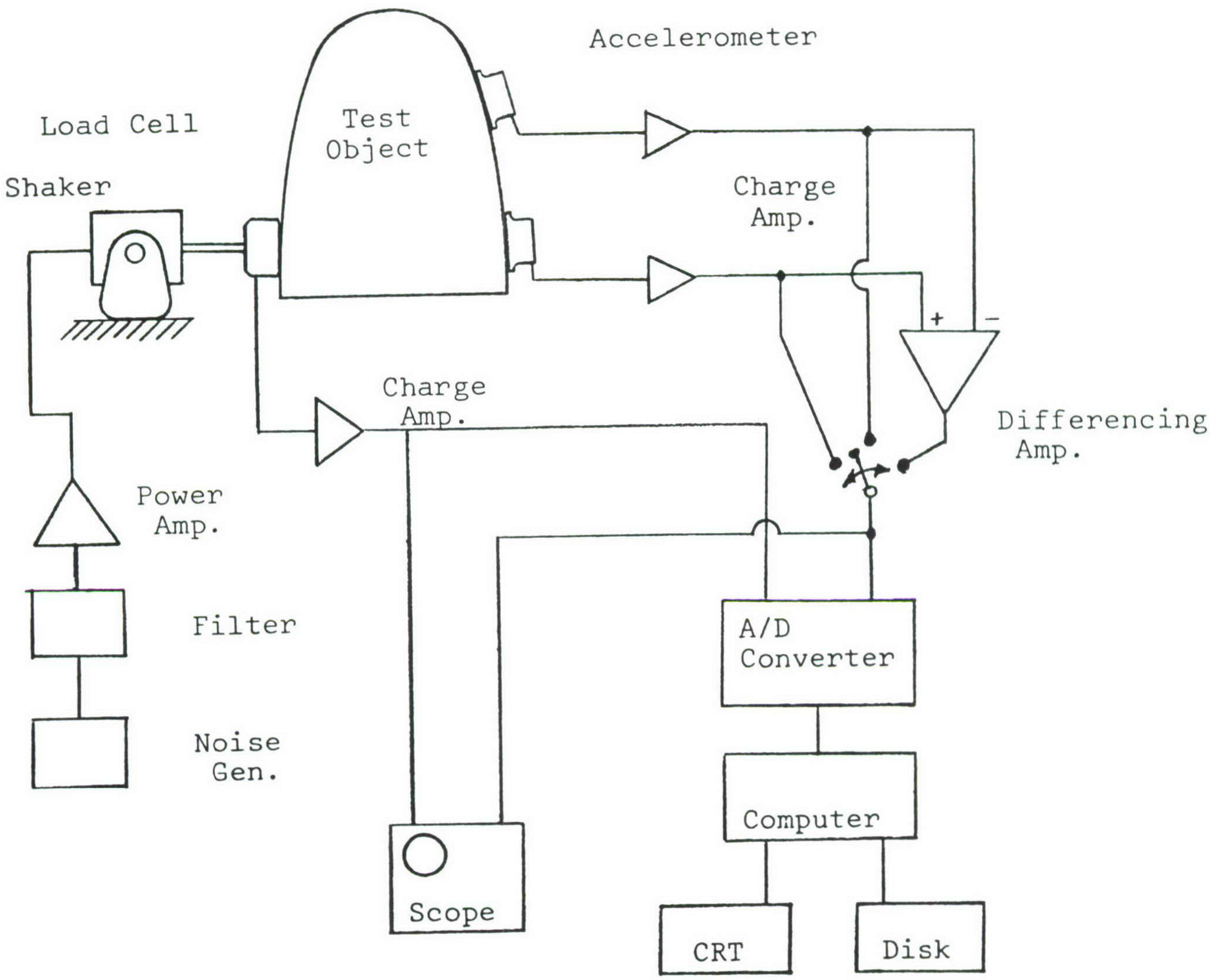

Figure 58   Schematic of Test Setup

TABLE 7

TEST EQUIPMENT

Item	Manufacturer	Model
Load Cell	Bruel & Kjaer	8200
Accelerometers	Endevco	2207-200
Charge Amp.	Endevco	2735
Dif. Amp.	Honeywell	122
Noise Generator	Wavetek	132
Variable Filter	Krohn-Hite	3323
Shaker	Unholtz-Dickie	Model 1 (50 lbf)
Power Amp.	Unholtz-Dickie	TA35I
A/D Converter	Time/Data	TDA-25
Computer	DEC	PDP 11/34
Scope	Tektronix	434

7.4 Results

Table 8 lists the natural frequencies measured in the test versus those predicted analytically. It should be emphasized that there is no way to know for certain which experimental mode corresponds to which analytical mode. For example, the eighth analytical mode (46.3 Hz) may correspond to either the seventh (45.5 Hz) or eighth (48.7 Hz) mode, and this could be determined only by a detailed investigation of the mode shape geometries. It should also be noted that the list of experimental modes is almost certainly incomplete due to the finite number of response points. The analytical model includes all modes up to a certain frequency, including any local modes that may have been missed in the test. "Generalized dynamic reduction" was the eigenvalue solution method that was chosen. If Guyan reduction had been used, with a judiciously selected analysis set, it probably would have been possible to eliminate these local modes.

PSD plots are shown in the following figures for three separate driving points as listed in Section 7.3. Figures 59 through 70 are experimental results and Figures 71 through 75 are analytical results. At best, there is some qualitative agreement between respective pairs of plots. Both exhibit peaks around 70 Hz. The analytical results show a peak around 90 Hz which is not seen in the experimental plots. Both also exhibit peaks in the area of 140 to 150 Hz. Table 9 lists r.m.s. values for several response PSD's. Correlation is fairly good for some of these values.

Power spectral density functions are plotted in linear amplitude-linear frequency format. This allows a direct interpretation of the area under the curve in terms of the mean square response. As a further aid to visualization of the frequency distribution of response, a quantity called the normalized cumulative r.m.s. response is plotted. It is a function of frequency defined as

TABLE 8

NATURAL FREQUENCIES OF THE FUSELAGE

Experimental	Mode No.	Analytical
45.5	7	22.7
48.7	8	46.3
70.1	9	71.9
79.7	10	74.2
83.0	11	79.3
109.8	12	85.1
111.8	13	88.4
113.9	14	88.9
121.9	15	90.9
126.6	16	95.5
130.0	17	97.1
133.3	18	112.0
137.0	19	112.2
140.0	20	116.4
148.7	21	118.0
155.9	22	120.7
	.	
	.	
	.	
	30	149.5

$$\text{cum. r.m.s.} = \sqrt{\frac{\int_o^f S(f)\,df}{\int_o^{f_{max}} S(f)\,df}} \qquad (7.1)$$

Since S(f), the PSD, is always positive, the cumulative r.m.s. is also, and will always range from zero at f=0 to unity at $f=f_{max}$. Thus, no scale is shown for it on the plots of Figures 59 to 70.

One would have to call this this test inconclusive with respect to evaluation of the Semi-Loof elements. The performance of the elements is masked by a number of other considerations which dominated this exercise. These questions include the following: (1) What was the true damping in the system? (2) What were the true support conditions? (3) What was the effect of the angular accelerometers and their mounts, in terms of both stiffness and inertia (not considered in the model)? (4) What local structural deformations might have been missed by the finite element model.

TABLE 9

R.M.S. VALUES OF PSD RESPONSES OF THE FUSELAGE

Drive Point	Response Point	Experimental	Analytical
1Y+	22Y+	5.5×10^{-5}	7.6×10^{-6}
1Y+	23X+	7.3×10^{-5}	2.3×10^{-5}
2Y-	32Z+	2.1×10^{-5}	4.1×10^{-6}
3X+	22Y+	8.5×10^{-6}	7.6×10^{-6}
3X+	23X+	3.0×10^{-6}	2.4×10^{-6}

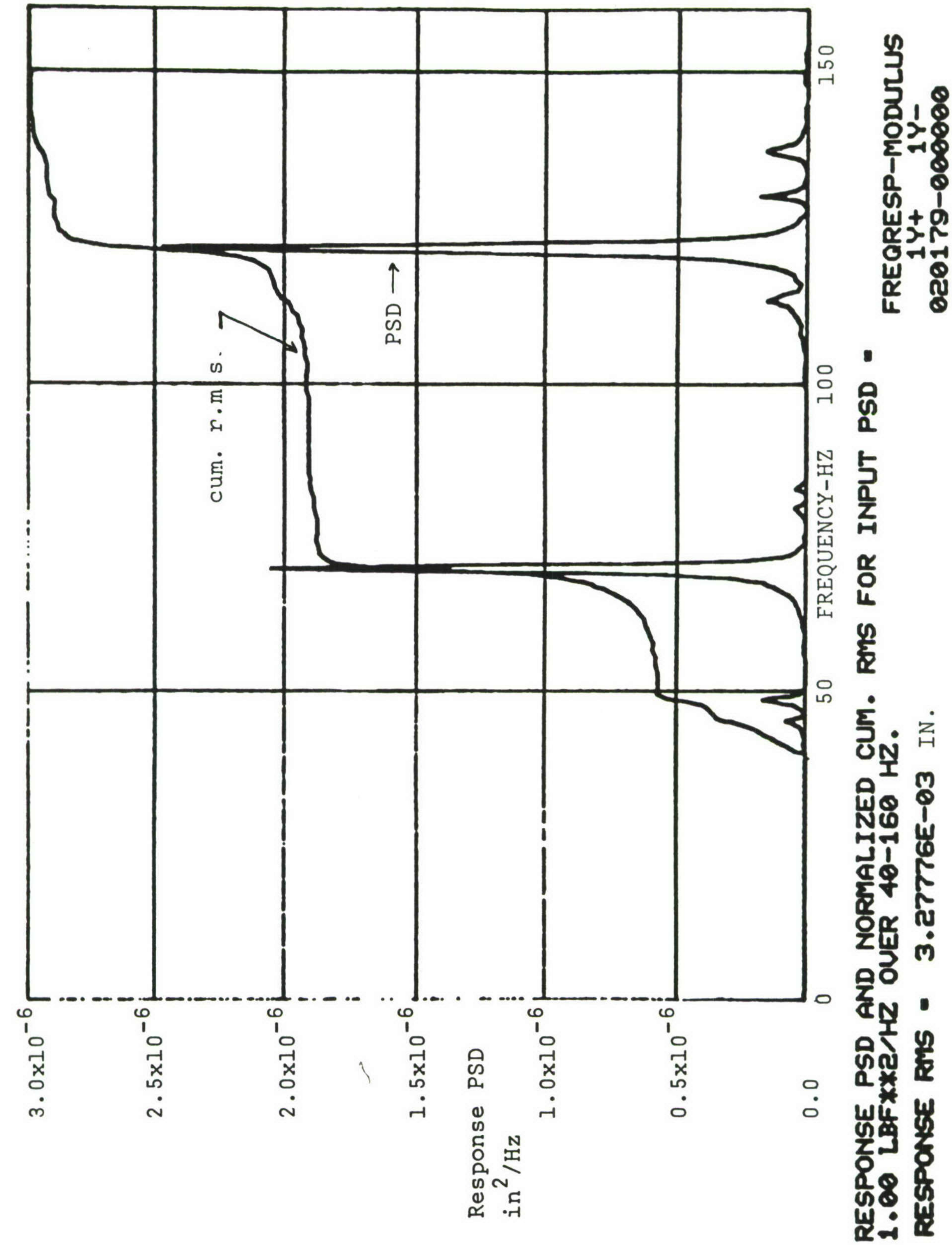

Figure 59 Experimental Results
Response Point 1, Y Translation
Driving Point 1, Y Translation

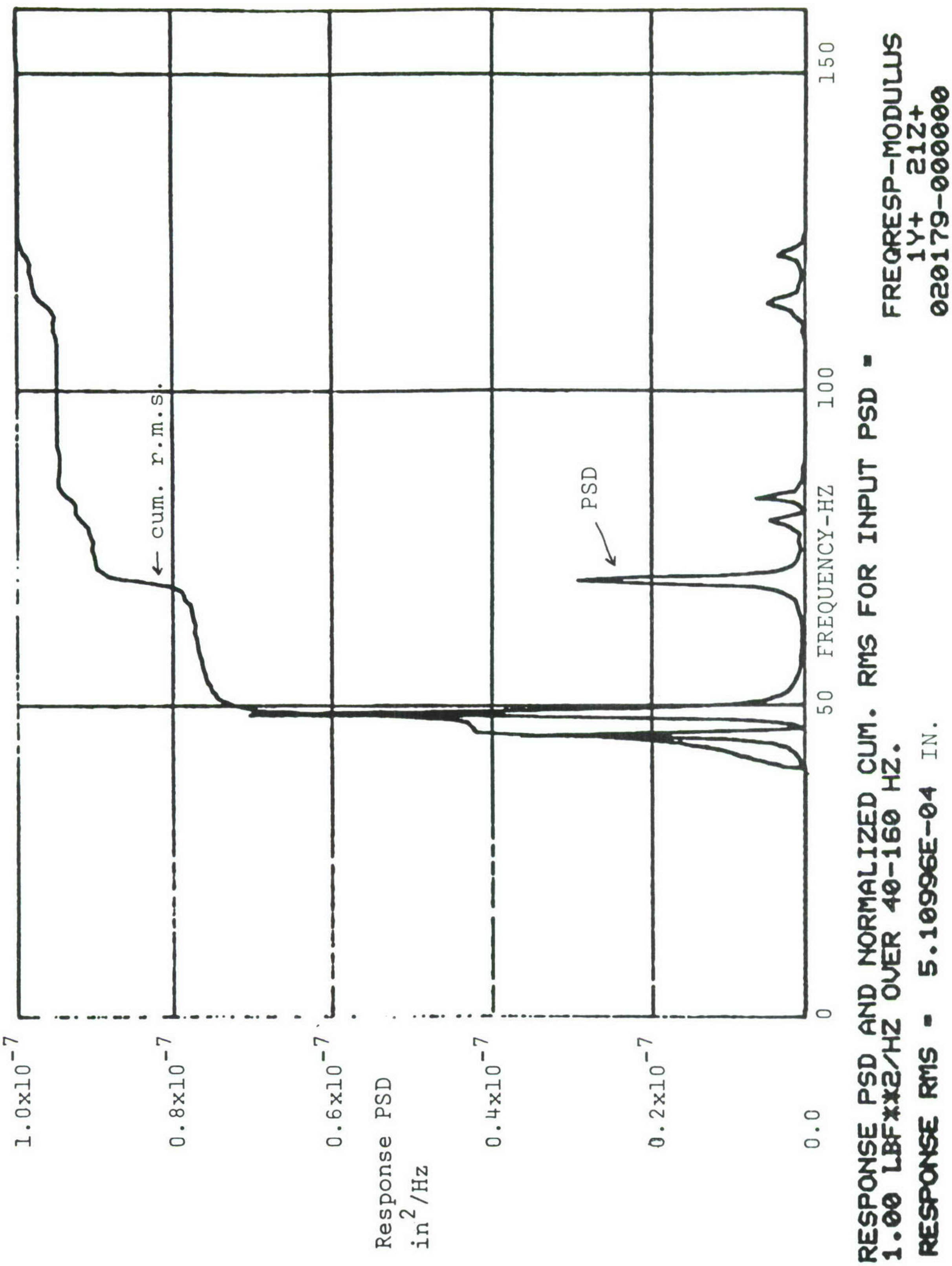

Figure 60 Experimental Results
Response Point 21, Z Translation
Driving Point 1, Y Translation

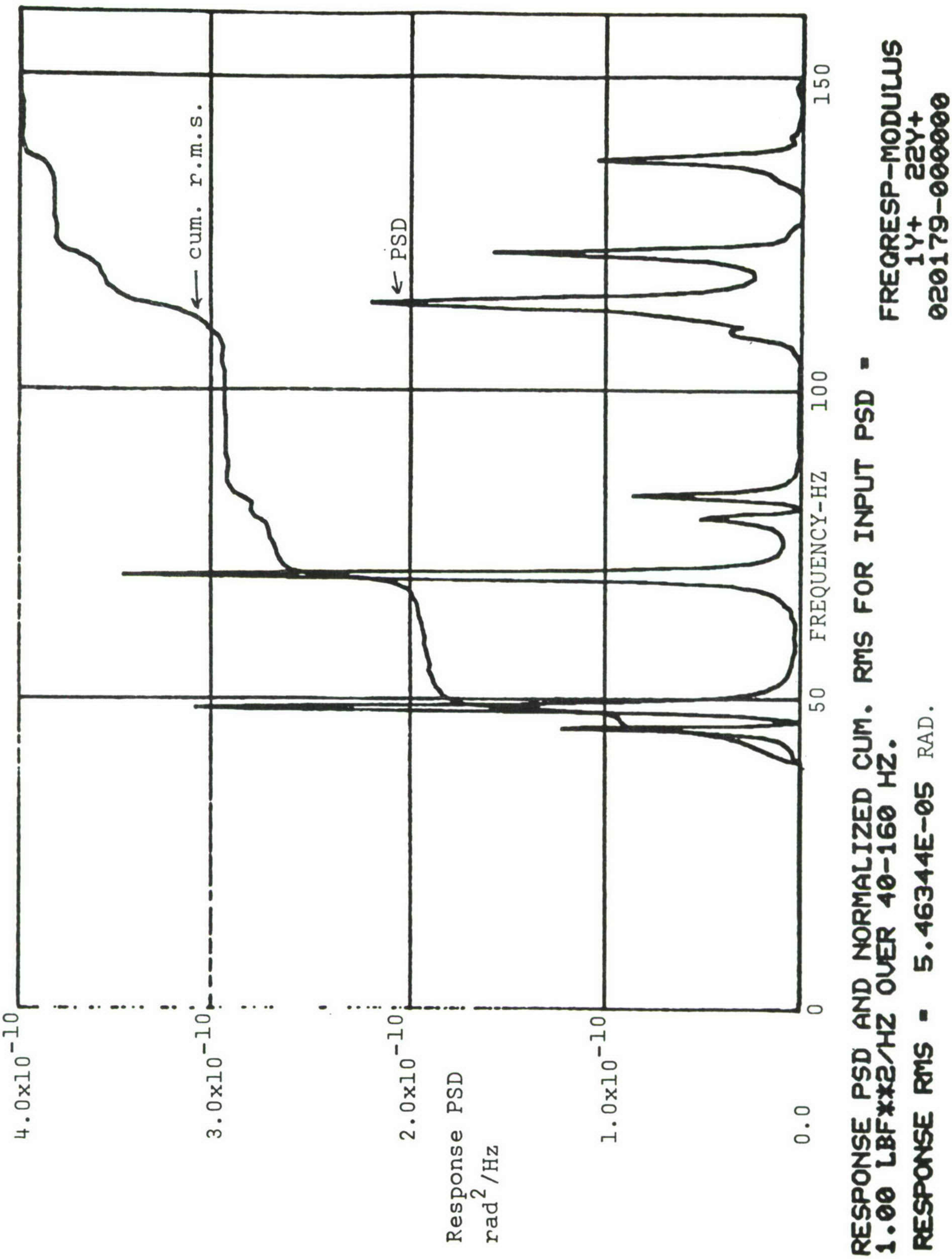

Figure 61 Experimental Results
Response Point 22, Rotation about Y
Driving Point 1, Y Translation

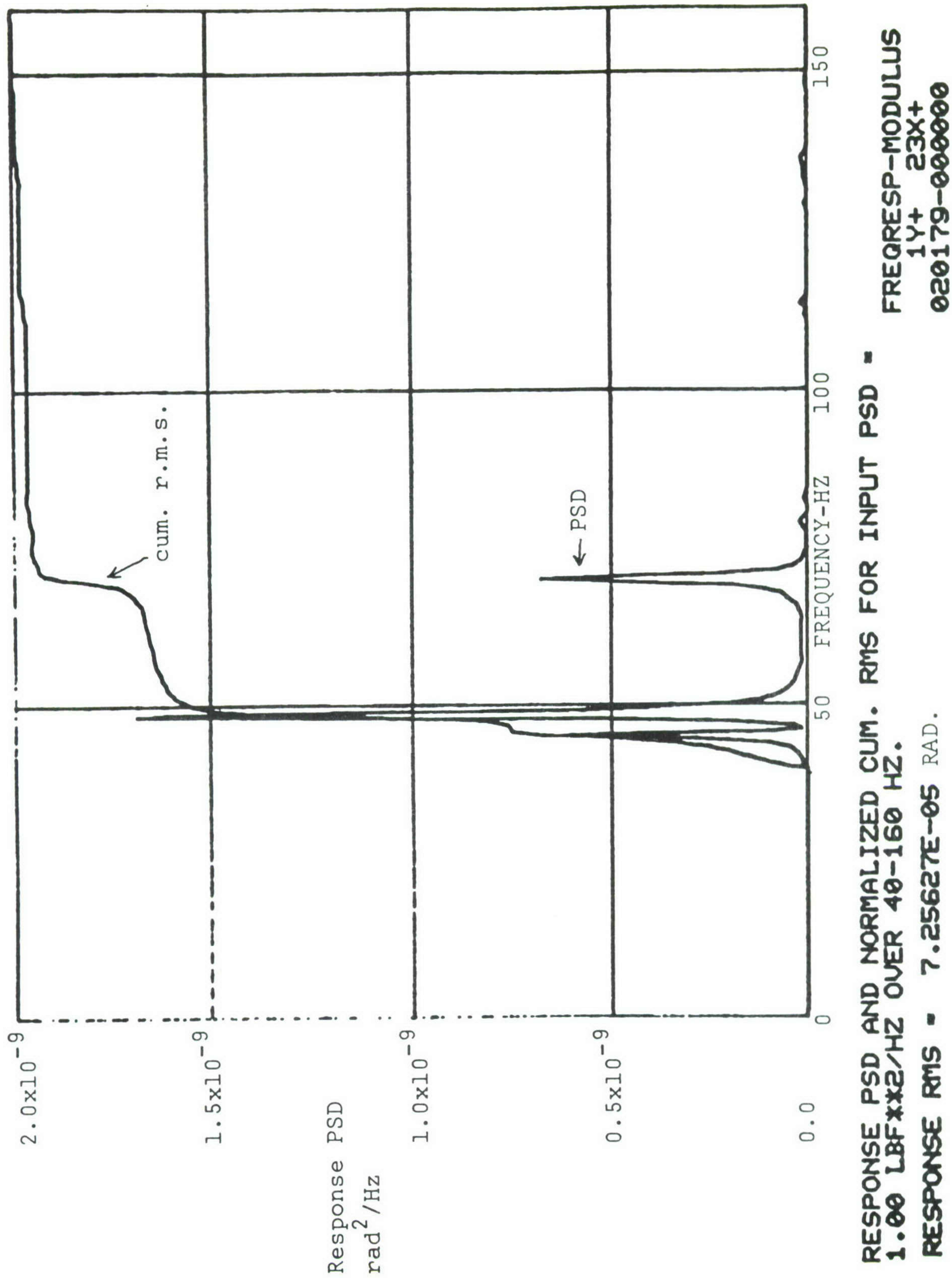

Figure 62 Experimental Results
Response Point 23, Rotation about X
Driving Point 1, Y Translation

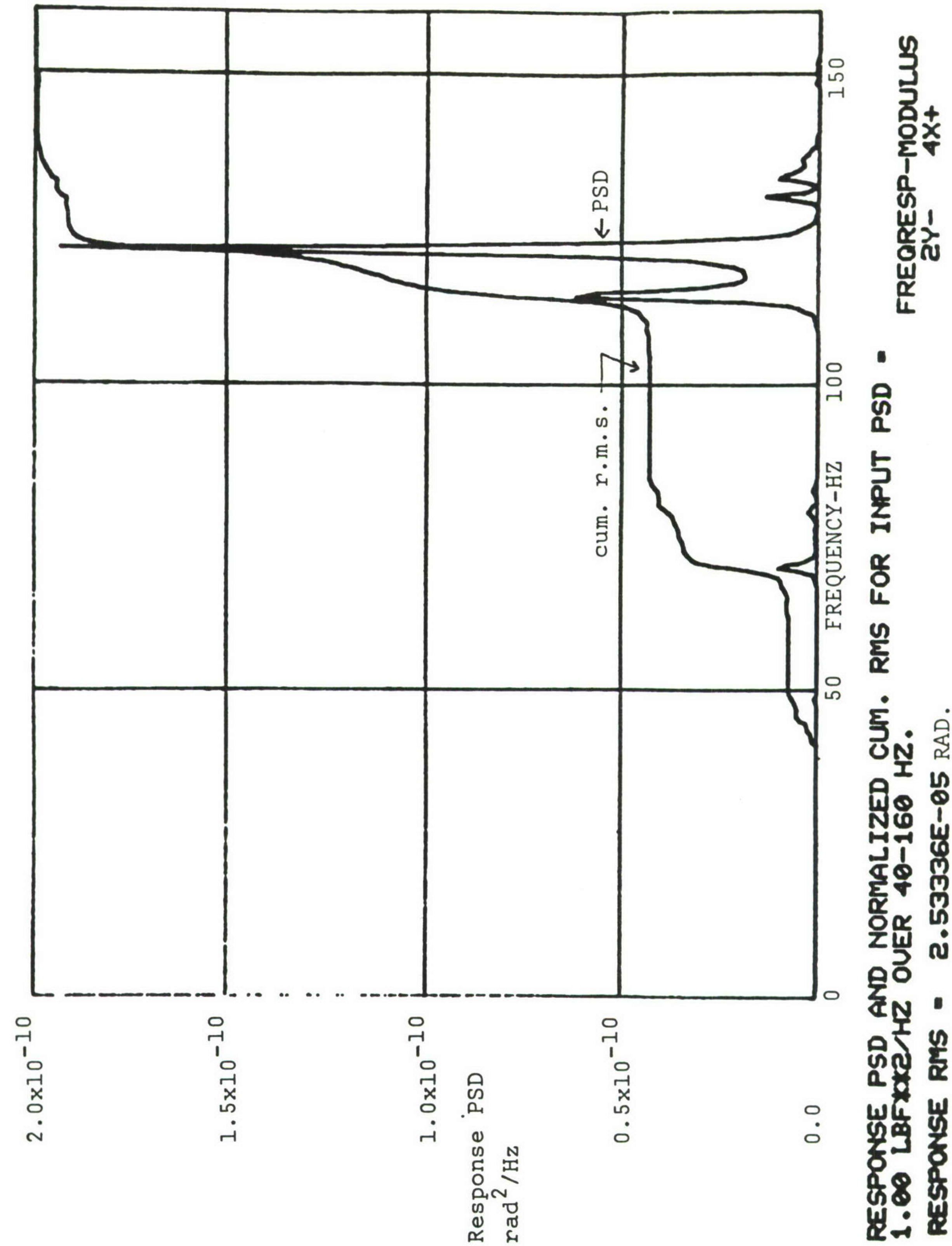

Figure 63 Experimental Results
Response Point 4, Rotation about X
Driving Point 2, Y Translation

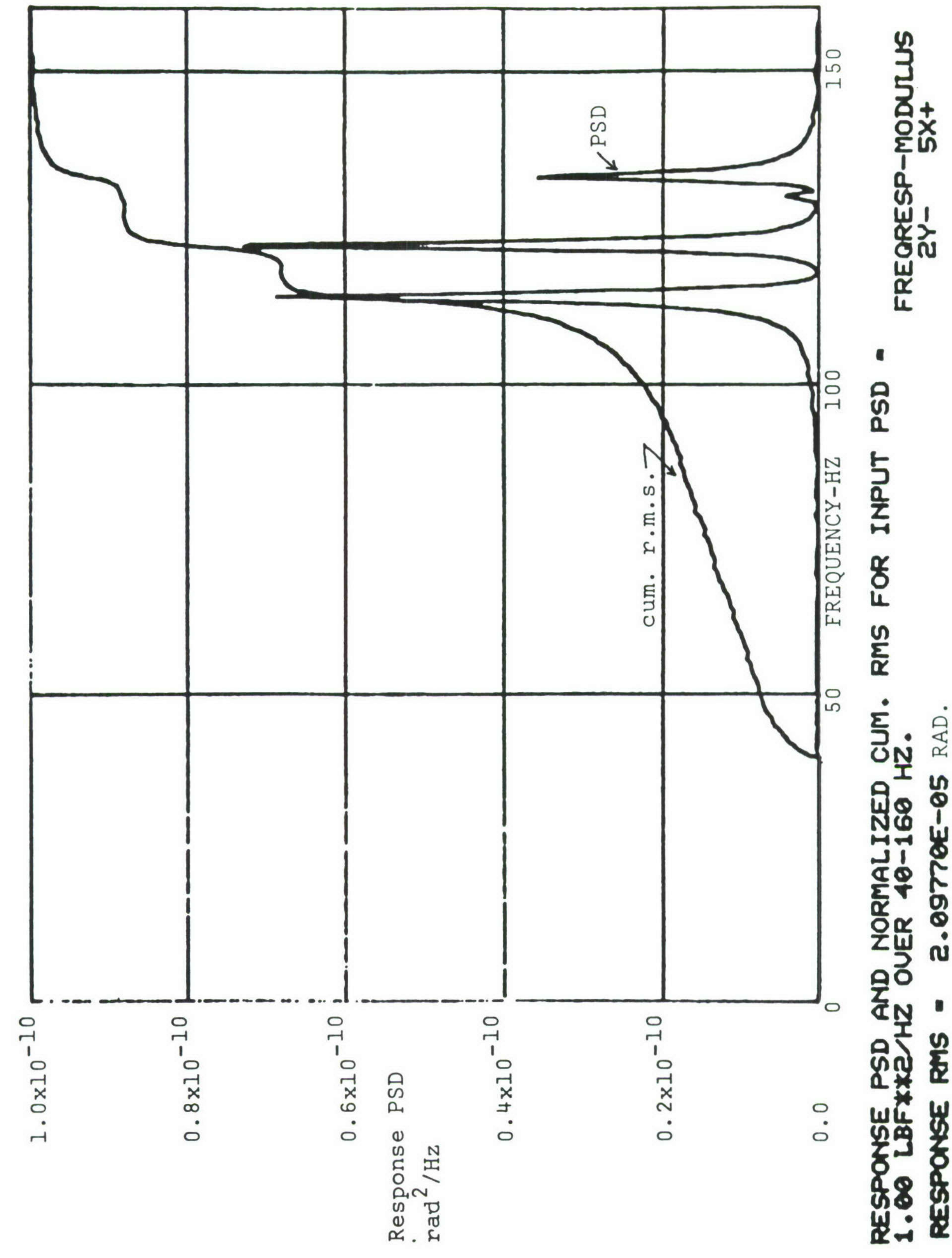

Figure 64 Experimental Results
Response Point 5, Rotation about X
Driving Point 2, Y Translation

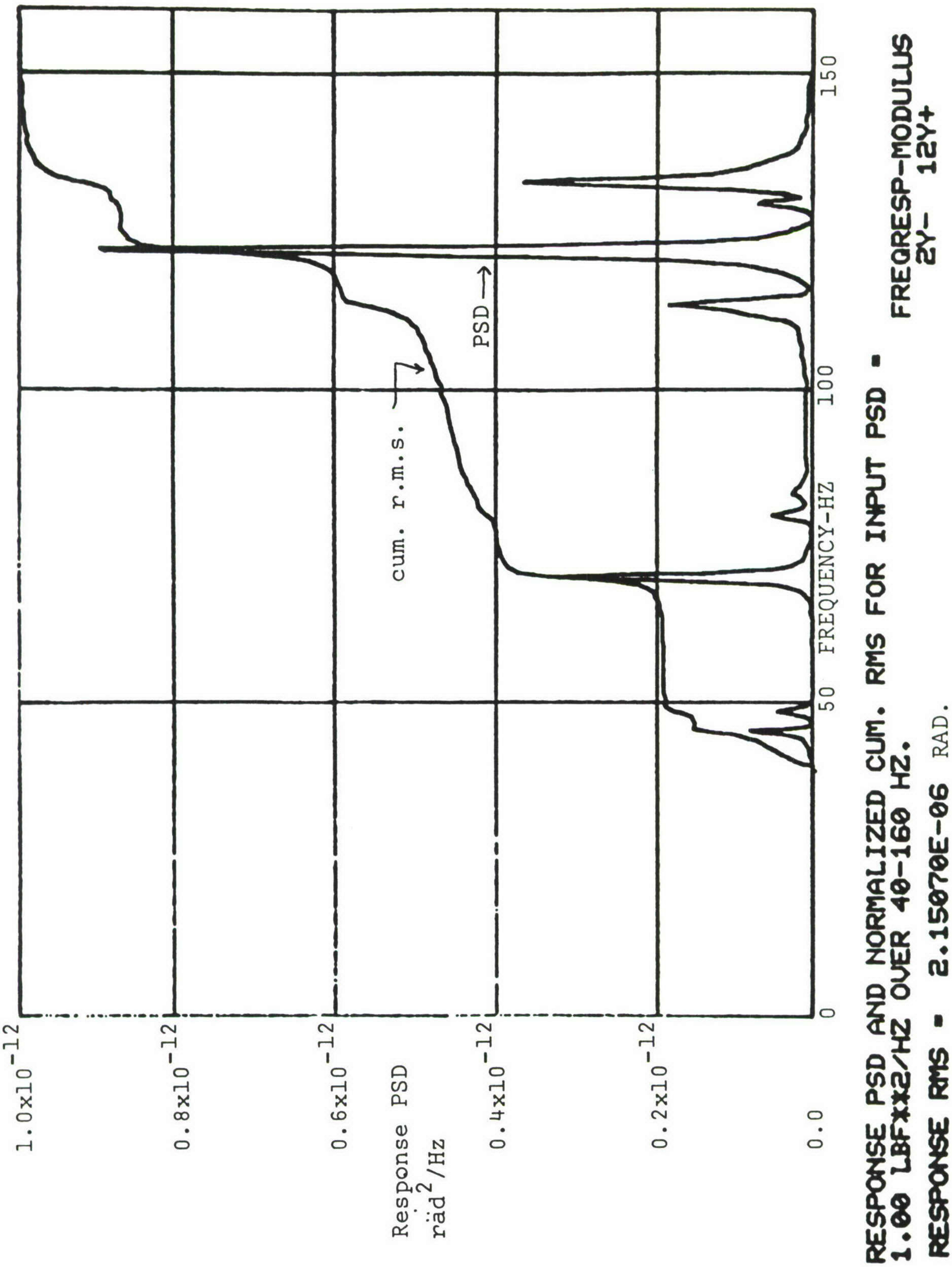

Figure 65 Experimental Results
Response Point 12, Rotation about Y
Driving Point 2, Y Translation

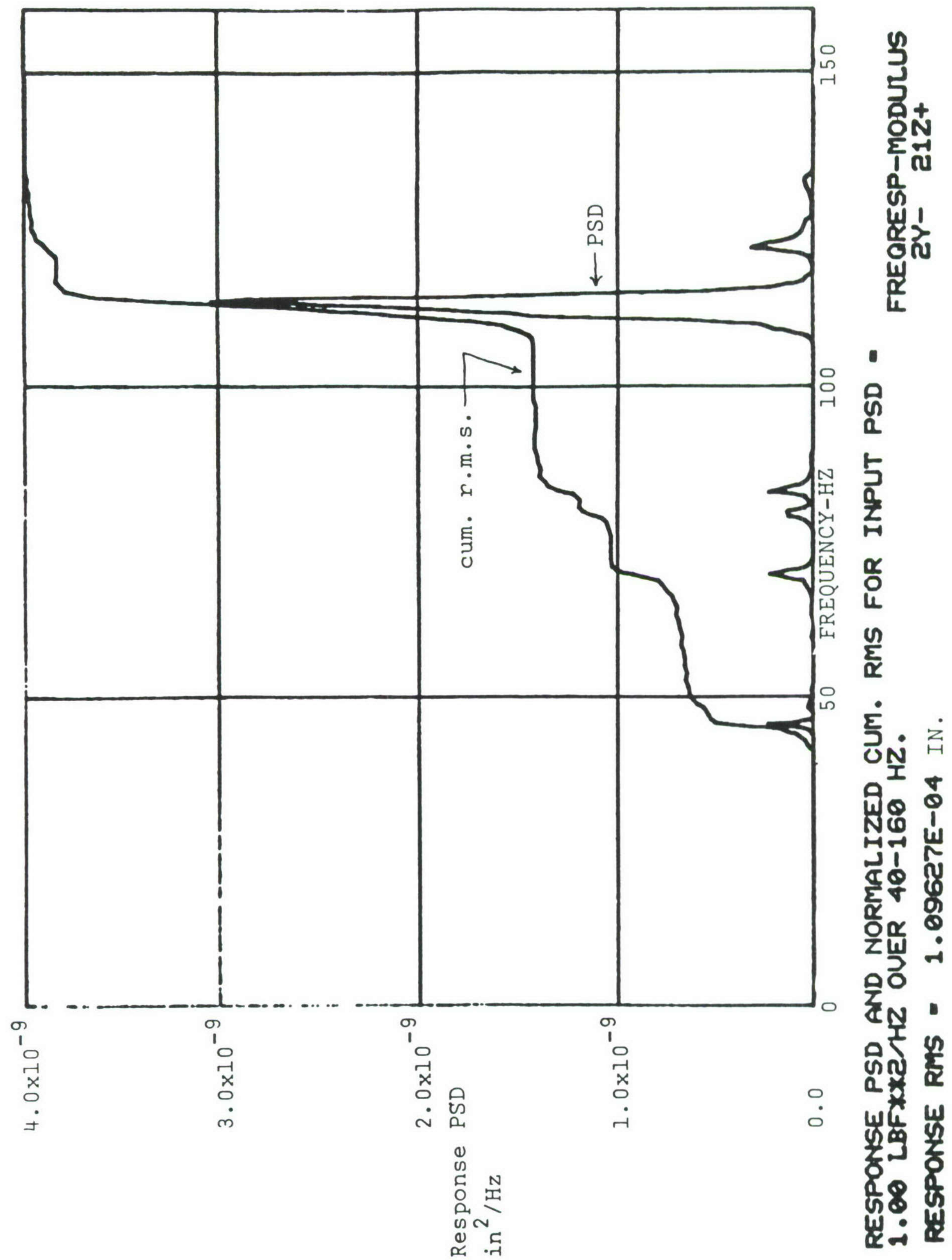

Figure 66 Experimental Results
Response Point 21, Z Translation
Driving Point 2, Y Translation

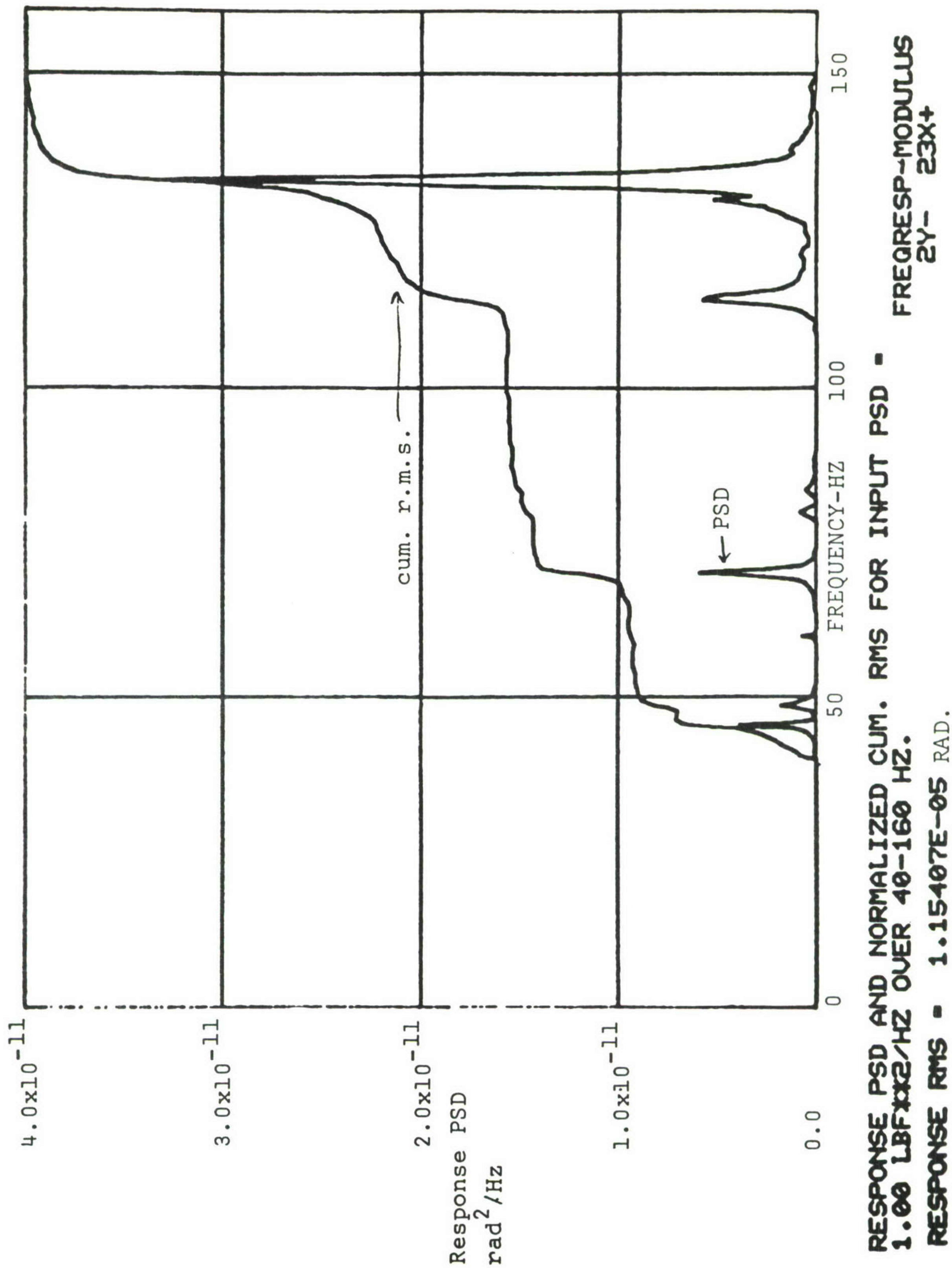

Figure 67 Experimental Results
Response Point 23, Rotation about X
Driving Point 2, Y Translation

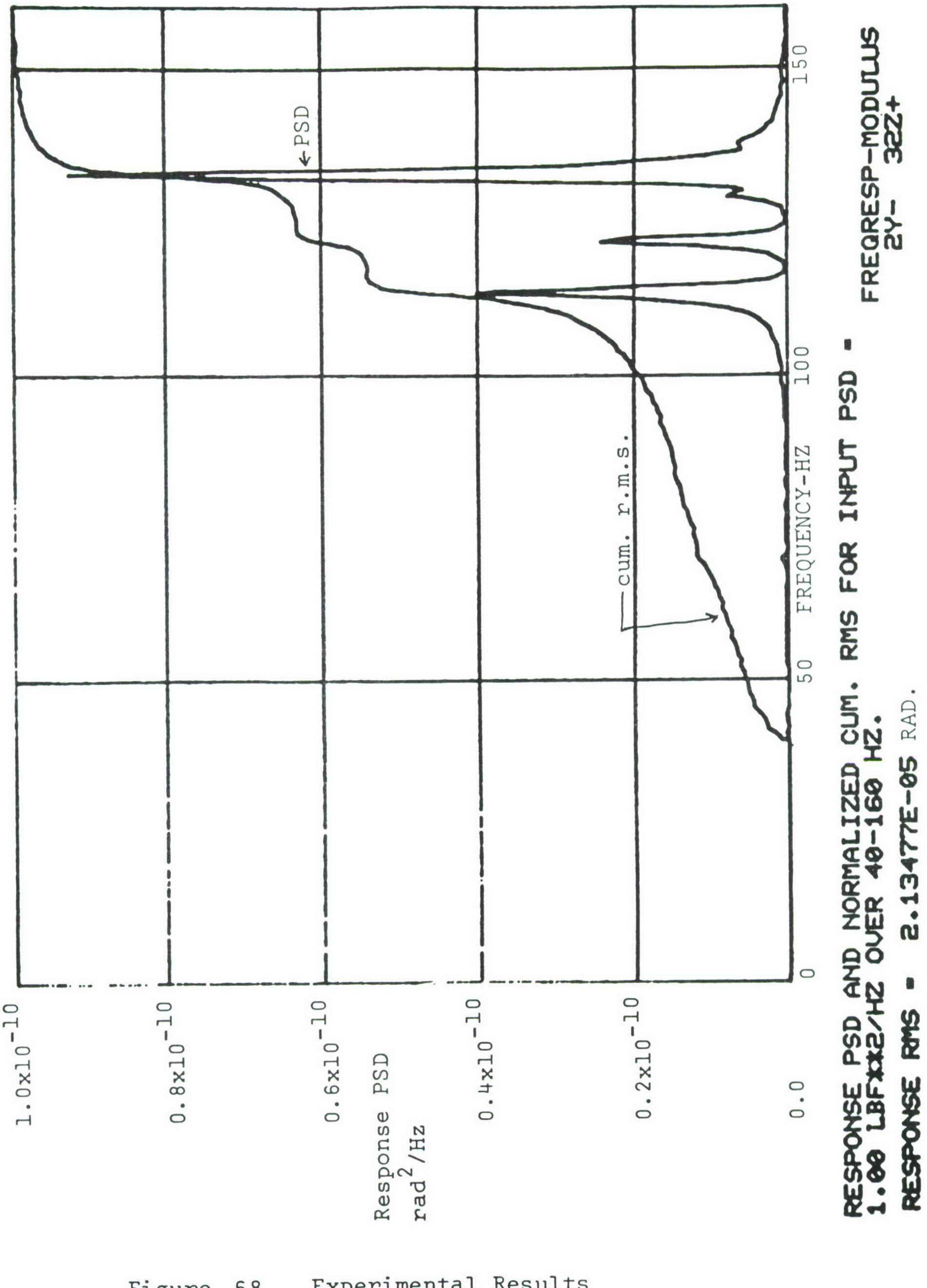

Figure 68 Experimental Results
Response Point 32, Rotation about Z
Driving Point 2, Y Translation

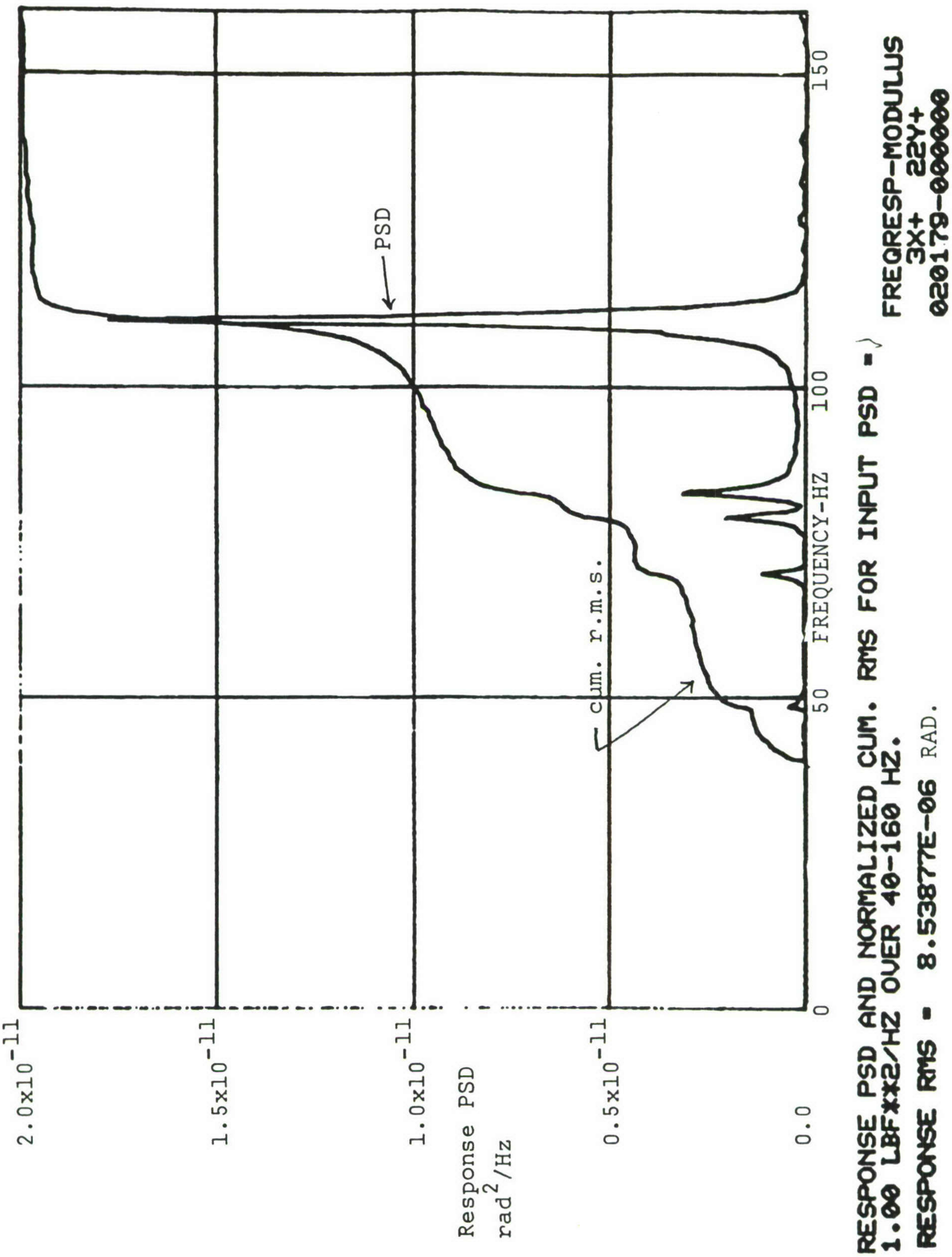

Figure 69 Experimental Results
Response Point 22, Rotation about X
Driving Point 3, X Translation

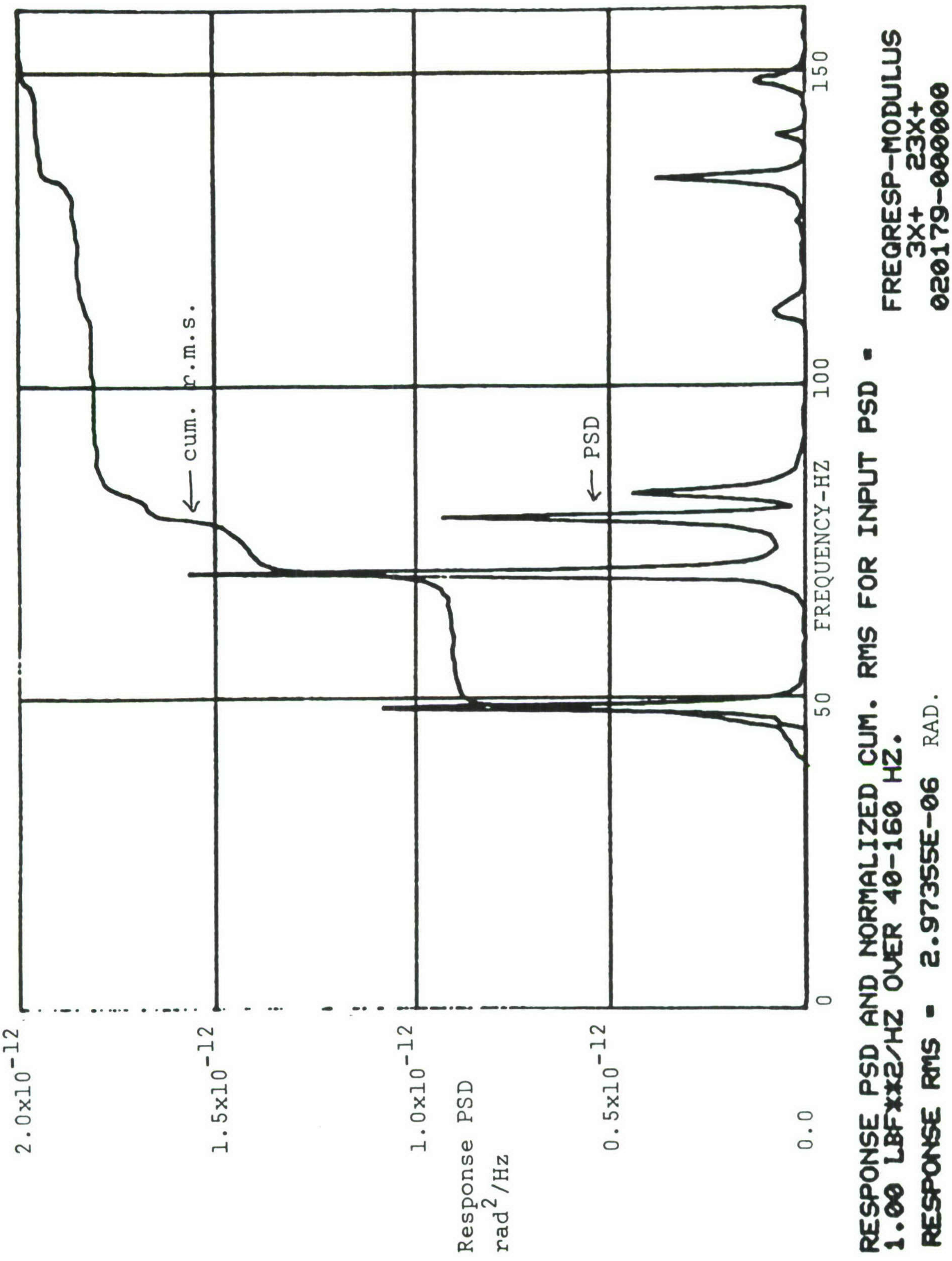

Figure 70 Experimental Results
Response Point 23, Rotation about Y
Driving Point 3, X Translation

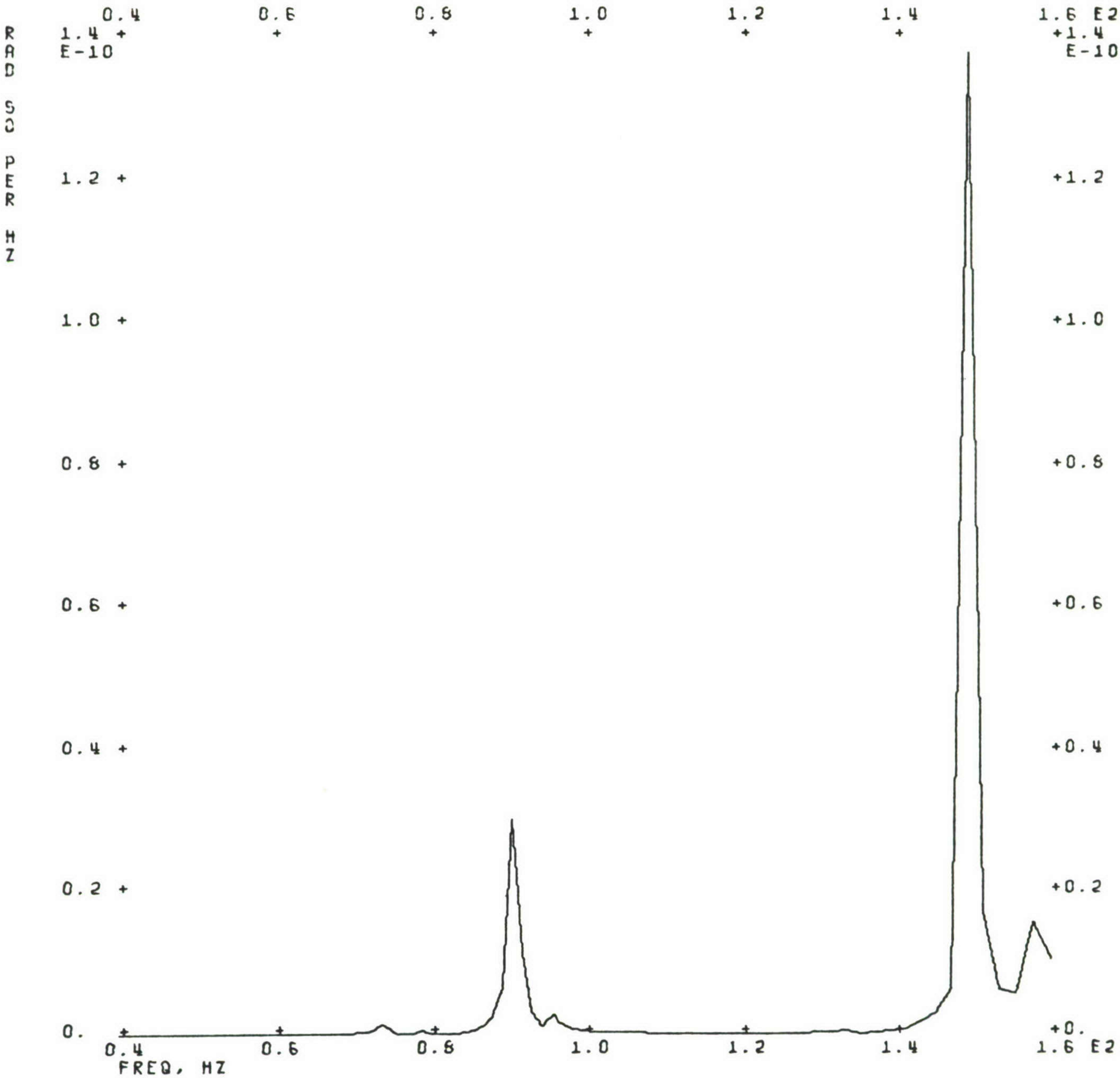

Figure 71 Analytical Results
Response Point 22, Rotation about Y
Driving Point 1, Y Translation

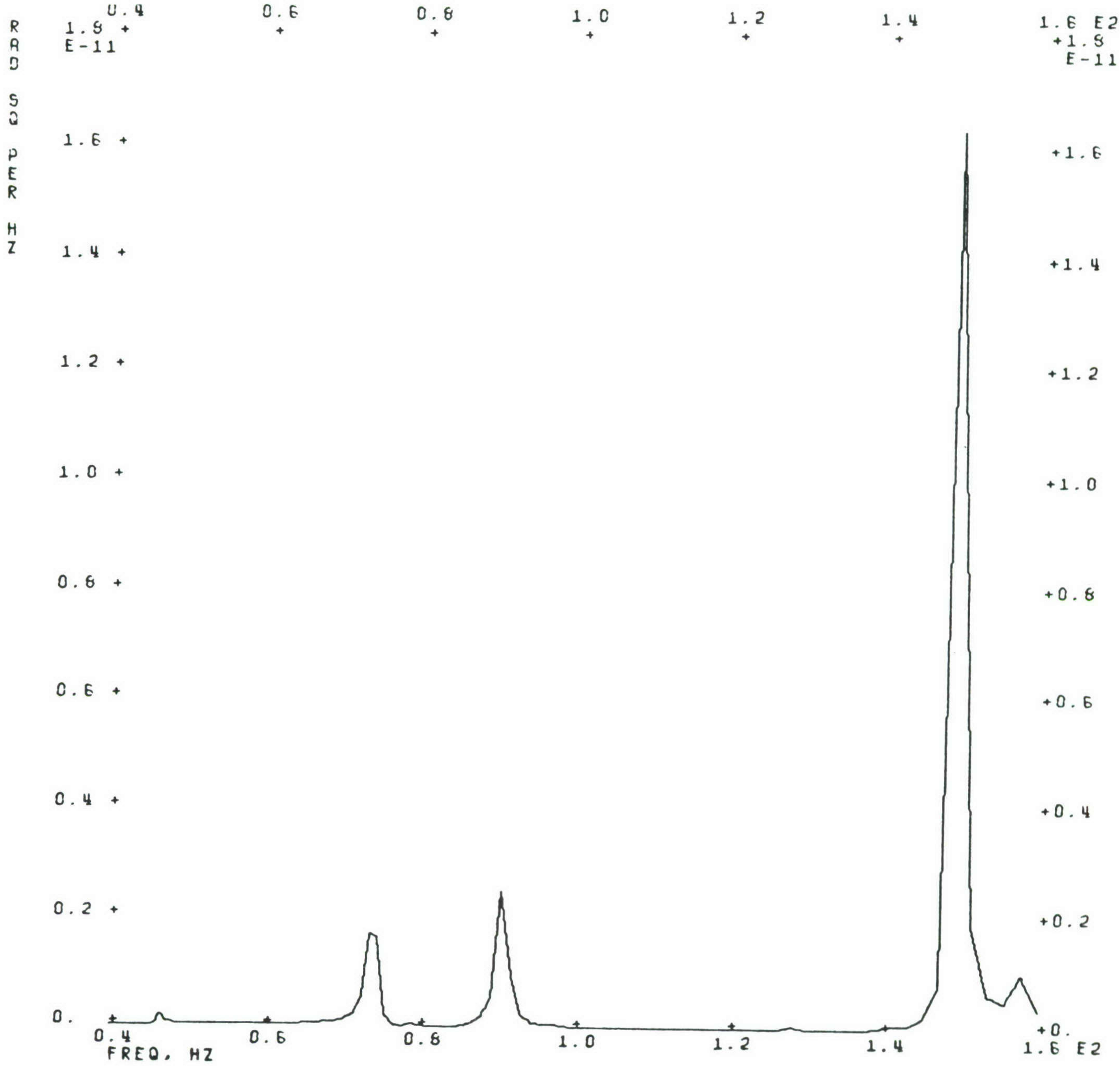

Figure 72 Analytical Results
Response Point 23, Rotation about X
Driving Point 1, Y Translation

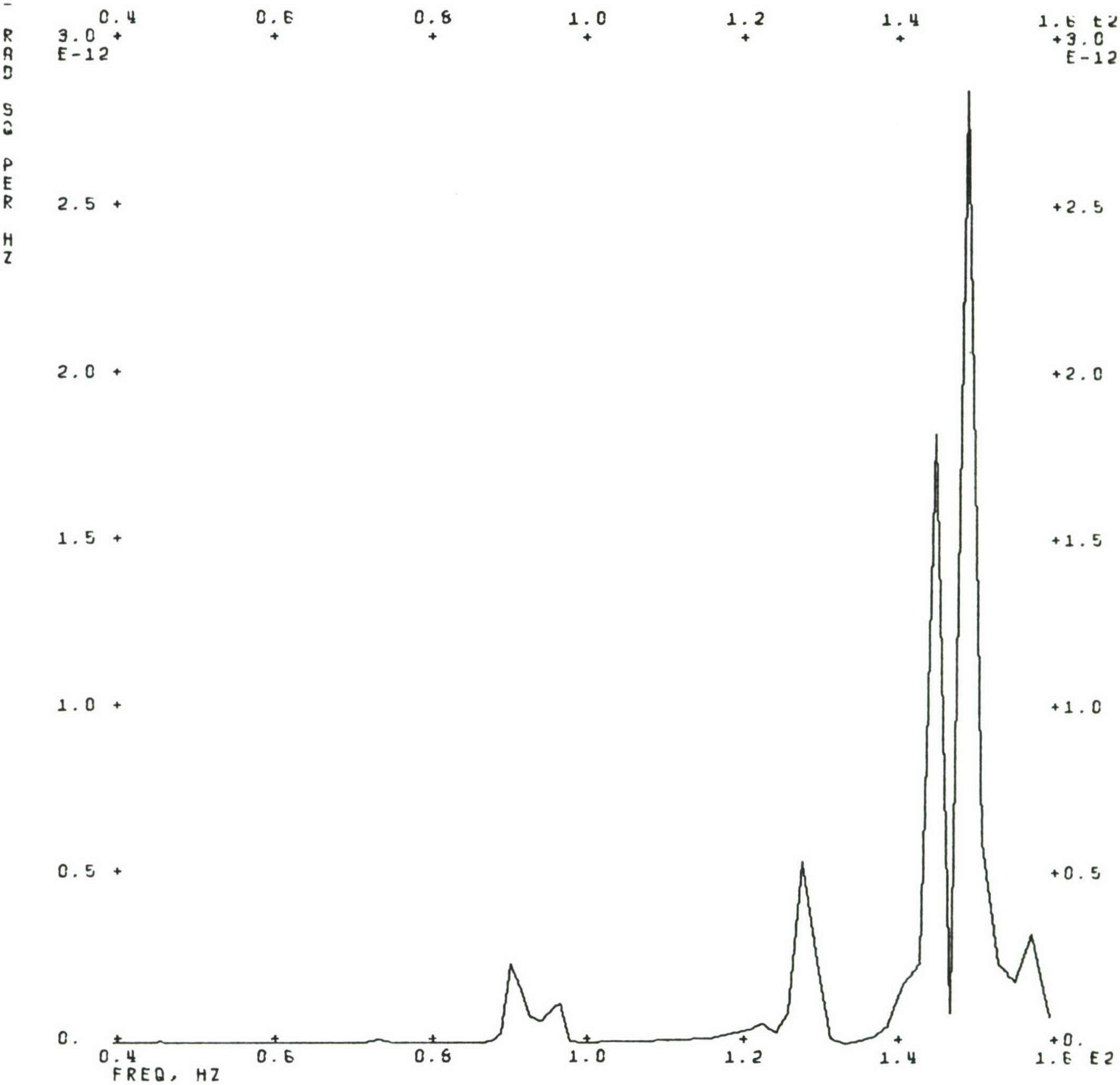

Figure 73 Analytical Results
Response Point 32, Rotation about Z
Driving Point 2, Y Translation

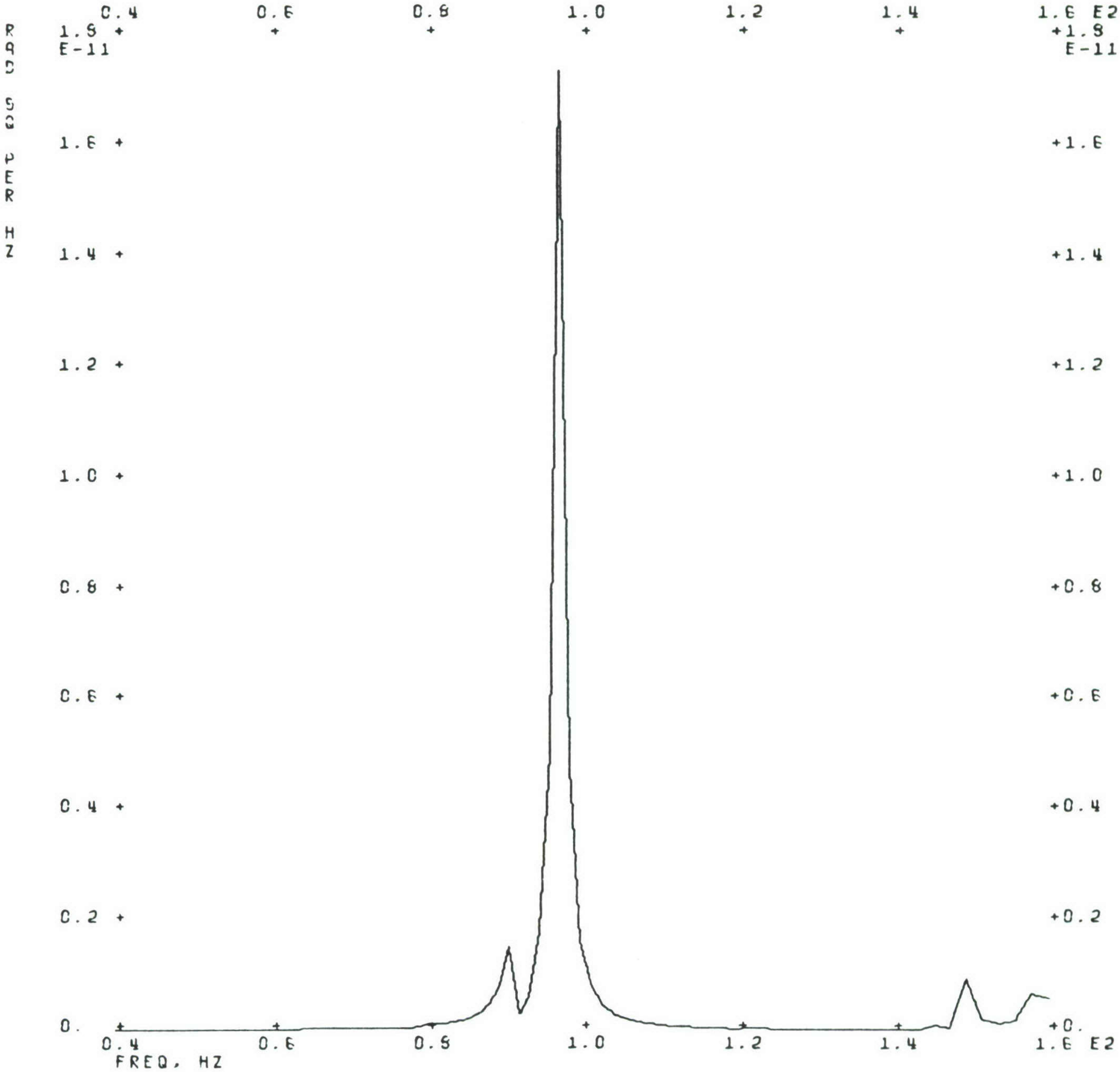

Figure 74 Analytical Results
Response Point 22, Rotation about Y
Driving Point 3, X Translation

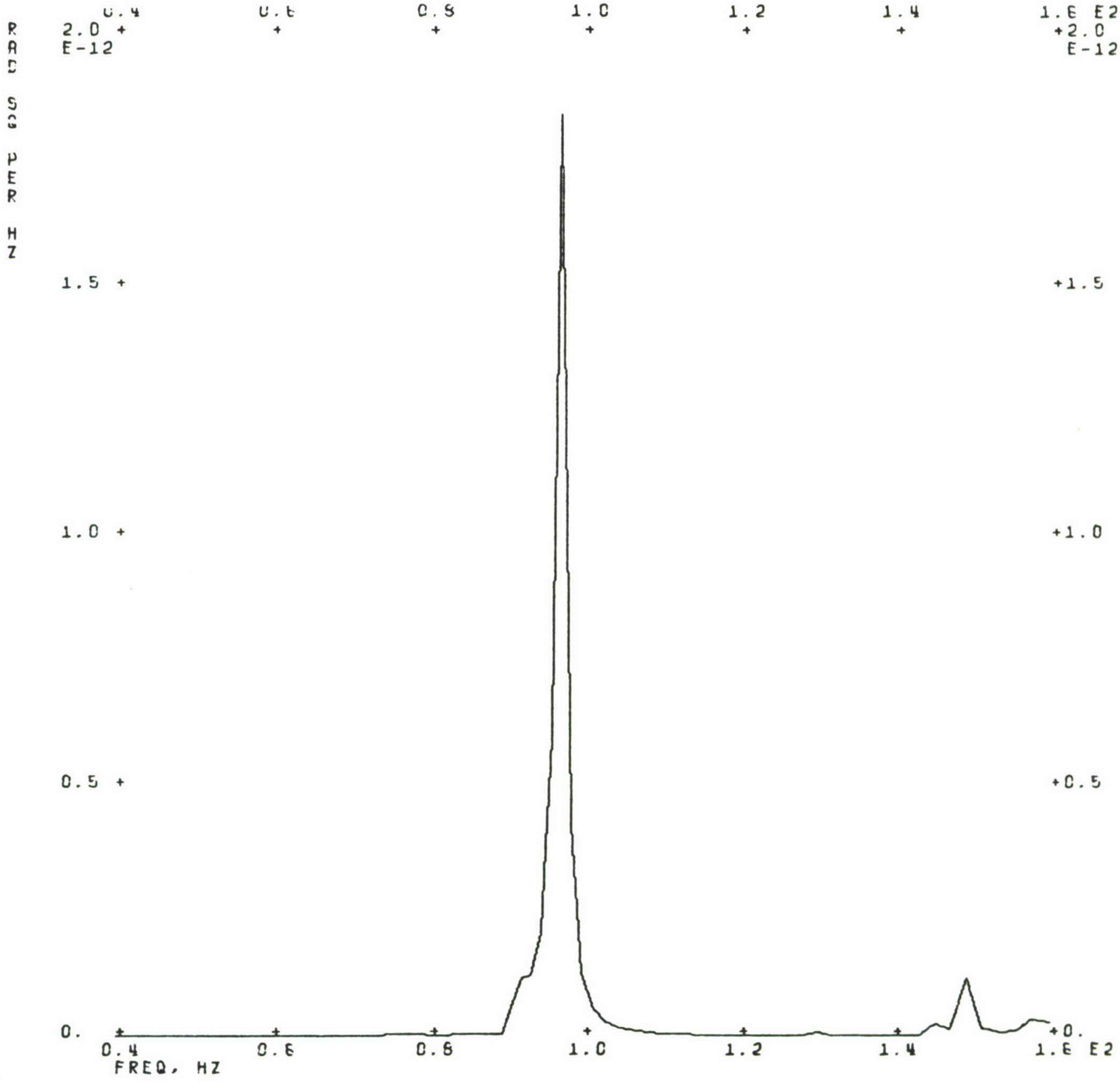

Figure 75 Analytical Results
Response Point 23, Rotation about X
Driving Point 3, X Translation

In retrospect, the fuselage analysis may not have been the ideal application for Semi-Loof given its present state of development. If the purpose of its development was to provide an advanced tool for analysis work, then it would have been informative to continue the policy followed in Phases I and II by modeling the same structure with both Semi-Loof and QUAD2 or other "standard" elements and then assessing the improvement in terms of accuracy per degree of freedom. Secondly, a smaller structure with equal complexity in terms of stiffeners, eccentricity, etc. would still have exercised the Semi-Loof elements just as well without the difficulties of getting large computer runs through a saturated central computer facility.

In spite of the disappointing results of the analysis, a number of valuable lessons were learned in the process. First, the participants emerged with a renewed appreciation of the amount of work involved in creating and debugging a large finite element model. Second, there was valuable feedback regarding some of the capabilities and input options needed in a large modeling job. In particular, these included convenient ways to specify beam orientations and offsets, and convenient specification of orthotropic (smeared stiffener) element orientation. Third, the exercise emphasized the number of variables or potential sources of discrepancy that can occur in an attempt to compare experimental to analytical results. Fourth, the Semi-Loof elements stood up well with respect to convenience of input and other operational details.

SECTION VIII
SUMMARY AND CONCLUSIONS

Angular vibration problems in aircraft have been studied in two distinct realms of vibration frequency. Low frequency problems have been studied from a deterministic viewpoint; that is, under the assumption that individual natural frequencies and mode shapes can be determined in some detail by analytical methods. Higher frequency problems have been approached in a statistical manner. The assumption here is that properties of individual modes cannot, and should not, be examined, but that aggregate response of mode groups can be estimated given only a limited structural description.

Considerable research and literature searching was carried out, but there was little to be found in the way of methods specifically addressed to angular vibration. Upon further reflection, it was decided that development work would have to be more general in nature, meaning that any new or improved methods would, for the most part, be relevant to vibration problems in general, and not just angular vibration.

The finite element method is the principal analytical tool currently in use for structural analysis. A number of advanced shell elements have been reported in the literature, but little of this progress has reached production users who mostly employ large, widely distributed codes such as NASTRAN. One set of curved shell elements known as "Semi-Loof" elements seemed especially promising. A skeleton computer program was obtained from its developer, Professor Bruce Irons. A preprocessing code was built around Irons' code to make it possible to use these elements with NASTRAN. This enables users to take full advantage of NASTRAN's capabilities. Small test problems showed encouraging results. A small stiffened panel was tested with results showing good agreement with Semi-Loof predictions. A large fuselage model was analyzed and tested, but with inconclusive results. A mathematical irregularity was encountered

in the quadrilateral element involving spurious mechanism modes. The problem was found to be avoidable, but still annoying.

The Semi-Loof pre- and post-processing programs are considered to be in production status, with careful attention having been given to input formats and error checking. Still, much more user experience will be needed before conclusive evaluations of these elements can be made. It is hoped that a real contribution has been made, not only to angular vibration methods, but to other shell analysis problems, as well.

For high frequency analysis, there is no widely accepted method with the flexibility and accuracy which finite elements allow in low frequency work. This is not surprising, considering the previously stated definition of the high frequency problem. During early literature searching, it was found that a rather diverse body of theory under the general name of Statistical Energy Analysis (SEA) had been developed during the 1960's in response to the difficulties of high frequency analysis. The method draws heavily on classical deterministic theories of acoustics, wave mechanics, and normal mode methods, and yet takes quite a unique view of vibration problems generally in that it uses component energies and intercomponent power flows as primary variables. SEA appeared to be well suited to the problem of predicting indirectly excited high frequency vibration of a piece of equipment mounted in an aircraft. The method is quite general and is not restricted to angular vibration.

It was decided that, due to the inexperience of the investigators with SEA, a small demonstration problem should be undertaken. The wave transmission method of SEA was used to predict equilibrium energy ratio and power transmission coefficient between two uniform plates coupled at a single degree of freedom. Comparison with experiment showed agreement which was quite encouraging in the light of the extensive assumptions involved. While physically simple, the experiment embodied the

typical factors which make high frequency predictions difficult. Mode counts were very high (over 600 total for the two plates) and individual mode shapes could not be determined. It was demonstrated how interactive digital FFT processing of measured data could be used to obtain the so-called coupling loss factors and internal loss factors of SEA. It was also demonstrated, and verified by experiment, that the basic assumptions of the wave transmission method can be utilized to estimate r.m.s. angular response given the component total energy for a uniform plate. While some software was developed in the course of the SEA experiment, it cannot yet be considered a production tool for the prediction of high frequency angular vibration.

Because of the extensive use of experimental methods for prediction of angular vibration, some effort was devoted to purely measurement problems. Differencing of output signals from translational accelerometers was identified as the most generally useful method of angular vibration measurement. Theoretical error analyses were performed to quantify the effects of intrachannel noise, interchannel gain and phase mismatch, and flexure of the mounting surface. It was concluded the measurement requirements involved in development of prediction methods could be satisfied by the differencing technique.

REFERENCES

1. Lyon, R. J., Statistical Energy Analysis for Designers, Part 1. Basic Theory and Part 2. The Engineering Application, AFFDL-TR-74-56. Part 1 - ADA 006 413, Part 2 - ADA 006 414.

2. Irons, B. M., "The Semi-Loof Shell Element," Finite Elements for Thin Shells and Curved Members, Chapter 11, ed. D. G. Ashwell and R. H. Gallagher, Wiley, London, 1976.

3. Zienkiewicz, The Finite Element Method in Engineering Service, McGraw-Hill, London, 1971.

4. Loof, H. W., "The Economical Computation of Large Structural Elements," Int. Symposium on Use of Computers in Structural Engineering, University of Newcastle-upon-Tyne, 1966.

5. Elaswaf, A., "An Application of the Semi-Loof Shell and Beam Elements," IASS World Conference on Space Enclosures.

6. Martins, R. A. F., and Owen, D. R. J., "Structural Instability and Natural Vibration Analysis of Thin Arbitrary Shells by Use of the Semi-Loof Element," J. Num. Methods in Engr., Volume 11, 1977, pp. 481-498.

7. Owen, D. R. J., and Martins, R. A. F., "Non-linear Analysis of Arbitrary Shell Structures by Use of the Semi-Loof Element."

8. NASTRAN Demonstration Problem Manual (Level 16.0), NASA SP-224(03), 1978.

9. Lyon, op cit, Section 3.2.

10. Remington, P. J., and Manning, J. E., "Comparison of Statistical Energy Analysis Power Flow Predictions with an 'Exact' Calculation," J. Acoustical Soc. Am., Vol. 57, No. 2, February 1975, pp. 374-379.

11. Manning, J. E., Cambridge Collaborative, Cambridge, Mass., personal communication.

12. Lyon, op cit, p. 38.

13. Lyon, op cit, Chapter 4.

14. Lyon, op cit, pp. 39-41.

15. Lee, Jr., and Whaley, P. W., Prediction of the Angular Vibration of Aircraft Structures, AFFDL-TR-76-56, Air Force Flight Dynamics Laboratory, Wright-Patterson AFB, Ohio, June 1976; also J. Sound and Vibration, Vol. 49, December 1976, pp. 541-549.

16. Klosterman, A., and Zimmerman, R., "Modal Survey Activity via Frequency Response Functions," Soc. Automotive Engineers, Paper No. 751068, National Aerospace Engineering and Manufacturing Meeting, Culver City, CA, Nov. 17-20, 1975.

17. Richardson, M., and Potter, R., "Identification of the Modal Properties of an Elastic Structure from Measured Transfer Function Data," Instrument Society of America, Paper 74250, 20th International Instrumentation Symposium, May 21-23, 1974, Albuquerque, New Mexico.

18. Otnes, R. K., and Enochson, L., Applied Time Series Analysis, Section 5.8, Wiley-Interscience, 1975.

19. Johnson, C. D., Gibson, W. C., Kienholz, D. A., and Paxson, E. B., Jr., "Interim Technical Report Angular Vibration of Aircraft, Phase II," Anamet Report 877.501C, October, 1978, under Contract No. F33615-77-C-3050.

20. Lyon, op cit, pp. 36-38.

21 Lyon, op cit, pp. 46-48.

22. Anamet Laboratories R & D Status Report, May 1978, Air Force Contract No. F33615-77-C-3050, on Angular Vibration of Aircraft.

23. Lee, J., and Whaley, P., "Prediction of the Angular Vibration of Aircraft Structures," J. Sound and Vibration (1976), Vol. 49, No. 4, pp. 541-549.

24. Anamet Laboratories R & D Status Report, June 1978, Air Force Contract No. F33615-77-C-3050, on Angular Vibration of Aircraft.

25. Whaley, P. W., and Obal, M. W., "Measurement of Angular Vibration Using Conventional Accelerometers," Shock and Vibration Bulletin, September 1977, pp. 97-107.

26. ten Wolde, T., Verheij, J. W., and Steenhoek, H. F., "Reciprocity Method for the Measurement of Mechano-Acoustical Transfer Functions," J. Sound and Vibration, Vol. 42, No. 1, 1975, pp. 49-55

REFERENCES (continued)

27. Bendat, J. S., and Piersol, A. G., Random Data: Analysis and Measurement Procedures, Wiley-Interscience, 1971, pp. 153-156.

28. Papoulis, A., Probability, Random Variables, and Stochastic Processes, McGraw-Hill, 1965, pp. 343-344.

29. Bendat and Piersol, op cit, pp. 141-147.

30. Lyon, op cit, p. 43.

31. Flügge, William, Stresses in Shells, Springer Vertag, Berlin, 1962, pp. 221-222.

32. Irons, B. M., "The Semi-Loof Shell Element," Symposium on Thin Shells and Curved Members, University College, Cardiff, Wales, April 1974.

APPENDIX A
SEMI-LOOF USER'S MANUAL

A.1 INTRODUCTION

This appendix is intended to supply all the information needed to prepare finite element models using Semi-Loof shell and beam elements. The reader is assumed to have read Section III of this report, which presents the background and mathematical nature of Semi-Loof elements. In addition, an "intermediate" level of NASTRAN expertise is assumed. This implies fairly extensive experience with medium- to large-scale modeling problems. No facility with the DMAP language is assumed, however. DMAP Alter packages described in this appendix are designed to be used as "black boxes."

The remainder of this appendix is organized as follows:

Section A.2 is a general discussion of the Semi-Loof element, reviewing the capabilities, assumptions, and precautions that users must have in mind.

Section A.3 gives instructions for preparing input data for PRELOOF, the Semi-Loof preprocessing routine. For the most part, this data is prepared in the NASTRAN "BULK DATA" format.

Section A.4 discusses POSTLOOF, the post-processing routine for recovery of rotations and stresses.

Section A.5 presents deck setups for CDC computers. The Semi-Loof coding has not been implemented on any other machines at this time.

Finally, Section A.6 is a compilation of programmer's notes for those who are interested in programming details.

Listings of control card procedures, Fortran source code for PRELOOF and POSTLOOF, and DMAP Alters appear in Appendix B.

A.2 GENERAL DISCUSSION

The following is a summary of the salient features of the Semi-Loof shell and beam elements from the user's point of view.

First, the shell elements are strictly for thin shell analysis, as reflected in the assumption of zero transverse shear strain at selected points on the shell. The decision as to what constitutes a thin shell is an engineering judgement, based on the R/t ratio. R is a radius of curvature for a curved shell, or a typical span for a flat plate. R/t should normally exceed 10 for a thin shell.

The shell elements represent both stretching and bending action. For flat plates, one may suppress one or the other of these actions. Assuming the plate lies in the x-y plane, one would constrain degrees of freedom 1 and 2 to eliminate stretching, or 3, 4, 5, and 6 for bending. (Even though 4, 5, and 6 are already suppressed by permanent single point constraints at corner nodes, and 6 at Loof nodes, it is not an error to constrain these redundantly on SPC cards. See the discussion of permanent SPC's in the next section.)

It is important to keep in mind the nature of the degrees of freedom for these elements. As explained in Section 3.4, each node point uses degrees of freedom 1, 2, and 3 as translations, like other NASTRAN elements, but dof 4, 5, and 6 are different. For the shell element, no rotation degrees of freedom are defined at corner points. This does not mean that rotations are zero at such points, but only that these rotations are not independent degrees of freedom. At mid-side nodes, dof 4 and 5 represent rotations about the tangent to the element side. These rotations are not actually located at the mid-side node, but at the Loof nodes, located at about 58% ($1/\sqrt{3}$) of the distance from the mid-side to either corner. Thus the values of dof 4 and 5 are not usually of interest at mid-side nodes, but their nature must be understood when it comes to applying constraints, loads, or especially joining other elements. If another NASTRAN bending element were joined to the mid-side node

of a Semi-Loof shell, the NASTRAN element would interpret dof 4 and 5 as rotations about the x and y axes at that node point, while the Semi-Loof element would interpret them as explained above. This error would not be detected by the software. The Semi-Loof beam element defines all three translations and three rotations in the normal NASTRAN manner at the two end points. The middle node uses dof 4 and 5 as Loof rotations for compatibility with the shell elements.

From this discussion it may be seen that the mid-side nodes are in a sense subservient to the corner nodes. That is, each mid-side node serves to define the shape of the arc joining two corner nodes. The fact that LOOF8 has eight nodes should not be construed to mean that LOOF8 is an eight-sided element. In setting up a model, one should first locate the corner nodes and then place the mid-side nodes at the center of each element edge. Although tests have shown that a considerable deviation in location from the center point can be tolerated without losing much accuracy, still there is usually no reason not to pick the center point, so this practice is recommended.

At this time, no studies have been made with regard to aspect ratios, and particularly, what is a practical upper bound on aspect ratio. No problem is anticipated, due to the iso-parametric formulation. It is known that no element side should not have too severe curvature. A 30° arc seems to be a good upper limit.

LOOF8 elements are preferred over LOOF6 triangle elements where the geometry permits. Two triangles would have five more degrees of freedom than a LOOF8 element covering the same area, and probably less accuracy.

A special feature of LOOF8 and LOOF6 is their accommodation of variation of element thickness and/or surface pressure over the surface of any element. In these cases, thicknesses and/or pressures are assigned to grid points, and the grid point values are interpolated over the element surface. For constant thick-ness elements, thicknesses are assigned on element connection

cards, and these values override any grid point thickness values. Variation of pressure would be useful for representing hydrostatic or hydrodynamic fluid pressures, for example.

LOOF8 and LOOF6 can reference isotropic and orthotropic material properties. In addition, there is a provision that is useful in modeling minor stiffening ribs in airframe structures. The most economical and realistic strategy in these cases is to "smear" the minor ribs, that is, to distribute their stiffness to the attached panel. This is done by calculating properties for an anisotropic panel that has the same stretching and bending stiffnesses as the panel-rib assemblage. This approach will, of course, not provide accurate local representation of deformations but should be a good overall model. The following formulas taken from Reference [31] may be useful in such cases:

$$
\begin{aligned}
A_{11} &= \frac{Et}{1-\nu^2} + \frac{EA_1}{b_1} \\
A_{22} &= \frac{Et}{1-\nu^2} + \frac{EA_2}{b_2} \\
A_{12} &= \frac{\nu Et}{1-\nu^2} \\
A_{33} &= \frac{Et}{2(1+\nu)} \\
B_{11} &= \frac{EA_1C_1}{b_1} \\
B_{22} &= \frac{EA_2C_2}{b_2} \\
D_{11} &= \frac{Et^3}{12(1-\nu^2)} + \frac{E(I_1 + A_1C_1^2)}{b_1} \\
D_{22} &= \frac{Et^3}{12(1-\nu^2)} + \frac{E(I_2 + A_2C_2^2)}{b_2} \\
D_{12} &= \frac{\nu Et^3}{12(1-\nu^2)} \\
D_{33} &= \frac{Et^3}{12(1+\nu)} + \frac{G}{2}\left(\frac{J_1}{b_1} + \frac{J_2}{b_2}\right)
\end{aligned}
\tag{A.1}
$$

Here A_{ij}, B_{ij}, and D_{ij} are force-strain parameters coupling force and moment resultants to strains and curvatures:

$$
\begin{Bmatrix} N_1 \\ N_2 \\ N_{12} \\ \hdashline M_1 \\ M_2 \\ M_{12} \end{Bmatrix} = \left[\begin{array}{ccc:ccc} A_{11} & A_{12} & 0 & B_{11} & 0 & 0 \\ A_{12} & A_{22} & 0 & 0 & B_{22} & 0 \\ 0 & 0 & A_{33} & 0 & 0 & 0 \\ \hdashline B_{11} & 0 & 0 & D_{11} & D_{12} & 0 \\ 0 & B_{22} & 0 & D_{12} & D_{22} & 0 \\ 0 & 0 & 0 & 0 & 0 & D_{33} \end{array} \right] \begin{Bmatrix} \varepsilon_1 \\ \varepsilon_2 \\ \varepsilon_{12} \\ \hdashline \chi_1 \\ \chi_2 \\ \chi_{12} \end{Bmatrix} \qquad (A.2)
$$

In these expressions, subscripts 1 and 2 represent two orthogonal directions. The beam properties referenced in Eq. (A.1) are

I_i = moment of inertia of a rib about its own center of gravity

A_i = area

b_i = spacing of ribs

C_i = eccentricity

J_i = torsion constant of a single rib

Also,

E,ν = material properties of both ribs and panel

t = panel thickness

Figure A-1 illustrates these properties

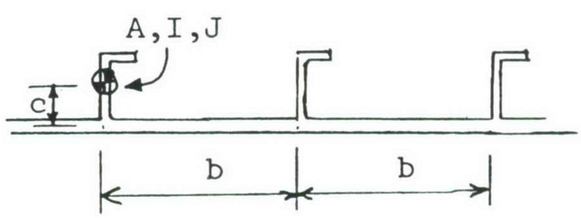

Figure A-1 Stiffened Panel Properties

It is important to get the signs of the B terms right. They are positive if the stiffeners are located on the positive side of the element; negative otherwise. The positive side is

determined by taking the cross product of unit vectors in the ξ and η directions (e.g. $\underset{\sim}{V}_\zeta = \underset{\sim}{V}_\xi \times \underset{\sim}{V}_\eta$, see Figure A-2). The resulting vector points outward on the positive side of the element. An equivalent indicator is to proceed around the perimeter of the element in the sequence prescribed on the CLOOF card and use the right-hand rule.

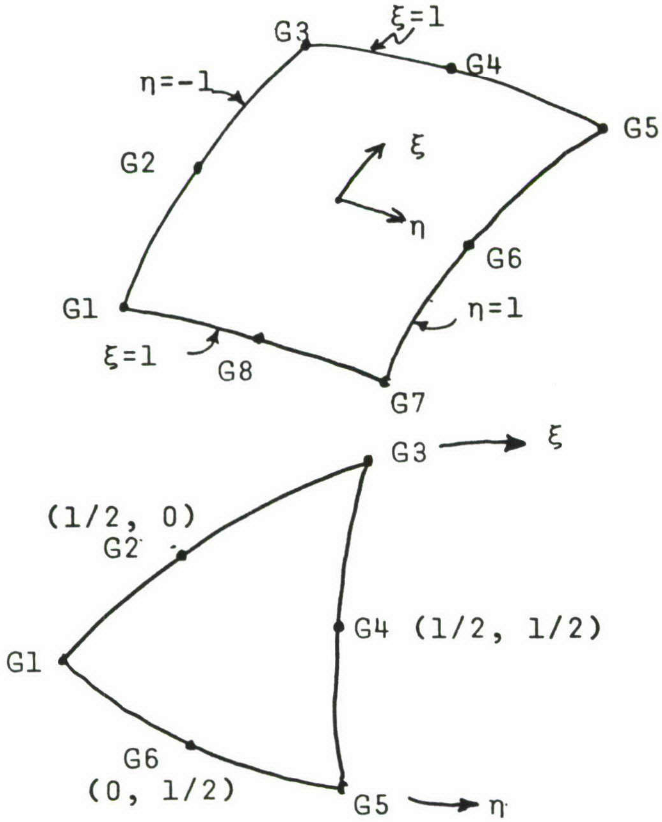

Figure A-2 Local Coordinates for LOOF8 and LOOF6 Elements

The LOOF3 curved beam element can represent non-prismatic beams. In this case, cross-section properties are prescribed at each node point and are interpolated quadratically over the length of the element.

The following items are not incorporated in the Semi-Loof elements at this time:

(1) Geometric stiffness
(2) Thermal loads
(3) Heat transfer matrices
(4) Line loads

Two computer programs have been written to interface Semi-Loof to NASTRAN: PRELOOF and POSTLOOF. PRELOOF reads the bulk data deck and interprets certain bulk data cards that describe Semi-Loof elements. It also recognizes GRID cards and certain other bulk data cards. It then generates and assembles stiffness matrices, mass matrices, and distributed loads and writes them on a binary file in a form suitable for input to NASTRAN. The data cards, with Semi-Loof connection and property cards deleted, are then passed to NASTRAN. NASTRAN then saves output information in a form that can be read by POSTLOOF which recovers angular deformations or stresses as requested by the user.

Most of this process of transferring files into and out of NASTRAN has been automated by means of control card procedures and DMAP Alters, and can be set up by the user with a minimum knowledge of computer control details. As mentioned earlier, a moderate amount of experience with NASTRAN is assumed, however. The following sections describe the steps required to use PRELOOF and POSTLOOF.

A.3 PRELOOF INPUT

Input to PRELOOF consists of a complete NASTRAN input file: Executive Control, Case Control, and Bulk Data. This file is read by PRELOOF, modified, and then passed on to NASTRAN for execution. Some of the data cards are recognized by PRELOOF and then removed from the deck, some are recognized and retained, and others are passed directly to NASTRAN without any processing. These cards are described below and summarized in Table A-1.

The UPDATE utility is used to manipulate the input deck, so the first card must always be

*DECK X

which is immediately followed by a title card. Then begins the Executive Control Deck, which contains the cards ID, TIME, APP, SOL, DIAG, etc., as in a normal NASTRAN run. Next there is provision for a number of options which govern PRELOOF. These are listed below, with the default option underlined:

\$LOOFECHO $\left\{\begin{matrix}\text{YES}\\ \underline{\text{NO}}\end{matrix}\right\}$	If yes, echo bulk data deck as read.
\$LOOFPLOT $\left\{\begin{matrix}\text{YES}\\ \underline{\text{NO}}\end{matrix}\right\}$	If yes, generate PLOTEL cards representing LOOF8 and LOOF6 elements. The PLOTEL element numbers are 10*N+i where N is the LOOF element number and i ranges from 1 to 8 for LOOF8 or 1 to 6 for LOOF6.
\$LOOFMAT $\left\{\begin{matrix}\underline{\text{YES}}\\ \text{NO}\end{matrix}\right\}$	If yes, generate matrices for NASTRAN. If no, process bulk data but do not generate matrices (e.g. for plots or debug).
\$LOOFDYN $\left\{\begin{matrix}\text{YES}\\ \underline{\text{NO}}\end{matrix}\right\}$	If yes, generate mass matrix for dynamics problem. If no, generate stiffness but not mass matrix.
\$LOOFDEBUG $\left\{\begin{matrix}\text{YES}\\ \underline{\text{NO}}\end{matrix}\right\}$	If yes, print out element matrices for diagnosis.
\$NASTRAN $\left\{\begin{matrix}\text{MSC}\\ \text{COSMIC}\end{matrix}\right\}$	Selects either MSC/NASTRAN or COSMIC NASTRAN. Default set to correspond to each particular installation.
\$LOOFGAUSS $\left\{\begin{matrix}\underline{2}\\ 3\end{matrix}\right\}$	Integration rule: 2 means 2x2, 3 means 3x3 integration.

$LOOFFACT $\begin{Bmatrix} \underline{0.0} \\ \chi \end{Bmatrix}$ Sets a factor to be used for a fifth point in 2x2 integration. 0.2 is a recommended value for χ when this option is used.

Following the $ option cards, the following must be included to access rigid format alters:

*READ RFALTS

followed by

ENDALTER
CEND

the end of the executive control deck.

Next is the case control, which is the same as for any NASTRAN run with the following exception: when pressure loads are generated by PRELOOF there must not be any LOAD cards in the case control deck. This implies only a single load case.

The bulk data deck is somewhat restricted in format as compared with normal NASTRAN capabilities which the reader is assumed to know. The following rules apply:

(1) The first field of each card must be left-adjusted.

(2) Among the cards recognized by PRELOOF (listed below), continuation cards must immediately follow their parents. Also, among these cards, only GRID may use the double field option (i.e. GRID*).

(3) The bulk data cards must be sorted into groups, with groups in the order listed below. Within each group, cards may be in any order as long as continuation cards immediately follow their parents.

Group 1: CORD2R, CORD2C, and CORD2S cards. These cards must reference the basic coordinate system in field 3.

Group 2: GRID cards (the double field GRID* may also be used). Only coordinate systems defined in group 1 (or the basic system) may be used. Permanent single-point constraints must <u>not</u> be used. They are established by PRELOOF.

Group 3: SEQGP cards. The BANDIT bandwidth optimization code has been modified to recognize CLOOF8, CLOOF6, and CLOOF3 cards.

Group 4: CLOOF8 and CLOOF6 element connection cards for quadrilateral and triangular Semi-Loof elements, respectively. These cards are described in detail on pages 235 through 238.

Group 5: CLOOF3 element connection cards for curved beam elements. See page 232 for format.

Group 6: PLOOF cards giving properties of isotropic LOOF8 and LOOF6 elements. See page 241.

Group 7: PLOOFX cards giving properties for anisotropic LOOF8 and LOOF6 elements. See page 243.

Group 8: PLOOF3 cards giving properties for LOOF3 elements. See page 242.

Group 9: MAT1 cards. As per the NASTRAN manual.

Group 10: MAT8 cards for homogeneous orthotropic shells (for smeared stiffeners see PLOOFX). See page 239.

Group 11: PLOAD4 cards defining pressures at grid points. See page 240.

Group 12: THLOOF cards defining thicknesses at grid points. See page 245.

Group 13: PARAM cards. Only PARAM WTMASS, which has the same function as in standard NASTRAN runs, is used.

Group 14: SPOINT cards. Scalar point identification numbers must be greater than the highest grid point number.

Following these cards, all bulk data cards not processed by PRELOOF are included. See Table A-1 for a summary of the foregoing.

TABLE A-1

SUMMARY OF PRELOOF INPUT DECK

```
*DECK X
title card
- - - - - - - - - - - - - - - - - - - - - - - - - - - - - -
ID                        Executive
TIME                        Control
APP                           Deck
SOL
DIAG
.
.
.
$LOOF options
*READ RFALTS
ENDALTER
CEND
- - - - - - - - - - - - - - - - - - - - - - - - - - - - - -
TITLE=----                Case
.                           Control
.                             Deck
.
BEGIN BULK
- - - - - - - - - - - - - - - - - - - - - - - - - - - - - -
CORD2R, CORD2C, CORD2S    Bulk
GRID                        Data
SEQGP                         Deck
CLOOF8, CLOOF6
CLOOF3
PLOOF
PLOOFX
PLOOF3
MAT1
MAT8
PLOAD4
THLOOF
PARAM
SPOINT
other Bulk Data Cards
ENDDATA
```

Input Data Card CLOOF3 Connections for LOOF3 Curved Beam Element

Description: Defines a Semi-Loof beam element of the structural model.

Format and Example:

1	2	3	4	5	6	7	8	9	10
CLOOF3	EID	MID	G1	G2	G3	P1	P2	P3	abc
CLOOF3	1401	1	502	502	503	7			ABC
+bc	F1,G0	F2	F3	F					def
+BC	0.	1.	0.	1					DEF
+ef	A1	B1	A2	B2	A3	B3			
+EF	-0.2								

Field	Contents
EID	Element identification number (Integer > 0).
MID	Identification number of a MAT1 material card (Integer > 0).
G1, G2, G3	Grid point identification numbers of connection points (Integer > 0, G1 ≠ G2 ≠ G3)
P1, P2, P3	Identification numbers of PLOOF3 cards defining section properties at G1, G2 and G3, respectively.
F1, F2, F3	Components of vector $\vec{V}$ at the end of the beam corresponding to grid point G1. $\vec{V}$, together with the vector from G1 to G3, define the principal bending plane of the element. (Straight beams only).
G0	Grid point identification number to optionally define $\vec{V}$ as the vector from G1 to G0.
F	Flag to specify the nature of fields 2, 3, 4 on the first continuation card as follows:

	2	3	4
F=1	F1	F2	F3
F=2	G0	blank	blank

CLOOF3 (Continued)

A1, A2, A3 Offset distance of grid point G1, G2, or G3, respectively, in plane 1. Positive if the sense of Ai is the same as the sense of X_2 (see sketch below).

B1, B2, B3 Offset distance of grid point G1, G2, or G3 respectively, in plane 2. Positive if the sense of Bi is the same as the sense of X_3 (see sketch below)

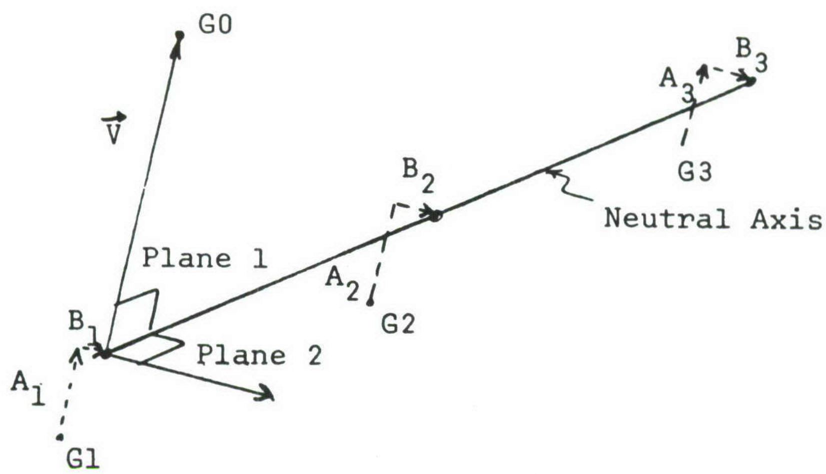

Straight Beam

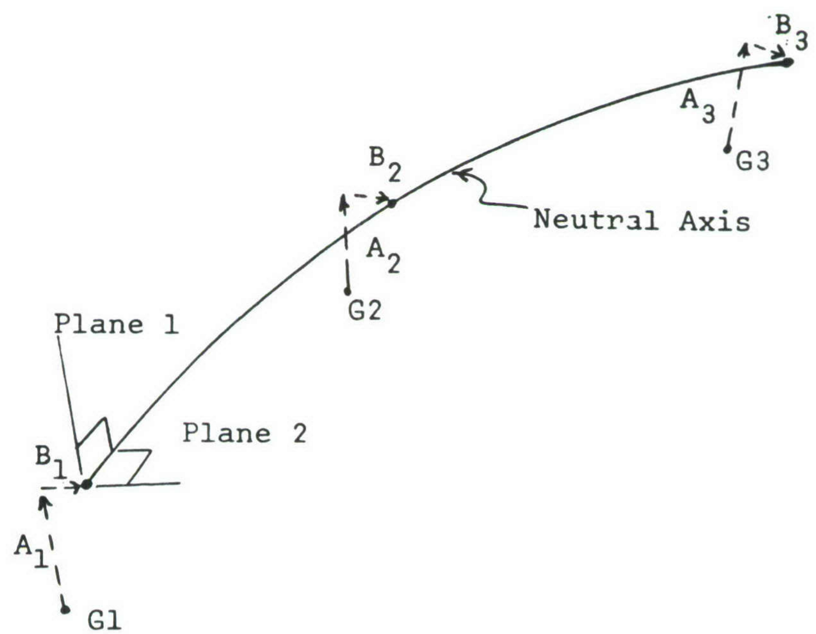

Curved Beam

Remarks:

1. Element identification numbers must be unique with respect to all other element identification numbers.

2. The center node G2 should be located near the center of the arc connection G1 to G3.

3. The continuation cards are optional.

4. Degrees of freedom 4 and 5 at node G2 represent Loof rotations and are not the grid point rotations normally used by NASTRAN.

5. The vector $\vec{V}$ is used only for straight beams. For curved beams, the principal plane is always the plane in which the curved beam lies. The principal plane is plane 1, corresponding to I1, C1 and D1 on the PLOOF3 card. Plane 2 corresponds to I2, C2 and D2.

Input Data Card CLOOF6 Connections for LOOF6 Element

Description: Defines a triangular Semi-Loof shell element of the structural model.

Format and Example:

1	2	3	4	5	6	7	8	9	10
CLOOF6	EID	PID	G1	G2	G3	G4	G5	G6	abc
CLOOF6	107	43	2	4	5	7	12	9	ABC
+bc	TH								
+BC	-14.0								

Field Contents

EID Element identification number (Integer > 0)

PID Identification number of a PLOOF property card (Integer > 0)

G1,...,G6 Grid point numbers of connection points (Integer > 0, G1 ≠ G2 ≠ ... ≠ G6)

TH Material property orientation angle in degrees (Real). The sketch below gives the sign conversion for TH.

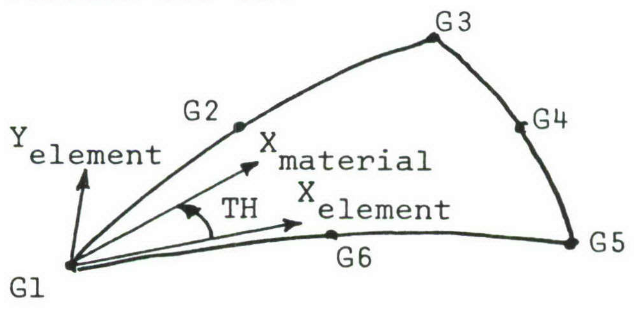

Remarks: 1. Element identification numbers must be unique with respect to all other element identification numbers.

2. Grid points G1 through G6 must be numbered consecutively around the perimeter of the element.

3. All interior angles must be less than 180°.

4. The Loof nodes G2, G4 and G6 should be located near the center of the arc connecting the respective corner points.

5. The continuation card is optional.

6. Degrees of freedom 4 and 5 at the Loof nodes represent Loof rotations and not the grid point rotations normally used by NASTRAN.

BULK DATA DECK

Input Data Card <u>CLOOF8</u> Connections for LOOF8 Element

Description: Defines a quadrilateral Semi-Loof shell element of the structural model.

Format and Example:

1	2	3	4	5	6	7	8	9	10
CLOOF8	EID	PID	G1	G2	G3	G4	G5	G6	abc
CLOOF8	16	101	104	105	106	109	110	112	ABC
+bc	G7	G8	TH						
+BC	114	102							

Field	Contents
EID	Element identification number (Integer > 0)
PID	Identification number of a PLOOF or PLOOFX property card (Integer > 0)
G1,...,G8	Grid point identification numbers of connection points (Integer > 0, G1 ≠ G2 ≠ ... ≠ G8)
TH	Material property orientation angle in degrees (Real). The sketch below gives the sign conversion for TH.

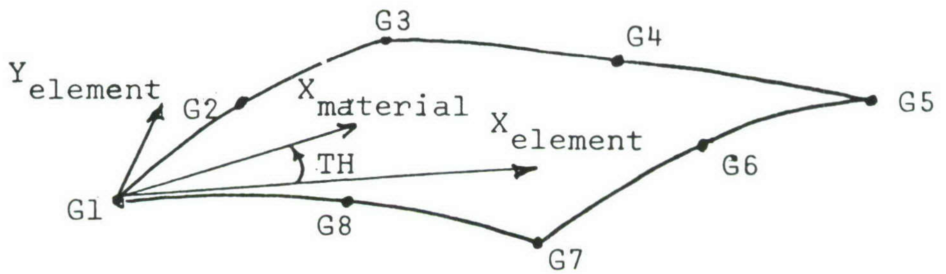

Remarks: 1. Element identification numbers must be unique with respect to all other element identification numbers.

2. Grid points G1 through G8 must be numbered consecutively around the perimeter of the element.

3. All interior angles must be less than 180°.

CLOOF8 (Continued)

4. Loof nodes G2, G4, G6 and G8 should lie near the mid point of the arc connecting the respective corner points.

5. Degrees of freedom 4 and 5 at the Loof nodes represent Loof rotations and not the grid point rotations normally used by NASTRAN.

Input Data Card MAT8 Material Property Definition, Form 8

Description: Defines the material properties for linear, temperature-independent, orthotropic materials.

Format and Example:

1	2	3	4	5	6	7	8	9	10
MAT8	MID	E11	E12	E22	G	RHO	X	X	
MAT8	1	10.2E6	3.2E6	8.2E6	4.1E6	0.2E-6			

Field Contents

MID Material identification number (Integer > 0)

E11, E12, E22, G — Elements of stress-strain matrix

$$\begin{Bmatrix} \sigma_1 \\ \sigma_2 \\ \tau_{12} \end{Bmatrix} = \begin{bmatrix} E_{11} & E_{12} & 0 \\ E_{12} & E_{22} & 0 \\ 0 & 0 & G \end{bmatrix} \begin{Bmatrix} \varepsilon_1 \\ \varepsilon_2 \\ \gamma_{12} \end{Bmatrix}$$

RHO Mass density

Input Data Card <u>PLOAD4</u> Distributed Loads for LOOF8 and LOOF6 Elements

<u>Description</u>: Specifies distributed pressure loads by grid points. All LOOF8 and LOOF6 elements connected to these grids have these loads applied.

<u>Format and Example</u>:

1	2	3	4	5	6	7	8	9	10
PLOAD4	P	G1	G2	G3	G4	G5	G6	G7	
PLOAD4	-0.1	17	18	22					

<u>Alternate Form</u>:

PLOAD4	P	GA	"THRU"	GB	X	X	X	X	
PLOAD4	112.0	100	THRU	110					

<u>Field</u> <u>Contents</u>

P Pressure value (Real)

G1,G2,...
GA, GB } Grid point numbers (Integer > 0)

<u>Remarks</u>:

1. There is no set identification number. Distributed loads on LOOF elements are not selected in the Case Control Deck.

2. In the alternate form, all grid points from GA through GB are given the specified load.

Input Data Card PLOOF Properties of LOOF8 Element

Description: Defines the properties of a Semi-Loof shell element. Referenced by CLOOF8 and CLOOF6 cards.

Format and Example:

1	2	3	4	5	6	7	8	9	10
PLOOF	PID	MID	THICK						
PLOOF	2	1							

Field	Contents
PID	Property identification number (Integer > 0)
MID	Material identification number of a MAT1 or MAT8 card (Integer > 0)
THICK	Element thickness (Real)

Remarks: 1. If THICK is omitted, thicknesses will be taken from THLOOF cards.

Input Data Card PLOOF3 Properties of a Semi-Loof Beam Element

Description: Defines the cross-sectional properties at one or more node points of a Semi-Loof curved beam element.

Format and Example:

1	2	3	4	5	6	7	8	9	10
PLOOF3	PID	A	I1	I2	J	C1	C2	D1	abc
PLOOF3	7	0.02	0.113	0.113	0.067	0.5	-0.5		+XY

+bc	D2								
+XY									

Field	Contents
PID	Property identification number (Integer > 0)
A	Cross-sectional area (Real > 0)
I1, I2	Moments of inertia (Real)
J	Torsion constant (Real)
C1, C2, D1, D2	Stress recovery coefficients (Real)

Remarks:

1. The stress recovery coefficients are the local coordinates defining fiber distances for which stresses may be recovered.

2. The continuation card is optional.

Input Data Card PLOOFX Orthotropic Membrane, Bending and Coupling Properties for LOOF8 and LOOF6 Elements

Description: Specifies a general force-strain law for a LOOF8 or LOOF6 element in matrix form.

Format and Example:

1	2	3	4	5	6	7	8	9	10
PLOOFX	PID	A11	A12	A13	A22	A23	A33	X	abc
PLOOFX		10.2E6	4.1E6		7.6E6		3.3E6		ABC
+bc	DENS	B11	B12	B13	B22	B23	B33	X	def
+BC	0.06								DEF
+ef	X	D11	D12	D13	D22	D23	D33	X	
DEF		5.2E6	0.9E6		3.2E6		1.8E6		

Field Contents

PID Property identification number (Integer > 0)

A_{ij}, B_{ij}, D_{ij} Matrices defining the force-strain law for the element as follows:

$$\begin{Bmatrix} N_1 \\ N_2 \\ N_{12} \\ --- \\ M_1 \\ M_2 \\ M_{12} \end{Bmatrix} = \left[\begin{array}{ccc:ccc} A_{11} & A_{12} & A_{13} & B_{11} & B_{12} & B_{13} \\ A_{12} & A_{22} & A_{23} & B_{12} & B_{22} & B_{23} \\ A_{13} & A_{23} & A_{33} & B_{13} & B_{23} & B_{33} \\ \hdashline B_{11} & B_{12} & B_{13} & D_{11} & D_{12} & D_{13} \\ B_{12} & B_{22} & B_{23} & D_{12} & D_{22} & D_{23} \\ B_{13} & B_{23} & B_{33} & D_{13} & D_{23} & D_{33} \end{array}\right] \begin{Bmatrix} \varepsilon_1 \\ \varepsilon_2 \\ \gamma_{12} \\ \\ \chi_1 \\ \chi_2 \\ \chi_{12} \end{Bmatrix}$$

PLOOFX (continued)

N_1, N_2, and N_{12} are in-plane force resultants and G_1, G_2, and γ_{12} are corresponding in-plane strains. M_1, M_2, and M_{12} are moment resultants, and χ_1, χ_2, and χ_{12} are corresponding curvatures.

DENS Effective mass per unit area for the shell

Remarks:

1. No material property card is referenced since material properties are implicit in the matrices A, B, D, and DENS.

2. The continuation cards may be omitted if no bending or coupling terms are desired.

BULK DATA DECK

Input Data Card THLOOF Grid-point Thicknesses

Description: Associates thicknesses with grid points for use by Semi-Loof shell elements.

Format and Example:

1	2	3	4	5	6	7	8	9	10
THLOOF	TH	GID	GID	GID	GID	GID	GID	GID	
THLOOF	0.07		4	7	6				

Alternate form:

THLOOF	TH	GID1	"THRU"	GID2					
THLOOF	0.2	16	THRU	48					

Field	Contents
TH	Thickness (Real > 0)
GID GID1 GID2	Grid-point identification number (Integer > 0, GID1 < GID2)

Remarks:
1. GID must be 0 or blank for omitted entries.
2. At least one positive GID must be present on each THLOOF card.

A.4 POSTLOOF INPUT

The POSTLOOF code serves to recover two kinds of information from solution vectors generated by NASTRAN: rotations and stresses. The solution vectors may be static displacements, eigenvectors, transient or frequency response vectors. If the NASTRAN output file contains more than one solution vector, information is recovered and printed successively for each vector.

The reason for recovering rotations in POSTLOOF is that node point rotations are not independent degrees of freedom with Semi-Loof shell elements, yet they may be of interest. Furthermore, rotations at arbitrary locations may be of interest, and these may be recovered as well. At node points, rotations are discontinuous between elements. The approach used for node points is to average the values indicated by all the elements that touch a given node point, except that when a LOOF3 beam element defines a rotation at a grid point, that value is used.

Stresses, if requested, are output at Gauss points only, which are optimal for stress calculations.

Input to POSTLOOF is as follows with default options underlined:

$NASTRAN $\left\{\begin{matrix}\text{MSC}\\ \text{COSMIC}\end{matrix}\right\}$ Default set for each installation.

$LOOFROT $\left\{\begin{matrix}\underline{\text{NONE}}\\ \text{GRIDS}\\ \text{n}\end{matrix}\right\}$ Where "NONE" suppresses recovery of rotations, "GRIDS" causes recovery at all grid points, and n is an integer indicating that rotations are requested at n specific locations, listed on n data cards immediately following.

Rotation recovery locations: (LOOFROT n option)

Col. 1-5	6-15	16-25
m_1	ξ_1	η_1
m_2	ξ_2	η_2
.	.	.
.	.	.
.	.	.
m_n	ξ_n	η_n

where m_i is an element number, and ξ_i, η_i are local coordinates for that element ($-1 \le \xi_i,\eta_i \le 1$ for LOOF8, $0 \le \xi_i,\eta_i \le 1$ for LOOF6). See Figure A-7 for local coordinates.

$LOOFSTRESS { NONE / ALL / R }	Where "NONE" suppresses recovery of stresses, "ALL" causes recovery for all elements, and n is an integer indicating that stresses are desired for n specific elements, listed on following data cards.

Stress recovery elements: ($LOOFSTRESS n option)

Col. 1-5	
	Where m_i is a LOOF8 or LOOF6 element number.
m_1	
m_2	
.	
.	
.	
m_n	

POSTLOOF can easily be tailored by the user-programmer for specific requirements. A POSTLOOF listing appears in Appendix B.

A.5 DECK SETUP

A complete Semi-Loof analysis consists of three major steps: PRELOOF, NASTRAN, and POSTLOOF. In order to relieve the user of the burden of operating system details, control card procedures ("procs") have been set up so that each step can be called by a single control card:

```
BEGIN(PRE,LOOF)
NASTRAN(DATA)ATTACH
BEGIN(POST,LOOF)
```

Proc "PRE" uses the UPDATE utility to fetch the DMAP alter package required by the user and insert it into the user's deck. PRELOOF is executed, and the NASTRAN program file is attached. Proc "POST" reads input and executes POSTLOOF.

DMAP alter packages are maintained in an UPDATE program library, which is automatically accessed by PRE. There are two alter packages for each rigid format (currently RF 1, 3, 11, 24, and 25 are supported): one for preprocessing and one for postprocessing. Deck names for each DMAP sequence are formed by concatenating the letters RF, the rigid format number, and either PRE or POST, e.g. RF3PRE or RF25POST. Each run will use an RFxxPRE sequence, an RFxxPOST sequence, or both. They are listed on an UPDATE *C card followed by an end-of-record card (7/8/9).

Finally, PRE attaches the NASTRAN program file. Thus, a complete deck setup for a run including all three processing steps would have the following form (assume rigid format 3 is being run):

Cards(s)	Remarks
job card, account cards	Follow installation rules.
ATTACH(LOOF,ID=xxxx)	Attach proc file using ID specified for a particular installation.
BEGIN(PRE,LOOF)	Assemble input and execute PRELOOF.
RFL(xxxxxx)	Request appropriate field length for NASTRAN.
NASTRAN(DATA)ATTACH	Execute NASTRAN.
BEGIN(POST,LOOF)	Execute POSTLOOF.
7/8/9	
*C RF3PRE,RF3POST	Fetch DMAP alter sequences.

Card(s)	Remarks
7/8/9	
*DECK X	
.	PRELOOF input as explained in Section A.3.
.	
.	
7/8/9	
.	POSTLOOF input as explained in Section A.4.
.	
.	
6/7/8/9	

Many users like to maintain large data decks in UPDATE program libraries. To accommodate this feature, PRE checks for the presence of a file named OLDPL and if one is present, it makes corrections to decks on that file using correction cards supplied by the user. In this case, a card such as

```
ATTACH(OLDPL,MYSEMILOOFDECK,ID=xxxx)
```

would precede BEGIN(PRE,LOOF) and the input record for PRELOOF would consist of UPDATE corrections such as

```
*ID FIXMYDECK
*I EXEC.10
*READ RFALTS
*D BULK.200
PARAM WTMASS .00259
7/8/9
```

For large problems, the user may desire to rerun NASTRAN without rerunning PRELOOF, or to rerun POSTLOOF without rerunning NASTRAN. To do this, the user must know what files are passed from one step to the next. Four files are involved:

File	Remarks
UT1	Contains stiffness matrices, mass matrices, and load vectors. Written by PRELOOF and read by NASTRAN. Binary format.
DATA	NASTRAN data deck after modification by PRELOOF. Written by PRELOOF and read by NASTRAN. Card image format.
LSTRES	Stress matrices and element connection tables. Written by PRELOOF and read by POSTLOOF. Binary format.

File	Remarks
UT2	Solution vector(s). Written by NASTRAN and read by POSTLOOF. Binary format.

Figure A-3 shows how these files pass information from PRELOOF to NASTRAN to POSTLOOF.

In running restart cases one must know what information must be regenerated and what information can be salvaged from previous runs. If any structural data changes, PRELOOF must be rerun and UT1 and DATA regenerated. Proc PRE checks for the presence of UT1 and if present, skips PRELOOF execution and just does UPDATE processing and attaches NASTRAN. If the NASTRAN restart facility is to be used, involving problem tapes and checkpoint dictionaries, one needs to know whether the rigid format will be restarted before or after the point at which UT1 is read in. If before, UT1 must either be generated or recovered from a previous run before executing NASTRAN. If after, UT1 is omitted, and the DMAP sequence used to read UT1 (i.e. RFxxPRE) is also omitted.

Now consider a sequence of runs for a large problem. Assume that input data is maintained on an UPDATE program library with deck names EXEC, CASE, and BULK, and that the following sequence of runs is executed:

1. Check out data and plot the undeformed structure.

2. Run static load check case.

3. Run dynamic case using NASTRAN checkpoint facility.

4. Restart NASTRAN without rerunning PRELOOF, save output from NASTRAN, then run POSTLOOF.

5. Rerun POSTLOOF.

The deck setups would be as follows:

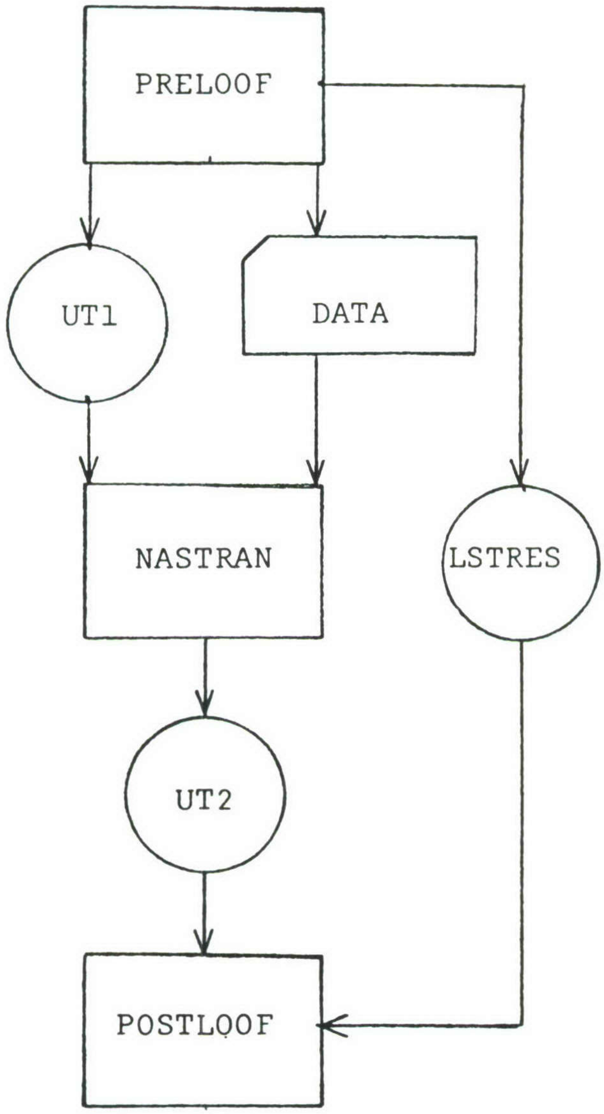

Figure A-3 Flow of Control from PRELOOF to NASTRAN to POSTLOOF

Run 1: Data Check and Plot

Card(s)	Remarks
job card, account card	
ATTACH(LOOF,ID=xxxx)	
ATTACH(OLDPL,BIGPROBLEM,ID=...)	
BEGIN(PRE,LOOF)	
RFL(160000)	
NASTRAN(DATA)ATTACH	
(plot control cards)	
7/8/9	
	Null input record for UPDATE. No DMAP sequences used since execution will halt right after plot generation.
7/8/9	
*ID FIXES	
*I EXEC.10	
$LOOFMAT NO	Suppress matrix generation.
$LOOFPLOT YES	Generate PLOTEL cards.
ALTER 23	Stop rigid format after plots.
EXIT$	
*I CASE.10	
OUTPUT(PLOT)	Plot commands.
.	
.	
*C EXEC,CASE,BULK	
6/7/8/9	

Run 2: Static Test Case (Rigid Format 1)

Card(s)	Remarks
job card, account card	
ATTACH(LOOF,ID=xxxx)	
ATTACH(OLDPL,BIGPROBLEM,ID=...)	
BEGIN(PRE,LOOF)	
RFL(160000)	
NASTRAN(DATA)ATTACH	
7/8/9	
*C RF1PRE	Get DMAP sequence for rigid format 1 preprocessing.
7/8/9	
*ID FIXES	
*I EXEC.10	
*READ RFALTS	Get DMAP sequence.
.	Other changes as needed.
.	
.	
*C EXEC,CASE,BULK	
6/7/8/9	

Run 3: Dynamic Run

Save PRELOOF output on tape, NASTRAN NPTP on tape, and checkpoint dictionary on permanent file.

Card(s)	Remarks
job card, account card	
ATTACH(LOOF,ID=xxxx)	
ATTACH(OLDPL,BIGPROBLEM,ID=...)	
BEGIN(PRE,LOOF)	
LABEL(SAVE,L=SAVEPRELOOF,VSN=xxx)	Tape to save UT1.
COPY(UT1,SAVE)	Save UT1 and LSTRES.
COPY(LSTRES,SAVE)	
REWIND(UT1)	
RETURN(LSTRES,SAVE)	
REQUEST(CHKPNT,*PF)	Permanent file for checkpoint dictionary.
LABEL(NPTP,W,L=NPTP,VSN=xxx)	New problem tape.
RFL(240000)	
NASTRAN(DATA,,CHKPNT)ATTACH	Punch output (checkpoint dictionary) routed to file CHKPNT.
CATALOG(CHKPNT,MYDICT,ID=xxxx)	
7/8/9	
*C RF3PRE,RF3POST	
7/8/9	
*ID FIXES	
*D EXEC.6	
SOL 3.0	Switch to rigid format 3.
CHKPNT YES	
*I EXEC.10	
*READ RFALTS	
.	Other changes as needed.
.	
.	
*C EXEC,CASE,BULK	
6/7/8/9	

Run 4: Restart NASTRAN, Execute POSTLOOF

Card(s)	Remarks
job card, account card	
ATTACH(RESTART,MYDICT,ID=xxxx)	Get checkpoint dictionary and old problem tape.
LABEL(OPTP,R,L,VSN=xxx)	
ATTACH(OLDPL,BIGPROBLEM,ID=xxx)	
UPDATE(Q,D,8,C=DATA,L=0)	Use UPDATE to set up DATA file.
LABEL(SAVE,W,L=SAVEUT2,VSN=xxx)	Tape to save file UT2.
COPY(UT2,SAVE)	

Card(s)	Remarks
REWIND(UT2)	
RETURN(SAVE)	
BEGIN(POST,LOOF)	
7/8/9	
*C RF3POST	
7/8/9	
*IC FIXES	
*D EXEC.6	
SOL 3,0	
*READ RESTART	Insert checkpoint dictionary.
*I EXEC.10	
*READ RFALTS	
.	Other changes as needed.
.	
.	
*I CASE.15	
BEGIN BULK	Do not retrieve bulk data from OLDPL. Insert bulk data additions and corrections after Case Control Deck.
.	
.	
.	
ENDDATA	
7/8/9	
$LOOFROT ALL	POSTLOOF input.
.	
.	
.	
6/7/8/9	

Run 5: Rerun POSTLOOF

job card, account card	
LABEL(SAVE1,R,L=SAVEPRELOOF,VSN=xxx)	
SKIPF(SAVE1,1,17)	Skip UT1.
COPY(SAVE1,LSTRES)	Recover LSTRES.
RETURN(SAVE)	
REWIND(LSTRES)	
LABEL(SAVE2,R,L=SAVEUT2,VSN=xxx)	Recover UT2.
COPY(SAVE2,UT2)	
RETURN(SAVE2)	
REWIND(UT2)	
BEGIN(POST,LOOF)	
7/8/9	
$LOOFROT ALL	POSTLOOF input.
.	
.	
.	
6/7/8/9	

A.6 PROGRAMMER'S NOTES

This section is a brief description of the programming techniques used in PRELOOF, a list of subroutines, and a list of important variables. A listing of the source codes for both PRELOOF and POSTLOOF can be found in Appendix B.

Because the amount of main storage required varies so much from one application to another, a dynamic core allocation procedure is used. Blank common space is added as needed by calls to subroutine MORCOR. The address of the newly acquired core relative to the beginning of blank common is available in variable NCORE, and this address is passed to a subroutine. For example, to allocate a new array C of size N by M, one would code the following:

```
COMMON A(1)
.
.
.
CALL MORCOR(N*M)
CALL SUBR(A(NCORE),N,M)
.
.
.
SUBROUTINE SUBR(C,N,M)
DIMENSION C(N,M)
```

Examples of this technique can be seen throughout PRELOOF.

PRELOOF checks input for errors. When a data card format error is detected, subroutine BUM notes the card which was erroneous. When any error is detected, a flag is set so that the job can be terminated after all input has been read.

Since grid point numbers, element numbers, etc., are arbitrary, a search procedure is needed so that the array entry corresponding to a given grid point or element can be located when the grid point number or element number is given. Function INDEX does this search, and returns a -1 if a match is not found, so that an error can be noted.

Since element matrices are accessed in random sequence during the assembly process, it is convenient to store these

matrices on random disk files. Element stiffness matrices are stored on unit 98, mass matrices on 99, and load vectors on 97. Utility subroutines READMS and WRITMS are used to access these files. This approach also allows two elements to share the same matrices if they are congruent.

The sequence of operations of PRELOOF is as follows:

The main program first calls INIT, which sets default values and reads $LOOF option cards. It then calls INPUT to read the bulk data deck.

INPUT calls FETCH once for each bulk data card. FETCH puts the alphanumeric card image in common block CARD, along with indicators to show whether that card is to be processed by PRELOOF. If so INPUT branches to the appropriate subroutine to decode information from the card images. These routines are:

```
CORD for CORD2R, CORD2C and CORD2S cards
GRID for GRID cards
SEQGP for SEQGP cards
ISHELL for CLOOF8 and CLOOF6 cards
IBEAM for CLOOF3 cards
CONGR for CONGR cards
IPSHEL for PLOOF cards
IPSHELX for PLOOFX cards
IPBEAM for PLOOF3 cards
IMAT for MAT1 and MAT8 cards
IPLOAD for PLOAD4 cards
ITHICK for THLOOF cards
PARAM for PARAM cards
ISPNT for SPOINT cards
```

All these routines use subroutine DCODE to decode 8-character fields in either integer, floating point, or alphabetic format, left or right adjusted. DCODE2 is available for 16-character fields.

PRELOOF then calls PROCESS to do some additional processing not handled by the input routines. First grid points are sequenced (unless SEQGP cards were present), using subroutine SORT. Then all shell elements are scanned, corner nodes are distinguished from mid-side nodes, and any attempts to use a node as a mid-side node of one element and a corner node of

another are noted. Appropriate permanent single-point constraints are generated. PLOTEL cards are generated if requested. Beam elements are then scanned in the same manner. Modified GRID cards are written out to file DATA.

PRELOOF then calls XSHELL, which controls shell element generation. XSHELL loops through all elements, gathering connection and property information, then calling QSHELL once for each element. After QSHELL has generated matrices, XSHELL stores them on disk and prints them out, if requested.

QSHELL loops through the Gauss points required for integration, calling ZHELL once for each Gauss point.

ZHELL calls HALOOF to generate shape functions and their derivatives, assembles the required functions into matrix B, assembles stiffnesses into matrix D, and computes the matrix product $B^T DB$, which is then accumulated onto the stiffness matrix. The mass matrix and load vector are handled in a similar fashion.

HALOOF is really the heart of the code. It generates values of all the shape functions and their required derivatives in array WSHEL, direction cosines in matrix FRAM, an area integrating factor in AREA, and a boundary integrating factor in SIDE. HALOOF calls SFR to obtain actual shape function values, then manipulates these to reduce out unwanted degrees of freedom. This subroutine was supplied by Prof. Irons, and more information about it may be found in his publications [2] and [32].

For beam elements, PRELOOF calls XBEAM, which controls beam element matrix generation. It calls ZBEAM once for each element. ZBEAM calls LOFBEM once for each integrating point, and LOFBEM in turn calls SFR1 to obtain shape function values. LOFBEM and SFR1 perform the same functions for beams as HALOOF and SFR do for shells.

Having generated element matrices, PRELOOF assembles them into global matrices. This is done by calls to ASSY, once for the stiffness matrix and once for the mass matrix, if requested.

ASSY generates six columns at a time and writes them out in a format compatible with NASTRAN (INPUTT2 module for COSMIC NASTRAN, INPUTT4 for MSC/NASTRAN).

If element load vectors have been computed, they are assembled into a master load vector by ASSL which writes out a single column.

The following is a list of the major variables used in PRELOOF. All array values are floating point.

Variable	Significance
NCORD	Number of coordinate systems
NUMNP	Number of node points
NSHELL	Number of LOOF8 and LOOF6 elements
NPSHEL	Number of PLOOF shell property cards
NPSHELX	Number of PLOOFX shell property cards
NSHLTY	Number of distinct shell element matrices
NBEAM	Number of beam elements
NPBEAM	Number of PLOOF3 beam property cards
NBMTY	Number of distinct beam element matrices
NMAT	Number of material properties
NSPOINT	Number of SPOINT's
CORD(3,5,NCORD)	Coordinate system data (1,1) External id. (2,1) Type = 1 = rectangular 2 = cylindrical 3 = spherical (i,2) Origin (i,j+2) Transformation matrix
GRID(13,NUMNP)	Grid point data (1) External id. (2) Location coordinate system id. (3 to 5) Location (location coordinate system) (6 to 8) Location (basic coordinate system) (9) Displacement coordinate system id. (10) Permanent single-point constraints (11) Sequence number (12) Pressure (13) Thickness
SEQ(NUMNP)	Same as GRID (11)

Variable	Significance	
SHELL(12,NSHELL)	Shell connections	
	(1)	External id.
	(2)	Property id.
	(3-10)	Grid point numbers (external id. initially, sequence numbers later)
	(11)	Element matrix number
	(12)	Material orientation angle for orthotropic materials
PSHELL(3,NPSHEL)	Isotropic shell properties	
	(1)	External id.
	(2)	Material id.
	(3)	Thickness
PSHELX(20,NPSHELX)	Anisotropic shell properties	
	(1)	External id.
	(2-7)	A matrix
	(8-13)	B matrix
	(14-19)	D matrix
	(20)	Area density
BEAM(21,NBEAM)	Beam connections	
	(1)	External id.
	(2)	Material id.
	(3-5)	Grid points (external id. initially, sequence numbers later)
	(6-8)	Property id. for cross-sections at the three grid points
	(9-14)	Offsets
	(15)	Element matrix number
	(16-18)	Not used
	(19-21)	Orientation vector
PBEAM(9)	Beam cross-section properties	
	(1)	External id.
	(2)	Area
	(3,4)	Moments of inertia
	(5)	Torsion constant
	(6-9)	Stress recovery coefficients
XMAT(6)	Material properties	
	(1)	External id.
	(2)	E_{11}
	(3)	E_{12}
	(4)	E_{22}
	(5)	G
	(6)	ρ

APPENDIX B

SEMI-LOOF PROGRAM LISTINGS

B.1 CONTROL CARD PROCEDURES

```
.PROC,UPDATE.
ATTACH(LOOFPL,ID=D740292,MR=1)
UPDATE(Q,P=LOOFPL)
FTN(I=COMPILE,B=NEW)
ATTACH(OLD,LOOFGO,ID=D740292,MR=1)
REWIND(OLD,NEW)
COPYL(OLD,NEW,LOOFGO)
RETURN(LOOFPL,COMPILE,OLD,NEW)
REVERT.
X
.PROC,PRE.
COMMENT.  PRELOOF,WPAFB
IFE,FILE(UT1,.NOT.(LO.OR.PF)),SKIPB.
ATTACH(RFALTER,LOOFALTER,ID=D740292,MR=1)
UPDATE(P=RFALTER,L=1,C=RFALTS,D,8)
RETURN(RFALTER)
UPDATE(D,8,C=PRE,L=1)
RETURN(RFALTS)
IFE,FILE(LOOFGO,.NOT.(LO.OR.PF)),SKIPA.
ATTACH(LOOFGO,ID=D740292,MR=1)
ENDIF(SKIPA)
LDSET(MAP=B/MAPFILE)
LOOFGO(PRE)
RETURN(LOOFGO,PRE,TAPE97,TAPE98,TAPE99)
ENDIF(SKIPB)
ATTACH(NASTRAN,ID=NASTRAN,MR=1)
LIBRARY(FORTRAN,SYSIO)
MAP(OFF)
RETURN(MAPFILE)
REVERT.
EXIT.
REWIND(MAPFILE)
COPY(MAPFILE,OUTPUT)
REVERT(ABORT)
X
.PROC,PLOT.
REDUCE.
ATTACH(M,MANDMCALCOMP,ID=D740292)
ATTACH(NASPLT,ID=D740292)
MAP(OFF)
REWIND(PLT2)
ROUTE(ANAPLT,DEF,DC=PR,ST=CSA,TID=TB)
LDSET(LIB=M)
NASPLT.
RETURN(ANAPLT,NASPLT,M)
REVERT.
X
```

```
.PROC,RESTORE,PROB=D740292.
LABEL(SAVE,R,L=LOOF,VSN=L04454)    REMOTE REQUEST, OWNER=D730368
REQUEST(LOOF,*PF)
COPYBF(SAVE,LOOF)
CATALOG(LOOF,ID=PROB,RP=999)
RETURN(LOOF)
REQUEST(LOOFGO,*PF)
COPYBF(SAVE,LOOFGO)
CATALOG(LOOFGO,ID=PROB,RP=999)
RETURN(LOOFGO)
COPYBF(SAVE,OLDPL)
REQUEST(NEWPL,*PF)
UPDATE(N,F,C=0)
CATALOG(NEWPL,LOOFALTER,ID=PROB,RP=999)
RETURN(OLDPL,NEWPL)
COPYBF(SAVE,OLDPL)
RETURN(SAVE)
UPDATE(N,C=0)
REQUEST(NEWPL,*PF)
CATALOG(NEWPL,LOOFPL,ID=PROB,RP=999)
RETURN(OLDPL,NEWPL)
X
W
```

B.2

DMAP ALTER LIBRARY

(Partial Listing)

```
$ *** ALTER MSC/NASTRAN, RIGID FORMAT 24 ***
$ *** TO ACCEPT FILES FROM PRELOOF FOR SEMI-LOOF ELEMENTS ***
$
$          PARAMS USED BY THIS ALTER ...
$
$          NAME       DEFAULT    REMARKS
$          ----       -------    -------
$
$          NSPOINT    0          NUMBER OF SPOINT-S IN THE MODEL
$
$          STIFFMAT   -1         POSITIVE VALUE INDICATES THAT PRELOOF
$                                GENERATED A STIFFNESS MATRIX
$
$          MASSMAT    -1         POSITIVE VALUE INDICATES THAT PRELOOF
$                                HAS GENERATED A MASS MATRIX.
$
$          LOADVEC    -1         POSITIVE VALUE INDICATES THAT PRELOOF
$                                GENERATED A LOAD VECTOR CORRESPONDING
$                                TO PRESSURE LOADING FOR THIS MODEL.
$
$          *NOTE* PRELOOF GENERATES ALL THESE PARAMS AUTOMATICALLY
$
ALTER 93
PARAM     //SUB/V,N,NOEXTRA/V,Y,NEXTRA=0/1 $
PARAM      //NOP/V,Y,STIFMAT=-1 $
COND       LBLNOK,STIFMAT $
INPUTT4    /KLGG,,,,/1/11 $
LABEL      LBLNOK $
EQUIV      KLGG,KGG/NOEXTRA $
COND       LBLNOX,NOEXTRA $
PARAM     //MPY/V,N,NDOF/V,Y,NEXTRA/6 $
PARAM     //ADD/V,N,MDOF/V,N,NDOF/V,Y,NSPOINT=0 $
PARAM     //SUB/V,N,LUSET2/V,N,LUSET/V,N,MDOF $
MATGEN    ,/RP/6/V,N,LUSET/V,N,LUSET2/V,N,MDOF $
MERGE      KLGG,,,RP,/KLGG1/ $
ADD        KLGG1,KGG/KGG1 $
EQUIV      KGG1,KGG/ALWAYS $
LABEL      LBLNOX $
PARAM      //NOP/V,Y,MASSMAT=-1 $
COND       LBLNOM,MASSMAT $
INPUTT4    /MLGG,,,,/1/11/0 $
EQUIV      MLGG,MGG/NOEXTRA $
COND       LBLNOM,NOEXTRA $
MERGE      MLGG,,,RP,/MLGG1/ $
ADD        MLGG1,MGG/MGG1 $
EQUIV      MLGG1,MGG/ALWAYS $
LABEL      LBLNOM $
```

```
ALTER 145
PARAM       //NOP/V,Y,LOADVEC=-1 $
COND        LBLNOPGL,LOADVEC $
INPUTT4     /PGL,,,,/1/11/0 $
EQUIV       PGL,PGLL/NOEXTRA $
COND        LBLNOP,NOEXTRA $
MERGE       PGL,,,,,RP/PGLL/0 $
LABEL       LBLNOP $
ADD         PGLL,PG/PGQ $
EQUIV       PGQ,PG/ALWAYS $
LABEL       LBLNOPGL $
```

```
$ *** ALTER MSC/NASTRAN, RIGID FORMAT 24 ***
$ *** TO PRODUCE FILES FOR POSTLOOF FOR SEMI-LOOF ELEMENTS ***
ALTER 160
OUTPUT4    UGV,,,,//0/12 $
```

```
$ *** ALTER MSC/NASTRAN, RIGID FORMAT 25 ***
$ *** TO ACCEPT FILES FROM PRELOOF FOR SEMI-LOOF ELEMENTS ***
$
$          PARAMS USED BY THIS ALTER ...
$
$          NAME      DEFAULT   REMARKS
$          ----      -------   -------
$
$          NSPOINT   0         NUMBER OF SPOINT-S IN THE MODEL
$
$          STIFFMAT  -1        POSITIVE VALUE INDICATES THAT PRELOOF
$                              GENERATED A STIFFNESS MATRIX
$
$          MASSMAT   -1        POSITIVE VALUE INDICATES THAT PRELOOF
$
$          *NOTE* PRELOOF GENERATES ALL THESE PARAMS AUTOMATICALLY
$
ALTER 76,80
PARAM      //AND/V,N,NOM/NOMGG/V,Y,MASSMAT=-1 $
COND       RFERR,NOM $
ALTER 83,83
PARAM      //AND/V,N,NOK/NOKGG/V,Y,STIFMAT=-1 $
ALTER 92
PARAM      //SUB/V,N,NOBLOW/V,Y,NSPOINT=0/1 $
PARAM      //SUB/V,N,LUSET2/LUSET/NSPOINT $
COND       LNOBLOW,NOBLOW $
MATGEN     ,/BLOW/6/LUSET/LUSET2/NSPOINT $
LABEL      LNOBLOW $
COND       NOLOOFK,STIFMAT $
INPUTT4    /KGG1,,,,/1/11 $
EQUIV      KGG1,KGG2/NOBLOW $
COND       NOLOOFK,NOBLOW $
MERGE      KGG1,,,,BLOW,/KGG2/ $
LABEL      NOLOOFK $
ADD        KGG2,KGG/KGGL $
EQUIV      KGGL,KGG/ALWAYS $
COND       NOLOOFM,MASSMAT $
INPUTT4    /MGG1,,,,/1/11/0 $
EQUIV      MGG1,MGG2/NOBLOW $
COND       NOLOOFM,NOBLOW $
MERGE      MGG1,,,,BLOW,/MGG2/ $
LABEL      NOLOOFM $
ADD        MGG2,MGG/MGGL $
EQUIV      MGGL,MGG/ALWAYS $
COND       LGPWG,GRDPNT $
GPWG       BGPDT,CSTM,EQEXIN,MGG/OGPWG/V,Y,GRDPNT=-1/C,Y,WTMASS $
OFP        OGPWG// $
LABEL      LGPWG $
```

B.3 PRELOOF PROGRAM LISTING

```
      PROGRAM PRELOOF(INPUT=201B,DATA=201B,OUTPUT=201B,UT1,LSTRES,
     .          TAPE3=DATA,TAPE4=UT1,TAPE7=LSTRES,
     .          TAPE1=INPUT,TAPE5=INPUT,TAPE6=OUTPUT,
     .          TAPE97,TAPE98,TAPE99)
C
C     MATRIX GENERATION PREPROCESSOR FOR SEMI-LOOF
C     SHELL AND BEAM ELEMENTS FOR USE IN NASTRAN
C     W.G. 12-78
C
      COMMON/CONTRL/ECHO,ERR,MATGEN,DYN,APPLD,PLOT,DBUG,BAD,NCORE,
     .     WTMASS,NASTY
      LOGICAL ECHO,ERR,MATGEN,DYN,APPLD,PLOT,DBUG,BAD
      COMMON/LOC/LCORD,LGRID,LSEQ,LSHELL,LBEAM,LPSHEL,LPSHELX,LPBEAM,
     .     LMAT,LPSPC
      COMMON/N/NCORD,NUMNP,NSHELL,NPSHEL,NPSHELX,NSHLTY,NBEAM,NPBEAM,
     .          NBMTY,NMAT,NSPOINT,MAXGRD,NDOF
      COMMON A(1)
      CALL INIT
C
C     READ STUFF IN; DO PARTIAL ERROR CHECK
C
      CALL INPUT
      IF (ERR) CALL SYSTEM(52,32H JOB ABORTED DUE TO ABOVE ERRORS)
C
C     DO SOME MORE PROCESSING
C
      CALL PROCESS(A(LGRID),A(LSHELL),A(LBEAM),A(LSEQ),A(LPSPC))
      IF (ERR) CALL SYSTEM(52,32H JOB ABORTED DUE TO ABOVE ERRORS)
      REWIND 3
C
C     GET MATRICES, IF WANTED
C
      IF (.NOT.MATGEN) STOP
C
C     RANDOM FILE INDICES
C
      NL=NSHLTY+NBMTY+1
      LSINDEX=NCORE
      CALL MORCOR(NL)
      LMINDEX=NCORE
      CALL MORCOR(NL)
      LLINDEX=NCORE
      CALL MORCOR(NL)
      CALL OPENMS(98,A(LSINDEX),NL,0)
      IF (DYN) CALL OPENMS(99,A(LMINDEX),NL,0)
      IF (APPLD) CALL OPENMS(97,A(LLINDEX),NL,0)
C
C SHELL ELEMENTS
C
      LELSTIF=NCORE
```

```
      CALL MORCOR(32*32)
      LELMASS=NCORE
      CALL MORCOR(32*32)
      LELOAD=NCORE
      CALL MORCOR(32)
      LELSTRS=NCORE
      CALL MORCOR(6*32)
      LSHAPE=NCORE
      CALL MORCOR(13*45)
      CALL XSHELL(A(LGRID),A(LSHELL),A(LPSHEL),A(LPSHELX),A(LMAT),
     .      A(LELSTIF),A(LELMASS),A(LELOAD),A(LELSTRS),
     .      A(LSINDEX),A(LSHAPE),A(LSEQ))
      NCORE=LELSTIF
C
C BEAM ELEMENTS
C
      LELSTIF=NCORE
      CALL MORCOR(17*17)
      LELMASS=NCORE
      CALL MORCOR(17*17)
      LELOAD=NCORE
      CALL MORCOR(17)
      LELSTFS=NCORE
      CALL MORCOR(17*6)
      LSHAPE=NCORE
      CALL MORCOR(13*45)
      CALL XBEAM(A(LGRID),A(LBEAM),A(LPBEAM),A(LMAT),
     .      A(LELSTIF),A(LELMASS),A(LELOAD),A(LELSTRS),
     .      A(LSINDEX),A(LSHAPE),A(LSEQ))
      IF (ERR) CALL SYSTEM(52,32H JOB ABORTED DUE TO ABOVE ERRORS)
      NCORE=LELSTIF
      NDOF=6*NUMNP+NSPUINT
      CALL MORCOR(32*32)
      LELMAT=NCORE
      CALL MORCOR(32*32)
      LBIG=NCORE
      CALL MORCOR(6*NDOF)
      CALL ASSY(4HSTIF,98,
     .      A(LBIG),A(LSHELL),A(LBEAM),A(LCORD),A(LGRID),A(LSEQ),
     .      A(LPSPC),A(LELMAT),A(LELMAT),NDOF)
      IF (ERR) CALL SYSTEM(52,32H JOB ABORTED DUE TO ABOVE ERRORS)
      IF (DYN)
     .CALL ASSY(4HMASS,99,
     .      A(LBIG),A(LSHELL),A(LBEAM),A(LCORD),A(LGRID),A(LSEQ),
     .      A(LPSPC),A(LELMAT),A(LELMAT),NDOF)
      IF (ERR) CALL SYSTEM(52,32H JOB ABORTED DUE TO ABOVE ERRORS)
      IF (NSPUINT.GT.0.AND.NASTY.EQ.1) CALL PARVEC
      IF (APPLD) CALL ASSL(4HLOAD,97,A(LBIG),
     .      A(LSHELL),A(LBEAM),A(LCORD),A(LGRID),A(LSEQ),
     .      A(LPSPC),A(LELMAT),A(LELMAT))
```

```
IF (ERR) CALL SYSTEM(52,32H JOB ABORTED DUE TO ABOVE ERRORS)
REWIND 4
REWIND 7
END
```

```
      SUBROUTINE DUMP(NAME,A,M,N,MN)
      DIMENSION A(M,N)
      CALL SYSTEM(51,5H DUMP)
      GO TO (10,20,30),MN
   10 DO 11 I=1,N
   11 PRINT 12,NAME,I,LOCF(A(1,I)),(A(J,I),J=1,M)
   12 FORMAT (1X,A10,I5,3X,O6/(5(1X,O20)))
      RETURN
   20 DO 21 I=1,N
   21 PRINT 22,NAME,I,LOCF(A(1,I)),(A(J,I),J=1,M)
   22 FORMAT (1X,A10,I5,3X,O6/(10E13.5))
      RETURN
   30 DO 31 I=1,N
   31 PRINT 32,NAME,I,LOCF(A(1,I)),(A(J,I),J=1,M)
   32 FORMAT (1X,A10,I5,3X,O6/(10I13))
      RETURN
      END
```

```
      SUBROUTINE MORCOR(N)
      COMMON/CONTRL/ECHO,ERR,MATGEN,DYN,APPLD,PLOT,DBUG,BAD,NCORE,
     .      WTMASS,NASTY
      LOGICAL ECHO,ERR,MATGEN,DYN,APPLD,PLOT,DBUG,BAD
      DIMENSION X(3)
      COMMON A(1)
      DATA LA,IFL/0,0/
      DATA KFL/4000B/
      IF (LA.GT.0) GO TO 5
      LA=LOCF(A)
      CALL MEM(IFL)
    5 NCORE=NCORE+N
   10 IF (NCORE+LA.LT.IFL-4) RETURN
      INCR=NCORE+LA-IFL+5
      INCR=(INCR+KFL-1)/KFL
      INCR=KFL*INCR
      IFL=IFL+INCR
      ENCODE(20,20,X) IFL
   20 FORMAT (4HRFL(,O6,1H))
      X(3)=0
      CALL REMARK(X)
      CALL MEM(IFL)
      GO TO 10
      END
```

```
          IDENT     MEM
          ENTRY     MEM
 MEM      BSSZ      1
          SA1       X1
          SX7       A1
          LX1       30D
          SA7       LSTAT
          BX6       X1
          SA6       STAT
          MEMORY    SCM,STAT,RECALL
          SA1       STAT
          SA2       LSTAT
          AX1       30D
          BX6       X1
          SA6       X2
          EQ        MEM
STAT      BSSZ      1
LSTAT     BSSZ      1
          END
```

```
      FUNCTION INDEX(LIST,N,L,ITEM)
C
C     FINDS A NUMBER IN A LIST (E.G. GRID POINT NUMBERS)
C
      DIMENSION LIST(L,1)
      REAL LIST,ITEM
      DO 10 INDEX=1,N
      IF (LIST(1,INDEX).EQ.ITEM) RETURN
   10 CONTINUE
      INDEX=-1
      RETURN
      END
```

```
      SUBROUTINE BUM
      COMMON/CONTRL/ECHO,ERR,MATGEN,DYN,APPLD,PLOT,DBUG,BAD,NCORE,
     .     WTMASS,NASTY
      LOGICAL ECHO,ERR,MATGEN,DYN,APPLD,PLOT,DBUG,BAD
      COMMON/CARD/NAME,CARD(400),MXCARD,NCARD,NTYPE,NSUB,NO
C
C     ERROR MESSAGE FOR BAD BULK DATA CARD
C
      IF (.NOT.ECHO) PRINT 10,NO,NAME,(CARD(I),I=1,NCARD)
   10 FORMAT (I10,1H.,5X,9A8/(24X,8A8))
      PRINT 20,NO
   20 FORMAT (29H *** FORMAT ERROR ON CARD NO.,I5)
      ERR=.TRUE.
      RETURN
      END
```

```
          IDENT      MOVER          (A,IC,B,JC,N)
          ENTRY      MOVER
          VFD        30/0HMOVER,30/5
*
*        COMPASS PROGRAM FOR TRANSFER OF DATA  (FTN COMPILER)
*
*                    EQUIVALENT FORTRAN SUBROUTINE
*     SUBROUTINE MOVER (A,IC,B,JC,N)
*     DIMENSION A(1),B(1)
*     IF(N.EQ.0) RETURN
*     I=1
*     J=1
*     DO 100 K=1,N
*     B(J)=A(I)
*     I=I+IC
* 100 J=J+JC
*     RETURN
*     END
*
MOVER     BSSZ       1
          SA5        A1+4           ADS(N) TO X5
          SB1        1
          SB3        2              2 TO B3
          SA2        X5             N TO X2
          SA3        A1+B1
          SX6        B1             1 TO X6
          SA4        A3+B3          ADS(JC) TO X4
          SA3        X3             IC TO X3
          SA5        A1+B3          ADS(B) TO X5
          SB4        X2             N TO B4
          SA4        X4             JC TO X4
          SB7        X3             IC TO B7
          BX7        X6*X2          MOD(N,2) TO X7
          SX6        B3             2 TO X6
          SB6        X4             JC TO B6
          LE         B4,B0,MOVER    RETURN IF N=0 OR N IS NEGATIVE
          ZR         X7,EVEN
          SA3        X1             ODDD, MOVE FIRST ELEMENT
          SB4        B4-B1
          SX1        X1+B7
          BX7        X3
          SX2        B4             N TO X2
          SA7        X5
          SX5        X5+B6
EVEN      BX7        X6*X2          MOD(N,4) TO X7
          SB5        B3+B3          4 TO B5
          ZR         X7,FOUR
          SA3        X1
          SA4        X1+B7
          SX1        X1+B7
```

```
         SB4       B4-B3
         BX6       X3
         SX1       X1+B7
         LX7       X4
         SA6       X5
         SA7       X5+B6
         SX5       X5+B6
         SX5       X5+B6
FOUR     GE        B0,B4,MOVER
         SX0       X5
         SB2       B0
         SA3       X1+B7
         SB7       B7+B7
         SA4       X1+B7
         SA2       X1
         SA5       A3+B7
         SX1       X0+B6
         SB7       B7+B7
         SB6       B6+B6
         EQ        B7,B0,ZERO        TEST FOR ZERO INCREMENT
         EQ        B0,B0,MIDD
LOOP     SA2       A2+B7
         SA3       A3+B7
         SA4       A4+B7
         SA5       A5+B7
MIDD     BX6       X2
         SB4       B4-B5
         LX7       X3
         SA6       X0+B2
         SA7       X1+B2
         SB2       B2+B6
         BX6       X4
         LX7       X5
         SA6       X0+B2
         SA7       X1+B2
         SB2       B2+B6
         GT        B4,LOOP
         EQ        B0,B0,MOVER
ZERO     BX6       X2
         LX7       X2
LOOP2    SA6       X0+B2
         SA7       X1+B2
         SB2       B2+B6
         SB4       B4-B5
         SA6       X0+B2
         SA7       X1+B2
         SB2       B2+B6
         GT        B4,LOOP2
         EQ        B0,B0,MOVER
         END
```

```
          IDENT     SCPROD     (N,IC,JC,A,B,SUM)
          VFD       36/0HSCPROD,24/6
          ENTRY     SCPROD
*                             COMPASS PROGRAM FOR SCALAR PRODUCT (FTN)
*                             I=J=1,   SUM=0
*                             DO 10 K=1,N
*                             SUM=SUM+A(I)*B(J)
*                             I=I+IC
*                          10 J=J+JC
SCPROD    BSSZ      1
          SB7       1              B7 REMAINS 1
          SA5       X1             N TO X5
          SA2       A1+B7          ADS(IC) TO X2
          MX6       0              CLEAR SUM1
          SA3       A2+B7          ADS(JC) TO X3
          SX7       B7             1 TO X7 FOR ODD-EVEN TEST
          SB1       X5             N TO B1
          SA4       A3+B7          ADS(A) TO X4
          BX0       X5*X7          MOD(N,2) TO X0
          SA5       A4+B7          ADS(B) TO X5
          SA2       X2             IC TO X2
          SA3       X3             JC TO X3
          SA1       X4             A(1) TO X1
          SA4       A5+B7          ADS(SUM) TO X4
          SB2       X2             IC TO B2
          SB3       X3             JC TO B3
          SA2       X5             B(1) TO X2
          SB6       X4             ADS(SUM) TO B6
          ZR        X0,EVEN        SKIP TO EVEN IF N EVEN
          RX6       X1*X2          N IS ODD      SUM1=A(1)*B(1)
          SA1       A1+B2          A(2) TO X1
          SA2       A2+B3          B(2) TO X2
          SB1       B1-B7          N=N-1
EVEN      EQ        B1,LAST        QUIT IF N IS NOW ZERO
          SX5       B1             X5=N
          SA3       A1+B2          A(I+1)TO X3
          SX7       B7+B7          2 TO X7
          SA4       A2+B3          B(I+1) TO X4
          BX0       X5*X7          MOD(N,4) TO X0
          SB2       B2+B2          2*IC TO B2
          MX7       0              CLEAR SUM2
          SB3       B3+B3          2*JC TO B3
          SB5       X0            MOD(N,4) TO B5
          SB1       B1+B5          N=N+MOD(N,4)
          MX0       0              CLEAR X0
          SB4       4              4 TO B4 FOR LOOP DECREMENT
          BX5       X7             CLEAR X5
          GT        B5,B0,TEST     SKIP TO TEST IF MOD(N,4)=2
          RX0       X1*X2          X0=A(1)*B(1)
          EQ        TWO            IF MOD(N,4) IS 0, START IN MIDDLE
```

```
LOOP     RX0    X1*X2         X0=A(I)*B(I)
         SA1    A1+B2         X1=A(I+2)
         NX6    X6            NORMALIZE SUM1
         SA2    A2+B3         X2=B(I+2)
         FX7    X7+X5         SUM2=SUM2+A(I-1)*B(I-1)
         RX5    X3*X4         X5=A(I+1)*B(I+1)
         SB1    B1-B4         N=N-4
         SA3    A3+B2         X3=A(I+3)
         NX7    X7            NORMALIZE SUM2
         SA4    A4+B3         X4=B(I+3)
         FX6    X6+X0         SUM1=SUM1+A(I)*B(I)
         RX0    X1*X2         X0=A(I+2)*B(I+2)
TWO      SA1    A1+B2         X1=A(I+4)
         SA2    A2+B3         X2=B(I+4)
         FX7    X7+X5         SUM2=SUM2+A(I+1)*B(I+1)
         NX6    X6            NORMALIZE SUM1
         RX5    X3*X4         X5=A(I+3)*B(I+3)
         SA3    A3+B2         X3=A(I+5)
         SA4    A4+B3         X4=B(I+5)
         NX7    X7            NORMALIZE SUM2
TEST     FX6    X6+X0         SUM1=SUM1+A(I+2)*B(I+2)
         LT     B4,B1,LOOP    RECYCLE IF 4 LT N
         RX0    X1*X2         CLEANUP BEGINS
         NX1    X6
         FX7    X7+X5
         RX5    X3*X4
         NX3    X7
         FX2    X0+X1
         NX6    X2
         FX4    X3+X5
         NX7    X4
         FX6    X6+X7         SUM=SUM1+SUM2
         NX6    X6
LAST     SA6    B6
         EQ     SCPROD
         END
```

```
         IDENT      REDCLP            (N,IC,JC,FAC,A,B)
         VFD        36/0HREDCLP,24/6
         ENTRY      REDCLP
REDCLP   BSSZ       1
*
*
*          GAUSSIAN REDUCTION LOOP.       FTN COMPILER
*
*          FORTRAN EQUIVALENT
*
*      SUBROUTINE REDCLP (N,IC,JC,FAC,A,B)
*      DIMENSION A(1),B(1)
*      I=1
*      J=1
*      DO 100 K=1,N
*      B(J)=B(J)-FAC*A(I)
*      I=I+IC
*  100 J=J+JC
*
*
         SA2        X1                N TO X2
         SB3        2                 2 TO B3
         SA3        A1+1              ADS(IC) TO X3
         SX6        1                 1 TO X6
         SA5        A1+B3             ADS(JC) TO X5
         SB2        X2                N TO B2
         SA4        A3+B3             ADS(FAC) TO X4
         SA3        X3                IC TO X3
         BX7        X6*X2             MOD(N,2) TO X7
         SA2        A5+B3             ADS(A) TO X2
         SA1        X5                JC TO X1
         SA5        A4+B3             ADS(B) TO X5
         SA4        X4                FAC TO X4
         SB7        X3                IC TO B7
         SB4        X1                JC TO B4
         BX0        X4                FAC TO X0
         SA4        X5                B TO X4
         SB1        X1+B4             2*JC TO B1
         SA1        X2                A TO X1
         SA2        X2+B7             A(1+IC) TO X2
         SB7        X3+B7             2*IC TO B7
         RX1        X0*X1             FIRST MULTIPLY
         ZR         X7,EVEN           SKIP IF N IS EVEN
         FX4        X4-X1             FINISH FIRST OPERATION IF N ODD
         SB2        B2-1              DECREMENT B2
         SA1        A1+B7             A(1+2*IC) TO X1
         NX6        X4                NORMALIZE(X4) TO X6
         SA6        A4                X6 TO B(1)
         ZR         B2,REDCLP         RETURN IF N=1
         RX1        X0*X1             X0*X1 TP X1
```

```
         SA4      A4+B1          B(1+2*JC) TO X4
EVEN     RX3      X0*X2          X0*X2 TO X3
         SA5      X5+B4          B(1+JC) TO X5
         GE       B3,B2,DONE     NO LOOP IF N=2 OR N=3
LOOP     FX4      X4-X1
         SA2      A2+B7
         SA1      A1+B7
         NX6      X4
         SA4      A4+B1
         FX3      X5-X3
         SA5      A5+B1
         NX7      X3
         SB2      B2-B3
         SA6      A4-B1
         RX1      X0*X1
         RX3      X0*X2
         SA7      A5-B1
         LT       B3,B2,LOOP
DONE     FX4      X4-X1
         NX6      X4
         FX5      X5-X3
         SA6      A4
         NX7      X5
         SA7      A5
         EQ       B0,B0,REDCLP
         END
```

```
      SUBROUTINE INIT
C
C     WADES THRU EXEC + CASE DECKS, SETS DEFAULT VALUES, READS
C     $LOOF OPTIONS, INITIALIZES STUFF
C
      COMMON/CONTRL/ECHO,ERR,MATGEN,DYN,APPLD,PLOT,DBUG,BAD,NCORE,
     .      WTMASS,NASTY
      LOGICAL ECHO,ERR,MATGEN,DYN,APPLD,PLOT,DBUG,BAD
      COMMON/LOC/LCORD,LGRID,LSEQ,LSHELL,LBEAM,LPSHEL,LPSHELX,LPBEAM,
     .      LMAT,LPSPC
      COMMON/CARD/NAME,CARD(400),MXCARD,NCARD,NTYPE,NSUB,NO
      COMMON/TITLE/TITLE(8)
      COMMON/GAUSS/NGAUS,GFACT
      COMMON/N/NCORD,NUMNP,NSHELL,NPSHEL,NPSHELX,NSHLTY,NBEAM,NPBEAM,
     .          NBMTY,NMAT,NSPOINT,MAXGRD,NDOF
      DIMENSION STATUS(6)
      DATA YES,NEIN/3HYES,3H NO/
      READ(5,1) TITLE
    1 FORMAT (8A10)
      IF (EOF(5).NE.0) STOP
      CALL MOVER(0,0,LCORD,1,9)
      CALL MOVER(0,0,NCORD,1,12)
      NCORE=1
      PLOT=.FALSE.
      ECHO=.FALSE.
      MATGEN=.TRUE.
      APPLD=.FALSE.
      ERR=.FALSE.
      DYN=.FALSE.
      DBUG=.FALSE.
      NGAUS=2
      GFACT=0
      WTMASS=1.
      NASTY=2
      MXCARD=400
      NO=0
    5 READ(1,10) (CARD(I),I=1,8)
   10 FORMAT (8A10)
      IF (EOF(1).NE.0) GO TO 40
      WRITE(3,10) (CARD(I),I=1,8)
      IF (CARD(1).EQ.10HBEGIN BULK) GO TO 20
      PLOT=PLOT.OR.(CARD(1).EQ.10H$LOOFPLOT .AND.CARD(2).EQ.3HYES)
      ECHO=ECHO.OR.(CARD(1).EQ.10H$LOOFECHO .AND.CARD(2).EQ.3HYES)
      DBUG=DBUG.OR.(CARD(1).EQ.10H$LOOFDEBUG.AND.CARD(2).EQ.4H YES)
      MATGEN=MATGEN.AND.CARD(1).NE.10H$LOOFMAT N
      IF (CARD(1).EQ.10H$LOOFGAUSS.AND.CARD(2).EQ.2H 3) NGAUS=3
      IF (CARD(1).EQ.10H$LOOFFACT ) GFACT=DCODE(CARD(2),2,BAD)
      DYN=DYN.OR.CARD(1).EQ.10H$LOOFDYN Y
      IF (CARD(1).EQ.10H$NASTRAN C) NASTY=1
      IF (CARD(1).EQ.10H$NASTRAN M) NASTY=2
```

```
      GO TO 5
   20 CALL MOVER(NEIN,0,STATUS,1,6)
      IF (MATGEN) STATUS(1)=YES
      IF (DYN) STATUS(2)=YES
      IF (APPLD) STATUS(3)=YES
      IF (ECHO) STATUS(4)=YES
      IF (PLOT) STATUS(5)=YES
      IF (DBUG) STATUS(6)=YES
      WRITE(6,30) TITLE,STATUS,NGAUS,NGAUS,GFACT
   30 FORMAT (47H1 PRELOOF -- PREPROCESSOR FOR SEMILOOF ELEMENTS//
     .       1X,8A10//21H OPTIONS IN EFFECT --//
     .       20H MATRIX GENERATION               ,T30,A3/
     .       20H DYNAMICS                        ,T30,A3/
     .       20H DISTRIBUTED LOAD                ,T30,A3/
     .       20H ECHO                            ,T30,A3/
     .       20H PLOT                            ,T30,A3/
     .       20H DEBUG                           ,T30,A3/
     .       20H INTEGRATION RULE            ,T30,I1,1HX,I1/
     .       20H INTEGRATION FACTOR            T27,F6.4)
      IF (ECHO) WRITE(6,35)
   35 FORMAT (///15X,27HB U L K   D A T A   E C H O)
      RETURN
   40 CALL SYSTEM(52,20H BULK DATA MISSING    )
      END
```

```
      SUBROUTINE INPUT
C
C     READS BULK DATA DECK, INTERPRETS CARDS PERTINENT TO SEMILOOF,
C     ECHOES OTHERS, DOES SOME ERROR CHECKS AND TABLE SETUPS.
C
      COMMON/CARD/NAME,CARD(400),MXCARD,NCARD,NTYPE,NSUB,NO
      COMMON/CONTRL/ECHO,ERR,MATGEN,DYN,APPLD,PLOT,DBUG,BAD,NCORE,
     .      WTMASS,NASTY
      LOGICAL ECHO,ERR,MATGEN,DYN,APPLD,PLOT,DBUG,BAD
      COMMON/LOC/LCORD,LGRID,LSEQ,LSHELL,LBEAM,LPSHEL,LPSHELX,LPBEAM,
     .      LMAT,LPSPC
      COMMON/N/NCORD,NUMNP,NSHELL,NPSHEL,NPSHELX,NSHLTY,NBEAM,NPBEAM,
     .          NBMTY,NMAT,NSPOINT,MAXGRD,NDOF
      COMMON A(1)
      LTYPE=1
C
C     FETCH UP A BULK DATA CARD
C
   10 CALL FETCH
      IF (NTYPE) 9000,10,15
   15 IF (NTYPE.GE.LTYPE) GO TO 30
      IF (.NOT.ECHO) PRINT 17,NO,NAME,(CARD(I),I=1,NCARD)
   17 FORMAT (I10,1H.,5X,9A8/(24X,8A8))
      PRINT 20,NO
   20 FORMAT (42H *** BULK DATA OUT OF ORDER, IGNORING CARD,I5)
      ERR=.TRUE.
      GO TO 10
   30 LTYPE=NTYPE
C
C     SEMILOOF CARD RECOGNIZED.  BRANCH TO APPROPRIATE ROUTINE
C
      GO TO
     .(100,200,300,400,500,600,700,800,900,1000,1100,1200,1300,1400),
     .NTYPE
C
C     CORD2X CARDS
C
  100 IF (LCORD.EQ.0) LCORD=NCORE
      CALL MORCOR(15)
      CALL CORD(A(LCORD))
      GO TO 10
C
C     GRID CARDS
C
  200 IF (LGRID.EQ.0) LGRID=NCORE
      CALL MORCOR(13)
      CALL GRID(A(LCORD),A(LGRID))
      GO TO 10
C
C     SEQUENCE CARDS
```

```
C
  300 IF (LSEG.EQ.0) LSEG=NCORE
      IF (LSEG.EQ.NCORE) CALL MORCOR(NUMNP)
      CALL SEGGP(A(LSEG),A(LGRID))
      GO TO 10
C
C     CLOOF8 AND CLOOF6 CARDS
C
  400 IF (LSHELL.EQ.0) LSHELL=NCORE
      CALL MORCOR(12)
      CALL ISHELL(A(LSHELL),A(LGRID))
      GO TO 10
C
C     CLOOF3
C
  500 IF (LBEAM.EQ.0) LBEAM=NCORE
      CALL MORCOR(21)
      CALL IBEAM(A(LBEAM),A(LGRID))
      GO TO 10
C
C     CONGRUENCE CARDS
C
  600 CALL CONGR(A(LGRID),A(LSHELL),A(LBEAM))
      GO TO 10
C
C     PLOOF
C
  700 IF (LPSHEL.EQ.0) LPSHEL=NCORE
      CALL MORCOR(3)
      CALL IPSHEL(A(LPSHEL))
      GO TO 10
C
C     PLOOFX
C
  800 IF (LPSHELX.EQ.0) LPSHELX=NCORE
      CALL MORCOR(20)
      CALL IPSHELX(A(LPSHELX))
      GO TO 10
C
C     PLOOF3
C
  900 IF (LPBEAM.EQ.0) LPBEAM=NCORE
      CALL MORCOR(9)
      CALL IPBEAM(A(LPBEAM))
      GO TO 10
C
C     MAT1 OR MAT8
C
 1000 IF (LMAT.EQ.0) LMAT=NCORE
      CALL MORCOR(6)
```

```
      CALL IMAT(A(LMAT))
      GO TO 10
C
C     PLOAD4
C
 1100 CALL IPLOAD(A(LGRID))
      APPLD=.TRUE.
      GO TO 10
C
C     THLOOF
C
 1200 CALL ITHICK(A(LGRID))
      GO TO 10
C
C     PARAM
C
 1300 CALL PARAM
      GO TO 10
C
C     SPOINT
C
 1400 CALL ISPNT
      GO TO 10
C
 9000 LPSPC=NCORE
      CALL MORCOR(NUMNP)
      IF (LSEQ.NE.0) RETURN
      LSEQ=NCORE
      CALL MORCOR(NUMNP)
      CALL MOVER(0,0,A(LSEQ),1,NUMNP)
      RETURN
      END
```

```
      SUBROUTINE FETCH
C
C     READS A BULK DATA CARD, PLUS ANY CONTINUATIONS, AND CHECKS
C     AGAINST LIST OF KNOWN CARDS
C
      COMMON/CONTRL/ECHO,ERR,MATGEN,DYN,APPLD,PLOT,DBUG,BAD,NCORE,
     .     WTMASS,NASTY
      LOGICAL ECHO,ERR,MATGEN,DYN,APPLD,PLOT,DBUG,BAD
      COMMON/CARD/NAME,CARD(400),MXCARD,NCARD,NTYPE,NSUB,NO
      DIMENSION BUFFER(8)
      DIMENSION LL(20),NN(20),MM(20),MECH(20)
      LOGICAL DUP
      LOGICAL MECH,FULL
      DATA PLUS,STAR/1H+,1H*/
      DATA LL/8HCORD2R  ,
     2        8HCORD2C  ,
     3        8HCORD2S  ,
     4        8HGRID    ,
     5        8HGRID*   ,
     6        8HSEQGP   ,
     7        8HCLOOF8  ,
     8        8HCLOOF6  ,
     9        8HCLOOF3  ,
     .        8HCONGR   ,
     .        8HPLOOF   ,
     .        8HPLOOFX  ,
     .        8HPLOOF3  ,
     .        8HMAT1    ,
     .        8HMAT8    ,
     .        8HPLOAD4  ,
     .        8HTHLOOF  ,
     .        8HPARAM   ,
     .        8HSPOINT  /
      DATA NN/1,
     .        1,
     .        1,
     .        2,
     .        2,
     .        3,
     .        4,
     .        4,
     .        5,
     .        6,
     .        7,
     .        8,
     .        9,
     .        10,
     .        10,
     .        11,
     .        12,
```

```
     .         13,
     .         14/
      DATA MM/1,
     .         2,
     .         3,
     .         1,
     .         2,
     .         1,
     .         1,
     .         2,
     .         1,
     .         1,
     .         1,
     .         1,
     .         1,
     .         1,
     .         2,
     .         1,
     .         1,
     .         1,
     .         1/
      DATA MECH/
     9              .TRUE.,
     .              .TRUE.,
     .              .TRUE.,
     .              .FALSE.,
     .              .FALSE.,
     .              .TRUE.,
     .              .FALSE.,
     .              .FALSE.,
     .              .FALSE.,
     .              .FALSE.,
     .              .FALSE.,
     .             .FALSE.,
     .              .FALSE.,
     .              .TRUE.,
     .              .FALSE.,
     .              .FALSE.,
     .              .FALSE.,
     .             .TRUE.,
     .              .TRUE./
      DATA KNOWN/19/
      DATA FULL/.FALSE./
      IF (.NOT.FULL) READ(1,10) BUFFER
   10 FORMAT (8A10)
      IF (EOF(1).NE.0.OR.BUFFER(1).EQ.7HENDDATA) GO TO 200
      FULL=.TRUE.
      DECODE(80,20,BUFFER) NAME,(CARD(I),I=1,8),C,CONT
   20 FORMAT (9A8,A1,A7)
      IF (NAME.EQ.6HPLOOF2) NAME=6HPLOOFX
```

```
      CALL LSHIFT(CARD,8)
      NO=NO+1
      FULL=.FALSE.
      DO 30 K=1,KNOWN
      IF (NAME.EQ.LL(K)) GO TO 40
   30 CONTINUE
      NTYPE=0
      NSUB=0
      DUP=.TRUE.
      GO TO 50
   40 NTYPE=NN(K)
      NSUB=MM(K)
      DUP=MECH(K)
C
C     PASS THIS CARD TO NASTRAN
C
   50 IF (DUP) WRITE(3,20) NAME,(CARD(I),I=1,8),C,CONT
C
C     AND ECHO, IF DESIRED
C
      IF (ECHO) PRINT 60,NO,NAME,(CARD(I),I=1,8),C,CONT
   60 FORMAT (I10,1H.,5X,9A8,A1,A7)
      L2=8
   70 READ(1,10) BUFFER
      FULL=.TRUE.
      IF (EOF(1).NE.0) GO TO 200
      L1=L2+1
      L2=L1+7
   80 FORMAT (A1,A7,8A8,A1,A7)
      DECODE(80,80,BUFFER) CHAR,CONT2,(CARD(L),L=L1,L2),C,CONT3
      CALL LSHIFT(CARD(L1),8)
      IF (CHAR.NE.PLUS.AND.CHAR.NE.STAR) GO TO 120
      FULL=.FALSE.
      IF (DUP) WRITE(3,80) CHAR,CONT2,(CARD(L),L=L1,L2),C,CONT3
      IF (ECHO) PRINT 90,CHAR,CONT2,(CARD(L),L=L1,L2),C,CONT3
   90 FORMAT (16X,A1,A7,8A8,A1,A7)
      IF (CONT2.EQ.CONT) GO TO 110
      PRINT 100,NO
  100 FORMAT (48H *** CONTINUATION CARD OUT OF ORDER FOR CARD NO.,I5)
      L1=L1-8
      L2=L2-8
      GO TO 70
  110 CONT=CONT3
      GOTO 70
  120 NCARD=L2-8
      IF (NCARD.LE.MXCARD) RETURN
      PRINT 130,NO
  130 FORMAT (13H *** CARD NO.,I5,10H TOOO LONG)
      IF (.NOT.ECHO) PRINT 60,NO,NAME,(CARD(I),I=1,8)
      L2=MXCARD
```

```
      RETURN
  200 NTYPE=-1
      RETURN
      END
```

```
      SUBROUTINE LSHIFT(CARD,N)
      DIMENSION CARD(1)
      INTEGER BLANK
      DATA MASK/77 00 00 00 00 00 00 00 00 00B/
      DATA BLANK/1L /
      DO 20 I=1,N
      DO 10 J=1,8
      IF ((CARD(I).AND.MASK).NE.BLANK) GO TO 20
      CARD(I)=SHIFT(CARD(I),6)
   10 CONTINUE
   20 CONTINUE
      RETURN
      END
```

```
      REAL FUNCTION DCODE(ITEM,TYPE,ERR)
      IMPLICIT INTEGER (A-Z)
      LOGICAL BAD,ERR
      DIMENSION CHAR(8)
      DATA PLUS,MINUS,ZERO,NINE,BLANK,E,PERIOD/
     .          1H+,1H-,1H0,1H9,1H ,1HE,1H./
      DECODE(8,5,ITEM) CHAR
    5 FORMAT (8A1)
      GO TO (100,200,300),TYPE
C
C     INTEGER
C
  100 L=-1
      BAD=.FALSE.
      DO 110 I=1,8
      C=CHAR(9-I)
      IF (C.NE.BLANK.AND.L.LT.0) L=I-1
      IF (C.GE.ZERO.AND.C.LE.NINE) GO TO 110
      IF (C.EQ.PLUS.OR.C.EQ.MINUS) GO TO 110
      IF (C.EQ.BLANK) GO TO 110
      BAD=.TRUE.
  110 CONTINUE
      IF (BAD) GO TO 400
      IC=ITEM
      IF (L.GT.0) IC=SHIFT(ITEM,60-6*L)
      DECODE(8,120,IC) M
  120 FORMAT (I8)
      DCODE=M
      GO TO 400
C
C     FLOATING POINT
C
  200 BAD=.FALSE.
      L=-1
      DO 210 I=1,8
      C=CHAR(9-I)
      IF (C.NE.BLANK.AND.L.LT.0) L=I-1
      IF (C.GE.ZERO.AND.C.LE.NINE) GO TO 210
      IF (C.EQ.PLUS.OR.C.EQ.MINUS) GO TO 210
      IF (C.EQ.E.OR.C.EQ.BLANK) GO TO 210
      IF (C.EQ.PERIOD) GO TO 210
      BAD=.TRUE.
  210 CONTINUE
      IF (BAD) GO TO 400
      IC=ITEM
      IF (L.GT.0) IC=SHIFT(ITEM,60-6*L)
C     CROSS YOUR FINGERS
      DECODE(8,220,IC) DCODE
  220 FORMAT (E8.0)
      GO TO 400
```

```
C
C     ALPHA
C
  300 BAD=.FALSE.
      IF (CHAR(1).NE.BLANK) GO TO 315
      DO 310 I=2,8
      IF (CHAR(I).NE.BLANK) GO TO 320
  310 CONTINUE
  315 ENCODE(8,5,DCODE) CHAR
      GO TO 400
  320 I1=I-1
      ENCODE(8,5,DCODE) (CHAR(J),J=1,8),(BLANK,J=1,I1)
  400 ERR=ERR.OR.BAD
      RETURN
      END
```

```
      REAL FUNCTION DCODE2(ITEM,TYPE,ERR)
      IMPLICIT INTEGER (A-Z)
      LOGICAL BAD,ERR
      DIMENSION ITEM(2)
      DIMENSION CHAR(16)
      DIMENSION TEMP(2)
      DATA PLUS,MINUS,ZERO,NINE,BLANK,E,PERIOD/
     .          1H+,1H-,1H0,1H9,1H ,1HE,1H./
      DECODE(18,10,ITEM) CHAR
   10 FORMAT (8A1,2X,8A1)
      GO TO (100,200,300),TYPE
C
C     INTEGER
C
  100 L=-1
      BAD=.FALSE.
      DO 110 I=1,16
      C=CHAR(17-I)
      IF (C.NE.BLANK.AND.L.LT.0) L=I-1
      IF (C.GE.ZERO.AND.C.LE.NINE) GO TO 110
      IF (C.EQ.PLUS.OR.C.EQ.MINUS) GO TO 110
      IF (C.EQ.BLANK) GO TO 110
      BAD=.TRUE.
  110 CONTINUE
      DCODE2=0
      IF (L.EQ.-1) RETURN
      IF (BAD) GO TO 400
      DCODE2=0
      IF (L) 160,140,130
  130 L16=16-L
      ENCODE(16,240,TEMP) (BLANK,I=1,L),(CHAR(I),I=1,L16)
      GO TO 150
  140 ENCODE(16,240,TEMP) CHAR
  150 DECODE(16,270,TEMP) DCODE2
  160 GO TO 400
C
C     FLOATING POINTS
C
  200 BAD=.FALSE.
      L=-1
      DO 210 I=1,16
      C=CHAR(17-I)
      IF (C.NE.BLANK.AND.L.LT.0) L=I-1
      IF (C.GE.ZERO.AND.C.LE.NINE) GO TO 210
      IF (C.EQ.PLUS.OR.C.EQ.MINUS) GO TO 210
      IF (C.EQ.BLANK.OR.C.EQ.E) GO TO 210
      IF (C.EQ.PERIOD) GO TO 210
      BAD=.TRUE.
  210 CONTINUE
      IF (BAD) GO TO 400
```

```
      DCODE2=0
      IF (L) 280,250,230
  230 L16=16-L
      ENCODE(16,240,TEMP) (BLANK,I=1,L),(CHAR(I),I=1,L16)
  240 FORMAT (16A1)
      GO TO 260
  250 ENCODE(16,240,TEMP) CHAR
  260 DECODE(16,270,TEMP) DCODE2
  270 FORMAT (E16.0)
  280 GO TO 400
C
C     ALPHA
C
  300 BAD=.FALSE.
      IF (CHAR(1).NE.BLANK) GO TO 315
      DO 310 I=2,16
      IF (CHAR(I).NE.BLANK) GO TO 320
  310 CONTINUE
  315 ENCODE(8,240,DCODE2) (CHAR(I),I=1,8)
      GO TO 400
  320 IF (I.GT.9) GO TO 330
      I7=I+7
      ENCODE(8,240,DCODE2) (CHAR(J),J=I,I7)
      GO TO 400
  330 I9=I-9
      ENCODE(8,240,DCODE2) (CHAR(J),J=I,16),(BLANK,J=1,I9)
  400 ERR=ERR.OR.BAD
      RETURN
      END
```

```
      SUBROUTINE SWING(A,ITYPE)
      DIMENSION A(3)
      IF (ITYPE.EQ.1) RETURN
      IF (ITYPE.NE.2) GO TO 10
      THETA=A(2)*3.1415927/180
      A(2)=A(1)*SIN(THETA)
      A(1)=A(1)*COS(THETA)
      RETURN
   10 IF (ITYPE.NE.3) RETURN
      THETA=A(2)*3.1415927/180
      PHI=A(3)*3.1415927/180
      A(3)=A(1)*COS(THETA)
      P=A(1)*SIN(THETA)
      A(2)=P*SIN(PHI)
      A(1)=P*COS(PHI)
      RETURN
      END
```

```
      SUBROUTINE TMATRX(T,A,B,C)
      DIMENSION T(3,3),A(3),B(3),C(3)
      DO 10 J=1,3
        T(J,2)=C(J)-A(J)
10      T(J,3)=B(J)-A(J)
      CALL NORMAL(T(1,3))
      CALL CROSS(T(1,3),T(1,2),T(1,2))
      CALL NORMAL(T(1,2))
      CALL CROSS(T(1,2),T(1,3),T(1,1))
      RETURN
      END
```

```
SUBROUTINE CROSS(A,B,C)
DIMENSION A(3),B(3),C(3)
C1=A(2)*B(3)-B(2)*A(3)
C2=-(A(1)*B(3)-B(1)*A(3))
C3=A(1)*B(2)-B(1)*A(2)
C(1)=C1
C(2)=C2
C(3)=C3
RETURN
END
```

```
SUBROUTINE NORMAL(X)
DIMENSION X(3)
E=SQRT(X(1)*X(1)+X(2)*X(2)+X(3)*X(3))
IF (E.EQ.0) RETURN
X(1)=X(1)/E
X(2)=X(2)/E
X(3)=X(3)/E
RETURN
END
```

```
      SUBROUTINE CORD(TRANS)
C
C     INTERPRETS CORD BULK DATA CARDS AND SETS UP COORDINATE
C     TRANSFORMATION TABLES
C
      DIMENSION TRANS(3,5,1)
      COMMON/CONTRL/ECHO,ERR,MATGEN,DYN,APPLD,PLOT,DBUG,BAD,NCORE,
     .     WTMASS,NASTY
      LOGICAL ECHO,ERR,MATGEN,DYN,APPLD,PLOT,DBUG,BAD
      COMMON/CARD/NAME,CARD(400),MXCARD,NCARD,NTYPE,NSUB,NO
      COMMON/N/NCORD,NUMNP,NSHELL,NPSHEL,NPSHELX,NSHLTY,NBEAM,NPBEAM,
     .          NBMTY,NMAT,NSPOINT,MAXGRD,NDOF
      DIMENSION AA(3),BB(3),CC(3)
      IF (NCARD.LT.9) GO TO 20
      NCORD=NCORD+1
      TRANS(1,1,NCORD)=DCODE(CARD,1,BAD)
      TRANS(2,1,NCORD)=NSUB
      DO 10 I=1,3
      AA(I)=DCODE(CARD(2+I),2,BAD)
      BB(I)=DCODE(CARD(5+I),2,BAD)
   10 CC(I)=DCODE(CARD(8+I),2,BAD)
      J=DCODE(CARD(2),1,BAD)
      BAD=BAD.OR.J.NE.0
      IF (BAD) GO TO 20
      CALL TMATRX(TRANS(1,3,NCORD),AA,BB,CC)
      CALL MOVER(AA,1,TRANS(1,2,NCORD),1,3)
      RETURN
   20 CALL BUM
      RETURN
      END
```

```
      SUBROUTINE GRID(CORD,GRD)
      DIMENSION CORD(3,5,1),GRD(13,1)
C
C     INTERPRETS GRID CARDS AND SETS UP TABLES
C
      COMMON/CONTRL/ECHO,ERR,MATGEN,DYN,APPLD,PLOT,DBUG,BAD,NCORE,
     .     WTMASS,NASTY
      LOGICAL ECHO,ERR,MATGEN,DYN,APPLD,PLOT,DBUG,BAD
      COMMON/CARD/NAME,CARD(400),MXCARD,NCARD,NTYPE,NSUB,NO
      COMMON/N/NCORD,NUMNP,NSHELL,NPSHEL,NPSHELX,NSHLTY,NBEAM,NPBEAM,
     .           NBMTY,NMAT,NSPOINT,MAXGRD,NDOF
      DIMENSION XYZ(3)
      NUMNP=NUMNP+1
      BAD=.FALSE.
      IF (NSUB.EQ.2) GO TO 10
C
C     SINGLE FIELD
C
      GRD(1,NUMNP)=DCODE(CARD(1),1,BAD)
      GRD(2,NUMNP)=DCODE(CARD(2),1,BAD)
      GRD(3,NUMNP)=DCODE(CARD(3),2,BAD)
      GRD(4,NUMNP)=DCODE(CARD(4),2,BAD)
      GRD(5,NUMNP)=DCODE(CARD(5),2,BAD)
      GRD(9,NUMNP)=DCODE(CARD(6),1,BAD)
      GRD(10,NUMNP)=DCODE(CARD(7),1,BAD)
      GO TO 20
C
C     DOUBLE FIELD
C
   10 GRD(1,NUMNP)=DCODE2(CARD(1),1,BAD)
      GRD(2,NUMNP)=DCODE2(CARD(3),1,BAD)
      GRD(3,NUMNP)=DCODE2(CARD(5),2,BAD)
      GRD(4,NUMNP)=DCODE2(CARD(7),2,BAD)
      GRD(5,NUMNP)=DCODE2(CARD(9),2,BAD)
      GRD(9,NUMNP)=DCODE2(CARD(11),1,BAD)
      GRD(10,NUMNP)=DCODE2(CARD(13),1,BAD)
   20 IF (.NOT.BAD) GO TO 30
      CALL BUM
      RETURN
   30 MAXGRD=MAX0(MAXGRD,IFIX(GRD(1,NUMNP)))
      IF (NUMNP.EQ.1) GO TO 38
      N1=NUMNP-1
      DO 32 I=1,N1
      IF (GRD(1,I).EQ.GRD(1,NUMNP)) GO TO 35
   32 CONTINUE
      GO TO 38
   35 PRINT 36,IFIX(GRD(1,NUMNP))
   36 FORMAT (19H *** DUPLICATE GRID,I6)
      ERR=.TRUE.
      RETURN
```

```
   38 DO 40 I=1,3
      GRD(I+5,NUMNP)=GRD(I+2,NUMNP)
   40 GRD(I+10,NUMNP)=0
      GRD(2,NUMNP)=0
      GRD(9,NUMNP)=0
      IF (GRD(2,NUMNP).LE.0) GO TO 80
      JCORD=INDEX(CORD,NCORD,15,GRD(2,NUMNP))
      IF (JCORD.GT.0) GO TO 60
      M=GRD(1,NUMNP)
      N=GRD(2,NUMNP)
      PRINT 50,M,N
   50 FORMAT ( 9H *** GRID,I8,37H REFERENCES UNKNOWN COORDINATE SYSTEM,
     .       I8)
      ERR=.TRUE.
      GO TO 80
C
C     CONVERT LOCATION TO BASIC COORDINATES
C
   60 CALL MOVER(GRD(3,NUMNP),1,XYZ,1,3)
      CALL SWING(XYZ,IFIX(CORD(2,1,JCORD)))
      DO 70 I=1,3
      CALL SCPROD(3,3,1,CORD(1,3,JCORD),XYZ,XX)
      GRD(2,NUMNP)=JCORD
   70 GRD(5+I,NUMNP)=XX+CORD(I,2)
   80 IF (GRD(9,NUMNP).LE.0) RETURN
      JCORD=INDEX(CORD,NCORD,15,GRD(9,NUMNP))
      IF (JCORD.GT.0) GO TO 90
      IF (JCORD.GT.0) RETURN
      M=GRD(1,NUMNP)
      N=GRD(9,NUMNP)
      PRINT 50,M,N
      ERR=.TRUE.
      RETURN
   90 GRD(9,NUMNP)=JCORD
      RETURN
      END
```

```
      SUBROUTINE SEQGP(SEQ,GRD)
C
C     READS SEQUENCE CARDS
C
      DIMENSION SEQ(1),GRD(13,1)
      INTEGER SEQ
      COMMON/CONTRL/ECHO,ERR,MATGEN,DYN,APPLD,PLOT,DBUG,BAD,NCORE,
     .     WTMASS,NASTY
      LOGICAL ECHO,ERR,MATGEN,DYN,APPLD,PLOT,DBUG,BAD
      COMMON/CARD/NAME,CARD(400),MXCARD,NCARD,NTYPE,NSUB,NO
      COMMON/N/NCORD,NUMNP,NSHELL,NPSHEL,NPSHELX,NSHLTY,NBEAM,NPBEAM,
     .          NBMTY,NMAT,NSPOINT,MAXGRD,NDOF
      BAD=.FALSE.
      DO 20 I=1,7,2
      GR=DCODE(CARD(I),1,BAD)
      SQ=DCODE(CARD(I+1),1,BAD)
      IF (GR.EQ.0) GO TO 20
      J=INDEX(GRD,NUMNP,13,GR)
      IF (J.NE.-1) GO TO 10
    5 BAD=.TRUE.
      GO TO 20
   10 IF (SQ.LT.0.OR.SQ.GT.NUMNP) GO TO 5
      SEQ(J)=SQ
   20 CONTINUE
      IF (BAD) CALL BUM
      RETURN
      END
```

```
      SUBROUTINE ISHELL(SHELL,GRD)
C
C     PROCESSES CLDJF8 AND CLDDF6 CARDS
C
      DIMENSION SHELL(12,1),GRD(13,1)
      COMMON/CONTRL/ECHO,ERR,MATGEN,DYN,APPLD,PLOT,DBUG,BAD,NCORE,
     .       WTMASS,NASTY
      LOGICAL ECHO,ERR,MATGEN,DYN,APPLD,PLOT,DBUG,BAD
      COMMON/CARD/NAME,CARD(400),MXCARD,NCARD,NTYPE,NSUB,NO
      COMMON/N/NCORD,NUMNP,NSHELL,NPSHEL,NPSHELX,NSHLTY,NBEAM,NPBEAM,
     .            NBMTY,NMAT,NSPOINT,MAXGRD,NDOF
      BAD=.FALSE.
      NSHELL=NSHELL+1
      SHELL(9,NSHELL)=0
      SHELL(10,NSHELL)=0
      NNOD=8
      IF (NSUB.EQ.2) NNOD=6
      N2=NNOD+2
      BAD=NCARD.LT.N2
      DO 10 I=1,N2
   10 SHELL(I,NSHELL)=DCODE(CARD(I),1,BAD)
      SHELL(11,NSHELL)=NSHELL
      SHELL(12,NSHELL)=0
      IF (NCARD.GE.N2+1) SHELL(12,NSHELL)=DCODE(CARD(N2+1),2,BAD)
      IF (.NOT.BAD) GO TO 15
      CALL BUM
      RETURN
C
C     GET GRIDS
C
   15 DO 30 I=3,N2
      L=SHELL(I,NSHELL)
      J=INDEX(GRD,NUMNP,13,FLOAT(L))
      SHELL(I,NSHELL)=J
      IF (J.NE.-1) GO TO 30
      PRINT 20,IFIX(SHELL(1,NSHELL)),L
   20 FORMAT (12H *** ELEMENT,I8,24H REFERENCES UNKNOWN GRID,I10)
      ERR=.TRUE.
   30 CONTINUE
      RETURN
      END
```

```
      SUBROUTINE IBEAM(BEAM,GRD)
C
C     PROCESSES CLDJF3 CARDS
C
      DIMENSION BEAM(21,1),GRD(13,1)
      COMMON/CONTRL/ECHO,ERR,MATGEN,DYN,APPLD,PLOT,DBUG,BAD,NCORE,
     .      WTMASS,NASTY
      LOGICAL ECHO,ERR,MATGEN,DYN,APPLD,PLOT,DBUG,BAD
      COMMON/CARD/NAME,CARD(400),MXCARD,NCARD,NTYPE,NSUB,NO
      COMMON/N/NCORD,NUMNP,NSHELL,NPSHEL,NPSHELX,NSHLTY,NBEAM,NPBEAM,
     .           NBMTY,NMAT,NSPOINT,MAXGRD,NDOF
      DIMENSION F(3)
      BAD=.FALSE.
      NBEAM=NBEAM+1
      DO 10 I=1,8
   10 BEAM(I,NBEAM)=DCODE(CARD(I),1,BAD)
      IF (BEAM(7,NBEAM).EQ.0) BEAM(7,NBEAM)=BEAM(6,NBEAM)
      IF (BEAM(8,NBEAM).EQ.0) BEAM(8,NBEAM)=BEAM(6,NBEAM)
      CALL MOVER(0,0,BEAM(16,NBEAM),1,6)
      BEAM(15,NBEAM)=NBEAM
      IF (BAD) CALL BUM
      IF (NCARD.LT.12) RETURN
      IF=DCODE(CARD(12),1,BAD)
      IF (IF.EQ.0) GO TO 45
      BAD=BAD.OR.(IF.NE.1.AND.IF.NE.2)
      IF (BAD) GO TO 100
      GO TO (20,30),IF
   20 DO 22 I=1,3
   22 F(I)=DCODE(CARD(8+I),2,BAD)
      IF (BAD) GO TO 100
      GO TO 40
   30 L=DCODE(CARD(9),1,BAD)
      IF (BAD) GO TO 100
      J=INDEX(GRD,NGRID,13,L)
      IF (J.EQ.-1) GO TO 80
      DO 32 I=1,3
   32 F(I)=GRD(5+I,J)
   40 CALL SCALAR(F,F,FSQ)
      IF (FSQ.EQ.0.) GO TO 100
      FSQ=SQRT(FSQ)
      DO 42 I=1,3
   42 BEAM(18+I,NBEAM)=F(I)/FSQ
   45 CALL MOVER(0,0,BEAM(9,NBEAM),1,6)
      IF (NCARD.LE.16) GO TO 60
      DO 50 I=17,22
   50 BEAM(I-8,NBEAM)=DCODE(CARD(I),2,BAD)
   60 DO 70 I=3,5
      L=BEAM(I,NBEAM)
      J=INDEX(GRD,NUMNP,13,FLOAT(L))
      BEAM(I,NBEAM)=J
```

```
      IF (J.EQ.-1) GO TO 80
   70 CONTINUE
      RETURN
   80 PRINT 90,IFIX(BEAM(1,NBEAM)),L
   90 FORMAT (12H *** ELEMENT,I8,24H REFERENCES UNKNOWN GRID,I10)
      ERR=.TRUE.
      RETURN
  100 CALL BUM
      RETURN
      END
```

```
      SUBROUTINE CONGR(GRD,SHELL,BEAM)
C
C     PROCESSES  CONGR CARDS
C
      DIMENSION GRD(13,1),SHELL(12,1),BEAM(18,1)
      COMMON/CONTRL/ECHO,ERR,MATGEN,DYN,APPLD,PLOT,DBUG,BAD,NCORE,
     .       WTMASS,NASTY
      LOGICAL ECHO,ERR,MATGEN,DYN,APPLD,PLOT,DBUG,BAD
      COMMON/CARD/NAME,CARD(400),MXCARD,NCARD,NTYPE,NSUB,NO
      COMMON/N/NCORD,NUMNP,NSHELL,NPSHEL,NPSHELX,NSHLTY,NBEAM,NPBEAM,
     .           NBMTY,NMAT,NSPOINT,MAXGRD,NDOF
      EL1=DCODE(CARD(1),1,BAD)
      J1=INDEX(SHELL,NSHELL,12,EL1)
      IF (J1.LT.0) GO TO 30
      DO 10 I=2,NCARD
      EL=DCODE(CARD(I),1,BAD)
      IF (BAD) GO TO 10
      IF (EL.EQ.0) GO TO 10
      J=INDEX(SHELL,NSHELL,12,EL)
      BAD=BAD.OR.J.LT.0
      IF (.NOT.BAD) SHELL(11,J)=SHELL(11,J1)
   10 CONTINUE
      IF (BAD) CALL BUM
      RETURN
   30 J1=INDEX(BEAM,NBEAM,18,EL1)
      BAD=J1.LT.0
      DO 40 I=2,NCARD
      EL=DCODE(CARD(I),1,BAD)
      IF (BAD) GO TO 40
      IF (EL.EQ.0) GO TO 40
      J=INDEX(BEAM,NBEAM,18,EL)
      BAD=BAD.OR.J.LT.0
      IF (.NOT.BAD) BEAM(15,J)=BEAM(15,J1)
   40 CONTINUE
      IF (BAD) CALL BUM
      RETURN
      END
```

```
      SUBROUTINE IPSHEL(PSHELL)
C
C     PROCESSES PLOOF CARDS -- SHELL PROPERTIES
C
      DIMENSION PSHELL(3,1)
      COMMON/CONTRL/ECHO,ERR,MATGEN,DYN,APPLD,PLOT,DBUG,BAD,NCORE,
     .     WTMASS,NASTY
      LOGICAL ECHO,ERR,MATGEN,DYN,APPLD,PLOT,DBUG,BAD
      COMMON/CARD/NAME,CARD(400),MXCARD,NCARD,NTYPE,NSUB,NO
      COMMON/N/NCORD,NUMNP,NSHELL,NPSHEL,NPSHELX,NSHLTY,NBEAM,NPBEAM,
     .         NBMTY,NMAT,NSPOINT,MAXGRD,NDOF
      BAD=.FALSE.
      NPSHEL=NPSHEL+1
      PSHELL(1,NPSHEL)=DCODE(CARD(1),1,BAD)
      PSHELL(2,NPSHEL)=DCODE(CARD(2),1,BAD)
      PSHELL(3,NPSHEL)=DCODE(CARD(3),2,BAD)
      IF (BAD) CALL BUM
      RETURN
      END
```

```
      SUBROUTINE IPSHELX(PSHELL)
C
C     PROCESSES PLOOFX CARDS -- ANISOTROPIC SHELL
C
      DIMENSION PSHELL(20,1)
      COMMON/CONTRL/ECHO,ERR,MATGEN,DYN,APPLD,PLOT,DBUG,BAD,NCORE,
     .       WTMASS,NASTY
      LOGICAL ECHO,ERR,MATGEN,DYN,APPLD,PLOT,DBUG,BAD
      COMMON/N/NCORD,NUMNP,NSHELL,NPSHEL,NPSHELX,NSHLTY,NBEAM,NPBEAM,
     .            NBMTY,NMAT,NSPOINT,MAXGRD,NDOF
      COMMON/CARD/NAME,CARD(400),MXCARD,NCARD,NTYPE,NSUB,NO
      BAD=.FALSE.
      IF (NCARD.LT.7) GO TO 40
      NPSHELX=NPSHELX+1
      PSHELL(1,NPSHELX)=DCODE(CARD(1),1,BAD)
      DO 10 I=2,7
   10 PSHELL(I,NPSHELX)=DCODE(CARD(I),2,BAD)
      PSHELL(20,NPSHELX)=DCODE(CARD(9),2,BAD)
      CALL MOVER(0,0,PSHELL(8,NPSHELX),1,12)
      IF (NCARD.LT.15) GO TO 35
      DO 20 I=10,15
   20 PSHELL(I-2,NPSHELX)=DCODE(CARD(I),2,BAD)
      IF (NCARD.LT.23) GO TO 35
      DO 30 I=18,23
   30 PSHELL(I-4,NPSHELX)=DCODE(CARD(I),2,BAD)
   35 IF (.NOT.BAD) RETURN
   40 CALL BUM
      RETURN
      END
```

```
      SUBROUTINE IPBEAM(PBEAM)
C
C     PROCESSES PLOJF3 CARDS -- BEAM PROPERTIES
C
      DIMENSION PBEAM(9,1)
      COMMON/CONTRL/ECHO,ERR,MATGEN,DYN,APPLD,PLOT,DBUG,BAD,NCORE,
     .      WTMASS,NASTY
      LOGICAL ECHO,ERR,MATGEN,DYN,APPLD,PLOT,DBUG,BAD
      COMMON/CARD/NAME,CARD(400),MXCARD,NCARD,NTYPE,NSUB,NO
      COMMON/N/NCORD,NUMNP,NSHELL,NPSHEL,NPSHELX,NSHLTY,NBEAM,NPBEAM,
     .           NBMTY,NMAT,NSPOINT,MAXGRD,NDOF
      NPBEAM=NPBEAM+1
      BAD=.FALSE.
      PBEAM(1,NPBEAM)=DCODE(CARD(1),1,BAD)
      DO 10 I=2,8
   10 PBEAM(I,NPBEAM)=DCODE(CARD(I),2,BAD)
      PBEAM(9,NPBEAM)=0
      IF (NCARD.GE.9) PBEAM(9,NPBEAM)=DCODE(CARD(9),2,BAD)
      BAD=BAD.OR.PBEAM(2,NPBEAM).LE.0
      IF (BAD) CALL BUM
      RETURN
      END
```

```
      SUBROUTINE IMAT(XMAT)
      DIMENSION XMAT(6,1)
      COMMON/CONTRL/ECHO,ERR,MATGEN,DYN,APPLD,PLOT,DBUG,BAD,NCORE,
     .      WTMASS,NASTY
      LOGICAL ECHO,ERR,MATGEN,DYN,APPLD,PLOT,DBUG,BAD
      COMMON/CARD/NAME,CARD(400),MXCARD,NCARD,NTYPE,NSUB,NO
      COMMON/N/NCORD,NUMNP,NSHELL,NPSHEL,NPSHELX,NSHLTY,NBEAM,NPBEAM,
     .           NBMTY,NMAT,NSPOINT,MAXGRD,NDOF
      REAL NU
      NMAT=NMAT+1
      BAD=.FALSE.
      XMAT(1,NMAT)=DCODE(CARD(1),1,BAD)
      IF (NSUB.EQ.2) GO TO 10
      E=DCODE(CARD(2),2,BAD)
      G=DCODE(CARD(3),2,BAD)
      NU=DCODE(CARD(4),2,BAD)
      RHO=DCODE(CARD(5),2,BAD)
      IF (G.EQ.0) G=E/(2*(1+NU))
      IF (NU.EQ.0) NU=E/(2*G)-1
      BAD=BAD.OR.NU.GE..5.OR.NU.LE.-1
      IF (.NOT.BAD) GO TO 5
      CALL BUM
      RETURN
    5 XMAT(2,NMAT)=E/(1-NU*NU)
      XMAT(3,NMAT)=NU*XMAT(2,NMAT)
      XMAT(4,NMAT)=XMAT(2,NMAT)
      XMAT(5,NMAT)=G
      XMAT(6,NMAT)=RHO
      RETURN
   10 DO 20 I=2,6
   20 XMAT(I,NMAT)=DCODE(CARD(I),2,BAD)
      IF (BAD) CALL BUM
      RETURN
      END
```

```
      SUBROUTINE IPLOAD(GRD)
C
C     PROCESSES PLOAD4 CARDS -- PRESSURES BY GRID POINTS
C
      DIMENSION GRD(13,1)
      COMMON/CONTRL/ECHO,ERR,MATGEN,DYN,APPLD,PLOT,DBUG,BAD,NCORE,
     .       WTMASS,NASTY
      LOGICAL ECHO,ERR,MATGEN,DYN,APPLD,PLOT,DBUG,BAD
      COMMON/CARD/NAME,CARD(400),MXCARD,NCARD,NTYPE,NSUB,NO
      COMMON/N/NCORD,NUMNP,NSHELL,NPSHEL,NPSHELX,NSHLTY,NBEAM,NPBEAM,
     .             NBMTY,NMAT,NSPOINT,MAXGRD,NDOF
      BAD=.FALSE.
      VALUE=DCODE(CARD(2),2,BAD)
      THRU=DCODE(CARD(4),3,BAD)
      IF (THRU.EQ.4HTHRU) GO TO 100
      DO 30 I=3,8
      GR=DCODE(CARD(I),1,BAD)
      IF (.NOT.BAD) GO TO 5
      CALL BUM
      GO TO 30
    5 IF (GR.EQ.0) GO TO 30
      J=INDEX(GRD,NUMNP,13,GR)
      IF (J.NE.-1) GO TO 20
      PRINT 10,IFIX(GR)
   10 FORMAT (40H *** PLOAD4 CARD REFERENCES UNKNOWN GRID,I8)
      ERR=.TRUE.
      RETURN
   20 GRD(12,J)=VALUE
   30 CONTINUE
      RETURN
  100 GR1=DCODE(CARD(3),1,BAD)
      GR2=DCODE(CARD(5),1,BAD)
      BAD=BAD.OR.GR2.LT.GR1
      IF (.NOT.BAD) GO TO 110
      CALL BUM
      RETURN
  110 J1=INDEX(GRD,NUMNP,13,GR1)
      J2=INDEX(GRD,NUMNP,13,GR2)
      GR=GR+1
      IF (J1.GT.0) GO TO 120
      PRINT 10,J1
      BAD=.TRUE.
  120 IF (J2.GT.0) GO TO 130
      PRINT 10,J2
      BAD=.TRUE.
  130 IF (.NOT.BAD) GO TO 140
      CALL BUM
      RETURN
  140 J=INDEX(GRD,NUMNP,13,GR)
      IF (J.EQ.-1) GO TO 150
```

```
      SUBROUTINE ITHICK(GRD)
      DIMENSION GRD(13,1)
C
C     PROCESS THLDOF CARDS (SHELL THICKNESS BY NODE POINT)
C
      COMMON/CONTRL/ECHO,ERR,MATGEN,DYN,APPLD,PLOT,DBUG,BAD,NCORE,
     .       WTMASS,NASTY
      LOGICAL ECHO,ERR,MATGEN,DYN,APPLD,PLOT,DBUG,BAD
      COMMON/CARD/NAME,CARD(400),MXCARD,NCARD,NTYPE,NSUB,NO
      COMMON/N/NCORD,NUMNP,NSHELL,NPSHEL,NPSHELX,NSHLTY,NBEAM,NPBEAM,
     .            NBMTY,NMAT,NSPOINT,MAXGRD,NDOF
      BAD=.FALSE.
      VALUE=DCODE(CARD(2),2,BAD)
      THRU=DCODE(CARD(4),3,BAD)
      IF (THRU.EQ.4HTHRU) GO TO 100
      DO 30 I=3,8
      GR=DCODE(CARD(I),1,BAD)
      IF (.NOT.BAD) GO TO 5
      CALL BUM
      GO TO 30
    5 IF (GR.EQ.0) GO TO 30
      J=INDEX(GRD,NUMNP,13,GR)
      IF (J.NE.-1) GO TO 20
      PRINT 10,IFIX(GR)
   10 FORMAT (40H *** THLDOF CARD REFERENCES UNKNOWN GRID,I8)
      ERR=.TRUE.
      GO TO 30
   20 GRD(12,J)=VALUE
   30 CONTINUE
      RETURN
  100 GR1=DCODE(CARD(3),1,BAD)
      GR2=DCODE(CARD(5),1,BAD)
      BAD=BAD.OR.GR2.LT.GR1
      IF (.NOT.BAD) GO TO 110
      CALL BUM
      RETURN
  110 J1=INDEX(GRD,NUMNP,13,GR1)
      J2=INDEX(GRD,NUMNP,13,GR2)
      IF (J1.GT.0) GO TO 120
      PRINT 10,J1
      BAD=.TRUE.
  120 IF (J2.GT.0) GO TO 130
      PRINT 10,J2
      BAD=.TRUE.
  130 IF (.NOT.BAD) GO TO 140
      CALL BUM
      RETURN
  140 J=INDEX(GRD,NUMNP,13,GR)
      IF (J.EQ.-1) GO TO 150
      GRD(12,J)=VALUE
```

```
      SUBROUTINE PARAM
      COMMON/CARD/NAME,CARD(400),MXCARD,NCARD,NTYPE,NSUB,NO
      COMMON/CONTRL/ECHO,ERR,MATGEN,DYN,APPLD,PLOT,DBUG,BAD,NCORE,
     .      WTMASS,NASTY
      LOGICAL ECHO,ERR,MATGEN,DYN,APPLD,PLOT,DBUG,BAD
      BAD=.FALSE.
      A=DCODE(CARD(1),3,BAD)
      IF (A.NE.6HWTMASS) GO TO 10
      WTMASS=DCODE(CARD(2),2,BAD)
   10 IF (BAD) CALL BUM
      RETURN
      END
```

```
      SUBROUTINE ISPNT
      COMMON/CONTRL/ECHO,ERR,MATGEN,DYN,APPLD,PLOT,DBUG,BAD,NCORE,
     .       WTMASS,NASTY
      LOGICAL ECHO,ERR,MATGEN,DYN,APPLD,PLOT,DBUG,BAD
      COMMON/N/NCORD,NUMNP,NSHELL,NPSHEL,NPSHELX,NSHLTY,NBEAM,NPBEAM,
     .            NBMTY,NMAT,NSPOINT,MAXGRD,NDOF
      COMMON/CARD/NAME,CARD(400),MXCARD,NCARD,NTYPE,NSUB,NO
      BAD=.FALSE.
      IF (CARD(2).EQ.4HTHRU) GO TO 20
      DO 10 I=2,8
      J=DCODE(CARD(I),1,BAD)
      IF (J.EQ.0) GO TO 10
      BAD=BAD.OR.J.LE.MAXGRD
      NSPOINT=NSPOINT+1
   10 CONTINUE
      IF (BAD) CALL BUM
      RETURN
   20 J1=DCODE(CARD(1),1,BAD)
      J2=DCODE(CARD(3),1,BAD)
      BAD=BAD.OR.J2.LT.J1.OR.J1.LE.MAXGRD
      IF (BAD) GO TO 30
      NSPOINT=NSPOINT+J2-J1+1
      RETURN
   30 CALL BUM
      RETURN
      END
```

```
      SUBROUTINE PROCESS(GRID,SHELL,BEAM,ISEQ,IPSPC)
      DIMENSION GRID(13,1),SHELL(12,1),BEAM(21,1),ISEQ(1),IPSPC(1)
      COMMON/CONTRL/ECHO,ERR,MATGEN,DYN,APPLD,PLOT,DBUG,BAD,NCORE,
     .     WTMASS,NASTY
      LOGICAL ECHO,ERR,MATGEN,DYN,APPLD,PLOT,DBUG,BAD
      COMMON/N/NCORD,NUMNP,NSHELL,NPSHEL,NPSHELX,NSHLTY,NBEAM,NPBEAM,
     .         NBMTY,NMAT,NSPOINT,MAXGRD,NDOF
      COMMON/LOC/LCORD,LGRID,LSEQ,LSHELL,LBEAM,LPSHEL,LPSHELX,LPBEAM,
     .     LMAT,LPSPC
      COMMON/TITLE/TITLE(8)
      COMMON A(1)
      CALL MOVER(-1,0,IPSPC,1,NUMNP)
C
C     SEQUENCE GRID POINTS
C
      IF (ISEQ(1).NE.0) GO TO 10
      LTEMP=NCORE
      CALL MORCOR(NUMNP)
      CALL SORT(GRID,A(LTEMP),ISEQ)
      NCORE=LTEMP
10    IF (NSHELL.EQ.0) GO TO 90
C
C     SHELL ELEMENTS
C
      NSHLTY=0
      DO 80 I=1,NSHELL
C
C       FIGURE OUT IF THIS IS A QUAD OR TRIANGLE
C
        LNODZ=8
        IF (SHELL(10,I).EQ.0) LNODZ=6
        IF (SHELL(11,I).EQ.1) NSHLTY=NSHLTY+1
        LK=LNODZ+2
        KL=LNODZ+1
C
C       IDENTIFY LOOP NODES
C
        DO 50 K=3,KL,2
          LL=SHELL(K,I)
          IF (LL.EQ.0) GO TO 50
          MM=SHELL(K+1,I)
          NN=SHELL(K+2,I)
          IF (K.EQ.KL) NN=SHELL(3,I)
          IF (.NOT.PLOT) GO TO 35
          IP1=10*SHELL(1,I)+K-2
          IP2=IP1+1
          LLL=GRID(1,LL)
          MMM=GRID(1,MM)
          NNN=GRID(1,NN)
          WRITE(3,20) IP1,LLL,MMM,IP2,MMM,NNN
```

```
   20       FORMAT (6HPLOTEL,I9,2(3I8,8X))
   35       IF (IPSPC(LL).NE.6) GO TO 40
            WRITE(6,30) IFIX(GRID(1,LL))
   30         FORMAT (9H *** GRID,I8,
     .        39H USED AS BOTH LOOF NODE AND CORNER NODE)
            ERR=.TRUE.
40          IPSPC(LL)=456
50          CONTINUE
          DO 70 K=4,LK,2
            LL=SHELL(K,I)
            IF (LL.EQ.0) GO TO 70
            IF (IPSPC(LL).NE.456) GO TO 60
            WRITE(6,30) IFIX(GRID(1,LL))
            ERR=.TRUE.
60          IPSPC(LL)=6
70          CONTINUE
80        CONTINUE
C
C      BEAM ELEMENTS
C
90     IF (NBEAM.EQ.0) GO TO 150
       NBMTY=0
       DO 140 I=1,NBEAM
         IF (BEAM(15,I).EQ.1) NBMTY=NBMTY+1
C
C        IDENTIFY LOOF NODES
C
         DO 110 K=3,5,2
           LL=BEAM(K,I)
           IF (LL.EQ.0) GO TO 110
           IF (IPSPC(LL).NE.6) GO TO 100
           WRITE(6,30) IFIX(GRID(1,LL))
           ERR=.TRUE.
 100       IPSPC(LL)=0
 110     CONTINUE
         K=4
           LL=BEAM(K,I)
           IF (LL.EQ.0) GO TO 130
           IF (IPSPC(LL).NE.456.AND.IPSPC(LL).NE.0) GO TO 120
           WRITE(6,30) IFIX(GRID(1,LL))
           ERR=.TRUE.
 120       IPSPC(LL)=6
 130       CONTINUE
 140     CONTINUE
   150   WRITE(7) TITLE,NUMNP,NSHELL,NPSHEL,NSHLTY,NBEAM,NPBEAM,
     .              NBMTY,NMAT
         IF (NSHELL.GT.0) WRITE(7) ((SHELL(J,I),J=1,12),I=1,NSHELL)
         IF (NBEAM.GT.0) WRITE(7) ((BEAM(J,I),J=1,15),I=1,NBEAM)
       DO 190 I=1,NUMNP
         GRID(11,I)=ISEQ(I)
```

```
      IF (IPSPC(I).NE.-1) GO TO 170
      PRINT 160,IFIX(GRID(1,I))
 160    FORMAT (19H ** WARNING -- GRID,I8,
     .          31H HAS NO LOOF ELEMENTS CONNECTED  )
      IPSPC(I)=0
 170  WRITE(3,180) IFIX(GRID(1,I)),IFIX(GRID(2,I)),GRID(3,I),
     .          GRID(4,I),I,I,GRID(5,I),IFIX(GRID(9,I)),IPSPC(I)
180   FORMAT (5HGRID*,I9,2I16,2E16.9,2H+G,I3/2H*G,I3,T9,E16.9,2I16)
190   CONTINUE
     IF (MATGEN) WRITE(3,195)
 195 FORMAT (17HPARAM   STIFMAT 1)
     IF (DYN) WRITE(3,200)
 200 FORMAT (17HPARAM   MASSMAT 1)
     IF (APPLD) WRITE(3,210)
 210 FORMAT (17HPARAM   LOADVEC 1)
     IF (NSPOINT.GT.0) WRITE(3,220) NSPOINT
 220 FORMAT (16HPARAM   NSPOINT ,I8)
     WRITE(3,230)
 230 FORMAT (7HENDDATA)
     RETURN
     END
```

```
      SUBROUTINE SORT(GRID,IGRD,ISEQ)
      DIMENSION GRID(13,1),IGRD(1),ISEQ(1)
C
C     SORT GRID POINTS ACCORDING TO EXTERNAL G.P. NO.
C
      COMMON/N/NCORD,NUMNP,NSHELL,NPSHEL,NPSHELX,NSHLTY,NBEAM,NPBEAM,
     .          NBMTY,NMAT,NSPOINT,MAXGRD,NDOF
      LOGICAL SWAP
      DO 5 I=1,NUMNP
      IGRD(I)=GRID(1,I)
5     ISEQ(I)=I
      N1=NUMNP-1
   10 SWAP=.FALSE.
      DO 20 I=1,N1
      IF (IGRD(I).LT.IGRD(I+1)) GO TO 20
      L=ISEQ(I)
      ISEQ(I)=ISEQ(I+1)
      ISEQ(I+1)=L
      L=IGRD(I)
      IGRD(I)=IGRD(I+1)
      IGRD(I+1)=L
      SWAP=.TRUE.
   20 CONTINUE
      IF (SWAP) GO TO 10
      DO 30 I=1,NUMNP
   30 IGRD(ISEQ(I))=I
      CALL MOVER(IGRD,1,ISEQ,1,NUMNP)
      RETURN
      END
```

```
      SUBROUTINE XSHELL(GRD,SHELL,PSHELL,PSHELLX,XMAT,ELSTIF,ELMASS,
     .          ELOAD,
     .      ELSTRES,SINDEX,SHAPE,SEQ)
C
C     DRIVES SHELL ELEMENT MATRIX GENERATOR
C
      DIMENSION GRD(13,1),SHELL(12,1),PSHELL(3,1),PSHELLX(20,1),
     .          XMAT(6,1)
      DIMENSION ELSTIF(32,32),ELMASS(32,32)
      DIMENSION ELOAD(32),ELSTRES(6,32)
      DIMENSION SINDEX(1),SEQ(1)
      INTEGER SEQ
      DIMENSION LNODS(8),PRESS(8)
      INTEGER SINDEX
      COMMON/CONTRL/ECHO,ERR,MATGEN,DYN,APPLD,PLOT,DBUG,BAD,NCORE,
     .      WTMASS,NASTY
      LOGICAL ECHO,ERR,MATGEN,DYN,APPLD,PLOT,DBUG,BAD
      COMMON/N/NCORD,NUMNP,NSHELL,NPSHEL,NPSHELX,NSHLTY,NBEAM,NPBEAM,
     .          NBMTY,NMAT,NSPOINT,MAXGRD,NDOF
      DIMENSION ELXYZ(9,4)
      DIMENSION AA(6),BB(6),DD(6)
      IF (NSHELL.EQ.0) RETURN
C
C     LOOP ON ELEMENTS
C
      DO 200 I=1,NSHELL
C
C     GET MATRIX INDEX AND SEE IF MATRICES FOR THIS CONGRUENCE
C     GROUP HAVE BEEN GENERATED YET
C
      LSEQ=SHELL(11,I)
      IF (SINDEX(LSEQ+1).NE.0) GO TO 200
      LPROP=INDEX(PSHELL,NPSHEL,3,SHELL(2,I))
      IF (LPROP.LE.0) GO TO 20
      LTYPE=1
      LMAT=INDEX(XMAT,NMAT,6,PSHELL(2,LPROP))
      THIK=PSHELL(3,LPROP)
      CALL MOVER(XMAT(1,LMAT),1,AA,1,6)
      DENS=XMAT(6,LMAT)
      IF (LMAT.GT.0) GO TO 40
      WRITE(6,10) IFIX(PSHELL(1,LPROP)),IFIX(PSHELL(3,LPROP))
   10 FORMAT (19H *** SHELL PROPERTY,I6,
     .          28H REFERENCES UNKNOWN MATERIAL,I6)
      ERR=.TRUE.
      GO TO 200
   20 LPROP=INDEX(PSHELLX,NPSHELX,20,SHELL(2,I))
      IF (LPROP.GT.0) GO TO 30
      WRITE(6,25) IFIX(SHELL(1,I)),IFIX(SHELL(2,I))
   25 FORMAT (18H *** SHELL ELEMENT,I8,
     .          28H REFERENCES UNKNOWN PROPERTY,I8)
```

```
      ERR=.TRUE.
      GO TO 200
   30 LTYPE=2
      CALL MOVER(PSHELLX(2,LPROP),1,AA,1,6)
      CALL MOVER(PSHELLX(8,LPROP),1,BB,1,6)
      CALL MOVER(PSHELLX(14,LPROP),1,DD,1,6)
      DENS=PSHELLX(20,LPROP)
      THIK=1.0
C
C     GATHER UP EIGHT (SIX) CORNER-POINT PROPERTIES
C
   40 CALL MOVER(0,0,ELXYZ(9,1),9,4)
      LNODS(7)=0
      LNODS(8)=0
      DO 60 J=1,8
        NOD=SHELL(J+2,I)
        IF (NOD.EQ.0) GO TO 65
        SHELL(J+2,I)=SEQ(NOD)
        LNODS(J)=NOD
        PRESS(J)=GRD(12,NOD)
        DO 50 K=1,3
   50     ELXYZ(J,K)=GRD(K+2,NOD)
   60   ELXYZ(J,4)=GRD(13,NOD)
C
C     THICKNESS ASSOCIATED WITH SHELL OVERRIDES G.P. VALUE
C
65    IF (THIK.NE.0) CALL MOVER(THIK,0,ELXYZ(1,4),1,8)
C
C     HERE WE GO
C
      CALL QSHELL(ELXYZ,LNODS,LTYPE,DENS,AA,BB,DD,SHELL(12,I),
     .     PRESS,ELSTIF,ELMASS,ELOAD,ELSTRES,SHAPE,LVABZ)
      IF (.NOT.BAD) GO TO 67
      WRITE(6,66) IFIX(SHELL(1,I))
   66 FORMAT (18H *** SHELL ELEMENT,I6,17H HAS BAD GEOMETRY)
      ERR=.TRUE.
      GO TO 200
C
C     DUMP OUT MATRICES TO DISK
C
   67 CALL WRITMS(98,ELSTIF,32*32,LSEQ)
      IF (DYN) CALL WRITMS(99,ELMASS,32*32,LSEQ)
      IF (APPLD) CALL WRITMS(97,ELOAD,32,LSEQ)
      IF (.NOT.DBUG) GO TO 200
C
C     DEBUG PRINTOUT
C
      WRITE(6,70) I
   70 FORMAT (*0STIFFNESS MATRIX FOR SHELL ELEMENT*,I4)
      DO 80 J=1,LVABZ
```

```
 80 WRITE(6,90) J,(ELSTIF(J,K),K=1,LVABZ)
 90 FORMAT (* ROW*,I3/(8E15.6))
    WRITE(6,100) I
100 FORMAT (*0STRESS MATRIX FOR SHELL ELEMENT*,I4)
    DO 110 J=1,6
110 WRITE(6,90) J,(ELSTRES(J,K),K=1,LVABZ)
    IF (.NOT.DYN) GO TO 140
    WRITE(6,120) I
120 FORMAT (*0MASS MATRIX FOR SHELL ELEMENT*,I4)
    DO 130 J=1,LVABZ
130 WRITE(6,90) J,(ELMASS(J,K),K=1,LVABZ)
140 IF (.NOT.APPLD) GO TO 200
    WRITE(6,150) I,(ELOAD(J),J=1,LVABZ)
150 FORMAT (*0LOAD VECTOR FOR SHELL ELEMENT*,I3/(8E15.6))
200 CONTINUE
    RETURN
    END
```

```
      SUBROUTINE QSHELL(XYZI,LNODS,LTYPE,DENS,AA,BB,DD,ANGLE,PRESS,
     .      ELSTIF,ELMASS,ELOAD,ELSTRES,WSHEL,LVABZ)
      DIMENSION XYZI(6,4),LNODS(8),AA(6),BB(6),DD(6),PRESS(8),
     1      ELSTIF(32,32),ELMASS(32,32),ELOAD(32)
      DIMENSION ELSTRES(6,32)
      COMMON/GAUSS/NGAUS,GFACT
      COMMON/N/NCORD,NUMNP,NSHELL,NPSHEL,NPSHELX,NSHLTY,NBEAM,NPBEAM,
     .          NBMTY,NMAT,NSPOINT,MAXGRD,NDOF
      COMMON/CONTRL/ECHO,ERR,MATGEN,DYN,APPLD,PLOT,DBUG,BAD,NCORE,
     .      WTMASS,NASTY
      LOGICAL ECHO,ERR,MATGEN,DYN,APPLD,PLOT,DBUG,BAD
      DIMENSION ABD(6,6)
      DIMENSION CGAUS3(3)
      DATA PI/3.1415927/
      DATA XGAUS3,XGAUS2/.77549 66692 4148, .57735 02691 8962/
      DATA CGAUS3/.55555555555556,.88888888888889,.55555555555556/
      LNODZ=8
      IF (LNODS(7).EQ.0) LNODZ=6
      LVABZ=4*LNODZ
      DATA THIK/0./
      CALL MOVER(0,0,ELSTIF,1,32*32)
      CALL MOVER(0,0,ELMASS,1,32*32)
      CALL MOVER(0,0,ELOAD,1,32)
C
C FILL IN STRESS-STRAIN MATRIX
C
      CALL MOVER(0,0,ABD,1,36)
      IF (LTYPE.EQ.2) GO TO 110
      ABD(1,1)=AA(2)
      ABD(1,2)=AA(3)
      ABD(2,1)=AA(3)
      ABD(2,2)=AA(4)
      ABD(3,3)=AA(5)
      GO TO 130
  110 ABD(1,1)=AA(1)
      ABD(1,2)=AA(2)
      ABD(2,1)=AA(2)
      ABD(1,3)=AA(3)
      ABD(3,1)=AA(3)
      ABD(2,2)=AA(4)
      ABD(2,3)=AA(5)
      ABD(3,2)=AA(5)
      ABD(3,3)=AA(6)
      ABD(1,4)=BB(1)
      ABD(1,5)=BB(2)
      ABD(2,4)=BB(2)
      ABD(1,6)=BB(3)
      ABD(3,4)=BB(3)
      ABD(2,5)=BB(4)
      ABD(2,6)=BB(5)
```

```
      ABD(3,5)=BB(5)
      ABD(3,6)=BB(6)
      DO 120 I=1,3
      DO 120 J=1,3
  120 ABD(I+3,J)=ABD(J,I+3)
      ABD(4,4)=DD(1)
      ABD(4,5)=DD(2)
      ABD(5,4)=DD(2)
      ABD(4,6)=DD(3)
      ABD(6,4)=DD(3)
      ABD(5,5)=DD(4)
      ABD(5,6)=DD(5)
      ABD(6,5)=DD(5)
      ABD(6,6)=DD(6)
  130 IF (ANGLE.EQ.0) GO TO 150
      C=COS(ANGLE*180/PI)
      S=SIN(ANGLE*180/PI)
      C2=C*C
      S2=S*S
      C4=C2*C2
      S4=S2*S2
      DO 140 I=1,4,3
      DO 140 J=1,4,3
      A11=ABD(I,J)
      A12=ABD(I,J+1)
      A22=ABD(I+1,J+1)
      ABD(I,J)=A11*C4+A12*S2*C2+A22*S4
      ABD(I,J+1)=(A11+A22-2*A12)*S2*C2
      ABD(J+1,I)=ABD(I+1,J)
  140 ABD(I+1,J+1)=A11*S4+A12*S2*C2+A22*C4
C
  150 IF (LNODZ.EQ.6) GO TO 40
      IF (NGAUS.EQ.3) GO TO 20
C
C QUADRILATERAL, 4-POINT GAUSS INTEGRATION
C
      IF (GFACT.EQ.0) WRITE(7) 4,LPROP
      IF (GFACT.NE.0) WRITE(7) 5,LPROP
      DO 10 IX=1,2
      DO 10 JY=1,2
      CALL ZHELL(XGAUS2*(3-2*IX),XGAUS2*(3-2*JY),
     .      XYZ1,ABD,LTYPE,PRESS,DENS,WSHEL,ELSTRES,ELSTIF,ELMASS,ELOAD,
     .      LNODS,LNODZ,LVABZ,1.-GFACT/4.)
       IF (BAD) RETURN
   10 CONTINUE
C
C OPTIONAL EXTRA POINT AT CENTER (QUAD)
C
       IF (GFACT.NE.0.) CALL ZHELL(0.,0.,
     .      XYZT,ABD,LTYPE,PRESS,DENS,WSHEL,ELSTRES,ELSTIF,ELMASS,ELOAD,
```

```
           LNODS,LNODZ,LVABZ,GFACT)
      IF (BAD) RETURN
      GO TO 55
C
C  QUADRILATERAL, 9-POINT GAUSS INTEGRATION
C
   20 WRITE(7) 9,LPROP
      DO 30 IX=1,3
      DO 30 JY=1,3
      CALL ZHELL(XGAUS3*(2-IX),XGAUS3*(2-JY),
     .     XYZT,ABD,LTYPE,PRESS,DENS,WSHEL,ELSTRES,ELSTIF,ELMASS,ELOAD,
     .     LNODS,LNODZ,LVABZ,CGAUS3(IX)*CGAUS3(JY))
      IF (BAD) RETURN
   30 CONTINUE
      GO TO 55
C
C 3-POINT GAUSS INTEGRATION ON TRIANGLE
C
   40 WRITE(7) 3,LPROP
      DO 50 JT=1,3
      CALL ZHELL(((4-JT)*(JT-1))/4.,MOD(JT,2)/2.,
     .     XYZT,ABD,LTYPE,PRESS,DENS,WSHEL,ELSTRES,ELSTIF,ELMASS,ELOAD,
     .     LNODS,LNODZ,LVABZ,1.)
      IF (BAD) RETURN
   50 CONTINUE
   55 DO 60 J=1,LVABZ
      DO 60 I=1,J
      ELSTIF(J,I)=ELSTIF(I,J)
   60 ELMASS(J,I)=ELMASS(I,J)
      RETURN
      END
```

```
      SUBROUTINE ZHELL(XI,ETA,XYZT,ABD,LTYPE,PRESS,DENS,WSHEL,
     .          ELSTRES,ELSTIF,ELMASS,ELOAD,LNODS,LNODZ,LVABZ,FACT)
      DIMENSION XYZT(9,4),LNODS(6),ABD(6,6),ELSTRES(6,32),
     .     ELSTIF(32,32),ELMASS(32,32),ELOAD(32)
      COMMON/N/NCORD,NUMNP,NSHELL,NPSHEL,NPSHELX,NSHLTY,NBEAM,NPBEAM,
     .          NBMTY,NMAT,NSPOINT,MAXGRD,NDOF
      COMMON/CONTRL/ECHO,ERR,MATGEN,DYN,APPLD,PLOT,DBUG,BAD,NCORE,
     .     WTMASS,NASTY
      LOGICAL ECHO,ERR,MATGEN,DYN,APPLD,PLOT,DBUG,BAD
      DIMENSION D(6,6),FRAM(3,3),POINT(3),XITA(2),WSHEL(13,45),B(6,45)
      XITA(1)=XI
      XITA(2)=ETA
    6 CALL HALOOF(1,AREA,XYZT,FRAM,POINT,SIDE,THIK,WSHEL,XITA,LNODS,
     *     LNODZ,LVABZ,LNODZ)
      BAD=.FALSE.
      IF (AREA.EQ.-69.) GO TO 60
C
C B MATRIX
C
      DO 8 N=1,LVABZ
      B(1,N)=WSHEL(4,N)
      B(2,N)=WSHEL(7,N)
      B(3,N)=WSHEL(5,N)+WSHEL(6,N)
      B(4,N)=WSHEL(10,N)
      B(5,N)=WSHEL(12,N)
    8 B(6,N)=2.0*WSHEL(11,N)
C
C D MATRIX
C
      CALL MOVER(ABD,1,D,1,36)
      IF (LTYPE.EQ.2) GO TO 15
      DO 10 I=1,3
      DO 10 J=1,3
      D(I,J)=D(I,J)*THIK
   10 D(I+3,J+3)=D(I,J)*THIK*THIK/12.
C
C STRESS AND STIFFNESS MATRICES
C
   15 DO 30 J=1,LVABZ
      DO 20 K=1,6
      CALL SCPROD(6,1,1,D(1,K),B(1,J),XX)
   20 ELSTRES(K,J)=XX*AREA
      DO 30 I=1,J
      CALL SCPROD(6,1,1,ELSTRES(1,J),B(1,I),BDB)
   30 ELSTIF(I,J)=ELSTIF(I,J)+FACT*BDB
      WRITE(7) ELSTRES,WSHEL,POINT,FRAM,THIK
C
C LOAD VECTOR
C
      IF (APPLD)
```

```
      .CALL REDCLP(LVABZ,3,1,-AREA*PRESS*FACT,WSHEL(3,1),ELOAD)
C
C MASS MATRIX
C
      IF (.NOT.DYN) GO TO 50
      AA=DENS*AREA*THIK*WTMASS
      DO 40 J=1,LVABZ
      DO 40 I=1,J
      CALL SCPROD(3,1,1,WSHEL(1,I),WSHEL(1,J),BB)
   40 ELMASS(I,J)=ELMASS(I,J)+AA*BB
   50 RETURN
   60 BAD=.TRUE.
      RETURN
      END
```

```
      SUBROUTINE XBEAM(GRID,BEAM,PBEAM,XMAT,
     .      ELSTIF,ELMASS,ELOAD,ELSTRES,SINDEX,SHAPE,ISEQ)
      DIMENSION GRID(13,1),BEAM(21,1),PBEAM(9,1),XMAT(6,1),
     .      ELSTIF(17,17),ELMASS(17,17),ELOAD(17),SINDEX(1),SHAPE(1),ISEQ(1)
     .      (1)
C
C     DRIVER FOR BEAM ELEMENT MATRIX GENERATOR
C
      COMMON A(1)
      COMMON/CONTRL/ECHO,ERR,MATGEN,DYN,APPLD,PLOT,DBUG,BAD,NCORE,
     .      WTMASS,NASTY
      LOGICAL ECHO,ERR,MATGEN,DYN,APPLD,PLOT,DBUG,BAD
      COMMON/N/NCORD,NUMNP,NSHELL,NPSHEL,NPSHELX,NSHLTY,NBEAM,NPBEAM,
     .           NBMTY,NMAT,NSPOINT,MAXGRD,NDOF
      DIMENSION ELXYZ(3,3),AREA(3),XI1(3),XI2(3),XJ(3),ZNORM(3),ZBIN(3),
     .      PRESS(3),LNODB(3)
      INTEGER SINDEX
      IF (NBEAM.EQ.0) RETURN
      LETRANS=NCORE
      CALL MORCOR(17*17)
      LQ=NCORE
      CALL MORCOR(17*17)
      DO 130 I=1,NBEAM
      LSEQ=BEAM(15,I)
      IF (SINDEX(LSEQ+NSHLTY+1).NE.0) GO TO 130
      LMAT=INDEX(XMAT,NMAT,1,BEAM(2,I))
      IF (LMAT.GT.0) GO TO 20
      WRITE(6,10) IFIX(BEAM(1,I))
   10 FORMAT (17H *** BEAM ELEMENT,I6,
     .           28H REFERENCES UNKNOWN MATERIAL,I6)
      ERR=.TRUE.
      GO TO 130
   20 BAD=.FALSE.
      DO 50 J=1,3
      NOD=BEAM(J+2,I)
      BEAM(J+2,I)=ISEQ(NOD)
      LNODB(J)=NOD
      IPB=INDEX(PBEAM,NPBEAM,9,BEAM(5+J,I))
      BAD=.FALSE.
      DO 30 K=1,3
   30 ELXYZ(J,K)=GRID(2+K,LNODB(J))
      AREA(J)=PBEAM(2,IPB)
      XI1(J)=PBEAM(3,IPB)
      XI2(J)=PBEAM(4,IPB)
      XJ(J)=PBEAM(5,IPB)
      ZNORM(J)=BEAM(7+2*J,I)
      ZBIN(J)=BEAM(8+2*J,I)
      IF (IPB.GT.0) GO TO 50
      WRITE(6,40) IFIX(BEAM(1,I)),IFIX(BEAM(5+J,I))
 40   FORMAT (17H *** BEAM ELEMENT,I6,28H REFERENCES UNKNOWN PROPERTY,I6)
```

```
     .      )
      BAD=.TRUE.
50    CONTINUE
      ERR=ERR.OR.BAD
      IF (BAD) GO TO 130
      CALL ZBEAM(ELXYZ,XMAT(1,LMAT),AREA,XI1,XI2,XJ,PRESS,ZNORM,ZBIN,
     .        BEAM(19,I),LNODB,
     .        ELSTIF,ELMASS,ELOAD,ELSTRES,A(LETRANS),A(LQ),SHAPE)
      CALL WRITMS(98,ELSTIF,17*17,LSEQ+NSHLTY)
      IF (DYN) CALL WRITMS(99,ELMASS,17*17,LSEQ+NSHLTY)
      IF (APPLD) CALL WRITMS(97,ELOAD,17,LSEQ+NSHLTY)
      IF (.NOT.BAD) GO TO 55
      WRITE(6,54) IFIX(BEAM(1,I))
   54 FORMAT (17H *** BEAM ELEMENT,I6,17H HAS BAD GEOMETRY)
      ERR=.TRUE.
      GO TO 130
   55 IF (.NOT.DBUG) GOTO 130
      WRITE(6,60) I
   60 FORMAT (*0STIFFNESS MATRIX FOR BEAM  ELEMENT*,I4)
      DO 70 J=1,17
   70 WRITE(6,80) J,(ELSTIF(J,K),K=1,17)
   80 FORMAT (* ROW*,I3/(8E15.6))
      IF (.NOT.DYN) GO TO 110
      WRITE(6,90) I
   90 FORMAT (*0MASS MATRIX FOR BEAM  ELEMENT*,I4)
      DO 100 J=1,17
  100 WRITE(6,80) J,(ELMASS(J,K),K=1,17)
110   IF (.NOT.APPLD) GO TO 130
      WRITE(6,120) I,ELOAD
120   FORMAT (*0LOAD VECTOR FOR BEAM  ELEMENT*,I3/(8E15.6))
130   CONTINUE
C
C     GIVE BACK BORROWED CORE
C
      NCORE=LETRANS
      RETURN
      END
```

```
      SUBROUTINE ZBEAM(XYZI,XMAT,ZAREA,ZXI1,ZXI2,ZXJ,ZPRESS,ZNORM,ZBIN,
     .      ORIENT,LNODB,
     .      ELSTIF,ELMASS,ELOAD,ELSTRES,ETRANS,Q,WBEAM)
      DIMENSION XYZI(3,3),XMAT(6),
     .          ZAREA(3),ZXI1(3),ZXI2(3),ZXJ(3),ZPRESS(3),ZNORM(3),ZBIN(3),
     .      ),ORIENT(3),LNODB(3),
     .      ELSTIF(17,17),ELMASS(17,17),ELOAD(17),ELSTRES(6,32),ETRANS(17,17),
     .      ,17),
     .      Q(17,17),WBEAM(13,45)
C
C     GETS BEAM STIFFNESS, MASS, AND/OR LOAD MATRICES
C
      DIMENSION XGAUS(5),CGAUS(5),B(6,32),T(3,3,3),OFFSET(3,3)
      REAL NU
      DIMENSION FRAM(3,3),D(6),POINT(3)
      COMMON/N/NCORD,NUMNP,NSHELL,NPSHEL,NPSHELX,NSHLTY,NBEAM,NPBEAM,
     .          NBMTY,NMAT,NSPOINT,MAXGRD,NDOF
      COMMON/CONTRL/ECHO,ERR,MATGEN,DYN,APPLD,PLOT,DBUG,BAD,NCORE,
     .      WTMASS,NASTY
      LOGICAL ECHO,ERR,MATGEN,DYN,APPLD,PLOT,DBUG,BAD
      DATA XGAUS/-.577350269,0.577350269,-.7745966692,.7745966692,0./
      DATA CGAUS/2*1.,2*.555555556,.888888889/
      DATA LVABZ/17/
      NU=XMAT(3)/XMAT(2)
      E=(1-NU*NU)*XMAT(2)
      G=XMAT(5)
      DENS=XMAT(6)
      CALL MOVER(0,0,ELSTIF,1,17*17)
      CALL MOVER(0,0,ELMASS,1,17*17)
      CALL MOVER(0,0,ELOAD,1,17)
C
C     LOOP ON GAUSS POINTS, END POINTS, AND MIDDLE POINT
C
      DO 70 IGAUS=1,5
      XI=XGAUS(IGAUS)
      CALL GCBSF1(XI,POINT)
C
C     INTERPOLATE CROSS-SECTION PROPERTIES
C
      AREA=0.
      XI1=0.
      XI2=0.
      XJ=0.
      PRESS=0.
      DO 10 J=1,3
        AREA=AREA+ZAREA(J)*POINT(J)
        XI1=XI1+ZXI1(J)*POINT(J)
        XI2=XI2+ZXI2(J)*POINT(J)
        PRESS=PRESS+ZPRESS(J)*POINT(J)
10      XJ=XJ+ZXJ(J)*POINT(J)
```

```
C
C     INDICATE CROSS-SECTION ORIENTATION
C
      CALL MOVER(0,0,FRAM,1,9)
      CALL MOVER(ORIENT,1,FRAM,1,3)
C
C     GET SHAPE FUNCTIONS
C
      CALL LOFBEM(1,LVABZ,SIDE,XYZT,FRAM,POINT,WBEAM,XI,3,3,3,LNODB)
      BAD=.FALSE.
      IF (SIDE.EQ.-69.) GO TO 120
      IF (XI.EQ.0.) CALL MOVER(FRAM,1,T(1,1,2),1,9)
      FACMOD=E*SIDE*CGAUS(IGAUS)
      FACSHE=G*FACMOD/E
C
C     FORM STRAIN-DISPLACEMENT TERMS
C
      CALL MOVER(WBEAM(4,1),13,B(1,1),6,LVABZ)
      CALL MOVER(WBEAM(8,1),13,B(2,1),6,LVABZ)
      CALL MOVER(WBEAM(9,1),13,B(3,1),6,LVABZ)
      CALL MOVER(WBEAM(11,1),13,B(4,1),6,LVABZ)
      CALL MOVER(WBEAM(12,1),13,B(5,1),6,LVABZ)
      CALL MOVER(WBEAM(10,1),13,B(6,1),6,LVABZ)
C
C     STIFFNESS TERMS
C
      D(1)=FACMOD*AREA
      D(2)=FACMOD*XI1
      D(3)=FACMOD*XI2
      D(4)=FACSHE*AREA/1.2
      D(5)=FACSHE*AREA/1.2
      D(6)=FACSHE*XJ
C
C     LOAD TERMS
C
      IF (IGAUS.LT.3.AND.APPLD.AND.PRESS.NE.0)
     .CALL REDCLP(LVABZ,1,3,1,-SIDE*PRESS,ELOAD,WBEAM(3,1))
C
C     STIFFNESS MATRIX
C
      IF (IGAUS.GT.2) GO TO 30
      DO 20 J=1,LVABZ
      DO 20 I=1,J
   20 ELSTIF(I,J)=ELSTIF(I,J)+B(1,J)*D(1)*B(1,I)+
     )           B(4,J)*D(4)*B(4,I)+B(5,J)*D(5)*B(5,I)
      GO TO 50
   30 DO 40 J=1,LVABZ
      DO 40 I=1,J
   40 ELSTIF(I,J)=ELSTIF(I,J)+B(2,J)*D(2)*B(2,I)+
                 B(3,J)*D(3)*B(3,I)+B(6,J)*D(6)*B(6,I)
```

```
      GO TO 70
C
C     MASS MATRIX
C
   50 IF (.NOT.DYN) GO TO 70
      AA=DENS*SIDE*AREA*WTMASS
      DO 60 J=1,LVABZ
      DO 60 I=1,J
      CALL SCPROD(3,1,1,WBEAM(1,I),WBEAM(1,J),BB)
   60 ELMASS(I,J)=ELMASS(I,J)+AA*BB
   70 CONTINUE
C
C     FILL IN SYMMETRIC TERMS
C
      DO 80 J=1,LVABZ
      DO 80 I=1,J
      ELSTIF(J,I)=ELSTIF(I,J)
   80 ELMASS(J,I)=ELMASS(I,J)
C
C     HANDLE OFFSET TRANSFORMATION
C
      DO 90 I=1,3
      IF (ZNORM(I).NE.0.) GO TO 100
      IF (ZBIN(I).NE.0.) GO TO 100
90    CONTINUE
      RETURN
100   CALL LOFBEM(1,LVABZ,SIDE,XYZT,T(1,1,1),POINT,WBEAM,-1.,3,3,3,LNODB)
     .      )
      CALL LOFBEM(1,LVABZ,SIDE,XYZT,T(1,1,3),POINT,WBEAM,1.,3,3,3,LNODB)
      DO 110 I=1,3
      DO 110 J=1,3
110   OFFSET(I,J)=T(J,2,I)*ZNORM(I)+T(J,3,I)*ZBIN(I)
      CALL TRANS(ETRANS,OFFSET)
      CALL TRIPLE(ETRANS,ELSTIF,ETRANS,17,17,Q)
      RETURN
  120 BAD=.TRUE.
      RETURN
      END
```

```
SUBROUTINE TRANS(E,A)
DIMENSION E(17,17),A(3,3)
CALL MOVER(0,0,E,1,17*17)
CALL MOVER(1.,0,E,18,17)
E(1,13)=-A(1,3)
E(1,14)=A(1,2)
E(2,12)=A(1,3)
E(2,14)=-A(1,1)
E(3,12)=-A(1,2)
E(3,13)=A(1,1)
E(4,7)=-A(2,3)/2.
E(4,8)=-A(2,3)/2.
E(6,7)=A(2,1)/2.
E(6,8)=A(2,1)/2.
E(9,16)=-A(3,3)
E(9,17)=A(3,2)
E(10,15)=A(3,3)
E(10,17)=-A(3,1)
E(11,15)=-A(3,2)
E(11,16)=A(3,1)
RETURN
END
```

```
      SUBROUTINE ASSY(NAME,IN,BIG,SHELL,BEAM,CORD,GRID,SEQ,
     .            IPSPC,SMAT,BMAT,NBIG)
      DIMENSION BIG(NBIG,6),SHELL(12,1),BEAM(21,1),CORD(3,5,1),
     .       GRID(13,1),SEQ(1),IPSPC(1),SMAT(32,32),BMAT(17,17)
      INTEGER SEQ
C
C     ASSEMBLE MASTER STIFFNESS OR MASS MATRIX
C
      COMMON/N/NCORD,NUMNP,NSHELL,NPSHEL,NPSHELX,NSHLTY,NBEAM,NPBEAM,
     .            NBMTY,NMAT,NSPOINT,MAXGRD,NDOF
      COMMON/CONTRL/ECHO,ERR,MATGEN,DYN,APPLD,PLOT,DBUG,BAD,NCORE,
     .       WTMASS,NASTY
      LOGICAL ECHO,ERR,MATGEN,DYN,APPLD,PLOT,DBUG,BAD
      DIMENSION TI1(3,3),TI2(3,3),TJ1(3,3),TJ2(3,3),Q(3,3)
      DIMENSION MANE(2)
C
C     MATRICES ISH AND IBM GIVE INDICES INTO SHELL AND BEAM ELEMENT
C     STIFFNESS MATRICES GIVEN LOCAL NODE NUMBER (SHELL - 1 TO 8,
C     BEAM - 1 TO 3) AND DOF NUMBER (1 TO 6)
C
      COMMON/ASS/ISH(6,8),IBM(6,3)
      DATA ISH/
     1       1,2,3,0,0,0,
     2       4,5,6,7,8,0,
     3       9,10,11,0,0,0,
     4       12,13,14,15,16,0,
     5       17,18,19,0,0,0,
     6       20,21,22,23,24,0,
     7       25,26,27,0,0,0,
     8       28,29,30,31,32,0/
      DATA IBM/
     1       1,2,3,12,13,14,
     2       4,5,6,7,8,0,
     3       9,10,11,15,16,17/
      GO TO (10,20),NASTY
   10 MANE(1)=NAME
      MANE(2)=4H
      CALL OU2INI(4,MANE,NDOF,NDOF,6,ICNTR,10000,NDOF,1,1,101)
      GO TO 25
   20 CALL OU4INI(4,NDOF,NDOF,6,1,NAME)
C
C     PRIMARY LOOP OVER NODES
C
   25 NCOL=0
      DO 210 I=1,NUMNP
C
C        CLEAR SPACE FOR 6 COLUMNS FOR THIS NODE (ALL ROWS)
C
         CALL MOVER(0,0,BIG,1,6*NDOF)
         IF (NSHELL.EQ.0) GO TO 100
```

```
C
C        SEARCH FOR SHELL ELEMENTS THAT TOUCH THIS NODE
C
         DO 70 K=1,NSHELL
           LNODZ=8
           IF (SHELL(9,K).EQ.0) LNODZ=6
           DO 60 L=1,LNODZ
             LNOD=SHELL(L+2,K)
             IF (LNOD.NE.I) GO TO 60
C
C            FOUND ONE (CORNER L OF ELEMENT K), GET ELEMENT MATRIX
C
             CALL READMS(IN,SMAT,32*32,IFIX(SHELL(11,K)))
C
C            LOOP ON 6 DOF FOR THAT NODE
C
             DO 50 LL=1,6
C
C              SEE IF THIS DOF IS ACTIVE FOR THIS NODE
C              IF SO GET INDEX INTO ELEMENT MATRIX
C
               LLL=ISH(LL,L)
               IF (LLL.EQ.0) GO TO 50
C
C              LOOP ON ALL 8 (6) NODES FOR COUPLING TERMS
C
               DO 40 M=1,LNODZ
                 DO 30 MM=1,6
                   MMM=ISH(MM,M)
                   IF (MMM.EQ.0) GO TO 30
C
C                  GET ROW NO. FOR MASTER MATRIX
                   MNOD=SHELL(M+2,K)
C
                   IBIG=6*(MNOD-1)+MM
                   BIG(IBIG,LL)=BIG(IBIG,LL)+SMAT(LLL,MMM)
   30              CONTINUE
   40            CONTINUE
   50          CONTINUE
   60        CONTINUE
   70      CONTINUE
C
C        SAME SONG + DANCE FOR BEAM ELEMENTS
C
         IF (NBEAM.EQ.0) GO TO 180
  100    DO 170 K=1,NBEAM
           DO 160 L=1,3
             LNOD=BEAM(L+2,K)
             IF (LNOD.NE.I) GO TO 160
             CALL READMS(IN,BMAT,17*17,IFIX(BEAM(15,K))+NSHLTY)
```

```
          DO 150 LL=1,6
            LLL=IBM(LL,L)
            IF (LLL.EQ.0) GO TO 150
            DO 140 M=1,3
              DO 130 MM=1,6
                MMM=IBM(MM,M)
                IF (MMM.EQ.0) GO TO 130
                MNOD=BEAM(M+2,K)
                IBIG=6*(MNOD-1)+MM
                BIG(IBIG,LL)=BIG(IBIG,LL)+BMAT(LLL,MMM)
  130           CONTINUE
  140         CONTINUE
  150       CONTINUE
  160     CONTINUE
  170   CONTINUE
C
C      TRANSFORM TO OUTPUT COORDINATES
C
180     IG=SEQ(I)
        CALL MOVER(0,0,TI1,1,9)
        CALL MOVER(1.,0,TI1,4,3)
        CALL MOVER(0,0,TI2,1,9)
        CALL MOVER(1.,0,TI2,4,3)
        ICORD=GRID(9,IG)
        IF (ICORD.GT.0) CALL MOVER(CORD(1,3,ICORD),1,TI1,1,9)
        IF (ICORD.GT.0.AND.IPSPC(IG).NE.6)
     .        CALL MOVER(CORD(1,3,ICORD),1,TI2,1,9)
        DO 190 J=1,NUMNP
          JG=SEQ(J)
          CALL MOVER(0,0,TJ1,1,9)
          CALL MOVER(1.,0,TJ1,4,3)
          CALL MOVER(0,0,TJ2,1,9)
          CALL MOVER(1.,0,TJ2,4,3)
          JCORD=GRID(9,JG)
          IF (ICORD.EQ.0.AND.JCORD.EQ.0) GO TO 190
          CALL MOVER(CORD(1,3,JCORD),1,TJ1,1,9)
          IF (IPSPC(JG).NE.6)
     .          CALL MOVER(CORD(1,3,JCORD),1,TJ2,1,9)
          CALL TRIPLE(TJ1,BIG(6*J-5,1),TI1,NDOF,3,Q)
          CALL TRIPLE(TJ1,BIG(6*J-5,4),TI2,NDOF,3,Q)
          CALL TRIPLE(TJ2,BIG(6*J-2,1),TI1,NDOF,3,Q)
          CALL TRIPLE(TJ2,BIG(6*J-2,4),TI2,NDOF,3,Q)
190       CONTINUE
C
C       WE NOW HAVE 6 COLS OF THE MASTER MATRIX ASSEMBLED
C       TIME TO WRITE THEM OUT
C
        DO 200 J=1,6
          NCOL=NCOL+1
          IF (NASTY.EQ.1)
```

```
     .      CALL OU2COL(4,BIG(1,J),NDOF,NDOF,ICNTR,IRPOS,NAME)
            IF (NASTY.EQ.2)
     .      CALL OU4COL(4,BIG(1,J),NDOF,NDOF,NCOL,NAME)
200         CONTINUE
210      CONTINUE
      RETURN
      END
```

```
      SUBROUTINE ASSL(NAME,IN,BIG,SHELL,BEAM,CORD,GRID,SEQ,
     .          IPSPL,SLOAD,BLOAD)
      DIMENSION BIG(1),SHELL(12,1),BEAM(21,1),CORD(3,5,1),GRID(13,1),
     .          SEQ(1),IPSPL(1),SLOAD(32),BLOAD(32)
      INTEGER SEQ
      COMMON/N/NCORD,NUMNP,NSHELL,NPSHEL,NPSHELX,NSHLTY,NBEAM,NPBEAM,
     .          NBMTY,NMAT,NSPOINT,MAXGRD,NDOF
      COMMON/CONTRL/ECHO,ERR,MATGEN,DYN,APPLD,PLOT,DBUG,BAD,NCORE,
     .      WTMASS,NASTY
      LOGICAL ECHO,ERR,MATGEN,DYN,APPLD,PLOT,DBUG,BAD
      DIMENSION Q(3,3)
      DIMENSION MANE(2)
      COMMON A(1)
      COMMON/ASS/ISH(6,8),IBM(6,3)
      GO TO (4,5),NASTY
    4 MANE(1)=NAME
      MANE(2)=0
      CALL OO2INI(4,MANE,NDOF,1,2,ICNTR,10000,NDOF,1,1,101)
      GO TO 8
    5 CALL OO4INI(4,NDOF,1,2,1,NAME)
    8 CALL MOVER(0,0,BIG,1,NDOF)
      DO 200 I=1,NUMNP
         IF (NSHELL.EQ.0) GO TO 50
         DO 40 K=1,NSHELL
            DO 30 L=1,8
               LNOD=SHELL(L+2,K)
               IF (GRID(11,LNOD).NE.I) GO TO 30
               CALL READMS(IN,SLOAD,32,IFIX(SHELL(11,K)))
               DO 10 LL=1,6
                  LLL=ISH(LL,L)
                  IF (LLL.EQ.0) GO TO 10
                  IBIG=6*(GRID(11,LNOD)-1)+LL
                  BIG(IBIG)=BIG(IBIG)+SLOAD(LLL)
   10             CONTINUE
   30          CONTINUE
   40       CONTINUE
         IF (NBEAM.EQ.0) GO TO 150
   50    DO 140 K=1,NBEAM
            DO 130 L=1,3
                  LNOD=BEAM(L+2,K)
               IF (GRID(11,LNOD).NE.I) GO TO 130
               CALL READMS(IN,BLOAD,17,IFIX(BEAM(15,K))+NSHLTY)
               DO 110 LL=1,6
                  LLL=IBM(LL,L)
                  IF (LLL.EQ.0) GO TO 110
                     IBIG=6*(GRID(11,LNOD)-1)+LL
                  BIG(IBIG)=BIG(IBIG)+BLOAD(LLL)
  110             CONTINUE
  130          CONTINUE
  140       CONTINUE
```

```
150     IG=SEQ(I)
        ICORD=GRID(9,IG)
        CALL MOVER(0,0,T1,1,9)
        CALL MOVER(1.,0,T1,4,3)
        CALL MOVER(0,0,T2,1,9)
        CALL MOVER(1.,0,T2,4,3)
        IF (ICORD.EQ.0) GO TO 200
        CALL MOVER(CORD(1,3,ICORD),1,T1,1,9)
        IF (IPSPC(IG).NE.6)
               CALL MOVER(CORD(1,3,ICORD),1,T2,1,9)
        CALL DOUBLE(BIG(6*I-5),T1,NDOF,3,Q)
        IF (NASTY.EQ.2) CALL OU4COL(4,BIG,NDOF,1,1,NAME)
  200   CONTINUE
      IF (NASTY.EQ.1) CALL OU2COL(4,BIG,NDOF,1,ICNTR,IRPOS,MANE)
      IF (NASTY.EQ.2) CALL OU4COL(4,BIG,NDOF,1,1,NAME)
      END
```

```
      SUBROUTINE PARVEC
      COMMON/CONTRL/ECHO,ERR,MATGEN,DYN,APPLD,PLOT,DBUG,BAD,NCORE,
     .      NTMASS,NASTY
      LOGICAL ECHO,ERR,MATGEN,DYN,APPLD,PLOT,DBUG,BAD
      COMMON/N/NCORD,NUMNP,NSHELL,NPSHEL,NPSHELX,NSHLTY,NBEAM,NPBEAM,
     .          NBMTY,NMAT,NSPOINT,MAXGRD,NDOF
      DIMENSION NAME(2)
      COMMON A(1)
      DATA NAME/4HPARV,2HEC/
      NBUF=NCORE
      CALL MORCOR(NDOF)
      CALL MOVER(0,0,A(NBUF),1,6*NUMNP)
      CALL MOVER(1.0,0,A(NBUF+6*NUMUMNP),1,NSPOINT)
      CALL OU2INI(4,NAME,1,NDOF,2,ICNTR,10000,NDOF,2,1,101)
      CALL OU2COL(4,A(NBUF),1,NDOF,ICNTR,IRPOS,NAME)
      NCORE=NBUF
      RETURN
      END
```

```
      SUBROUTINE OU4COL(NRU,A,NROWS,NCOLS,NCOLN,NAME)
C     OU4COL 030375-1525
C     REVISED FOR MSC LEVEL 26
      DIMENSION A(1)
      DO 20 I=1,NROWS
      IF(A(I).NE.0.)GO TO 30
   20 CONTINUE
      IF (NCOLN.LT.NCOLS) RETURN
      GO TO 70
   30 NSTART=I
      DO 60 I=NSTART,NROWS
      IF(A(I).NE.0.)NSTOP=I
   60 CONTINUE
      NW=NSTOP-NSTART+1
      WRITE(NRU) NCOLN,NSTART,NW,(A(I),I=NSTART,NSTOP)
      IF(NCOLN.LT.NCOLS)RETURN
   70 NDUM1=NCOLS+1
      NDUM2=1
      DUM=-69.
      WRITE(NRU) NDUM1,NDUM2,NDUM2,DUM
      PRINT 1000,NAME,NRU
 1000 FORMAT(21H OU4COL***DATA BLOCK ,A10,
     +17H WRITTEN TO UNIT ,I2)
      RETURN
      END
```

```
      SUBROUTINE OU4INI(NRU,NROWS,NCOLS,NFORM,NTYPE,NAME)
C     OU4INI 030375-1520
C     REVISED FOR MSC LEVEL 26
      WRITE(NRU) NCOLS,NROWS,NFORM,NTYPE
      PRINT 100,NAME,NRU
  100 FORMAT(32H OU4INI***HEADER FOR DATA BLOCK ,A10,
     +17H WRITTEN TO UNIT ,I2)
      RETURN
      END
```

```
      SUBROUTINE OU2COL(NRU,A,NCOLS,NROWS,ICNTR,IRPOS,MNAME)
C     OU2COL 092374-1605
C
C     WRITE REAL S.P. NON-ZERO VALUES OF A MATRIX COLUMN IN
C     OUTPUT2 FORMAT-MUST CALL OU2INI BEFORE THIS TO
C     WRITE HEADER ON OUTPUT2 MATRIX FILE
C
C     9/18/74... GET
C
      DIMENSION A(1),ISAME(4),IRPOS(1),MNAME(2)
C
      DATA ISAME/1,0,0,264201/,IEOR/131071/
C
      ICNTR=ICNTR-1
      IF(IABS(ICNTR+2).GT.NCOLS) GO TO 40
      WRITE(NRU) NROWS
      WRITE(NRU) (A(I),I=1,NROWS)
      WRITE(NRU)ICNTR
   30 IF(IABS(ICNTR+2).NE.NCOLS) RETURN
      NWRDS=0
      WRITE(NRU) NWRDS
      PRINT 60,MNAME,NRU
   60 FORMAT(22H OU2COL*** DATA BLOCK ,2A4,
     +17H WRITTEN TO TAPE ,I2)
      RETURN
40    PRINT 50,(MNAME(I),I=1,2)
50    FORMAT(51H OU2COL*** ATTEMPT TO WRITE MORE COLUMNS THAN EXIST,
     +12H FOR MATRIX ,2A4)
      END
```

```
      SUBROUTINE OU2INI(NRU,MNAME,NCOLS,NROWS,IFORM,ICNTR,IDNSTY,MCOL,
     +ITYPE,ISKIP,IPOS)
C     OU2INI 092374-1600
C
C     WRITE HEADER INFORMATION IN OUTPUT2 FORMAT
C      CALL OU2COL AFTER THIS TO OUTPUT2 A MATRIX
C     CALL O2USET TO OUTPUT2 USET
C
C     9/18/74...GET
C
      DIMENSION NAST(7),MNAME(2)
C
      DATA NAST/4HNAST,4HRAN ,4HFORT,4H TAP,4HE ID,4H COD,4HE - /
      DATA LABL/4HXXXX/
C
  901 FORMAT(3(1X,I2))
C
      IF(ISKIP.NE.0) GO TO 10
      REWIND NRU
      NWRDS=3
      WRITE(NRU)NWRDS
      CALL DATE (DAT)
      DECODE(9,901,DAT)IMO,IDA,IYR
      WRITE(NRU)IMO,IDA,IYR
      NWRDS=7
      WRITE(NRU)NWRDS
      WRITE(NRU)(NAST(I),I=1,7)
      NWRDS=2
      WRITE(NRU)NWRDS
      WRITE(NRU)LABL,LABL
      ICNTR=-1
      WRITE(NRU)ICNTR
      ICNTR=0
      WRITE(NRU)ICNTR
   10 NWRDS=2
      WRITE(NRU)NWRDS
      WRITE(NRU)(MNAME(I),I=1,2)
      ICNTR=-1
      WRITE(NRU)ICNTR
      NWRDS=8
      WRITE(NRU)NWRDS
      WRITE(NRU)IPOS,NCOLS,NROWS,IFORM,ITYPE,MCOL,IDNSTY
     .      ,1
      ICNTR=-2
      WRITE(NRU)ICNTR
      PRINT 20,MNAME,NRU
   20 FORMAT(33H OU2INI*** HEADER FOR DATA BLOCK ,2A4,
     +17H WRITTEN TO TAPE ,I2)
      RETURN
      END
```

```
      SUBROUTINE TRIPLE(A,X,B,N,M,Q)
      DIMENSION A(M,M),X(N,M),B(M,M),Q(M,M)
C
C                                                 T
C     COMPUTE TRIPLE MATRIX PRODUCT Q=A XB
C
      DO 20 I=1,M
        DO 20 L=1,M
          Q(I,L)=0.
          DO 20 J=1,M
            XB=0.
            DO 10 K=1,M
10            XB=XB+X(J,K)*B(K,L)
   20       Q(I,L)=Q(I,L)+A(J,I)*XB
      DO 30 I=1,M
        DO 30 J=1,M
30        X(I,J)=Q(I,J)
      RETURN
      END
```

```
      SUBROUTINE DOUBLE(X,A,N,M,Q)
      DIMENSION X(N,M),A(M,M),Q(M,M)
C
C     COMPUTE MATRIX PRODUCT Q=XA, STORE Q IN X
C
      DO 10 I=1,M
        DO 10 K=1,M
          Q(I,K)=0.
          DO 10 J=1,M
10          Q(I,K)=Q(I,K)+X(I,J)*A(J,K)
      DO 20 I=1,M
        DO 20 J=1,M
20        X(I,J)=Q(I,J)
      RETURN
      END
```

```
      SUBROUTINE HALOOF(NEL, AREA, ELXYZT, FRAM, POINT, SIDE, THIK,
     .     WSHEL, XITA, LNODS, LNODZ, LVABZ, NODEL)
C
C*** TO CREATE SHAPE FUNCTION ARRAY WSHEL, FOR SEMILOOF SHELL ELEMENT.
C
C*** WRITTEN BY BRUCE IRONS, JULY 1972, WASHINGTON D.C.
C
      DIMENSION AREAV(3), FRAME(3,3), GENSID(6,4),
     1   SHEAR(11,43), SIGT(3), SWOP(6), THIKDD(3,3), TRANS(2,2),
     2   VLOOF(3,36), WCORN(10,3), WLOOF(10,3), XGAUS(4,4), XILOOF(9,4),
     3   XLOCAL(2), XYZDD(3,3), XYZPRE(8,4)
      DIMENSION ELXYZT(9,4), FRAM(3,3), POINT(3), WSHEL(13,45),
     .     XITA(2), LNODS(NODEL,NEL)
      EQUIVALENCE (T11,TRANS(1,1)), (T12,TRANS(1,2)),
     1   (T21,TRANS(2,1)), (T22,TRANS(2,2))
      DATA GENSID/1., -1., 0., 3*-.5, 0., 1., -1., 4*1., 0., -1.,
     1   4*0., 1., 0., -1., 2*1./,XILOOF/.211324866, 2*.788675134,
     2   .211324866, 2*0., .3333333333, 4*0., .211324866, 2*.788675134,
     3   .211324866, .3333333333, 2*0., -.577350269, .577350269, 2*1.,
     4   .577350269, -.577350269, 2*-1., 0., 2*-1., -.577350269,
     5   .577350269, 2*1., .577350269, -.577350269, 0. /,
     6   XGAUS/0., 4*.5, 0., 2*.5, -.577350269, 2*.577350269,
     7   3*-.577350269, 2*.577350269/, XYZPRE/32*0.0/, NOZPRE/0/
C
C*** GENERATE NSTAGE TO DEFINE PATH THROUGH HALOOF.
C
       N   ERROR = 1
       IF(LNODZ.NE.6. AND .LNODZ.NE.8) GO TO 99
       NSTAGE = 4
       IF(LNODZ.NE.NOZPRE) NSTAGE = 2
       NOZPRE = LNODZ
       DO 2 LNOD = 1,LNODZ
       DO 2 NX = 1,4
       IF(ELXYZT(LNOD,NX).NE.XYZPRE(LNOD,NX)) NSTAGE = 2
     2 CONTINUE
       IF(NSTAGE.EQ.4) GO TO 18
C
C*** INITIALIZATION FOR NEW ELEMENT, NSTAGE = 1. FIND CENTRE COORDINATES
C
       LIMZ = (3*LNODZ)/2 - 1
       LVABZ = 4*LNODZ
       LNODZA = LNODZ + 1
       LVABZA = LVABZ + 1
       LVABZZ = LVABZ + LIMZ
       DO 3 L = LNODZA,LIMZ
       DO 3 J = 1,LVABZZ
     3 SHEAR(L,J) = 0.0
       DO 5 NX = 1,4
       GASH = 0.0
       LNODZ1 = LNODZ/2
```

```
      DO 4  KORN =  1, LNODZ1
      DO 4 K = 1,2
    4 GASH = GASH
     1    + 8.0*ELXYZT(2*KORN+K-2,NX)/FLOAT(216*K-408-LNODZ*(21*K-41))
    5 ELXYZT(9,NX) = GASH
C
C*** DIAGNOSTICS FOR A NEW ELEMENT. RELATE COORDINATES TO CENTRE.
C
      DO 10 I = 1, LNODZ
      N   ERROR = 2
      IF(ELXYZT(I,4).LE.0.0) GO TO 99
      IF(I.EQ.LNODZ) GO TO 9
      JA = I + 1
      DO 8 J = JA, LNODZ
      N   ERROR = 3
      IA = IABS(LNODS(I,NEL))
      IB = IABS(LNODS(J,NEL))
      IF(IA .EQ. IB) GO TO 99
      DO 7 K = 1,3
      IF(ELXYZT(I,K).NE.ELXYZT(J,K)) GO TO 8
    7 CONTINUE
      N   ERROR = 4
      GO TO 99
    8 CONTINUE
    9 DO 10 NX = 1,4
      IF(NX.NE.4) ELXYZT(I,NX) = ELXYZT(I,NX) - ELXYZT(9,NX)
   10 XYZPRE(I,NX) = ELXYZT(I,NX)
C
C*** CREATE SWOP = 1.0 OR -1.0, TO IMPLEMENT SIGN CHANGES AT LOOF NODES.
C
C*** ALSO INTERPOLATE TO ESTIMATE NORMAL THICKNESSES AT LOOF NODES.
C
      VLOOF(1,LVABZA) = ELXYZT(9,4)
      DO 12 NSIDE = 1,6
   12 SWOP(NSIDE) = 1.0
      LAST = LNODZ - 1
      DO 14 NEXT = 1, LNODZ, 2
      MID = LAST + 1
      IA = IABS(LNODS(NEXT,NEL))
      IB = IABS(LNODS(LAST,NEL))
      IF(IA .LT. IB) SWOP(MID/2) = -1.0
      VLOOF(1,4*LAST-3) = .455341801*ELXYZT(LAST,4)
     1    + .666666667*ELXYZT(MID,4) - .122008468*ELXYZT(NEXT,4)
      VLOOF(1,4*MID-3) = -.122008468*ELXYZT(LAST,4)
     1    + .666666667*ELXYZT(MID,4) + .455341801*ELXYZT(NEXT,4)
C
C*** ALSO CHECK THAT MIDSIDE NODES ARE REASONABLY CENTRAL.
C
      GASH = 0.0
      GISH = 0.0
```

```
      GUSH = 0.0
      DO 13 I = 1,3
      ELMID = ELXYZT(MID,I)
      GASH = GASH + (ELXYZT(NEXT,I)-ELMID)**2
      GISH = GISH + (ELXYZT(LAST,I)-ELMID)**2
   13 GUSH = GUSH + (ELXYZT(LAST,I)+ELXYZT(NEXT,I)-ELMID-ELMID)**2
      N    ERROR = 5
C     IF(ABS(GASH-GISH).GT.0.040*(GASH+GISH)) GO TO 99
      N    ERROR = 6
C     IF(GUSH.GT.0.25*(GASH+GISH)) GO TO 99
   14 LAST = NEXT
C     WRITE(6,602) SWOP, (VLOOF(1,I), I = 1, LVABZA, 4)
C602  FORMAT(/7H SWOP =,6F6.3//26H THICKNESSES AT LOOF NODES/1X,9F13.8)
C
C*** ORGANISE LOOP AROUND LOOF NODES, FOR NSTAGE = 2
C
C*** DO 76 NSTAGE = 2,4 (IN EFFECT)
   15 NLOOF = 0
   16 NLOOF = NLOOF + 1
C*** DO 67 NLOOF = 1, LNODZ+1 IF NSTAGE = 2,
C***  OR DO 67 NLOOF = 1, (3*LNODZ)/2 IF NSTAGE = 3,
      DO 17 I = 1,2
      IF(NSTAGE.EQ.2. OR .NLOOF.LE.LNODZ)
     1   XLOCAL(I) = XILOOF(NLOOF,LNODZ+I-6)
C
C*** AND ALSO AROUND INTEGRATING POINTS IF NSTAGE = 3,
C
      IF(NSTAGE.EQ.3. AND .NLOOF.GT.LNODZ)
     1   XLOCAL(I) = XGAUS(NLOOF-LNODZ,LNODZ+I-6)
   17 CONTINUE
      GO TO 23
C
C*** OTHERWISE, ORGANISE SINGLE-SHOT OPTION, FOR NSTAGE = 4,
C
C*** TEST WHETHER INPUT POINT IS A LOOF NODE, PLUS OR MINUS 0.0001,
C
   18 DO 19 I = 1,2
   19 XLOCAL(I) = XITA(I)
      NLOOF = LNODZA
      DO 22 MAYBE = 1,LNODZ
      DO 20 I = 1,2
      IF(ABS(XLOCAL(I)-XILOOF(MAYBE,LNODZ+I-6)).GT.0.0001) GO TO 22
   20 CONTINUE
      NLOOF = MAYBE
   22 CONTINUE
      IF(NLOOF.LE.LNODZ) WRITE(6,604) NLOOF
  604 FORMAT(/36H INPUT POINT RECOGNISED AS LOOF NODE,I3)
C
C*** CREATE VALUES AND XI,ETA DERIVATIVES OF X,Y,Z IN XYZDD, T IN THIKDD
C
```

```
   23 CONTINUE
 606  FORMAT(/13H *** NSTAGE =,I2,10H,  NLOOF =,I3,7H,  XI =,F12.8,
     1    8H,  ETA =,F12.8)
      CALL SFR(XLOCAL, WCORN, WLOOF, NSTAGE, LNODZ)
      K = 0
      DO 27 I = 1,3
      DO 26 J = 1,3
      GASH = 0.0
      DO 24 L = 1,LNODZ
   24 GASH = GASH + WCORN(L+K,I)*ELXYZT(L,J)
      XYZDD(J,I) = GASH
      IF(NSTAGE.EQ.2) GO TO 26
      GASH = 0.0
      DO 25 L = 1,LNODZA
   25 GASH = GASH + WLOOF(L+K,I)*VLOOF(J,4*L-1)
      THIKDD(J,I) = GASH
   26 CONTINUE
   27 K = 1
C     WRITE(6,608) XYZDD
C608  FORMAT(/6H XYZDD/(1X,3F15.10))
C     IF(NSTAGE.EQ.3) WRITE(6,610) THIKDD
C610  FORMAT(/7H THIKDD/(1X,3F15.10))
C
C*** CREATE VECTOR AREA = VAREA, AT GIVEN POINT XI, ETA.
C
      CALL VECTOR(XYZDD(1,2), XYZDD(1,3), AREAV(1))
      CALL SCALAR(AREAV(1), AREAV(1), AREASQ)
      N   ERROR = 7
      IF(AREASQ.EQ.0.0) GO TO 99
      AREA = SQRT(AREASQ)
C     WRITE(6,612) AREA, AREAV
C612  FORMAT(/7H AREA =,F13.10,10X,13HAREA VECTOR =,3F13.10)
C
C*** NORMALISE VECTOR AREA INTO FRAME, COL.3, AS LOCAL UNIT NORMAL Z.
C
C*** COLUMN 2 OF FRAME BECOMES UNIT Y AROUND EDGE.
C
      DO 30 I = 1,3
      FRAME(I,3) = AREAV(I)/AREA
      GASH = 0.0
      DO 29 J = 1,2
   29 GASH = GASH + GENSID((NLOOF+1)/2,LNODZ+J-6)*XYZDD(I,J+1)
   30 FRAME(I,2) = GASH
C
C*** NORMALISE Y, AND IMPLEMENT SWOP BY REVERSING SIGN OF Y.
C
C*** PUT APPROXIMATE VECTOR THICKNESS ETC. INTO VLOOF, FOR NSTAGE = 2
C
      N   ERROR = 8
      CALL SCALAR(FRAME(1,2), FRAME(1,2), SIDESQ)
```

```
      IF(SIDESQ.EQ.0.0) GO TO 99
      SIDE = SQRT(SIDESQ)
      DO 31 I = 1,3
      FRAME(I,2) = FRAME(I,2)*SWOP((NLOOF+1)/2)/SIDE
      IF(NSTAGE.NE.2) GO TO 31
      VLOOF(I,4*NLOOF-2) = FRAME(I,2)
      VLOOF(I,4*NLOOF-1) = FRAME(I,3)*VLOOF(I,4*NLOOF-3)
      VLOOF(I,4*NLOOF) = FRAME(I,3)
   31 CONTINUE
C
C*** AND COLUMN 1 IS UNIT X, THE OUTWARD POINTING IN-PLANE NORMAL.
C
      CALL VECTOR(FRAME(1,2), FRAME(1,3), FRAME(1,1))
      IF (ABS(XITA(1)).EQ.1..OR.ABS(XITA(2)).EQ.1.) RETURN
C     WRITE(6,614) ((FRAME(J,I), I = 1,3), J = 1,3)
C614  FORMAT(/44H COLS OF FRAME ARE UNIT LOCAL CARTESIAN AXES//
C    1   (1X,3F13.10))
C
C*** CHECK THAT NORMALS ARE REASONABLY PARALLEL, WHILE NSTAGE = 2.
C
      IF(NSTAGE.GT.2) GO TO 35
      IF(NLOOF.EQ.1) GO TO 67
      KZ = 4*NLOOF-4
      DO 32 K = 4, KZ, 4
      CALL VECTOR(VLOOF(1,4*NLOOF), VLOOF(1,K), POINT(1))
      CALL SCALAR(POINT(1), POINT(1), COSSQ)
      N   ERROR = 9
C     IF(COSSQ.GT.0.75) GO TO 99
   32 CONTINUE
C
C*** PLACE CONTRIBUTION OF CENTRAL NODE IN VLOOF (NSTAGE = 2 ONLY)
C
C*** COMPLETE LOOP NLOOF = 1 TO LNODZ+1 FOR NSTAGE = 2.
C
      IF(NLOOF.LE.LNODZ) GO TO 67
      THIKC = VLOOF(1,LVABZA)
      DO 33 I = 1,3
      DO 33 J = 1,2
   33 VLOOF(I,LVABZ+J) = FRAME(I,J)*THIKC
      GO TO 67
C
C*** CREATE THE 2X2 JACOBIAN MATRIX, AND INVERT IT. (NSTAGE = 3 OR 4)
C
   35 DO 36 J = 1,2
      DO 36 I = 1,2
      CALL SCALAR(FRAME(1,I), XYZDD(1,J+1), TRANS(J,I))
   36 CONTINUE
C     WRITE(6,616) TRANS
C616  FORMAT(/6H TRANS/(1X,2F13.10))
      GASH = T11
```

```
      T11 = T22/AREA
      T22 = GASH/AREA
      T12 = -T12/AREA
      T21 = -T21/AREA
C     WRITE(6,616) TRANS
C
C*** TRANSFORM WCORN AND WLOOF INTO LOCAL X,Y DERIVATIVES.
C
      DO 41 N = 1,LNODZA
      DO 41 I = 1,2
      GASH = 0.0
      GISH = 0.0
      DO 40 J = 1,2
      GASH = GASH + TRANS(I,J)*WCORN(N+11,J)
   40 GISH = GISH + TRANS(I,J)*WLOOF(N+11,J)
      WCORN(N,I+1) = GASH
   41 WLOOF(N,I+1) = GISH
C     WRITE(6,618)
C618  FORMAT(/16H WCORN AND WLOOF/)
C     DO 42 I = 1,3
C  42 WRITE(6,620) (WCORN(N,I), N = 1,LNODZA)
C620  FORMAT(1X,9F13.10)
C     DO 43 I = 1,3
C  43 WRITE(6,620) (WLOOF(N,I), N = 1,LNODZA)
C
C*** PUT THICKNESS AND DERIVATIVES INTO LOCAL COORDINATE SYSTEM.
C
      DO 45 I = 1,3
      DO 44 J = 1,2
      POINT(J) = 0.0
      DO 44 K = 1,2
   44 POINT(J) = POINT(J) + TRANS(J,K)*THIKDD(I,K+1)
      DO 45 J = 1,2
   45 THIKDD(I,J+1) = POINT(J)
      DO 48 J = 1,3
      DO 47 I = 1,3
      CALL SCALAR(THIKDD(1,J), FRAME(1,I), POINT(I))
   47 CONTINUE
      DO 48 I = 1,3
   48 THIKDD(I,J) = POINT(I)
C     WRITE(6,622) THIKDD
C622  FORMAT(/17H THICKNESS VECTOR,3F12.7//17H X-DERIVATIVES    ,3F12.7//
C    1  17H Y-DERIVATIVES    ,3F12.7)
      THIK = THIKDD(3,1)
      N   ERROR = 10
      IF(THIK.LE.0.0) GO TO 99
C
C*** FIND THE CHANGE IN LOCAL X,Y DERIVATIVES ACROSS THICKNESS OF SHELL.
C
      DO 57 LNOD = 1,LNODZA
```

```
      IF(NSTAGE.NE.4) GO TO 51
      DO 50 I = 2,3
      GASH = 0.0
      DO 49 J = 1,2
   49 GASH = GASH - THIKDD(J,1)*WCORN(LNOD,J+1)
   50 POINT(I) = GASH
C
C*** CREATE WSHEL = SHAPE FUNCTION ARRAY, DISPLACEMENT TERMS FIRST.
C
   51 KORN = (LNOD+1)/2
      DO 54 K = 1,3
      KOL = 2*KORN + 3*LNOD + K - 5
      IF(LNOD.GT.LNODZ) KOL = 5*LNODZ + 2 + K
      DO 53 N = 1,3
      FACT = FRAME(K,N)
      WSHEL(N,KOL) = WCORN(LNOD,1)*FACT
      IF(NSTAGE.EQ.4. AND .N.EQ.3) FACT = 0.0
      DO 53 ND = 2,3
   53 WSHEL(N+N+ND,KOL) = WCORN(LNOD,ND)*FACT
      DO 54 N = 1,2
      DO 54 ND = 2,3
      WSHEL(N+7,KOL) = WSHEL(N+7,KOL)
     1   - THIKDD(ND-1,1)*WSHEL(N+N+ND,KOL)/THIK
      IF(NSTAGE.EQ.4) WSHEL(N+N+ND+6,KOL) = (POINT(ND)*FRAME(K,N)
     1   + THIKDD(3,ND)*WCORN(LNOD,N+1)*FRAME(K,3))/THIK
   54 CONTINUE
C
C*** INTRODUCE ROTATION TERMS WITH BENDING ACTION INTO WSHEL.
C
      DO 57 L = 1,2
      KOL = (L-1)*4*LNODZ + (2-L)*6*KORN + LNOD
      IF(LNOD.GT.LNODZ) KOL = 5*LNODZ + 3 - L
      DO 56 N = 1,2
      CALL SCALAR(VLOOF(1,4*LNOD+L-4), FRAME(1,N), FACT)
      WSHEL(N+7,KOL) = FACT*WLOOF(LNOD,1)/THIK
      IF(NSTAGE.NE.4) GO TO 56
      DO 55 ND = 2,3
   55 WSHEL(N+N+ND+6,KOL) = FACT*WLOOF(LNOD,ND)/THIK
   56 CONTINUE
      DO 57 NROW = 1,7
   57 WSHEL(NROW,KOL) = 0.0
C
C*** COMBINE LAST THREE COLUMNS OF WSHEL TO CREATE NORMAL DEFLECTION.
C
      IF(LNODZ.EQ.6) GO TO 61
      IZ = 3*NSTAGE + 1
      DO 60 I = 1,IZ
      GASH = 0.0
      DO 59 K = 1,3
   59 GASH = GASH + WSHEL(I,42+K)*VLOOF(K,4*LNODZ+4)
```

```
   60 WSHEL(1,43) = GASH
C      WRITE(6,624) (N, (WSHEL(K,N), K = 1,13), N = 1, LVABZZ)
C624   FORMAT(/15H WSHEL ORIGINAL/9X,1HU,8X,1HV,8X,1HW,8X,2HUX,7X,2HUY,
C     1    7X,2HVX,7X,2HVY,7X,2HUZ,7X,2HVZ,6X,3HUXZ,6X,3HUYZ,6X,3HVXZ,6X,
C     2    3HVYZ/68X,18HOR UZ+WX  OR VZ+WY/(I4,13F9.5))
   61 IF(NSTAGE.EQ.4) GO TO 86
C
C*** CREATE ARRAY SHEAR, FOR INTRODUCING THE CONSTRAINTS (NSTAGE = 3)
C
      IF(NLOOF.GT.LNODZ) GO TO 63
      DO 62 I = 1,LVABZZ
      SHEAR(NLOOF,I) = WSHEL(9,I)
      SHEAR(11,I) = SHEAR(11,I) + WSHEL(8,I)*SIDE*THIK*SWOP((NLOOF+1)/2)
   62 CONTINUE
      GO TO 67
   63 DO 66 KOL = 1,LVABZZ
      DO 66 NXY = 1,2
      GASH = SHEAR(LNODZ+NXY,KOL)
      DO 65 MXY = 1,2
      CALL SCALAR(FRAME(1,MXY), VLOOF(1,4*LNODZ+NXY), FACT)
   65 GASH = GASH + WSHEL(MXY+7,KOL)*AREA*THIK*FACT
   66 SHEAR(LNODZ+NXY,KOL) = GASH
C
C*** COMPLETE LOOP AROUND LOOF NODES ETC, TO CREATE VLOOF OR SHEAR.
   67 IF(NLOOF.LE.LNODZ. OR .
     1   (NSTAGE.EQ.3. AND .NLOOF.LT.(3*LNODZ)/2)) GO TO 16
      IF(NSTAGE.NE.2) GO TO 76
C
C*** CREATE PLUS-MINUS SUM OF THICKNESS VECTORS AT LOOF NODES (NSTAGE=2)
C
      DO 70 I = 1,3
      GASH = 0.0
      DO 68 N = 3,LVABZ,4
   68 GASH = -GASH + VLOOF(I,N)
      SIGT(I) = GASH
C
C*** AND THE 3X3 MATRIX ASSOCIATED WITH IT, STORED IN XYZDD.
C
      DO 70 J = 1,3
      GASH = 0.0
      IF(I.EQ.J) GASH = FLOAT(LNODZ)
      DO 69 N = 2,LVABZ,4
   69 GASH = GASH - VLOOF(I,N)*VLOOF(J,N)
   70 XYZDD(I,J) = GASH
C      WRITE(6,626) SIGT, XYZDD
C626   FORMAT(/24H PLUS-MINUS ERROR VECTOR,3F12.8//
C     1    25H MATRIX FOR CORRECTING IT,3F12.8,2(/25X,3F12.8))
C
C*** GET THE ADJUGATE OF THIS 3X3 SYMMETRIC POSITIVE DEFINITE MATRIX.
C
```

```
      K = 3
      DO 71 I = 1,3
      CALL VECTOR(XYZDD(1,I), XYZDD(1,6-I-K), FRAME(1,K))
   71 K = I
      CALL SCALAR(XYZDD(1,1), FRAME(1,1), DETERM)
      DO 73 I = 1,3
      CALL SCALAR(FRAME(1,I), SIGT(1), PROD)
   73 POINT(I) = PROD/DETERM
C     WRITE(6,628) FRAME, POINT
C628  FORMAT(/9H ADJUGATE,3(/1X,3F12.8)//10H SOLUTIONS,3F12.8)
C
C*** CORRECT VECTOR THICKNESSES IN VLOOF.
C
      FACT = 1.0
      DO 75 N = 2,LVABZ,4
      FACT = -FACT
      CALL SCALAR(POINT(1), VLOOF(1,N), PROD)
      DO 74 I = 1,3
   74 VLOOF(I,N+1) = VLOOF(I,N+1) - FACT*(POINT(I)-PROD*VLOOF(I,N))
C
C*** CREATE DIFFERENTIAL DISPLACEMENT VECTORS TO DEFINE ROTATIONS.
C
C*** THIS COMPLETES WORK FOR NSTAGE = 2.
C
      TFIRST = VLOOF(1,N-1)
      CALL VECTOR(VLOOF(1,N), VLOOF(1,N+1), VLOOF(1,N-1))
      DO 75 I = 1,3
   75 VLOOF(I,N) = VLOOF(I,N)*TFIRST
      NZ = 4*LNODZA
C     WRITE(6,630) (N, (VLOOF(I,N), I = 1,3), N = 1,NZ)
C630  FORMAT(/6H VLOOF/(1X,I3,6X,3F15.10))
      NSTAGE = 3
      GO TO 15
C
C*** SHEAR HAS BEEN CREATED IN NLOOF LOOP FOR NSTAGE = 3.
C
C*** CHOOSE PIVOT FOR REDUCING ARRAY SHEAR, AND DO ROW INTERCHANGE.
C
   76 CONTINUE
C     WRITE(6,632)
C632  FORMAT(/6H SHEAR)
C     DO 77 N = 1,LVABZZ
C  77 WRITE(6,634) N, (SHEAR(I,N), I = 1,LIMZ)
C634  FORMAT(I4,11F10.6)
      DO 83 LIM = 1,LIMZ
      KP = LVABZ + LIM
      PIVOT = 0.0
      DO 79 L = LIM,LIMZ
      IF(ABS(PIVOT).GT.ABS(SHEAR(L,KP))) GO TO 79
      LBIG = L
```

```
      PIVOT = SHEAR(LBIG,KP)
   79 CONTINUE
      DO 80 K = 1,LVABZZ
      CHANGE = SHEAR(LBIG,K)
      SHEAR(LBIG,K) = SHEAR(LIM,K)
   80 SHEAR(LIM,K) = CHANGE/PIVOT
C
C*** REDUCE ARRAY SHEAR TO CREATE CONSTRAINT MATRIX,
C
C*** THIS COMPLETES WORK FOR NSTAGE = 3.
C
      DO 82 NROW = 1,LIMZ
      FACT = SHEAR(NROW,KP)
      IF(NROW.EQ.LIM. OR .FACT.EQ.0.0) GO TO 82
      DO 81 KOL = 1,LVABZZ
   81 SHEAR(NROW,KOL) = SHEAR(NROW,KOL) - FACT*SHEAR(LIM,KOL)
   82 CONTINUE
   83 CONTINUE
C     WRITE(6,636)
C636  FORMAT(/22H SHEAR AFTER REDUCTION)
C     DO 85 N = 1,LVABZZ
C  85 WRITE(6,634) N, (SHEAR(I,N), I = 1,LIMZ)
      NSTAGE = 4
      GO TO 18
C
C*** USE ARRAY SHEAR TO CONSTRAIN WSHEL AT THE GIVEN POINT XI,ETA.
C
   86 DO 88 I = 1,LVABZ
      DO 88 J = 1,13
      GASH = WSHEL(J,I)
      DO 87 K = 1,LIMZ
   87 GASH = GASH - WSHEL(J,K+LVABZ)*SHEAR(K,I)
   88 WSHEL(J,I) = GASH
C     WRITE(6,638)
C640  FORMAT(I4,13F9.5)
C638  FORMAT(/18H WSHEL CONSTRAINED)
C
C*** IMPLEMENT SWOP TO EXCHANGE TWO NORMAL SLOPES.
C
      DO 92 N = 8, LVABZ, 8
      IF(SWOP(N/8).EQ.1.0) GO TO 92
      DO 91 J = 1,13
      CHANGE = WSHEL(J,N)
      WSHEL(J,N) = WSHEL(J,N-1)
   91 WSHEL(J,N-1) = CHANGE
   92 CONTINUE
C     WRITE(6,642)
C642  FORMAT(/14H WSHEL SWOPPED)
C     DO 94 N = 1,LVABZ
C  94 WRITE(6,640) N, (WSHEL(J,N), J = 1,13)
```

```
C
C*** ASSEMBLE UXZ, UYZ, VXZ, VYZ TO CREATE WXX, WXY, WYY.
C
C      WRITE(6,644)
C644   FORMAT(/30H WSHEL WITH SECOND DERIVATIVES)
       DO 96 N = 1,LVABZ
       WSHEL(10,N) = -WSHEL(10,N)
       WSHEL(11,N) = -0.5*(WSHEL(11,N)+WSHEL(12,N))
       WSHEL(12,N) = -WSHEL(13,N)
C      WRITE(6,640) N, (WSHEL(J,N), J = 1,12)
   96 CONTINUE
C
C*** PUT POINT, FRAM IN COMMON, ALSO AREA, SIDE WITH INTEGRATING FACTORS
C
       AREA = AREA*(FLOAT(LNODZ)-5.6)/2.4
       SIDE = SIDE*FLOAT(LNODZ-4)/4.0
       DO 98 I = 1,3
       POINT(I) = XYZDD(1,1) + ELXYZT(9,I)
       DO 98 J = 1,3
   98 FRAM(I,J) = FRAME(I,J)
       RETURN
C
C*** WRITE DIAGNOSTIC ERROR MESSAGE.
C
   99 WRITE(6,699) NERROR
  699  FORMAT(/6H ERROR,I5,18H IN SEGMENT HALOOF)
       AREA=-69.
       END
```

```
      SUBROUTINE SFR(XLOCAL, WCORN, WLOOF, NSTAGE, LNODZ)
C
C*** SHAPE FUNCTION SUBROUTINE TO SERVE HALOOF.
C
      DIMENSION MD(4), TERMV(46), WCORN(10,3), WLOOF(10,3), XLOCAL(2)
      COMMON/COEF/COEF(247)
      DATA MD/8, 43, 90, 171/
      DATA TERMV /46*0./
C
C*** INITIALIZE AND PREPARE TO CALCULATE TERMV = POLYNOMIAL TERMS.
C
      XI = XLOCAL(1)
      ETA = XLOCAL(2)
C     WRITE(6,604) XI, ETA
C604  FORMAT(/5H XI =,F15.10,6X,5HETA =,F15.10)
      IA = 2
C
C*** CREATE POLYNOMIAL TERMS AND XI, ETA DERIVATIVES.
C
      TERMV(1) = 0.0
      TERMV(2) = 1.0
      NZ = (LNODZ+NSTAGE-3)/2
      DO 6 N = 1, NZ
      IAN = IA + N
      N2 = N + 15
      N3 = N + 30
      DO 4 J = IA,IAN
      TERMV(J+N) = TERMV(J)*XI
      TERMV(J+N2) = TERMV(J)*FLOAT(IAN-J)
    4 TERMV(J+N3) = TERMV(J-1)*FLOAT(J-IA)
      IA = IAN
    6 TERMV(IA+N) = TERMV(IA-1)*ETA
C
C*** CREATE SPECIAL COMBINATIONS FOR LOOF NODES, ETC.
C
      DO 8 I = 8, 38, 15
      IF(LNODZ.EQ.6) TERMV(I) =
     1   2.0*(TERMV(I)-TERMV(I+3)) + 3.0*(TERMV(I+1)-TERMV(I+2))
      IF(LNODZ.EQ.8) TERMV(I) = TERMV(I+2)
      IF(LNODZ.EQ.8) TERMV(I+2) = TERMV(I+6)
    8 CONTINUE
C
C*** USE TERMV TO FIND WCORN AND WLOOF AND XI, ETA DERIVATIVES.
C
      NFOISZ = (NSTAGE+1)/2
      DO 18 NFOIS = 1, NFOISZ
      NZ = (3*LNODZ)/2 + NFOIS - 4
      IF(NZ.NE.10) GO TO 12
      NZ = 9
      DO 10 I = 10,40,15
```

```
   10 TERMV(I) = TERMV(I+3) - TERMV(I+5)
   12 K = 0
      DO 18 I = 1,3
      DO 16 N = 1,NZ
      GASH = 0.0
      MDEL = MD(LNODZ+NFOIS-6) + N*NZ - 15*I
      MA = 16*I-14
      MZ = 15*I+NZ-14
      DO 14 M = MA, MZ
   14 GASH = GASH + TERMV(M)*COEF(M+MDEL)
      IF(NFOIS.EQ.1) WCORN(N+K,I) = GASH
      IF(NFOIS.EQ.2) WLOOF(N+K,I) = GASH
   16 CONTINUE
   18 K = 1
C     WRITE(6,606)
C606  FORMAT(/16H WCORN AND WLOOF/)
C     DO 22 I = 1,3
C  22 WRITE(6,608) (WCORN(N,I), N = 1,LNODZ+1)
C     DO 24 I = 1,3
C  24 WRITE(6,608) (WLOOF(N,I), N = 1,LNODZ+1)
C608  FORMAT(1X,9F13.10)
      RETURN
C
C*** ERROR DIAGNOSTICS, IF POINT LIES OUTSIDE ELEMENT.
C
   99 WRITE(6,610) XI, ETA
  610 FORMAT(/30H ERROR 11 IN SEGMENT SFR, XI =,F15.9,3X,5HETA =,F15.9)
      STOP
      END
```

```
      BLOCK DATA
C
C*** TO INITIALIZE COEFFICIENTS FOR CORNER-MIDSIDE AND LOOF VERSIONS
C
C*** OF QUADRATIC TRIANGLE AND QUADRILATERAL FOR SUBROUTINE SFR.
C
      DIMENSION COEFA(166), COEFB(81)
      COMMON/COEF/COEF(247)
      EQUIVALENCE (COEF(1), COEFA(1)), (COEF(167),COEFB(1))
      DATA COEFA/ 1.,-3.,-3., 2., 4., 2., 0., 4., 0.,-4.,-4., 0., 0.,
     1 -1., 0., 2., 0., 0., 0., 0., 0., 0., 4., 0., 0., 0.,-1., 0., 0.,
     2  2., 0., 0., 4., 0.,-4.,-4.,   0.910683603, 1.577350269,
     3 -6.041451884,-6.196152423, 2.464101615, 8.928203230, 1.732050808,
     4 -0.244016936, 0.422649731, 2.041451884, 4.196152423,-4.464101615,
     5 -4.928203230,-1.732050808, 0.333333333,-1.422649731,-2.577350269,
     6 -1.464101615, 5.000000000, 5.464101615, 1.732050808, 0.333333333,
     7 -2.577350269,-1.422649731, 5.464101615, 5.000000000,-1.464101615,
     8 -1.732050808,-0.244016936, 2.041451884, 0.422649731,-4.928203230,
     9 -4.464101615, 4.196152423, 1.732050807, 0.910683602,-6.041451884,
     1  1.577350269, 8.928203230, 2.464101615,-6.196152422,-1.732050807,
     2 -1.,6.,6.,-6.,-6.,-6.,0.,-.25,0.,0.,.25,.25,.25,-.25,-.25,0.,
     3 .5,0.,-.5,-.5,0.,0.,0.,.5,0.,-.25,0.,0.,.25,-.25,.25,.25,-.25,0.,
     4 .5,.5,0.,0.,0.,-.5,-.5,0.,0.,-.25,0.,0.,.25,.25,.25,.25,.25,0.,
     5 .5,0.,.5,-.5,0.,0.,0.,-.5,0.,-.25,0.,0.,.25,-.25,.25,-.25,.25,0.,
     6  .5,-.5,0.,0.,0.,-.5,.5,0.,0.,1.,0.,0.,-1.,0.,-1.,0.,0.,1./
       DATA COEFB/ 0.000000000, 0.216506351,-0.375000000,-0.093750000,
     1  0.216506351, 0.281250000,-0.649519053, 0.375000000,-0.324759526,
     2 -0.000000000,-0.216506351,-0.375000000,-0.093750000,-0.216506351,
     3  0.281250000, 0.649519053, 0.375000000, 0.324759526, 0.000000000,
     4  0.375000000, 0.216506351, 0.281250000,-0.216506351,-0.093750000,
     5 -0.375000000,-0.649519053,-0.324759526, 0.000000000, 0.375000000,
     6 -0.216506351, 0.281250000, 0.216506351,-0.093750000,-0.375000000,
     7  0.649519053, 0.324759526,-0.000000000,-0.216506351, 0.375000000,
     8 -0.093750000, 0.216506351, 0.281250000, 0.649519053,-0.375000000,
     9 -0.324759526, 0.000000000, 0.216506351, 0.375000000,-0.093750000,
     1 -0.216506351, 0.281250000,-0.649519053,-0.375000000, 0.324759526,
     2 -0.000000000,-0.375000000,-0.216506351, 0.281250000,-0.216506351,
     3 -0.093750000, 0.375000000, 0.649519053,-0.324759526,-0.000000000,
     4 -0.375000000, 0.216506351, 0.281250000, 0.216506351,-0.093750000,
     5 .375,-.649519053,.324759526,1.,0.,0.,-.75,0.,-.75,0.,0.,0./
       END
```

```
      SUBROUTINE VECTOR(U, V, W)
C
C*** TO COMPUTE VECTOR PRODUCT U*V INTO AREA W.
C
      DIMENSION U(3), V(3), W(3)
      K = 3
      DO 2 I = 1,3
      W(6-I-K) = U(K)*V(I) - U(I)*V(K)
    2 K = I
      RETURN
      END
```

```
      SUBROUTINE SCALAR(U, V, PROD)
C
C*** TO COMPUTE SCALAR PRODUCT OF VECTORS U AND V.
C
      DIMENSION U(3), V(3)
      PROD = 0.0
      DO 2 I = 1,3
    2 PROD = PROD + U(I)*V(I)
      RETURN
      END
```

```
      SUBROUTINE LOFBEM(NEL, LVABZ, SIDE, ELXYZT, FRAM,POINT, WBEAM,
     .      XI, NODEL, NDIM, LNODZ, LNODS)
C
C***  WRITTEN BY BRUCE IRONS AND FERNANDO ALBUQUERQUE
C***  SWANSEA, 1/7/1973
C
C
C***  TO ERATE SHAPE FUNCTION ARRAY WBEAM, FOR SEMILOOF BEAM ELEMENT
C
      LOGICAL KNOWFR
      DIMENSION LNODS(NODEL,NEL)
      DIMENSION ELXYZT(NODEL,NDIM)
      DIMENSION POINT(3), FRAM(3,3), WBEAM(13,45)
      DIMENSION FRAME(3,3), LNOPRE(6), SHEAR(10,21), VLOOF(3,6)
      DIMENSION WCORN(3,2), WLOOF(4,2), XILOOF(5)
      DATA XILOOF /-.577350269, .577350269,
     2 -.7745966692, .7745966692, 0.0/, LNOPRE/6*0/
C
C***  GENERATE NSTAGE
C
      N   ERROR = 1
      IF(LVABZ . NE.  17 .AND. LVABZ .NE.  19) GO TO 99
      IF( LVABZ .EQ. 17) KONST = 4
      IF( LVABZ .EQ. 19) KONST = 2
      NSTAGE = 3
      DO 2 N = 1, LNODZ
      IF(LNODS(N,NEL) .NE. LNOPRE(N)) NSTAGE = 1
    2 LNOPRE(N) = LNODS(N,NEL)
    3 XLOCAL = XI
      GO TO ( 4, 99, 24) , NSTAGE
C
C***   INITIALIZATION AND DIAGNOSTICS
C
    4 DO 10 I=2,3
      JJ = I-1
      DO 8 J = 1, JJ
      N ERROR = 2
      IA = IABS(LNODS(I,NEL))
      IB = IABS(LNODS(J,NEL))
      IF(IA .EQ. IB) GO TO 99
    8 CONTINUE
   10 CONTINUE
C
C***  CHECK THAT MIDSIDE IS NEAR THE MIDLE AND THAT ELEMENT IS
C     NOT TOO CURVED
C
      GASH = 0.0
      GISH = 0.0
      GUSH = 0.0
      DO 12 I = 1,3
```

```
      GASH = GASH + (ELXYZT(3,I) - ELXYZT(2,I))**2
      GISH = GISH + (ELXYZT(2,I) -ELXYZT(1,I))**2
   12 GUSH = GUSH + (ELXYZT(3,I) - 2.0*ELXYZT(2,I) +ELXYZT(1,I))**2
C
C***  CREATE UNIT BINORMAL Z OUT OF PLANE OF ELEMENT = COL. 3 OF FRAME
C
      KNOWFR=.FALSE.
      DO 13 I=1,3
      FRAME(I,1)=FRAM(I,1)
   13 KNOWFR=KNOWFR.OR.FRAM(I,1).NE.0.
      DO 14 I = 1,3
      IF (.NOT.KNOWFR) FRAME(I,1)=ELXYZT(1,I)-2.*ELXYZT(2,I)+ELXYZT(3,I)
   14 FRAME(I,2) = ELXYZT(3,I) - ELXYZT(1,I)
C
      DO 16 I = 1,4
      IF (.NOT.KNOWFR) FRAME(I-1,1)=FRAME(I-1,1)+1.0
      CALL VECTOR(FRAME(1,1), FRAME(1,2), FRAME(1,3))
      CALL SCALAR ( FRAME(1,3), FRAME(1,3), ZSQ)
      IF(ZSQ .GT. 0.0) GO TO 18
   16 CONTINUE
      N   ERROR = 5
      GO TO 99
   18 DO 20 I = 1,3
   20 FRAME(I,3) = FRAME(I,3)/SQRT(ZSQ)
C
C***  ORGANIZE LOOP AND END NODES TO CREATE VLOOF , THEN SHEAR
C
   21 NLOOF = 0
   22 NLOOF = NLOOF + 1
C
C***  DO 56 NLOOF = 1,2 IF NSTAGE= 1, BUT NLOOF = 1,5 IF NSTAGE = 2
C
      XLOCAL = XILOOF ( NLOOF )
   24 CALL SFR1(XLOCAL, WCORN, WLOOF)
C
C***  COMPLETE FRAME X IS ALONG TANGENT TO BEAM
C
      DO 28 I = 1,3
      GASH = 0.0
      DO 26 N = 1,3
   26 GASH = GASH + ELXYZT(N,I)*WCORN(N,2)
   28 FRAME(I,1) = GASH
      CALL SCALAR ( FRAME(1,1), FRAME(1,1), SIDESQ)
      N  ERROR= 6
      IF(SIDESQ .EQ. 0.0) GO TO 99
      SIDE = SQRT(SIDESQ)
      DO 30 I = 1,3
   30 FRAME(I,1) = FRAME(I,1)/SIDE
C
C***  AND UNIT Y, IN COL 2 OF FRAME, IS NORMAL TO BOTH
```

```
C
      CALL VECTOR( FRAME(1,3), FRAME(1,1), FRAME(1,2))
C     WRITE(6,608) ((FRAME(J,I),I = 1,3), J = 1,3)
C 608 FORMAT(/44H COLS OF FRAME ARE UNIT LOCAL CARTESIAN AXES,
C    1//(1X,3F13.10))
      GO TO ( 31, 34, 34), NSTAGE
C
C***  APPEND FRAME TO VLOOF , HENCE ENDING TASK WITH NSTAGE = 1
C
   31 DO 32 I = 1,3
      DO 32 J = 1,3
   32 VLOOF(I,3*(NLOOF-1)+J) = FRAME(I,J)
      GO TO 56
C
C***  TRANSFORM DERIVATIVES OF WCORN AND WLOOF IN XILOOF
C
   34 DO 36 N = 1,3
   36 WCORN(N,2) = WCORN(N,2)/SIDE
C      WRITE(6,612)
C 612 FORMAT(/16H WCORN AND WLOOF/)
C     DO 37 I = 1,2
C  37 WRITE(6,614) (WCORN(N,I), N =1,3)
C 614 FORMAT(1X, 4F13.10)
      DO 38 N = 1,4
   38 WLOOF(N,2) = WLOOF(N,2)/SIDE
C     DO 39 I = 1,2
C  39 WRITE(6,614) (WLOOF(N,I), N = 1,4)
C
C***  INITIALIZE WBEAM TO ZERO
C
      DO 40 I = 1,12
      DO 40 J = 1,24
   40 WBEAM (I,J) = 0.0
C
C***  INTRODUCE TERMS FOR DISPLACEMENT INTO COL 1 TO 11 OF WBEAM
C
      DO 42 NOD = 1,3
      DO 42 IUVW = 1,3
      KOL = 3*(NOD-1) + IUVW
      IF ( NOD .EQ. 3) KOL = KOL+2
      WBEAM (IUVW,KOL) = WCORN(NOD,1)
      WBEAM(4,KOL) = WCORN(NOD,2)*FRAME(IUVW,1)
      DO 42 NSHEAR =1,2
   42 WBEAM(NSHEAR+10,KOL) = WCORN(NOD,2)*FRAME(IUVW,NSHEAR+1)
C
C***  INTRODUCE ROTATION TERMS INTO WBEAM
C
      DO 46 NOD = 1,4
      DO 46 IUVW = 1,3
      KOL = 3*NOD+IUVW+8
```

```
      IF( NOD .GE. 3) KOL = KOL+1
      DO 44 IXYZ = 1,3
   44 WBEAM(IXYZ+4,KOL) = WLOOF(NOD,1) * FRAME(IUVW,IXYZ)
      WBEAM(8,KOL) = WLOOF(NOD,2)*FRAME(IUVW,3)
      WBEAM(9,KOL) = -WLOOF(NOD,2)*FRAME(IUVW,2)
      WBEAM(10,KOL) = WLOOF(NOD,2)*FRAME(IUVW,1)
      WBEAM(11,KOL) =-WLOOF(NOD,1)*FRAME(IUVW,3)
   46 WBEAM(12,KOL) = WLOOF(NOD,1)*FRAME(IUVW,2)
C
C***  CREATE LOCAL ROTATION TERMS IN BEAM FOR NSTAGE = 2
C
      DO 51 NOD = 3,4
      DO 51 I = 1,3
      IF (I .EQ. 1) KOL = NOD+4
      IF(I .GT. 1) KOL = 2*NOD+I+10
      DO 51 NROW = 1,12
      GASH = 0.0
      DO 50 J = 1,3
   50 GASH = GASH + WBEAM(NROW,3*NOD+J+9)*VLOOF(J,3*(NOD-3)+I)
   51 WBEAM(NROW,KOL) = GASH
C     WRITE(6,617) (N, (WBEAM(K,N), K= 1,12), N = 1,24)
C 617 FORMAT(/15H WBEAM ORIGINAL/9X,1HU,8X,1HV,8X,1HW,
C    1  8X,2HDS,7X,4HROTX,5X,4HROTY,5X,4HROTZ,
C    2  3X,6HCURVXY,3X,6HCURVXZ,2X,7HTORCURV,4X,5HSHEXY,4X,5HSHEXZ ,
C    3 /(I4,12F9.5))
      GO TO ( 99,53,70), NSTAGE
C
C***  INTRODUCE THE BENDING CURVATURES INTO SHEAR
C
   53 DO 54 KOL = 1,21
      DO 54 IYZ = 1,2
   54 SHEAR(2*NLOOF+IYZ-2,KOL) = WBEAM(10+IYZ,KOL)
C***  COMPLETE LOOP FOR NLOOF , WITH NSTAGE = 1 OR 2
C
   56 IF(NLOOF .LT. 2) GO TO 22
      NSTAGE = NSTAGE + 1
      IF(NSTAGE .EQ. 2) GO TO 21
C     WRITE(6,618)
C 618 FORMAT(14H INITIAL SHEAR)
C     DO 57 N = 1,21
C  57 WRITE(6,620) N, (SHEAR(I,N) , I = 1,8)
C 620 FORMAT(I4 ,10F10.6)
C
C***  FINALIZE THE MATRIX SHEAR , IN FIRST FOUR ROWS
C
      DO 58 KOL = 1,12
      DO 58 IYZ = 1 , 2
      SHEAR(IYZ,KOL) = SHEAR(IYZ,KOL)
   58 SHEAR(IYZ+2,KOL) = SHEAR(IYZ+2,KOL)
C     WRITE(6,619)
```

```
C 619 FORMAT(12H FINAL SHEAR)
C     DO 59 N = 1,21
C  59 WRITE(6,620) N, (SHEAR(I,N), I = 1,10)
C
C***  CHOOSE PIVOT FOR REDUCING ARRAY SHEAR AND DO ROW INTERCHANGE
C
      DO 66 LIM = 1,KONST
      KP = LVABZ + LIM
      PIVOT = 0.0
      DO 60 L = LIM,KONST
      IF(ABS(PIVOT) .GT. ABS(SHEAR(L,KP)))  GO TO 60
      LBIG = L
      PIVOT = SHEAR(LBIG,KP)
   60 CONTINUE
      DO 61 K = 1,21
      CHANGE = SHEAR(LBIG,K)
      SHEAR(LBIG,K) = SHEAR(LIM,K)
   61 SHEAR(LIM,K) = CHANGE/PIVOT
C
C***  REDUCE ARRAY SHEAR TO CREATE CONSTRAINT MATRIX
C
      DO 64 NROW = 1, KONST
      FACT = SHEAR(NROW,KP)
      IF(NROW .EQ. LIM .OR. FACT .EQ. 0.0) GO TO 64
      DO 62 KOL = 1,21
   62 SHEAR(NROW,KOL) = SHEAR(NROW,KOL) - FACT*SHEAR(LIM,KOL)
   64 CONTINUE
   66 CONTINUE
C     WRITE(6,621)
C 621 FORMAT(/22H SHEAR AFTER REDUCTION)
C     DO 67 N = 1,21
C  67 WRITE(6,623) N, (SHEAR(I,N), I = 1,KONST)
C 623 FORMAT(I4,4F10.6)
      GO TO 3
C
C***  USE ARRAY SHEAR TO CONSTRAIN WBEAM AT THE GIVEN POINT XI
C
   70 DO 74 I = 1,LVABZ
      DO 74 J = 1,12
      GASH = WBEAM(J,I)
      DO 72 K = 1,KONST
   72 GASH = GASH -WBEAM(J,K+LVABZ)*SHEAR(K,I)
   74 WBEAM(J,I) = GASH
C     WRITE(6,622)
C 622 FORMAT(/18H WBEAM CONSTRAINED)
C
C***  INTRODUCE SIGN CONVENTION FOR LOOF ROTATIONS
C
       IA = IABS(LNODS(3,NEL))
      IB = IABS(LNODS(1,NEL))
```

```
      IF(IA .GT. IB) GO TO 77
      DO 75 J = 1,12
      CHANGE = WBEAM(J,7)
      WBEAM(J,7) = -WBEAM(J,8)
   75 WBEAM(J,8) = -CHANGE
C     WRITE(6,626)
C 626 FORMAT(/14H WBEAM SWOPPED)
C     DO 76 N = 1,LVABZ
C  76 WRITE (6,624) N, (WBEAM(J,N), J= 1,12)
C 624 FORMAT(I4,12F9.5)
C
C***  COMPUTE POINT , AND PASS FRAME INTO FRAM IN COMMON
C
   77 DO 80 I = 1,3
      GASH = 0.0
      DO 78 J = 1,3
      GASH = GASH + WCORN(J,1) * ELXYZT(J,I)
   78 FRAM(I,J) = FRAME(I,J)
   80 POINT(I) = GASH
      RETURN
   99 WRITE (6,699) NERROR
  699 FORMAT(/7H1 ERROR,I5,18H IN SEGMENT LOFBEM)
      SIDE=-69.
      END
```

```
      SUBROUTINE GCBSF1( XI, P)
C
C***   ROUTINE GIVES QUADRATIC INTERPOLATION FUNCTIONS IN XI.
C
      DIMENSION P(3)
      G = XI
      P(1) = .5 * G * (-1. + G )
      P(2) = 1. - G * G
      P(3) = .5 * G * ( 1. + G )
      RETURN
      END
```

```
      SUBROUTINE SFR1(XI, WCORN, WLOOF)
C
C***  SHAPE FUNCTION SUBROUTINE TO SERVE LOFBEM
      DIMENSION COEF(56), TERMV(4), WCORN(3,2), WLOOF(4,2)
C
C
C***  DEFINE COEFFICIENTS FOR SHAPE FUNCTIONS AND DERIVATIVES
C
      DATA COEF / 0., -.5, .5, 0.,
     11., 0., -1., 0.,
     2 0., .5, .5, 0.,
     3-.5, 1., 0., 0.,
     40., -2., 0., 0.,
     5.5, 1., 0., 0.,
     6 -0.25, 0.25, 0.75, -0.75,
     7 -0.25, -0.25, 0.75, 0.75,
     8.75, -1.2990381, -.75, 1.299038,
     9.75, 1.2990381, -.75, -1.2990381,
     1 0.25, 1.5, -2.25, 0.0,
     2 -0.25, 1.5, 2.25, 0.0,
     3-1.2990381, -1.5, 3.8971143, 0.,
     41.2990381, -1.5, -3.8971143, 0./ , TERMV(1)/1.0/
C
C***   DIAGNOSTICS AND CREATE POWERS OF XI = XLOCAL
C
C 600 FORMAT(/9H XLOCAL =, F12.6)
C     WRITE(6,600) XI
      IF(XI.LT.-1.0 .OR. XI .GT. 1.0) GO TO 99
      DO 2 I = 1,3
    2 TERMV(I+1) = TERMV(I)*XI
C
C*** CREATE WCORN WITH XI DERIVATIVES
C
      DO 10 IDIF = 1,2
      DO 6 NOD = 1,3
      IDEL = 12*IDIF + 4*NOD - 16
      GASH = 0.0
      DO 4 I = 1,3
    4 GASH = GASH+TERMV(I)*COEF(I+IDEL)
    6 WCORN(NOD,IDIF) = GASH
C
C***  CREATE WLOOF WITH XI DERIVATIVES
C
      DO 10 NOD = 1,4
      IDEL = 16*IDIF+4*NOD+4
      GASH = 0.0
      DO 8 I =1,4
    8 GASH = GASH + TERMV(I) *COEF(I+IDEL)
   10 WLOOF(NOD,IDIF) = GASH
      RETURN
```

```
C
C***  ERROR DIAGNOSTICS
C
   99 WRITE(6,602)
  602 FORMAT(34H1ERROR IN SFR, XI IS OUTSIDE RANGE)
      END
```

B.4 POSTLOOF LISTING

```
*DECK POSTLOO
      PROGRAM POSTLOO(UT2,LSTRES,INPUT,OUTPUT,TAPE3,
     .        TAPE1=LSTRES,TAPE2=UT2,TAPE5=INPUT,TAPE6=OUTPUT)
C
C     PROGRAM TO RECOVER STRESSES FOR SEMI-LOOF SHELL AND BEAM
C     ELEMENTS USING NASTRAN.  SEMI-LOOF PRE-PROCESSOR IS THE
C     COMPANION PROGRAM
C
      COMMON/N/NUMNP,NSHELL,NBEAM,NSHLTY,NBMTY,NGAUS
C     COMMON A(1)
      COMMON A(20000)
      DIMENSION TITLE(8)
      REWIND 1
      REWIND 2
      READ(1) TITLE,NUMNP,NSHELL,NSHLTY,NBEAM,NBMTY,NGAUS
      CALL DATE(DA)
      CALL TIME(TI)
      NINDEX=1
      NU=NINDEX+9*NSHELL+1
      CALL IN4INI(2,NCOLS,NROWS,NFORM,NTYPE,0,1)
      NLNODS=NU+NROWS
      NNP=NLNODS+10*NSHELL
      NNSEL=NLNODS+NSHLTY
      NLAST=NNSEL+NSHELL
      CALL RFL(NLAST)
      CALL INIT(A(NINDEX),A(NLNODS),A(NNP),A(NNSEL))
      DO 20 I=1,NCOLS
      CALL IN4COL(2,A(NU),NCOLS,NROWS,11,NFIN,NERR,0)
   20 CALL STRESS(TITLE,DA,TI,1,A(NU),A(NLNODS),A(NNP))
      END
*DECK INIT
      SUBROUTINE INIT(INDEX,LNODS,NP)
      DIMENSION INDEX(1),LNODS(10,1),NP(1)
      COMMON/N/NUMNP,NSHELL,NBEAM,NSHLTY,NBMTY,NGAUS
      COMMON/BLOCK/BLOCK(790)
    1 CALL OPENMS(3,INDEX,9*NSHLTY+1,0)
      READ(1) ((LNODS(J,I),J=1,10),I=1,NSHELL)
      DO 10 I=1,NSHLTY
      READ(1) LT,NP(LT)
      NPP=NP(LT)
      DO 10 J=1,NPP
      READ(1) BLOCK
   10 CALL WRITMS(3,BLOCK,790,9*LT+J-9)
      READ(1) ((LNODS(J,I),J=1,10),I=1,NSHELL)
      RETURN
      END
```

```
*DECK STRESS
      SUBROUTINE STRESS(TITLE,DATE,TIME,ICASE,U,LNODS,NP)
      DIMENSION U(1),LNODS(10,1),NP(1)
      DIMENSION TITLE(8)
      COMMON/BLOCK/STRESM(6,32),WSHEL(13,45),POINT(3),FRAM(3,3),THIK
      COMMON/N/NUMNP,NSHELL,NBEAM,NSHLTY,NBMTY
      DIMENSION ELDISP(32),S(3,6),FF(6)
      DIMENSION ISH(6,8)
      DATA ISH/1,2,3,0,0,0,
     .         4,5,6,7,8,0,
     .         9,10,11,0,0,0,
     .         12,13,14,15,16,0,
     .         17,18,19,0,0,0,
     .         20,21,22,23,24,0,
     .         25,26,27,0,0,0,
     .         28,29,30,31,32,0/
      DATA PI/3.1415927/
      IF (NSHELL.EQ.0) GO TO 300
C
C     SHELL ELEMENTS
C
      IJ=0
      DO 200 I=1,NSHELL
C
C       GET ELEMENT DISPLACEMENTS
C
        DO 115 J=1,8
          L=LNODS(J+2,I)
          IF (L.EQ.0) GO TO 115
          DO 110 K=1,6
            MDOF=6*(L-1)+K
            LDOF=ISH(K,J)
            IF (LDOF.NE.0) ELDISP(LDOF)=U(MDOF)
  110       CONTINUE
  115     CONTINUE
C
C       LOOP ON GAUSS POINTS
C
        NGAUS=NP(LNODS(2,I))
        DO 170 J=1,NGAUS
          CALL READMS(3,STRESM,790,9*LNODS(2,I)+J-9)
          IJ=IJ+1
C
C         GET 6 FORCE RESULTANTS IN LOCAL COORD
C
          DO 120 K=1,6
  120       CALL SCPROD(32,6,1,STRESM(K,1),ELDISP,FF(K))
C
C         LOOP ON Z=H/2, 0, -H/2 FOR COMBINED BENDING-STRETCHING
C
```

```
      Z=THIK/2
      T3=THIK**3
      DO 140 K=1,3
C
C       GET SX, SY, TXY
C
        DO 130 L=1,3
  130     S(K,L)=FF(L)/THIK+FF(L+3)*12*Z/T3
C
C       GET PRINCIPAL STRESSES
C
        SS=(S(K,1)+S(K,2))/2.
        TT=(S(K,1)-S(K,2))/2.
        RR=SQRT(TT*TT+S(K,3)**2)
        S(K,4)=SS+RR
        S(K,5)=SS-RR
        S(K,6)=0.
        IF (S(K,3).NE.0..OR.TT.NE.0.)
     .  S(K,6)=0.5*ATAN2(-S(K,3),TT)*180/PI
  140   Z=Z-THIK/2
      IF (MOD(IJ,8).EQ.1)
     . WRITE(6,150) TITLE,ICASE,DATE,TIME
  150 FORMAT (26H1SEMI-LOOF STRESS RECOVERY//1X,8A10/
     . T100,4HCASE,I3,2(2X,A10)//
     . 8H ELEMENT,T12,8HLOCATION,T31,11HLOCAL X/Y/Z,T55,
     . 23H** FORCE  RESULTANTS **,T90,
     . 40H** STRESSES SX/SY/TXY/SMAX/SMIN/ANGLE **/
     . T55,9HFX/FY/FXY,T69,9HMX/MY/MXY,T91,3HTOP,T105,6HMIDDLE,
     . T120,6HBOTTOM)
      WRITE(6,160) I,POINT(1),(FRAM(K,1),K=1,3),FF(1),FF(4),
     .                           (S(K,1),K=1,3)
  160 FORMAT (/I5,T10,2HX=,E10.4,T26,3HX=(,3F7.4,1H),
     .     T53,E12.6,T68,E12.6,T85,3E15.6)
      WRITE(6,161) POINT(2),(FRAM(K,2),K=1,3),FF(2),FF(5),
     .                           (S(K,2),K=1,3)
  161 FORMAT (T10,2HY=,E10.4,T26,3HY=(,3F7.4,1H),
     .     T53,E12.6,T68,E12.6,T85,3E15.6)
      WRITE(6,162) POINT(3),(FRAM(K,3),K=1,3),FF(3),FF(6),
     .                           (S(K,3),K=1,3)
  162 FORMAT (T10,2HZ=,E10.4,T26,3HZ=(,3F7.4,1H),
     .     T53,E12.6,T68,E12.6,T85,3E15.6)
      WRITE(6,163) ((S(L,K),L=1,3),K=4,6)
  163 FORMAT (2(T85,3E15.6/),T82,3F15.2)
  170 CONTINUE
  200 CONTINUE
  300 RETURN
      END
W
```

APPENDIX C

DETAILED DESCRIPTION OF SOFTWARE USED IN STATISTICAL ENERGY ANALYSIS EXPERIMENT

C.1 GENERAL

The experimental investigation of the wave transmission method for implementing an SEA model was carried out using a minicomputer-based data analysis system. The computer and peripheral A/D converters replace a rather large amount of special-purpose analog gear which would otherwise be required and at the same time allow much greater flexibility in data analysis. However, to fully explain the procedure, some description of the software is needed. This description, along with source code listings, is provided in this appendix. It should be noted that the group of programs, while quite easy to use, does not represent a finished product. It is presented simply as the least ambiguous way of describing the experimental data processing.

The programs are written in Time Series Language (TSL), a proprietory language developed by Time/Data Division of Genrad. A working familiarity with the language, with standard vendor-supplied subroutines and with the DEC RT-11 operating system, is assumed. As written, the programs run on a Time/Data Model TDA-25 system and require a cartridge disc peripheral (DEC model RK05 or equivalent) and Tektronix 4000 series CRT terminal.

In the next section a brief functional description of each subroutine is given. Following that, a list of the subroutine groups which make up each load module is given along with the required subroutine call formats. Finally, source listings are given for all TSL subroutines. No listing for vendor-supplied machine language routines are given since these are not normally available to the user.

C.2 SUBROUTINE DESCRIPTIONS

The total program package is too large to fit in memory at one time. It is divided into groups of subroutines which are loaded and run as needed for various tasks. Since the TSL interpreter does not allow automatic handling of overlays, the groups must be loaded under manual control from the keyboard. In this section each subroutine is described individually.

Subroutine Name: ADSET
Description: Vendor-supplied machine language driver for A/D converters. In the current application it is accessed only through other vendor-supplied TSL subroutines which provide a simple operator interface.

Subroutine Name(s): SETADS, SETUP, PARAM, IO, IOALL
Description: Standard subroutines from the vendor-supplied TSL applications library which set, retrieve, store, and list all control parameters for the A/D peripheral. They are described in the TSL user manual for TDA-25 systems.

Subroutine Name: RTIO
Description: Vendor-supplied machine language subroutine to allow storage and retrieval of data on the system disc. It is described in the vendors application note.

Subroutine Name: DISPLY
Description: Vendor-supplied machine language routine to provide graphical display of data. It is described in the TSL manual.

Subroutine Name: CPHASE
Description: Vendor-supplied machine language subroutine which performs linear phase correction on cross-spectral density functions. It is used to compensate for non-simultaneous

sampling of the multiplexed analog signals and is described in the TDA-25 system documentation.

Subroutine Name: TRAN1

Description: Computes mobility function from acceleration signal on channel 2 and force signal on channel 1. Uses setup conditions previously stored under subroutine SETUP. Prompts operator for channel scale factors EU_A and EU_B in engineering units per volt and returns the mobility function in consistent engineering units (CEU's). Simultaneously computes coherence and channel 1 autopower spectral density.

Subroutine Name: NORM1

Description: Called by TRAN1 to provide proper normalization of mobility (EU_A-SEC/EU_B), coherence (nondimensional), and channel 1 autopower (EU_A^2/Hz.).

Subroutine Name: CLF

Description: Computes coupling loss factor by the wave transmission formula:

$$\omega\eta_{AB} = \frac{1}{m_A} \frac{R_e(\overline{H}_B)}{\left|\overline{H}_A + \overline{H}_B + H_c\right|^2}$$

where

$$\left.\begin{array}{l}\overline{H}_A = H_A(f_c) \\ \overline{H}_B = H_B(f_c)\end{array}\right\}$$ complex coupling point mobilities of bodies A and B previously measured under TRAN1, frequency-averaged under AVGRB, and stored on disc.

m_A = mass of body A

$H_c(f) = \dfrac{i\,2\pi\,f}{k_c}$

k_c = coupling stiffness

$i = \sqrt{-1}$

f_c = center frequency of averaging band

Subroutine Name: CLFD

Description: Computes coupling loss factor by the same wave transmission formula as does CLF except that a direct connection between bodies A and B is assumed. This implies $k_c = \infty$ and $H_c = 0$.

Subroutine Name: AVGRB

Description: Performs a running average on a real or complex TSL block. When used on a complex block, the real and imaginary parts are smoothed separately. Averaging window width is specified in the call but must be $1/2^k$ times the width of the block. The value deposited in the destination block at a particular discrete frequency f_c is an approximation to

$$\overline{H}(f_c) = \frac{1}{\Delta f} \int_{f_c-\frac{\Delta f}{2}}^{f_c+\frac{\Delta f}{2}} H(f)\, df$$

The approximation comes about from the fact that H(f) is obtained by measurement using discrete Fourier transform methods and is therefore known only as a discrete frequency series approximation to the true continuous function. The definite integration is approximated by a finite sum over a portion of the series.

Subroutine Name: DISPL2

Description: Displays unaveraged and averaged functions on the same plot scale as dotted and solid lines, respectively.

Subroutine Name: EBEA

Description: Computes predicted ratio of smoothed energy spectral densities $\overline{E}_A(f_c)/\overline{E}_B(f)$ from data files for $\omega\eta_{AB}$ and $\omega\eta_B$ previously computed and stored on disc. Uses the formula

$$\frac{\overline{E}_B(f_c)}{\overline{E}_A(f_c)} = \frac{\omega\eta_{AB}}{\omega\eta_B + \omega \frac{N_A}{N_B} \eta_{AB}}$$

Subroutine Name: PTRAN

Description: Computes transmitted power from force and acceleration signals at coupling point. Requests scale factors EU_A and EU_B for channels A and B in engineering units per volt. Expects force signal on channel A and returns the spectral density of transmitted power in (EU_A - EU_B - sec/Hz.).

Subroutine Name: LVXPS

Description: Called by PTRAN to compute the complex cross power spectral density between velocity and force by using signals proportional to acceleration and force.

Subroutine Name: NORM3

Description: Called by LVXPS to normalize the discrete cross power spectrum to account for channel scale factors, record length, number of records per ensemble, and double-sided DFT.

Subroutine Name: ENERGY

Description: Computes and stores a file of velocity power spectral densities and mass weighting coefficients which are later used by routine EADD to compute the total energy of a vibrating structure. Uses signals proportional to acceleration and computes for two points at a time. Prompts operator for channel scale factors and accelerometer locations.

Subroutine Name: PSDV2

Description: Called repeatedly by ENERGY to compute velocity power spectral density.

Subroutine Name: NORM2

Description: Called by PSDV2 to normalize velocity PSD to single-sided $(EU - SEC)^2/Hz$. EU represents a scale factor in acceleration engineering units per volt for channel A or B as previously input under prompt from ENERGY.

Subroutine Name: EADD

Description: Uses an RTIO file of velocity PSD's previously stored by ENERGY to compute the energy spectral density for a component. Mass weighting coefficients are stored as the zero frequency entries of the velocity PSD's.

C.3 CALLING FORMATS

In this section the call formats are given for the various subroutines. The sequence in which they are presented represents a typical acquisition and processing run as described in section 3.4.3. It will be assumed that the system of units being used is force, length, and time in lbf., inches, and seconds. Consistent units for acceleration and force scale factors are thus (in/sec^2)/volt and lbf/volt. In the following, prompts from computer are underlined and operator inputs are in capital letters. It is assumed that step 1 of the procedure is complete and that the RT-11 monitor and TSL interpreter are loaded and running. Storage of data is assumed to be done manually under calls to the subroutines of RTIO except for the multiple velocity PSD's measured in step 3 of section 3.4.3 which are stored under program control. RTIO usage is a standard TSL operation and will not be described further. Optional subroutine arguments are indicated by brackets. RT-11 file names and other text strings are enclosed in single quotes. All functions except point velocity PSD's are most conveniently stored in individual RT-11 files.

The description begins at step 2 of section 3.4.3.

CALL	EXPLANATION
>LOAD'PTRANL'	Loads all required subroutines for measuring transmitted power.
>SETUP	Initiates a question-and-answer session to establish data acquisition conditions.
>PTRAN	Starts program to measure the spectral density of transmitted power.

INPUT FORCE (CH A) CEU/V — Operator connects force signal to channel A input and responds with scale factor and carriage return (CR).

INPUT ACCEL (CH B) CEU/V — Operator responds similarly for acceleration channel.

The spectral density of transmitted power is then measured, placed in a real floating point block B8, displayed on the system CRT, and control is returned to the operator. He may inspect and store the function as desired.

>CLEAR

>LOAD 'NRGL' — Load all subroutines needed to measure component energy.

>SETUP — Establish A/D conditions.

>ENERGY 'E_i Filename', 'text', recnum, mass [,'N']

'E_i Filename' — RT-11 file for storage of velocity PSD's at various points on the structure. Point number is used as file record number.

'text' — Descriptive text string for E_i file.

recnum — Total number of desired records (new file) or next record to be filled (existing file).

mass — Mass coefficient to be stored with each velocity PSD. This version of the software assumes the same mass is associated with each point.

'N'	Denotes new file. Omit to resume filling an existing file.
CH A EU/VOLT CH B EU/VOLT	Operator inputs accelerometer scale factors for channels A and B each terminated by (CR).
CH A TO POINT 1 CH B TO POINT 2	Operator mounts accelerometers and initiates measurement with (CR). Machine measures velocity PSD's, displays them, stores them in appropriate file records if ok'ed by the operator, and issues prompts to move accelerometers to the next two points.

>CLEAR

>LOAD 'EADDL'	Loads subroutines to compute smoothed spectral density of component energy from point velocity PSD's and mass coefficients stored under ENERGY.

>EADD 'E_i Filename', firstrec, lastrec

'E_i Filename'	File of point velocity PSD's and mass coefficients previously created under ENERGY.
firstrec	Point number of first velocity PSD to be included in mass weighted sum.
lastrec	Point number of last velocity PSD to be included in mass weighted sum.

Subroutine EADD will compute the spectral density of the total component energy as a mass-weighted sum of the point velocity PSD's and place it in real floating point block B8. The function is next frequency averaged.

$\underline{>}$AVGRB B8, B9, avgfct

B8	Source block to be frequency averaged, in this case B8.
B9	Destination block where frequency averaged function is placed.
avgfct	Desired ratio of maximum DFT analysis frequency to averaging bandwidth.

The smoothed and unsmoothed component energy function may now be inspected and stored as desired under manual control. This completes step 3 of section 3.4.3.

The structures are next uncoupled and the shaker and transducing equipment rearranged to measure the admittance at the coupling point to body B.

$\underline{>}$CLEAR

$\underline{>}$LOAD 'HZACQL'	Loads all subroutines required for mobility measurement. To save core, AVGRB is not yet loaded.
$\underline{>}$SETUP	Establish A/D parameters.
$\underline{>}$TRAN1	Initiates program to measure $H_B(f)$.

INPUT FORCE (CH A) CEU/V — Operator connects force signal to channel A input, inputs scale factor and (CR).

INPUT ACCEL (CH B) CEU/V — Operator responds similarly for acceleration channel.

The program performs the measurements and computations to obtain $H_B(f)$. It is placed in a complex floating point block B8, displayed, and control is returned to the operator. The operator will normally inspect it and use RTIO calls to store it on disc as appropriate. The shaker and transducing are moved to body A and the process repeated to obtain $H_A(f)$. To obtain smoothed versions of H_A and H_B, the subroutine AVGRB is loaded.

$\geq$BLKCLR

$\geq$LOAD'AVGRB'

The functions $H_A(f)$ and $H_B(f)$ are read into memory by manual calls to RTIO and smoothed versions $\overline{H}_A(f_c)$ and $\overline{H}_B(f_c)$ are computed using AVGRB just as was done for component energy functions. AVGRB will handle either real or complex blocks. $\overline{H}_A(f_c)$ and $\overline{H}_B(f_c)$ are manually stored as usual. This completes step 6 of section 3.4.3.

$\geq$CLEAR

$\geq$LOAD 'CLFL'

$\geq$CLF 'H_AFile', 'H_B File', k_c, m_A

'H_AFile' — File where $\overline{H}_A(f_c)$ was stored previously.

'H_BFile'	File where $H_B(f_c)$ was stored previously.
k_c	Coupling stiffness
m_A	Mass of body A.

The power transfer coefficient $2\pi f_c \eta_{AB}$ is computed from $\bar{H}_A(f_c)$, $\bar{H}_B(f_c)$, k_c and m_A by CLF using equation 3.56 of this report. This is the predicted value of normalized transmitted power $<\pi_{AB}>_t/<E_A>_t$.

The actual value of frequency-dependent internal loss factor $\eta_B(f_c)$ is formed under manual control from the keyboard. The smoothed spectral densities of transmitted power and component B energy are read into memory and their ratio is formed. This is $2\pi f_c \eta_B(f_c)$ which is then written to disc.

The predicted energy ratio is next computed using the predicted coupling loss factor and actual internal loss factor.

$\underline{>}$CLEAR

$\underline{>}$LOAD 'EBEAL'	Loads all subroutines needed to compute $<E_B>_t/<E_A>_t$

EBEA '$\omega\eta_{AB}$File', '$\omega\eta_B$File', A_A/A_B

'$\omega\eta_{AB}$File'	File where predicted weighted coupling loss factor has previously been stored.
'$\omega\eta_B$File'	File where actual weighted internal loss factor of plate B has been previously stored.
A_A/A_B	Area ratio of plates

The predicted value of $<E_B>_t/<E_A>_t$ is computed using eq. 3.8 of this report. It is placed in a real floating block B8, displayed, and control is returned to the operator. He may then inspect and store the function as desired.

The actual values of normalized transmitted power $<\pi_{AB}>_t/<E_A>_t$ and normalized receptor energy $<E_B>_t/<E_A>_t$ are computed under manual control from the keyboard. The quantity $<\pi_{AB}>_t$ is simply the smoothed spectral density of transmitted power times the smoothing bandwidth. A similar interpretation holds for $<E_B>_t$ and $<E_A>_t$. Since the same smoothing band was used throughout, the desired ratio is easily found. The previously measured and smoothed spectral densities are read into memory and divided. The ratio functions are then written back onto disc.

Predicted and measured values for all comparison values are now available. The standard TSL plot routine was used for making most of the figures of Chapter 3.0.

C.4 PROGRAM LISTING

Subroutine tables for each load module and source listing for each TSL subroutine are as follows.

```
LOAD 'HZACQL'
:PSTAB
IOP          63
IOALL       460
SETUP        70
PARAM       116
SETADS      169
HLET         34
ADSET      1415
CPHASE      199
NORM1        57
DISPLY     1800
OPEN        816
CLOSE        32
WRITEH      168
READH       362
WRITEB       53
READB        61
WAITIO       29
SPFUN        40
STORE        26
TRAN1       247
TOTAL-6217
>
```

```
LOAD 'CLFL'
:PSTAB
OPEN        816
CLOSE        32
WRITEH      168
READH       362
WRITEB       53
READB        61
WAITIO       29
SPFUN        40
DISPLY     1800
CLF         175
AVGRB       196
DISPL2      122
TOTAL-3854
>
```

```
LOAD 'PTRANL'
:PSTAB
OPEN        816
CLOSE        32
WRITEH      168
READH       362
WRITEB       53
READB        61
WAITIO       29
SPFUN        40
PARAM       116
IOALL       460
SETUP        70
ADSET      1415
SETADS      169
HLET         34
DISPLY     1800
IOP          63
CPHASE      199
LUXPS       330
NORM3        33
PTRAN       108
STORE        26
TOTAL-6384
>
```

```
LOAD 'NRGL'
:PSTAB
OPEN        816
CLOSE        32
WRITEH      168
READH       362
WRITEB       53
READB        61
WAITIO       29
SPFUN        40
DISPLY     1800
ADSET      1415
SETADS      169
HLET         34
SETUP        70
IOALL       460
PARAM       116
IOP          63
ENERGY      541
PSDV2       168
NORM2        81
TOTAL-6478
>
```

```
LOAD 'EADDL'
:PSTAB
OPEN        816
CLOSE        32
WRITEH      168
READH       362
WRITEB       53
READB        61
WAITIO       29
SPFUN        40
DISPLY     1800
LABEL        77
AVGRB       154
STORE        26
DISPL2       53
EADD        183
TOTAL-3854
>
```

```
LOAD 'EBEAL'
:PSTAB
OPEN        816
CLOSE        32
WRITEH      168
READH       362
WRITEB       53
READB        61
WAITIO       29
SPFUN        40
DISPLY     1800
DISPL3      122
EBEA         88
TOTAL-3571
>
```

```
LIST IOP
CREATE IOP
10 PRINT P0,': ',';'
20 GOTO I3,30,100
30 INPUT 'KB',P1
40 ARG I0
50 IF I0,4,110,110,60
60 IF P1,P3,10,70,70
70 IF P1,P4,110,110,10
100 PRINT P2,'=',P1
110 RETURN
END
>
```

```
LIST IOALL
CREATE IOALL
10 IOP 'FRAME SIZE',I15,'I15',128,8192
20 STACK 100,115,0,1.,3,150,165,.5,165,100,0,1.,2,1,1,165,150
30 IOP 'CHANNEL CODE 1=A 2=B 3=AB',I14,'I14',1,3
40 IOP 'BANDWIDTH',R15,'R15',0,80000.
50 IF R15,25000,80,80,60
60 PRINT 'NO FILTERS'
70 IOP 'SAMPLE RATE',R14,'R14',1,160000.
80 IOP 'CHANNEL A LEVEL, VOLTS',R13,'R13',0,16
90 IOP 'CHANNEL B LEVEL, VOLTS',R12,'R12',0,16
100 IOP 'BUFFER CODE 0=SINGLE 1=DOUBLE',I13,'I13',0,1
110 IOP 'TRIGGER 0=OFF 1=FIRST 2=EACH FRAME',I12,'I12',0,2
120 IF I12,170,170,130
130 IOP 'TRIGGER SOURCE 0=A 1=B 2=EXT',I11,'I11',0,2
140 IOP 'TRIGGER SLOPE 0=POS 1=NEG 2=+OR- 3=DIG',I10,'I10',0,3
150 IOP 'TRIGGER LEVEL %',R11,'R11',-99,99
160 IOP 'TRANSIENT CAPTURE % (0=OFF)',R10,'R10',0,99
170 IOP 'COUPLING 0=AC 1=DC',I9,'I9',0,1
180 IOP 'AVERAGE REMOVAL 0=OFF 1=REMOVE',I8,'I8',0,1
190 IOP 'ZERO INSERTION 0=OFF 1=ON',I7,'I7',0,1
200 IOP 'ERROR TRAPS 0=ENABLE 1=DISABLE',I6,'I6',0,1
210 IOP 'FRAME COUNT',I5,'I5'
220 IOP 'HANNING WINDOW 0=OFF 1=ON',I4,'I4',0,1
230 RETURN
END
>
```

```
LIST SETADS
-CREATE SETADS
10 BLKCLR
20 STACK 100,101,102
30 HLET I0,I14,'XXA B AB'
40 STACK 25000.,R15,31,250
50 ADSET 'SU',B0,I15,I0,R0,R13,'VB',R12
60 IF R15,25000,80,80,70
70 ADSET 'SF',R14,'FL',0
80 HLET I0,I9,'ACDC'
90 HLET I1,I8,'DDED'
100 HLET I2,I7,'DZEZ'
110 ADSET 'CL',I0,I1,I2
120 HLET I0,I6,'ETDT'
130 HLET I1,I13,'SBDB'
140 ADSET I0,I1
150 IF I12,210,210,160
160 HLET I0,I12,'XXTFTE'
170 PROD I1,I11,4
180 SUM I1,I1,I10
190 HLET I1,I1,'APANABADBPBNBBBDEPENEBED'
200 ADSET I0,I1,R11,'TC',R10
210 STACK 152,151,150
220 RETURN
END
>
```

```
LIST SETUP
CREATE SETUP
10 ERASE
20 ARG I3
30 GOTO I3,40,60
40 IOALL
50 RETURN
60 ARG 0,P0,I3
70 IF I3,8,80,100,80
80 PRINT 'BAD FILE SPEC'
90 RETURN
100 INPUT P0,I15,I14,I13,I12,I11,I10,I9,I8,I7,I6,I5,I4,R15,R14,R13,R-
12,R11,R10
110 END
120 RETURN
END
>
```

```
LIST PARAM
CREATE PARAM
10 ARG I3
20 GOTO I3,30,90
30 ERASE
40 PRINT 'CURRENT SETUP'
50 PRINT
60 LET I3,1
70 IOALL
80 RETURN
90 ARG 0,P0,I3
100 IF I3,8,110,130,110
110 PRINT 'BAD FILE SPEC'
120 RETURN
130 WRITE P0,I15,',',I14,',',I13,',',I12,',',I11,',',I10,',',I9
140 WRITE P0,I8,',',I7,',',I6,',',I5,',',I4,',',R15,',',R14,',',R13,-
',',R12,',',R11,',',R10
150 END
160 RETURN
END
>
```

```
LIST EBEA
CREATE EBEA
10 REMARK "ETAAB .CLF","ETAB .NAD",AA/AB
20 OPEN P0
30 READH
40 READH B8
50 READB B8
60 OPEN P1
70 READH
80 READH B9
90 READB B9
100 CLOSE
105 MOVE B8,B10
110 MLCONR P2,B10
120 ADD B9,B10
130 DIV B10,B8
140 DISPLY B8,'EX',0,1000,'L25','SC',1.,'G','R'
150 RETURN
END
>
```

```
>LIST EADD
CREATE EADD
5 REMARK "EIFILE",FIRSTREC,LASTREC
10 BLKCLR
20 OPEN 0,P0,'B'
30 READH 0,B7
40 READB 0,B7,'R',0
50 MOVE B7,B8
60 ZERO B8
100 FOR I0,P1,P2
110 READB 0,B7,'R',I0
120 LET R6,B7,0
130 LET B7,0,0.
140 MLCONR R6,B7
150 ADD B7,B8
160 NEXT I0
170 MOVE B8,B7
180 BIBSET B7,5,I15
190 BIBSET B7,6,R1
200 QUOT R1,R1,2.
210 QUOT R1,R1,I15
215 MLCONR R1,B7
220 INTG B7
225 DIF I15,I15,1
230 LET R2,B7,I15
250 PRINT 'INPUT AVG. FACTOR'
260 INPUT R14
265 DISPLY B8,'YLAB','NRG/HZ','R'
270 AVGRB B8,B9,R14
280 BEAMP 550,700
290 PRINT 'TOTAL ENERGY = ',R2,'  C.E.U.'
300 RETURN
END
>
```

```
LIST NORM2
CREATE NORM2
10 REMARK GIVES S.S. EU**2/HZ
20 BIBSET B7,6,R7
30 BIBSET B7,5,I3
40 QUOT R7,R7,4.
50 QUOT R7,I3,R7
60 QUOT R7,R7,I5
70 PROD R14,R8,R8
80 PROD R14,R7,R14
90 MLCONR R14,B7
100 PROD R14,R9,R9
110 PROD R14,R7,R14
120 MLCONR R14,B8
130 PROD R7,I5,R7
140 QUOT R7,2.,R7
150 RETURN
END
>
```

```
LIST PSDV2
CREATE PSDV2
10 LET I14,3
20 SETADS
30 FOR I0,1,I5
40 ADSET 'SA'
50 DFT B0,I4
60 DFT B1,I4
70 ASPEC B0,B7
80 ASPEC B1,B8
90 NEXT I0
100 NORM2
110 PROD R1,6.283,R7
120 MOVE B7,B10
130 STCONR R1,B10
140 LET B10,0,0.
150 INTG B10
160 MUL B10,B10
170 LET B10,0,1.
180 FOR I0,0,2
190 LET B7,I0,0.
200 LET B8,I0,0.
210 NEXT I0
220 DIV B10,B7
230 DIV B10,B8
240 DISPLY B7,'YLAB','S(F)','R'
250 DISPLY B7,'GLAB','VELOCITY PSD','R'
260 DISPLY B7,'M','EX',0,R15,'G','R'
270 DISPLY B8,'NG','M','EX',0,R15,'G','R'
280 RETURN
END
>
```

```
LIST ENERGY
CREATE ENERGY
3 REMARK 'EFILE','TEXT',MAX OR
4 REMARK  NEXTREC,MASS,['N']
10 BLKCLR
20 PRINT 'CH A EU/VOLT'
30 INPUT R8
40 PRINT 'CH B EU/VOLT'
50 INPUT R9
60 ARG I0
70 IF I0,4,250,250,90
80 REMARK INITIALIZE NEW FILE
90 SETADS
100 ADSET 'SA'
110 DFT B0
120 ASPEC B0,B7
130 ZERO B7
140 OPEN P0,'N','B'
145 WRITEH B7,P1
150 SUM I2,P2,1
160 FOR I1,1,I2
180 WRITEB B7
190 NEXT I1
200 CLOSE
210 LET I1,1
220 SUM I2,I1,1
230 GOTO 270
240 REMARK OLD FILE:SET POINTERS
250 LET I1,P2
260 SUM I2,I1,1
270 REMARK ACQUIRE DATA FOR PSDV FILE
280 LET R6,P3
290 PRINT 'CH.A TO POINT ',I1
300 PRINT 'CH.B TO POINT ',I2
310 HOLIN
320 PRINT '(CR) TO BEGIN'
330 HOLIN I3
340 IF I3,13,330,350,330
350 PRINT 'NOW ACQUIRING'
360 PSDV2
370 REMARK STORE MASS AS DC VALUE
380 LET B7,0,R6
390 LET B8,0,R6
400 OPEN P0,'B'
420 WRITEB B7,I0,'R',I1
440 WRITEB B8,I0,'R',I2
460 IF I0,0,470,490,470
470 PRINT 'WRITEB ERROR'
480 RETURN
490 PRINT 'WHAT NOW?'
500 PRINT '     PROCEED   (PR)'
510 PRINT '     REPEAT    (RE)'
520 PRINT '     PAUSE     (PA)'
530 PRINT '     EXIT      (EX)'
540 HINPUT I3,'PR','RE','PA','EX'
550 IF I3,1,560,610,560
560 IF I3,2,570,290,570
570 IF I3,3,580,650,580
580 IF I3,4,590,640,590
590 PRINT 'WHAT?'
600 GOTO 540
610 SUM I1,I1,2
620 SUM I2,I1,1
630 GOTO 290
640 RETURN
650 PRINT 'DISPLAY A OR B?'
660 HINPUT I3,'A','B'
670 IF I3,1,680,710,680
680 IF I3,2,690,730,690
690 PRINT 'WHAT?'
700 GOTO 660
710 DISPLY B7,'M','EX',0,R15,'G'
720 GOTO 490
730 DISPLY B8,'M','EX',0,R15,'G'
740 GOTO 490
750 RETURN
END
>
```

```
LIST PTRAN
CREATE PTRAN
10 PRINT 'PTRAN MEASURES POWER '
15 PRINT 'FLOW INTO BODY 2 FROM'
17 PRINT 'FORCE AND ACCELERATION'
18 PRINT 'AT THE COUPLING POINT'
30 PRINT
35 PRINT 'INPUT FORCE (CH A) CEU/V'
50 INPUT R8
60 PRINT 'INPUT ACCEL (CH B) CEU/V'
75 INPUT R9
80 LUXPS
90 RETURN
END
>
```

```
LIST NORM3
CREATE NORM3
10 BIBSET B7,6,R7
12 QUOT R0,I15,R7
14 QUOT R0,R0,I5
20 PROD R0,R0,R8
30 PROD R0,R0,R9
100 MLCONR R0,B7
110 RETURN
END
>
```

```
LIST LUXPS
CREATE LUXPS
10 REMARK COMPUTE L-A XPS
20 LET I14,3
30 SETADS
40 FOR I0,1,I5
50 ADSET 'SA'
60 DFT B0,I4
70 DFT B1,I4
80 CSPEC B0,B1,B7
90 NEXT I0
100 CPHASE B7,1
110 NORM3
120 REMARK CREATE OMEGA IN B10
130 IMAG B7,B8
140 MOVE B8,B10
150 BIBSET B7,6,R7
160 QUOT R1,I15,R7
170 QUOT R1,6.283,R1
180 STCONR R1,B10
190 LET B10,0,0.
200 INTG B10
210 LET B10,0,1.
220 REMARK COMPUTE TRANSMITTED POWER
230 REMARK AND ITS SPECTRAL DENSITY
240 DIV B10,B8
250 QUOT R2,R1,6.283
260 LET B8,0,0.
270 LET B8,1,0.
280 MLCONR 2.,B8
290 MOVE B8,B7
300 MLCONR R2,B7
310 INTG B7
320 BIBSET B7,5,I0
330 DIF I0,I0,1
340 LET R3,B7,I0
350 REMARK  DISPLAY OUTPUT
360 DISPLY B8,'EX',0,R15,'YLAB',' ','
G','R'
370 BEAMP 20,600
380 PRINT 'TRANSMITTED'
390 BEAMP 0,580
400 PRINT 'POWER SPECTRAL'
410 BEAMP 40,560
420 PRINT 'DENSITY'
430 BEAMP 412,740
440 PRINT 'TRANSMITTED POWER = ',R3,'
 C.E.U.'
450 BEAMP 650,710
460 PROD R4,R3,1000000.
470 PRINT ' = ',R4,'MICRO CEU'
480 RETURN
END
>
```

```
LIST DISPL2
CREATE DISPL2
10 REMARK  XMAX,YMAX,IFLOG
20 ARG I7
30 IF I7,3,40,70,70
40 DISPLY B8,'P','EX',0,P0,'SC',P1,'G','R'
50 DISPLY B9,'C','EX',0,P0,'SC',P1,'NG','G','R'
60 GOTO 90
70 DISPLY B8,'P','L50','EX',0,P0,'SC',P1,'G','R'
80 DISPLY B9,'C','NG','L50','EX',0,P0,'SC',P1,'G','R'
90 BEAMP 550,740
100 PRINT 'AVGNG BW. = ',R1,' HZ.'
110 RETURN
END
>
```

```
LIST AVGRB
CREATE AVGRB
10 REMARK  SRCBLK,DSTBLK,AVGFCT
20 MOVE P0,P1
30 ZERO P1
40 BIBSET P0,5,I15
50 BIBSET P0,6,R1
60 QUOT R1,R1,2.
70 QUOT R1,R1,P2
80 QUOT I14,I15,P2
90 DIF I13,I15,I14
100 DIF I13,I13,1
110 QUOT I12,I14,2
120 FOR I11,0,I13
130 BIBSET P0,4,I8
140 BLKDEF B0,I14,I8,P0,I11
150 MOVE B0,B1
160 INTG B1
170 DIF I10,I14,1
180 IF I8,1,190,190,240
190 LET R0,B1,I10
200 QUOT R0,R0,I14
210 SUM I9,I12,I11
220 LET P1,I9,R0
230 GOTO 280
240 LET C0,B1,I10
245 QUOT R2,1.,I14
250 STACK 202,300,9,350
260 SUM I9,I12,I11
270 LET P1,I9,C0
280 NEXT I11
290 DISPLY P0,'P','G','R'
300 DISPLY P1,'NG','G','R'
310 BEAMP 550,740
320 PRINT 'AVGNG BDWTH = ',R1,' HZ.'
330 RETURN
END
>
```

```
>LIST CLF
CREATE CLF
5 REMARK "HAFILE","HBFILE",KC,MA
10 OPEN P0
20 READH
30 READH B10
40 READB B10
50 CLOSE
60 PRINT
70 OPEN P1
80 READH
90 READH B11
100 READB B11
110 CLOSE
120 ASPEC B10,B8
130 ZERO B8
140 ASPEC B10,B9
150 ZERO B9
160 ADD B11,B10
170 BIBSET B11,6,R7
180 BIBSET B11,5,I0
190 QUOT R1,R7,I0
200 PROD R1,R1,3.141
210 MOVE B11,B12
220 STCONR R1,B9
230 ZERO B8
240 COMPLX B9,B8,B12
250 MOVE B12,B11
260 INTG B11
270 SUB B12,B11
280 QUOT R2,1.,P2
290 MLCONR R2,B11
300 MOVE B11,B12
310 ADD B11,B10
320 ASPEC B10,B9
330 OPEN P1
340 READH B11
350 READB B11
360 CLOSE
370 REAL B11,B8
380 DIV B9,B8
390 QUOT R2,1.,P3
400 MLCONR R2,B8
420 RETURN
END
>
```

```
LIST TRAN1
CREATE TRAN1
10 LET I14,3
20 PRINT 'INPUT FORCE (CH A) CEU/V'
30 INPUT R8
40 PRINT 'INPUT ACCEL (CH B) CEU/V'
50 INPUT R9
60 SETADS
70 FOR I0,1,I5
80 ADSET 'SA'
90 DFT B0,I4
100 DFT B1,I4
110 CSPEC B0,B1,B7
120 ASPEC B0,B5
130 ASPEC B1,B6
140 NEXT I0
150 CPHASE B7,1
160 NORM1
170 MOVE B5,B1
180 MOVE B5,B0
190 BIBSET B0,6,R7
200 BIBSET B0,5,I0
210 QUOT R1,R7,I0
220 QUOT R1,R1,2
230 PROD R1,R1,6.283
240 STCONR R1,B0
250 STCONR R1,B1
260 INTG B0
270 SUB B1,B0
280 LET B0,0,R1
290 MLCONC (0.,-1.),B7
300 DIV B0,B7
310 DIV B0,B6
320 DIV B0,B6
330 FOR I0,0,2
340 LET B5,I0,B5,3
350 LET B6,I0,B6,3
360 LET B7,I0,B7,3
370 NEXT I0
380 BIBSET B7,5,I0
390 BLKDEF B8,I0,2,B0,0
400 MOVE B7,B8
410 DIV B5,B8
420 MOVE B7,B9
430 ASPEC B9,B9
440 DIV B5,B9
450 DIV B6,B9
460 DISPLY B8,'EX',0,R15,'G','R'
470 RETURN
END
>
```

```
LIST NORM1
CREATE NORM1
10 BIBSET B7,6,R7
20 QUOT R0,I15,R7
30 QUOT R0,R0,I5
40 MLCONR R8,B5
50 MLCONR R8,B5
60 MLCONR R9,B6
70 MLCONR R9,B6
80 MLCONR R8,B7
90 MLCONR R9,B7
100 MLCONR R0,B5
110 MLCONR R0,B6
120 MLCONR R0,B7
130 RETURN
END
>
```

```
LIST CLFD
CREATE CLFD
5 REMARK "HAFILE","HBFILE",MA
8 REMARK "DIRECT CONNECTION" VERSION OF CLF
10 OPEN P0
20 READH
30 READH B10
40 READB B10
50 CLOSE
70 OPEN P1
80 READH
90 READH B11
100 READB B11
110 CLOSE
160 ADD B11,B10
320 ASPEC B10,B9
330 OPEN P1
340 READH B11
350 READB B11
360 CLOSE
370 REAL B11,B8
380 DIV B9,B8
390 QUOT R2,1.,P2
400 MLCONR R2,B8
420 RETURN
END
>
```

APPENDIX D

FUSELAGE MODEL LISTING

```
FULL FUSELAGE FREE VIBRATION
ID FUS,MODE
$NASTRAN MSC
$LOOFFACT 0.2
$LOOFDYN YES
$LOOFECHO YES
SOL 25,0
CHKPNT YES
TIME 20
DIAG 8
CEND
TITLE=FULL FUSELAGE MODEL
SUBTITLE=FIRST MODE
ECHO=NONE
METHOD=2
DYNRED=2
DISP=ALL
BEGIN BULK
CORD2R         1       0      0.      0.      0.      0.      0.      1.+CC1
+CC1           1.     0.      0.
GRID         100       1  28.200   4.000   0.000
GRID        1100       1  28.200  -4.000   0.000
GRID         101       1  27.400   5.800   0.000
GRID        1101       1  27.400  -5.800   0.000
GRID         102       1  26.600   7.097   0.000
GRID        1102       1  26.600  -7.097   0.000
GRID         103       1   24.40    9.90     0.0
GRID        1103       1   24.40  -9.900     0.0
GRID         104       1  22.200  11.341   0.000
GRID        1104       1  22.200 -11.341   0.000
GRID         105       1  18.200  13.381   0.000
GRID        1105       1  18.200 -13.381   0.000
GRID         106       1  14.200  15.011   0.000
GRID        1106       1  14.200 -15.011   0.000
GRID         107       1  10.100  14.448   0.000
GRID        1107       1  10.100 -14.448   0.000
GRID         108       1   6.000  14.188   0.000
GRID        1108       1   6.000 -14.188   0.000
GRID         109       1   1.500  11.750   0.000
GRID        1109       1   1.500 -11.750   0.000
GRID         110       1  -3.408   7.787   0.000
GRID        1110       1  -3.408  -7.787   0.000
GRID         111       1  -4.120   5.003   0.000
GRID        1111       1  -4.120  -5.003   0.000
GRID         112       1  -5.240   0.000   0.000
GRID         113       1  26.600   7.710   6.250
GRID        1113       1  26.600  -7.710   6.250
GRID         114       1  22.200  12.420   6.250
GRID        1114       1  22.200 -12.420   6.250
GRID         115       1  14.200  15.860   6.250
```

GRID	1115	1	14.200	-15.860	6.250
GRID	116	1	6.000	15.410	6.250
GRID	1116	1	6.000	-15.410	6.250
GRID	117	1	-3.204	10.170	6.250
GRID	1117	1	-3.204	-10.170	6.250
GRID	118	1	-6.250	0.000	6.250
GRID	119	1	28.400	4.200	6.250
GRID	1119	1	28.400	-4.200	6.250
GRID	120	1	-4.750	7.590	6.250
GRID	1120	1	-4.750	-7.590	6.250
GRID	121	1	28.560	0.000	0.000
GRID	122	1	28.500	2.400	0.000
GRID	1122	1	28.500	-2.400	0.000
GRID	200	1	28.600	4.393	12.500
GRID	1200	1	28.600	-4.393	12.500
GRID	201	1	27.800	6.800	12.500
GRID	1201	1	27.800	-6.800	12.500
GRID	202	1	26.600	8.313	12.500
GRID	1202	1	26.600	-8.313	12.500
GRID	203	1	24.400	11.600	12.500
GRID	1203	1	24.400	-11.600	12.500
GRID	204	1	22.200	13.500	12.500
GRID	1204	1	22.200	-13.500	12.500
GRID	205	1	19.440	15.110	12.500
GRID	1205	1	19.440	-15.110	12.500
GRID	206	1	14.200	16.700	12.500
GRID	1206	1	14.200	-16.700	12.500
GRID	207	1	10.100	16.750	12.500
GRID	1207	1	10.100	-16.750	12.500
GRID	208	1	6.000	16.639	12.500
GRID	1208	1	6.000	-16.639	12.500
GRID	209	1	1.500	15.098	12.500
GRID	1209	1	1.500	-15.098	12.500
GRID	210	1	-3.000	12.558	12.500
GRID	1210	1	-3.000	-12.558	12.500
GRID	211	1	-5.120	10.345	12.500
GRID	1211	1	-5.120	-10.345	12.500
GRID	212	1	-7.240	0.000	12.500
GRID	213	1	26.600	9.240	19.500
GRID	1213	1	26.600	-9.240	19.500
GRID	214	1	22.200	14.200	19.500
GRID	1214	1	22.200	-14.200	19.500
GRID	215	1	14.200	16.840	19.500
GRID	1215	1	14.200	-16.840	19.500
GRID	216	1	4.550	16.720	19.500
GRID	1216	1	4.550	-16.720	19.500
GRID	217	1	-3.750	13.280	19.500
GRID	1217	1	-3.750	-13.280	19.500
GRID	218	1	-8.630	0.000	19.500
GRID	219	1	28.760	5.120	19.500

GRID	1219	1	28.760	-5.120	19.500
GRID	220	1	-7.200	2.750	12.500
GRID	1220	1	-7.200	-2.750	12.500
GRID	221	1	-7.200	1.750	12.500
GRID	1221	1	-7.200	-1.750	12.500
GRID	222	1	-8.580	3.000	19.500
GRID	1222	1	-8.580	-3.000	19.500
GRID	223	1	29.200	0.000	12.500
GRID	224	1	29.100	2.600	12.500
GRID	1224	1	29.100	-2.600	12.500
GRID	226	1	-5.80	3.0	19.50
GRID	1226	1	-5.80	-3.000	19.50
GRID	227	1	-6.80	3.0	19.50
GRID	1227	1	-6.80	-3.000	19.50
GRID	300	1	28.920	5.840	26.500
GRID	1300	1	28.920	-5.840	26.500
GRID	301	1	28.000	8.300	26.500
GRID	1301	1	28.000	-8.300	26.500
GRID	302	1	26.600	10.176	26.500
GRID	1302	1	26.600	-10.176	26.500
GRID	303	1	24.400	12.826	26.500
GRID	1303	1	24.400	-12.826	26.500
GRID	304	1	22.200	14.892	26.500
GRID	1304	1	22.200	-14.892	26.500
GRID	305	1	18.200	16.651	26.500
GRID	1305	1	18.200	-16.651	26.500
GRID	306	1	14.200	16.975	26.500
GRID	1306	1	14.200	-16.975	26.500
GRID	307	1	10.100	17.009	26.500
GRID	1307	1	10.100	-17.009	26.500
GRID	309	1	3.100	16.800	26.500
GRID	1309	1	3.100	-16.800	26.500
GRID	310	1	0.000	15.750	26.500
GRID	1310	1	0.000	-15.750	26.500
GRID	311	1	-4.500	14.000	26.500
GRID	1311	1	-4.500	-14.000	26.500
GRID	312	1	-10.000	0.000	26.500
GRID	313	1	26.600	10.890	33.000
GRID	1313	1	26.600	-10.890	33.000
GRID	314	1	21.600	15.500	33.000
GRID	1314	1	21.600	-15.500	33.000
GRID	315	1	14.200	17.500	33.000
GRID	1315	1	14.200	-17.500	33.000
GRID	316	1	4.550	17.330	33.000
GRID	1316	1	4.550	-17.330	33.000
GRID	318	1	-11.000	0.000	33.000
GRID	319	1	29.490	5.950	33.000
GRID	1319	1	29.490	-5.950	33.000
GRID	320	1	-9.950	3.250	26.500
GRID	1320	1	-9.950	-3.250	26.500

GRID	321	1	-9.000	7.000	26.500
GRID	1321	1	-9.000	-7.000	26.500
GRID	322	1	0.000	0.000	26.500
GRID	323	1	0.500	3.250	26.500
GRID	1323	1	0.500	-3.250	26.500
GRID	324	1	-7.980	9.170	33.000
GRID	1324	1	-7.980	-9.170	33.000
GRID	325	1	29.990	0.000	26.500
GRID	326	1	29.900	3.500	26.500
GRID	1326	1	29.900	-3.500	26.500
GRID	327	1	-2.00	3.25	26.50
GRID	1327	1	-2.00	-3.250	26.50
GRID	328	1	-7.25	3.25	26.50
GRID	1328	1	-7.25	-3.250	26.50
GRID	330	1	0.250	1.630	26.500
GRID	1330	1	0.250	-1.630	26.500
GRID	331	1	1.800	10.030	26.500
GRID	1331	1	1.800	-10.030	26.500
GRID	332	1	-4.500	8.630	26.500
GRID	1332	1	-4.500	-8.630	26.500
GRID	333	1	-2.250	1.630	26.500
GRID	1333	1	-2.250	-1.630	26.500
GRID	334	1	-4.500	3.250	26.500
GRID	1334	1	-4.500	-3.250	26.500
GRID	335	1	-10.000	1.630	26.500
GRID	1335	1	-10.000	-1.630	26.500
GRID	336	1	-7.250	1.630	26.500
GRID	1336	1	-7.250	-1.630	26.500
GRID	337	1	-5.000	0.000	26.500
GRID	338 1		3.20	17.20	33.00
GRID	13381		3.20	-17.20033.00	
GRID	339	1	0.000	0.000	33.000
GRID	340	1	-5.250	14.550	33.000
GRID	1340	1	-5.250	-14.550	33.000
GRID	341	1	0.250	1.630	33.000
GRID	1341	1	0.250	-1.630	33.000
GRID	400	1	30.050	6.060	39.500
GRID	1400	1	30.050	-6.060	39.500
GRID	401	1	28.000	9.200	39.500
GRID	1401	1	28.000	-9.200	39.500
GRID	402	1	26.500	11.600	39.500
GRID	1402	1	26.500	-11.600	39.500
GRID	403	1	24.400	13.565	39.500
GRID	1403	1	24.400	-13.565	39.500
GRID	404	1	21.000	16.100	39.500
GRID	1404	1	21.000	-16.100	39.500
GRID	405	1	18.200	17.296	39.500
GRID	1405	1	18.200	-17.296	39.500
GRID	406	1	14.200	18.027	39.500
GRID	1406	1	14.200	-18.027	39.500

GRID	407	1	10.100	18.116	39.500
GRID	1407	1	10.100	-18.116	39.500
GRID	408	1	6.000	17.859	39.500
GRID	1408	1	6.000	-17.859	39.500
GRID	409	1	4.500	17.768	39.500
GRID	1409	1	4.500	-17.768	39.500
GRID	410	1	3.200	17.592	39.500
GRID	1410	1	3.200	-17.592	39.500
GRID	411	1	-1.380	16.940	39.500
GRID	1411	1	-1.380	-16.940	39.500
GRID	412	1	-12.000	0.000	39.500
GRID	413	1	26.600	12.550	46.880
GRID	1413	1	26.600	-12.550	46.880
GRID	414	1	21.600	16.650	46.880
GRID	1414	1	21.600	-16.650	46.880
GRID	415	1	14.700	18.760	46.880
GRID	1415	1	14.700	-18.760	46.880
GRID	417	1	-6.500	15.570	46.880
GRID	1417	1	-6.500	-15.570	46.880
GRID	418	1	-13.000	0.000	46.880
GRID	419	1	30.325	6.580	46.880
GRID	1419	1	30.325	-6.580	46.880
GRID	420	1	-10.330	10.870	39.500
GRID	1420	1	-10.330	-10.870	39.500
GRID	421	1	-6.000	15.090	39.500
GRID	1421	1	-6.000	-15.090	39.500
GRID	422	1	0.000	0.000	39.500
GRID	423	1	-10.000	11.270	46.880
GRID	1423	1	-10.000	-11.270	46.880
GRID	426	1	14.450	17.710	46.880
GRID	1426	1	14.450	-17.710	46.880
GRID	427	1	10.350	17.630	46.880
GRID	1427	1	10.350	-17.630	46.880
GRID	428	1	3.100	15.870	46.880
GRID	1428	1	3.100	-15.870	46.880
GRID	429	1	-6.500	14.050	46.880
GRID	1429	1	-6.500	-14.050	46.880
GRID	430	1	0.000	0.000	46.880
GRID	431	1	1.600	8.800	39.500
GRID	1431	1	1.600	-8.800	39.500
GRID	500	1	30.600	7.100	54.250
GRID	1500	1	30.600	-7.100	54.250
GRID	501	1	28.600	11.000	54.250
GRID	1501	1	28.600	-11.000	54.250
GRID	502	1	26.600	13.500	54.250
GRID	1502	1	26.600	-13.500	54.250
GRID	503	1	24.400	16.114	54.250
GRID	1503	1	24.400	-16.114	54.250
GRID	504	1	22.200	17.200	54.250
GRID	1504	1	22.200	-17.200	54.250

```
GRID           505          1   18.200  19.000   54.250
GRID          1505          1   18.200 -19.000   54.250
GRID           506          1   15.200  19.500   54.250
GRID          1506          1   15.200 -19.500   54.250
GRID           507          1   14.700  17.400   54.250
GRID          1507          1   14.700 -17.400   54.250
GRID           508          1    3.070  14.143   54.250
GRID          1508          1    3.070 -14.143   54.250
GRID           509          1   -7.000  13.000   54.250
GRID          1509          1   -7.000 -13.000   54.250
GRID           510          1   -7.000  16.040   54.250
GRID          1510          1   -7.000 -16.040   54.250
GRID           511          1  -11.900  12.830   54.250
GRID          1511          1  -11.900 -12.830   54.250
GRID           512          1  -14.000   0.000   54.250
GRID      513       1        27.45    12.95    61.57
GRID          15131          27.45     -12.95061.57
GRID      514       1        22.20    17.21    61.57
GRID          15141          22.20     -17.21061.57
GRID           515          1   15.215  19.505   61.570
GRID          1515          1   15.215 -19.505   61.570
GRID           516          1  -14.520   9.455   61.570
GRID          1516          1  -14.520  -9.455   61.570
GRID           517          1   -8.250  16.570   61.570
GRID          1517          1   -8.250 -16.570   61.570
GRID           518          1  -15.000   0.000   61.570
GRID           519          1   31.150   6.950   61.570
GRID          1519          1   31.150  -6.950   61.570
GRID           520          1  -14.000   7.450   54.250
GRID          1520          1  -14.000  -7.450   54.250
GRID           521          1    0.000   0.000   54.250
GRID           522          1  -14.000   3.730   54.250
GRID          1522          1  -14.000  -3.730   54.250
GRID           528          1   31.300   4.300   54.250
GRID          1528          1   31.300  -4.300   54.250
GRID           529          1   31.500   0.000   54.250
GRID           530          1    8.700  15.800   54.250
GRID          1530          1    8.700 -15.800   54.250
GRID           531          1   14.950  18.450   54.250
GRID          1531          1   14.950 -18.450   54.250
GRID           532          1   -2.000  13.570   54.250
GRID          1532          1   -2.000 -13.570   54.250
GRID           533          1   -7.000  14.500   54.250
GRID          1533          1   -7.000 -14.500   54.250
GRID           534          1   14.850  16.700   61.570
GRID          1534          1   14.850 -16.700   61.570
GRID           535          1    2.890  14.240   61.570
GRID          1535          1    2.890 -14.240   61.570
GRID           536          1   -8.250  13.130   61.570
GRID          1536          1   -8.250 -13.130   61.570
```

GRID	537	1	1.540	7.070	54.250
GRID	1537	1	1.540	-7.070	54.250
GRID	538	1	-3.500	6.500	54.250
GRID	1538	1	-3.500	-6.500	54.250
GRID	539	1	-10.500	10.230	54.250
GRID	1539	1	-10.500	-10.230	54.250
GRID	540	1	-7.000	0.000	54.250
GRID	541	1	0.000	0.000	61.570
GRID	600	1	31.700	6.800	68.880
GRID	1600	1	31.700	-6.800	68.880
GRID	601	1	30.500	9.500	68.880
GRID	1601	1	30.500	-9.500	68.880
GRID	602	1	28.300	12.400	68.880
GRID	1602	1	28.300	-12.400	68.880
GRID	603	1	25.250	14.760	68.880
GRID	1603	1	25.250	-14.760	68.880
GRID	604	1	22.200	17.220	68.880
GRID	1604	1	22.200	-17.220	68.880
GRID	605	1	19.000	19.000	68.880
GRID	1605	1	19.000	-19.000	68.880
GRID	606	1	15.230	19.510	68.880
GRID	1606	1	15.230	-19.510	68.880
GRID	607	1	15.000	16.000	68.880
GRID	1607	1	15.000	-16.000	68.880
GRID	608	1	2.700	14.331	68.880
GRID	1608	1	2.700	-14.331	68.880
GRID	609	1	-9.500	13.250	68.880
GRID	1609	1	-9.500	-13.250	68.880
GRID	610	1	-9.500	17.100	68.880
GRID	1610	1	-9.500	-17.100	68.880
GRID	611	1	-13.640	15.320	68.880
GRID	1611	1	-13.640	-15.320	68.880
GRID	612	1	-16.000	0.000	68.880
GRID	613	1	28.950	12.300	76.760
GRID	1613	1	28.950	-12.300	76.760
GRID	614	1	22.200	18.110	76.760
GRID	1614	1	22.200	-18.110	76.760
GRID	615	1	14.720	20.230	76.760
GRID	1615	1	14.720	-20.230	76.760
GRID	616	1	-10.000	17.550	76.760
GRID	1616	1	-10.000	-17.550	76.760
GRID	617	1	-16.270	13.730	76.760
GRID	1617	1	-16.270	-13.730	76.760
GRID	618	1	-16.750	0.000	76.760
GRID	619	1	31.700	7.000	76.760
GRID	1619	1	31.700	-7.000	76.760
GRID	620	1	-16.000	3.000	68.880
GRID	1620	1	-16.000	-3.000	68.880
GRID	621	1	-15.040	11.460	68.880
GRID	1621	1	-15.040	-11.460	68.880

GRID	622	1	0.000	0.000	68.880
GRID	623	1	-16.270	9.320	76.760
GRID	1623	1	-16.270	-9.320	76.760
GRID	624	1	32.450	0.000	68.880
GRID	625	1	32.400	4.000	68.880
GRID	1625	1	32.400	-4.000	68.880
GRID	626	1	9.000	15.200	68.880
GRID	1626	1	9.000	-15.200	68.880
GRID	627	1	15.120	17.760	68.880
GRID	1627	1	15.120	-17.760	68.880
GRID	628	1	-3.400	13.790	68.880
GRID	1628	1	-3.400	-13.790	68.880
GRID	629	1	-9.500	15.180	68.880
GRID	1629	1	-9.500	-15.180	68.880
GRID	630	1	1.350	7.170	68.880
GRID	1630	1	1.350	-7.170	68.880
GRID	631	1	-4.750	6.630	68.880
GRID	1631	1	-4.750	-6.630	68.880
GRID	632	1	-12.270	12.360	68.880
GRID	1632	1	-12.270	-12.360	68.880
GRID	633	1	-8.000	0.000	68.880
GRID	634	1	14.550	16.700	76.760
GRID	1634	1	14.550	-16.700	76.760
GRID	635	1	0.300	14.920	76.760
GRID	1635	1	0.300	-14.920	76.760
GRID	636	1	-10.000	13.880	76.760
GRID	1636	1	-10.000	-13.880	76.760
GRID	637	1	10.53	16.25	76.76
GRID	1637	1	10.53	-16.250	76.76
GRID	638	1	4.38	15.42	76.76
GRID	1638	1	4.38	-15.420	76.76
GRID	700	1	31.700	7.200	84.630
GRID	1700	1	31.700	-7.200	84.630
GRID	701	1	30.800	9.900	84.630
GRID	1701	1	30.800	-9.900	84.630
GRID	702	1	29.600	12.200	84.630
GRID	1702	1	29.600	-12.200	84.630
GRID	703	1	26.400	15.800	84.630
GRID	1703	1	26.400	-15.800	84.630
GRID	704	1	22.200	19.000	84.630
GRID	1704	1	22.200	-19.000	84.630
GRID	705	1	18.200	20.300	84.630
GRID	1705	1	18.200	-20.300	84.630
GRID	706	1	14.200	21.000	84.630
GRID	1706	1	14.200	-21.000	84.630
GRID	708	1	-2.10	17.60	84.63
GRID	1708	1	-2.10	-17.600	84.63
GRID	709	1	6.050	20.800	84.630
GRID	1709	1	6.050	-20.800	84.630
GRID	710	1	-2.100	19.700	84.630

GRID	1710	1	-2.100	-19.700	84.630
GRID	711	1	-10.500	14.500	84.630
GRID	1711	1	-10.500	-14.500	84.630
GRID	712	1	-10.500	18.000	84.630
GRID	1712	1	-10.500	-18.000	84.630
GRID	713	1	29.950	12.200	93.630
GRID	1713	1	29.950	-12.200	93.630
GRID	714	1	22.200	19.500	93.630
GRID	1714	1	22.200	-19.500	93.630
GRID	715	1	14.200	21.750	93.630
GRID	1715	1	14.200	-21.750	93.630
GRID	716	1	6.000	21.550	93.630
GRID	1716	1	6.000	-21.550	93.630
GRID	717	1	-1.050	20.550	93.630
GRID	1717	1	-1.050	-20.550	93.630
GRID	718	1	-11.650	18.090	93.630
GRID	1718	1	-11.650	-18.090	93.630
GRID	719	1	32.500	7.000	93.630
GRID	1719	1	32.500	-7.000	93.630
GRID	720	1	14.100	17.400	84.630
GRID	1720	1	14.100	-17.400	84.630
GRID	721	1	6.05	18.65	84.63
GRID	1721	1	6.05	-18.650	84.63
GRID	722	1	-2.100	15.500	84.630
GRID	1722	1	-2.100	-15.500	84.630
GRID	723	1	-17.500	0.000	84.630
GRID	724	1	-2.100	0.000	84.630
GRID	725	1	-13.000	17.500	84.630
GRID	1725	1	-13.000	-17.500	84.630
GRID	726	1	-17.500	16.000	84.630
GRID	1726	1	-17.500	-16.000	84.630
GRID	727	1	-17.50	9.50	84.63
GRID	1727	1	-17.50	-9.500	84.63
GRID	728	1	10.100	21.000	84.630
GRID	1728	1	10.100	-21.000	84.630
GRID	729	1	6.050	16.500	84.630
GRID	1729	1	6.050	-16.500	84.630
GRID	730	1	10.100	17.150	84.630
GRID	1730	1	10.100	-17.150	84.630
GRID	731	1	1.900	20.200	84.630
GRID	1731	1	1.900	-20.200	84.630
GRID	732	1	1.98	16.00	84.63
GRID	1732	1	1.98	-16.000	84.63
GRID	733	1	-5.300	19.100	84.630
GRID	1733	1	-5.300	-19.100	84.630
GRID	734	1	-17.50	1.50	84.63
GRID	1734	1	-17.50	-1.500	84.63
GRID	735	1	-17.50	3.00	84.63
GRID	1735	1	-17.50	-3.000	84.63
GRID	736	1	-2.10	1.50	84.63

```
GRID          1736          1    -2.10   -1.500    84.63
GRID           737          1   32.740    0.000   84.630
GRID           738          1   32.400    4.300   84.630
GRID          1738          1   32.400   -4.300   84.630
GRID           739          1   -12.20     1.50    84.63
GRID          1739          1   -12.20   -1.500    84.63
GRID           740          1    -14.1     0.00    84.63
GRID           741          1   -2.100    3.000   92.630
GRID          1741          1   -2.100   -3.000   92.630
GRID           742          1   -2.100    0.000   93.130
GRID           743          1   -2.100   15.500   88.130
GRID          1743          1   -2.100  -15.500   88.130
GRID           744          1  -17.500    0.000   89.130
GRID           745          1  -17.500    0.000   93.630
GRID           746          1   -17.50     6.00    93.63
GRID          1746          1   -17.50   -6.000    93.63
GRID    747      1            -17.50  3.0      89.13
GRID          17471           -17.50      -3.00089.13
GRID           748          1  -17.500   16.700   89.130
GRID          1748          1  -17.500  -16.700   89.130
GRID           749          1  -17.500   16.750   93.630
GRID          1749          1  -17.500  -16.750   93.630
GRID           750          1  -11.080   18.050   89.130
GRID          1750          1  -11.080  -18.050   89.130
GRID           751          1    -6.30    15.00    84.63
GRID          1751          1    -6.30  -15.000    84.63
GRID           752          1    -10.5    16.25    84.63
GRID          1752          1    -10.5  -16.250    84.63
GRID           753          1   14.150   19.200   84.630
GRID          1753          1   14.150  -19.200   84.630
GRID           754          1    -2.10     3.00    84.63
GRID          1754          1    -2.10   -3.000    84.63
GRID           755          1    -2.10     9.25    84.63
GRID          1755          1    -2.10   -9.250    84.63
GRID    756      1            -17.50  3.0      93.63
GRID          17561           -17.50      -3.00093.63
GRID           757          1  -17.500   13.160   93.630
GRID          1757          1  -17.500  -13.160   93.630
GRID           758          1   -2.100    7.300   90.380
GRID          1758          1   -2.100   -7.300   90.380
GRID           759          1   -2.100    7.240   87.510
GRID          1759          1   -2.100   -7.240   87.510
GRID           760          1   -2.100    0.000   88.880
GRID           761          1   -16.58    12.05    93.63
GRID          1761          1   -16.58  -12.050    93.63
GRID    763      1            -15.80  0.0      84.63
GRID           764          1   -6.880   18.900   89.130
GRID          1764          1   -6.880  -18.900   89.130
GRID           765          1   -5.830   19.750   98.130
GRID          1765          1   -5.830  -19.750   98.130
```

```
GRID            766         1 -14.450  17.420  93.630
GRID           1766         1 -14.450 -17.420  93.630
GRID            767         1 -12.230  18.130  98.130
GRID           1767         1 -12.230 -18.130  98.130
GRID            768         1 -17.130  17.130  98.130
GRID           1768         1 -17.130 -17.130  98.130
GRID            769         1   -10.50    8.75   84.63
GRID           1769         1   -10.50  -8.750   84.63
GRID            770         1   -10.50    3.00   84.63
GRID           1770         1   -10.50  -3.000   84.63
GRID            771         1   -14.00    3.00   84.63
GRID           1771         1   -14.00  -3.000   84.63
GRID            772         1    -6.30    3.00   84.63
GRID           1772         1    -6.30  -3.000   84.63
GRID            773         1    -14.0   15.25   84.63
GRID           1773         1    -14.0 -15.250   84.63
GRID            774         1    -7.05    0.00   84.63
GRID            800         1  33.300   6.800 102.630
GRID           1800         1  33.300  -6.800 102.630
GRID            801         1  32.000   9.800 102.630
GRID           1801         1  32.000  -9.800 102.630
GRID            802         1  30.300  12.300 102.630
GRID           1802         1  30.300 -12.300 102.630
GRID            803         1  26.730  16.440 102.630
GRID           1803         1  26.730 -16.440 102.630
GRID            804         1  22.200  20.000 102.630
GRID           1804         1  22.200 -20.000 102.630
GRID            805         1  18.200  21.500 102.630
GRID           1805         1  18.200 -21.500 102.630
GRID            806         1  14.200  22.500 102.630
GRID           1806         1  14.200 -22.500 102.630
GRID            807         1  10.100  22.500 102.630
GRID           1807         1  10.100 -22.500 102.630
GRID            808         1   6.000  22.300 102.630
GRID           1808         1   6.000 -22.300 102.630
GRID            809         1   3.000  21.881 102.630
GRID           1809         1   3.000 -21.881 102.630
GRID    810       1       0.      21.4    102.630
GRID           18101      0.      -21.400102.630
GRID    811       1       -6.4    20.     102.63
GRID           18111      -6.4    -20.000102.63
GRID            812         1 -12.800  18.171 102.630
GRID           1812         1 -12.800 -18.171 102.630
GRID            813         1  29.150  14.050 112.130
GRID           1813         1  29.150 -14.050 112.130
GRID            814         1  21.750  20.400 112.130
GRID           1814         1  21.750 -20.400 112.130
GRID            815         1  14.200  22.700 112.130
GRID           1815         1  14.200 -22.700 112.130
GRID            816         1   6.000  22.650 112.130
```

GRID	1816	1	6.000	-22.650	112.130
GRID	817	1	0.000	21.800	112.130
GRID	1817	1	0.000	-21.800	112.130
GRID	818	1	-11.400	19.320	112.130
GRID	1818	1	-11.400	-19.320	112.130
GRID	819	1	33.050	6.350	112.130
GRID	1819	1	33.050	-6.350	112.130
GRID	820	1	-17.000	17.500	102.630
GRID	1820	1	-17.000	-17.500	102.630
GRID	821	1	-15.000	17.900	102.630
GRID	1821	1	-15.000	-17.900	102.630
GRID	826	1	-16.00	12.80	107.63
GRID	1826	1	-16.00	-12.800	107.63
GRID	822	1	-13.650	18.890	112.130
GRID	1822	1	-13.650	-18.890	112.130
GRID	823	1	34.000	0.000	102.630
GRID	824	1	33.800	4.500	102.630
GRID	1824	1	33.800	-4.500	102.630
GRID	825	1	-15.750	18.550	112.130
GRID	1825	1	-15.750	-18.550	112.130
GRID	900	1	32.800	5.900	121.630
GRID	1900	1	32.800	-5.900	121.630
GRID	901	1	31.100	11.100	121.630
GRID	1901	1	31.100	-11.100	121.630
GRID	902	1	28.000	15.800	121.630
GRID	1902	1	28.000	-15.800	121.630
GRID	903	1	24.400	18.900	121.630
GRID	1903	1	24.400	-18.900	121.630
GRID	904	1	21.300	20.800	121.630
GRID	1904	1	21.300	-20.800	121.630
GRID	905	1	18.200	22.000	121.630
GRID	1905	1	18.200	-22.000	121.630
GRID	906	1	14.200	22.900	121.630
GRID	1906	1	14.200	-22.900	121.630
GRID	907	1	10.100	23.200	121.630
GRID	1907	1	10.100	-23.200	121.630
GRID	908	1	6.000	23.000	121.630
GRID	1908	1	6.000	-23.000	121.630
GRID	909	1	3.000	22.700	121.630
GRID	1909	1	3.000	-22.700	121.630
GRID	910	1	0.000	22.200	121.630
GRID	1910	1	0.000	-22.200	121.630
GRID	911	1	-5.000	21.714	121.630
GRID	1911	1	-5.000	-21.714	121.630
GRID	912	1	-10.000	20.459	121.630
GRID	1912	1	-10.000	-20.459	121.630
GRID	920	1	-14.500	19.600	121.630
GRID	1920	1	-14.500	-19.600	121.630
GRID	921	1	-12.300	20.000	121.630
GRID	1921	1	-12.300	-20.000	121.630

```
GRID          922         1   33.300    0.000  121.630
GRID          923         1   33.000    3.600  121.630
GRID         1923         1   33.000   -3.600  121.630
GRID          150         1    37.70     3.43    12.50
GRID          151         1     30.2    -3.43    12.50
SEQGP    150     584     151     585
CLOOF8          1         1      100      101      102      113      202      201+CC1
+CC1          200       119
CLOOF8       1001      1001     1100     1101     1102     1113     1202     1201+CC1001
+CC1001      1200      1119
CLOOF8          2         1      102      103      104      114      204      203+CC2
+CC2          202       113
CLOOF8       1002      1001     1102     1103     1104     1114     1204     1203+CC1002
+CC1002      1202      1113
CLOOF8          3         1      104      105      106      115      206      205+CC3
+CC3          204       114
CLOOF8       1003      1001     1104     1105     1106     1115     1206     1205+CC1003
+CC1003      1204      1114
CLOOF8          4         1      106      107      108      116      208      207+CC4
+CC4          206       115
CLOOF8       1004      1001     1106     1107     1108     1116     1208     1207+CC1004
+CC1004      1206      1115
CLOOF8          5         1      108      109      110      117      210      209+CC5
+CC5          208       116
CLOOF8       1005      1001     1108     1109     1110     1117     1210     1209+CC1005
+CC1005      1208      1116
CLOOF8          6         1      110      111      112      118      212      221+CC6
+CC6          220       120
CLOOF8       1006      1001     1110     1111      112      118      212     1221+CC1006
+CC1006      1220      1120
CLOOF8          7         4      200      201      202      213      302      301+CC7
+CC7          300       219
CLOOF8       1007      1004     1200     1201     1202     1213     1302     1301+CC1007
+CC1007      1300      1219
CLOOF8          8         2      202      203      204      214      304      303+CC8
+CC8          302       213
CLOOF8       1008      1002     1202     1203     1204     1214     1304     1303+CC1008
+CC1008      1302      1213
CLOOF8          9         2      204      205      206      215      306      305+CC9
+CC9          304       214
CLOOF8       1009      1002     1204     1205     1206     1215     1306     1305+CC1009
+CC1009      1304      1214
CLOOF8         10         2      206      207      208      216      309      307+CC10
+CC10         306       215
CLOOF8       1010      1002     1206     1207     1208     1216     1309     1307+CC1010
+CC1010      1306      1215
CLOOF8         11         2      208      209      210      217      311      310+CC11
+CC11         309       216
CLOOF8       1011      1002     1208     1209     1210     1217     1311     1310+CC1011
+CC1011      1309      1216
```

```
CLOOF8        12        3      210      211      220      222      320      321+CC12
+CC12        311      217
CLOOF8      1012     1003     1210     1211     1220     1222     1320     1321+CC1012
+CC1012     1311     1217
CLOOF8        13        4      300      301      302      313      402      401+CC13
+CC13        400      319
CLOOF8      1013     1004     1300     1301     1302     1313     1402     1401+CC1013
+CC1013     1400     1319
CLOOF8        14        5      302      303      304      314      404      403+CC14
+CC14        402      313
CLOOF8      1014     1005     1302     1303     1304     1314     1404     1403+CC1014
+CC1014     1402     1313
CLOOF8        15        5      304      305      306      315      406      405+CC15
+CC15        404      314
CLOOF8      1015     1005     1304     1305     1306     1315     1406     1405+CC1015
+CC1015     1404     1314
CLOOF8        16        5      306      307      309      316      408      407+CC16
+CC16        406      315
CLOOF8      1016     1005     1306     1307     1309     1316     1408     1407+CC1016
+CC1016     1406     1315
CLOOF8        19        5      320      335      312      318      412      420+CC19
+CC19        421      324
CLOOF8      1019     1005     1320     1335      312      318      412     1420+CC1019
+CC1019     1421     1324
CLOOF8        20        4      400      401      402      413      502      501+CC20
+CC20        500      419
CLOOF8      1020     1004     1400     1401     1402     1413     1502     1501+CC1020
+CC1020     1500     1419
CLOOF8        21        5      402      403      404      414      504      503+CC21
+CC21        502      413
CLOOF8      1021     1005     1402     1403     1404     1414     1504     1503+CC1021
+CC1021     1502     1413
CLOOF8        22        5      404      405      406      415      506      505+CC22
+CC22        504      414
CLOOF8      1022     1005     1404     1405     1406     1415     1506     1505+CC1022
+CC1022     1504     1414
CLOOF8        23        5      421      420      412      418      512      522+CC23
+CC23        520      423
CLOOF8      1023     1005     1421     1420      412      418      512     1522+CC1023
+CC1023     1520     1423
CLOOF8        24        4      500      501      502      513      602      601+CC24
+CC24        600      519
CLOOF8      1024     1004     1500     1501     1502     1513     1602     1601+CC1024
+CC1024     1600     1519
CLOOF8        25        7      502      503      504      514      604      603+CC25
+CC25        602      513
CLOOF8      1025     1007     1502     1503     1504     1514     1604     1603+CC1025
+CC1025     1602     1513
CLOOF8        26        7      504      505      506      515      606      605+CC26
+CC26        604      514
```

CLOOF8	1026	1007	1504	1505	1506	1515	1606	1605+CC1026
+CC1026	1604	1514						
CLOOF8	27	11	510	511	520	516	621	611+CC27
+CC27	610	517						
CLOOF8	1027	1011	1510	1511	1520	1516	1621	1611+CC1027
+CC1027	1610	1517						
CLOOF8	28	4	600	601	602	613	702	701+CC28
+CC28	700	619						
CLOOF8	1028	1004	1600	1601	1602	1613	1702	1701+CC1028
+CC1028	1700	1619						
CLOOF8	29	7	602	603	604	614	704	703+CC29
+CC29	702	613						
CLOOF8	1029	1007	1602	1603	1604	1614	1704	1703+CC1029
+CC1029	1702	1613						
CLOOF8	30	7	604	605	606	615	706	705+CC30
+CC30	704	614						
CLOOF8	1030	1007	1604	1605	1606	1615	1706	1705+CC1030
+CC1030	1704	1614						
CLOOF8	31	2	610	611	621	617	726	725+CC31
+CC31	712	616						
CLOOF8	1031	1002	1610	1611	1621	1617	1726	1725+CC1031
+CC1031	1712	1616						
CLOOF8	32	2	621	620	612	618	723	734+CC32
+CC32	735	623						
CLOOF8	1032	1002	1621	1620	612	618	723	1734+CC1032
+CC1032	1735	1623						
CLOOF8	33	11	712	725	726	748	749	766+CC33
+CC33	718	750						
CLOOF8	1033	1011	1712	1725	1726	1748	1749	1766+CC1033
+CC1033	1718	1750						
CLOOF8	37	4	700	701	702	713	802	801+CC37
+CC37	800	719						
CLOOF8	1037	1004	1700	1701	1702	1713	1802	1801+CC1037
+CC1037	1800	1719						
CLOOF8	38	3	702	703	704	714	804	803+CC38
+CC38	802	713						
CLOOF8	1038	1003	1702	1703	1704	1714	1804	1803+CC1038
+CC1038	1802	1713						
CLOOF8	39	3	704	705	706	715	806	805+CC39
+CC39	804	714						
CLOOF8	1039	1003	1704	1705	1706	1715	1806	1805+CC1039
+CC1039	1804	1714						
CLOOF8	40	3	706	728	709	716	808	807+CC40
+CC40	806	715						
CLOOF8	1040	1003	1706	1728	1709	1716	1808	1807+CC1040
+CC1040	1806	1715						
CLOOF8	42	3	709	731	710	717	810	809+CC42
+CC42	808	716						
CLOOF8	1042	1003	1709	1731	1710	1717	1810	1809+CC1042
+CC1042	1808	1716						

CLOUF8	43	11	718	766	749	768	820	821+CC43
+CC43	812	767						
CLOUF8	1043	1011	1718	1766	1749	1768	1820	1821+CC1043
+CC1043	1612	1767						
CLOUF8	47	28	724	736	754	772	770	739+CC47
+CC47	740	774						
CLOUF8	1047	1028	724	1736	1754	1772	1770	1739+CC1047
+CC1047	740	774						
CLOUF8	48	19	754	755	722	751	711	769+CC48
+CC48	770	772						
CLOUF8	1048	1019	1754	1755	1722	1751	1711	1769+CC1048
+CC1048	1770	1772						
CLOUF8	49	3	220	221	212	218	312	335+CC49
+CC49	320	222						
CLOUF8	1049	1003	1220	1221	212	218	312	1335+CC1049
+CC1049	1320	1222						
CLOUF8	51	4	800	801	802	813	902	901+CC51
+CC51	900	819						
CLOUF8	1051	1004	1800	1801	1802	1813	1902	1901+CC1051
+CC1051	1900	1819						
CLOUF8	52	11	520	522	512	518	612	620+CC52
+CC52	621	516						
CLOUF8	1052	1011	1520	1522	512	518	612	1620+CC1052
+CC1052	1621	1516						
CLOUF8	53	19	722	708	710	733	712	752+CC53
+CC53	711	751						
CLOUF8	1053	1019	1722	1708	1710	1733	1712	1752+CC1053
+CC1053	1711	1751						
CLOUF8	54	10	802	803	804	814	904	903+CC54
+CC54	902	813						
CLOUF8	1054	1010	1802	1803	1804	1814	1904	1903+CC1054
+CC1054	1902	1813						
CLOUF8	55	10	804	805	806	815	906	905+CC55
+CC55	904	814						
CLOUF8	1055	1010	1804	1805	1806	1815	1906	1905+CC1055
+CC1055	1904	1814						
CLOUF8	56	10	806	807	808	816	908	907+CC56
+CC56	906	815						
CLOUF8	1056	1010	1806	1807	1808	1816	1908	1907+CC1056
+CC1056	1906	1815						
CLOUF8	57	10	808	809	810	817	910	909+CC57
+CC57	908	816						
CLOUF8	1057	1010	1808	1809	1810	1817	1910	1909+CC1057
+CC1057	1908	1816						
CLOUF8	58	10	810	811	812	818	912	911+CC58
+CC58	910	817						
CLOUF8	1058	1010	1810	1811	1812	1818	1912	1911+CC1058
+CC1058	1910	1817						
CLOUF8	61	16	521	538	509	539	520	522+CC61
+CC61	512	540						

CLOOF8	1061	1016	521	1538	1509	1539	1520	1522+CC1061
+CC1061	512	540						
CLOOF8	68	13	607	634	720	753	706	615+CC68
+CC68	606	627						
CLOOF8	1068	1013	1607	1634	1720	1753	1706	1615+CC1068
+CC1068	1606	1627						
CLOOF8	41	12	720	730	729	721	709	728+CC41
+CC41	706	753						
CLOOF8	1041	1012	1720	1730	1729	1721	1709	1728+CC1041
+CC1041	1706	1753						
CLOOF8	70	26	608	635	722	751	711	636+CC70
+CC70	609	628						
CLOOF8	1070	1026	1608	1635	1722	1751	1711	1636+CC1070
+CC1070	1609	1628						
CLOOF8	71	13	609	636	711	752	712	616+CC71
+CC71	610	629						
CLOOF8	1071	1013	1609	1636	1711	1752	1712	1616+CC1071
+CC1071	1610	1629						
CLOOF8	81	6	408	409	410	428	508	530+CC81
+CC81	507	427						
CLOOF8	1081	1006	1408	1409	1410	1428	1508	1530+CC1081
+CC1081	1507	1427						
CLOOF8	82	25	410	428	508	532	509	429+CC82
+CC82	421	411	90.					
CLOOF8	1082	1025	1410	1428	1508	1532	1509	1429+CC1082
+CC1082	1421	1411						
CLOOF8	86	13	507	534	607	627	606	515+CC86
+CC86	506	531						
CLOOF8	1086	1013	1507	1534	1607	1627	1606	1515+CC1086
+CC1086	1506	1531						
CLOOF8	87	26	507	534	607	626	608	535+CC87
+CC87	508	530						
CLOOF8	1087	1026	1507	1534	1607	1626	1608	1535+CC1087
+CC1087	1508	1530						
CLOOF8	88	26	508	535	608	628	609	536+CC88
+CC88	509	532						
CLOOF8	1088	1026	1508	1535	1608	1628	1609	1536+CC1088
+CC1088	1509	1532						
CLOOF8	89	13	509	536	609	629	610	517+CC89
+CC89	510	533						
CLOOF8	1089	1013	1509	1536	1609	1629	1610	1517+CC1089
+CC1089	1510	1533						
CLOOF8	118	14	422	431	410	338	309	331+CC118
+CC118	323	341	90.					
CLOOF8	1118	1014	422	1431	1410	1338	1309	1331+CC1118
+CC1118	1323	1341						
CLOOF8	119	14	521	537	508	428	410	431+CC119
+CC119	422	430	90.					
CLOOF8	1119	1014	521	1537	1508	1428	1410	1431+CC1119
+CC1119	422	430						

```
CLOOF8        120      14     622     630     608     535     508     537+CC120
+CC120        521     541     90.
CLOOF8       1120    1014     622    1630    1608    1535    1508    1537+CC1120
+CC1120       521     541
CLOOF8        131      15     742     741     758     759     754     736+CC131
+CC131        724     760
CLOOF8       1131    1015     742    1741    1758    1759    1754    1736+CC1131
+CC1131       724     760
CLOOF8        136      11     745     756     746     747     735     734+CC136
+CC136        723     744
CLOOF8       1136    1011     745    1756    1746    1747    1735    1734+CC1136
+CC1136       723     744
CLOOF8        137      11     746     757     749     748     726     727+CC137
+CC137        735     747
CLOOF8       1137    1011    1746    1757    1749    1748    1726    1727+CC1137
+CC1137      1735    1747
CLOOF8        169      11     323     331     309     310     311     332+CC169
+CC169        334     327
CLOOF8       1169    1011    1323    1331    1309    1310    1311    1332+CC1169
+CC1169      1334    1327
CLOOF8        176      32     309     338     410     411     421     340+CC176
+CC176        311     310
CLOOF8       1176    1032    1309    1338    1410    1411    1421    1340+CC1176
+CC1176      1311    1310
CLOOF8        180      12     729     732     722     708     710     731+CC180
+CC180        709     721
CLOOF8       1180    1012    1729    1732    1722    1708    1710    1731+CC1180
+CC1180      1709    1721
CLOOF8        181      19     740     739     770     771     735     734+CC181
+CC181        723     763
CLOOF8       1181    1019     740    1739    1770    1771    1735    1734+CC1181
+CC1181       723     763
CLOOF8        182      18     622     631     609     632     621     620+CC182
+CC182        612     633     55.
CLOOF8       1182    1018     622    1631    1609    1632    1621    1620+CC1182
+CC1182       612     633
CLOOF8        185      19     770     769     711     773     726     727+CC185
+CC185        735     771
CLOOF8       1185    1019    1770    1769    1711    1773    1726    1727+CC1185
+CC1185      1735    1771
CLOOF6  17       32      309     316     408     409     410     338
CLOOF6  1017     1032    1309    1316    1408    1409    1410    1338
CLOOF6  18       5       311     321     320     324     421     340
CLOOF6       1018    1005    1311    1321    1320    1324    1421    1340
CLOOF6         34      29     812     818     912     921     920     822
CLOOF6       1034    1029    1812    1818    1912    1921    1920    1822
CLOOF6         62      16     509     533     510     511     520     539
CLOOF6       1062    1016    1509    1533    1510    1511    1520    1539
CLOOF6  63       16      521     537     508     532     509     538
CLOOF6         69      27     720     730     729     637     607     634
```

```
CLOOF6       1069     1027     1720     1730     1729     1637     1607     1634
CLOOF6         75       31      110      117      210      211      220      120
CLOOF6       1075     1031     1110     1117     1210     1211     1220     1120
CLOOF6         80       25      406      426      507      427      408      407
CLOOF6       1080     1025     1406     1426     1507     1427     1408     1407
CLOOF6         83       13      421      429      509      533      510      417
CLOOF6       1083     1013     1421     1429     1509     1533     1510     1417
CLOOF6         84       13      406      426      507      531      506      415
CLOOF6       1084     1013     1406     1426     1507     1531     1506     1415
CLOOF6        116       20      220      227      334      328      320      222
CLOOF6       1116     1020     1220     1227     1334     1328     1320     1222
CLOOF6        117       14      422      341      323      330      322      339
CLOOF6       1117     1014      422     1341     1323     1330      322      339
CLOOF6        121        5      421      423      520      511      510      417
CLOOF6       1121     1005     1421     1423     1520     1511     1510     1417
CLOOF6        132       15      758      743      722      755      754      759
CLOOF6       1132     1015     1758     1743     1722     1755     1754     1759
CLOOF6        138       17      746      757      749      766      718      761
CLOOF6       1138     1017     1746     1757     1749     1766     1718     1761
CLOOF6        156       11      334      328      320      335      312      336
CLOOF6       1156     1011     1334     1328     1320     1335      312     1336
CLOOF6        157       11      812      821      820      825      920      822
CLOOF6       1157     1011     1812     1821     1820     1825     1920     1822
CLOOF6        161       30      710      717      810      765      718      764
CLOOF6       1161     1030     1710     1717     1810     1765     1718     1764
CLOOF6        162        3      710      733      712      750      718      764
CLOOF6       1162     1003     1710     1733     1712     1750     1718     1764
CLOOF6        163       30      810      811      812      767      718      765
CLOOF6       1163     1030     1810     1811     1812     1767     1718     1765
CLOOF6        167       11      322      330      323      327      334      333
CLOOF6       1167     1011      322     1330     1323     1327     1334     1333
CLOOF6        166       20      220      226      323      327      334      227
CLOOF6       1166     1020     1220     1226     1323     1327     1334     1227
CLOOF6        168       11      322      333      334      336      312      337
CLOOF6       1168     1011      322     1333     1334     1336      312      337
CLOOF6        170       11      334      332      311      321      320      328
CLOOF6       1170     1011     1334     1332     1311     1321     1320     1328
CLOOF6        183       18      609      629      610      611      621      632
CLOOF6       1183     1018     1609     1629     1610     1611     1621     1632
CLOOF6        184       18      622      630      608      628      609      631+CF184
+CF184       90.0
CLOOF6  1184    1018    622     1630    1608    1628    1609    1631    +CF1184
+CF1184 90.
CLOOF6        186       19      711      752      712      725      726      773
CLOOF6       1186     1019     1711     1752     1712     1725     1726     1773
CLOOF6        188        9      607      626      608      638      729      637
CLOOF6       1188     1009     1607     1626     1608     1638     1729     1637
CLOOF6        189       27      729      732      722      635      608      638
CLOOF6       1189     1027     1729     1732     1722     1635     1608     1638
CLOOF3        106        1      121      122      100        1        1        1+CL106
```

```
+CL106                                                                       +CO106
+CO106        1.390      0.0     1.390      0.0     1.390      0.0
CLOOF3         1106        1       121     1122      1100        1        1      1+CL 106
+CL 106                                                                      +CO 106
+CO 106       1.390      0.0     1.390      0.0     1.390      0.0
CLOOF3          207        1       223      224       200        6        6      6+CL207
+CL207                                                                        +CO207
+CO207        1.880      0.0     1.880      0.0     1.880      0.0
CLOOF3         1207        1       223     1224      1200        6        6      6+CL 207
+CL 207                                                                      +CO 207
+CO 207       1.880      0.0     1.880      0.0     1.880      0.0
CLOOF3          305        1       325      326       300       10       10     10+CL305
+CL305                                                                        +CO305
+CO305    1.7               1.7               1.7
CLOOF3         1305        1       325     1326      1300       10       10     10+CL 305
+CL 305                                                                      +CO 305
+CO 305   1.7               1.7               1.7
CLOOF3          504        1       529      528       500       18       18     18+CL504
+CL504                                                                        +CO504
+CO504    1.268             1.268             1.268
CLOOF3         1504        1       529     1528      1500       18       18     18+CL 504
+CL 504                                                                      +CO 504
+CO 504   1.268             1.268             1.268
CLOOF3          604        1       624      625       600       22       22     22+CL604
+CL604                                                                        +CO604
+CO604    1.55              1.55              1.55
CLOOF3         1604        1       624     1625      1600       22       22     22+CL 604
+CL 604                                                                      +CO 604
+CO 604   1.55              1.55              1.55
CLOOF3          703        1       737      738       700       26       26     26+CL703
+CL703                                                                        +CO703
+CO703    2.38              2.38              2.38
CLOOF3         1703        1       737     1738      1700       26       26     26+CL 703
+CL 703                                                                      +CO 703
+CO 703   2.38              2.38              2.38
CLOOF3          806        1       823      824       800       30       30     30+CL806
+CL806                                                                        +CO806
+CO806    1.95              1.95              1.95
CLOOF3         1806        1       823     1824      1800       30       30     30+CL 806
+CL 806                                                                      +CO 806
+CO 806   1.95              1.95              1.95
CLOOF3          907        1       922      923       900       34       34     34+CL907
+CL907                                                                        +CO907
+CO907    2.2               2.2               2.2
CLOOF3         1907        1       922     1923      1900       34       34     34+CL 907
+CL 907                                                                      +CO 907
+CO 907   2.2               2.2               2.2
CLOOF3          100        1       100      101       102        1        1      1+CL100
+CL100                                                                        +CO100
+CO100       -1.350      0.0    -1.350      0.0    -1.350      0.
```

```
CLOOF3     1100       1    1100    1101    1102       1       1      1+CL 100
+CL 100                                                               +CO 100
+CO 100  -1.350     0.0  -1.350     0.0  -1.350     0.
CLOOF3      101       1     102     103     104       2       2      2+CL101
+CL101                                                                +CO101
+CO101   -1.350     0.0  -1.350     0.0  -1.350     0.
CLOOF3     1101       1    1102    1103    1104       2       2      2+CL 101
+CL 101                                                               +CO 101
+CO 101  -1.350     0.0  -1.350     0.0  -1.350     0.
CLOOF3      102       1     104     105     106       3       3      3+CL102
+CL102                                                                +CO102
+CO102   -1.330     0.0  -1.330     0.0  -1.330     0.
CLOOF3     1102       1    1104    1105    1106       3       3      3+CL 102
+CL 102                                                               +CO 102
+CO 102  -1.330     0.0  -1.330     0.0  -1.330     0.
CLOOF3      103       1     106     107     108       4       4      4+CL103
+CL103                                                                +CO103
+CO103   -1.500     0.0  -1.500     0.0  -1.500     0.
CLOOF3     1103       1    1106    1107    1108       4       4      4+CL 103
+CL 103                                                               +CO 103
+CO 103  -1.500     0.0  -1.500     0.0  -1.500     0.
CLOOF3      104       1     108     109     110       5       5      5+CL104
+CL104                                                                +CO104
+CO104  -2.08    0.0     -2.08    0.0     -2.08    0.0
CLOOF3     1104       1    1108    1109    1110       5       5      5+CL 104
+CL 104                                                               +CO 104
+CO 104 -2.08    0.0     -2.08    0.0     -2.08    0.0
CLOOF3      105       1     110     111     112       5       5      5+CL105
+CL105                                                                +CO105
+CO105  -2.08    0.0     -2.08    0.0     -2.08    0.0
CLOOF3     1105       1    1110    1111     112       5       5      5+CL 105
+CL 105                                                               +CO 105
+CO 105 -2.08    0.0     -2.08    0.0     -2.08    0.0
CLOOF3      107       1     100     119     200      61      61     61+CL107
+CL107  1.       0.      0.      1                                    +CO107
+CO107  0.78     0.0     0.78     0.0     0.78     0.0
CLOOF3     2107       1    1100    1119    1200      61      61     61+CL1107
+CL1107 1.         0.0000.       1                                    +CO1107
+CO1107 0.78     0.0     0.78     0.0     0.78     0.0
CLOOF3      200       1     200     201     202       6       6      6+CL200
+CL200                                                                +CO200
+CO200   -1.880     0.0  -1.880     0.0  -1.880     0.
CLOOF3     1200       1    1200    1201    1202       6       6      6+CL 200
+CL 200                                                               +CO 200
+CO 200  -1.880     0.0  -1.880     0.0  -1.880     0.
CLOOF3      201       1     202     203     204       7       7      7+CL201
+CL201                                                                +CO201
+CO201   -2.130     0.0  -2.130     0.0  -2.130     0.
CLOOF3     1201       1    1202    1203    1204       7       7      7+CL 201
+CL 201                                                               +CO 201
```

```
+CO 201    -2.130     0.0  -2.130     0.0  -2.130      0.
CLOOF3        202       1     204     205     206       7       7      8+CL202
+CL202                                                                  +CO202
+CO202     -2.130     0.0  -2.130     0.0  -1.940      0.
CLOOF3       1202       1    1204    1205    1206       7       7      8+CL 202
+CL 202                                                                 +CO 202
+CO 202    -2.130     0.0  -2.130     0.0  -1.940      0.
CLOOF3        203       1     206     207     208       8       8      8+CL203
+CL203                                                                  +CO203
+CO203     -1.940     0.0  -1.940     0.0  -1.940      0.
CLOOF3       1203       1    1206    1207    1208       8       8      8+CL 203
+CL 203                                                                 +CO 203
+CO 203    -1.940     0.0  -1.940     0.0  -1.940      0.
CLOOF3        204       1     208     209     210       8       8      8+CL204
+CL204                                                                  +CO204
+CO204     -1.940     0.0  -1.940     0.0  -1.940      0.
CLOOF3       1204       1    1208    1209    1210       8       8      8+CL 204
+CL 204                                                                 +CO 204
+CO 204    -1.940     0.0  -1.940     0.0  -1.940      0.
CLOOF3        205       1     210     211     220       9       9      9+CL205
+CL205                                                                  +CO205
+CO205     -1.215     0.0  -1.215     0.0  -1.215      0.
CLOOF3       1205       1    1210    1211    1220       9       9      9+CL 205
+CL 205                                                                 +CO 205
+CO 205    -1.215     0.0  -1.215     0.0  -1.215      0.
CLOOF3        206       1     220     221     212       9       9      9+CL206
+CL206                                                                  +CO206
+CO206     -1.215     0.0  -1.215     0.0  -1.215      0.
CLOOF3       1206       1    1220    1221     212       9       9      9+CL 206
+CL 206                                                                 +CO 206
+CO 206    -1.215     0.0  -1.215     0.0  -1.215      0.
CLOOF3        208       1     200     219     300      61      61     61+CL208
+CL208  1.        0.        0.        1                                 +CO208
+CO208  0.78      0.0       0.78      0.0       0.78      0.0
CLOOF3       2208       1    1200    1219    1300      61      61     61+CL1208
+CL1208 1.             0.0000.        1                                 +CO1208
+CO1208 0.78      0.0       0.78      0.0       0.78      0.0
CLOOF3        209       1     311     217     210      47      48     48+CL209
+CL209  0.        1.        0.        1                                 +CO209
+CO209  -.76      0.0       -.923     0.0       -.923     0.0
CLOOF3       2209       1    1311    1217    1210      47      48     48+CL1209
+CL1209 0.           -1.0000.         1                                 +CO1209
+CO1209 -.76      0.0       -.923     0.0       -.923     0.0
CLOOF3        250       1     334     332     311      57      57     57+CL250
+CL250  0.        0.        1.        1                                 +CO250
+CO250  -1.41     0.0       -1.41     0.0       -1.41     0.0
CLOOF3       2250       1    1334    1332    1311      57      57     57+CL1250
+CL1250 0.             0.0001.        1                                 +CO1250
+CO1250 -1.41     0.0       -1.41     0.0       -1.41     0.0
CLOOF3        251       1     722     635     608      53      66     67+CL251
```

```
+CL251   0.       1.       0.       1                                            +CO251
+CO251   .50      0.0      .24      0.0      .113     0.0
CLOOF3       2251        1    1722     1635     1608        53        66       67+CL1251
+CL1251  0.            -1.0000.     1                                           +CO1251
+CO1251  .50      0.0      .24      0.0      .113     0.0
CLOOF3        252        1     711      771      740        74        74       74+CL252
+CL252                                                                          +CO252
+CO252   -.40     0.0      -.40     0.0      -.40     0.0
CLOOF3       1252        1    1711     1771      740        74        74       74+CL 252
+CL 252                                                                         +CO 252
+CO 252  -.40     0.0      -.40     0.0      -.40     0.0
CLOOF3        300        1     300      301      302        10        11       11+CL300
+CL300                                                                          +CO300
+CO300     -1.500      0.0  -1.500      0.0   -1.500        0.
CLOOF3       1300        1    1300     1301     1302        10        11       11+CL 300
+CL 300                                                                         +CO 300
+CO 300    -1.500      0.0  -1.500      0.0   -1.500        0.
CLOOF3        301        1     302      303      304        11        11       12+CL301
+CL301                                                                          +CO301
+CO301     -1.500      0.0  -1.500      0.0   -1.270        0.
CLOOF3       1301        1    1302     1303     1304        11        11       12+CL 301
+CL 301                                                                         +CO 301
+CO 301    -1.500      0.0  -1.500      0.0   -1.270        0.
CLOOF3        302        1     304      305      306        12        12       12+CL302
+CL302                                                                          +CO302
+CO302     -1.270      0.0  -1.270      0.0   -1.270        0.
CLOOF3       1302        1    1304     1305     1306        12        12       12+CL 302
+CL 302                                                                         +CO 302
+CO 302    -1.270      0.0  -1.270      0.0   -1.270        0.
CLOOF3        303        1     306      307      309        13        13       13+CL303
+CL303                                                                          +CO303
+CO303     -1.040      0.0  -1.040      0.0   -1.040        0.
CLOOF3       1303        1    1306     1307     1309        13        13       13+CL 303
+CL 303                                                                         +CO 303
+CO 303    -1.040      0.0  -1.040      0.0   -1.040        0.
CLOOF3        304        1     309      310      311        13        13       13+CL304
+CL304                                                                          +CO304
+CO304   -1.04    0.0      -1.04    0.0      -1.04    0.0
CLOOF3       1304        1    1309     1310     1311        13        13       13+CL 304
+CL 304                                                                         +CO 304
+CO 304  -1.04    0.0      -1.04    0.0      -1.04    0.0
CLOOF3        306        1     300      319      400        61        61       61+CL306
+CL306   1.       0.       0.       1                                           +CO306
+CO306   0.78     0.0      0.78     00.0     0.78     0.0
CLOOF3       2306        1    1300     1319     1400        61        61       61+CL1306
+CL1306  1.            0.0000.      1                                           +CO1306
+CO1306  ^.78     0.0      0.78     00.0     0.78     0.0
CLOOF3        307        1     309      310      311        13        13       13+CL307
+CL307                                                                          +CO307
+CO307     -1.040      0.0  -1.040      0.0   -1.040        0.
```

```
CLOOF3      1307         1     1309     1310     1311       13        13        13+CL 307
+CL 307                                                                            +CO 307
+CO 307   -1.040       0.0   -1.040      0.0   -1.040       0.         .
CLOOF3       308         1      421      340      311       45        45        46+CL308
+CL308   0.        1.        0.       1                                          +CO308
+CO308   -.80     0.0       -.80     0.0       -.80     0.0
CLOOF3      2308         1     1421     1340     1311       45        45        46+CL1308
+CL1308  0.            -1.0000.         1                                        +CO1308
+CO1308  -.80     0.0       -.80     0.0       -.80     0.0
CLOOF3       309         1      312      318      412       81        80        79+CL309
+CL309   1.        0.        0.       1                                          +CO309
+CO309     -0.57       0.0    -0.63      0.0    -0.69       0.
CLOOF3      2309         1      312      318      412       81        80        79+CL1309
+CL1309  1.             0.0000.         1                                        +CO1309
+CO1309    -0.57       0.0    -0.63      0.0    -0.69       0.
CLOOF3       400         1      400      401      402       14        14        15+CL400
+CL400                                                                           +CO400
+CO400    -1.185       0.0   -1.185      0.0   -1.440       0.
CLOOF3      1400         1     1400     1401     1402       14        14        15+CL 400
+CL 400                                                                          +CO 400
+CO 400   -1.185       0.0   -1.185      0.0   -1.440       0.
CLOOF3       401         1      402      403      404       15        15        16+CL401
+CL401                                                                           +CO401
+CO401    -1.440       0.0   -1.440      0.0   -2.071       0.
CLOOF3      1401         1     1402     1403     1404       15        15        16+CL 401
+CL 401                                                                          +CO 401
+CO 401   -1.440       0.0   -1.440      0.0   -2.071       0.
CLOOF3       402         1      404      405      406       16        16        16+CL402
+CL402                                                                           +CO402
+CO402    -2.071       0.0   -2.071      0.0   -2.071       0.
CLOOF3      1402         1     1404     1405     1406       16        16        16+CL 402
+CL 402                                                                          +CO 402
+CO 402   -2.071       0.0   -2.071      0.0   -2.071       0.
CLOOF3       403         1      406      407      408       16        17        17+CL403
+CL403                                                                           +CO403
+CO403    -2.071       0.0   -2.268      0.0   -2.268       0.
CLOOF3      1403         1     1406     1407     1408       16        17        17+CL 403
+CL 403                                                                          +CO 403
+CO 403   -2.071       0.0   -2.268      0.0   -2.268       0.
CLOOF3       404         1      408      409      410       17        17        17+CL404
+CL404                                                                           +CO404
+CO404    -2.268       0.0   -2.268      0.0   -2.268       0.
CLOOF3      1404         1     1408     1409     1410       17        17        17+CL 404
+CL 404                                                                          +CO 404
+CO 404   -2.268       0.0   -2.268      0.0   -2.268       0.
CLOOF3       405         1      410      411      421       17        17        17+CL405
+CL405                                                                           +CO405
+CO405    -2.268       0.0   -2.268      0.0   -2.268       0.
CLOOF3      1405         1     1410     1411     1421       17        17        17+CL 405
+CL 405                                                                          +CO 405
```

```
+CO 405    -2.268      0.0  -2.268      0.0  -2.268      0.
CLOOF3        406        1      400      419      500      61       61       61+CL406
+CL406  1.       0.       0.       1                                           +CO406
+CO406  0.78     0.0      0.78     0.0      0.78     0.0
CLOOF3       2406        1     1400     1419     1500      61       61       61+CL1406
+CL1406 1.              0.0000.        1                                       +CO1406
+CO1406 0.78     0.0      0.78     0.0      0.78     0.0
CLOOF3        407        1      510      417      421      43       43       43+CL407
+CL407  0.       1.       0.       1                                           +CO407
+CO407  0.0      -.75     0.0      -.75     0.0      -.75
CLOOF3       2407        1     1510     1417     1421      43       43       43+CL1407
+CL1407 0.             -1.0000.        1                                       +CO1407
+CO1407 0.0      -.75     0.0      -.75     0.0      -.75
CLOOF3        408        1      509      429      421      42       42       42+CL408
+CL408  0.       1.       0.       1                                           +CO408
+CO408  0.0      .75      0.0      .75      0.0      .75
CLOOF3       2408        1     1509     1429     1421      42       42       42+CL1408
+CL1408 0.             -1.0000.        1                                       +CO1408
+CO1408 0.0      .75      0.0      .75      0.0      .75
CLOOF3        409        1      410      431      422      73       73       73+CL409
+CL409  0.       0.       1.       1                                           +CO409
+CO409  0.0      .94      0.0      .94      0.0      .94
CLOOF3       2409        1     1410     1431      422      73       73       73+CL1409
+CL1409 0.              0.0001.        1                                       +CO1409
+CO1409 0.0      .94      0.0      .94      0.0      .94
CLOOF3        410        1      412      418      512      79       80       81+CL410
+CL410  1.       0.       0.       1                                           +CO410
+CO410     -0.69      0.0   -0.63      0.0   -0.57       0.
CLOOF3       2410        1      412      418      512      79       80       81+CL1410
+CL1410 1.              0.0000.        1                                       +CO1410
+CO1410    -0.69      0.0   -0.63      0.0   -0.57       0.
CLOOF3        500        1      500      501      502      19       19       19+CL500
+CL500                                                                         +CO500
+CO500    -1.880      0.0  -1.880      0.0  -1.880      0.
CLOOF3       1500        1     1500     1501     1502      19       19       19+CL 500
+CL 500                                                                        +CO 500
+CO 500   -1.880      0.0  -1.880      0.0  -1.880      0.
CLOOF3        501        1      502      503      504      19       20       20+CL501
+CL501                                                                         +CO501
+CO501    -1.880      0.0  -2.500      0.0  -2.500      0.
CLOOF3       1501        1     1502     1503     1504      19       20       20+CL 501
+CL 501                                                                        +CO 501
+CO 501   -1.880      0.0  -2.500      0.0  -2.500      0.
CLOOF3        502        1      504      505      507      20       20       20+CL502
+CL502                                                                         +CO502
+CO502    -2.500      0.0  -2.500      0.0  -  0.0      0.
CLOOF3       1502        1     1504     1505     1507      20       20       20+CL 502
+CL 502                                                                        +CO 502
+CO 502   -2.500      0.0  -2.500      0.0  -  0.0      0.
CLOOF3        503        1      507      530      508      21       21       21+CL503
```

```
+CL503
+CO503     -1.470       0.0   -1.470       0.0   -1.470       0.                        +CO503
CLOUF3       1503         1     1507      1530     1508        21        21         21+CL 503
+CL 503
+CO 503    -1.470       0.0   -1.470       0.0   -1.470       0.                        +CO 503
CLOUF3        506         1      500       519      600        61        61         61+CL506
+CL506  1.        0.        0.        1
+CO506  0.0       0.78      0.0       0.78      0.0       0.78                        +CO506
CLOUF3       2506         1     1500      1519     1600        61        61         61+CL1506
+CL1506 1.             0.0000.        1
+CO1506 0.0       0.78      0.0       0.78      0.0       0.78                        +CO1506
CLOUF3        507         1      610       517      510        43        43         43+CL507
+CL507  0.        1.        0.        1
+CO507  0.0       -.75      0.0       -.75      0.0       -.75                        +CO507
CLOUF3       2507         1     1610      1517     1510        43        43         43+CL1507
+CL1507 0.            -1.0000.        1
+CO1507 0.0       -.75      0.0       -.75      0.0       -.75                        +CO1507
CLOUF3        508         1      609       536      509        42        42         42+CL508
+CL508  0.        1.        0.        1
+CO508  0.0       .75       0.0       .75       0.0       .75                         +CO508
CLOUF3       2508         1     1609      1536     1509        42        42         42+CL1508
+CL1508 0.            -1.0000.        1
+CO1508 0.0       .75       0.0       .75       0.0       .75                         +CO1508
CLOUF3        509         1      512       518      612        82        83         84+CL509
+CL509  1.        0.        0.        1
+CO509  .77       0.0       1.26      0.0       1.71      0.0                         +CO509
CLOUF3       2509         1      512       518      612        82        83         84+CL1509
+CL1509 1.             0.0000.        1
+CO1509 .77       0.0       1.26      0.0       1.71      0.0                         +CO1509
CLOUF3        600         1      602       603      604        23        23         24+CL600
+CL600
+CO600     -1.630       0.0   -1.630       0.0   -2.500       0.                        +CO600
CLOUF3       1600         1     1602      1603     1604        23        23         24+CL 600
+CL 600
+CO 600    -1.630       0.0   -1.630       0.0   -2.500       0.                        +CO 600
CLOUF3        601         1      604       605      607        24        24         24+CL601
+CL601
+CO601     -2.500       0.0   -2.500       0.0      1.0       0.                        +CO601
CLOUF3       1601         1     1604      1605     1607        24        24         24+CL 601
+CL 601
+CO 601    -2.500       0.0   -2.500       0.0      1.0       0.                        +CO 601
CLOUF3        602         1      600       601      602        23        23         23+CL602
+CL602
+CO602     -1.630       0.0   -1.630       0.0   -1.630       0.                        +CO602
CLOUF3       1602         1     1600      1601     1602        23        23         23+CL 602
+CL 602
+CO 602    -1.630       0.0   -1.630       0.0   -1.630       0.                        +CO 602
CLOUF3        603         1      607       626      608        25        25         25+CL603
+CL603
+CO603     -0.941       0.0   -0.941       0.0   -0.941       0.                        +CO603
```

```
CLOOF3      1603       1    1607    1626    1608      25      25      25+CL 603
+CL 603                                                                  +CO 603
+CO 603   -0.941     0.0  -0.941     0.0  -0.941      0.
CLOOF3       605       1     608     628     609      25      25      25+CL605
+CL605                                                                   +CO605
+CO605    -0.941     0.0  -0.941     0.0  -0.941      0.
CLOOF3      1605       1    1608    1628    1609      25      25      25+CL 605
+CL 605                                                                  +CO 605
+CO 605   -0.941     0.0  -0.941     0.0  -0.941      0.
CLOOF3       606       1     600     619     700      61      61      61+CL606
+CL606  1.      0.      0.      1                                        +CO606
+CO606  0.78    0.0     0.78    0.0     0.78    0.0
CLOOF3      2606       1    1600    1619    1700      61      61      61+CL1606
+CL1606 1.          0.0000.     1                                        +CO1606
+CO1606 0.78    0.0     0.78    0.0     0.78    0.0
CLOOF3       607       1     712     616     610      43      43      43+CL607
+CL607  0.      1.      0.      1                                        +CO607
+CO607  0.0     -.75    0.0     -.75    0.0     -.75
CLOOF3      2607       1    1712    1616    1610      43      43      43+CL1607
+CL1607 0.          -1.0000.    1                                        +CO1607
+CO1607 0.0     -.75    0.0     -.75    0.0     -.75
CLOOF3       608       1     711     636     609      42      42      42+CL608
+CL608  0.      1.      0.      1                                        +CO608
+CO608  0.0     .75     0.0     .75     0.0     .75
CLOOF3      2608       1    1711    1636    1609      42      42      42+CL1608
+CL1608 0.          -1.0000.    1                                        +CO1608
+CO1608 0.0     .75     0.0     .75     0.0     .75
CLOOF3       700       1     700     701     702      26      27      27+CL700
+CL700                                                                   +CO700
+CO700    -2.380     0.0  -2.490     0.0  -2.490      0.
CLOOF3      1700       1    1700    1701    1702      26      27      27+CL 700
+CL 700                                                                  +CO 700
+CO 700   -2.380     0.0  -2.490     0.0  -2.490      0.
CLOOF3       701       1     702     703     704      27      27      28+CL701
+CL701                                                                   +CO701
+CO701    -2.490     0.0  -2.490     0.0  -2.775      0.
CLOOF3      1701       1    1702    1703    1704      27      27      28+CL 701
+CL 701                                                                  +CO 701
+CO 701   -2.490     0.0  -2.490     0.0  -2.775      0.
CLOOF3       702       1     704     705     720      28      28      28+CL702
+CL702                                                                   +CO702
+CO702    -2.775     0.0  -2.775     0.0     0.0      0.
CLOOF3      1702       1    1704    1705    1720      28      28      28+CL 702
+CL 702                                                                  +CO 702
+CO 702   -2.775     0.0  -2.775     0.0     0.0      0.
CLOOF3       704       1     700     719     800      61      61      61+CL704
+CL704  1.      0.      0.      1                                        +CO704
+CO704  0.78    0.0     0.78    0.0     0.78    0.0
CLOOF3      2704       1    1700    1719    1800      61      61      61+CL1704
+CL1704 1.          0.0000.     1                                        +CO1704
```

```
+C01704 0.78     0.0      0.78     0.0      0.78     0.0
CLOOF3       705        1      812      767      718       40       40       40+CL705
+CL705  1.       0.       0.       1                                            +C0705
+C0705  0.0      2.0      0.0      2.0      0.0      2.0
CLOOF3      2705        1     1812     1767     1718       40       40       40+CL1705
+CL1705 1.             0.0000.     1                                            +C01705
+C01705 0.0      2.0      0.0      2.0      0.0      2.0
CLOOF3       706        1      718      750      712       40       40       40+CL706
+CL706  1.       0.       0.       1                                            +C0706
+C0706  0.0      2.0      0.0      2.0      0.0      2.0
CLOOF3      2706        1     1718     1750     1712       40       40       40+CL1706
+CL1706 1.             0.0000.     1                                            +C01706
+C01706 0.0      2.0      0.0      2.0      0.0      2.0
CLOOF3       707        1      754      772      770       50       51       52+CL707
+CL707  0.       0.       1.       1                                            +C0707
+C0707  -.73     0.0      -1.07    0.0      -1.38    0.0
CLOOF3      2707        1     1754     1772     1770       50       51       52+CL1707
+CL1707 0.             0.0001.     1                                            +C01707
+C01707 -.73     0.0      -1.07    0.0      -1.38    0.0
CLOOF3  708      1        735      623      612      49       49       49       +CL708
+CL708  1.       0.       0.       1                                            +C0708
+C0708  1.28     0.0      1.28     0.0      1.28     -3.0
CLOOF3      2708        1     1735     1623      612       49       49       49+CL1708
+CL1708 1.             0.0000.     1                                            +C01708
+C01708 1.28     0.0      1.28     0.0      1.28     -3.0
CLOOF3       709        1      746      756      745       54       54       54+CL709
+CL709  1.       0.       0.       1
CLOOF3      2709        1     1746     1756      745       54       54       54+CL1709
+CL1709 1.             0.0000.     1                                            +C01709
+C01709 1.28     0.0      1.28     0.0      1.28     -3.0
CLOOF3       710        1      820      768      749       59       59       59+CL710
+CL710  0.       1.       0.       1
CLOOF3      2710        1     1820     1768     1749       59       59       59+CL1710
+CL1710 0.            -1.0000.     1                                            +C01710
+C01710 1.28     0.0      1.28     0.0      1.28     -3.0
CLOOF3       711        1      722      743      758       53       53       75+CL711
+CL711                                                                          +C0711
+C0711  -.50     .20      -.50     .20      -.50     .20
CLOOF3      1711        1     1722     1743     1758       53       53       75+CL 711
+CL 711                                                                         +C0 711
+C0 711 -.50     .20      -.50     .20      -.50     .20
CLOOF3       712        1      758      741      742     75       75        75 +CL712
+CL712                                                                          +C0712
+C0712  -.50     .20      -.50     .20      -.50     .20
CLOOF3      1712        1     1758     1741      742       75       75       75+CL 712
+CL 712                                                                         +C0 712
+C0 712 -.50     .20      -.50     .20      -.50     .20
CLOOF3       713        1      720      730      729       85       85       85+CL713
+CL713  0.       0.       1.       1                                            +C0713
+C0713  0.0      -1.28    0.0      -1.28    0.       -1.28
```

```
CLOOF3      2713       1     1720     1730     1729       85       85      85+CL1713
+CL1713 0.          0.0001.       1                                           +CO1713
+CO1713 0.0      -1.28    0.0      -1.28    0.       -1.28
CLOOF3       714       1      729      732      722       85       86      87+CL714
+CL714  0.       0.       1.       1                                          +CO714
+CO714  0.0      -1.28    0.0      -1.97    0.0      -2.45
CLOOF3      2714       1     1729     1732     1722       85       86      87+CL1714
+CL1714 0.          0.0001.       1                                           +CO1714
+CO1714 0.0      -1.28    0.0      -1.97    0.0      -2.45
CLOOF3       717       1      770      771      735       52       78      78+CL717
+CL717  0.       0.       1.       1                                          +CO717
+CO717  -1.38    0.0      -1.50    0.0      -1.50    0.0
CLOOF3      2717       1     1770     1771     1735       52       78      78+CL1717
+CL1717 0.          0.0001.       1                                           +CO1717
+CO1717 -1.38    0.0      -1.50    0.0      -1.50    0.0
CLOOF3  806     1        823      824      800      30       30       30      +CL806
+CL806                                                                        +CO806
+CO806  -1.95    0.       -1.95    0.       -1.95    0.
CLOOF3      1806       1      823     1824     1800       30       30      30+CL 806
+CL 806                                                                       +CO 806
+CO 806 -1.95    0.       -1.95    0.       -1.95    0.
CLOOF3       800       1      800      801      802       30       31      31+CL800
+CL800                                                                        +CO800
+CO800     -1.950      0.0  -1.535      0.0  -1.535       0.
CLOOF3      1800       1     1800     1801     1802       30       31      31+CL 800
+CL 800                                                                       +CO 800
+CO 800    -1.950      0.0  -1.535      0.0  -1.535       0.
CLOOF3       801       1      802      803      804       31       31      32+CL801
+CL801                                                                        +CO801
+CO801     -1.535      0.0  -1.535      0.0  -1.280       0.
CLOOF3      1801       1     1802     1803     1804       31       31      32+CL 801
+CL 801                                                                       +CO 801
+CO 801    -1.535      0.0  -1.535      0.0  -1.280       0.
CLOOF3       802       1      804      805      806       32       32      32+CL802
+CL802                                                                        +CO802
+CO802     -1.280      0.0  -1.280      0.0  -1.28        0.
CLOOF3      1802       1     1804     1805     1806       32       32      32+CL 802
+CL 802                                                                       +CO 802
+CO 802    -1.280      0.0  -1.280      0.0  -1.28        0.
CLOOF3       803       1      806      807      808       33       33      33+CL803
+CL803                                                                        +CO803
+CO803     -1.410      0.0  -1.410      0.0  -1.410       0.
CLOOF3      1803       1     1806     1807     1808       33       33      33+CL 803
+CL 803                                                                       +CO 803
+CO 803    -1.410      0.0  -1.410      0.0  -1.410       0.
CLOOF3       804       1      808      809      810       33       33      33+CL804
+CL804                                                                        +CO804
+CO804     -1.410      0.0  -1.410      0.0  -1.410       0.
CLOOF3      1804       1     1808     1809     1810       33       33      33+CL 804
+CL 804                                                                       +CO 804
```

```
+CO 804    -1.410      0.0   -1.410      0.0   -1.410      0.
CLOOF3        805        1      810      811      812      33        33      33+CL805
+CL805                                                                        +CO805
+CO805     -1.410      0.0   -1.410      0.0   -1.410      0.
CLOOF3       1805        1     1810     1811     1812      33        33      33+CL 805
+CL 805                                                                       +CO 805
+CO 805    -1.410      0.0   -1.410      0.0   -1.410      0.
CLOOF3        807        1      812      821      820      58        58      58+CL807
+CL807                                                                        +CO807
+CO807      -2.31      0.0    -2.31      0.0    -2.31      0.
CLOOF3       1807        1     1812     1821     1820      58        58      58+CL 807
+CL 807                                                                       +CO 807
+CO 807     -2.31      0.0    -2.31      0.0    -2.31      0.
CLOOF3        808        1      920      822      812      39        39      39+CL808
+CL808
CLOOF3       1808        1     1920     1822     1812      39        39      39+CL 808
+CL 808                                                                       +CO 808
+CO 808     -2.31      0.0    -2.31      0.0    -2.31      0.
CLOOF3        809        1      800      819      900      61        61      61+CL809
+CL809  1.       0.       0.       1                                          +CO809
+CO809  0.78     0.0      0.78     0.0      0.78     0.0
CLOOF3       2809        1     1800     1819     1900      61        61      61+CL1809
+CL1809 1.          0.0000.        1                                          +CO1809
+CO1809 0.78     0.0      0.78     0.0      0.78     0.0
CLOOF3  810      1        920      826      746      41       41      41      +CL810
+CL810  1.       0.       0.       1                                          +CO810
+CO810  0.0      1.15     0.0      0.0      1.04     0.0
CLOOF3       2810        1     1920     1826     1746      41        41      41+CL1810
+CL1810 1.          0.0000.        1                                          +CO1810
+CO1810 0.0      1.15     0.0      0.0      1.04     0.0
CLOOF3        811        1      746      747      723      41        41      41+CL811
+CL811  1.       0.       0.       1                                          +CO811
+CO811  1.04     0.0      1.04     0.0      2.0      0.0
CLOOF3       2811        1     1746     1747      723      41        41      41+CL1811
+CL1811 1.          0.0000.        1                                          +CO1811
+CO1811 1.04     0.0      1.04     0.0      2.0      0.0
CLOOF3        900        1      900      901      902      35        35      35+CL900
+CL900                                                                        +CO900
+CO900      -2.61      0.0   -2.610      0.0   -2.610      0.
CLOOF3       1900        1     1900     1901     1902      35        35      35+CL 900
+CL 900                                                                       +CO 900
+CO 900     -2.61      0.0   -2.610      0.0   -2.610      0.
CLOOF3        901        1      902      903      904      36        36      36+CL901
+CL901                                                                        +CO901
+CO901     -3.120      0.0   -3.120      0.0   -3.120      0.
CLOOF3       1901        1     1902     1903     1904      36        36      36+CL 901
+CL 901                                                                       +CO 901
+CO 901    -3.120      0.0   -3.120      0.0   -3.120      0.
CLOOF3        902        1      904      905      906      36        36      36+CL902
+CL902                                                                        +CO902
```

```
+CU902    -3.120     0.0  -3.120     0.0  -3.120     0.
CLOOF3      1902       1    1904    1905    1906      36      36    36+CL 902
+CL 902                                                                +CO 902
+CO 902   -3.120     0.0  -3.120     0.0  -3.120     0.
CLOOF3       903       1     906     907     908      37      37    37+CL903
+CL903                                                                 +CO903
+CO903    -2.750     0.0  -2.750     0.0  -2.750     0.
CLOOF3      1903       1    1906    1907    1908      37      37    37+CL 903
+CL 903                                                                +CO 903
+CO 903   -2.750     0.0  -2.750     0.0  -2.750     0.
CLOOF3       904       1     908     909     910      37      37    37+CL904
+CL904                                                                 +CO904
+CO904    -2.750     0.0  -2.750     0.0  -2.750     0.
CLOOF3      1904       1    1908    1909    1910      37      37    37+CL 904
+CL 904                                                                +CO 904
+CO 904   -2.750     0.0  -2.750     0.0  -2.750     0.
CLOOF3       905       1     910     911     912      37      37    38+CL905
+CL905                                                                 +CO905
+CO905    -2.750     0.0  -2.750     0.0  -1.500     0.
CLOOF3      1905       1    1910    1911    1912      37      37    38+CL 905
+CL 905                                                                +CO 905
+CO 905   -2.750     0.0  -2.750     0.0  -1.500     0.
CLOOF3       906       1     912     921     920      38      38    38+CL906
+CL906                                                                 +CO906
+CO906    -1.500     0.0  -1.500     0.0  -1.500     0.
CLOOF3      1906       1    1912    1921    1920      38      38    38+CL 906
+CL 906                                                                +CO 906
+CO 906   -1.500     0.0  -1.500     0.0  -1.500     0.
PLOOF         11       1    0.04
PLOOF         12       1     .11
PLOOF         13       1     .06
PLOOF         15       1     .14
PLOOF         17       1    .075
PLOOF         19       1     .12
PLOOF         20       1     .07
PLOOF       1011       1    0.04
PLOOF       1012       1     .11
PLOOF       1013       1     .06
PLOOF       1015       1     .14
PLOOF       1017       1    .075
PLOOF       1019       1     .12
PLOOF       1020       1     .07
PLOOFX  1       4.637+5 1.549+5 0.0     6.68+5  0.0     1.544+5         +PL1
+PL1    5.86E-3 0.      0.      0.      -7.56+4 0.      0.              +PLL1
+PLL1           61.83   20.65   0.0     4.75+4  0.0     72.48
PLOOFX  2       4.637+5 1.549+5 0.0     1.031+6 0.0     1.544+5         +PL2
+PL2    9.32E-3 0.      0.      0.      -2.10+5 0.      0.              +PLL2
+PLL2           61.83   20.65   0.0     1.318+5 0.0     1.295+2
PLOOFX  3       4.637+5 1.549+5 0.0     7.396+5 0.0     1.544+5         +PL3
+PL3    6.54E-3 0.      0.      0.      -1.021+5                        +PLL3
```

```
+PLL3              61.83    20.65    0.0        64.08    0.0        84.09
PLOOFX    4        9.411+5  1.549+5  0.0        4.637+5  0.0        1.544+5             +PL4
+PL4      8.46E-3  -2.11+5                                                              +PLL4
+PLL4              1.607+5  20.65    0.0        61.83    0.0        3.364+2
PLOOFX    5        4.637+5  1.549+5  0.0        7.642+5  0.0        1.544+5             +PL5
+PL5      6.78E-3  0.       0.       0.         -1.112+50.          0.                  +PLL5
+PLL5              61.83    20.65    0.0        6.98+4   0.0        87.91
PLOOFX    6        1.266+6  2.323+5  0.0        6.956+5  0.0        2.316+5             +PL6
+PL6      9.34E-3  -2.576+50.        0.         0.       0.         0.                  +PLL6
+PLL6              1.971+5  69.69     0.0       2.087+2  0.0        4.914+2
PLOOFX    7        4.637+5  1.549+5  0.0        7.191+5  0.0        1.544+5             +PL7
+PL7      6.54-3   0.       0.       0.         -9.451+40.          0.                  +PLL7
+PLL7              61.83    20.65    0.0        5.934+4  0.0        80.92
PLOOFX    8        1.005+6  2.323+5  0.0        6.956+5  0.0        2.316+5             +PL8
+PL8      8.82-3   -6.798+40.        0.         0.       0.         0.                  +PLL8
+PLL8              2.976+4  69.70     0.0       2.087+2   0.0       2.355+2
PLOOFX     9       1.015+6   2.323+5 0.0         6.956+5 0.0         2.316+5            +PL9
+PL9      8.82-3   -1.213+5 0.       0.         0.       0.         0.                  +PLL9
+PLL9              7.67+4    69.70    0.0        2.087+2  0.0        1.887+2
PLOOFX    10       4.637+5  1.549+5  0.0        6.767+5  0.0        1.544+5             +PL10
+PL10     5.04-3   0.       0.       0.         -7.876+4            0.                  +PLL10
+PLL10             61.83    20.64    0.0        4.946+4  0.0        74.31
PLOOFX    14       7.547+5  1.549+5  0.0        4.637+5  0.0        1.544+5             +PL14
+PL14     6.69-3   -1.129+5          0.         0.       0.         0.                  +PLL14
+PLL14             7.168+4  20.65    0.0        61.83    0.0        96.17
PLOOFX    16       1.307+6  1.549+5  0.0        4.637+5  0.0        1.544+5             +PL16
+PL16     1.19-2   -2.278+50.        0.         0.       0.         0.                  +PLL16
+PLL16             7.922+4  20.65    0.0        61.83    0.0        8.386+3
PLOOFX    18       7.384+5  1.549+5  0.0        4.637+5  0.0        1.544+5             +PL18
+PL18     6.53-3   -5.768+4                                                             +PLL18
+PLL18             2.515+4  20.65    0.0        61.83    0.0        126.97
PLOOFX    1001     4.637+5  1.549+5  0.0        6.68+5   0.0        1.544+5             +PL1
+PL1      5.86E-3  0.       0.       0.          7.56+4  0.         0.                  +PLL1
+PLL1              61.83    20.65    0.0        4.75+4   0.0        72.48
PLOOFX    1002     4.637+5  1.549+5  0.0        1.031+6  0.0        1.544+5             +PL2
+PL2      9.32E-3  0.       0.       0.          2.10+5  0.         0.                  +PLL2
+PLL2              61.83    20.65    0.0        1.318+5  0.0        1.295+2
PLOOFX    1003     4.637+5  1.549+5  0.0        7.396+5  0.0        1.544+5             +PL3
+PL3      6.54E-3  0.       0.       0.          1.021+5                                +PLL3
+PLL3              61.83    20.65    0.0        64.08    0.0        84.09
PLOOFX    1004     9.411+5  1.549+5  0.0        4.637+5  0.0        1.544+5             +PL4
+PL4      8.46E-3   2.11+5                                                              +PLL4
+PLL4              1.607+5  20.65    0.0        61.83    0.0        3.364+2
PLOOFX    1005     4.637+5  1.549+5  0.0        7.642+5  0.0        1.544+5             +PL5
+PL5      6.78E-3  0.       0.       0.          1.112+50.          0.                  +PLL5
+PLL5              61.83    20.65    0.0        6.98+4   0.0        87.91
PLOOFX    1006     1.266+6  2.323+5  0.0        6.956+5  0.0        2.316+5             +PL6
+PL6      9.34E-3   2.576+5                                                             +PLL6
+PLL6              1.971+5  69.69     0.0       2.087+2  0.0        4.914+2
PLOOFX    1007     4.637+5  1.549+5  0.0        7.191+5  0.0        1.544+5             +PL7
```

```
+PL7      6.34-3    0.        0.        0.        9.451+4
+PLL7               61.83     20.65     0.0       5.934+4 0.0       80.92             +PLL7
PLOOFX    1008      1.005+6 2.323+5 0.0         6.956+5 0.0       2.316+5           +PL8
+PL8      8.82-3    6.798+4                                                         +PLL8
+PLL8               2.976+4 69.70       0.0     2.087+2   0.0     2.355+2
PLOOFX    1009      1.015+6   2.323+5 0.0       6.956+5 0.0       2.316+5           +PL9
+PL9      8.82-3    1.213+5                                                         +PLL9
+PLL9               7.67+4    69.70     0.0     2.087+2   0.0     1.887+2
PLOOFX    1010      4.637+5 1.549+5 0.0         6.767+5 0.0       1.544+5           +PL10
+PL10     5.04-3                                7.876+4                             +PLL10
+PLL10              61.83     20.64     0.0     4.946+4 0.0       74.31
PLOOFX    1014      7.547+5 1.549+5 0.0         4.637+5 0.0       1.544+5           +PL14
+PL14     6.69-3    1.129+5                                                         +PLL14
+PLL14              7.168+4 20.65       0.0     61.83     0.0     96.17
PLOOFX    1016      1.307+6 1.549+5 0.0         4.637+5 0.0       1.544+5           +PL16
+PL16     1.19-2    2.278+5                                                         +PLL16
+PLL16              7.922+4 20.65       0.0     61.83     0.0     8.386+3
PLOOFX    1018      7.384+5 1.549+5 0.0         4.637+5 0.0       1.544+5           +PL18
+PL18     6.53-3    5.768+4                                                         +PLL18
+PLL18              2.515+4 20.65               61.83             126.97
PLOOFX    25        1.260+6 2.323+5 0.0         6.956+5 0.0       2.316+5           +PL25
+PL25     9.34E-3   2.576+50.           0.      0.        0.      0.                +PLL25
+PLL25              1.971+5 69.69       0.0     2.087+2 0.0       4.914+2
PLOOFX    26        1.005+6 2.323+5 0.0         6.956+5 0.0       2.316+5           +PL26
+PL26     8.82-3    6.798+40.           0.      0.        0.      0.                +PLL26
+PLL26              2.976+4 69.70       0.0     2.087+2   0.0     2.355+2
PLOOFX    27        1.015+6   2.323+5 0.0       6.956+5 0.0       2.316+5           +PL27
+PL27     8.82-3    1.213+5 0.          0.      0.        0.      0.                +PLL27
+PLL27              7.67+4    69.70     0.0     2.087+2   0.0     1.887+2
PLOOFX    28        1.307+6 1.549+5 0.0         4.637+5 0.0       1.544+5           +PL28
+PL28     1.19-2    2.278+50.           0.      0.        0.      0.                +PLL28
+PLL28              7.922+4 20.65       0.0     61.83     0.0     8.386+3
PLOOFX    29        4.637+5 1.549+5 0.0         6.767+5 0.0       1.544+5           +PL29
+PL29     5.04-3    0.        0.        0.      7.876+4           0.                +PLL29
+PLL29              61.83     20.64     0.0     4.946+4 0.0       74.31
PLOOFX    30        4.637+5 1.549+5 0.0         7.396+5 0.0       1.544+5           +PL30
+PL30     6.54E-3   0.        0.        0.      1.021+5                             +PLL30
+PLL30              61.83     20.65     0.0     64.08     0.0     84.09
PLOOFX    31        4.637+5 1.549+5 0.0         6.68+5    0.0     1.544+5           +PL31
+PL31     5.86E-3   0.        0.        0.      7.56+4  0.        0.                +PLL31
+PLL31              61.83     20.65     0.0     4.75+4    0.0     72.48
PLOOFX    32        4.637+5 1.549+5 0.0         7.642+5 0.0       1.544+5           +PL32
+PL32     6.78E-3   0.        0.        0.      1.112+50.         0.                +PLL32
+PLL32              61.83     20.65     0.0     6.98+4    0.0     87.91
PLOOFX    1025      1.206+6 2.323+5 0.0         6.956+5 0.0       2.316+5           +PL1025
+PL1025   9.34E-3   -2.576+50.          0.      0.        0.      0.                +PLL102
+PLL1025            1.971+5 69.69       0.0     2.087+2 0.0       4.914+2
PLOOFX    1026      1.005+6 2.323+5 0.0         6.956+5 0.0       2.316+5           +PL1026
+PL1026   8.82-3    -6.798+40.          0.      0.        0.      0.                +PLL102
+PLL1026            2.976+4 69.70       0.0     2.087+2   0.0     2.355+2
```

```
PLOOFX   1027     1.015+6  2.323+5 0.0       6.956+5 0.0      2.316+5           +PL1027
+PL1027 8.82-3   -1.213+5 0.       0.        0.      0.       0.                +PLL1027
+PLL1027          7.67+4   69.70    0.0       2.087+2  0.0     1.887+2
PLOOFX   1028     1.307+6 1.549+5 0.0        4.637+5 0.0      1.544+5           +PL1028
+PL1028 1.19-2   -2.278+50.        0.        0.      0.       0.                +PLL1028
+PLL1028          7.922+4 20.65    0.0       61.83   0.0      8.386+3
PLOOFX   1029     4.637+5 1.549+5 0.0        6.767+5 0.0      1.544+5           +PL1029
+PL1029 5.04-3    0.      0.       0.        -7.876+4         0.                +PLL1029
+PLL1029          61.83   20.64    0.0       4.946+4 0.0      74.31
PLOOFX   1030     4.637+5 1.549+5 0.0        6.68+5  0.0      1.544+5           +PL1030
+PL1030 6.54E-3 0.        0.       0.        -1.021+5                           +PLL1030
+PLL1030          61.83   20.65    0.0       64.08   0.0      84.09
PLOOFX   1031     4.637+5 1.549+5 0.0        6.68+5  0.0      1.544+5           +PL1031
+PL1031 5.86E-3 0.        0.       0.        -7.56+4 0.       0.                +PLL1031
+PLL1031          61.83   20.65    0.0       4.75+4  0.0      72.48
PLOOFX   1032     4.637+5 1.549+5 0.0        7.642+5 0.0      1.544+5           +PL1032
+PL1032 6.78E-3 0.        0.       0.        -1.112+50.       0.                +PLL1032
+PLL1032          61.83   20.65    0.0       6.98+4  0.0      87.91
PLOOF3          1   0.250   0.261  0.92-2 0.300-3
PLOOF3          2   0.252   0.255  0.0110 0.302-3
PLOOF3          3   0.285   0.276  0.0122 0.465-3
PLOOF3          4   0.266   0.319  0.0112 0.319-3
PLOOF3  5          .33     .710    .418-2  .400-3
PLOOF3          6   5.360   9.630  0.29+1 0.898-0
PLOOF3          7   3.890   6.960  1.1700 0.435-0
PLOOF3          8   2.420   5.570  0.8830 0.646-1
PLOOF3          9   1.830   2.630  0.8120 0.416-1
PLOOF3         10   0.349   0.506  0.0116 0.654-3
PLOOF3         11   0.319   0.370  0.0113 0.598-3
PLOOF3         12   0.284   0.243  0.0108 0.532-3
PLOOF3         13   0.251   0.153  0.0103 0.470-3
PLOOF3         14   0.486   0.561  0.0845 0.104-2
PLOOF3         15   0.330   0.353  0.0118 0.703-3
PLOOF3         16   1.080   1.060  0.1430 0.218-1
PLOOF3         17   1.130   1.200  0.1540 0.248-1
PLOOF3         18   0.293   0.206  0.0165 0.550-3
PLOOF3         19   0.337   0.559  5.35-3 0.550-3
PLOOF3         20   0.424   1.180  7.39-3 0.693-3
PLOOF3         21   0.284   0.310  0.76-2 0.464-3
PLOOF3         22   0.347   0.389  0.0312 0.567-3
PLOOF3         23   0.316   0.423  0.0108 0.516-3
PLOOF3         24   0.438   1.270  0.0117 0.716-3
PLOOF3         25   0.242   0.125  0.0120 0.454-3
PLOOF3         26   0.376   1.130  0.0489 0.379-3
PLOOF3         27   0.485   2.170  0.0646 0.489-3
PLOOF3         28   0.830   3.250  0.0856 0.299-2
PLOOF3         29   0.904   4.680  0.0578 0.348-2
PLOOF3         30   0.389   0.300  0.0257 0.392-3
PLOOF3         31   0.298   0.335  0.0173 0.301-3
PLOOF3         32   0.184   0.145  2.21-3 0.186-3
```

```
PLOOF3          33    0.231     0.247    0.0101 0.233-3
PLOOF3          34    1.490     4.600    0.1870 0.508-1
PLOOF3          35    1.700     8.200    0.2350 0.633-1
PLOOF3          36    2.000     12.90    0.2450 0.723-1
PLOOF3          37    1.490     7.460    0.1800 0.427-1
PLOOF3          38    1.170     1.370    0.0691 0.366-1
PLOOF3          39    1.950     3.700    0.8520 0.414-1
PLOOF3  40      1.97    .447    4.27    .400-1
PLOOF3  41      1.58    1.27    .408    .399-1
PLOOF3  45      .504    .236    .134    .329-2
PLOOF3  46      .486    .197    .134    .317-2
PLOOF3  47      .347    .109    .151-4
PLOOF3  47      .347    .109    .151-1  .227-2
PLOOF3  48      .361    .106    .311-1  .236-2
PLOOF3  49      .151    .569-2  .683-1  .153-3
PLOOF3  50      0.75    .134    .017    0.052
PLOOF3  51      2.04    .415    .024    0.082
PLOOF3  52      3.09    1.49    .146    0.468
PLOOF3  53      .320    .728-1  .175-1  .194-2
PLOOF3  54      .460    .213-1  .863-1  .706-2
PLOOF3  55      .127    .509-1  .265-2  .106-3
PLOOF3  56      0.55    0.087   0.133   .007
PLOOF3  57      .150    .850-1  .617-2  .125-3
PLOOF3  58      2.14    2.50    2.08    .489-1
PLOOF3  59      .084    .468-2  .679-2  .696-4
PLOOF3  75      .320    .728-1  .180-1  .194-2
PLOOF3  78      3.60    2.70    .432    1.293
PLOOF3  61      .09     .019    2.79-5  1.09-4
PLOOF3  42      .39     .073    .002    .008
PLOOF3  43      .39     .002    .073    .008
PLOOF3  39      1.95    .852    3.70    .414-1
PLOOF3  66      .338    .267-1  .759-1  .205-2
PLOOF3  67      .270    .579    .617-1  .164-2
PLOOF3  73      .409    .205-1  .220    .165-2
PLOOF3  74      .284    .42-1   .42-1   .137-2
PLOOF3  79      .641    .182    .619-1  .692-2
PLOOF3  80      .619    .145    .614-1  .669-2
PLOOF3  81      .596    .11     .618-1  .643-2
PLOOF3  82      .253    .207-1  .613-1  .843-3
PLOOF3  83      .328    .997-1  .723-1  .109-2
PLOOF3  84      .403    .267    .793-1  .134-2
PLOOF3  85      .330    .284-1  .782-1  .145-2
PLOOF3  86      .400    .314-1  .266    .157-2
PLOOF3  87      .453    .331-1  .521    .165-2
MAT1    1       10.3E6  3.86E6          .103
PARAM   WTMASS  2.59E-3
PARAM   GRDPNT  0
RBE2    190     151     123456  150     200     223     1200
CONM2   192     150     1       11.55   -0.39   -3.43   -1.16           +CON192
+CON192   3.028           8.733                   134.05
```

```
DYNRED  2       150.0                                   50                      YES
EIGR    2       GIV                                     50                      1.E-9   +E2
+E2     MAX
EIGR    1       INV     0.0     30.0    3       3                               1.E-10  +E
+E      MAX
SPOINT  5001    THRU    5050
ASET1   0       5001    THRU    5050
SUPORT  774     123     112     12      922     2
ENDDATA
```


☆U.S.Government Printing Office: 1979 — 657-002/657